Appendix 16
Concrete I-Wall and Sheet Piling Material Recovery, Sampling and Testing: IHNC

Introduction

On Friday, 6 January 2006, samples of the concrete I-wall, reinforcing steel and sheet piling were taken from the I-wall on west bank of the Inner Harbor Navigation Canal. The location from which the materials were sampled was the west side of France Rd. near France Road Parkway. The primary objective of this exercise was to determine material properties of the I-wall concrete and reinforcing steel, and the sheet piling.

Material Sampling

An approximately eight foot long by 44 inch high section was sawcut from the top of the concrete I-wall as shown if Figure 16-1. The sample was taken from a location at approximately Station 0+44 and was labeled IPET-WE-EW 0+44.

Figure 16-1. Sawcutting Concrete Wall Sample

This sample was transported to the warehouse at the New Orleans District office. On 11 January, three six inch diameter concrete cores were taken from the wall sample by Beta Testing & Inspection for compressive testing.

An 8 by 24 inch sample was taken from the web each of two sheet piling at the site. (See Figures 16-2 and 16-3.) The pilings were labeled IHNC-SP-WS-B1 and IHNC-SP-WS-B2 and the corresponding samples were labeled IHNC-WS-B1A and IHNC-WS-B2A. The samples were provided to Beta Testing & Inspection for testing. The sheet piling was transported to the warehouse at the New Orleans District office.

Figure 16-2. Flame Cutting of Material Samples from Piling IHNC-SP-WS-B2

Figure 16-3. Flame Cutting Material Samples from Sheet Piling IHNC-SP-WS-B1

Four samples of reinforcing steel recovered from the I-wall at approximately Station 2+00 were also provided to Beta Testing and Inspection for testing. The samples were two pieces each of #4 and #6 rebar and were labeled IHNC WEST 4A, IHNC WEST 4B, IHNC WEST 6A and IHNC WEST 6B.

Test Results

Complete test results are detailed in the report by Beta Testing and Inspection included in Attachment A. The test data are summarized in Tables 16-1, 16-2, and 16-3. Material specifications for IHNC West I-wall system were not found despite extensive effort to locate them.

Table 16-1
Concrete Compressive Strength

Core Sample	Compressive Strength (psi)
IPET-WS-EW-1	5220
IPET-WS-EW-2	5850
IPET-WS-EW-3	6650

Table 16-2
Sheet Piling Tensile Properties

Sample	Yield Strength (ksi)	Tensile Strength (ksi)	Elongation in 8 in. (%)
IHNC-SP-WS-B1A	51.95	81.84	16.25
IHNC-SP-WS-B2A	61.10	89.94	15.83

The samples of the #6 rebars evidently contained small welds that were not observed during sampling. Consequently, the samples provided spurious test results and are not included here but are included in the report by Beta Testing & Inspection in Attachment A.

Sample	Bar Size	Yield Strength (ksi)	Tensile Strength (ksi)	Elongation in 8 in. (%)
IHNC-WEST-4A	4	51.00	81.00	14.12
IHNC-WEST-4B	4	48.50	79.00	14.12

Attachment A
Test Report from Beta Test & Inspection, LLC

Beta Testing & Inspection, LLC
Forensic Engineering Division

March 9, 2006

Paul F. Mlakar, Ph.D., P.E.

US Army Corps of Engineers
Engineer Research and Development Center
3909 Halls Ferry Road
Vicksburg, MS 39180

RE: Testing of IHNC West Side South of France Rd.
Ramp to 700' North of Benefit Street Gate
Final Report
BTI Report No.: 1054-ES010606

Dear Mr. Mlaker:

On January 6, 2006 at the referenced site, sheet pile samples and steel reinforcing bars were sampled. On January 11, 2006 concrete specimens were sampled at the US Army Corps of Engineers New Orleans District warehouse. BTI cut a total of three concrete cores from a wall section identified as IPET-WS-EW 0+44 Flood Side. Mark Cheek, P.E. of BTI witnessed the removal of 8"x 24" section from two different sheet piles and assumed responsible possession of the sheet pile samples and four reinforcing bars; two No.4 and two No.6. Representatives of BTI were informed by the Corps of Engineers that the material samples provided to BTI or obtained by BTI were portions of existing components taken from the IHNC West Side South of France Road Ramp to 700' North of Benefit Street Gate. All specimens were labeled, tagged, and secured prior to transporting. Samples were transported to Beta Testing & Inspection, LLC (BTI) laboratory for testing. Project Material data sheets and project specifications for the sampled materials were not provided. BTI has completed testing of concrete cores, steel sheet pile sections, and steel reinforcing bars.

Concrete Cores

Three cores were cut from the Flood side of sample panel IPET-WS-EW-O+44 Flood Side. The cores were obtained in accordance with procedures defined by ASTM C-42. Prior to compression testing each core was prepared in accordance with ASTM C-42, C-617, and C-39. Each core was then tested in compression to failure and the results recorded in accordance with ASTM C-39. See Table C.1 for results of the concrete core testing.

P.O. Box 2203 • Gretna, LA 70054 • (504) 227-2273 • fax (504) 227-2274
13801 Old Gentilly Road Suite #17 New Orleans, Louisiana 70129

Testing of IHNC West Side March 9, 2006

Table C.1

Sample panel MH38C1						
Core ID	Capped Length (in.)	Diameter (in)	Area (in^2)	l/d	Correction factor	Maximum load (lbs.)
IPET-WS-EW-1	9.9	5.62	24.8	1.76	0.98	132,000
	Compressive strength (psi)	Fracture type	Age (days)	Load application	Test date/time	Sample date/time
	5220	A	NA	vertical	1/12/06 11:00am	1/11/06 10:00am
Core ID	Capped Length (in.)	Diameter (in)	Area (in^2)	l/d	Correction factor	Maximum load (lbs.)
IPET-WS-EW-2	10.25	5.62	24.8	1.82	1.0	145,000
	Compressive strength (psi)	Fracture type	Age (days)	Load application	Test date/time	Sample date/time
	5850	B	NA	vertical	1/12/06 11:00am	1/11/06 11:00am
Core ID	Capped Length (in.)	Diameter (in)	Area (in^2)	l/d	Correction factor	Maximum load (lbs.)
IPET-WS-EW-3	9.69	5.62	24.8	1.72	0.97	170,000
	Compressive strength (psi)	Fracture type	Age (days)	Load application	Test date/time	Sample date/time
	6650	B	NA	vertical	1/12/06 11:00am	1/11/06 12:00am

Average compressive strength (psi)	5907

Testing of IHNC West Side

March 9, 2006

Steel Sheet Piling

A welder provided by Pittman Construction cut one 8"x 24" specimen from each of the two-sheet pile using an acetylene cutting torch. Mandina's Inspection a subcontractor of BTI then prepared and tested each specimen in tension to failure in accordance with ASTM A-370. For test results see table SP-1 and graph SP-1

Steel Reinforcing Bars

Four pieces of steel reinforcing bars were secured and transported to BTI's laboratory. The steel reinforcing bar samples ranged in size from No. 4 to No. 6 bars. Mandina's Inspection a subcontractor of BTI tested the rebar specimens to failure in accordance with ASTM A-615 & A370. For test results see table RB-1 and graph RB-1

Upon completion and acceptance of the testing program, all of the materials, tested and untested, will be sealed and returned to the New Orleans District Office of the US Army Corps of Engineers. Enclosed are copies of our laboratory accreditations and equipment calibration reports associated with the test performed. Should you have any questions regarding this letter or require additional information, please do not hesitate to contact us.

Sincerely,

Beta Testing & Inspection, LLC

Mark A. Cheek

Mark A. Cheek, P.E.
Vice-President

Enclosures

TABLE SP-1

MECHANICAL TESTING LABORATORY DIVISION

Mandrina's Insp. 2-24-06

MTL JOB NO. 4405.90

TENSILE NO. _____
BTI # 1054

SPECIMEN ID	WIDTH INCHES	THICKNESS SQ. IN.	AREA SQ. IN.	YIELD STR. POUNDS	YIELD STR. PSI	TENSILE STR. POUNDS	TENSILE STR. PSI	ELONGATION IN 8" GAGE PERCENT
HNC-SP-WS-B1-A	1.441	.356	.512	26600	51953	41900	81835	9.300 16.25%

TENSILE NO. _____
BTI # 1054

SPECIMEN ID	WIDTH INCHES	THICKNESS SQ. IN.	AREA SQ. IN.	YIELD STR. POUNDS	YIELD STR. PSI	TENSILE STR. POUNDS	TENSILE STR. PSI	ELONGATION IN 8" GAGE PERCENT
HNC-SP-WS-B2-A	1.487	.355	.527	32200	61100	47400	89948	9.267 15.83%

G:\WORDDATA\ISIFORMS\TTFY.LAB

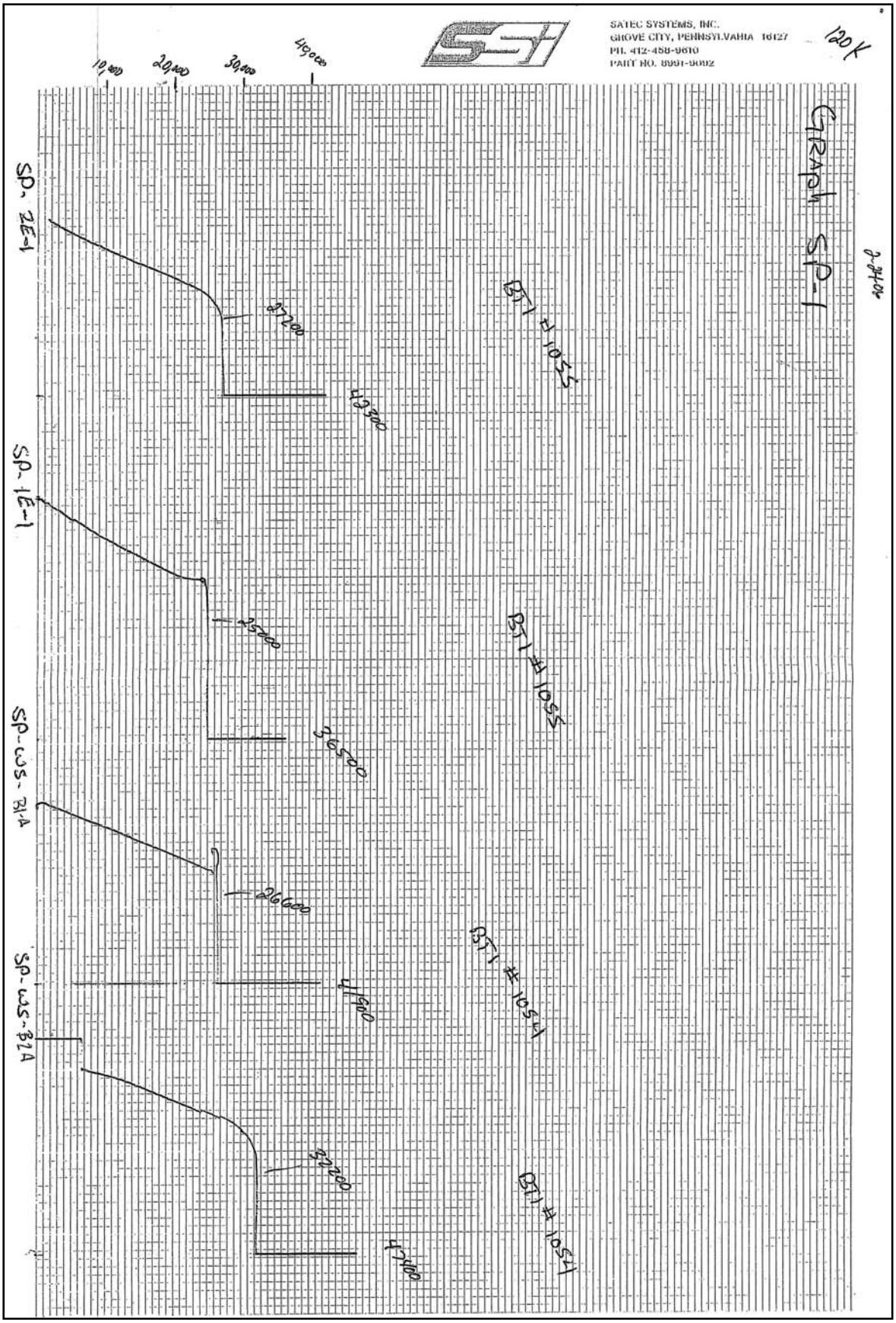

TABLE RB-1

MECHANICAL TESTING LABORATORY DIVISION

2-24-06

MTL JOB NO. Mandina's BSP. 4406.90

TENSILE NO. BTI # 1054

SPECIMEN ID	DIA. INCHES	AREA SQ. IN.	YIELD LOAD POUNDS	YIELD STR. PSI	ULTIMATE LOAD POUNDS	TENSILE STR. PSI	ELONGATION IN 8" GAGE PERCENT (8" Gage)	REDUCTION IN AREA PERCENT
IPET-RB #6A IHNC west (Pittman) St. 2+00	.750	.44	24700	56136	39300	89318	8.715 8.93%	~~.715~~ .595 .278 36.8%

* FAILED @ WELD

TENSILE NO. BTI # 1054

SPECIMEN ID	DIA. INCHES	AREA SQ. IN.	YIELD LOAD POUNDS	YIELD STR. PSI	ULTIMATE LOAD POUNDS	TENSILE STR. PSI	ELONGATION IN 8" GAGE PERCENT	REDUCTION IN AREA PERCENT
IPET-RB #6B IHNC west (Pittman) St. 2+00	.750	.44	25000	56818	36900	83863	8.415 5.18%	.669 .351 20.2%

* FAILED @ WELD

TENSILE NO. BTI # 1054

SPECIMEN ID	DIA. INCHES	AREA SQ. IN.	YIELD LOAD POUNDS	YIELD STR. PSI	ULTIMATE LOAD POUNDS	TENSILE STR. PSI	ELONGATION IN 2" GAGE PERCENT	REDUCTION IN AREA PERCENT
IPET-RB-4B (Pittman)(west) IHNC-west St. 2+00	.500	.20	9700	48500	15600	79000	9.130 14.12%	.279 .061 69.5%

TENSILE NO. BTI # 1054

SPECIMEN ID	DIA. INCHES	AREA SQ. IN.	YIELD LOAD POUNDS	YIELD STR. PSI	ULTIMATE LOAD POUNDS	TENSILE STR. PSI	ELONGATION IN 8" GAGE PERCENT	REDUCTION IN AREA PERCENT
IPET-RB-#4A (Pittman)(west) IHNC-west St. 2+00	.500	.20	10200	51000	16200	81000	9.130 14.12%	.266 .055 72.5%

G:\WORDDATA\SIFORMS\TT505.LAB

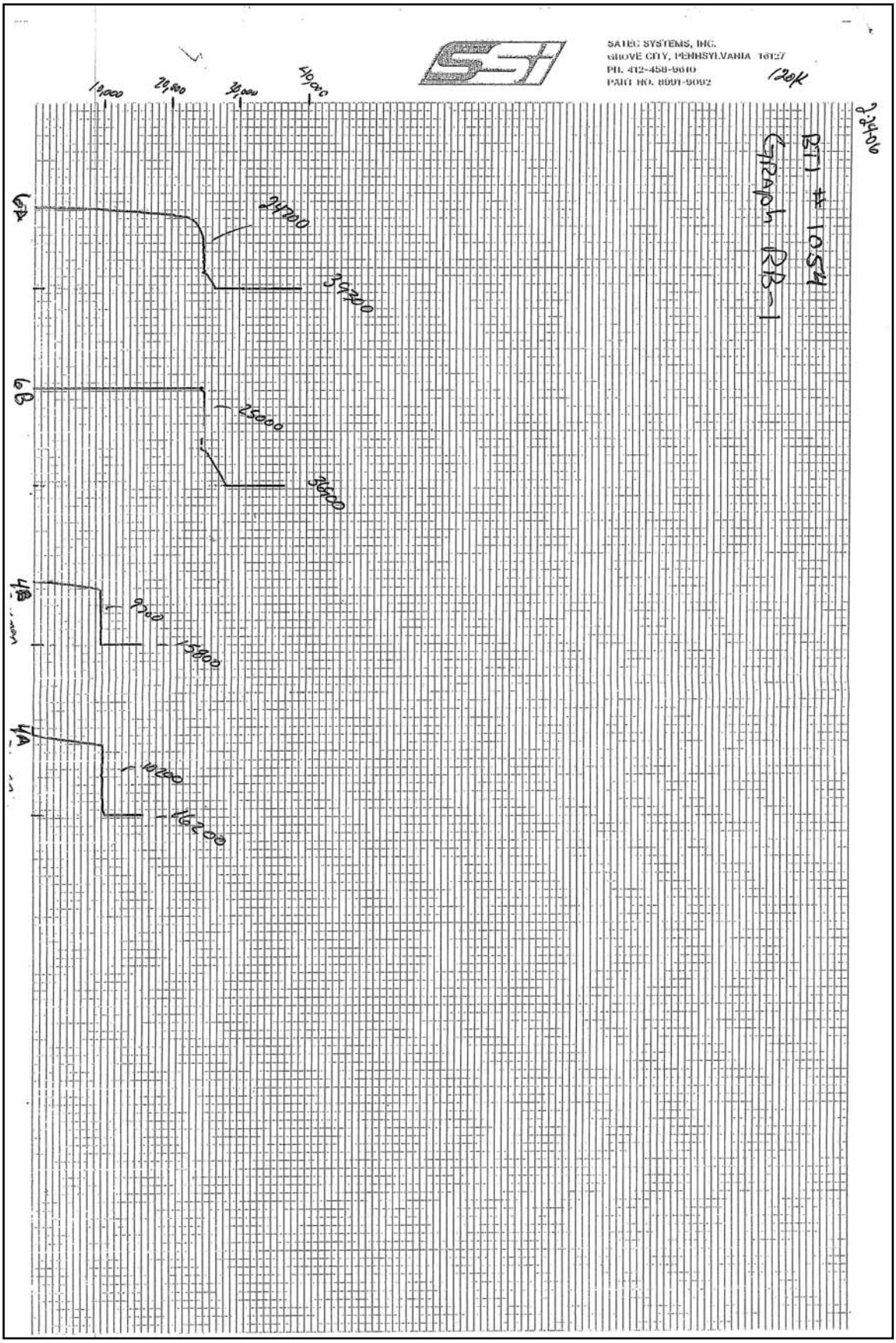

Beta Testing & Inspection, LLC
Forensic Engineering Division

March 9, 2006

Paul F. Mlakar, Ph.D., P.E.

US Army Corps of Engineers
Engineer Research and Development Center
3909 Halls Ferry Road
Vicksburg, MS 39180

RE: Testing of IHNC East Side, North Claiborne Ave. to Florida Ave.
Final Report
BTI Project No.: 1055
BTI Report No.: 1055-ES011306

Dear Mr. Mlaker:

On January 13, 2006 at the referenced site, sheet pile samples, steel reinforcing bars and concrete core specimens were sampled. BTI cut a total of three concrete cores from a wall section identified as IPET-IHNC-E 20+40. Mark Cheek, P.E. of BTI witnessed the removal of 9"x 25" section from two different sheet piles and assumed responsible possession of the sheet pile samples and four reinforcing bars; two No.4 and two No.7. Representatives of BTI were informed by the Corps of Engineers that the material samples provided to BTI or obtained by BTI were portions of existing components taken from the IHNC East Side, North Claiborne Ave. to Florida Ave project. All specimens were labeled, tagged, and secured prior to transporting. Samples were transported to Beta Testing & Inspection, LLC (BTI) laboratory for testing. Project Material data sheets and project specifications for the sampled materials were not provided. BTI has completed testing of concrete cores, steel sheet pile sections, and steel reinforcing bars.

Concrete Cores

Three cores were cut from the sample panel IPET-IHNC-E 20+40. The cores were obtained in accordance with procedures defined by ASTM C-42. Prior to compression testing each core was prepared in accordance with ASTM C-42, C-617, and C-39. Each core was then tested in compression to failure and the results recorded in accordance with ASTM C-39. See Table C.1 for results of the concrete core testing.

P.O. Box 2203 • Gretna, LA 70054 • (504) 227-2273 • fax (504) 227-2274
13801 Old Gentilly Road Suite #17 New Orleans, Louisiana 70129

Testing of IHNC East Side March 9, 2006

Table C.1

Sample panel MH38C1						
Core ID	Capped Length (in.)	Diameter (in)	Area (in^2)	l/d	Correction factor	Maximum load (lbs.)
IPET-IHNC-E1	11.2	5.62	24.8	1.99	1	97,000
	Compressive strength (psi)	Fracture type	Age (days)	Load application	Test date/time	Sample date/time
	3910	A	NA	vertical	1/18/06 10:00am	1/13/06 1:30pm
Core ID	Capped Length (in.)	Diameter (in)	Area (in^2)	l/d	Correction factor	Maximum load (lbs.)
IPET-IHNC-E2	11.2	5.62	24.8	2.0	1.0	95,500
	Compressive strength (psi)	Fracture type	Age (days)	Load application	Test date/time	Sample date/time
	3850	A	NA	vertical	1/12/06 10:15am	1/13/06 2:15pm
Core ID	Capped Length (in.)	Diameter (in)	Area (in^2)	l/d	Correction factor	Maximum load (lbs.)
IPET-IHNC-E3	11.2	5.62	24.8	1.99	1.0	100,500
	Compressive strength (psi)	Fracture type	Age (days)	Load application	Test date/time	Sample date/time
	4050	A	NA	vertical	1/12/06 10:30am	1/13/06 2:30pm

Average compressive strength (psi)	3940

Testing of IHNC East Side

March 9, 2006

Steel Sheet Piling

A welder provided by Cajun Constructors cut one 9"x 25" specimen from each of the two-sheet pile using an acetylene cutting torch. Mandina's Inspection a subcontractor of BTI then prepared and tested each specimen in tension to failure in accordance with ASTM A-370. For test results see table SP-1 and graph SP-1

Steel Reinforcing Bars

Four pieces of steel reinforcing bars were secured and transported to BTI's laboratory. The steel reinforcing bar samples ranged in size from No. 4 to No. 7 bars. Mandina's Inspection a subcontractor of BTI tested the rebar specimens to failure in accordance with ASTM A-615 & A370. For test results see table RB-1 and graph RB-1

Upon completion and acceptance of the testing program, all of the materials, tested and untested, will be sealed and returned to the New Orleans District Office of the US Army Corps of Engineers. Enclosed are copies of our laboratory accreditations and equipment calibration reports associated with the test performed. Should you have any questions regarding this letter or require additional information, please do not hesitate to contact us.

Sincerely,

Beta Testing & Inspection, LLC

Mark A. Cheek

Mark A. Cheek, P.E.
Vice-President

Enclosures

Table SP-1

MECHANICAL TESTING LABORATORY DIVISION

Mardinaia's Insp. 2.24.06

MTL JOB NO. 4405.90

TENSILE NO. _____
BT1 # 1055

SPECIMEN ID	WIDTH INCHES	THICKNESS SQ. IN.	AREA SQ. IN.	YIELD STR. POUNDS	YIELD STR. PSI	TENSILE STR. POUNDS	TENSILE STR. PSI	ELONGATION IN 8" GAGE PERCENT
IPET-SP-1E-1	1.445	.321	.463	25000	53995	36500	78833	9.200 15.0 %

TENSILE NO. _____
BT1 # 1055

SPECIMEN ID	WIDTH INCHES	THICKNESS SQ. IN.	AREA SQ. IN.	YIELD STR. POUNDS	YIELD STR. PSI	TENSILE STR. POUNDS	TENSILE STR. PSI	ELONGATION IN 8" GAGE PERCENT
IPET-SP-2E-1	1.452	.358	.519	27200	52408	42300	81502	9.326 16.5 %

TENSILE NO. _____

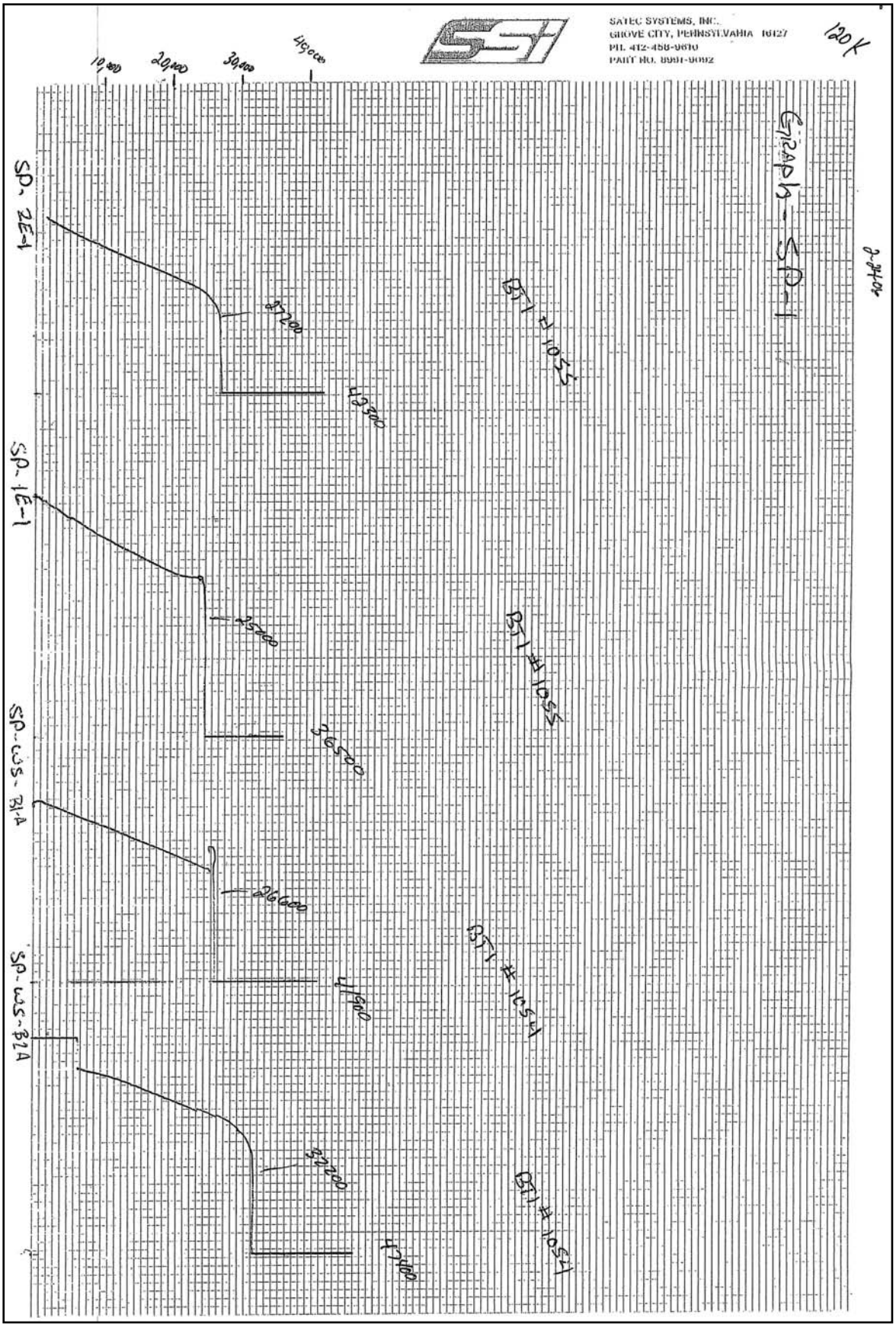

TABLE RB-1

MECHANICAL TESTING LABORATORY DIVISION

MTL JOB NO. Mandina's IHNC 4405.90 2-24-06

TENSILE NO. _____
BTI # 1055

SPECIMEN ID	DIA. INCHES	AREA SQ. IN.	YIELD LOAD POUNDS	YIELD STR. PSI	ULTIMATE LOAD POUNDS	TENSILE STR. PSI	ELONGATION IN 8" GAGE PERCENT	REDUCTION IN AREA PERCENT
IPET-RB-E1 IHNC)(EAST) (CAJun)	.875	.60	39500	65833	63100	105166	8.847 10.58%	.735 .424 3.6%

TENSILE NO. _____
BTI # 1055

SPECIMEN ID	DIA. INCHES	AREA SQ. IN.	YIELD LOAD POUNDS	YIELD STR. PSI	ULTIMATE LOAD POUNDS	TENSILE STR. PSI	ELONGATION IN 8" GAGE PERCENT	REDUCTION IN AREA PERCENT
IPET-RB-E2 IHNC)(EAST) CAJun	.875	.60	38500	64166	61600	102666	8.925 11.56%	.630 .311 12.9%

TENSILE NO. _____
BTI # 1055

SPECIMEN ID	DIA. INCHES	AREA SQ. IN.	YIELD LOAD POUNDS	YIELD STR. PSI	ULTIMATE LOAD POUNDS	TENSILE STR. PSI	ELONGATION IN 8" GAGE PERCENT	REDUCTION IN AREA PERCENT
IPET-RB-E3 IHNC)(EAST) CAJun	.500	.20	9200	46000	14800	74000	9.595 19.5%	.275 .055 70.5%

TENSILE NO. _____
BTI # 1055

SPECIMEN ID	DIA. INCHES	AREA SQ. IN.	YIELD LOAD POUNDS	YIELD STR. PSI	ULTIMATE LOAD POUNDS	TENSILE STR. PSI	ELONGATION IN 8" GAGE PERCENT	REDUCTION IN AREA PERCENT
IPET-RB-E4 IHNC)(EAST) (CAJun)	.500	.20	11000	55000	15400	77000	8.650 8.1%	.389 11.8%

G:\WORDDATA\ISIFORMS\TT505.LAB

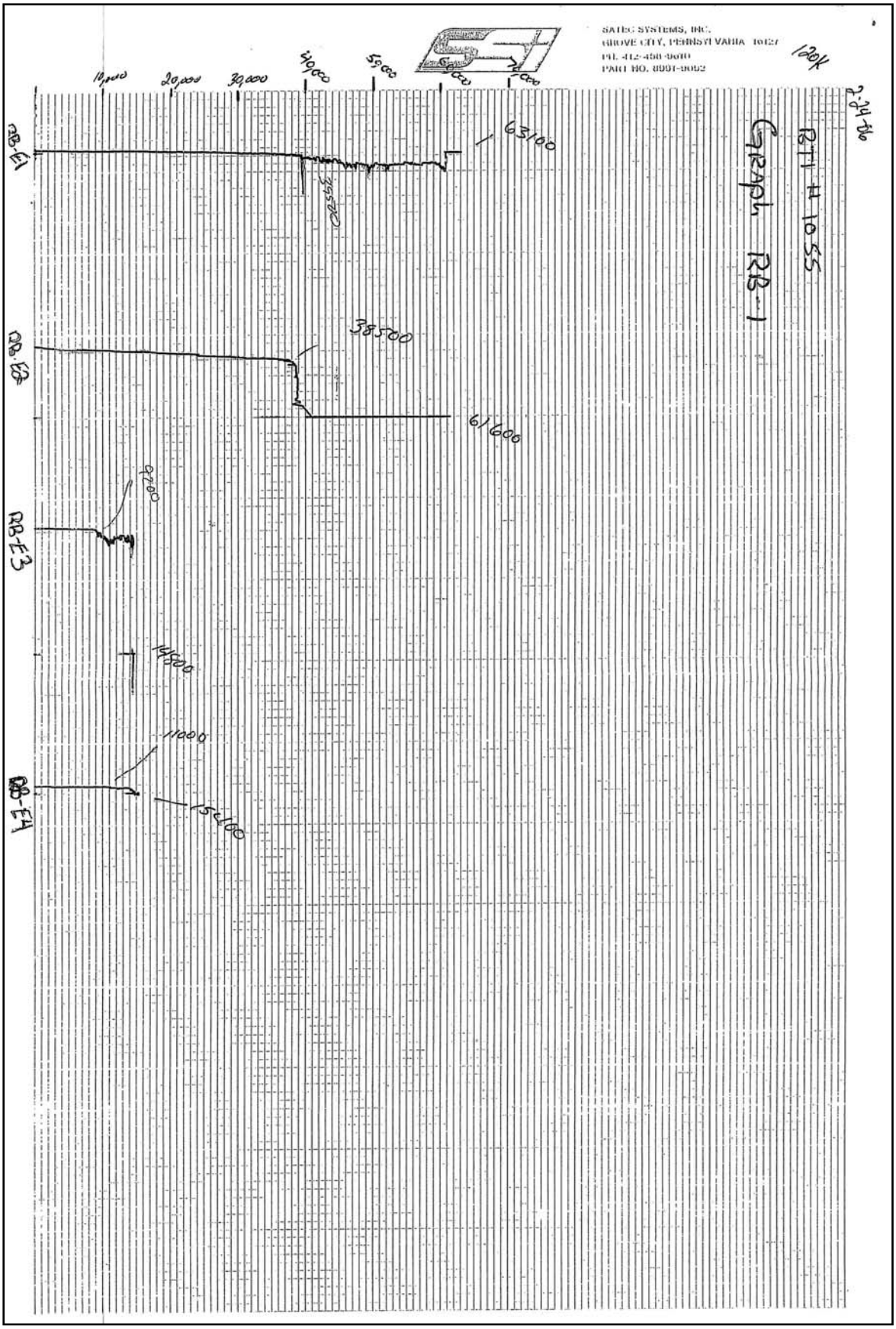

Appendix 17
Finite Element Seepage Study – Seepage Analysis for Foundation Breaches

Early in the IPET investigation of the breaches on the outflow canals, questions were raised about the underseepage in the marsh layer under the levee on the 17th Street Canal as the cause of the breach. For the breaches on London Avenue Canal, field observations indicated that underseepage in the sand layer under the marsh layer and the levees may have contributed to these breaches. Several other organizations investigating the levee breaches did some seepage analyses or speculated that either underseepage or through seepage caused the breaches. To address these concerns, a number of transient finite element seepage analyses were performed.

17th Street Canal Seepage Analysis

The seepage for the 17th Street Canal was conducted early in the IPET investigation of the performance of the floodwalls and levees. The focus of this initial seepage investigation was the time frame it would take for the marsh material to saturate and develop seepage pressures that could affect the stability of the floodwall and levee system. Early on in the investigation, the marsh material was referred to as peat.

The geological conditions in the New Orleans area are presented in Appendix V-2. A summary for the outfall canals are presented here. The soil conditions in the area of the New Orleans outfall canals has been determined through evaluation of existing and recently drilled engineering borings, earlier geologic mapping studies of the area (Dunbar et al. 1994 and 1995; Dunbar, Torrey, and Wakeley, 1999; Kolb, Smith, and Silva, 1975; Kolb, 1962; Kolb and Van Lopik, 1958; and Saucier, 1963 and 1994), and new studies performed since August 2005.

Geologic mapping of the surface and subsurface in the vicinity of the canal failures identifies distinct depositional environments, related to Holocene (less than 10,000 years old) sea-level rise and deposition of sediment by Mississippi River distributary channels during this period. Overlying the Pleistocene surface beneath the 17th Street Canal are approximately 50 to 60 ft of shallow water, fine-grained sediments consisting of bay sound or estuarine, beach, and lacustrine deposits as indicated in the cross section shown in Figure V-17-1. Overlying this shallow water sequence are approximately 10 to 20 ft of marsh and swamp deposits that correspond to the latter

stages of deltaic sedimentation as these deltaic deposits became subaerial. A buried barrier beach ridge extends in a southwest to northeast direction in the subsurface, along the southern shore of Lake Pontchartrain, as shown by the geologic map in Figure V-17-2. A stable sea level 10 to 15 ft lower than current levels permitted sandy sediments from the Pearl River to the east to be concentrated by longshore drift, and formed a sandy spit or barrier beach complex in the New Orleans area (Saucier, 1963, 1994). As shown by Figure V-17-2, the site of the levee breach at the 17th Street Canal is located on the northern side of the beach ridge where the sand ridge is thinner, and there is a layer of clay between the sand and the marsh layer, while both of the London Canal breaches are located over the thickest part of the barrier beach ridge complex, where the sand deposit lies directly beneath the marsh layer, as shown in Figure V-17-1.

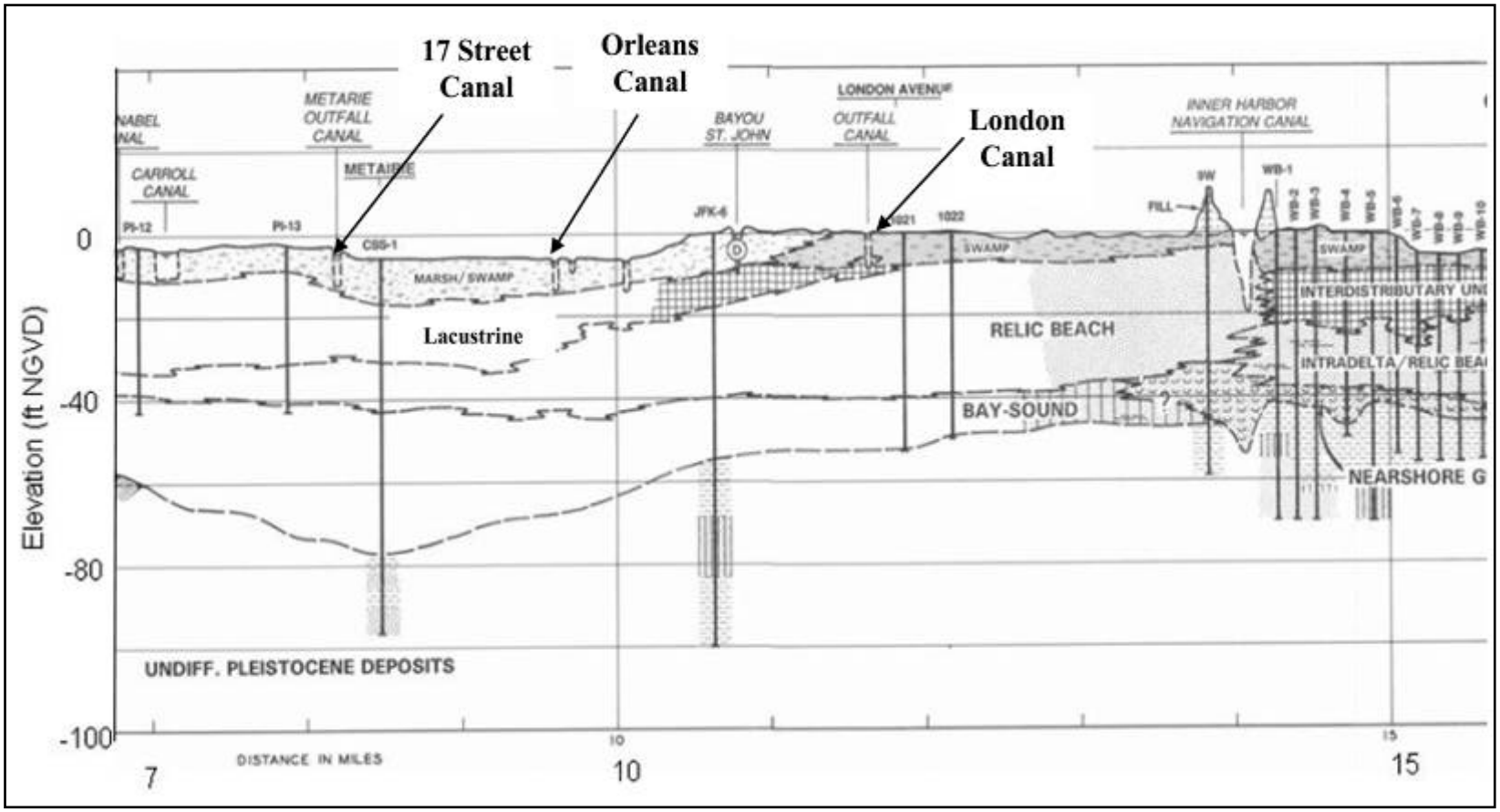

Figure V-17-1. Geological Cross Section Extending West to East Direction Across Western Jefferson Parish and Into Eastern Orleans Parish. Section runs from near the 17th Street Canal to the Inner Harbor Navigation Canal. Major outfall canals in Orleans Parish are noted on the section. Cross section shows the different environments of deposition in the subsurface overlying the Pleistocene (10,000 to 2 million years old) surface. Holocene (less than 10,000 years old) shallow water fill composed of between 50 to 60 feet of bay-sound (and/or estaurine), relic beach (i.e., buried Pine Island Barrier beach complex) and lacustrine or interdistributary deposits. Shallow water environments are overlain by 10 to 20 ft of marsh and swamp deposits. Detailed explanation of environments with discussion of lithogology and engineering properties is presented in Appendix A. Cross-section modified from east half of section C –C', Spanish Fort Quadrangle (Dunbar and others, 1994). Maps and cross-sections from the New Orleans area are available at *lmvmapping.erdc.usace.army.mil*.

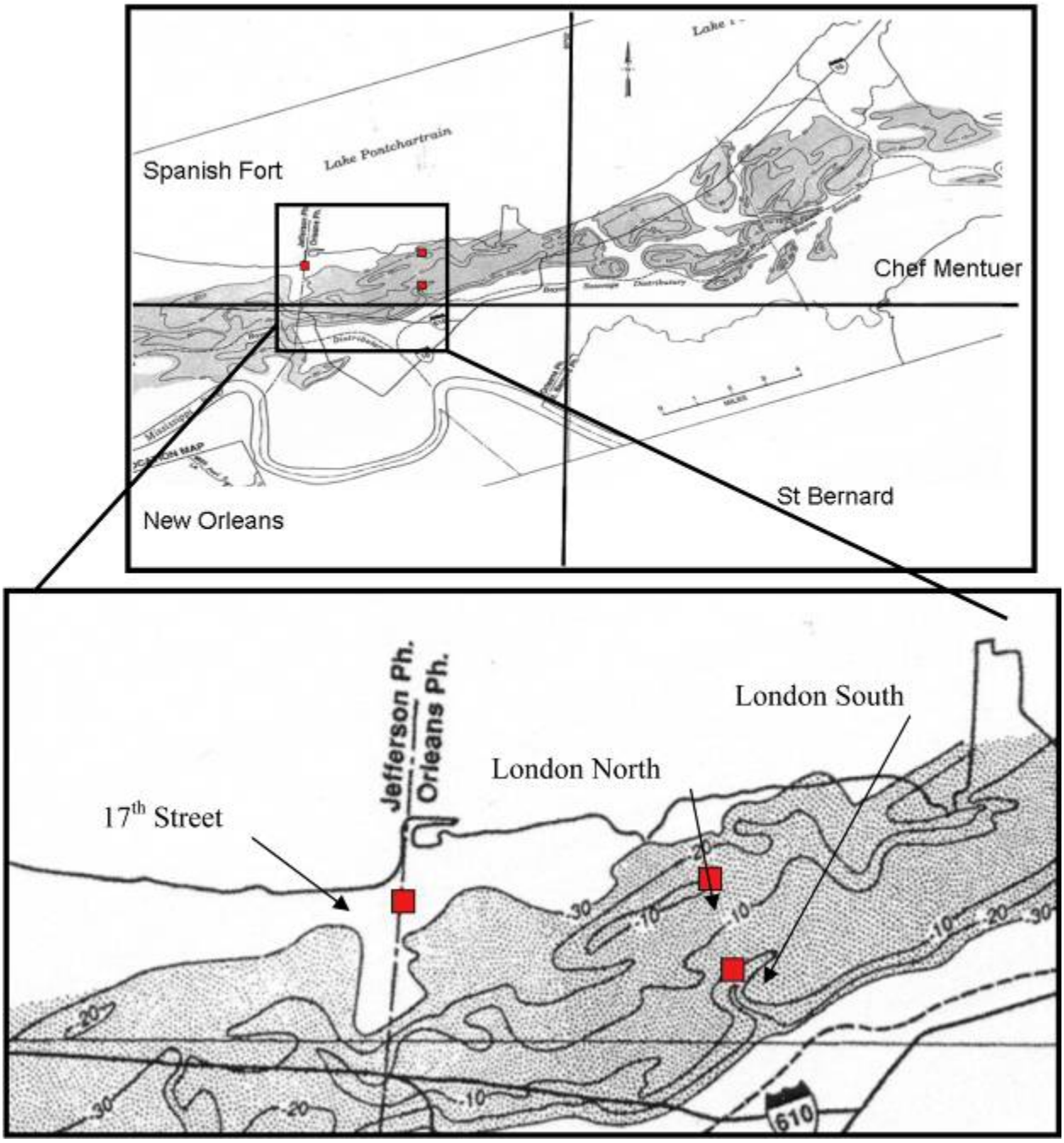

Figure V-17-2. Generalized contour map showing the Pine Island Beach, contour values are in Ft MSL (Saucier, 1994). Upper figure shows general trend of beach ridge in the New Orleans area, lower figure shows detailed view at the canals. London canal levee failures are located along the axis of the beach. The 17th Street Canal levee break is located on the protected or back barrier side of the beach ridge and consequently is dominated by fine-grained deposits corresponding to low-energy depositional-type settings. Extent of beach ridge shown extends across the Spanish Fort, Chef Mentuer, and New Orleans 15-min. USGS topographic quadrangles

The cross section for the seepage analysis is shown in Figure V-17-3. It was constructed early in the IPET investigation and was based on the best available information at the time. The levee was constructed of semi-compacted fat clay and is underlain by the marsh\swamp material (peat) of variable thickness ranging from 10 ft thick under the centerline of the levee to 16 ft thick outside the levee on the protected side. The marsh material is underlain by a lacustrine clay layer of approximately 20 ft thick. The next layer is a 20-ft-thick sand layer. The bottom of the cross section\model is the top of the bay sound clay layer. The values for permeability of the soil layers were initially estimated from the literature based on material type and are shown in Table V-17-1.

Table V-17-1
Permeability for 17th Street Seepage Analysis

Soil Type	Permeability, k (cm/sec)	Permeability, k (ft/hr)
Levee	1.0×10^{-6}	0.000118
Marsh/Peat	1.0×10^{-4}	0.0118
Sand	1.0×10^{-2}	1.18

Weber (1969) found that the permeability of marsh/peat material ranged from high of 0.01 ft/hr under a consolidation pressure of 1 ft of fill to a low of 0.0001 ft/hr under a consolidation pressure of 10 ft of fill. The permeability selected for these analyses is at the high side of the range of permeability values that Weber found, and the results will be conservative with regard to the time it takes to achieve given pore pressure values in the transient analyses.

The initial boundary conditions for the steady state solution prior to the hurricane were set to a water level of Elevation 0.0 on the canal side (right hand side of Figure V-21-3), to a water level of Elevation -7.0 on the far left boundary, and zero pressure for the elements on the protected side above Elevation -7.0. The zero pressure for the elements will require the finite element program to determine the free surface where the soil is fully saturated below it. A finite element analysis was performed to determine the free surface for the steady state solution; thus, establishing the initial conditions for the transient analysis of the surge in the canal from Hurricane Katrina.

A hypothetical hydrograph was used in these transient analyses because at the time of these analyses, the data for a more accurate hydrograph was not available. The hypothetical hydrograph consisted of the water level in the canal going from Elevation 0.0 ft to Elevation 11.5 ft in 8 hours, then held constant at Elevation 11.5 ft for 8 hours, and then going from Elevation 11.5 ft to Elevation 0.0 in 8 hours. This is more severe in terms of the time the high water level is maintained in the canal than the actual rise due to the surge the hurricane. The boundary conditions for the transient analyses are the hypothetical hydrograph applied as head values on the canal side, zero pressure for the elements on the protected side, and a water level of Elevation -7.0 on the far left boundary. The permeability of the sheet pile is assumed to be equal to the surrounding soil, which is a worst case scenario.

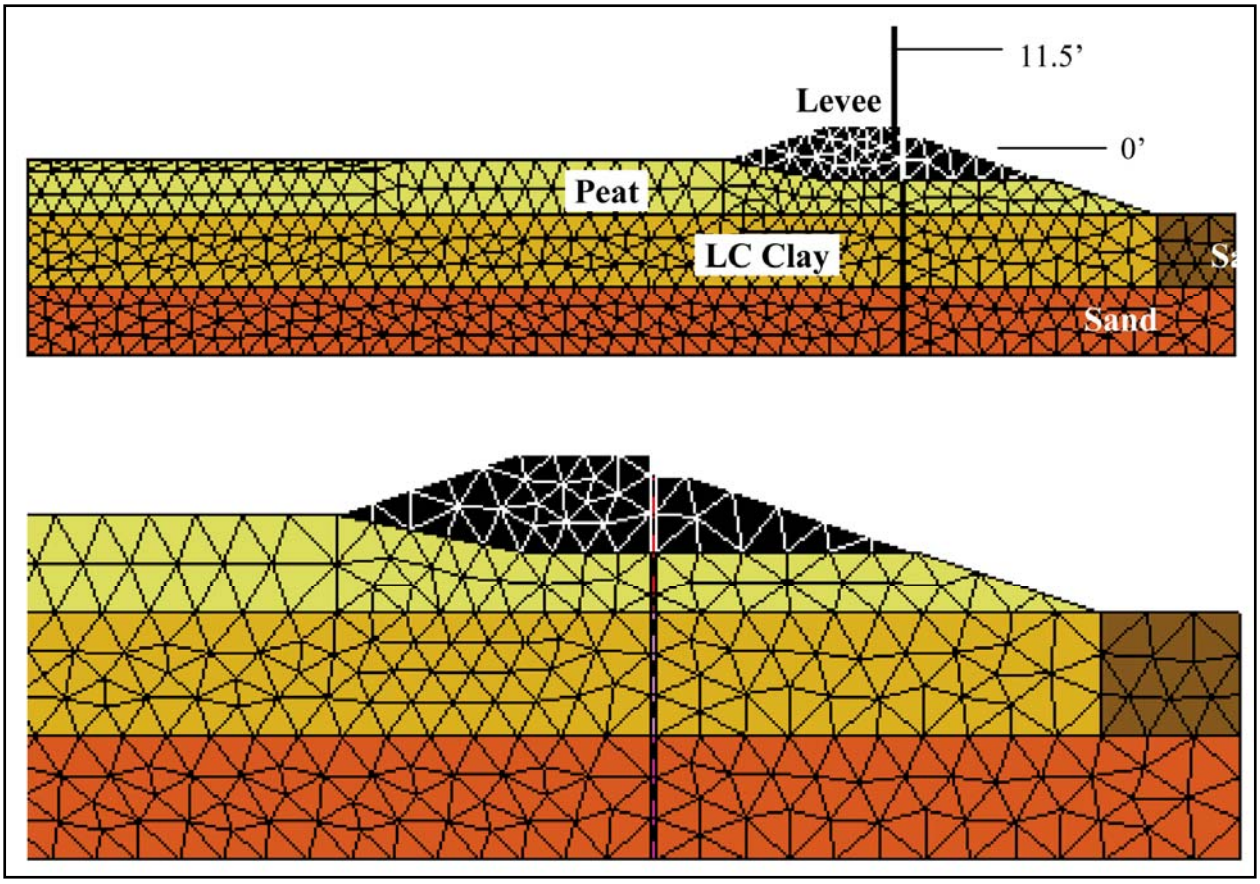

Figure V-17-3. Cross-section with mesh material types

Figure V-17-4 shows the node locations that will be used in the discussion of the results.

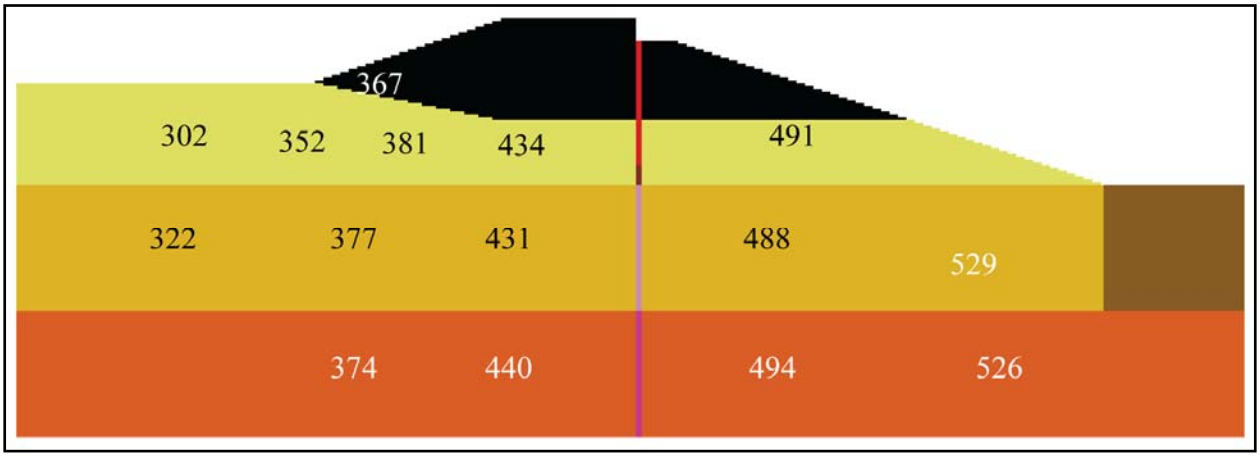

Figure V-17-4. Node numbers and locations.

Figure V-17-5 shows the total head values at the node locations in the marsh (peat) materials for the hypothetical hydrograph. Figure V-17-6 shows the total head values from the transient analysis as a percent of the total head values for the steady state solution.

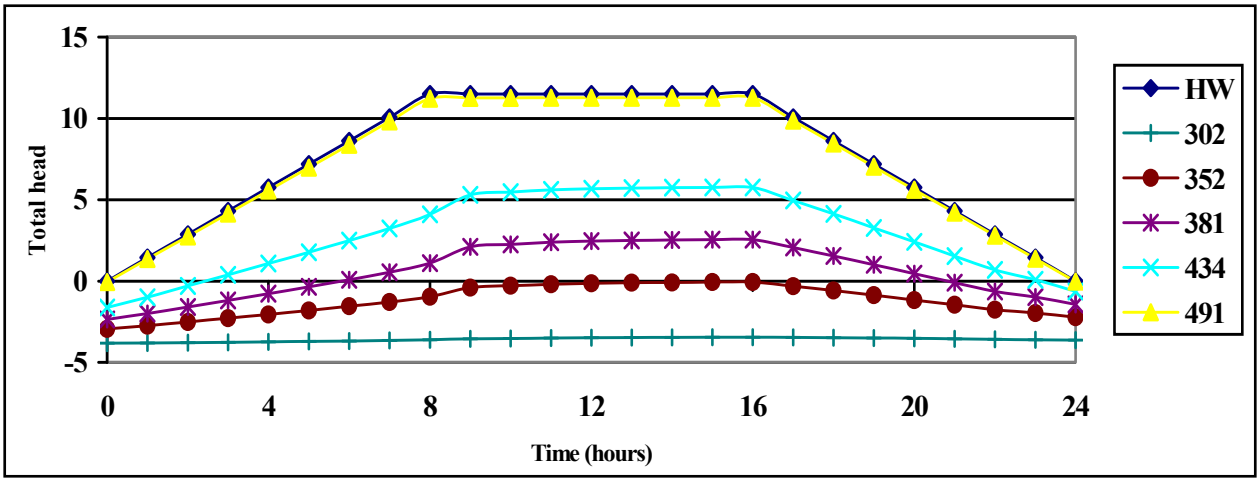

Figure V-17-5. Total head values in the marsh (peat) material.

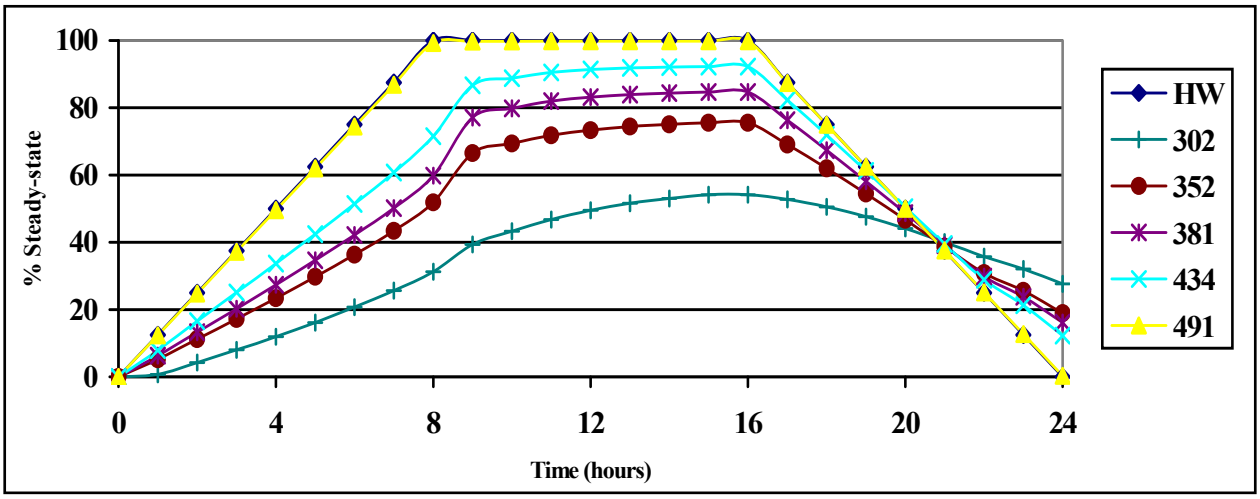

Figure V-17-6. Percent of steady state in the marsh (peat) material.

From the Figure V-17-6, it can be seen that the total head values are less than 60 percent of the steady state values on the protected side. For the actual hydrological conditions in the canal prior to the breach (0- to 8 hrs), the head values under the levee on the protected side would have been less than 60% of the steady state solution, and the head values on the protected side would have been less than 40%.

If the marsh (peat) materials under the levee was consolidated from the weight of the levee, the permeability could be reduced by a factor of 100, which would make it equal to the permeability of the levee. Figure V-17-7 shows the total head values from the transient analysis as a percent of the total head values for the steady state solution for the reduced permeability of the marsh (peat). It can be seen from this that the total head values are less than 10 percent of the steady state values on the protected side.

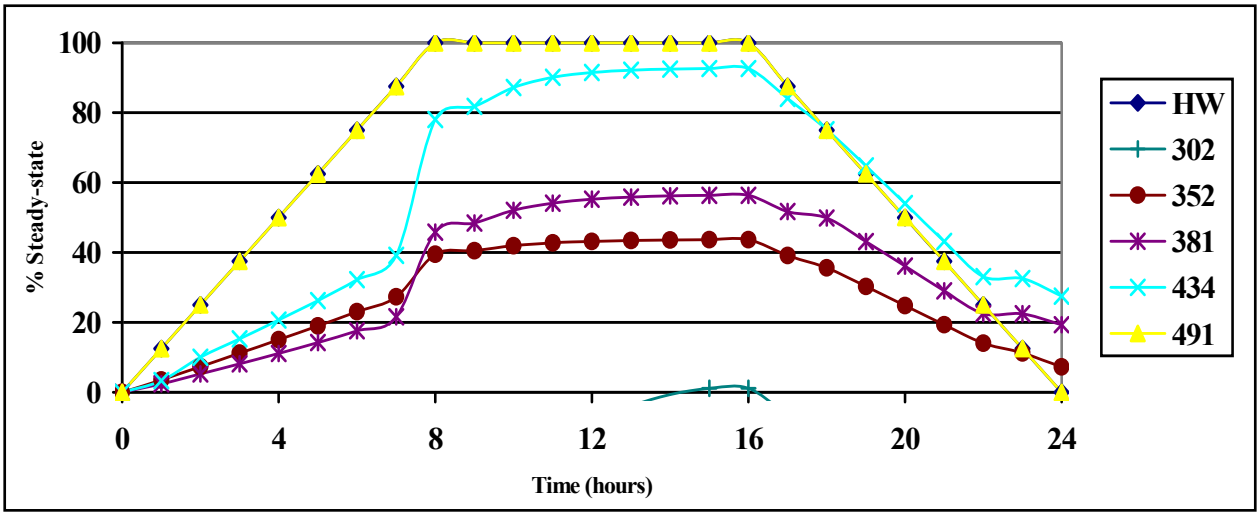

Figure V-17-7. Percent of steady state in the marsh (peat) material.

In summary, the time dependency of the seepage at the 17th Street breach due to the hurricane surge in the canal does affect the potential pore pressures found on the protected side when compared to steady state solution. Due to this time dependency, it is unlikely that seepage through levee or underseepage through the marsh (peat) had any significant affect on the cause of the breach.

London Avenue Canal Seepage Analyses

The focus of the seepage analyses for London Avenue Canal was to investigate what was the potential cause of the high uplift pressure in the sand layer. As presented earlier, and as shown by Figure V-17-2, the site of the levee breach on London Avenue Canal is located over the thickest part of the barrier beach ridge complex, where the sand deposit lies directly beneath the marsh layer, as shown in Figure V-17-1. This is in contrast to the foundation at 17th Street where the marsh layer is underlain by the lacustrine clay layer of approximately 20 ft thick, which separates the sand layer from the marsh layer. At the 17th Street canal, the lacustrine clay layer also separates the water in the canal from the sand layer. At the London Avenue Canal, the water in the canal is only separated from the sand layer by a 2 ft to 5 ft layer of silt in the bottom of the canal. If the sand layer has a direct connection to the canal, the uplift pressures in the sand will be directly proportional to the level of water in the canal because the sand layer is fully saturated, and the marsh and levee are 100 times less permeable than the sand layer. Another important part of the seepage investigation was to determine if the gap between the wall and canal side levee could cause the high uplift pressures on the protected side.

Figure V-17-8 shows the finite element mesh used for the seepage analyses performed for London Avenue canal, north breach. Figure V-17-9 shows the materials used in the first series of finite element seepage analyses of London Avenue Canal, north breach. Table V-17-2 presents the permeability values used in the first series of analyses. Table V-17-3 presents the boundary values for the first series of analyses.

Table V-17-2
Permeability Values

Material Number	Name	K (cm/sec)	K (ft/hr)
1	Levee Clay	1.0 (10^{-6})	0.000118
2	Top Soil – Protected Side	1.0 (10^{-6})	0.000118
3	Clay	1.0 (10^{-6})	0.000118
4	Peat – Levee Centerline	1.0 (10^{-6})	0.000118
5	Peat – Shallow Overburden	1.0 (10^{-4})	0.0118
6	Beach Sand	1.5 (10^{-2})	1.77
7	Equivalent 1-ft-thick Sheet Pile	1.6 (10^{-5})	0.002
8	Bay Sound Clay	1.0 (10^{-6})	0.000118

Table V-17-3
Boundary Conditions

Run Number	Canal Water Elevation (ft)	Drain Water Elevation (ft)	Bottom of Crack Elevation (ft)
1	1.07	-6.4	None
2	11.4	-1.4	None
3	11.4	-1.4	-12.9

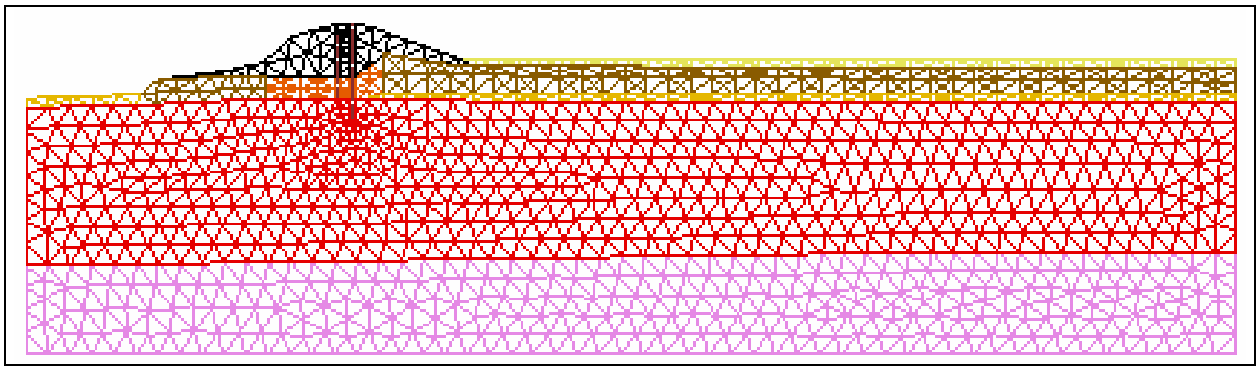

Finite Element Mesh

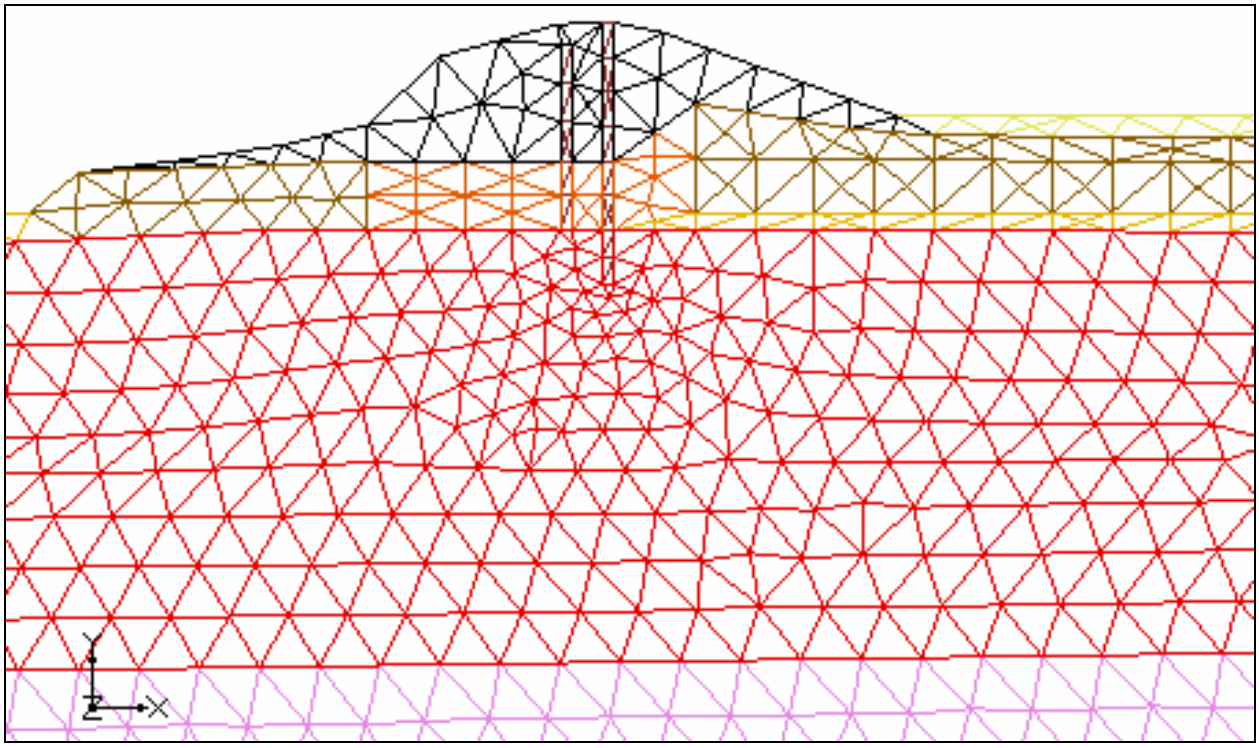

Zoom showing the sheet piles for the I-wall and the abandon wall

Figure V-17-8. Finite Element Mesh for the breach at London Avenue Canal north

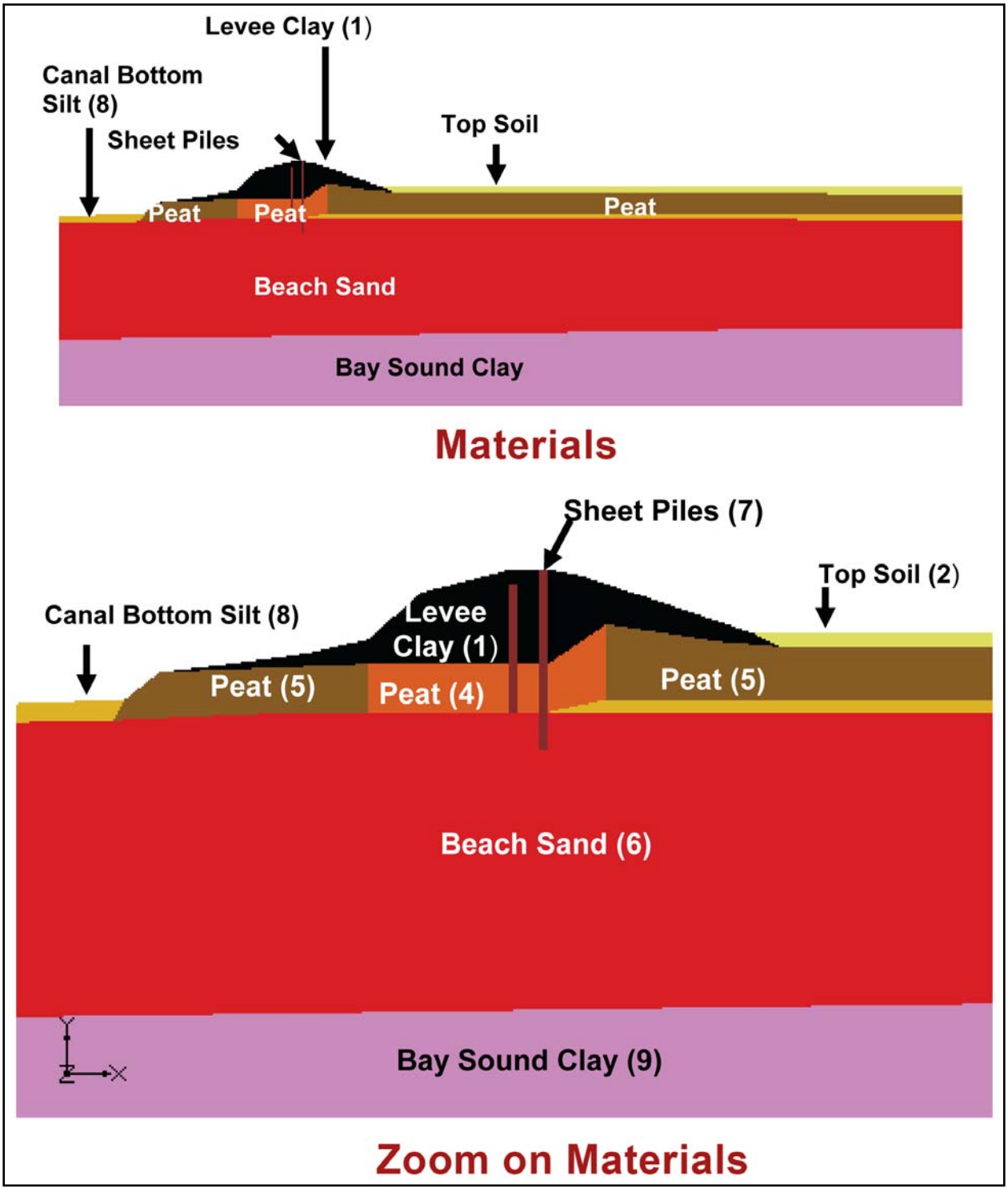

Figure V-17-9. Materials used in the first series of finite element seepage analyses.

The pre-flood results are presented in Figure V-17-10. The finite element seepage analysis results shows that sheet piles do almost nothing as illustrated by the two equipotential plots in Figure V-17-10. Most of the head loss is in the levee clay. The sheet piles are more pervious than the clay levee, so they offer no resistance to flow in the levee. The sheet pile supporting the

I-wall extends only 4.5 ft into the sand, making it of limited use for effecting the seepage conditions in the sand layer.

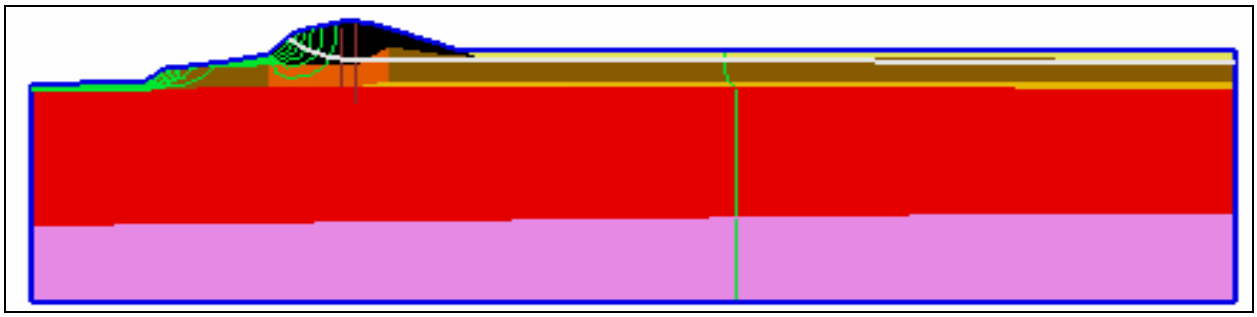

(a) With Sheet Pile

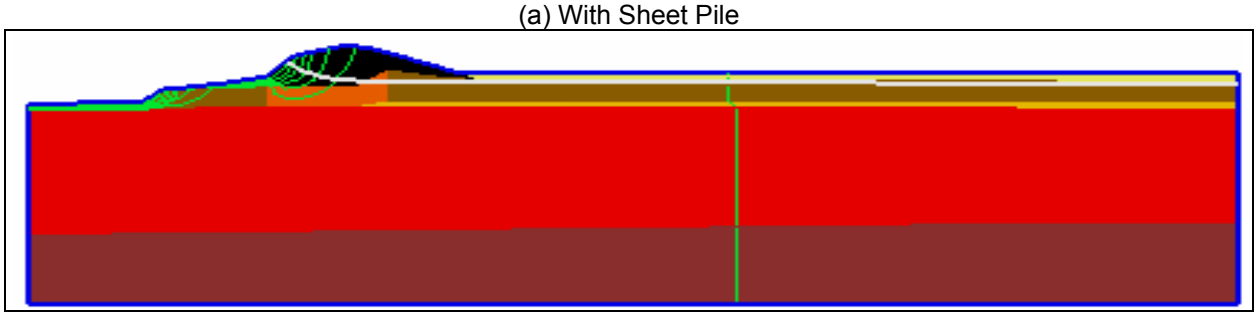

(b) Without Sheet Pile

Figure V-17-10. Pre-Flood Equipotential Lines

The flood results with no crack are presented in Figure V-17-11. Again, the finite element seepage analysis results shows that sheet piles do almost nothing, as illustrated by the two equipotential plots in Figure V-17-11. The difference in head from canal to protected side is 12.8 ft (11.4 ft – (-1.4 ft)). A significant amount of the head loss still occurs in the levee, with only contours 0 and –1 appearing in the sand.

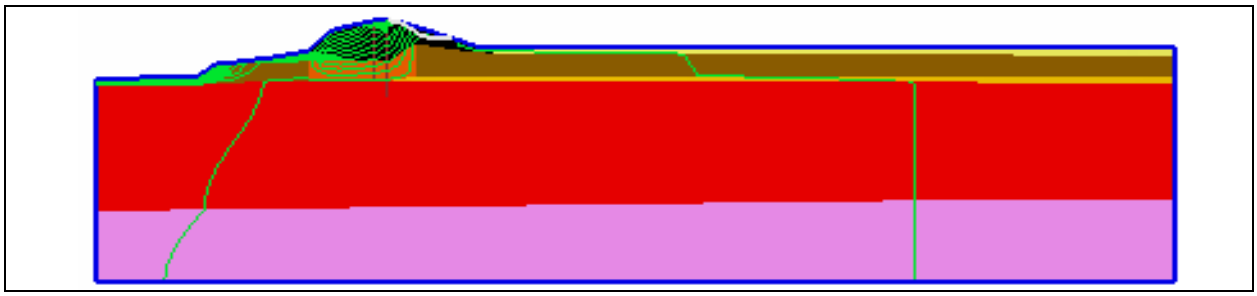

(a) With Sheet Pile

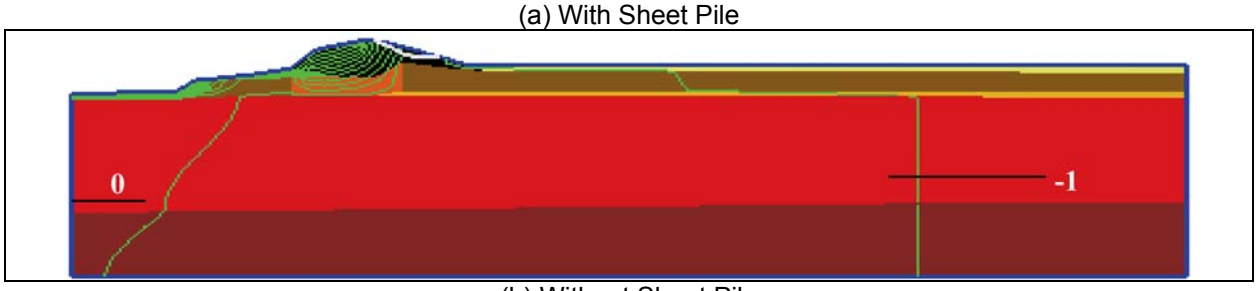

(b) Without Sheet Pile

Figure V-17-11. After-Flood Equipotential Lines with No Crack Formed

The flood results with a crack between the sheet pile and the canal side levee are presented in Figure V-17-11. The crack drove many more equipotential drops down into the sand as shown in Figure V-17-11. The sheet piles had more of an effect on the first total head contour in the sand. The first total head contour with the sheet pile is 8 ft, and without the sheet pile, is 9 ft. Thus, the head loss in the sand is even more without the sheet pile.

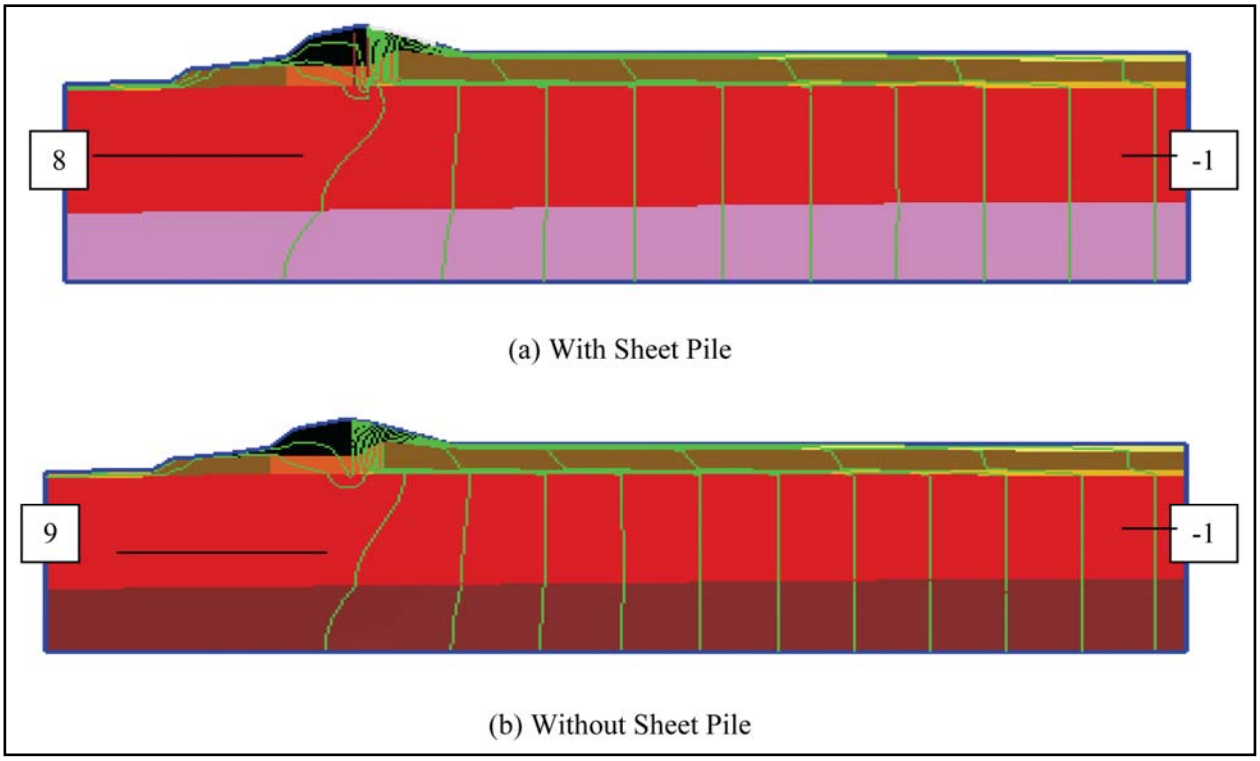

Figure V-17-12. After-Flood Equipotential Lines with Crack Formed

Another series of transient finite element seepage analyses were performed to validate that the steady-state assumptions are valid. Figure V-17-13 shows the rise portion of the IPET-constructed hydrograph for London Avenue Canal. This hydrograph is used to specify the water level on the canal side of the model and the time rise during the transient analysis.

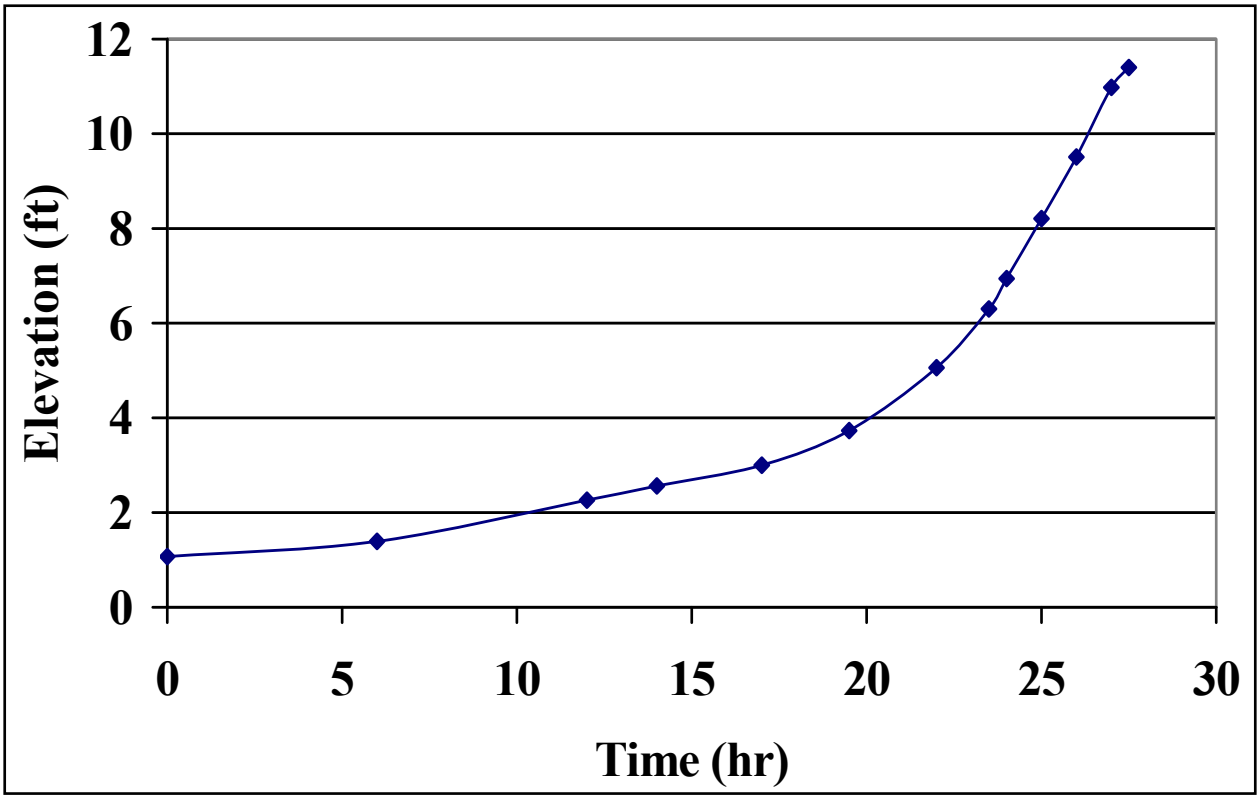

Figure V-17-13. Rise portion of the IPET-constructed hydrograph for London Avenue Canal

Figure V-17-14 shows a comparison of the results of the steady state analysis and the transient analysis. Visually, they appear virtually the same with regard to the equipotential lines. Table V-17-4 compares the location of where contours cross the top of the sand layer for steady-state and transient solutions and shows that the results for the two analyses are virtually the same. The results show that the steady-state analysis is sufficiently accurate for future analysis efforts.

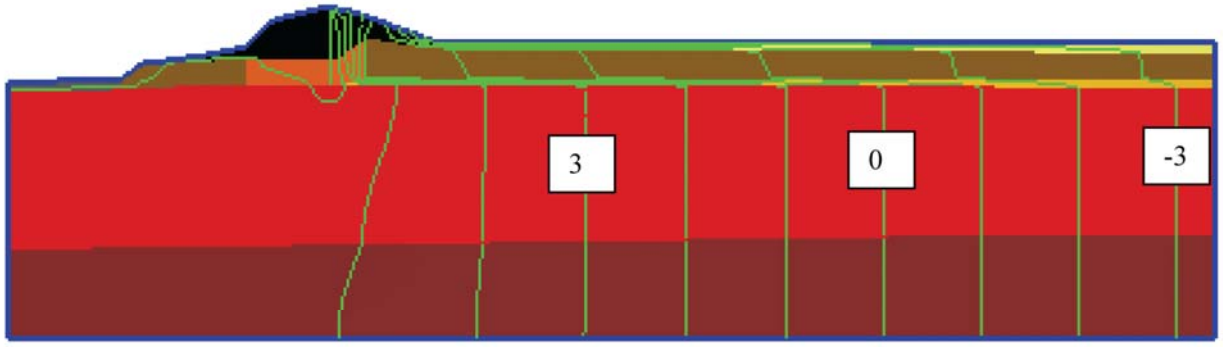

a.) Total Head for Steady-State Solution

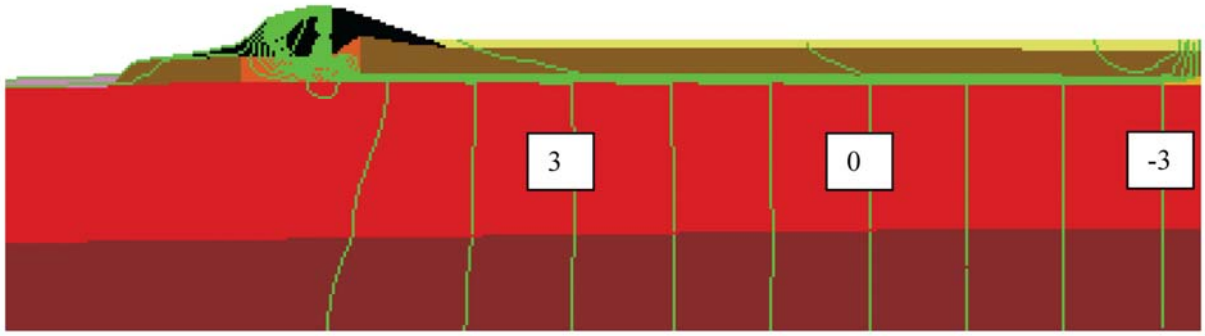

b.) Total Head for Transient Solution

Figure V-17-14.

Table V-17-4
Location where Contours Cross the Top of the Sand Layer for Steady-State and Transient Solutions, Canal Elevation = 7.0035 ft, Drain Elevation = –3.4 ft, Crack

Contour Level	X – Steady-State (ft)	X – Transient (ft)
-3	398.2	398.0
-2	376.2	375.7
-1	354.1	353.4
0	331.9	331.0
1	309.4	308.4
2	286.8	285.8
3	264.1	263.1
4	241.5	240.7
5	221.2	220.7

Inner Harbor Navigation Canal (IHNC) Seepage Analysis

In the IPET Final Draft Report (June 1, 2006), it noted that other possible modes of failure beside overtopping/erosion for the breaches of the IHNC I-wall along the Lower Ninth Ward included "sliding instability and piping and erosion from underseepage." The report goes on to say that "*Piping and erosion from underseepage is unlikely because the I-walls were founded in a clay levee fill, a marsh layer made up of organics, clay and silt, and a clay layer. Because of the thickness, the low permeabilities of these materials, and the relatively short duration of the storm, this failure mode was considered not likely and was eliminated as a possible mode of failure.*" In the NSF-Berkeley report (ILIT Final Report, July 31, 2006), they stated "*This greatly underestimates the permeability, and especially the laterally permeability of the marsh deposits. It also continues the very dangerous assumption that underseepage was not a serious problem for 'short duration' storm surge loading that plagued the original design of many sections of the New Orleans regional defense system, and led to use of sheetpile curtains that far too short to effectively (and safely) cut off underseepage flows.*"

The value of coefficient of permeability assigned to the marsh layer in the NSF-Berkeley report was 10^{-2} cm/sec. This is three orders of magnitude higher than the highest coefficient of permeability IPET determined from consolidation tests on undisturbed samples of the marsh layer, as shown in Figure V-17-15. Consolidation tests performed by IPET show that the coefficient of permeability of the marsh material decreases as consolidation pressure decreases, from a maximum of 10^{-5} cm/sec for low consolidation pressures, to values as low as 10^{-8} cm/sec for consolidation pressure equal to 4,000 psf.

Weber (1969) found a similar variation of permeability with effective overburden pressure using field permeability (piezometer) tests on peat in the California Delta, as shown in Figure V-17-15. Weber's peat coefficient of permeability values are roughly the same as the values determined from the IPET consolidation tests on marsh material from New Orleans, but the scatter of the values from consolidation tests is greater. The difference may be due to the fact that the consolidation tests represent point values, whereas the field tests represent average values for a larger volume of soil. There may also be some inherent differences between the materials.

The permeability values for the marsh materials used by NSF-Berkeley in their seepage analyses were at least **1,000** times too high. Their values are higher than the permeability values for the sand layer at the London Avenue Canal determined from field pump tests. The NSF-Berkeley report states, "*The values of lateral permeability used in these analyses were based on experience with similar geologic units from other regions, our own field observations, and the accumulated reports indicating high lateral permeability. A best-estimated coefficient of lateral permeability of $k_h \sim 10^{-2}$ cm/sec was modeled for the most open of the marsh sub-strata.*" There is no possible or plausible explanation for NSF-Berkeley's choice of permeability values for the marsh material. These permeability values were also used in all of their PLAXIS analyses, and they were higher than any other material, including the sand layers.

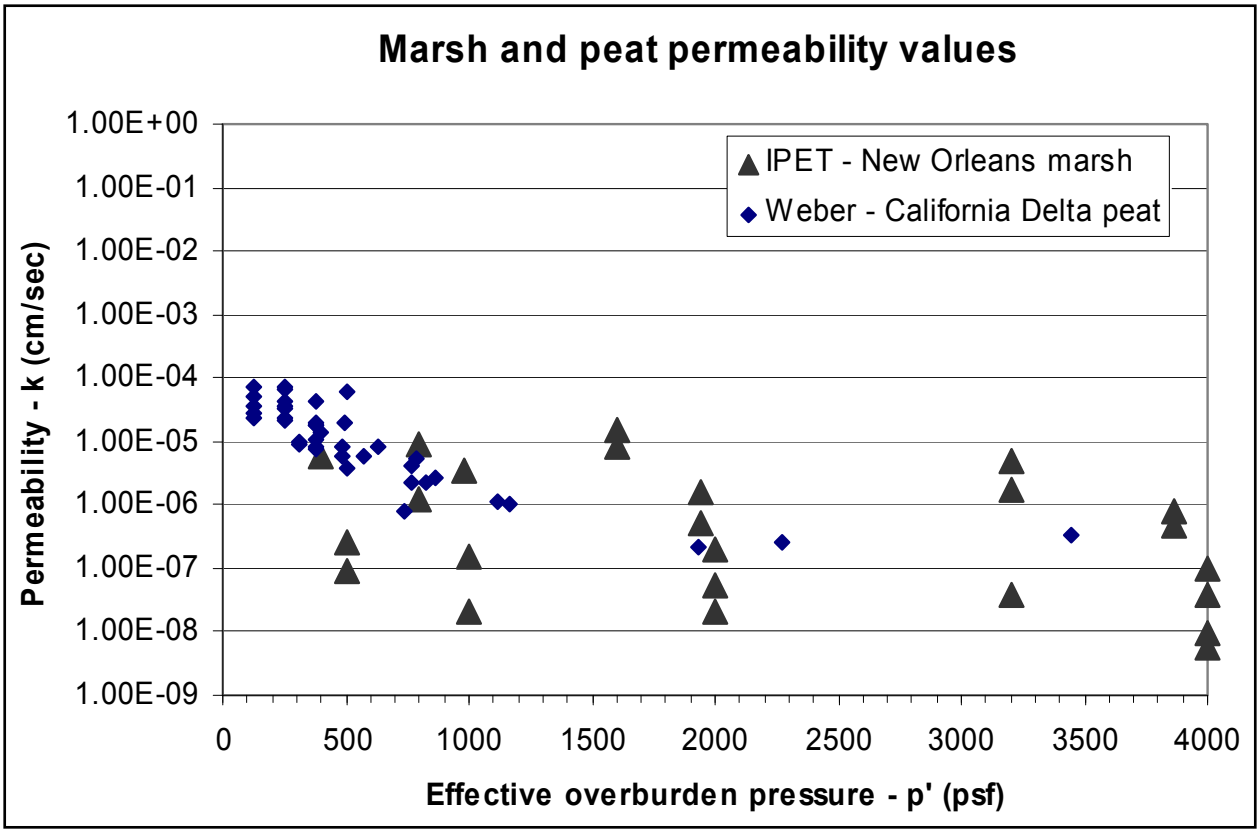

Figure V-17-15. Values of marsh permeability measured by IPET in consolidation tests on New Orleans marsh material, and by Weber (1969) in field piezometer tests on California Delta peat.

In order to demonstrate the effects of more realistic permeability values for the marsh material on the performance of the IHNC I-wall along the Lower Ninth Ward, the IPET team has conducted a series of transient finite element analyses.

The data available to assess the stratigraphy of the area includes borings from the General Design Memorandum (GDM), borings taken after the failure, and cone penetration tests taken after the failure. The locations of these borings and cone penetration tests are shown in Figure V-17-16. Note that all borings taken after the failure were at the levee toe. The GDM contains 10 borings on the levee centerline (2-U, 3, 4, 5, 6-U, and 7 in the vicinity of the breach), and four at the levee toe (2-UT, 3T, 4T, and 6UT). A centerline profile under the levee is represented in Figure V-17-17 and is based on both pre-Katrina and post-Katrina borings. This section shows 60 to 70 ft of predominantly fine-grained Holocene (i.e., less than 10,000 years old) shallow water and terrestrial sediments overlying the Pleistocene surface (i.e., older than 10,000 years). Holocene sediments are separated into various depositional environments in Figure V-17-17, based on soil texture, organic content, and other physical and engineering properties. Engineering properties of these layers are described in greater detail below.

The GDM borings indicate the levee fill properties for the north and south breach areas are similar, consisting of compacted CL and CH materials. The average moist unit weight of the fill was estimated to be 109 pcf.

Beneath the fill is a marsh unit about 17 ft thick. The marsh layer is composed of organic material from the cypress swamp that occupied the area, together with silt and clay deposited in the marsh. Because the upper 8 to 9 ft of this unit has different material properties than the lower portion, it was divided into two layers, Marsh 1 and Marsh 2. Water contents and saturated unit weights determined from samples of marsh material taken from the toe are shown in Figures V-17-18 and V-17-19, respectively. These figures clearly depict the differences in the marsh layers.

Water contents, unit weights, and undrained shear strengths are shown in Table V-17-5, and these properties for the Marsh 2 layer are shown in Table V-17-6. These properties are based on samples from post-Katrina borings at the levee toe. The average saturated unit weight of the Marsh 1 layer is about 105 pcf. Water contents of the Marsh 1 layer are as high as 80%. The average water content is approximately 49%. The average saturated unit weight of the Marsh 2 layer is about 80 pcf. Water contents of the Marsh 2 layer are as high as 442%. The average water content is approximately 175%. The marsh 1 layer is mostly CH material. The Marsh 2 layer is fibrous at the top, and more amorphous near the bottom, indicating more advanced decomposition of the older organic materials at depth.

Table V-17-5
Properties of Marsh 1 Layer from Post-Katrina Borings at Toe

Marsh 1 Layer					
Number of Samples = 16					
	Mean	Standard Deviation	COV	Max	Min
%w	49	17	0.342	80.2	21.9
Saturated Unit Weight (pcf)	104	9	0.081	120.5	92.2
S_u (psf)	550	214	0.389	3195	90.0

Table V-17-6
Properties of Marsh 2 Layer from Post-Katrina Borings at Toe

Marsh 2 Layer					
Number of Samples = 12					
	Mean	Standard Deviation	COV	Max	Min
%w	175	96	0.549	441.6	90.9
Saturated Unit Weight (pcf)	78.4	7	0.091	87.1	63.4
S_u (psf)	195.3	116	0.595	336	64.6

Table V-17-7
Properties of Interdistributary Clay from Post-Katrina Borings at Toe

Interdistributary Clay					
Number of Samples = 45					
	Mean	Standard Deviation	COV	Max	Min
%w	60	12	0.208	77.2	25
Saturated Unit Weight (pcf)	101.1	6	0.063	125	93.6

Beneath the marsh layers is a layer of interdistributary clay with an average Liquid Limit of about 79% and an average Plastic Limit of 26%. Based on consolidation test results presented in the GDM, the clay is normally consolidated throughout its depth. The average saturated unit weight of the clay is about 100 pcf, and the average water content is approximately 60%. Water content and unit weights are summarized in Table V-17-7.

Beneath the clay is a layer of Beach Sand. This layer is not involved in the observed or calculated mechanisms of instability, and its strength is therefore of little importance in stability analyses, except as a more resistant layer beneath the clay.

Figure V-17-20 shows the cross section of the north IHNC breach selected for the seepage analysis.

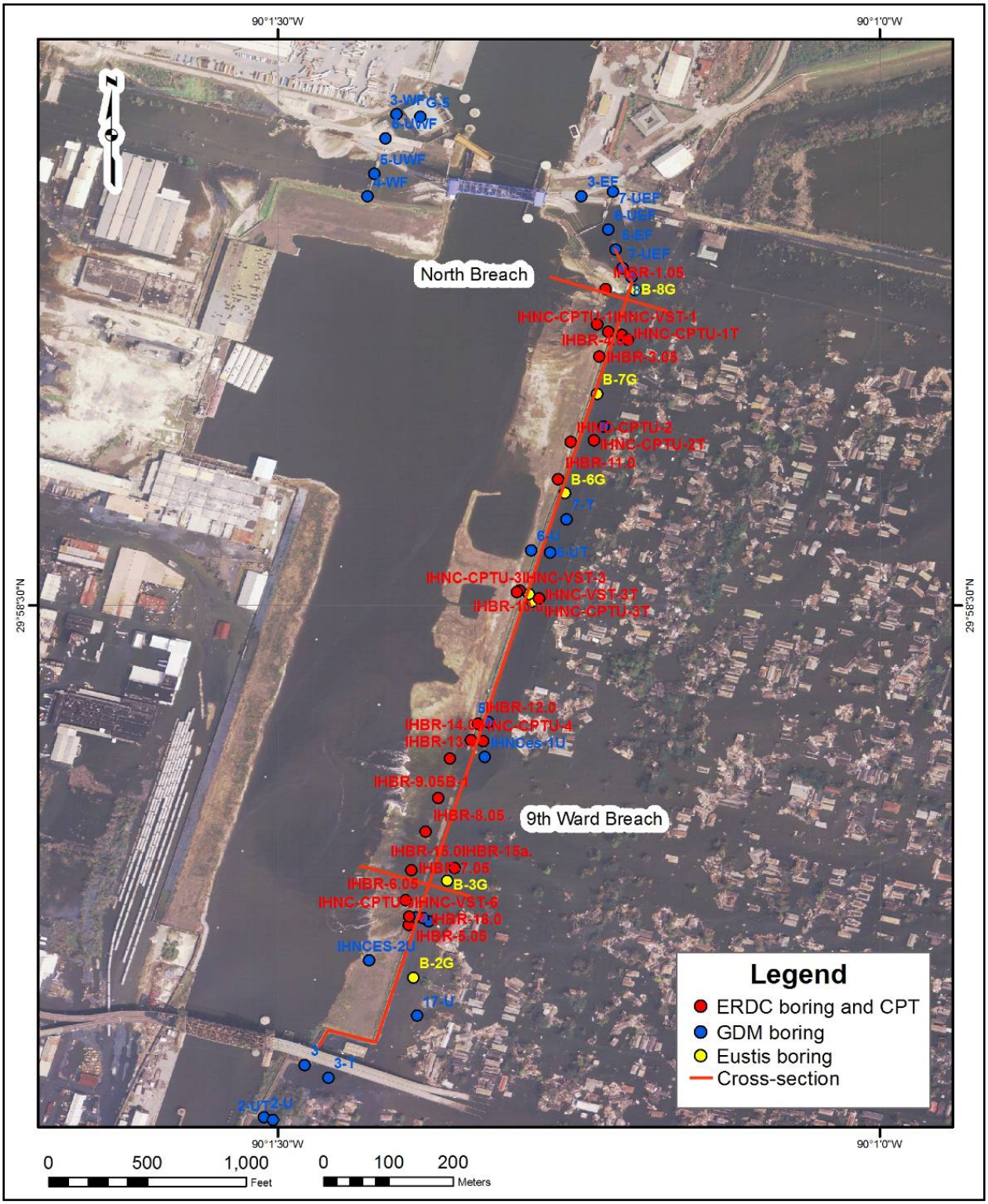

Figure V-17-16. IHNC – East Bank (Between Florida Ave. and North Claiborne Ave.), Boring and CPTU Location Map

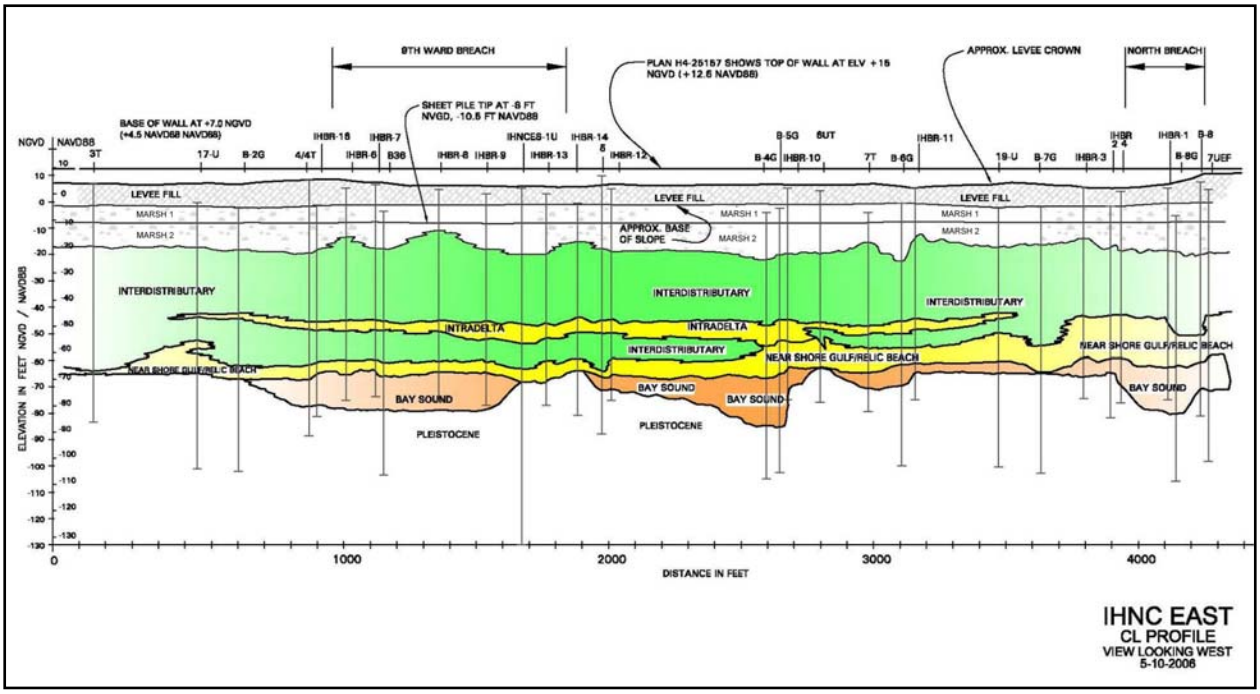

Figure V-17-17. IHNC East Bank, Centerline Geologic Section Showing South (Lower Ninth Ward) and North Breaches

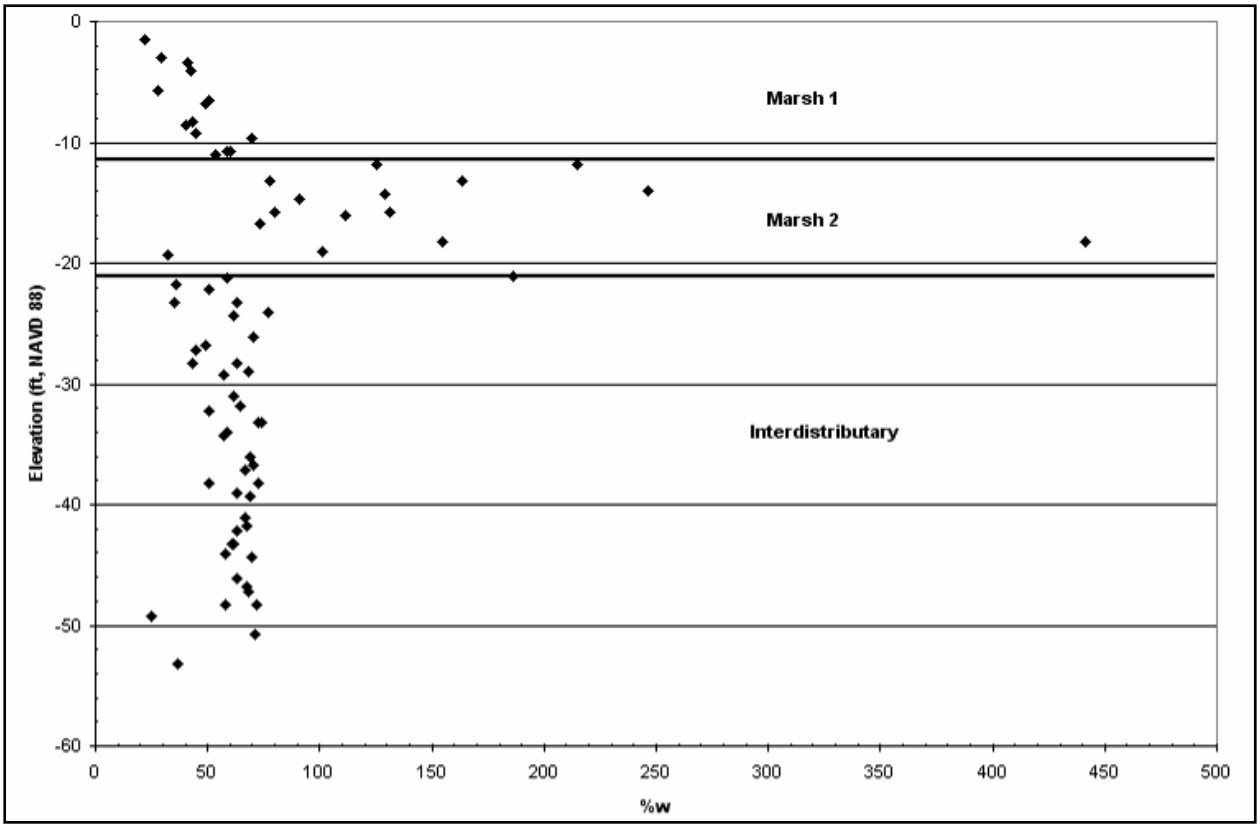

Figure V-17-18. IHNC – East Bank (Between Florida Ave. and North Claiborne Ave.), % w Versus Elevation (ft, NAVD 88) from Toe Borings

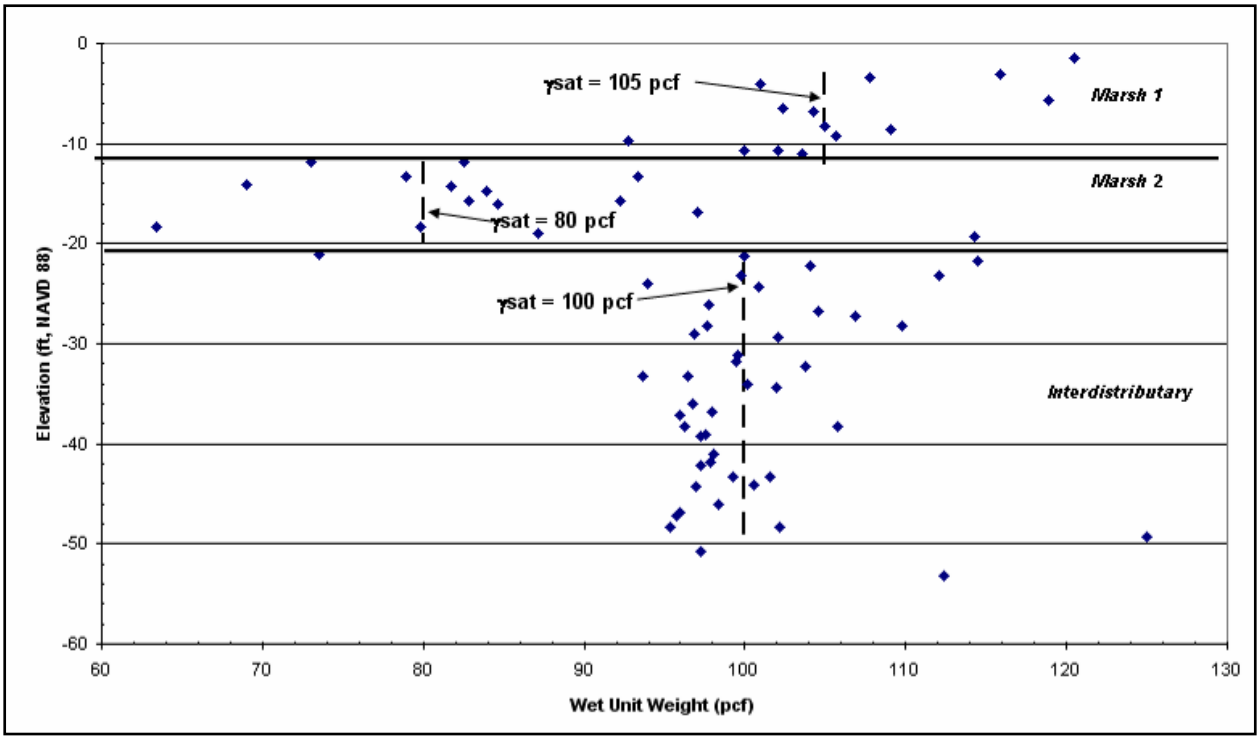

Figure V-17-19. IHNC – East Bank (Between Florida Ave. and North Claiborne Ave.), Wet Unit Weight versus Elevation (ft, NAVD 88) from Post-Katrina Borings

Figure V-17-20 shows the cross section of the north IHNC breach selected for the seepage analysis. Figure V-17-21 shows the finite element mesh used for the seepage analyses performed for the IHNC canal, north breach. Figure V-17-22 show the materials used in the first series of finite element seepage analyses of the IHNC canal, north breach and the coefficient of permeability values used in the first series of the analyses. Figure V-17-23 shows the rise portion of the IPET-constructed hydrograph for IHNC canal. This hydrograph is used to specify the water level on the canal side of the model and the time rise during the transient analysis. As the water level rise in the canal, the protected side boundary water is raised from -11.5 to -6.0 to simulate the shut down of the pumps and the heavy rainfall.

Figure V-17-24 shows the initial steady-state underseepage conditions used for the transient analysis. It is important to keep in mind that soil above the phreatic surface is not fully saturated; and in order for seepage flow to occur, the soil most become fully saturated, which requires time. Figure V-17-25 shows the steady-state solution for the canal water level at 12.5 (top of the wall) and the protected side at -6.0. The phreatic surface in the protected side levee does not intersect the protected side slope. The phreatic surface intersects the protected side water surface (elevation -6.0) at the toe of the levee (elevation -6.0). The exit gradient at the levee toe is less than 0.30.

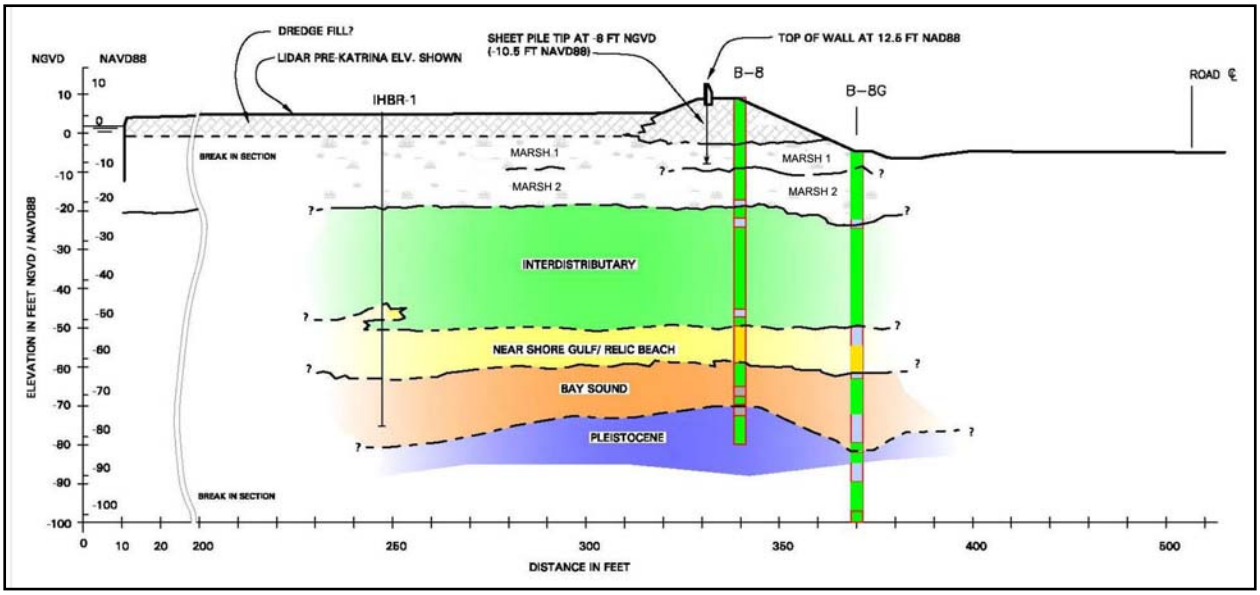

Figure V-17-20. Profile of the North Breach at IHNC East bank, View Looking North

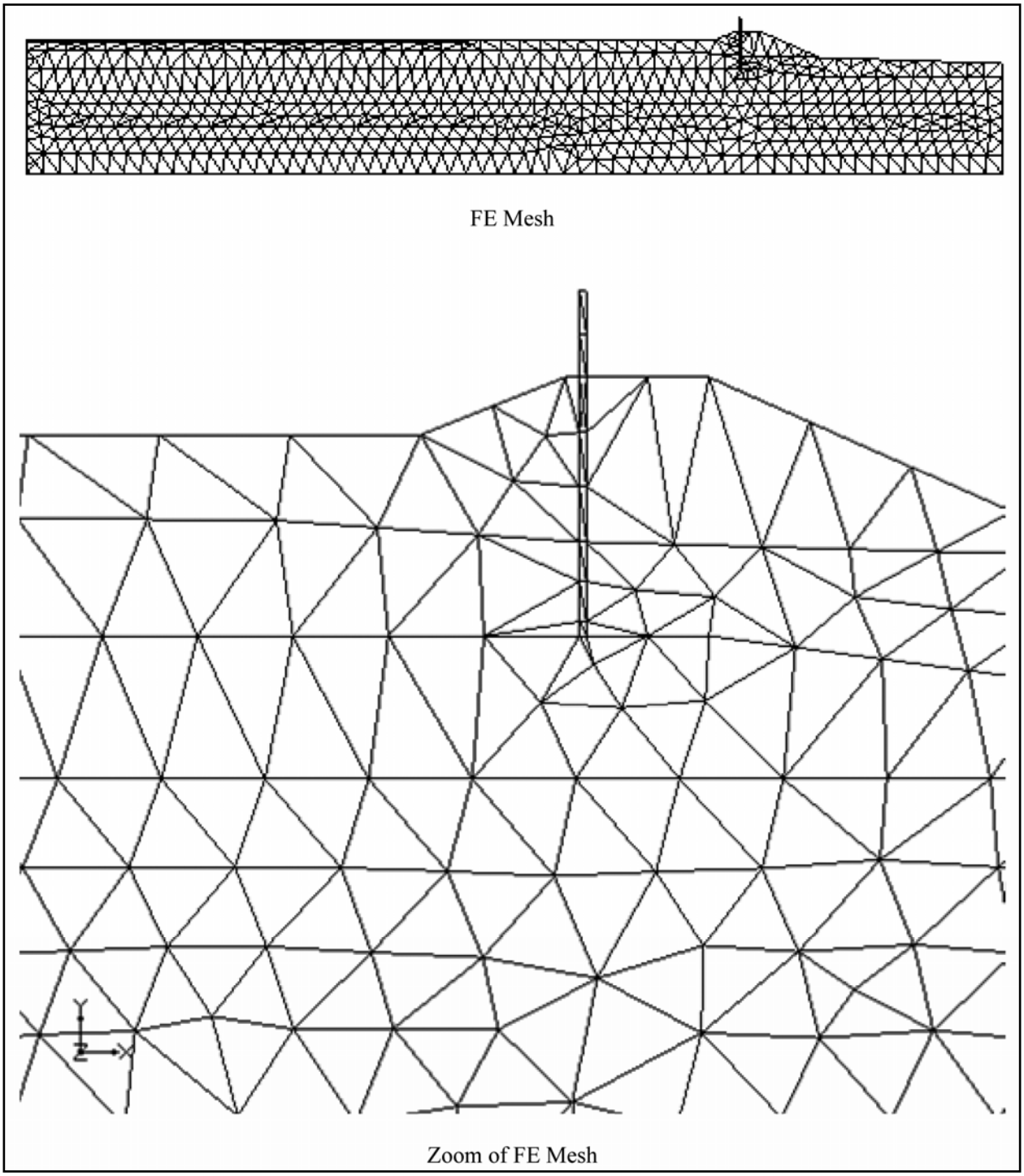

Figure V-17-21. Finite element mesh of the north breach of IHNC east bank.

Material Number	Name	K (ft/hr)
1	Levee Fill	0.000118
2	Marsh #1	0.00118
3	Marsh #2	0.00118
4	Wall #1	0.000118
5	Interdistributary	0.000118
6	Sand	1.77
7	Wall #2	0.00118

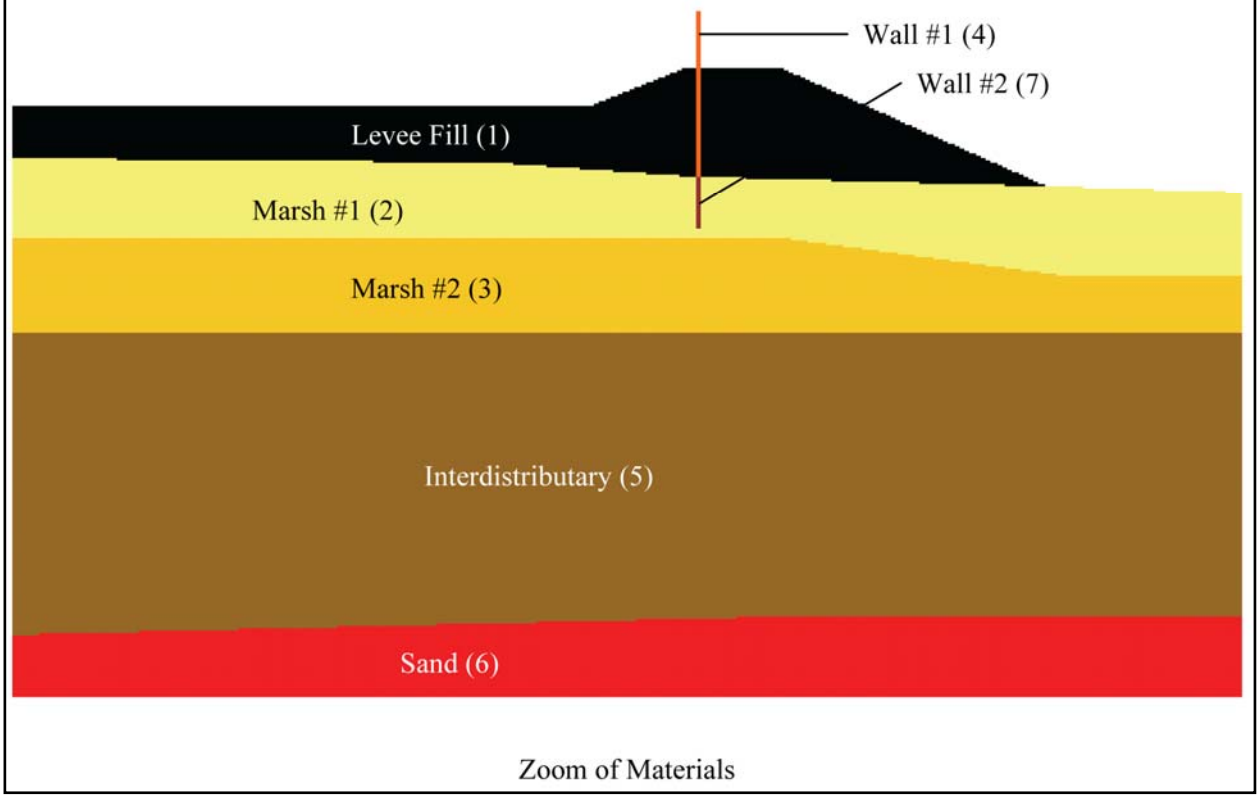

Figure V-17-22. Materials and coefficient of permeability values used in the first series of IHNC finite element seepage analyses.

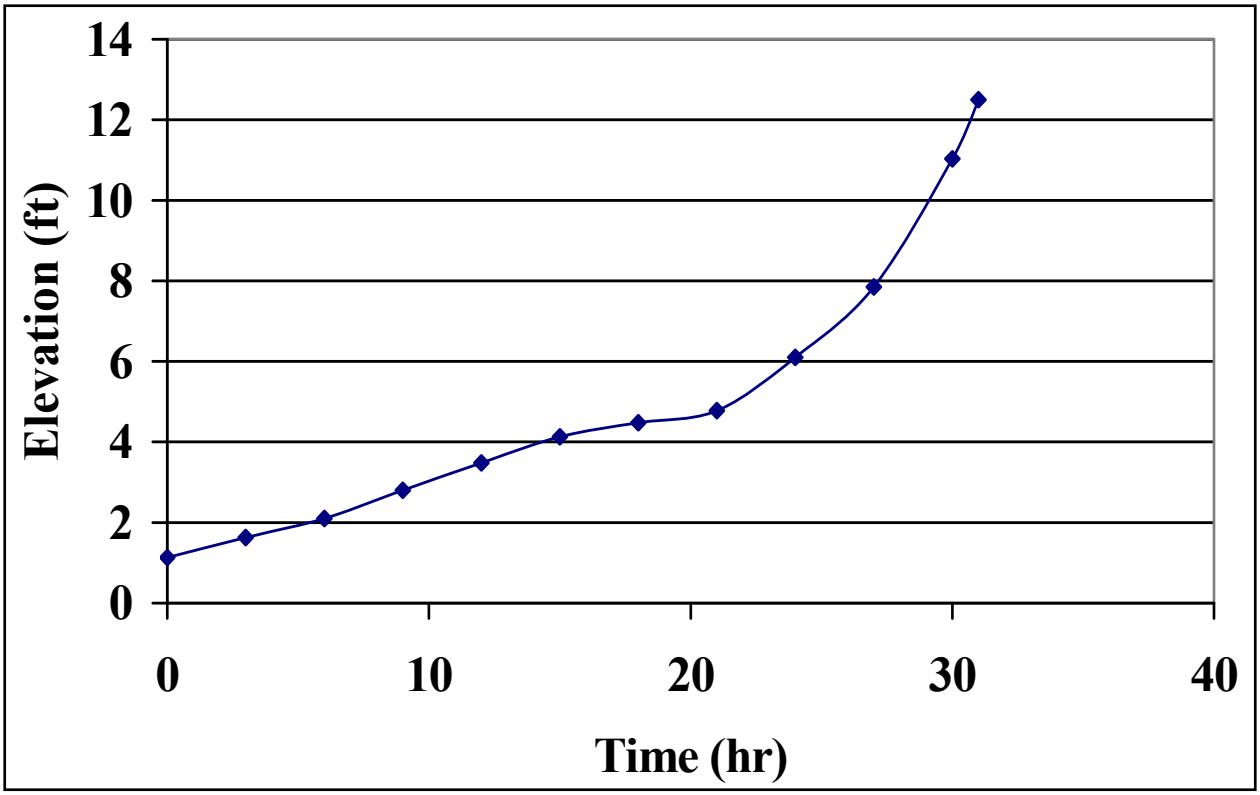

Figure V-17-23. Hydrograph starting 8/28/2005 at 12:00 AM

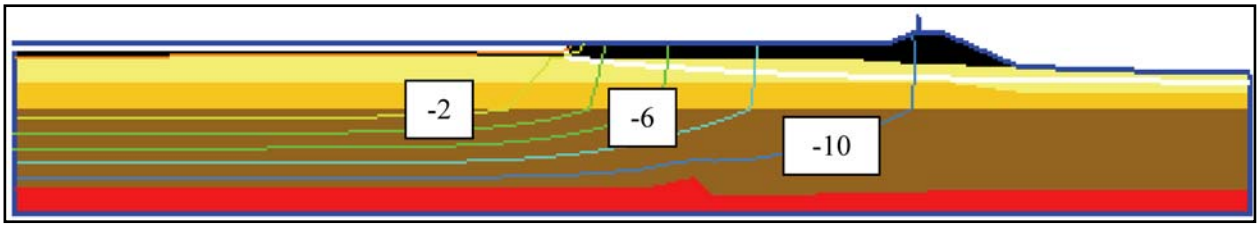

Figure V-17-24. Contours of Total Head for Steady-State Solution, Canal Elevation = 1.13 ft applied from x=0 to x = 202 ft, Head at Protected Side = -11.5 ft, (Equipotential Lines = -10, -8, -6, -4, -2, 0 ft)

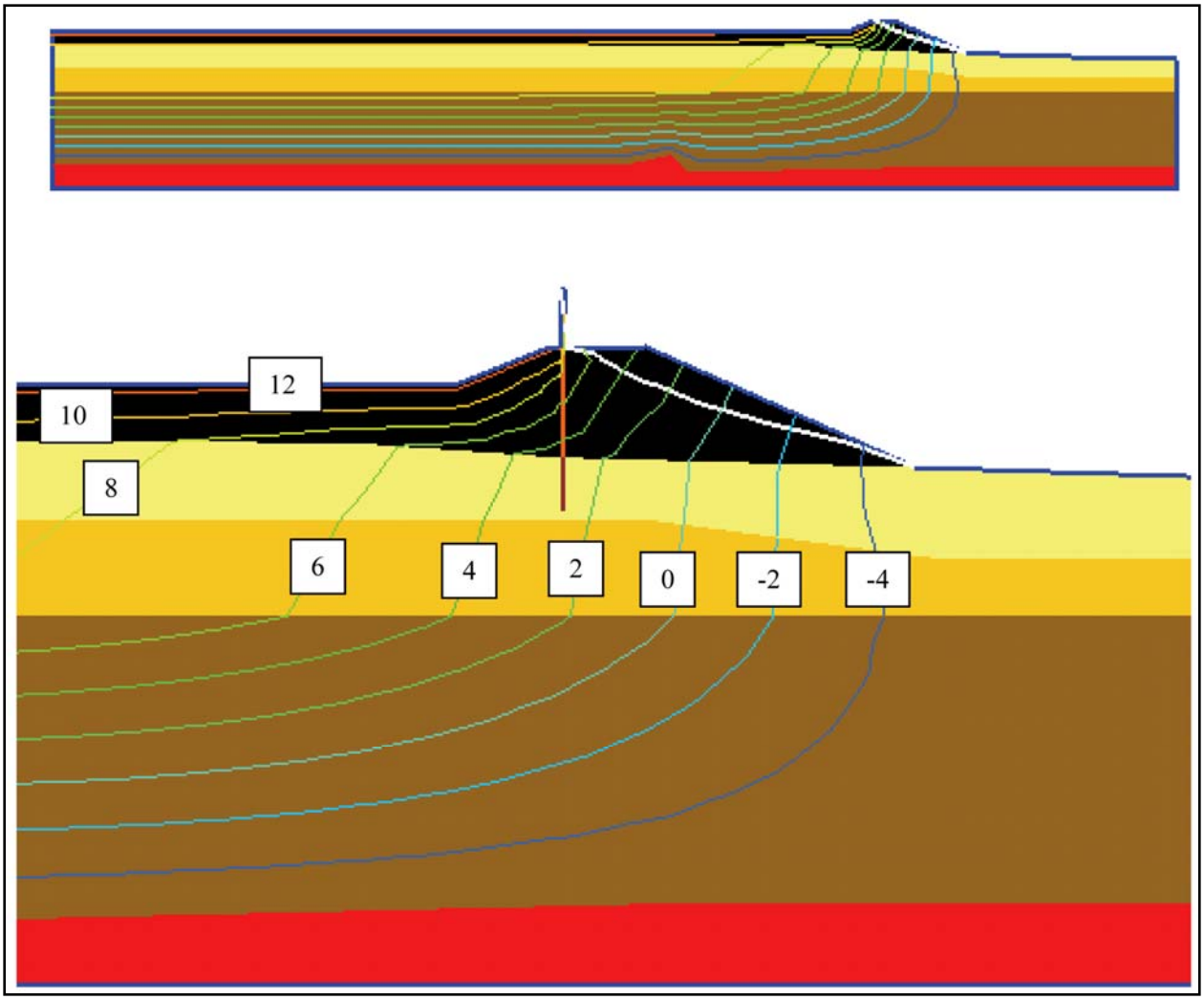

Figure V-17-25. Contours of Total Head for Steady-State Solution, Canal Elevation = 12.5 ft, Head at Protected Side = -6 ft (Equipotential Lines = -4, -2, 0, 2, 4, 6, 8, 10, 12 ft)

Figure V-17-26 shows the results of the transient finite element seepage analysis for the most realistic representation of the geometry and material property. It can be seen that the seepage conditions have not reached the steady-state condition. The levee on the canal side has not even reached full saturation.

As designed, the pre-Katrina site conditions were a clay blanket starting at the toe of the levee on the canal side. This is similar to the clay blanket used upstream of a dam to reduce underseepage and seepage pressures down stream. While unlikely, a worst case condition would be that the clay blanket had the same permeability as the marsh material, Figure V-17-27. Figure V-17-28 shows the initial steady-state underseepage conditions used for the transient analysis. V-17-29 shows the steady state solution for the canal water level at 12.5 (top of the wall) and the protected side at -6.0 for no clay blanket. The phreatic surface intersects the protected levee slope.

Figure V-17-30 shows the results of the transient finite element seepage analysis for the clay blanket with the same permeability as the marsh material. Again, the levee on the canal side does not even reach full saturation.

In order to answer questions raised by NRC based on NSF Berkeley analyses, another unrealistic set of conditions were assessed. These conditions included no clay blanket, and increasing the permeability of the marsh by 100 times beyond the highest limit of published values. Figure V-17-31 shows the steady state solution for the canal water level at 12.5 (top of the wall) and the protected side at -6.0 for 100 times increase in permeability. Figure V-17-32 shows the results of the transient finite element seepage analysis for the 100 times increase in marsh permeability. Even with this completely unrealistically high permeability, the seepage does not reach the steady state conditions.

Table V-17-8 shows a comparison of the exit gradient for the steady state condition and transient analysis of the storm surge in the canal. The transient solution has a 40 percent reduction in uplift pressure on the protected side as compared to the steady state analysis. The transient solution also has a 48 percent reduction in the exit gradient as compared to the steady state solution.

Table V-17-8
Comparison of Exit Gradient for Steady State Condition and Transient Analysis

	Total Head at Sheetpile on Protected Side (ft)	Uplift Force on Protected Side (kips)	Percent Reduction in Uplift from Steady State	Change in Head at Toe of Levee (ft)	Length of Seepage Path (ft)	Exit Gradient = H/L	Percent Reduction in Gradient from Steady State
Steady State	10	11.4		6-4.59=1.41	10.79-6=4.79	0.29	
Transient	6	6.8	40	6-5.30=0.70	10.79-6=4.79	0.15	48

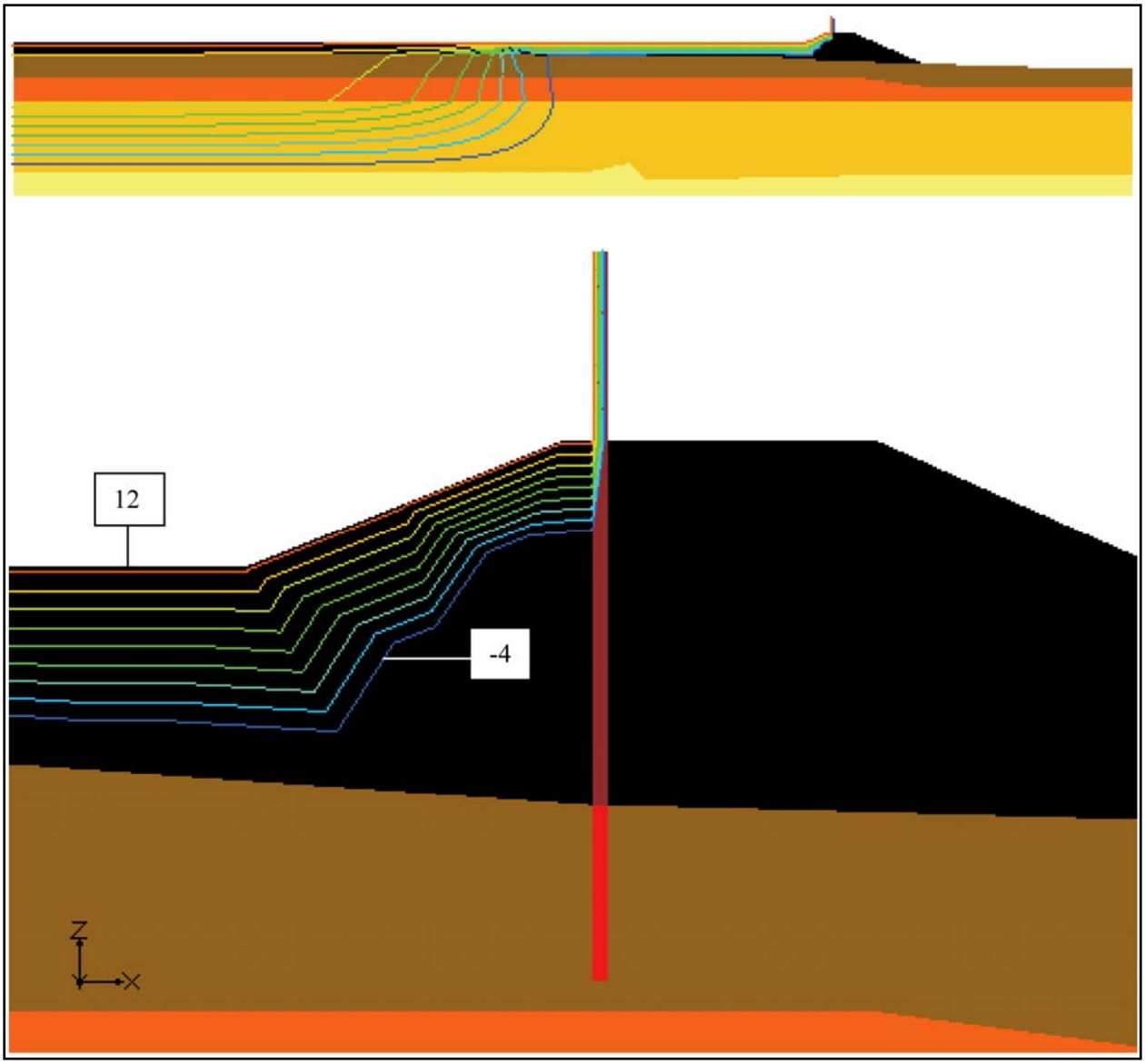

Figure V-17-26. Contours of Total Head for Transient Solution, Canal Elevation = 12.5 ft, Head at Protected Side = -6 ft (Equipotential Lines = -4, -2, 0, 2, 4, 6, 8, 10, 12 ft)

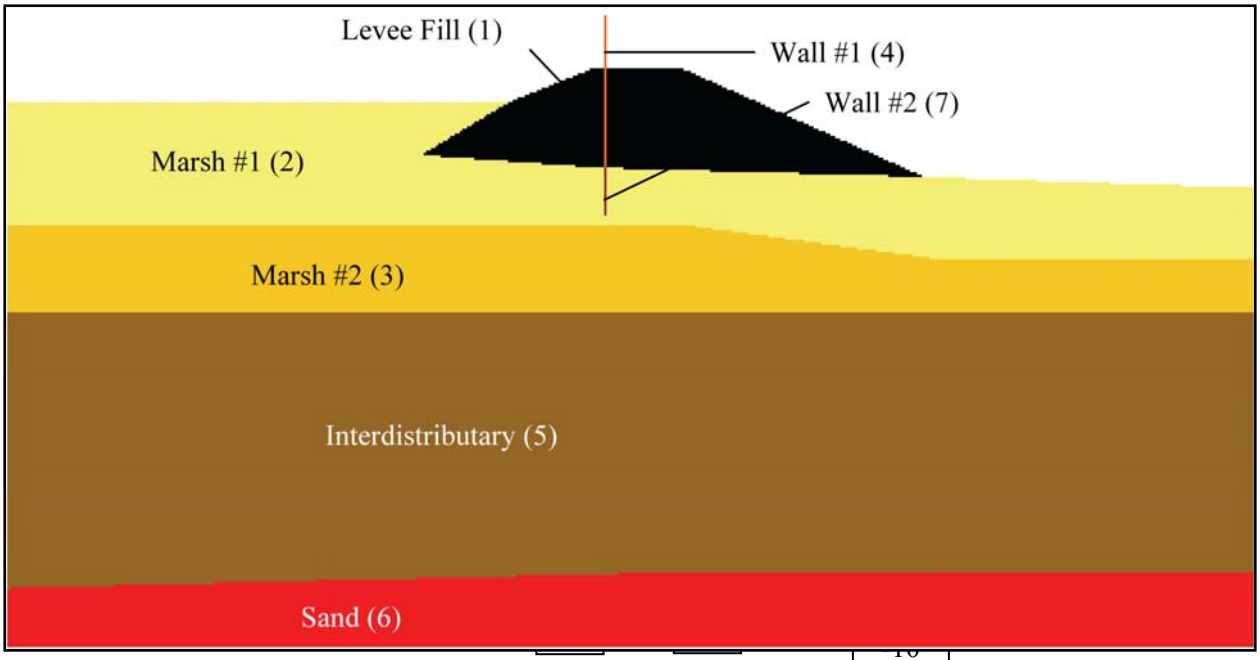

Figure V-17-27. Clay Blanket Assumed to have the same permeability as Marsh #1

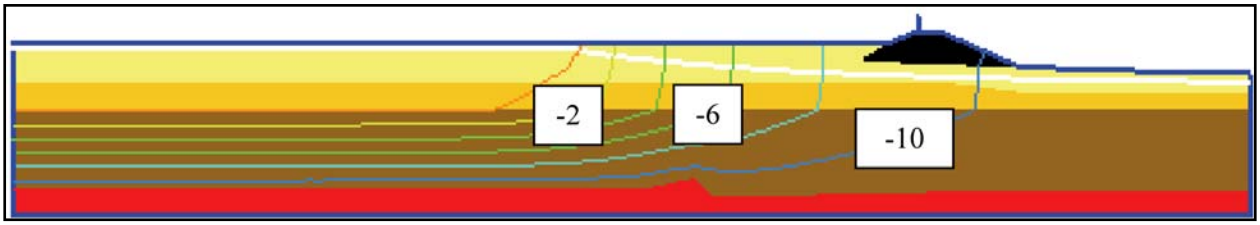

Figure V-17-28. 2D Contours of Total Head for Steady-State Solution, Canal Elevation = 1.13 ft applied from x=0 to x = 202 ft, Head at Protected Side = -11.5 ft (Equipotential Lines = -10, -8, -6, -4, -2, 0 ft)

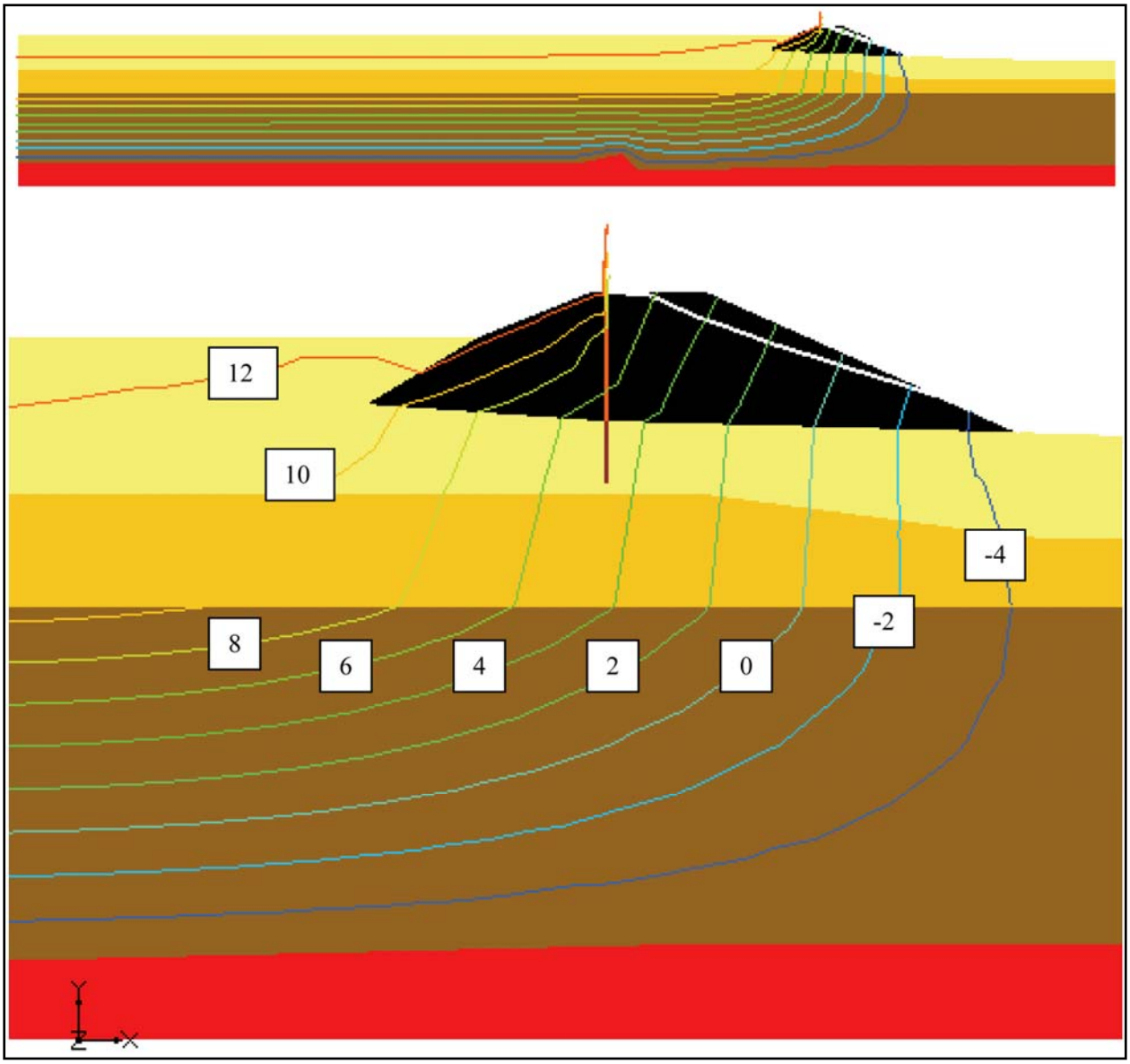

Figure V-17-29. Contours of Total Head for Steady-State Solution, Canal Elevation = 12.5 ft, Head at Protected Side = -6 ft (Equipotential Lines = -4, -2, 0, 2, 4, 6, 8, 10, 12 ft)

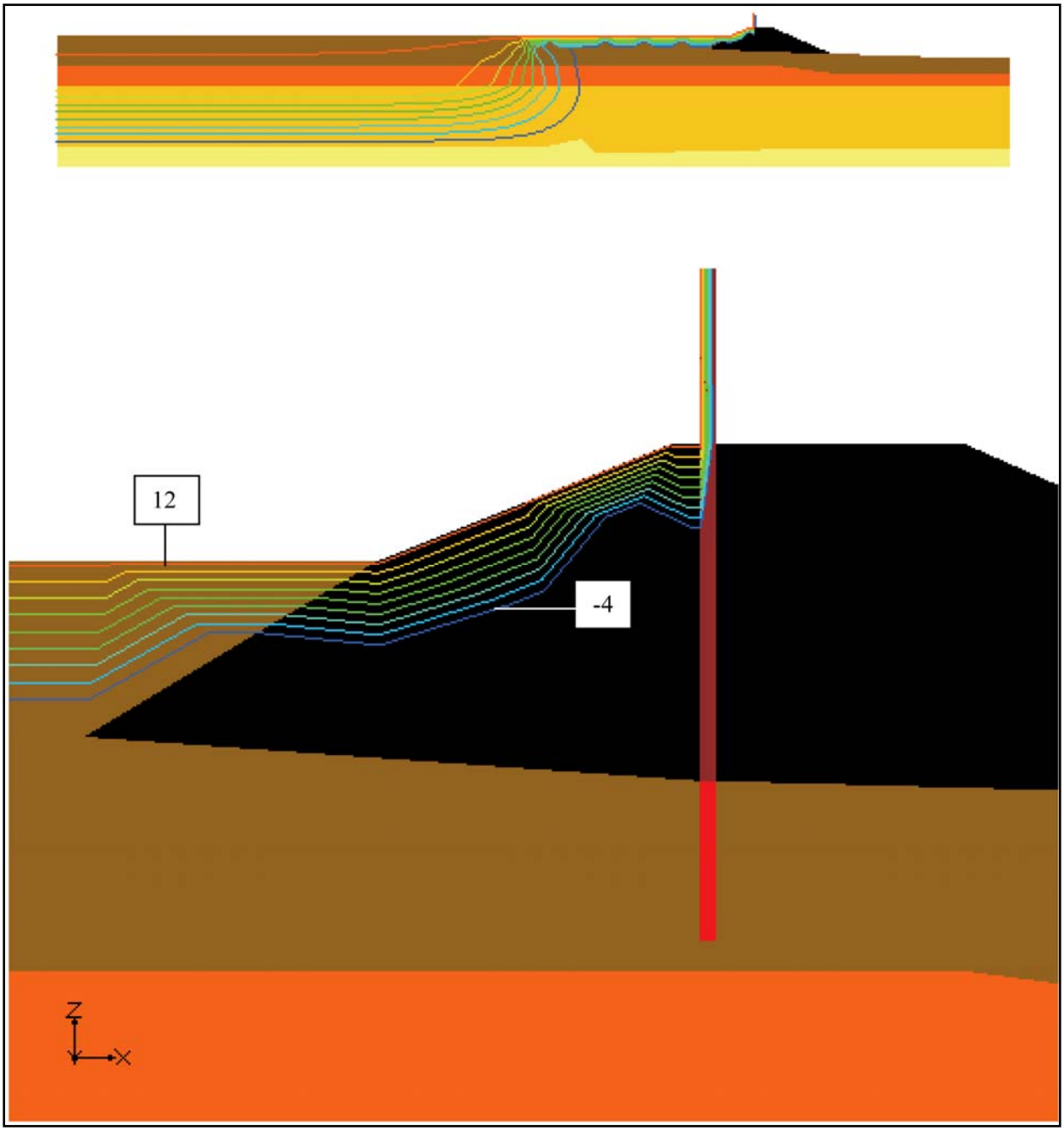

Figure V-17-30. Contours of Total Head for Transient Solution, Canal Elevation = 12.5 ft, Head at Protected Side = -6 ft (Equipotential Lines = -4, -2, 0, 2, 4, 6, 8, 10, 12 ft)

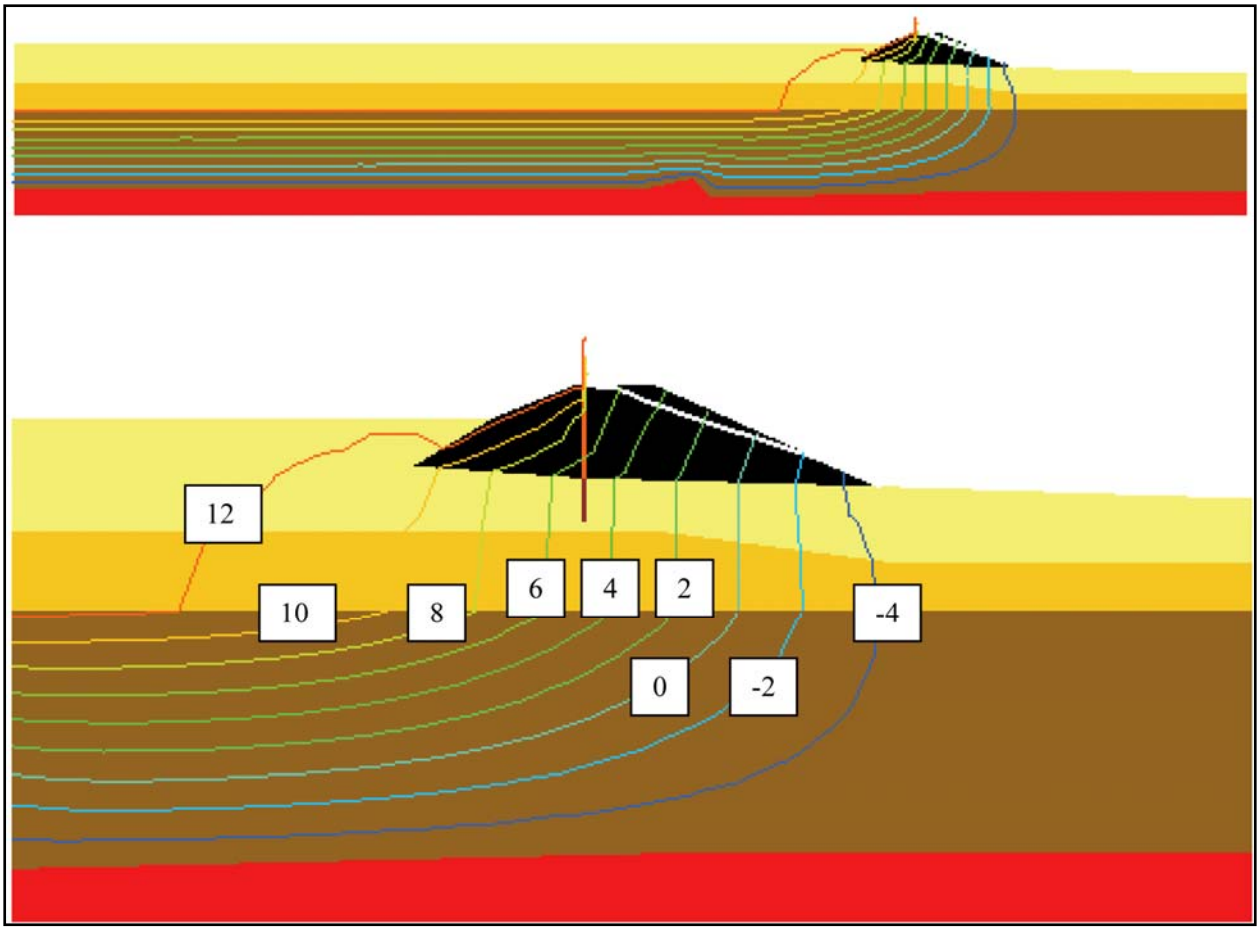

Figure V-17-31. Contours of Total Head for Steady-State Solution, Canal Elevation = 12.5 ft, Head at Protected Side = -6 ft (Equipotential Lines = -4, -2, 0, 2, 4, 6, 8, 10, 12 ft)

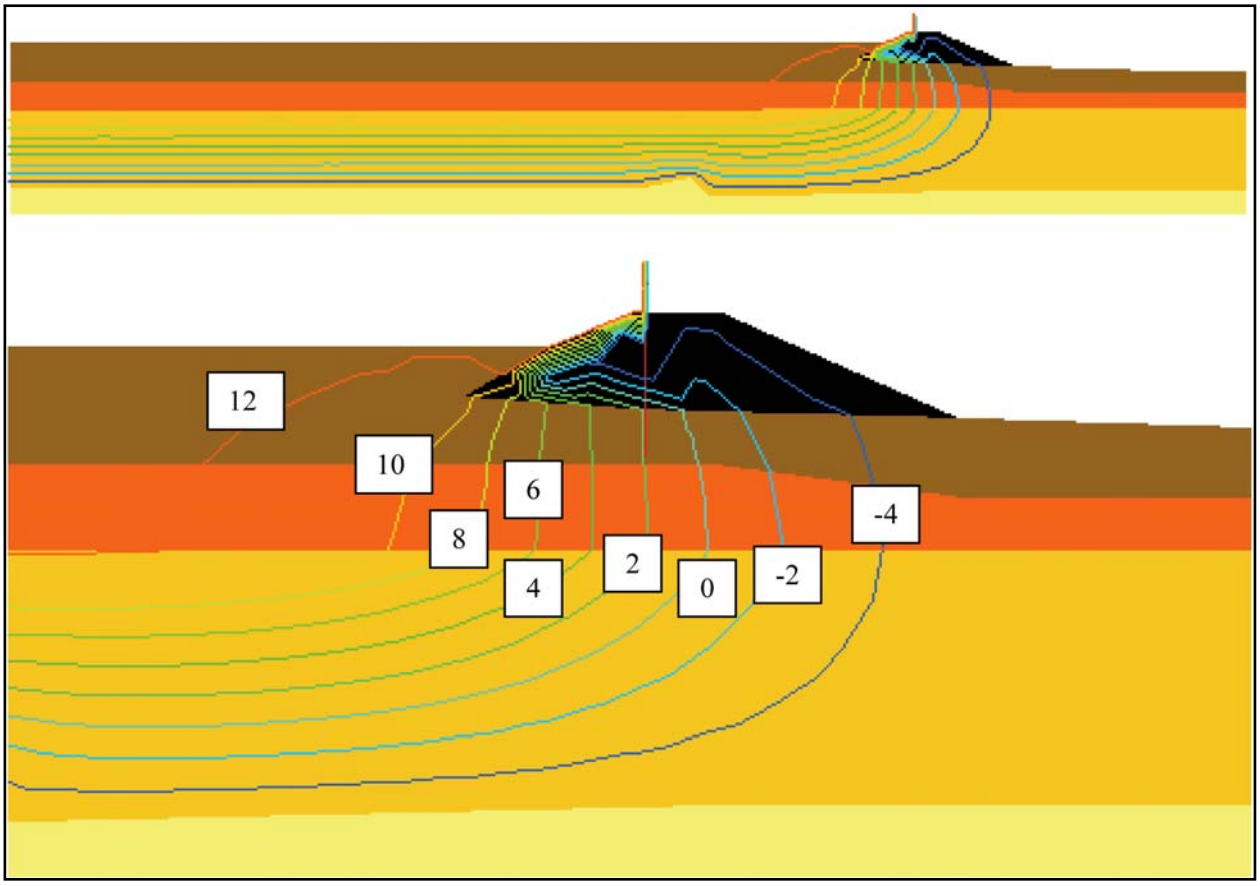

Figure V-17-32. Contours of Total Head for Transient Solution, Canal Elevation = 12.5 ft, Head at Protected Side = -6 ft (Equipotential Lines = -4, -2, 0, 2, 4, 6, 8, 10, 12 ft)

In conclusion, the NSF-Berkeley findings and recommendations on underseepage, especially regarding the IHNC breaches along the Lower Ninth Ward, stated in their 31 July 2006 final report, are based on unrealistic and unproven permeability values that led to faulty and deceptive analysis results, typical garbage in garbage out. The writers of the NSF-Berkeley report either did not completely read the IPET Draft Final Report or they intentionally ignored information that did not support their hypothesis. The NSF-Berkeley report states, "*Unfortunately, even IPET's own analyses do not suggest a high likelihood of failure of the north breach section at the canal water levels present as early as 5:00 am (approximately Elev. +9 feet, MSL), so this would not appear to be the explanation for the observed in the neighborhood. Instead, it is proposed that observed water rise on the inboard (protected) side Florida Avenue was more likely the result of large underseepage flows through the highly pervious "marsh" deposits along this frontage*."

IPET's slope stability analyses show that failure of the IHNC East Bank, North Breach at the Lower Ninth Ward could occur before the canal water level reached the top of the wall. There is clear evidence that water levels in the northern region of the Lower Ninth Ward, south of Florida Avenue, were rising early in the morning of August 29, 2005. Several eyewitness accounts had water flowing into houses and down streets between 0430 and 0500. Stopped clock data has the water level in this area at Elevation +3.0 by 0600, which makes the depth of water between 5 and

10 ft. These observed water levels and the associated volume of water needed to achieve them in the northern region of the Lower Ninth Ward, south of Florida Avenue, **did not come from underseepage** as suggested by the NSF-Berkeley report. This can only occur if the levee is breached, which is what the IPET Draft Final Report stated, "*Eyewitness reports indicate that water level in the 9th Ward near Florida Avenue was rising when the water level in the IHNC was still below the top of the wall. Stability analyses indicate that foundation failure would occur before overtopping at the north breach on the east side of the IHNC. This breach location is thus the likely source of the early flooding in the 9th Ward.*" Even with outrageously unrealistically high permeability values used by the NSF-Berkeley group, underseepage could not produce the volume of water observed in this area. The NSF-Berkeley group would have realized this if they had reviewed the hydrograph for the Lower Ninth Ward inundation presented in Appendix V-11 and reproduced here in Figure V-17-33.

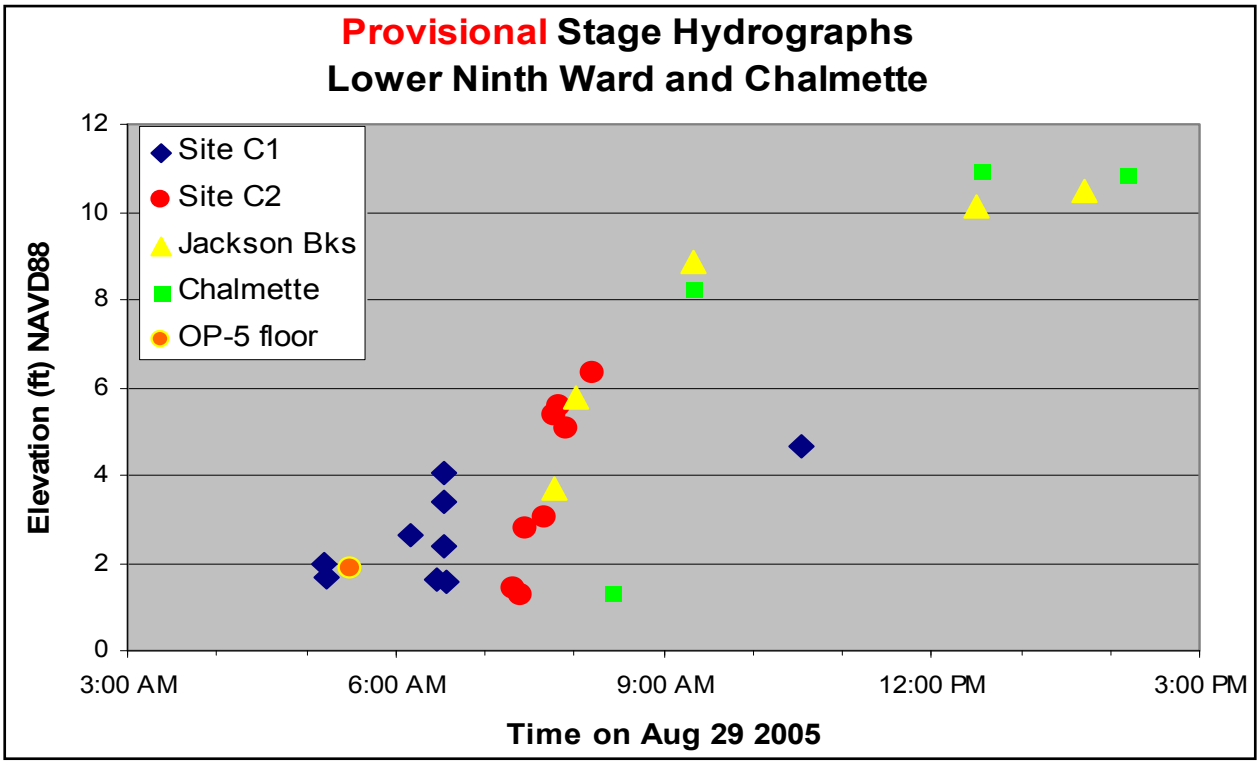

Figure V-17-33. Hydrograph for the Lower Ninth Ward Inundation

The IPET slope stability analyses show that the levee would become unstable when the water level in the canal reached approximately Elevation +11.2 NAVD 88. Figure V-17-34 shows the reprint of the hydrograph for the IHNC, Figure 129, IPET Volume IV – Storm, page IV-185. The hydrograph shows that the water level in the canal at 0500 could have been Elevation +11.0, depending on which gage reading is used. Based on the variability of the soil properties and the gage readings that make up the hydrograph, the IPET analyses **would appear** to provide a probable explanation for the observed water in the neighborhood and foundation failure that resulted in the north breach. In order for this foundation failure to develop, it did not require unrealistic underseepage to occur to cause the breach.

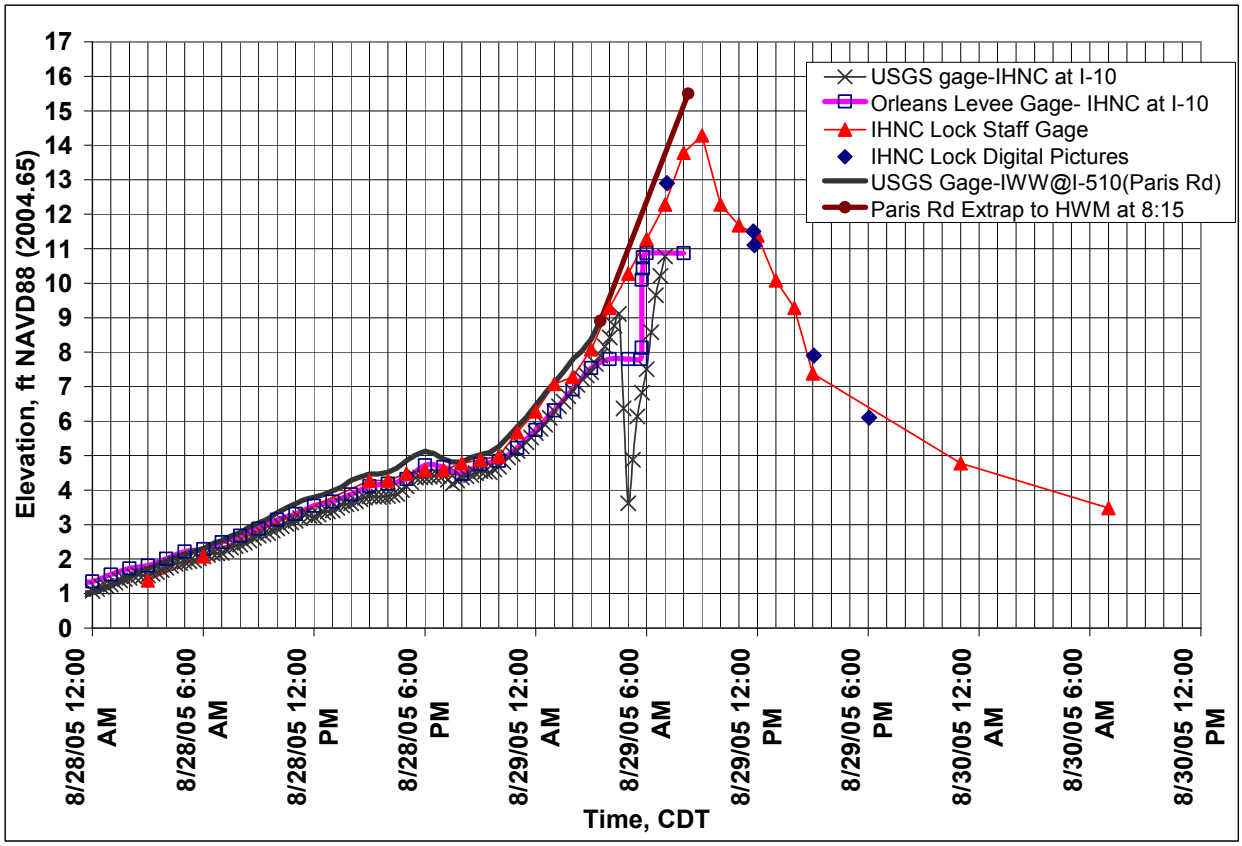

Figure V-17-34. Hydrograph for IHNC

This calls into question the rest of the NSF-Berkeley investigation of the breaches along the IHNC east bank Lower Ninth Ward. They stated that the failure of south breach was due to underseepage. The NSF-Berkeley group states the crevasse splay shown in the foreground of Figure V-17-35 (Figure 6.45, NSF-Berkeley report ILIT Final Report, July 31, 2006) was due to reverse underseepage. The NSF-Berkeley report states, "*Finally, clear and uncompromising evidence of the high lateral permeability of these deposits* ***at this site*** *is presented in Figure 6.45, which shows a well-developed classic crevasse splay that resulted from reverse underseepage through these same highly pervious marsh deposits as the ponded floodwaters drained out from the Lower Ninth Ward after the hurricane passed.*"

A much more plausible explanation for the crevasse splay shown in the foreground of Figure V-17-35 is that it was caused by erosion when the Lower Ninth Ward drained back into the canal, Figure V-17-36. While the NSF-Berkeley group tries to use unclear and compromised evidence from observations to bolster their underseepage hypothesis, they overlooked the direct comparison of field observations between the south breach at the east bank of the IHNC Lower Ninth Ward, Figure V-17-37, and the I-wall on Citrus back levee along the GIWW, Figures V-17-38, V-17-39, and V17-40. The NSF-Berkeley report stated that the damage along Citrus Back Levee was due to: "*Scour trenches developed along the full length of the floodwall on the protected side, as overtopping cascaded over the tops of the floodwalls. In many instances, these trenches were located several feet from the base of wall (indicating progressive*

tilting of the floodwalls, and thus the waters falling farther to the inboard side) and some had widths of 7 feet or more." They go on to state: "*These scour-induced trenches reduced the lateral support for the sheetpiles and the concrete floodwall they supported, and the lateral forces of the outboard side storm surge pushed the laterally unbraced floodwall sideways."*

Comparing the scour trench located on the protected side of what was the I-wall running along the east bank of IHNC, south breach Lower Ninth Ward shown in Figure V-17-37, with the scour trench on the protected side of the I-wall of the Citrus Back Levee shown in Figure V-17-38, and the IPET slope stability analysis for the I-wall at the east bank IHNC at south breach show it to be stable, with water to the top of the wall, one would have to conclude that the most plausible explanation for the breach is scour of the protected side support of the I-wall from overtopping.

While the IPET team believes it is the importance to consider all possible modes of failure, it is most important to consider realistic materials and scenarios in order to help future designers understand the failures of the New Orleans Hurricane Protection System that took place so that it is not repeated in the future.

Because the unrealistic permeability assigned to the marsh material for the NSF-Berkeley seepage analyses was at least 1,000 times too high, the results of the seepage analyses described in that report do not reflect the real seepage conditions in the field. Because it was assigned such a high permeability, the marsh layer appeared in those analyses to have very low resistance to seepage, and to respond very quickly to the rise in canal water level. This behavior is not consistent with the actual behavior of marsh material and peat, especially when consolidated under the weight of the levees. Based on this mistaken choice of marsh permeability, and the ensuing unrepresentative analytical results, the authors of the NSF-Berkeley report offered this advice regarding design analyses:

> *"Exoneration, a priori, of underseepage dangers should be discontinued immediately, and underseepage analyses should be required for the full regional flood protection system."*

This is misguided advice based on an assumed permeability for the marsh material that is at least three orders of magnitude higher than the actual permeability. Underseepage analyses performed using this inappropriate value of permeability are misleading, and do not provide a reasonable basis for design to prevent or mitigate underseepage problems.

Figure V-17-35. Aerial view of the south breach at east bank of the IHNC (at the west end of the Lower Ninth Ward), showing in crevasse splay generated by reverse drainage flow. (Figure 6.45, NSF-Berkeley report (ILIT Final Report, July 31, 2006)

Figure V-17-36. Aerial view of the south breach at east bank of the IHNC (at the west end of the Lower Ninth Ward), showing turbulent water flow coming out of the Lower Ninth Ward after the hurricane passed

Figure V-17-37. Scour and Erosion Leading to the Failure of the I-Wall on the IHNC adjacent to the South Breach (Lower Ninth Ward)

Figure V-17-38. Scour trench on the protected side of Citrus Back Levee I-wall. (Figure 7.14, NSF-Berkeley report (ILIT Final Report, July 31, 2006)

Figure V-17-39. Another section of the Citrus Back Levee I-wall showing erosion of the levee, lateral deflection, and tilting from overtopping

Figure V-17-40. Deflection and tilting of Citrus Back Levee I-wall

Seepage Analysis of the Levees along the Mississippi River Gulf Outlet (MRGO)

The levees along the Mississippi River Gulf Outlet adjacent to Lake Borgne suffered significant damage from erosion due to surge and wave action from Hurricane Katrina. The IPET assessment of the available data and associated information on the cause of the damage led to the finding that the damage was caused by erosion due to flow over the levees from the surge and wave action. The NSF-Berkeley report suggested that the erosion was due to "*seepage flow passing through the embankment section, and then eroding soil as it exits through the lower portion of the back side slope face"*. The report further states that "*This 'through flow' can cause significant erosion if the embankment soils are pervious, as was the case along significant portions of the MRGO frontage levees*". Figure V-17-41 shows the NSF-Berkeley illustration of the through flow erosion they suggest as one of the causes of the damage to levees along the MRGO.

In order for through flow to be the cause of the erosion of the MRGO levees, not only is it necessary to have a highly pervious levee soil, but a sufficient amount of time to allow the levee soils to become saturated and establish seepage through the levee. To examine the possibility of through flow as the cause of the erosion of the MRGO levees, a series of transient finite element

seepage analyses was performed to investigate if the rise in water level was sufficient to cause through seepage.

Contrary to the NSF-Berkeley report that stated that the levees along the MRGO were *"sand core,"* levees were constructed of hydraulic dredge material with considerable variability ranging from fat clays to silty sands, Figure V-17-42 to V-17-49 and Table V-17-9. This variability was not confined to just along the length, but also through the cross section. The levee cross sections had pockets of sands and silts. This makes it impossible to create a typical cross section to analyze. Therefore, one material type will be used for the levee cross section in an individual transient seepage analysis and then the coefficient of permeability will be varied in successive analyses to investigate how the through seepage will increase with greater permeability.

Table V-17-9
Soil borings and scour depth along selected MRGO levee reaches

Soil boring / surface soil type	Scour depth, ft	Water crest over crown, ft
9BU / med lean clay	5	2
11BU / soft fat clay	10	5
12BU / med lean clay	6	7
18UBD / silty sand	6	7
13BU / med fat clay	1	7
19UBD / silty sand	n/a (sheetpile reach)	7
ERDC / med fat clay	1	7
10-CUHA / silt	n/a (sheetpile reach)	6
10-CUI / med fat clay	0.5	6

Figure V-17-50 shows the cross section and initial coefficient of permeability used in the series of the transient finite element analysis. Figure V-17-51 shows the finite element mesh used for these analyses.

Figure V-17-52 shows the computed hydrograph for the hurricane storm surge and the associated wave action for a given location on the MRGO canal. The storm surge is the source of the through seepage. Figure V-17-53 shows the smooth hydrograph used in the transient analyses.

The initial boundary conditions for the steady state solution prior to the hurricane were set to a water level of Elevation 1.0 on the canal side (right hand side of Figure V-17-51), to a water level of Elevation 1.0 on the far left boundary, and zero pressure for the elements defining the levee and element on the protected side above Elevation 1.0.

Figure V-17-54 shows the steady-state solution for the MRGO canal water level at Elevation 18 and Elevation 1 on the far boundary on the protected side. The phreatic surface in the protected side levee does not intersect the protected side slope.

Figure V-17-55 shows the results of the transient analysis using the hydrograph in Figure V-17-53. It shows, as would be expected, there is not a sufficient amount of time to saturate the levee and establish through seepage.

The worst possible soil type for through seepage of the levee would be a clean sand. The levee soil type can be made into a clean sand by increasing the coefficient of the permeability in the model by 15,000. Figure V-17-56 shows the steady-state solution for the case of the coefficient of the permeability increased by 15,000. The phreatic surface intersects the protected side levee slope surface. Figure V-17-57 shows the computed hydraulic gradient for the steady-state solution for the case of the coefficient of the permeability increased by 15,000. The hydraulic gradient values at the toe and slope of the levee on the protected side are very low and unlikely to cause erosion of a grass covered slope.

Figure V-17-58 shows the results of the transient analysis using the hydrograph in Figure V-17-53. It shows there is not a sufficient amount of time to saturate the levee and establish through seepage.

Even if the levees along MRGO were totally constructed of a clean sand which they were not, the time that the water remained on the unprotected side of the levees due to the Hurricane Katrina surge before it overtopped the levees was not sufficient to establish through seepage and cause erosion of the levees.

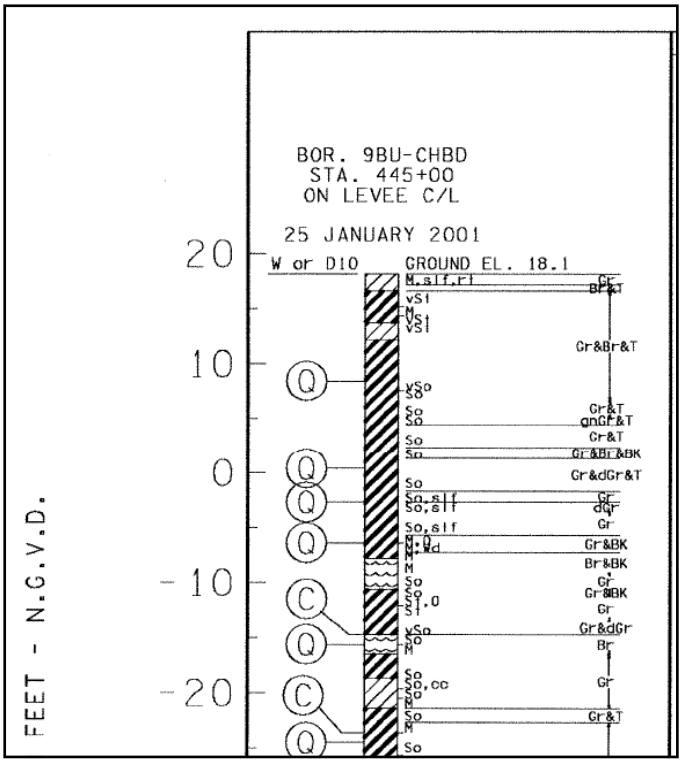

Figure V-17-42. Soil boring 9BU along MRGO (ft, NGVD)

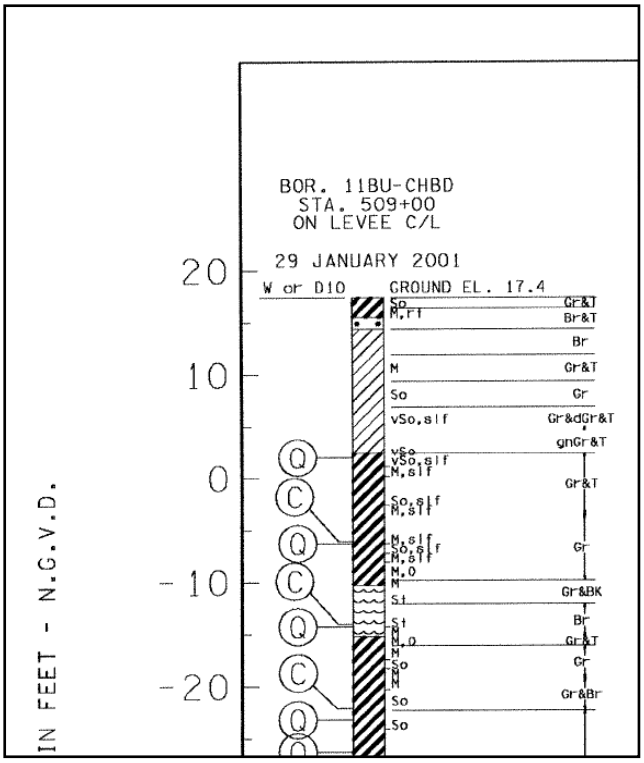

Figure V-17-43. Soil boring 11BU along MRGO

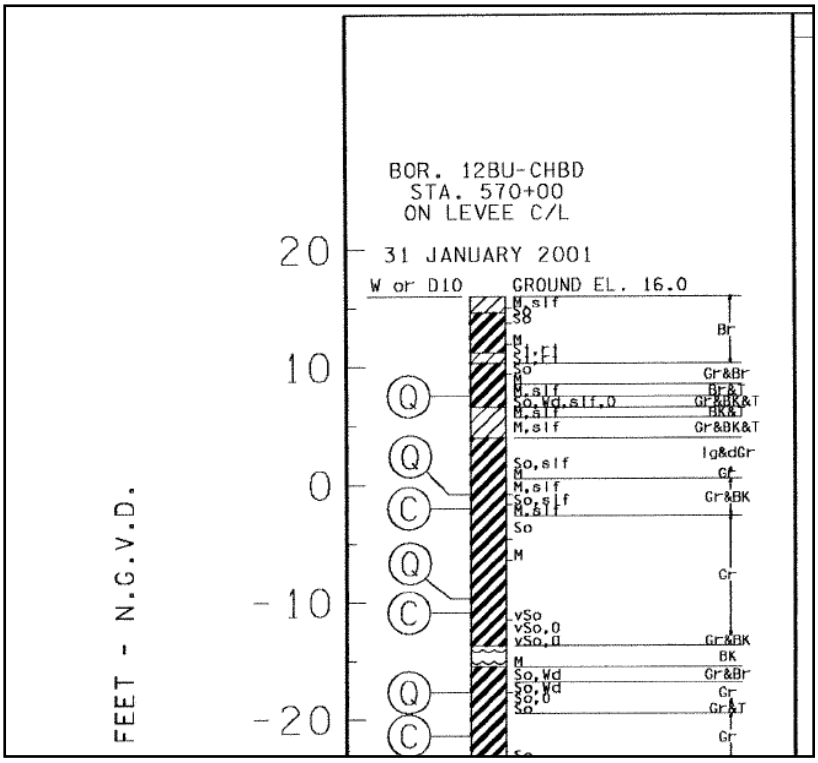

Figure V-17-44. Soil boring 12BU along MRGO

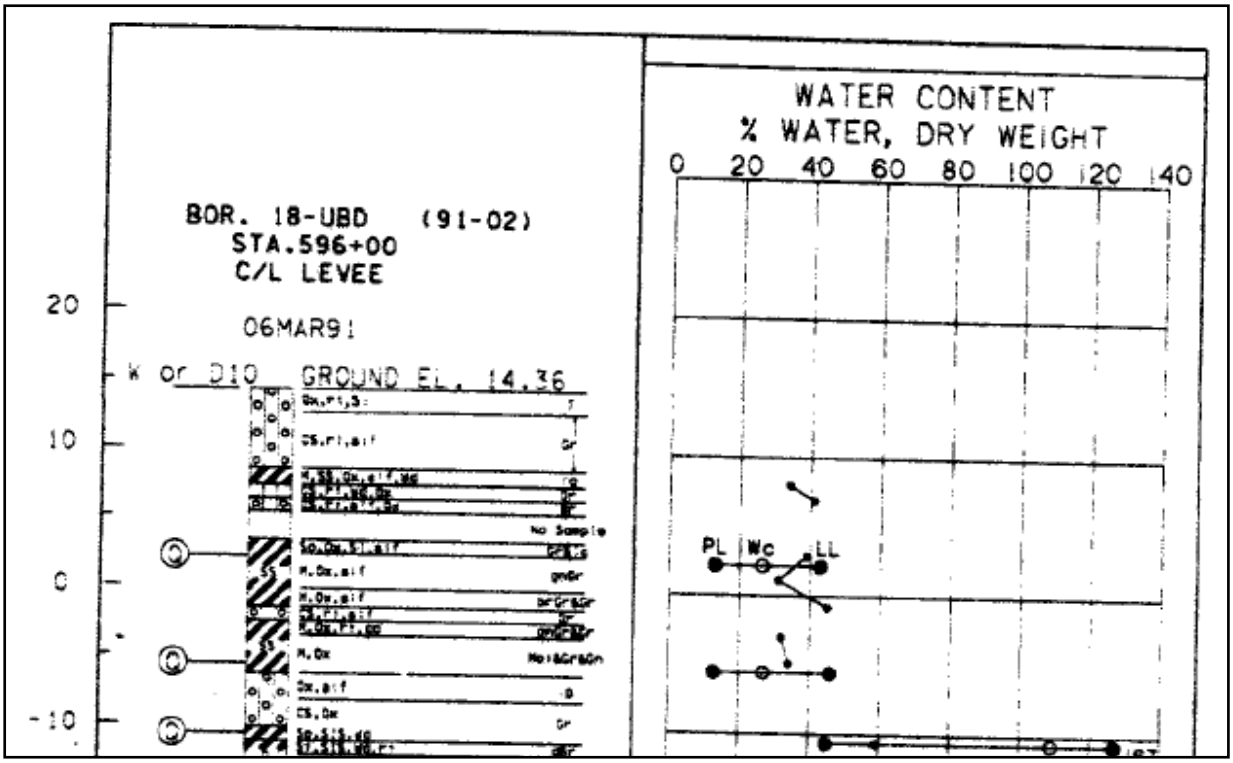

Figure V-17-45. Soil boring 18-UBD along MRGO

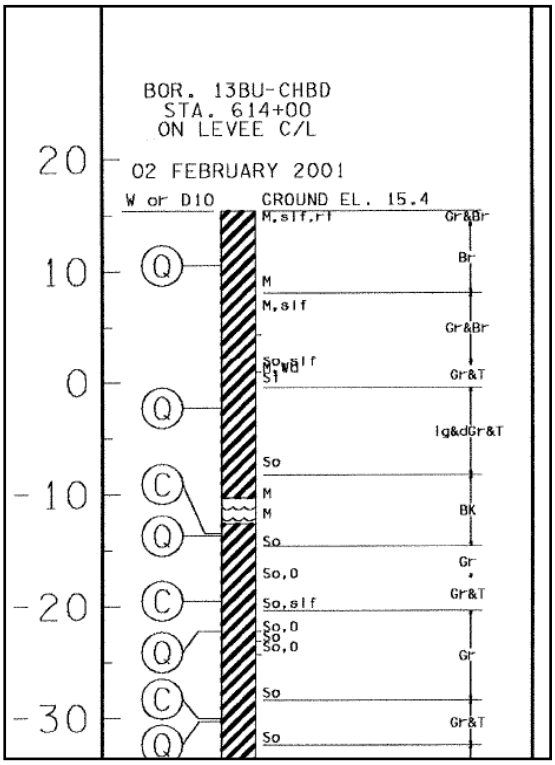

Figure V-17-46. Soil boring 13BU along MRGO

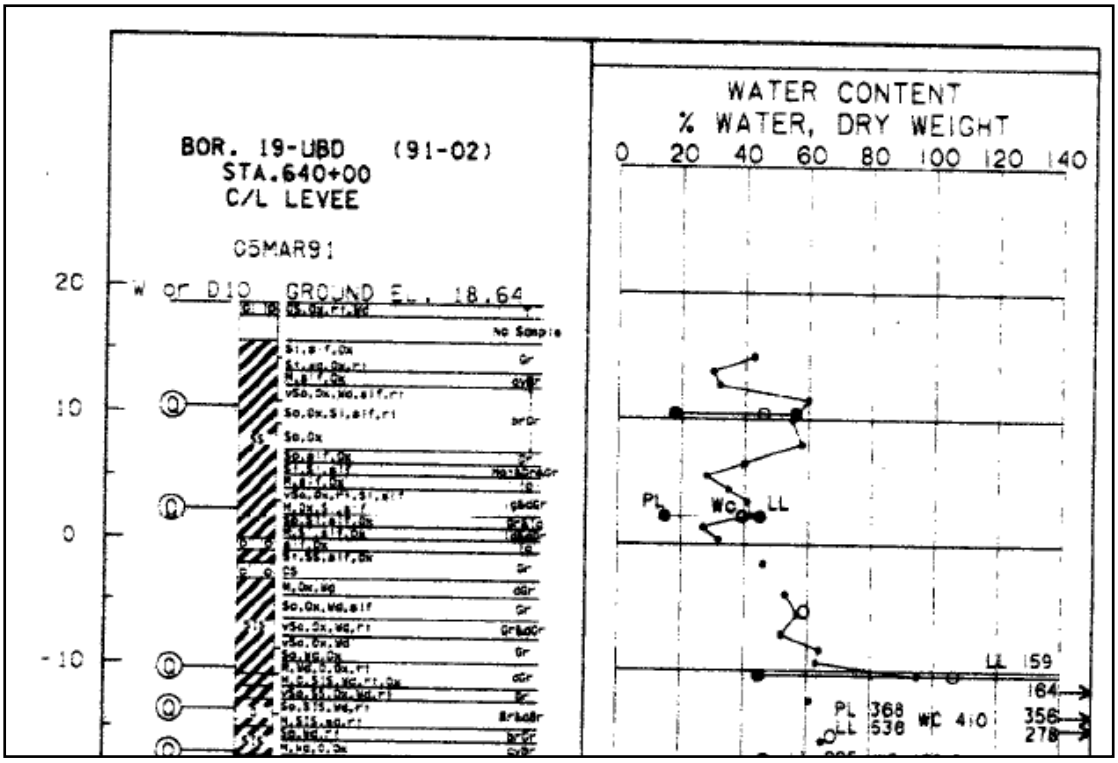

Figure V-17-47. Soil boring 19-UBD along MRGO

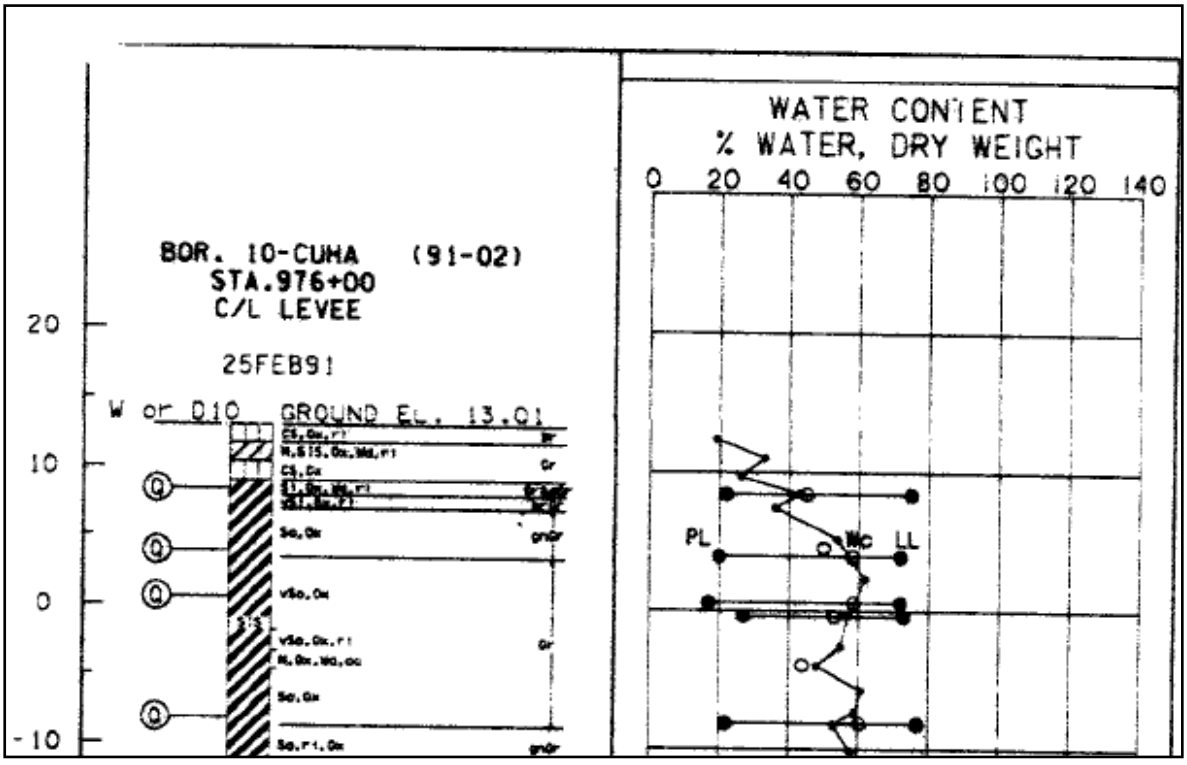

Figure V-17-48. Soil boring 10-CUHA along MRGO

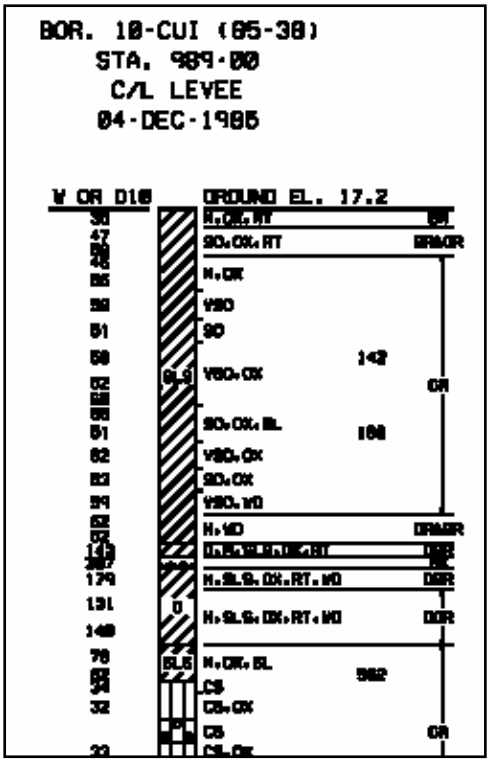

Figure V-17-49. Soil boring 10-CUI along MRGO

Material Number	Name	K (ft/hr)
1	Levee	0.000118
2	ML #1	0.00118
3	CH #1	0.000118
4	CH #2	0.000118
5	ML # 2	0.118

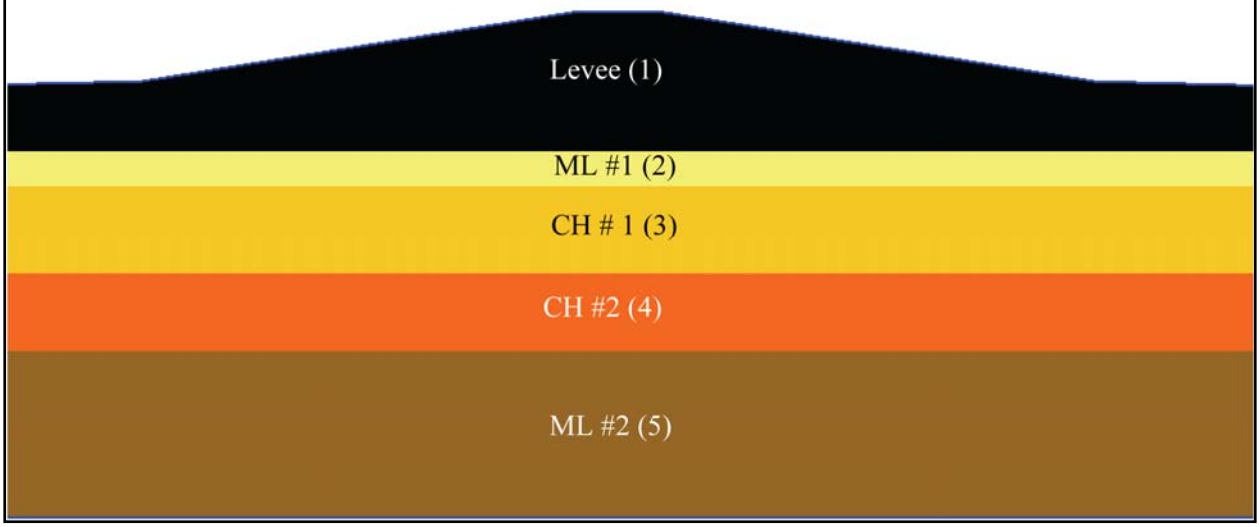

Figure V-17-50. Typical MRGO levee cross section.

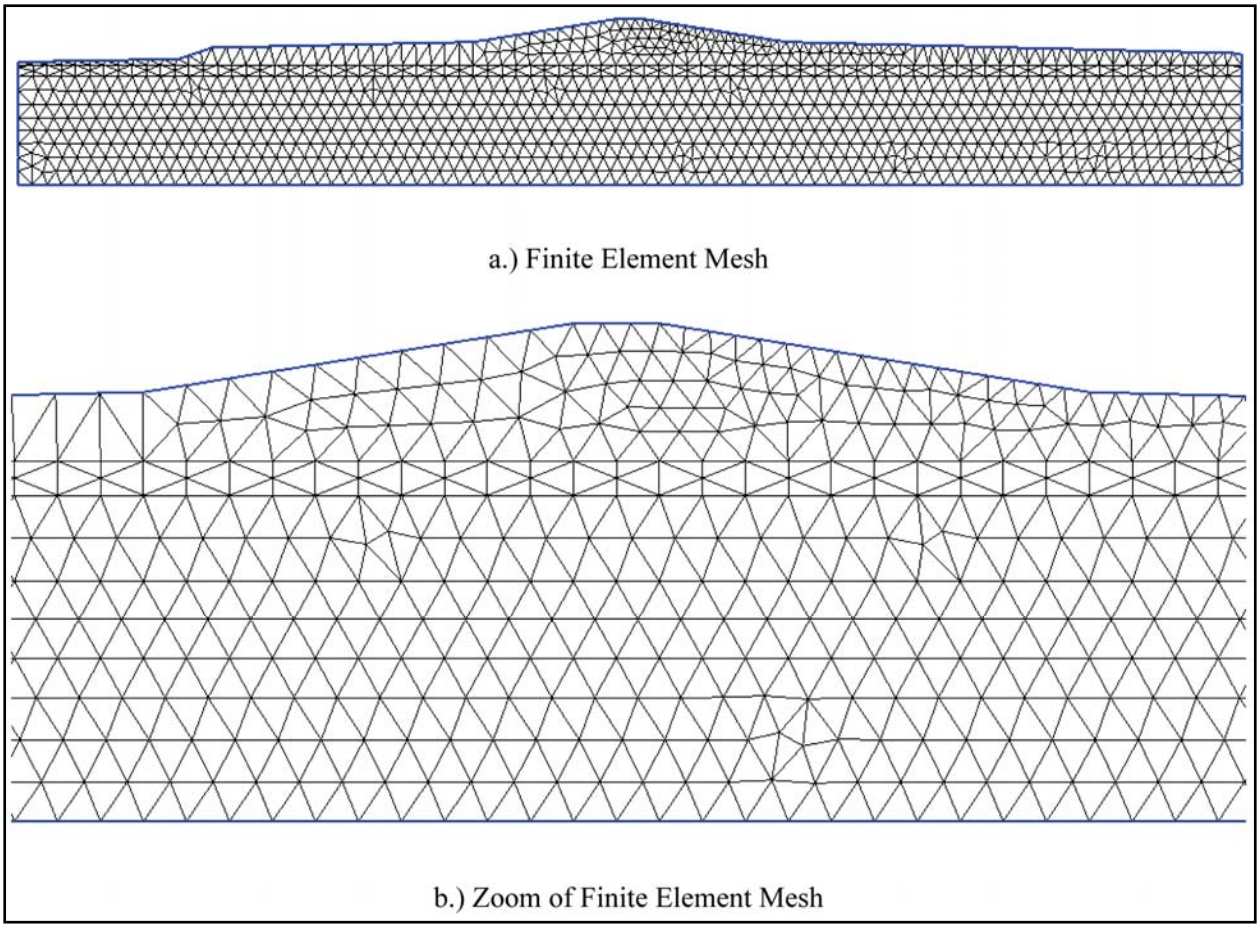

Figure V-17-51. The finite element mesh for the seepage MRGO levees.

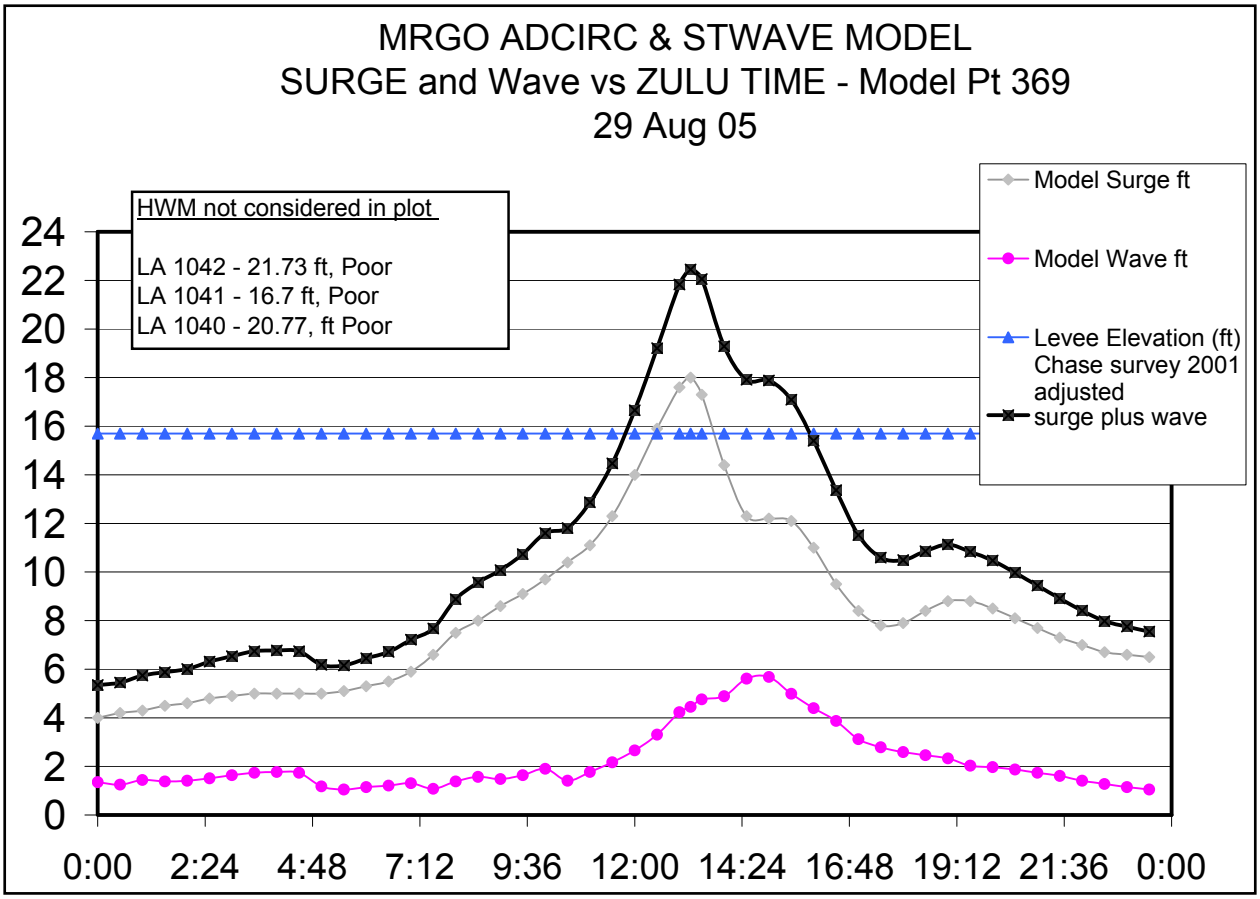

Figure V-17-52. Computed hydrograph showing water level due to the surge and wave action

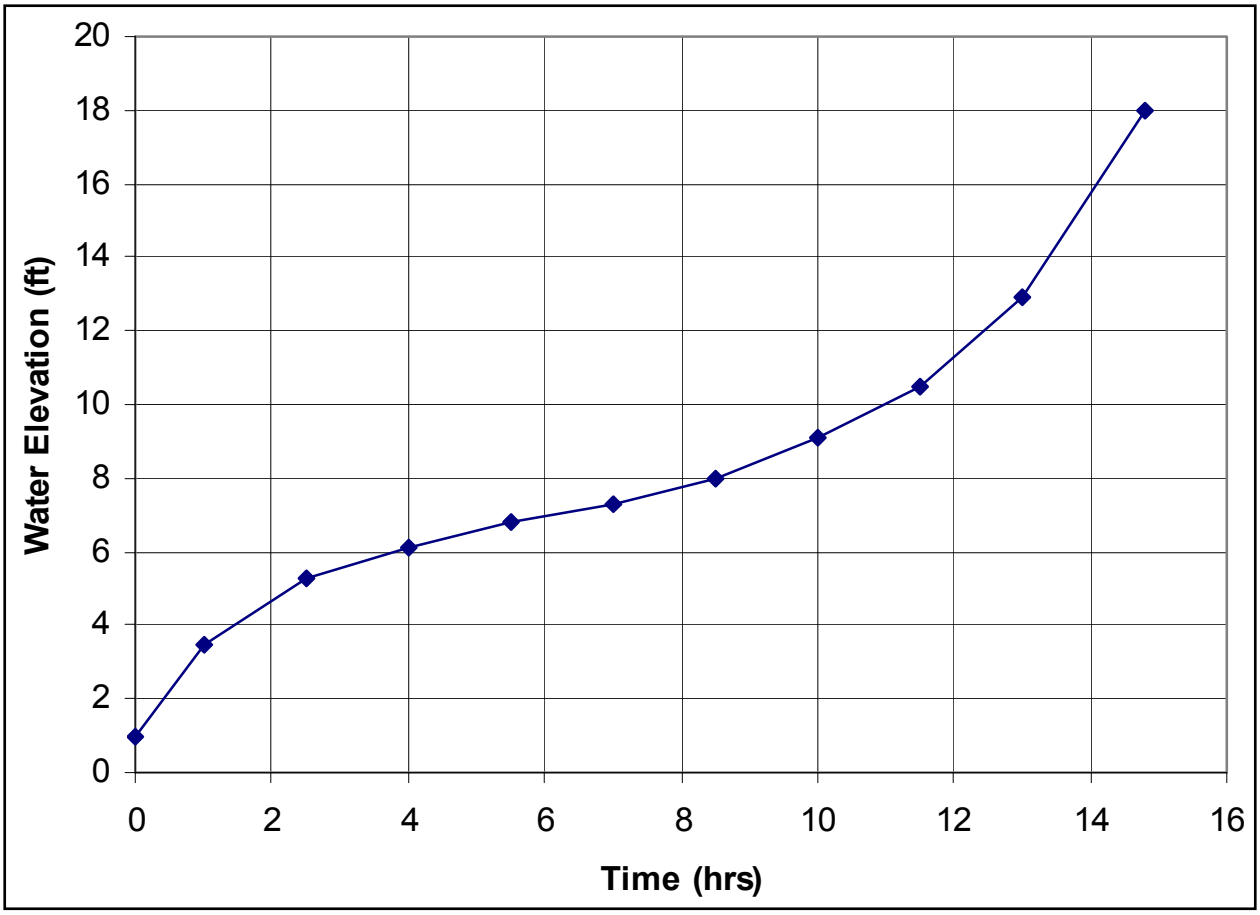

Figure V-17-53. Smoothed Hydrograph starting 8/28/2005 at 21:30

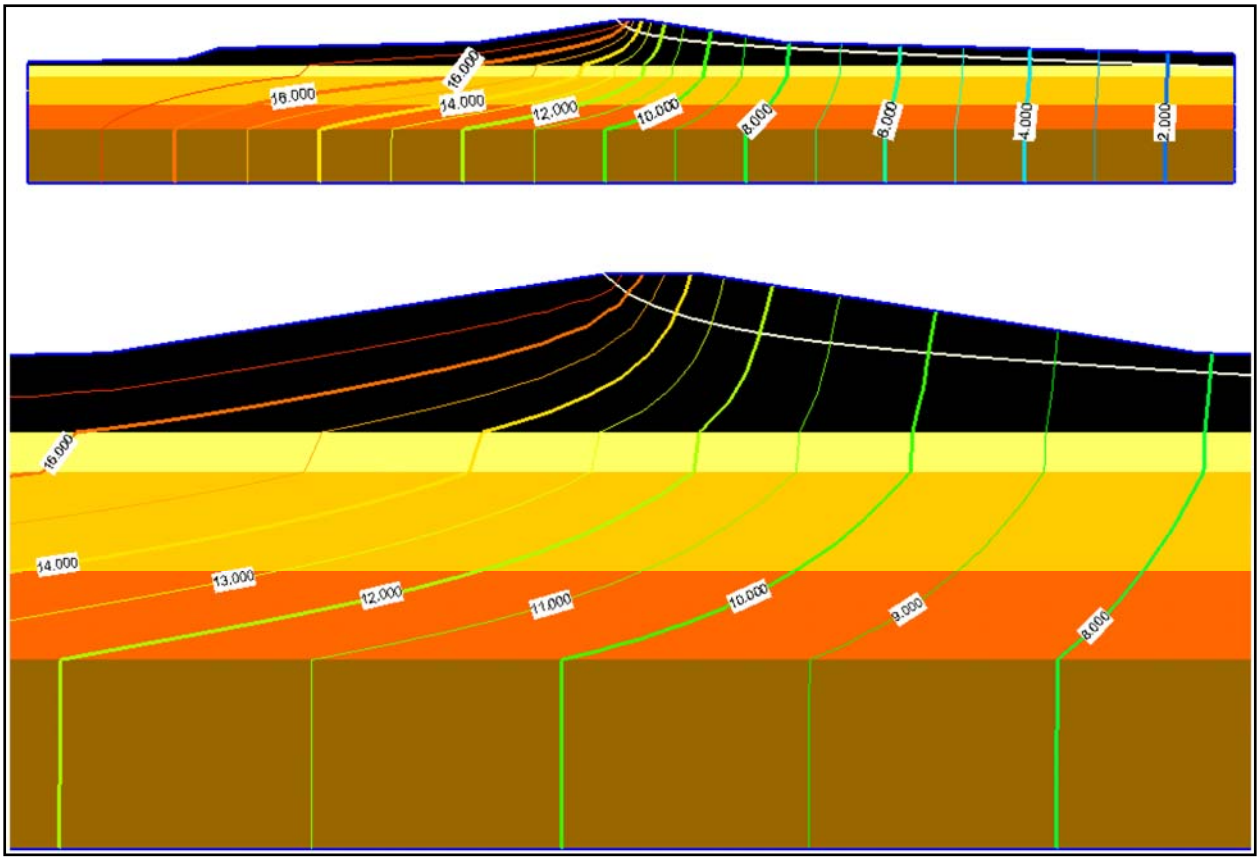

Figure V-17-54. Seep2D Contours of Total Head for Steady-State Solution Canal Elevation = 18 ft, Head at Protected Side = 1 ft

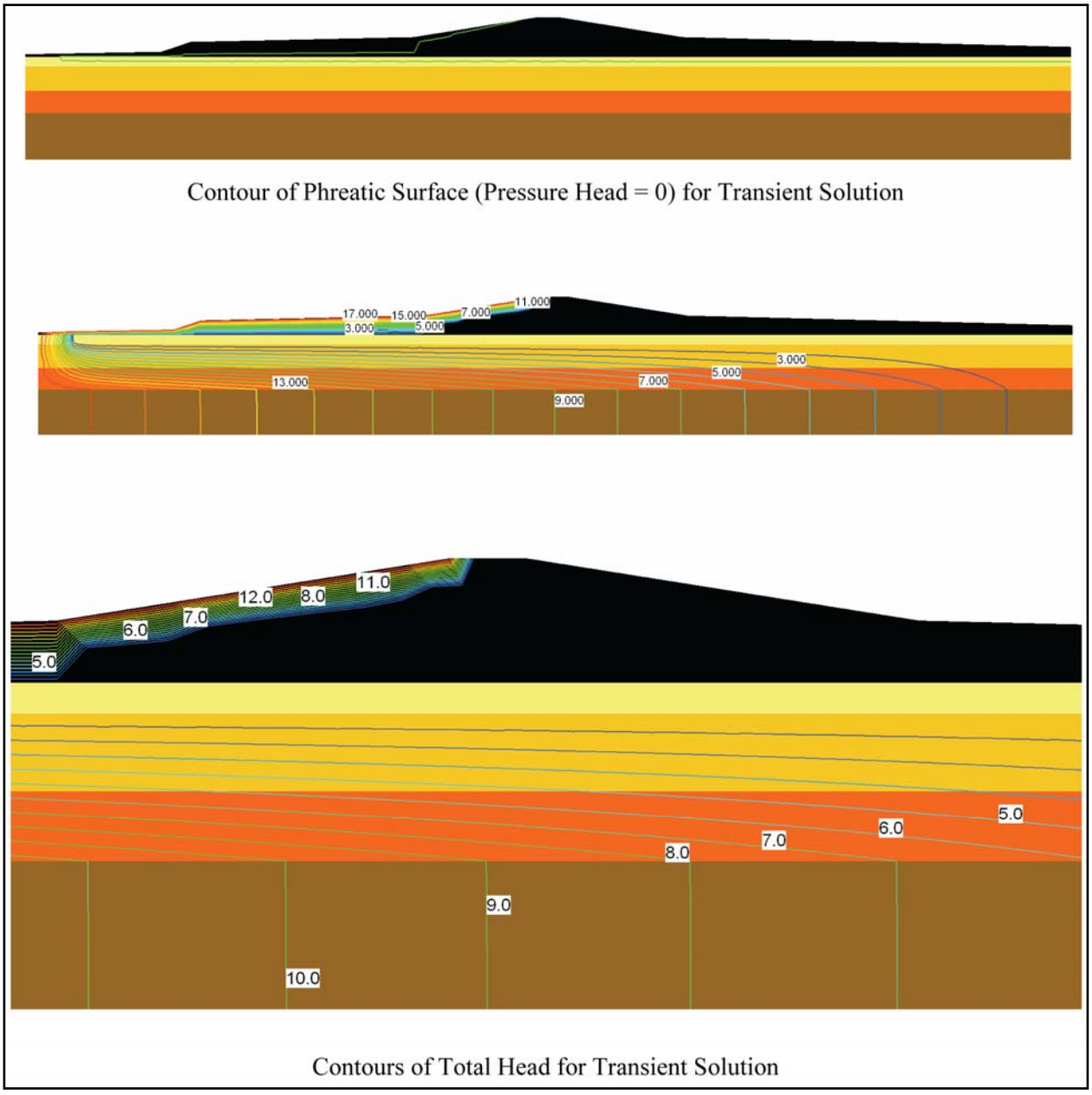

Figure V-17-55. Results of Transient Analysis for a clay levee with Canal Elevation = 18 ft, Head at Protected Side = 1 ft

Material Number	Name	K (ft/hr)
1	Levee	1.77
2	ML #1	0.00118
3	CH #1	0.000118
4	CH #2	0.000118
5	ML # 2	0.118

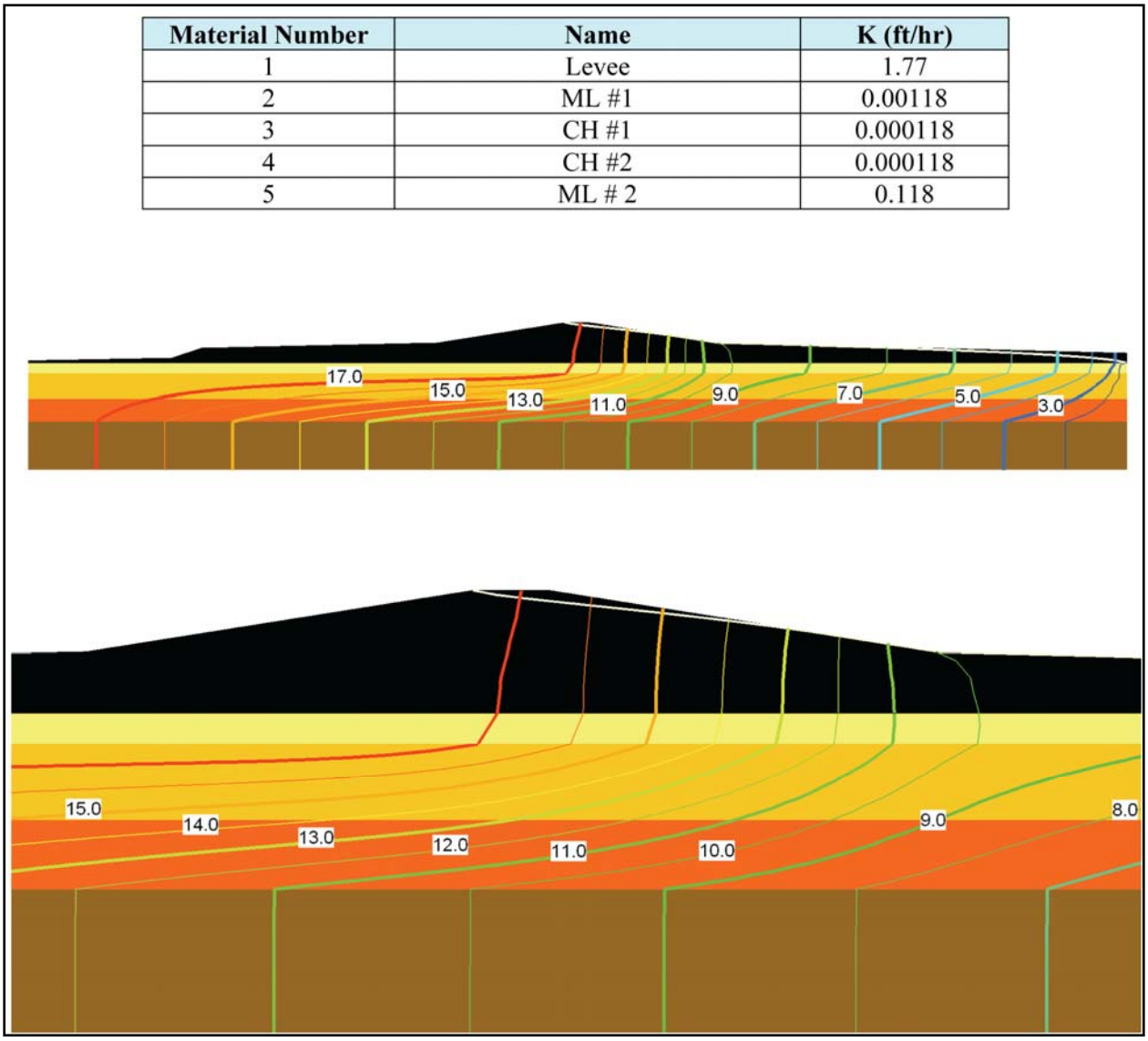

Figure V-17-56. Contours of Total Head for Steady-State Solution, Canal Elevation = 18 ft, Head at Protected Side = 1 ft

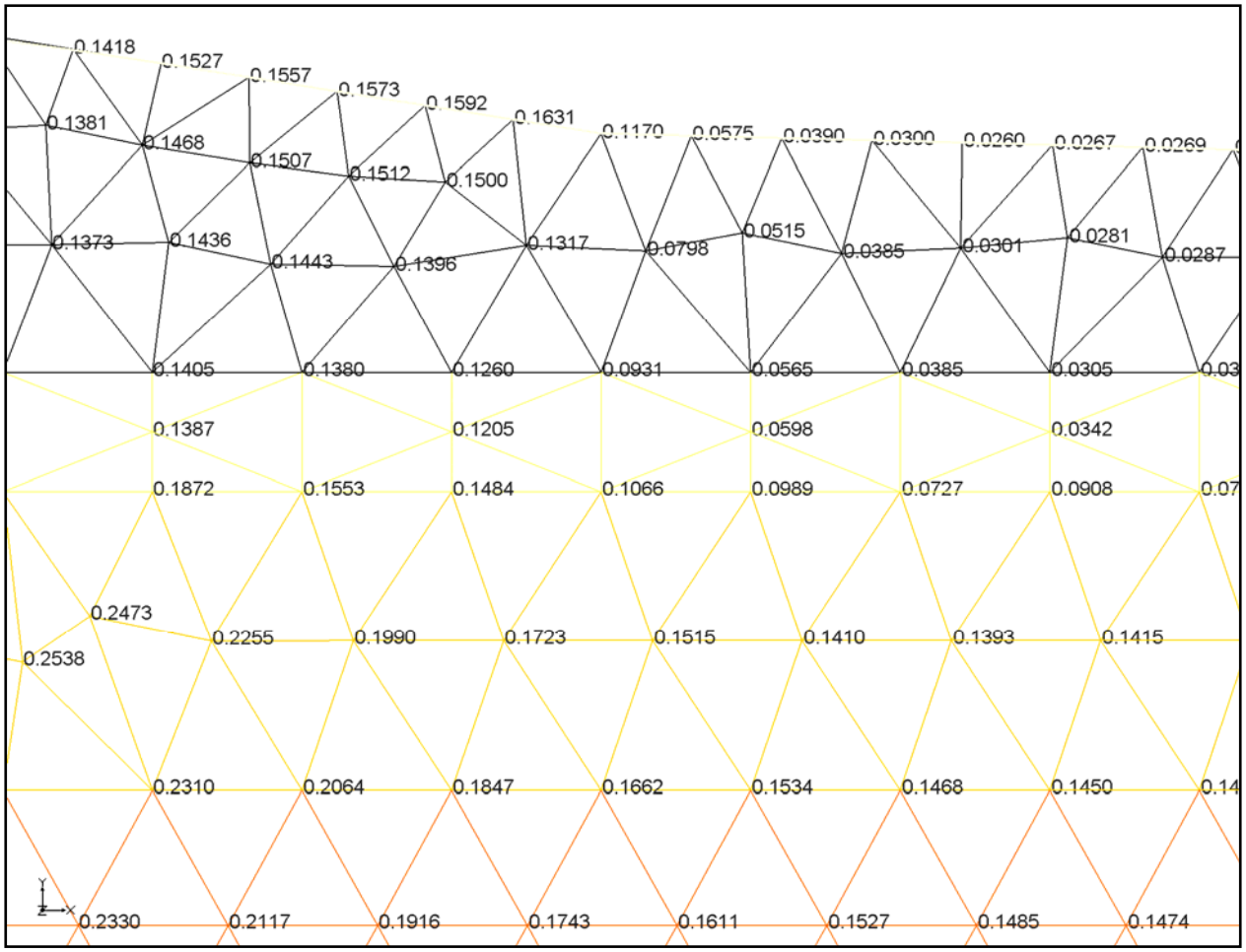

Figure V-17-57. Values of Gradient at Toe for Steady-State Solution, Canal Elevation = 18 ft, Head at Protected Side = 1 ft

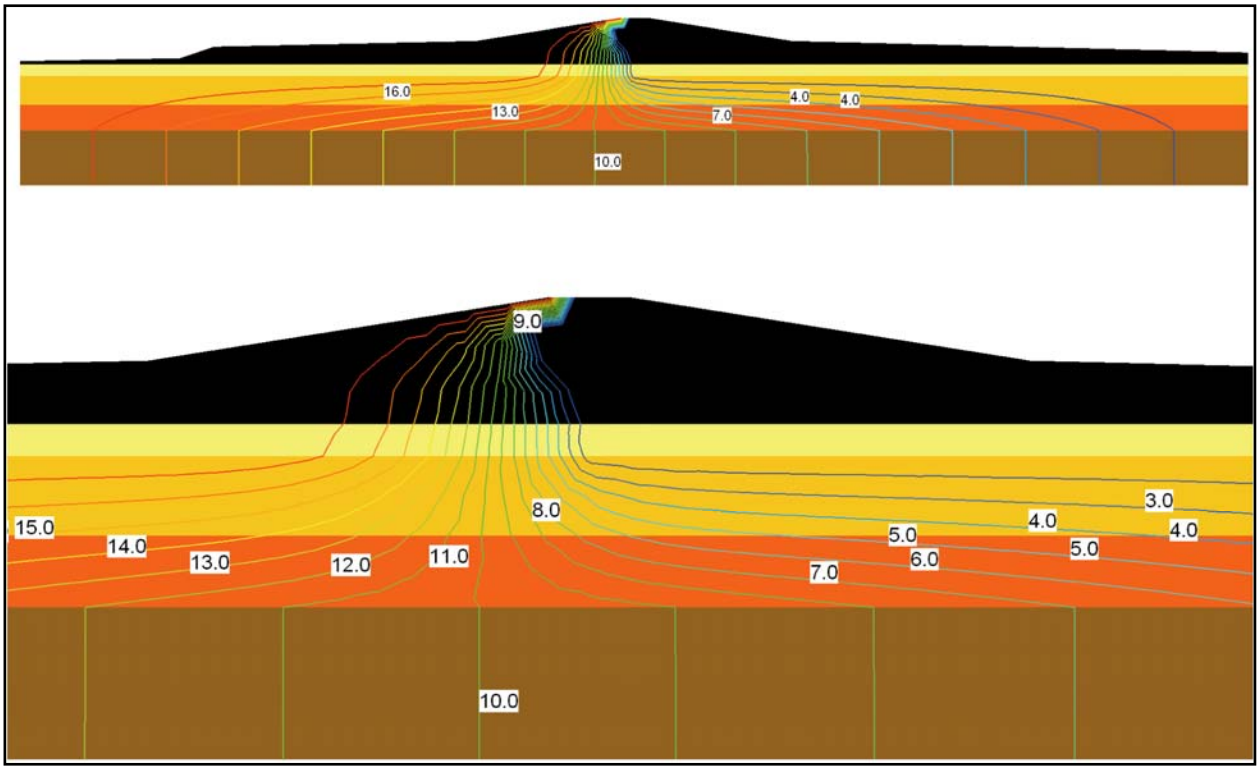

Figure V-17-58. Contours of Total Head for Transient Solution, Canal Elevation = 18 ft, Head at Protected Side = 1 ft

Appendix 18
New Orleans East and St. Bernard Parish Levee Performance Report

Overview

This document briefly discusses the physical characteristics of the New Orleans East (NOE) levees in Orleans Parish and the Chalmette (and Chalmette Extension) levees along the Mississippi River Gulf Outlet (MRGO) in St. Bernard Parish. The purpose of this report is to examine the differences between sections of levee that performed well and those sections that were severely eroded or destroyed by Hurricane Katrina. The main sources of data for this study were the original design documents and post-hurricane investigations conducted mostly by the New Orleans District Task Force Guardian (TFG) and members of the Interagency Performance Evaluation Team (IPET).

The Design Memorandum (DM) for each New Orleans hurricane protection project describes the local and site geology in addition to the design of the levees and associated floodwalls. Typical pre-construction geotechnical data are provided in the DM such as geologic cross sections of the levee design with associated borings, soil property tests and stability analyses. Post-construction changes occurred after the projects were initially constructed. For example, sections of the NOE Back Levee (BL) and Chalmette Levee and Extension levees were built by hydraulically filling soil in multiple lifts over many years. At the time of the 1971 design for the NOE BL levee enlargement the height of the existing levees averaged 10 ft above mean sea level. The 1971 proposed design elevations were 17 ft (NGVD). The levees were surveyed in 2001 and again in 2005 (after Katrina). The pre-storm elevations ranged from 16 to 20 ft (NAVD 88, 2004.65) and averaged 17 ft. Light detection and ranging (LIDAR) aerial surveys were adjusted by IPET personnel in 2006 and a digital elevation map (DEM) was created for the IPET. These DEM elevations were useful for comparing storm surge and wave heights to levee heights. Where these data were not available the levee heights were estimated from New Orleans District maps.

The TFG gathered an enormous amount of post-storm data including ground and aerial photos, damage survey reports, and post-Lidar surveys. These data were useful to delineate and describe the areas of good and poor performance during Katrina. Pre-Katrina LIDAR levee elevation profiles were compared with post-storm profiles to visually express this damage

phenomenon, using the Hillshading tool within a Geographical Information System (GIS). The storm surge and wave height were also compared to levee elevations and are briefly discussed. Surge and wave heights were estimated by the IPET Storm Team using numerical models ADCIRC and STWAVE respectively. The modeled values were compared to those detected by the IPET conducted High Water Mark Survey, which was assumed to be evidence of the actual maximum surge.

The Engineering Research and Development Center's Geotechnical and Structures Laboratory (ERDC\GSL) performed on-site erodibility tests on selected NOE and St. Bernard Parish levees that survived major storm damage. The erosion tests were performed per the ASTM D 5852-00 method (Standard Test Method for Erodibility Determination of Soil in the Field or in the Laboratory by the Jet Index Method) using an apparatus borrowed from the U.S. Department of Agriculture (USDA).

New Orleans East

Figure 1 is an aerial photograph illustrating the extent of the NOE basin or levee district. The major levee and floodwall segments are labeled in Figure 2 and enclose the entire NOE basin. These major segments are referred to generally as the IHNC, Citrus Lakefront, NOE Lakefront, New Orleans East (South Point to GIWW), New Orleans East Back Levee (NOE BL) and Citrus Back Levee. The NOE BL makes up the southeast portion of the levee system where most of the scour damage occurred, and is bounded to the east by the South Point Levee and to the west by the Citrus Back Levee.

Figure 1. General map of the New Orleans East (NOE) basin. Major levee segments are Lakefront Levees, NOE East Levee (South Point to GIWW), NOE Back Levee, Citrus Back Levee and IHNC levees.

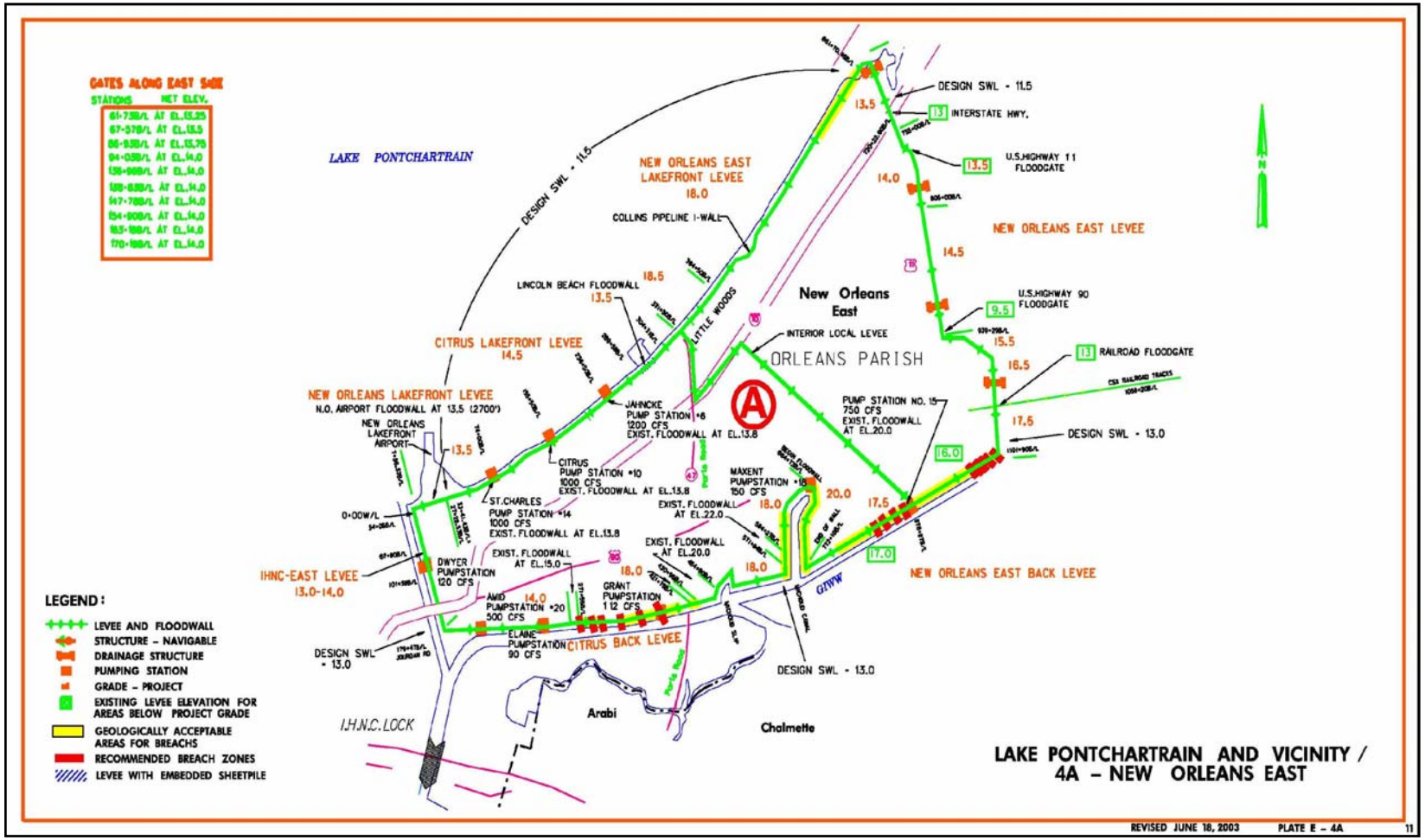

Figure 2. New Orleans East Levee system, bounded by the South Point to GIWW levee on the east and NOE Back and Citrus Back Levees to the south (from TFG)

Figure 2 also illustrates individual hurricane protection components of each major levee segment. The Back Levee protection components include three floodwalls, one pump station and a series of 18 gates along the Michoud Canal floodwall. The level of protection varies from 20.0 to 16.0 ft throughout the NOE BL. The static water level design was 13 ft. Levee segment elevations below design grade (pre-Katrina) are shown inside rectangles and occurred mostly along the NOE BL and the South Point Levee.

Figure 3 shows the breached levee segments (red lines) due to Katrina. Figure 4 is a map showing post-Katrina TFG repair contracts let for NOE Basin. This map shows the length of levee damage and the general type of damage. The most continuous damage is noted along the eastern portion of the NOE BL. Table 1 is a brief listing of restoration contract descriptions.

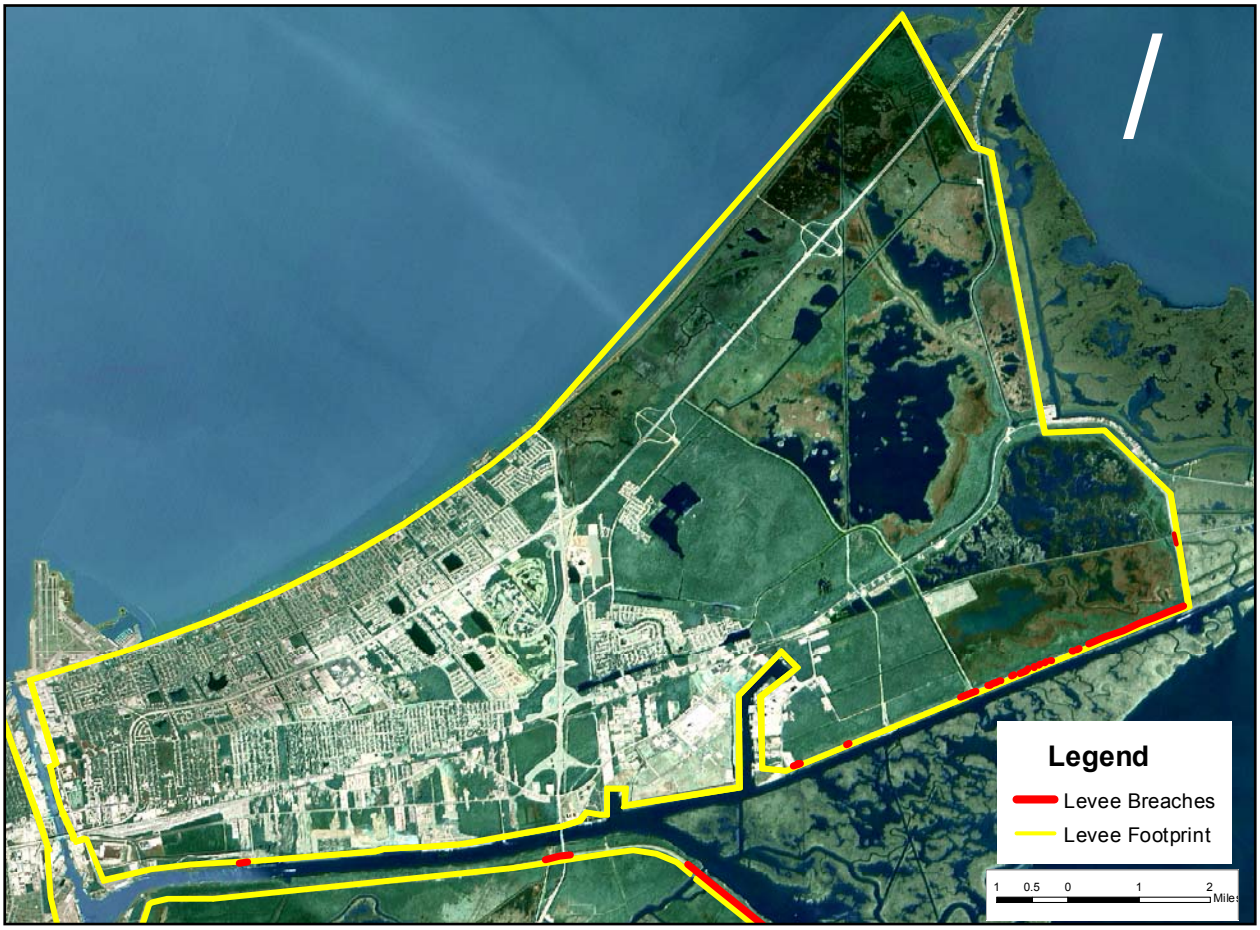

Figure 3. NOE basin post-Katrina breaches

Figure 4. TFG Damage Survey Report/ Project Information Report –highlighting areas of damage in red (diagram from TFG)

Table 1
General Description of Damage Within the NOE Basin

Repair Contract	Description
Project: NOE01 – East Back Levee Repair from Michoud Canal to CSX RR	Project NOE01 consists of rebuilding approximately 4.3 miles of the existing levee back up to its constructed grade with 680,000 CY of earthen material, then seeding and fertilizing. The entire reach of levee was brought up to an interim level of protection of elevation +10 by November 15, 2005
Project: NOE02 – Floodwall Repair at Pump Station 15	Project NOE02 includes removing the damaged steel sheet pile wall, installing a new concrete T-wall, filling in scour holes and bringing the damaged levee back up to pre-hurricane Katrina elevation.
Project: NOE03 – Floodwall Repair near Air Products Hydrogen Plant	Project NOE03 includes removing the damaged concrete I-wall and steel sheet pile wall, filling in scour holes, installing a new concrete I-Wall, and raising the damaged levee to pre-hurricane Katrina elevation and then seeding and fertilizing. The damaged reach was first brought up to an interim level of protection of elevation +10 by November 15, 2005 before final repairs are made.
Project: NOE04 – Citrus Back Levee Floodwall Repair	Project NOE04 includes removing the damaged concrete I-wall sections, filling in the scour holes, regrading the damaged levee, constructing new concrete wall, and putting in an earthen stability berm on the landside of the wall. The repaired levee section and stability berm will be seeded and fertilized. The damaged reach was first brought up to an interim level of protection of elevation +10 by December 1, 2005 before final repairs are made.
Project: NOE05 – CSX Railroad Floodgate Repair	Project NOE05 includes the removal of the existing concrete wall and railroad closure gate, filling the scoured areas, constructing a new closure gate and new concrete T-walls and I-walls, placement of rip rap, concrete slope paving and concrete roadway.
Project: NOE06 –Lakefront Airport Floodwall Scour Repairs	Project NOE06 consists of filling in and paving over the scour holes next to the concrete wall. It also includes filling in the scour hole and paving the damaged road section with concrete at the interface of the Floodgate L-15 concrete wall and levee.
Project: NOE07 – Lake Pontchartrain Lakefront Levee Scour Repair	Project NOE07 includes intermittent scour repair along approximately 19 miles of earthen levee along the Lake Pontchartrain Lakefront and the eastern boundary of the Bayou Savage National Wildlife Preserve. The work consists of filling in the scour areas with semi-compacted fill, reshaping where needed, and seeding and fertilizing.
Project: NOE08 – Drainage and Floodgate Structures Scour Repairs From Southpoint to the GIWW	Project NOE08 includes filling in the scour holes and capping with gabion structures to prevent future erosion. The gabion structures are wire baskets filled with stone interlocked to form a surface erosion barrier
Project: NOE09 – Floodwall Scour Repairs from Michoud Slip to Michoud Canal	Project NOE09 includes filling in the scour holes next to the wall with embankment material, installing bedding material, and concrete slope paving above the scour to prevent future erosion. Also includes adding an earthen stability berm on both flood and protected sides of the wall. The project also consists of intermittent repairs to damaged concrete and various joints and gates in the walls.

2001 and 2001 LIDAR Surveys

Figures 5 through 7 illustrate a digital graphic technique called Hillshading that expresses LIDAR survey elevations in a quasi-three-dimensional (3D) aspect. The figures illustrate the 3D structure of the levee footprint, from the protected toe, up the slope to the crown and back down the floodside of the levee to its unprotected toe. Figure 5 shows the intact (pre-Katrina) condition of a selected levee section at the intersection of the NOE BL and South Point levees. The light green line along the South Point Levee is the levee crown which is continuous in the pre-storm condition. The dark blue line is the levee crown along the NOE BL and is slightly higher than the South Point levee. The elevations are contoured with respect to a 2001 datum used by a survey contractor (Chance, 2001) and are not corrected for later subsidence. The 2001 survey had a 1.0-ft resolution. Figure 6 is the post-storm survey (2005) which had a 2.0-ft resolution and was referenced to a different control point. These data were not adjusted or corrected, but reflect the raw survey data as in Figure 5.

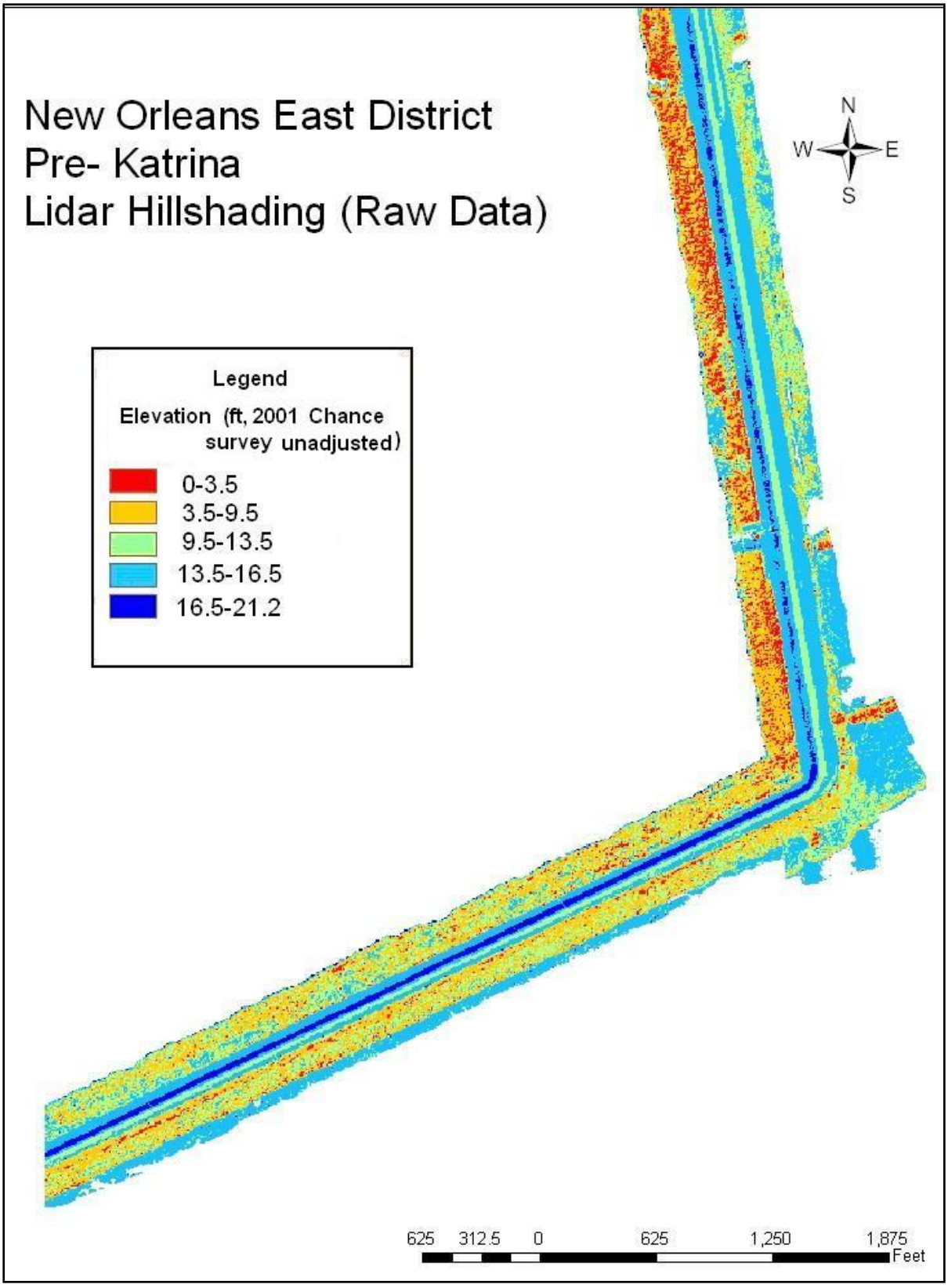

Figure 5. Hillshading from Pre-Katrina LIDAR, at intersection of the South Point-GIWW and NOE Back Levee (southeast corner of the New Orleans East basin)

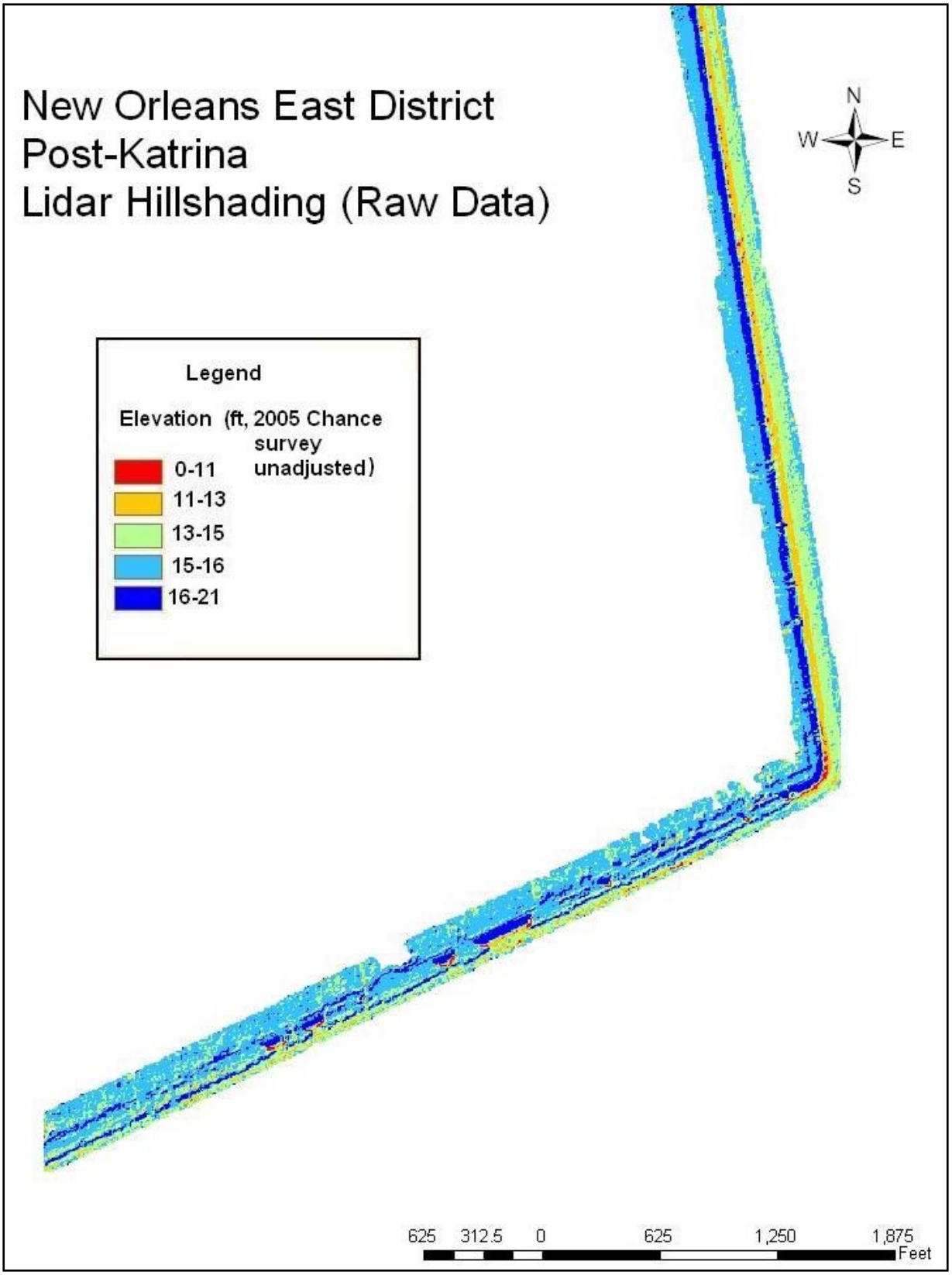

Figure 6. Hillshading from Post-Katrina LIDAR at southeast corner of New Orleans East basin

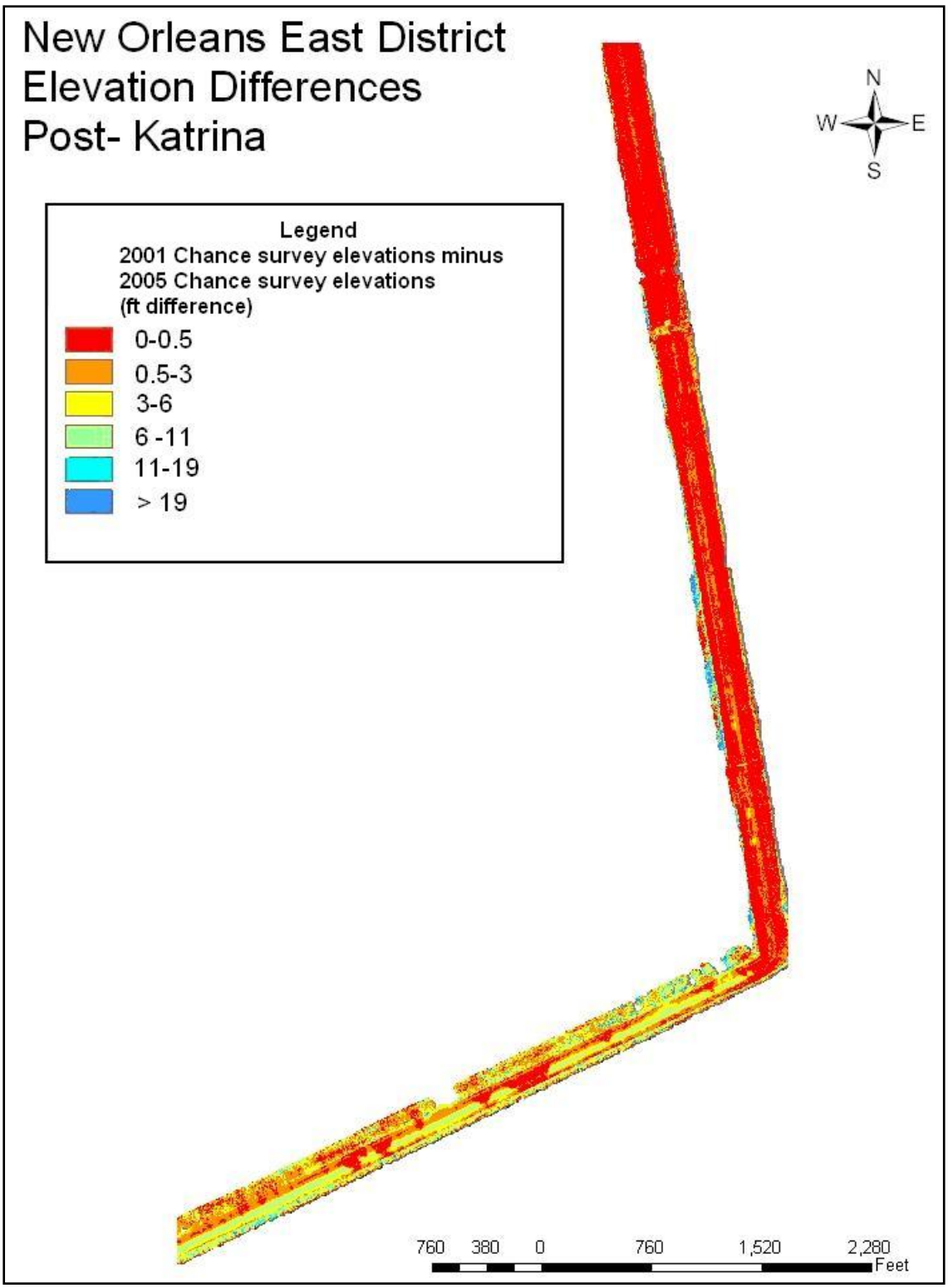

Figure 7. Hillshading from Pre-Katrina LIDAR minus Post-Katrina LIDAR at the southeast corner of New Orleans East basin. Figure created from raw LIDAR data, thus noise and outliers not removed from dataset. Red areas indicate less than 0.5 ft difference between survey elevations, but is actually expresses the difference in dataset control points. Thus, the red areas probably indicate zero changes in elevations.

The post survey visually illustrates the dramatic loss of levee material from the NOE BL crown, presumably from overtopping. Most of the portion east of pump station 15 along the NOE BL was demolished. However, the South Point levee still has its basic levee shape. Figure 7 shows the mathematical difference of the two previous figures (pre-storm minus post-storm surfaces) and illustrates scour depth. The area of most severe scour occurs along the eastern portion of the NOE BL. Figure 7 implies that scour has occurred along the South Point levee (red contour 0.-0.5 ft) but this is probably an artifact of the surveys having different control points. Actually, South Point levee had very minor scour.

The LIDAR data along the levee crown can also be expressed as an elevation profile. Figure 8 is a plan view of the LIDAR stationing used in this investigation. Figures 9 through 12 show selected post storm LIDAR survey data along the NOE BL. These data allow comparison of scour depths to construction methods and associated soil types, in addition to wave height and surge elevation.

Figure 8. LIDAR stationing used in this report, starting at Lakefront levee and ending at the Michoud Slip along the GIWW. ERDC erosion test location under the I-510 Bridge is shown.

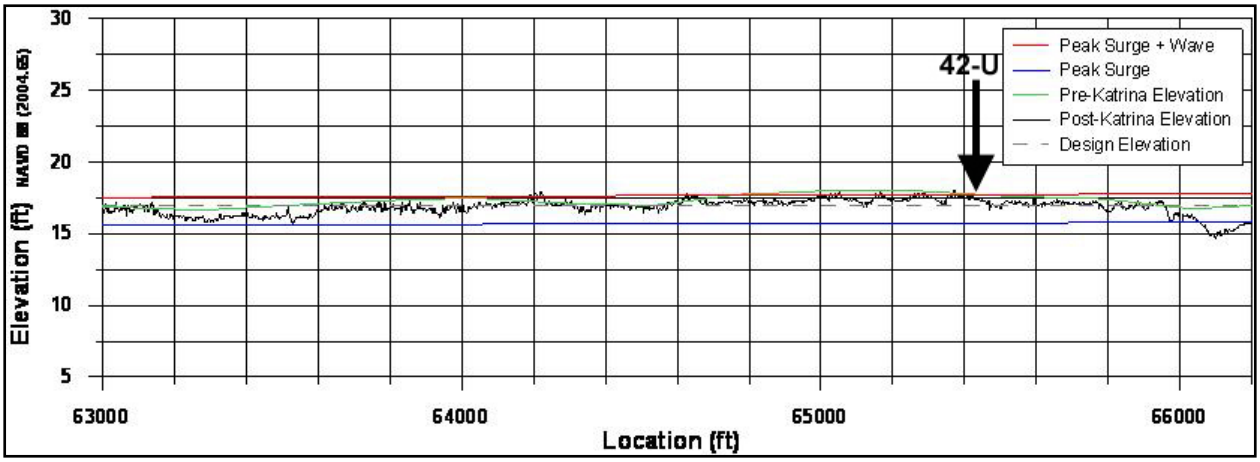

Figure 9. A typical post-Katrina LIDAR profile along the NOE Back Levee west of Pump Station 15. Soil boring 42-U is annotated at approximate B/L Sta 832+00.

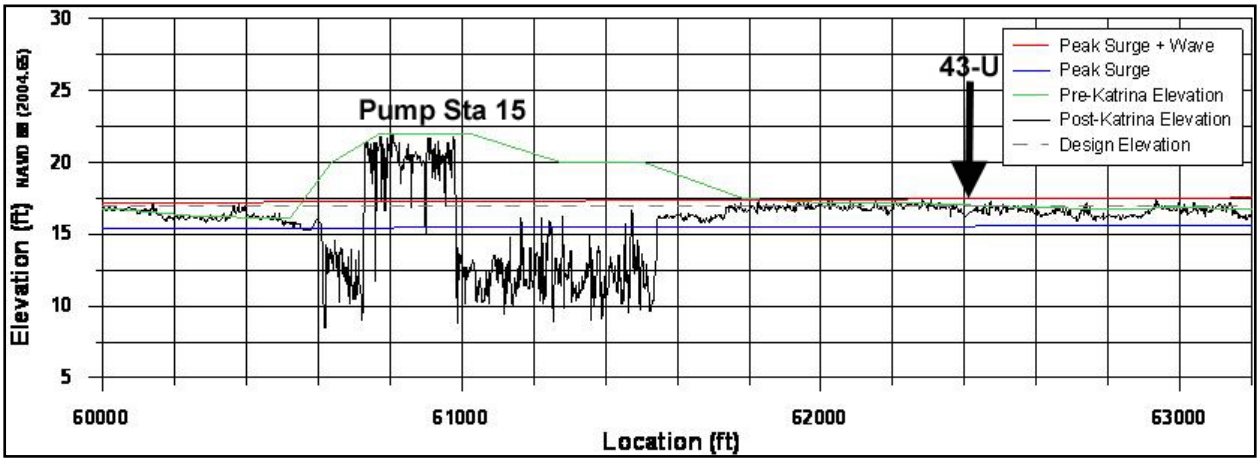

Figure 10. Another typical post-Katrina LIDAR profile along the NOE Back Levee west of Pump Station 15. Soil boring 43-U is annotated at approximate B/L Sta 872+00.

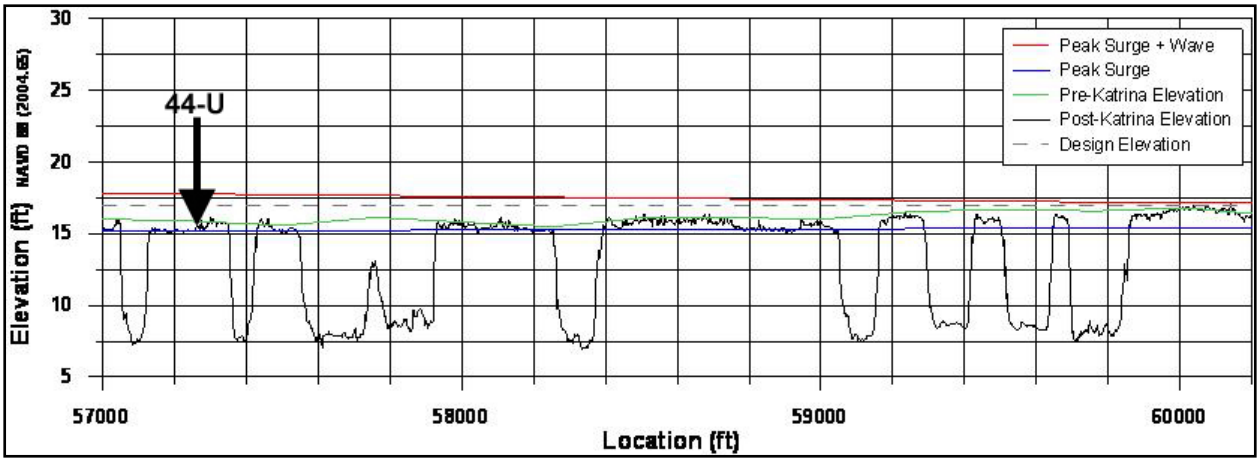

Figure 11. A typical post-Katrina LIDAR profile along the NOE Back Levee east of Pump Station 15. Soil boring 44-U is annotated at approximate B/L Sta 913+00. Note the numerous breach locations and significant scouring along this reach.

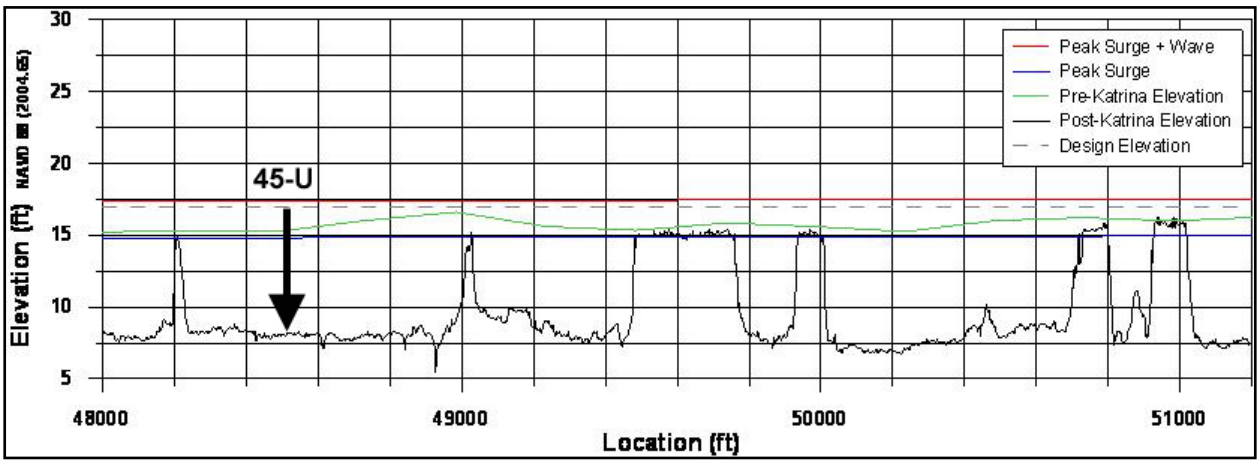

Figure 12. Another typical post-Katrina LIDAR profile along the NOE Back Levee east of Pump Station 15. Soil boring 45-U is annotated at approximate B/L Sta 1003+00 near the intersection of the South Point to GIWW levee (NOE). Note the numerous breach locations and significant scouring along this reach.

Scour depths vary tremendously along the selected profiles starting at the Michoud Canal, moving east along the GIWW and ending at the South Point Levee. The average pre-storm elevation of the NOE BL was 16.0 ft (NVGD88, 2004.65) to the east of the pump station and 17.0 ft (NVGD88, 2004.65) to the west of the pump station (see Figure 2). The average scour to the east of the pump station was 8 ft with approximately 75% of the levee scoured to this depth. The maximum scour in this segment was approximately 15 ft. In contrast the western portion of the NOE BL earthen levee performed well. Approximately 99 percent of the western NOE BL was scoured just 0.5 to 2.0 ft. Table 2 lists the stationing and elevations of the structural components in the NOE BL.

Table 2
Elevation and Extent of Structural Components in NOE BL

NOE BL station		Structure	Approximate Elevation
Start	End		
772+00	874+42	Levee	17.5
874+42	875+62	I-Wall	20
875+62	878+12	T-Wall	23
878+12	879+32	I-Wall	20
879+32	1006+59.2	Levee	17.5

The variable levee performance in the NOE basin was most likely because of differences in levee construction (hydraulic fill versus truck hauled), levee soil types (sandy versus clayey), differences in surge and wave heights during the storm (hydraulic loading), or other contributing factors. Levee construction, soil types, and hydraulic loading issues for selected portions of NOE levees are hereinafter discussed.

Construction Methods, Soil Types and Hydraulic Forces

Construction methods of the levees were investigated and a map of hauled versus hydraulically filled levees is shown as Figure 13. This map was compared to the levee breach map (Figure 3) and it was noted that levees constructed of hydraulic fill coincided with breached levees. In general, levees built of hydraulic fill performed poorly, while levees built primarily of hauled and semi-compacted fill generally suffered minor or moderate scour. Levee soil types shown on historic soil boring logs were analyzed to corroborate such a general conclusion.

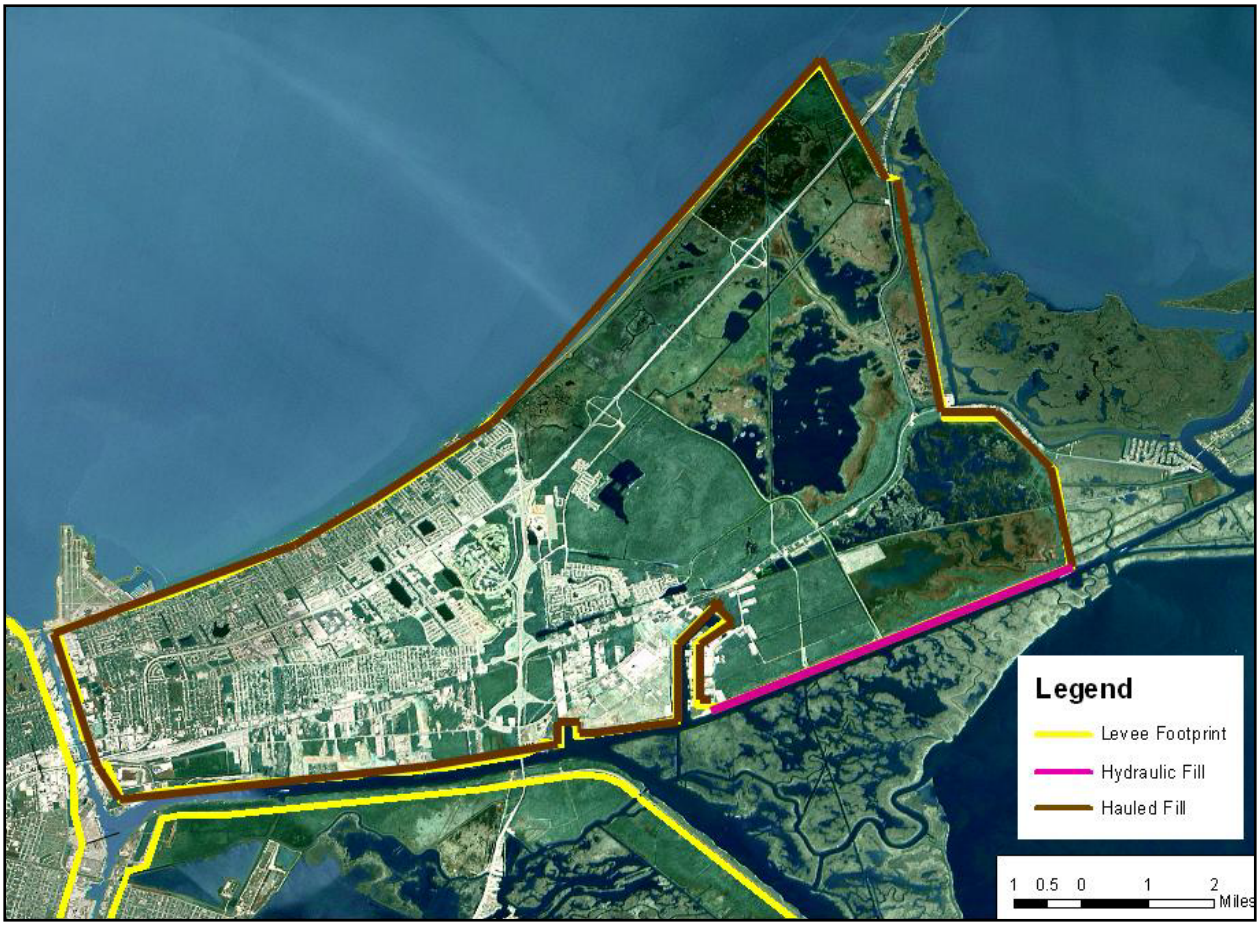

Figure 13. NOE Levee construction materials (from USACE DM NOE Back Levee, Citrus Back Levee, South Point to GIWW levee, Lakefront Levees, IHNC levees after 1969)

Four soil borings located on Figure 14 (42-U, 43-U, 44-U, 45-U - 2001) were drilled in 2001 after the final lift was constructed to approximate elevation 19 ft above msl. The borings show that the levee materials at the crown surface (the final soil construction lift) were silts, sands and lean clays. Borings 42-U and 43-U (Figure 15) were west of the pump station 15 (previous figures 9 and 10), and borings 44-U and 45-U (Figure 16) were east of the pump station 15 (previous figures 11 and 12). Figure 17 shows descriptions of the soil types. Borings 44-U and 45-U had more fat clay layers in the top 10 ft than the other two borings (42-U and 43-U), but the presence of fat clay layers was not necessarily indicative of higher erosion resistance since the levees east of pump station 15 typically had higher erosion, scour, and breaching frequency than the west side.

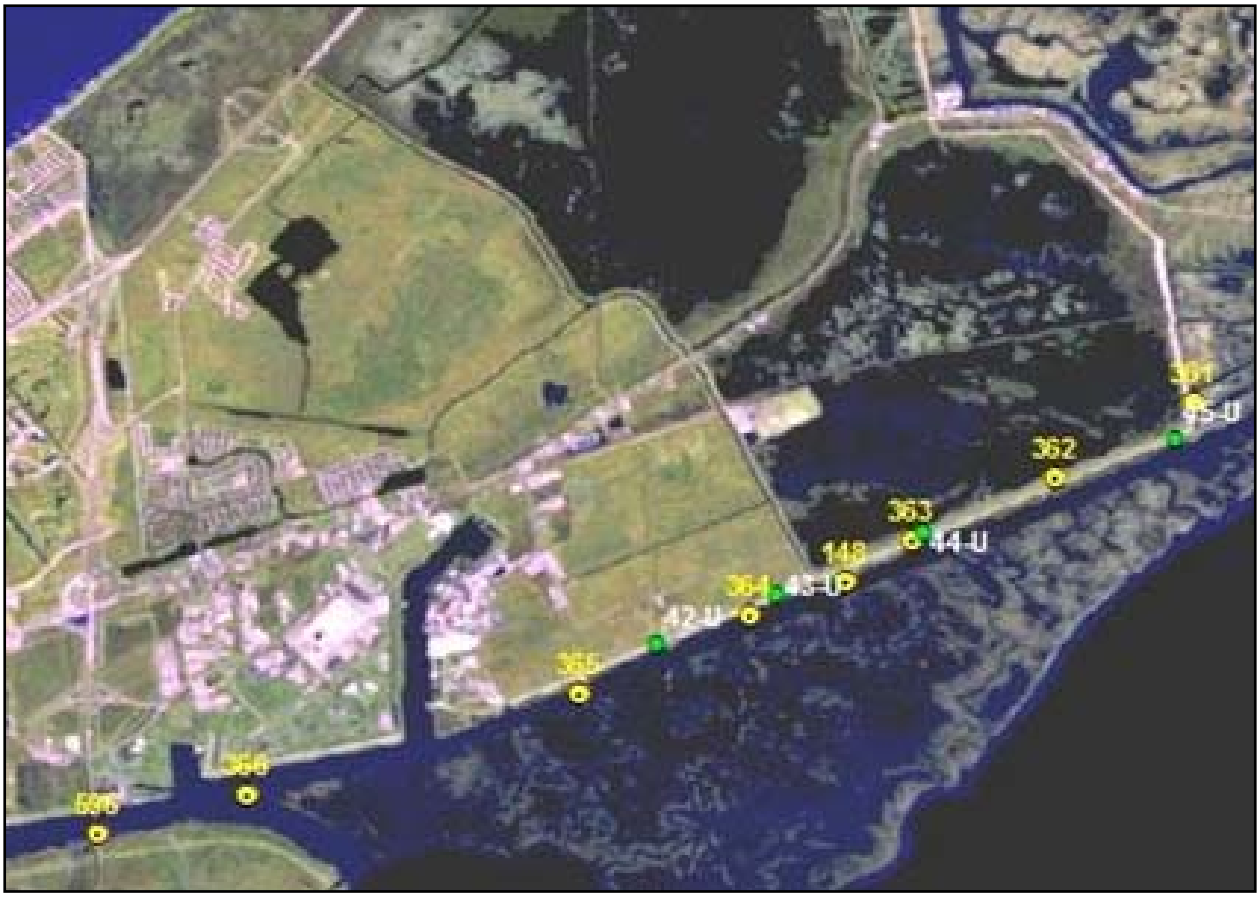

Figure 14. Location of undisturbed borings (42-U, 43-U, 44-U, 45-U) drilled in 2001 along the NOE Back Levee

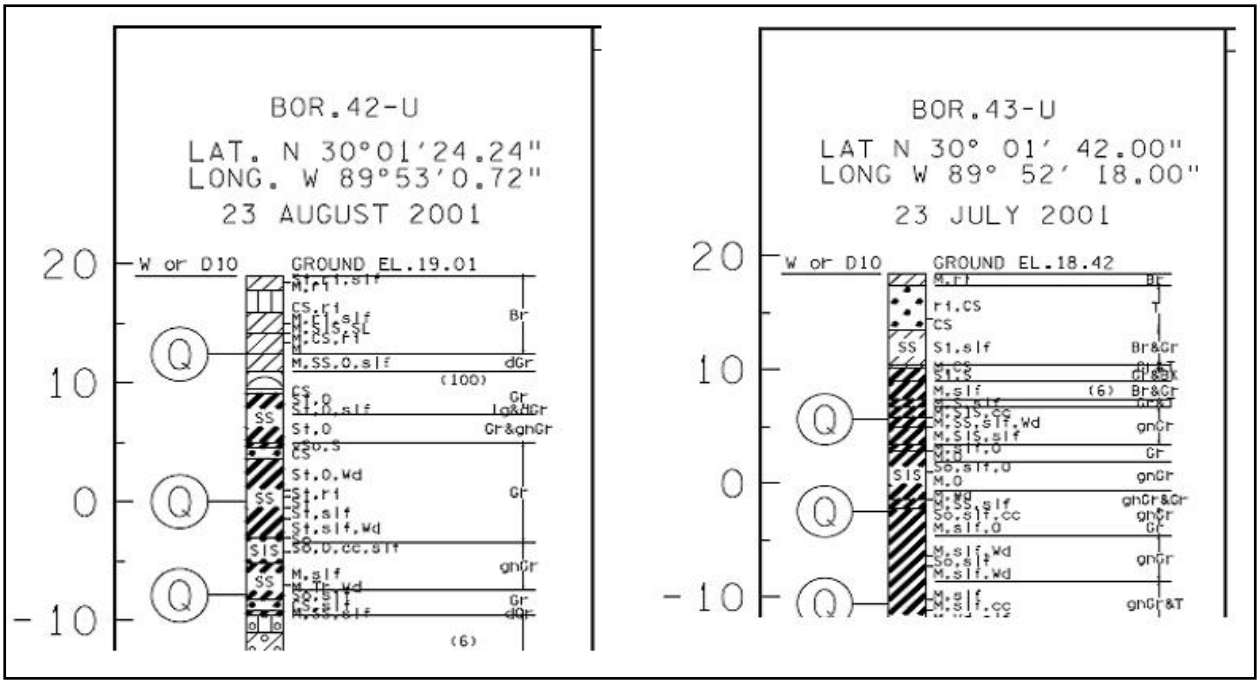

Figure 15. NOE Back Levee soil borings 42-U and 43-U taken west of Pump Station 15

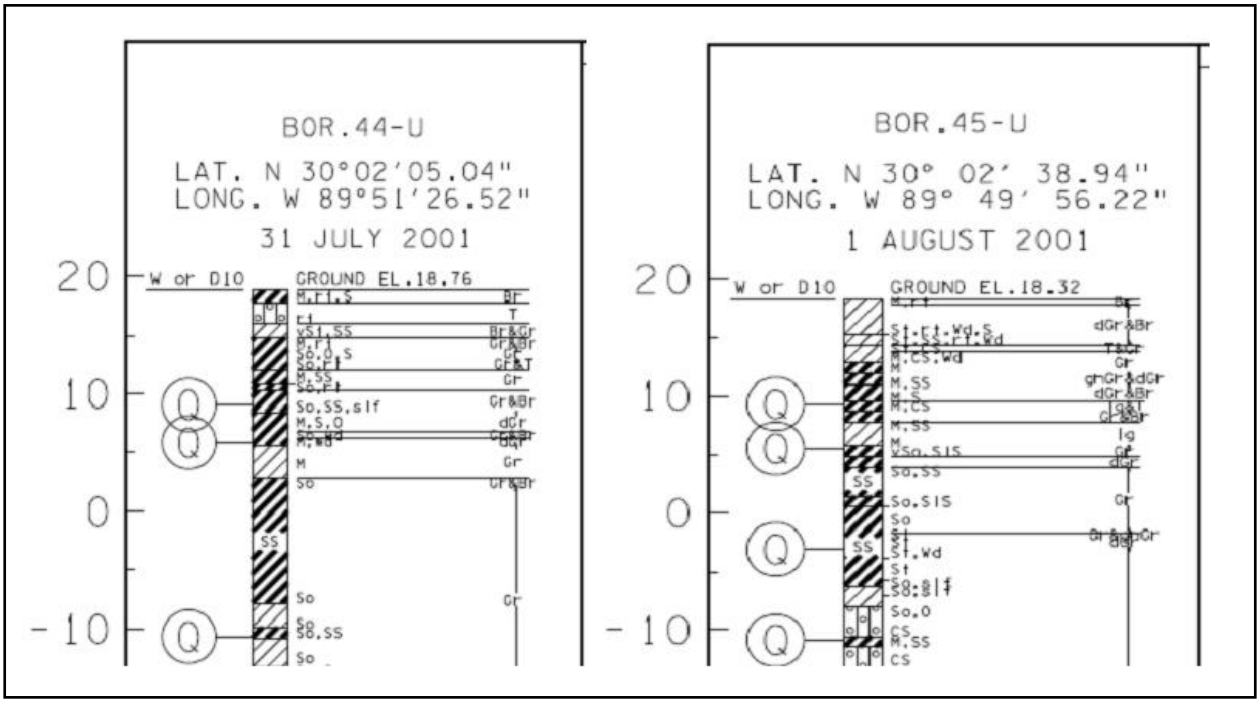

Figure 16. NOE Back Levee soil borings 43-U and 45-U taken east of Pump Station 15

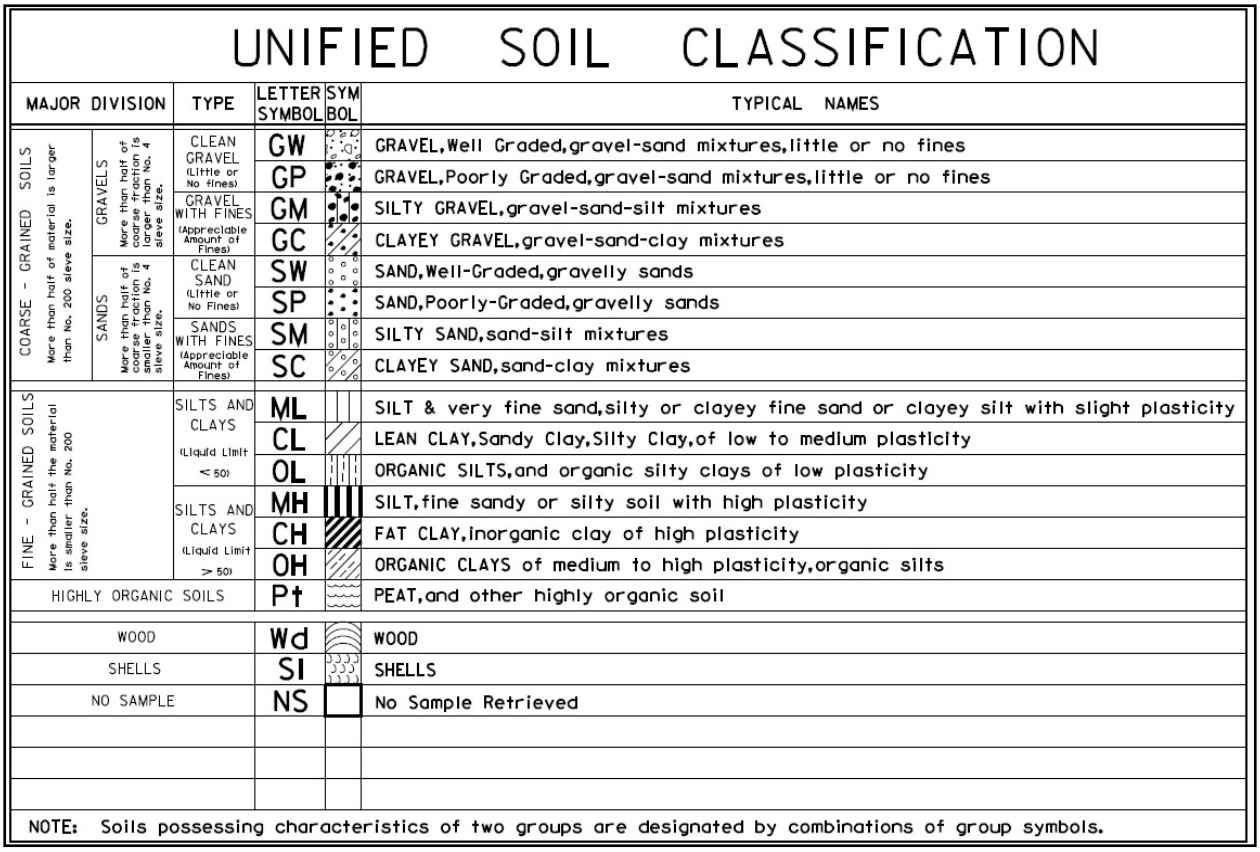

Figure 17. Description of boring log symbols

Hydraulic analyses (surge and wave estimation) were conducted by IPET Storm Team for the purpose of "hindcasting" the storm surge and wave heights. Surge analyses were conducted using the numerical model "ADCIRC". Wave heights were estimated using the numerical model "STWAVE". Figure 18 shows numerical model data points where surge and wave estimates were calculated for the NOE Basin Levee system. Herein, data points were selected (Figure 19) along the GIWW and along the South Point Levee system for comparison of storm water elevation to levee elevations and the likely correlation to levee performance.

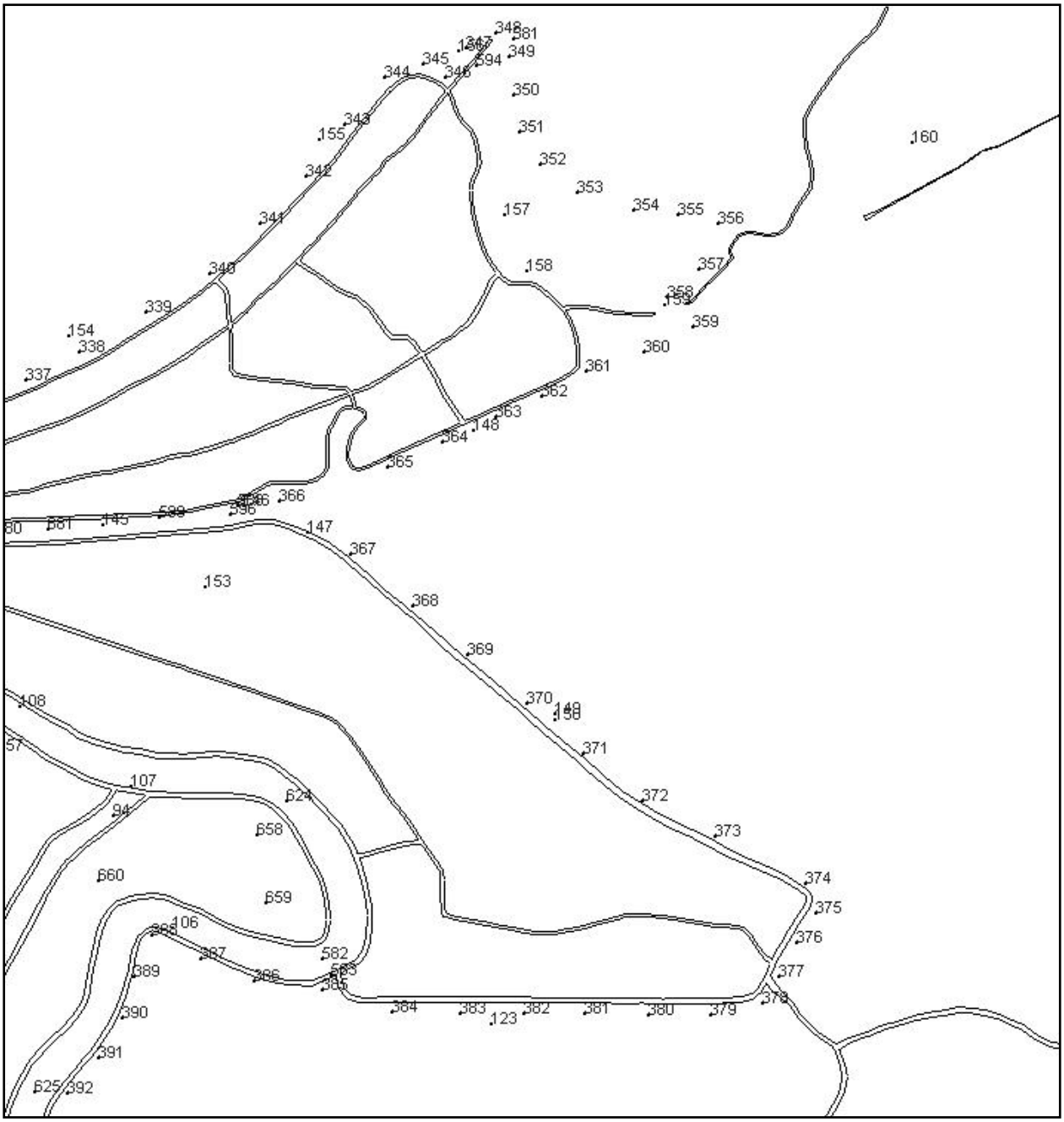

Figure 18. ERDC hydraulic model data points for the NOE Levee System

Figure 19. Selected hydraulic data points for surge analyis (350, 351 and 349 are shown on Figure 18)

Table 3 shows the model-calculated surge maximum elevation and the wave heights associated with the maximum surge, in addition to the measured high-water marks surveyed near these points, and the surveyed levee elevations. The high water mark data points were sparse and are described in another IPET report. The calculated maximum surge, "interpreted" surge after consideration of the high water mark survey, the interpreted surge plus the wave height, and levee elevations are plotted in two figures (Figure 20 and 21). Figure 20 is a plot of the data along the north bank of the GIWW between Paris road and the intersection of the GIWW and the South Point levee. Figure 21 is a similar plot expressing data along the South Point levee, (i.e., the eastern boundary of the NOE basin). Note that the interpreted surge data mimic the trend of the calculated surge data.

Table 3
Calculation of interpreted surge from ADCIRC numerical model and High Water Mark survey for selected model data points

NOE Back Levees, table of surge and wave data								
ADCIC Model Point	**Latitude**	**Longitude**	**ADCIRC Model max surge (ft NAVD 88, 2004.65)**	**STWAVE Model wave height (ft) at max water level**	**Closest HWM value (ft NAVD 88 (2004.65))**	**Interpreted Surge from HWM and ADCIRC (ft, NAVD 88, 2004.65)**	**Interpreted Surge plus wave ht at Max water level**	**Levee Elevation (ft) 2001 Chance Survey, adjusted**
596	30.004139	-89.938667	15.2	2.03	15.4	15.5	17.53	15.6
366	30.008200	-89.923897	14.9	2.56	15.4,18.2	16	18.56	16.84
365	30.018400	-89.890984	14.6	2.53	15.4, 18.2	16	18.53	18.1
364	30.026340	-89.874229	14.3	2.53	15.4, 18.2	15.6	18.13	16.85
148	30.029604	-89.864881	14.0	2.49	15.4, 15.7	15.4	17.89	16.59
363	30.033979	-89.858070	13.9	2.56	15.7	15.2	17.76	15.87
362	30.040150	-89.843964	13.7	2.66	15.7	15	17.66	16.65
361	30.047791	-89.830162	13.5	2.69	15.7	15	17.69	16.95
NOE Southpoint to GIWW, table of surge and wave data								
South Point Levee model data point	**Latitude**	**Longitude**	**ADCIRC Model max surge (ft NAVD 88, 2004.65)**	**STWAVE Model wave height (ft) at max water level**	**Closest HWM value (ft NAVD 88 (2004.65))**	**Interpreted Surge from HWM and ADCIRC (ft, NAVD 88, 2004.65)**	**Interpreted Surge plus wave ht at Max water level**	**Levee Elevation (ft) 2001 Chance Survey, adjusted**
158	30.078615	30.078615	12.7	1.12	15.7	14.2	15.32	16.56
157	30.095602	30.095602	12.7	1.64	15.7	13	14.64	15.39
351	30.121361	30.121361	12.7	2	13.4	12.3	14.3	15.33
350	30.132311	30.132311	12.7	2.17	11.4	12	14.17	14.54
349	30.144039	30.144039	12.3	1.64	11.4	12.5	14.14	14.96

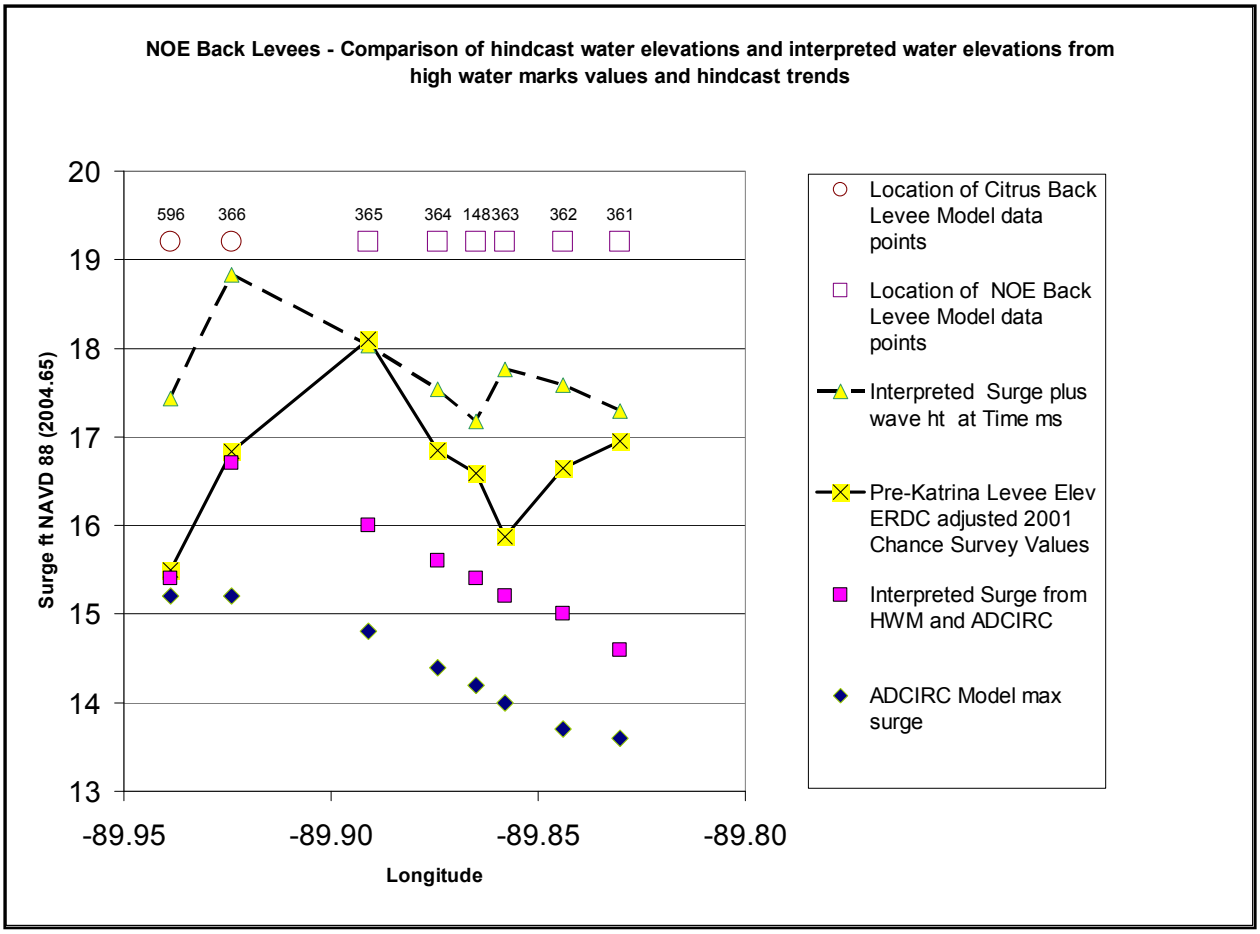

Figure 20. Data from Table 3 plotted with levee elevations derived from pre-Katrina LIDAR (Chance, 2001) for Citrus Back Levee and NOE Back Levee

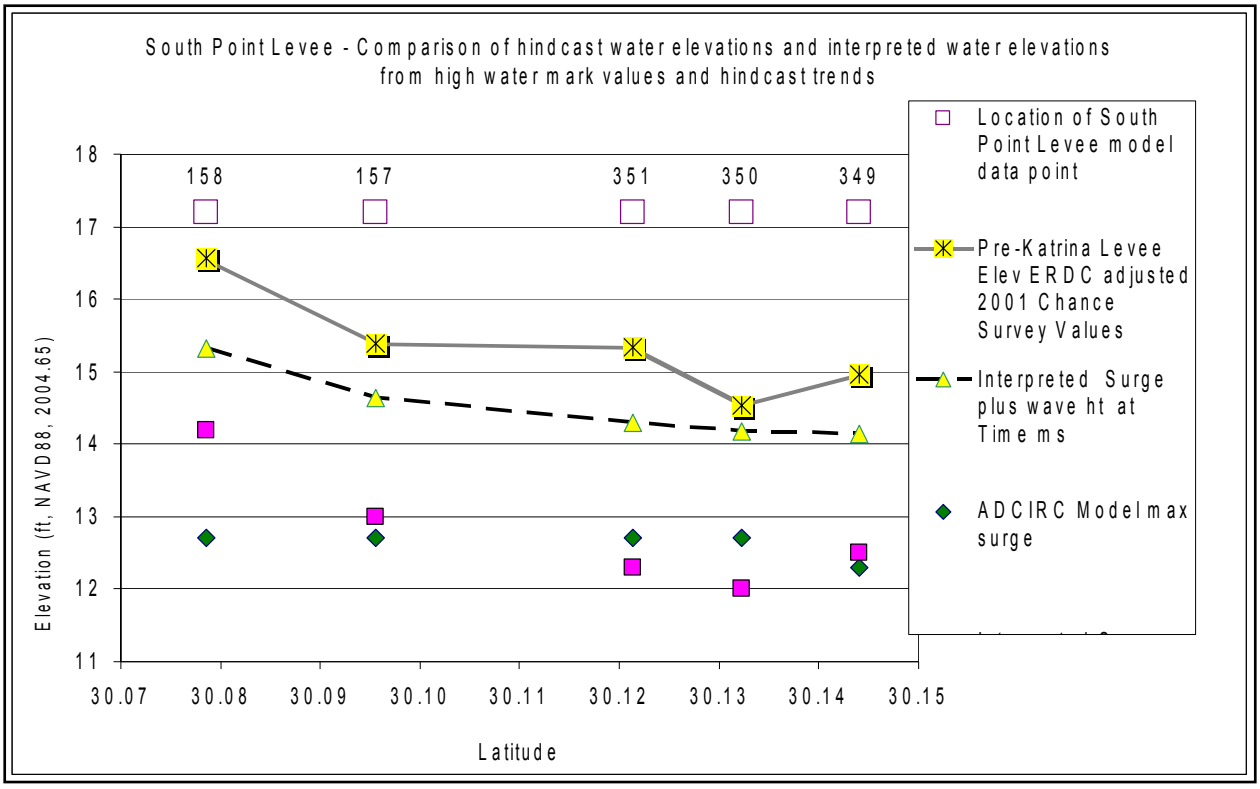

Figure 21. Data from Table 3 plotted with levee elevation derived from pre-Katrina LIDAR (Chance 2001) for South Point Levee

Figure 20 includes two data points within the Citrus Back Levee and the remaining points are within the NOE BL system. The point locations are designated by circles and squares on the plot, respectively. Figure 20 shows the interpreted surge plus wave height exceeds the levee elevation along the entire reach. The maximum overtopping occurs at point 363 (approximately 2 ft) and the minimum is at point 596 (0.2 ft). The eastern section of this reach suffered major erosion and breaching while west of data point 364 the levee performed well with little scour of the earthen levees. The NOE BL is hydraulically filled and extends from the Michoud Canal to the South Point levee. The NOE BL height increases westward from data point 364, which may explain the decrease of erosion from data point 364 to 365. The Citrus BL was subjected to an interpreted 1.5 ft of overtopping but had little erosion, possibly because it was constructed of hauled and semi-compacted fill.

ERDC conducted a set of in-situ erodibility at approximately data point 596. The tests were conducted under the I-510 bridge (located in previous figure 8) using the ASTM Jet Index Test which verified the high resistance to erosion at this site (Wibowo et al 2006). The existing levee under the I-510 bridge was constructed from fat clays and lean clays with dry densities ranging up to 103 lb/cu ft and subsequently had minimal erosion damage.

Figure 21 compares the maximum storm water levels (interpreted surge plus wave height) with levee elevation along the South Point levee system. The data implies little to no overtopping along this system and the LIDAR profiles indicate little to no erosion or breaches along the earthen levee. The levee elevations were approximately 1-ft above the maximum water levels.

Breaching occurred at the CSX railroad gate (a transition structure), and minor erosion occurred at drainage structures. Figure 22 shows a LIDAR plot of levee section near Highway 90, and Figure 23 shows an intact levee along this reach, typical of the South Point to GIWW levee.

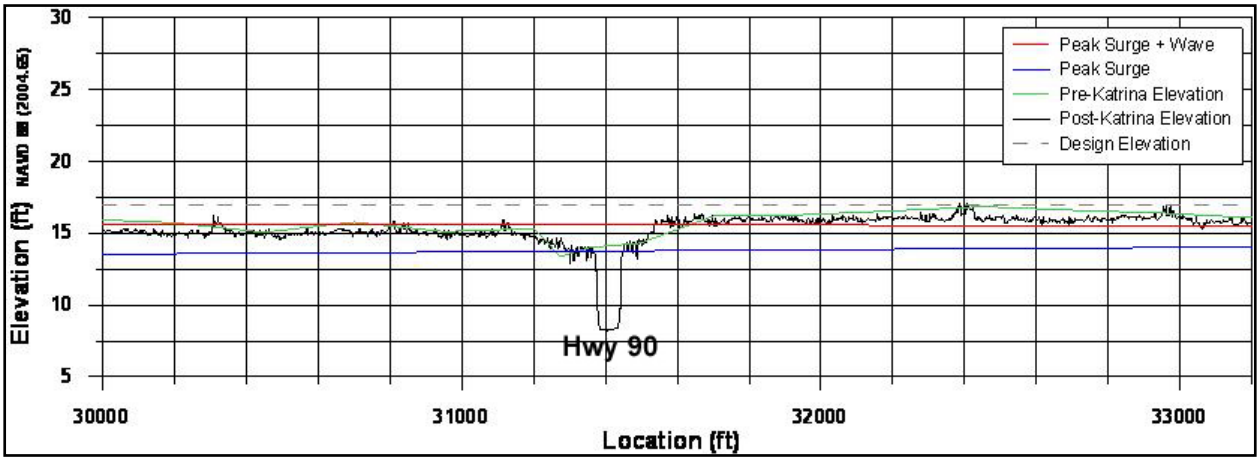

Figure 22. NOE Levee LIDAR profile near the Hwy 90 crossing. Note the slightly lower levee elevation along the reach north of Hwy 90 (left side in above figure) which allowed minimal wave overtopping but not surge overtopping. Minimal erosion occurred along the entire South Point to GIWW levee as typified in above figure.

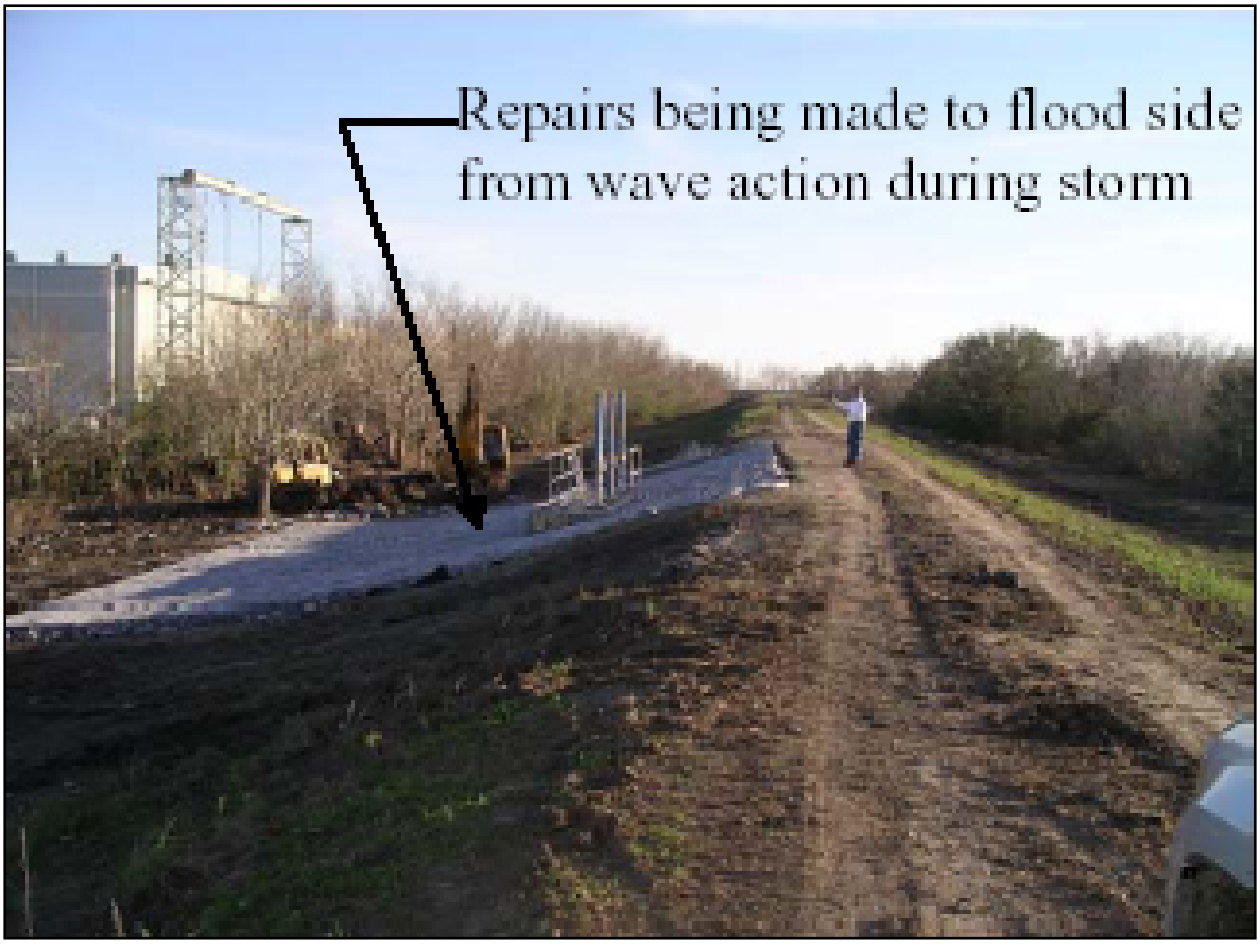

Figure 23. NOE South Point to GIWW Levee north of the Hwy 90 crossing at Drainage Structure N19 (approximate So.Point to GIWW B/L Sta 927+70) with minor floodside erosion. Landside erosion was minimal. (Photo from IPET)

Chalmette and Chalmette Extensions, St. Bernard Parish

The portion of the levee that protects St. Bernard Parish and a small section of eastern Orleans Parish was designed to protect 75 sq. miles of urban and industrial lands. Figure 24 illustrates the components of the hurricane protection plan for St. Bernard Parish. The levee portion was constructed with a 10-foot crown width and side slopes of 1 on 3. The height of the levee varies but is in the range of 10 – 12 feet above natural ground or 17 to 19 ft el NAVD 88, May 2002. There are also floodwall segments along the line of protection that consist of sheet-pile walls or concrete I-walls constructed on the top of sheet-pile. There are two control structures with sector gates (Bienvenue and Dupre) that were constructed to allow tidal fluctuations in the marsh lands behind the hurricane project. There are also six road closure structures located where a highway or road pass through the line of protection and one railroad closure. In addition there is one gravity drainage structure along the southern section of the hurricane levee. The line of protection was designed to provide protection from the Standard Project Hurricane (approximately a fast moving Category 3 storm) (TFG 2005). The Levee

District is classified as an urban Flood Control Works (FCW), and all the primary project features were categorized as “acceptable” per their last inspection in May 2005.

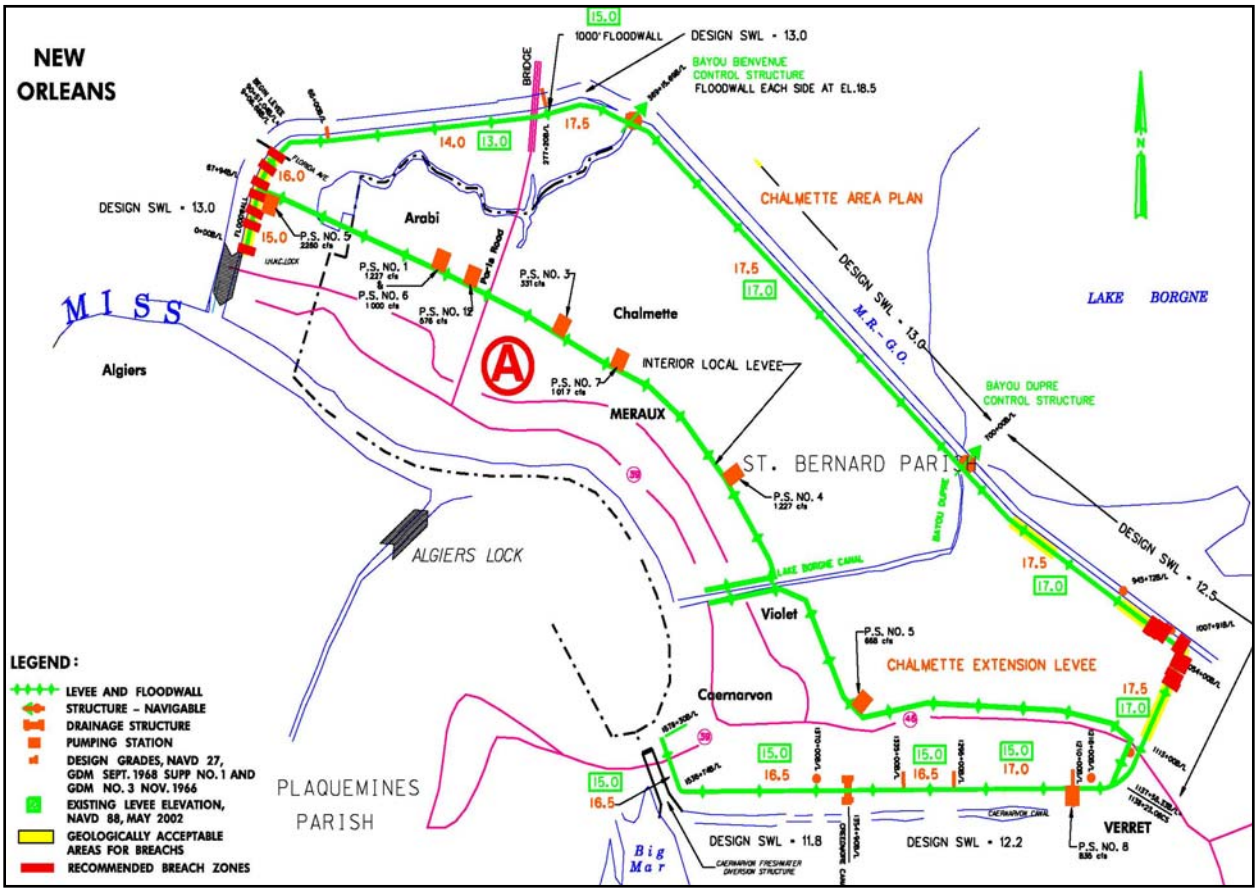

Figure 24. St. Bernard Parish hurricane protection plan map (from TFG)

The hurricane produced storm surge levels at the levee along the Mississippi River Gulf Outlet (MRGO) at elevation 19.0 ft (NAVD 88, 2004.65), approximately. The average elevation of the existing levee crown was at a nominal 17.0 ft (NAVD 88, 2004.65). Numerous breaches in addition to scour and severe erosion occurred along this stretch of levee as a result of the overtopping. There was also major damage to the two control structures. Figure 25 outlines the major levee damages (in red) and the TFG repair projects. The following table describes the damages and repair contract information (TFG 2005).

Figure 25. TFG map showing damaged levees and restoration contracts (from TFG)

Table 4
General Description of Damage Within the Chalmette Basin, St. Bernard and Orleans Parish (See Figure X)

Repair Contract	Description
STBO1 - Lake Pontchartrain - Prepare Levee Foundation (St. Bernard Parish).	Project STB01 includes site preparation work in the areas of levee damage between the Bayou Bienvenue and Bayou Dupre Control Structures. The contracted work (rental agreement contract) is complete.
STBO2 - Lake Pontchartrain – Borrow Area Preparation (St. Bernard Parish)	Project STB02 includes site preparation work in the borrow areas between the Bayou Bienvenue and Bayou Dupre Control Structures. The borrow area is a strip of land adjacent to the levee, which was used as a disposal area during the construction of the MRGO canal. This rental agreement contract has not been fully utilized – some borrow area preparation work has been accomplished as part of STB01 work (same contractor).
STB03 - Levee Restoration East of Bayou Dupre - MRGO Baseline Station 714+55 to 1007+91 (St. Bernard Parish)	Project STB03 includes repairing a 5.6-mile reach of levee along the MRGO extending east from the Bayou Dupre Control Structure. The entire levee reach will be restored to the design grade elevation, requiring the placement of an estimated 1,120,000 cubic yards of fill material. The borrow area for this fill material is a strip of land adjacent to the levee, which was used as a disposal area during the construction of the MRGO canal.
STB04 - MRGO Baseline Station 380+00 to 705+00 - Between Bayou Depre and Bayou Bienvenue Control Structures (St. Bernard Parish)	Project STB04 includes repairing a 6.2-mile reach of levee along the MRGO between the Bayou Bienvenue and the Bayou Dupre Control Structures. The entire levee reach will be restored to the design grade elevation, requiring the placement of an estimated 652,000 cubic yards of fill material. The borrow area for this fill material is a strip of land adjacent to the levee, which was used as a disposal area during the construction of the MRGO canal.
STB05 – Levee Restoration Miscellaneous Gates and Floodwall Repairs – IHNC to Bayou Bienvenue (Orleans Basin)	Project STB05 includes repair of minor scour on the backside of the levee and structural and structural backfill scour adjacent to floodwalls and four closure structures, which are located between the Bayou Bienvenue Control Structure to the GIWW lock. An estimated 26,000 cubic yards of fill material will be required for this work, which is being furnished by the contactor.
STB06 – Repairs and Modifications - Bayou Dupre Control Structure (St. Bernard Parish).	Project STB06 includes repair of structural damage and loss of structural backfill at the Bayou Dupre Control Structure. A significant scour hole is to be filled with 17,500 cubic yards of granular backfill and protected with grouted riprap. An estimated 22,500 tons of riprap and 13,400 cubic yards of embankment fill will be required for the repairs. All materials are to be furnished by the contractor.
STB07 – Repairs and Modifications – Bayou Bienvenue Control Structure (Orleans Parish).	Project STB07includes repair of structural damage and loss of structural backfill at the Bayou Bienvenue Control Structure. A significant scour hole is to be filled with 28,600 cubic yards of granular backfill and protected with grouted riprap. An estimated 32,100 tons of riprap and 3,400 cubic yards of embankment fill will be required for the repairs. All materials are to be furnished by the contractor.
STB08 - MRGO to Caernarvon Levee Miscellaneous Scour Repair (St. Bernard Parish)	The work includes repair of minor scour on the backside of the levee from the Mississippi River Gulf Outlet (MRGO) to Caernarvon, which is about 10.8 miles in length. An estimated 36,000 cubic yards of fill material will be required for this work
STB09 - Repair Creedmore Structure (St. Bernard Parish)	The work includes constructing a cofferdam and removing debris from the structure to permit closure of the gates and inspection of the structure to determine if further repairs are necessary.

Figure 26 shows the breach locations for St. Bernard Parish, which includes near 70% of the levee along MRGO. Figure 27 highlights the levees construction methods, including hauled, hydraulically filled and walled reaches. Note the breach locations in Figures 26 coincide with the reaches constructed using hydraulic fill. Several pre-Katrina soil borings along the levee crown are provided in Figures 28 through 35, between Bayou Bienvenue (Station 370+00 levee C/L) to the southeastern corner of the parish (Station 999+67 levee C/L). Note that the top surface layers are composed of variable soil types ranging from sand to fat clays.

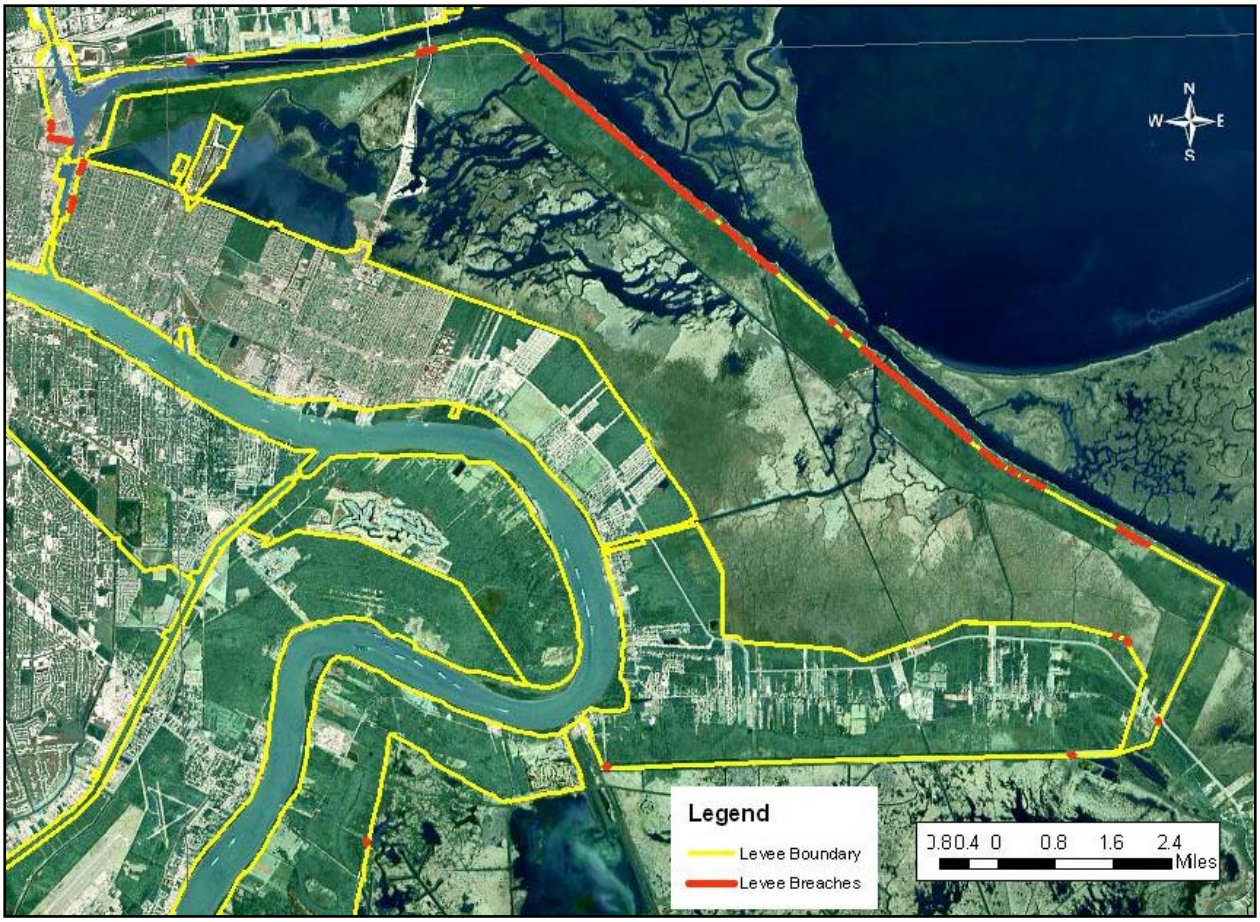

Figure 26. St. Bernard Parish breach locations.

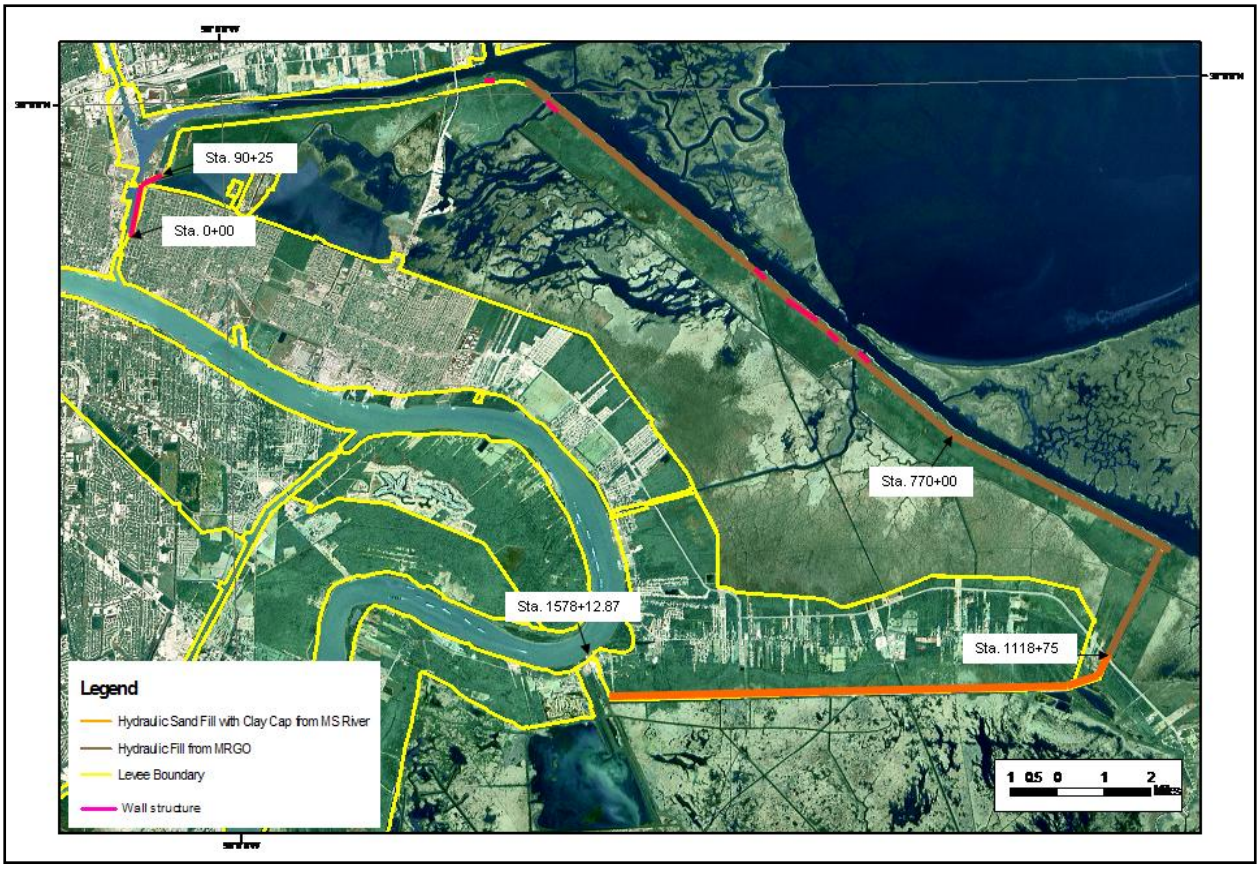

Figure 27. Constructed levee soil sources

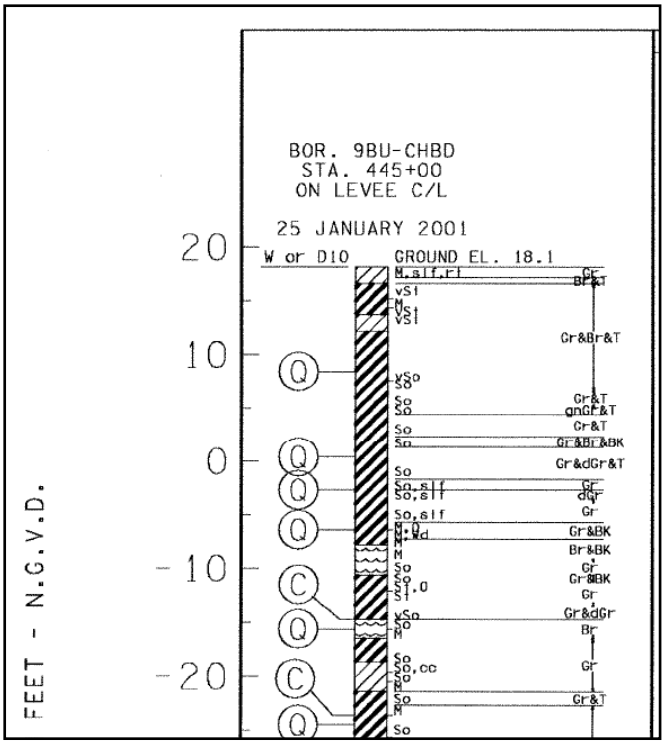

Figure 28. Soil boring 9BU along MRGO (ft, NGVD)

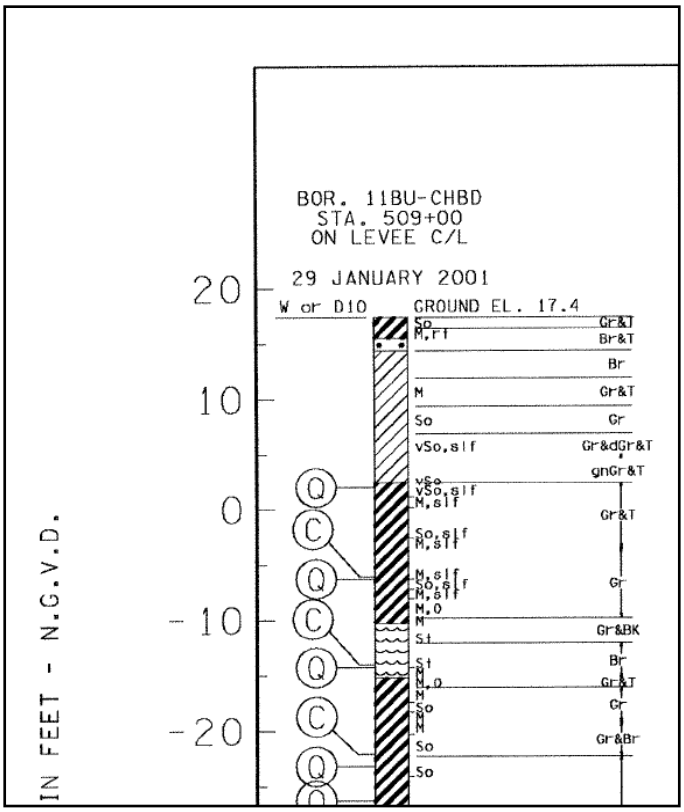

Figure 29. Soil boring 11BU along MRGO

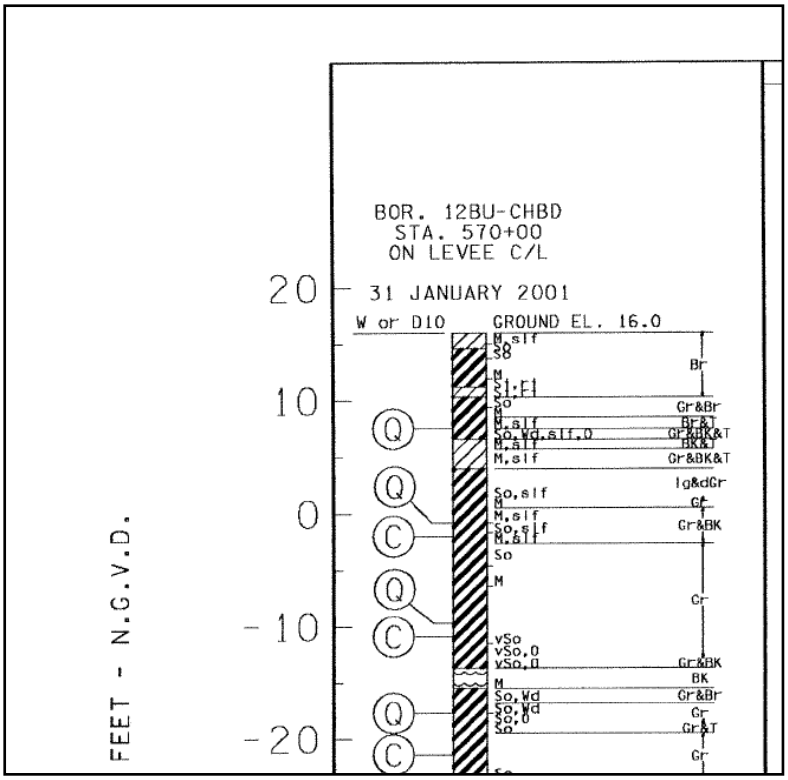

Figure 30. Soil boring 12BU along MRGO

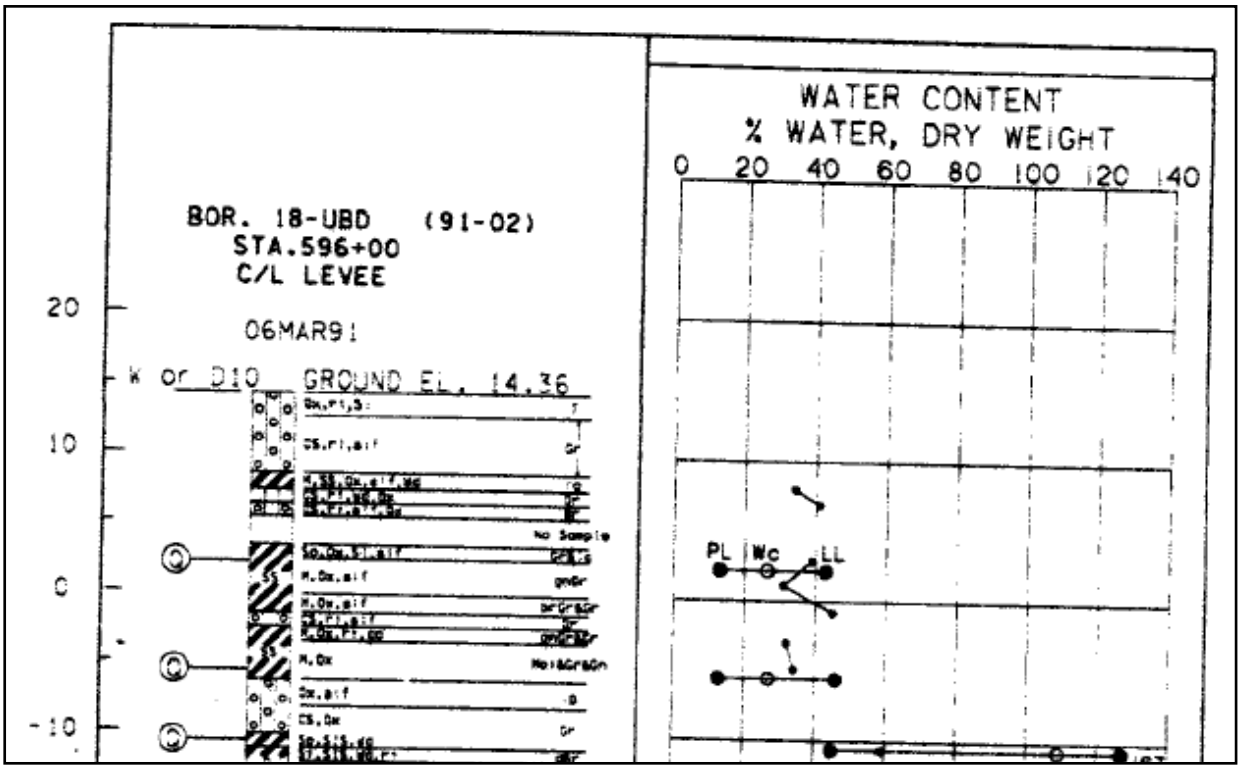

Figure 31. Soil boring 18-UBD along MRGO

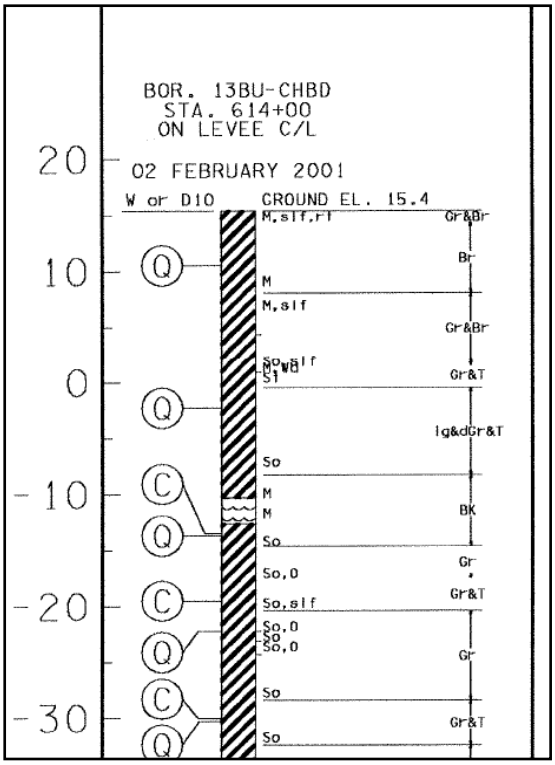

Figure 32. Soil boring 13BU along MRGO

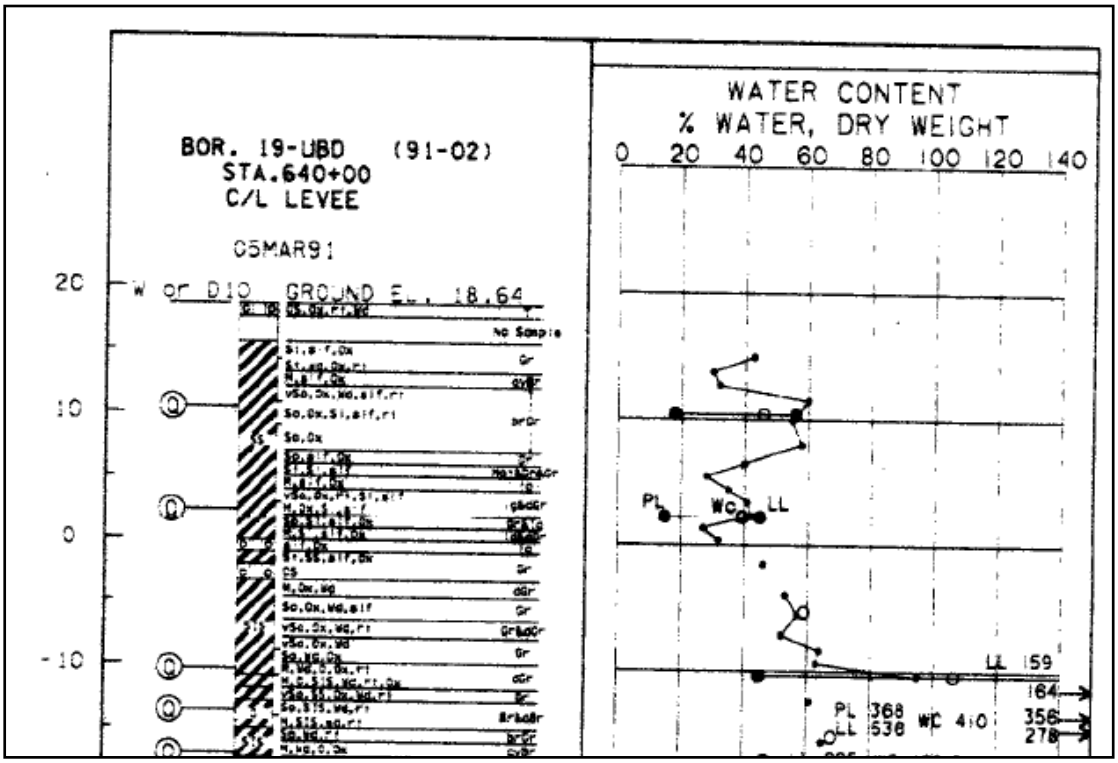

Figure 33. Soil boring 19-UBD along MRGO

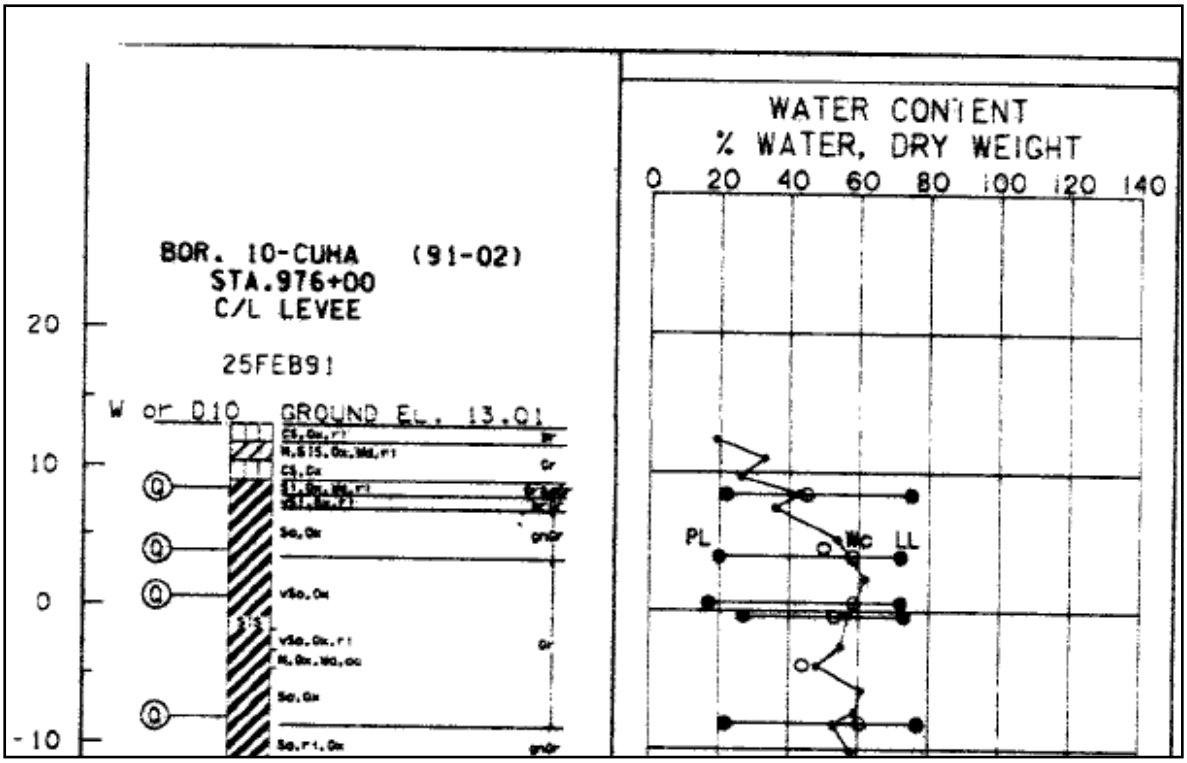

Figure 34. Soil boring 10-CUHA along MRGO

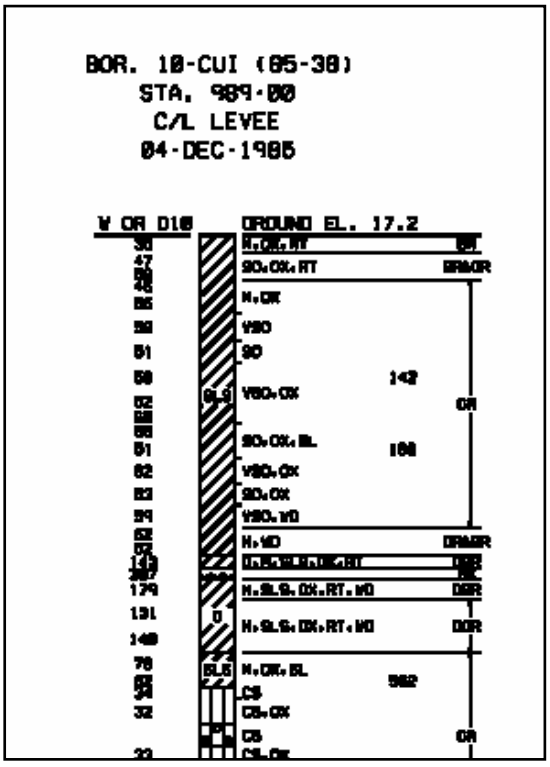

Figure 35. Soil boring 10-CUI along MRGO

2001 and 2005 LIDAR Levee Profile Surveys

Figure 36 shows a LIDAR stationing map for portions of the St. Bernard levee system. To establish possible correlations between soil type and erosion depth, the LIDAR data are plotted as levee profiles along 3000-ft reaches (Figures 37 through 45). Levee reaches of high scour are easily identified using these profiles. The above boring locations are identified on the profiles to facilitate the correlation between soil and erosion. In addition, Figure 43 shows the location of one set of erodibility tests performed by ERDC/GSL (Wibowo, et al 2006); the ASTM Jet Index Test. The tests indicated high resistance to erosion at this site and the LIDAR also shows little scour at this location. The existing levee at this location was constructed with a fat clay (CH) surface as noted by the test engineers.

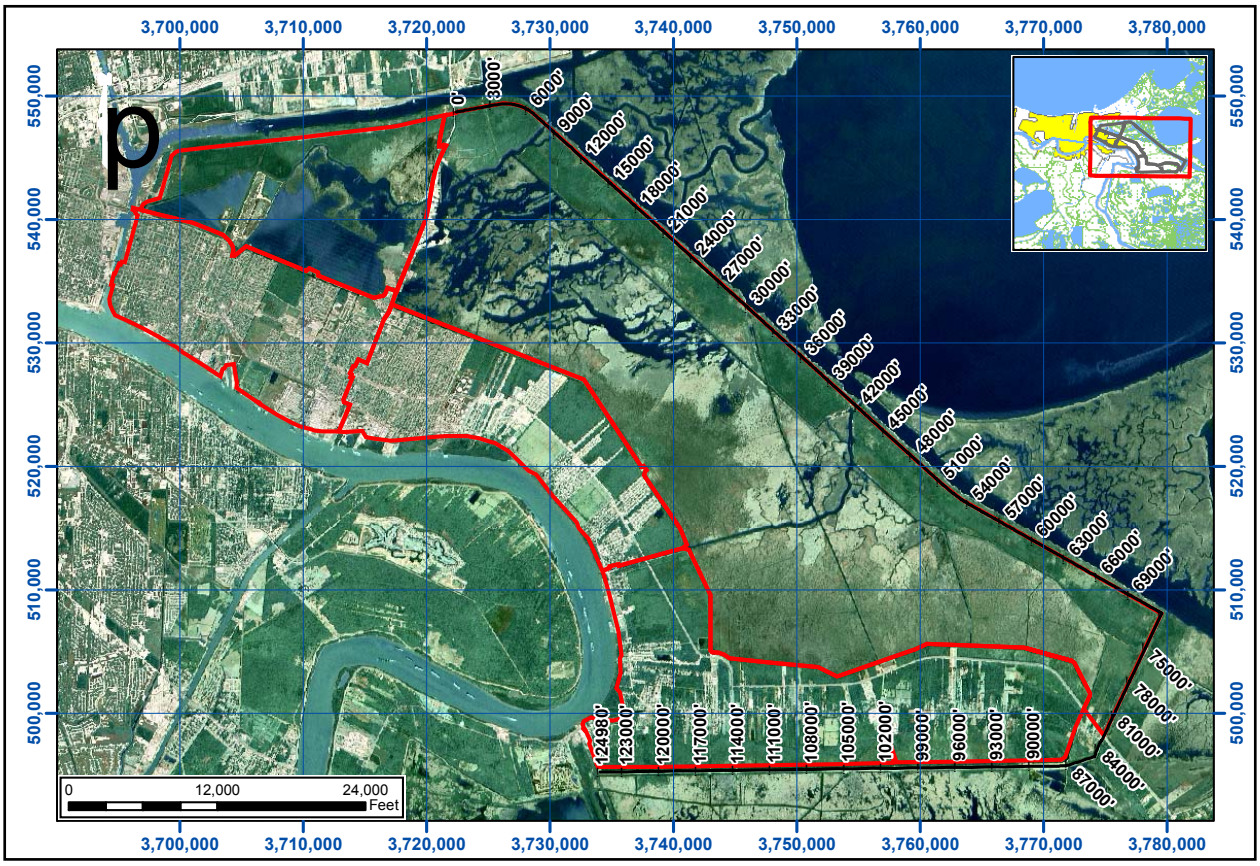

Figure 36. St. Bernard Parish LIDAR stationing map with ERDC erosion test locations

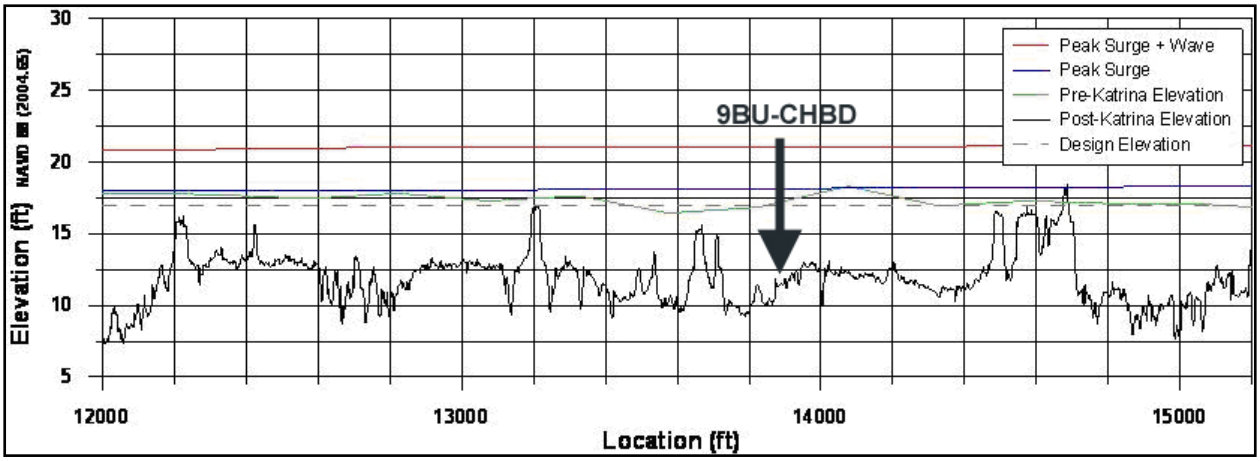

Figure 37. LIDAR plot showing soil boring 9BU-CHBD approximate location. Erosion depth was approximately 5 ft.

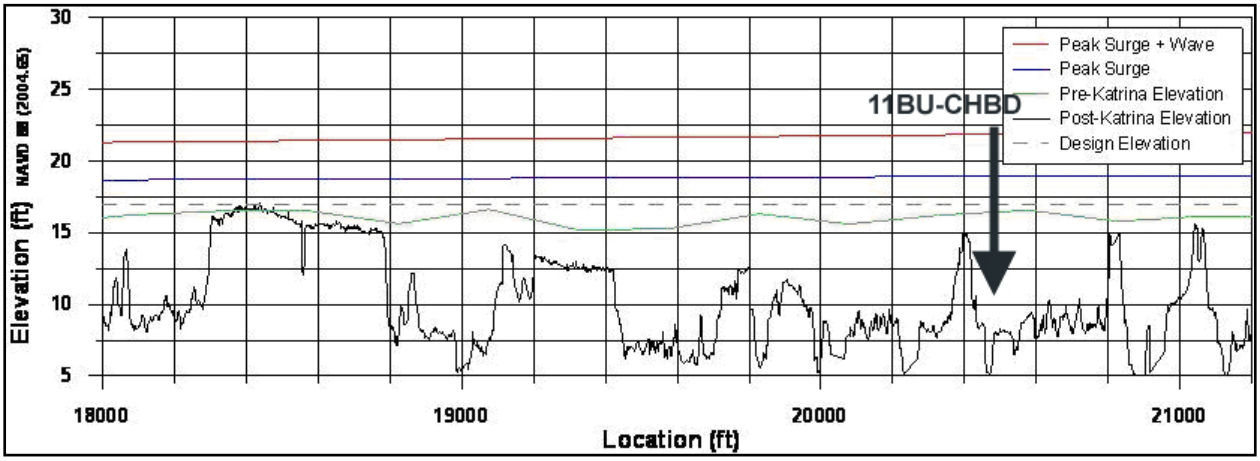

Figure 38. LIDAR plot showing soil boring 11BU-CHBD approximate location. Erosion depth was approximately 10 ft.

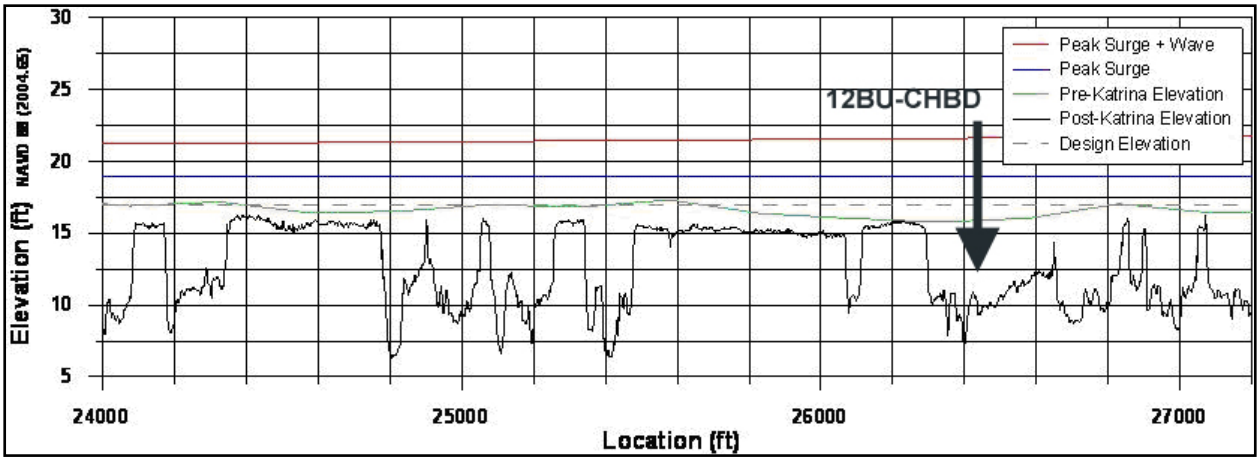

Figure 39. LIDAR plot showing approximate location of soil boring 12BU-CHBD. Approximate erosion depth was 6 ft.

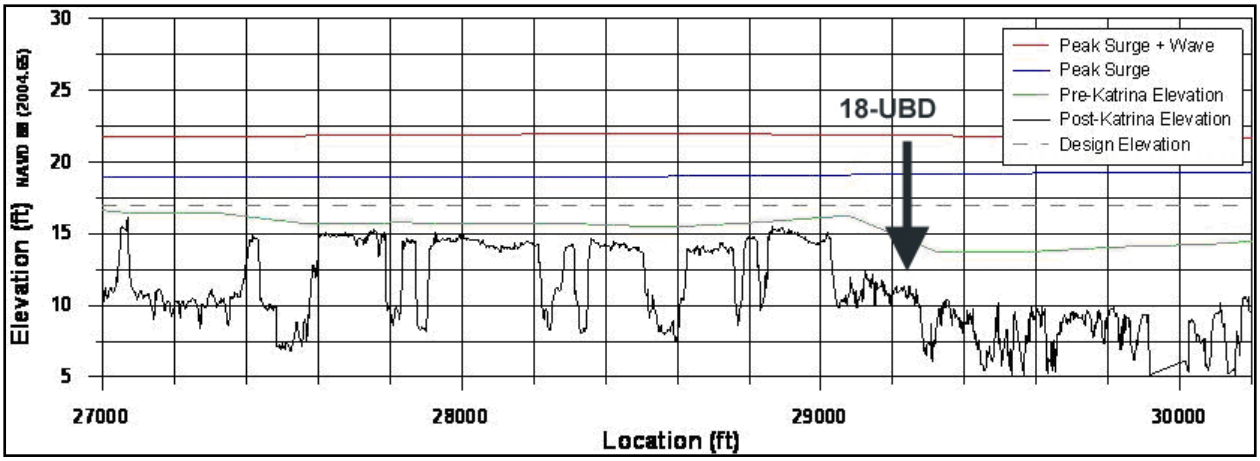

Figure 40. LIDAR plot showing approximate location of soil boring 18-UBD. Approximate erosion depth was 6 ft.

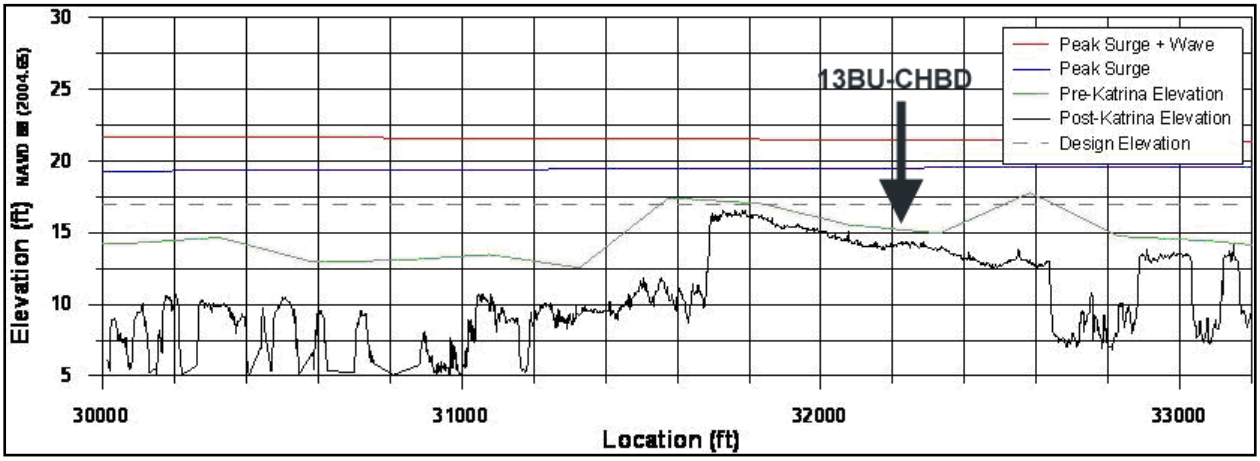

Figure 41. LIDAR plot showing soil boring 13BU-CHBD approximate location. Erosion depth was approximately 1 ft.

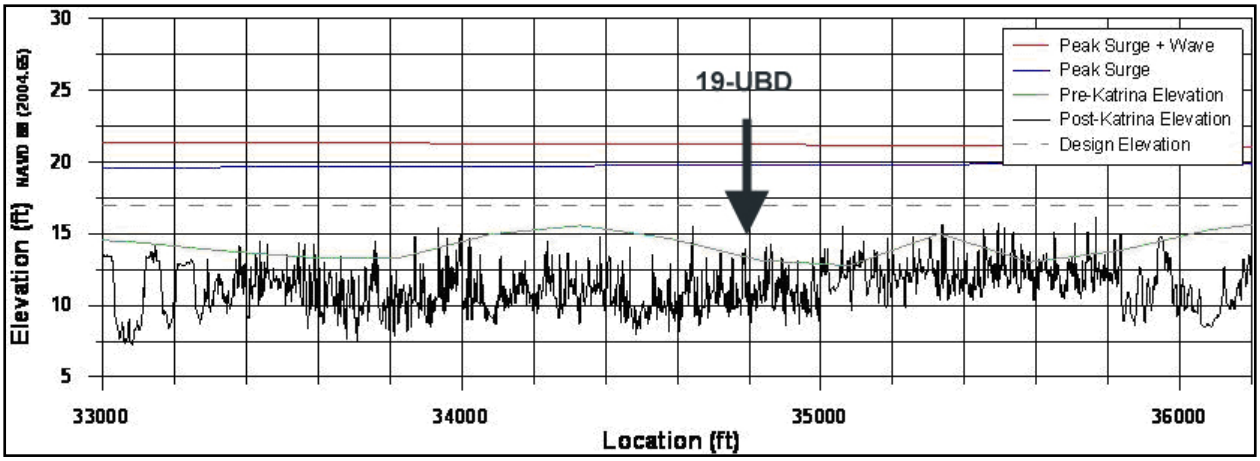

Figure 42. LIDAR plot showing soil boring 19-UBD approximate location. Note that the crown elevation was about 19 ft in 1991. Pre-Katrina elevation was approximately 13 ft, indicating 6 ft subsidence in about 14 years. Sheetpiling was present at this location as indicated by the LIDAR signature.

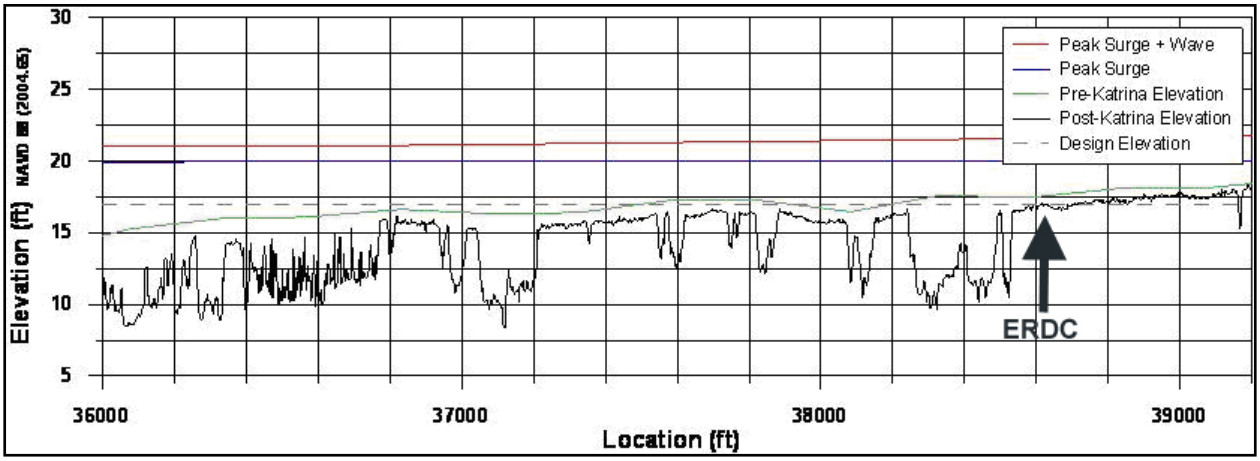

Figure 43. LIDAR plot showing approximate location of ERDC erosion tests on the crown of the surviving post-Katrina levee.

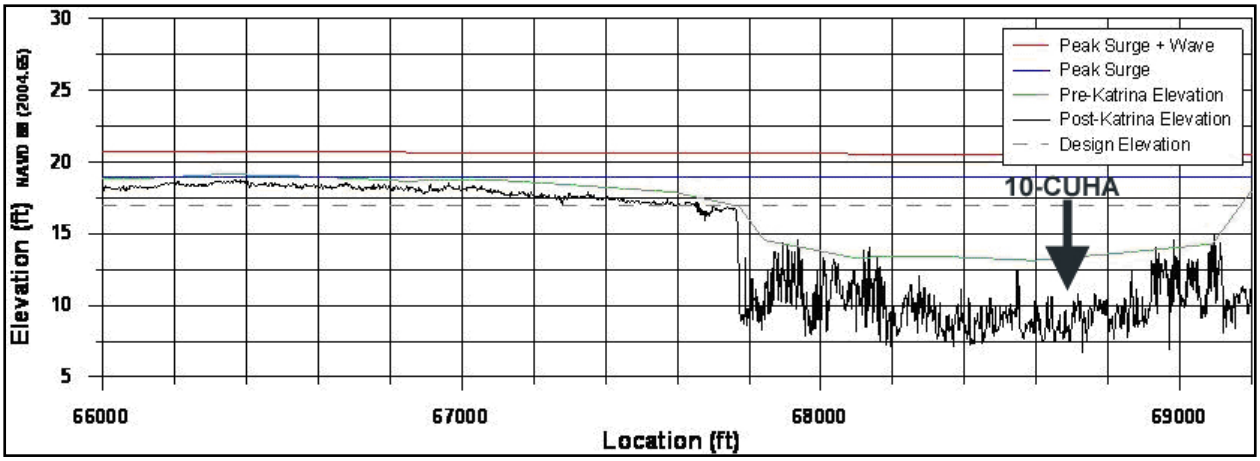

Figure 44. LIDAR plot showing approximate location of soil boring 10-CUHA. Pre-Katrina crown elevation was 13 ft in 1991, and post-Katrina elevation was approximately 6 ft lower, indicating crown subsidence (settlement) in the 14 year period combined with Katrina scour. Sheetpiling was present at this location as indicated by the LIDAR signature.

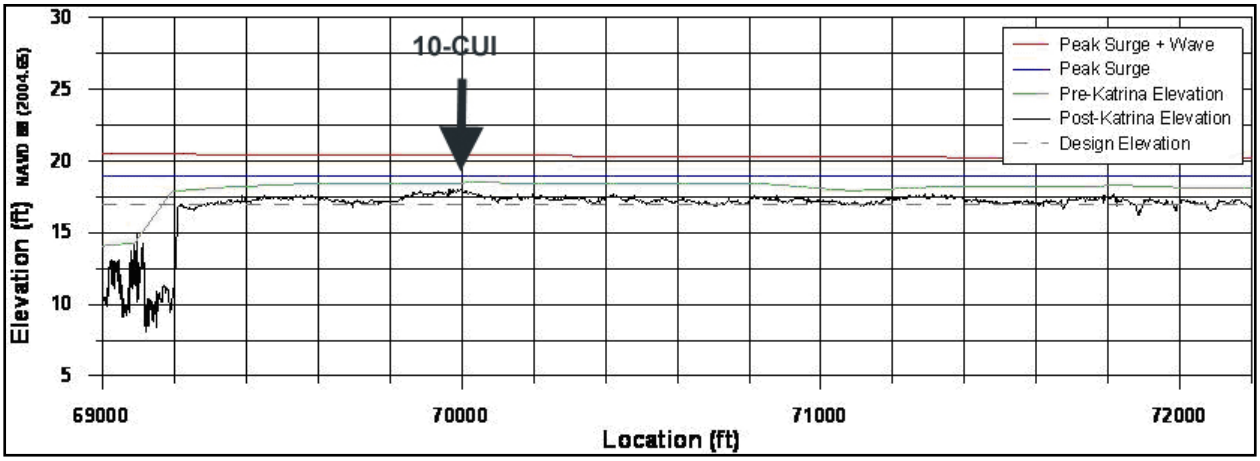

Figure 45. LIDAR plot showing approximate location of soil boring 10-CUI drilled in 1985. Erosion damage was minimal.

The soil type, scour depth, and hydraulic loading data from the above figures (37 thru 45) are generalized in Table 5. The levee crown surface soil types and consistencies (strengths) are shown with approximate scour depths and approximate surge plus wave heights. Figure 46 is a plot of the Table 5 data, and shows the relations between soil type, soil strength, hydraulic loading, and erosion depths at selected points along the levee crown. Note that no strong correlation between erosion depth and hydraulic loading was observed. From these selected points (Table 5), it appears that soil consistency (strength) and soil type correlate with erosion depth and hydraulic loading. The soil consistency is correlated in that soft fat clays performed poorly (i.e. had deeper erosion) compared to medium fat clays, and the medium fat clays performed better than the medium lean clays. The soil strengths (consistencies) are directly comparable to construction compaction effort. For example, a compacted clayey soil will have higher density and strength than an uncompacted clayey soil at the same water content.

Table 5
Soil Borings, Scour Depth, and Hydraulic Loading Along Selected MRGO Levee Reaches

Soil boring / surface soil type	Scour depth, ft	Water crest over crown, ft	Nearest numerical model data point
9BU / med lean clay	5	2	367
11BU / soft fat clay	10	5	368
12BU / med lean clay	6	7	369
18UBD / silty sand	6	7	369
13BU / med fat clay	1	7	369
19UBD / silty sand	n/a (sheetpile reach)	7	369 - 370
ERDC / med fat clay	1	7	370
10-CUHA / silt	n/a (sheetpile reach)	6	373
10-CUI / med fat clay	0.5	6	373

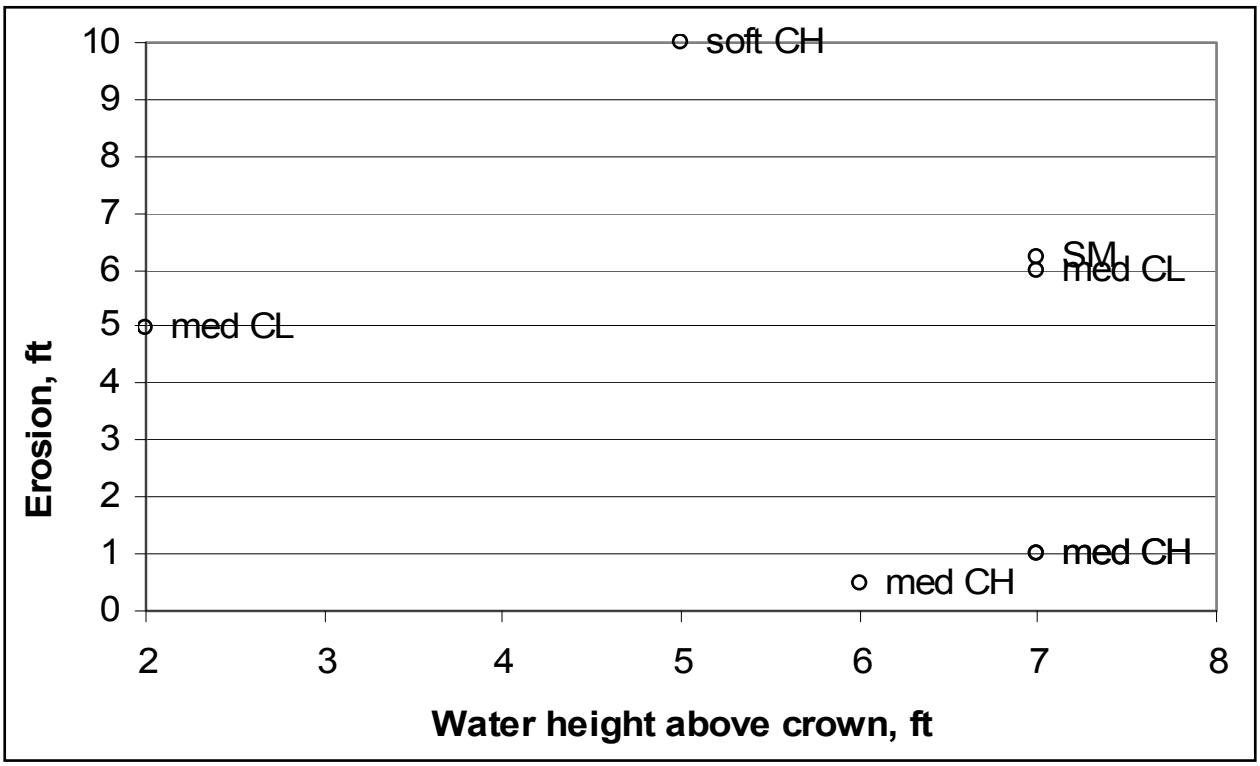

Figure 46. Scour depths versus surge/wave loading at selected points along the MRGO levee. Crown soil type and consistency are labeled (med = medium consistency, SM = silty sand, CL = lean clay, and CH = fat clay)

St. Bernard Hydraulic Analysis –Surge, Wave and Levee Elevations

Figure 47 shows selected numerical data points extracted from the IPET Storm Team hydraulic analyses. Numerical models ADCIRC and STWAVE were used to estimate the surge

and wave hydrographs, respectively, associated with hurricane Katrina. Table 6 shows the model calculated storm surge maximum elevation and wave heights associated with the maximum surge, in addition to measured high-water marks surveyed near these points and surveyed levee elevations. The high water mark data points were sparse and are described in another IPET report. The maximum surge, interpreted surge after consideration of the high water mark survey, the interpreted surge plus the wave height, and levee elevations are plotted in three figures (Figures 48, 49 and 50). The figures separate the data into straight line reaches of levee (with some overlap) for ease of illustration. For example, Figure 48 shows the data along the MRGO. The data shows the calculated maximum surge is approximately 2.5 ft lower than the interpreted surge when the high water mark survey is considered. Note that the interpreted surge also expresses the trend calculated by the numerical model. Figure 48 also dramatizes the height of water flow over this reach of levee by comparing levee elevation to the interpreted maximum storm water level (i.e., interpreted surge elevation plus calculated wave height).

Figure 47. St. Bernard ADCIRC model points for hindcasting

Table 6
Calculation of Interpreted Surge Along MRGO From ADCIRC Numerical Model and High Water Mark Survey for Selected Model Data Points Shown in Figure 47

St. Bernard Parish - Chalmette (MRGO), Table of Surge and Wave Data								
MRGO ADCIRC Model Point	Latitude	Longitude	ADCIRC Model max surge (ft NAVD 88, 2004.65)	STWAVE Model wave height (ft) at Max water level	Closest HWM value (ft NAVD 88 (2004.65))	Interpreted Surge from HWM and ADCIRC (ft, NAVD 88, 2004.65)	Interpreted Surge plus wave ht at computed Max water level	Levee Elevation (ft) 2001 Chance Survey, adjusted
147	29.99857	-89.915208	15.4	2.13	18.17	18	20.13	16.85
367	29.99198	-89.9020386	15.7	3.25	18.17	18	21.25	17.81
368	29.97585	-89.883049	16.2	3.28	18.17	18.5	21.78	16.17
369	29.96123	-89.8664703	16.4	4.76	21.2, 20.8, 16.8	18.5	23.26	15.46
370	29.946	-89.848381	16.6	4.1	21.2, 20.8, 16.8	19.5	23.6	16.08
371	29.93063	-89.831192	16.7	4.07	21.2, 20.8, 16.8	19.5	23.57	18.67
372	29.91631	-89.8129501	16.9	3.9	21.2, 20.8, 16.8	19.3	23.2	17.69
373	29.90545	-89.7909393	16.9	3.84	21.2, 20.8, 16.8	19	22.84	17.06
375	29.88171	-89.760398	16.6	3.7	18.7, 18.1	18.8	22.5	18.55
376	29.87277	-89.766243	16.4	1.67	18.7, 18.1	18.6	20.27	18.41
St. Bernard Parish - Southern Reach of Chalmette Extension, Table of Surge and Wave Data								
Verrette ADCIRC Model Point	Latitude	Longitude	ADCIRC Model max surge (ft NAVD 88, 2004.65)	STWAVE Model wave height (ft) at Max water level	Closest HWM value (ft NAVD 88 (2004.65))	Interpreted Surge from HWM and ADCIRC (ft, NAVD 88, 2004.65)	Interpreted Surge plus wave ht at computed Max water level	Levee Elevation (ft) 2001 Chance Survey, adjusted
375	29.88171	-89.760398	16.6	3.7	18.7, 18.1	18.8	22.5	18.55
376	29.87277	-89.766243	16.4	1.67	18.7, 18.1	18.6	20.27	18.41
377	29.86247	-89.7717438	16.3	1.71	18.7, 18.1	18.6	20.31	18.30
378	29.85422	-89.7767181	15.7	1.77	13.7, 18.7, 18.1	18	19.77	19.00
380	29.85045	-89.8112488	15	1.44	13.7	14	15.44	15.50
St. Bernard Parish, Near Verret to Caernarvon Surge and Wave Data								
Cearnarvon ADCIRC Model Point	Latitude	Longitude	ADCIRC Model max surge (ft NAVD 88, 2004.65)	STWAVE Model wave height (ft) at max water level	Closest HWM value (ft NAVD 88 (2004.65))	Interpreted Surge from HWM and ADCIRC (ft, NAVD 88, 2004.65)	Interpreted Surge plus wave ht at Max water level	Levee Elevation (ft) 2001 Chance Survey, adjusted
378	29.85422	-89.7767181	15.7	1.77	13.7, 18.7, 18.1	18	19.77	19.00
380	29.85045	-89.8112488	15	1.44	13.7	14	15.44	15.50
381	29.85096	-89.8310013	14.8	1.31	12.9	13	14.31	15.00
382	29.85113	-89.8495483	14.6	1.25	11.7, 12.0	12	13.25	15.00
383	29.85113	-89.868606	14.3	1.25	12	12	13.25	16.50
384	29.85155	-89.8896713	13.9	1.41	11.8, 11.8	11.8	13.21	17.00
385	29.85834	-89.9107132	13.3	1.51	10.5, 11.8	11.5	13.01	15.00

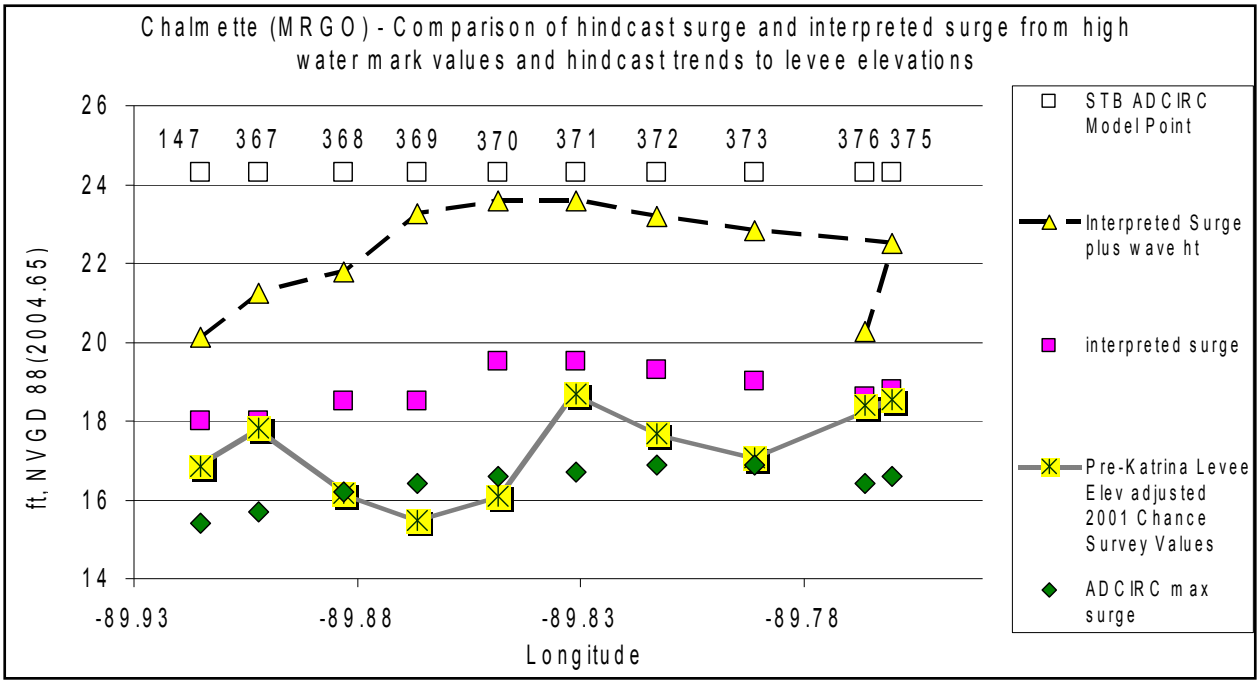

Figure 48. Estimated surges compared to levee elevations from North to South along the MRGO, St. Bernard Parish. Data point locations shown in Figure 47.

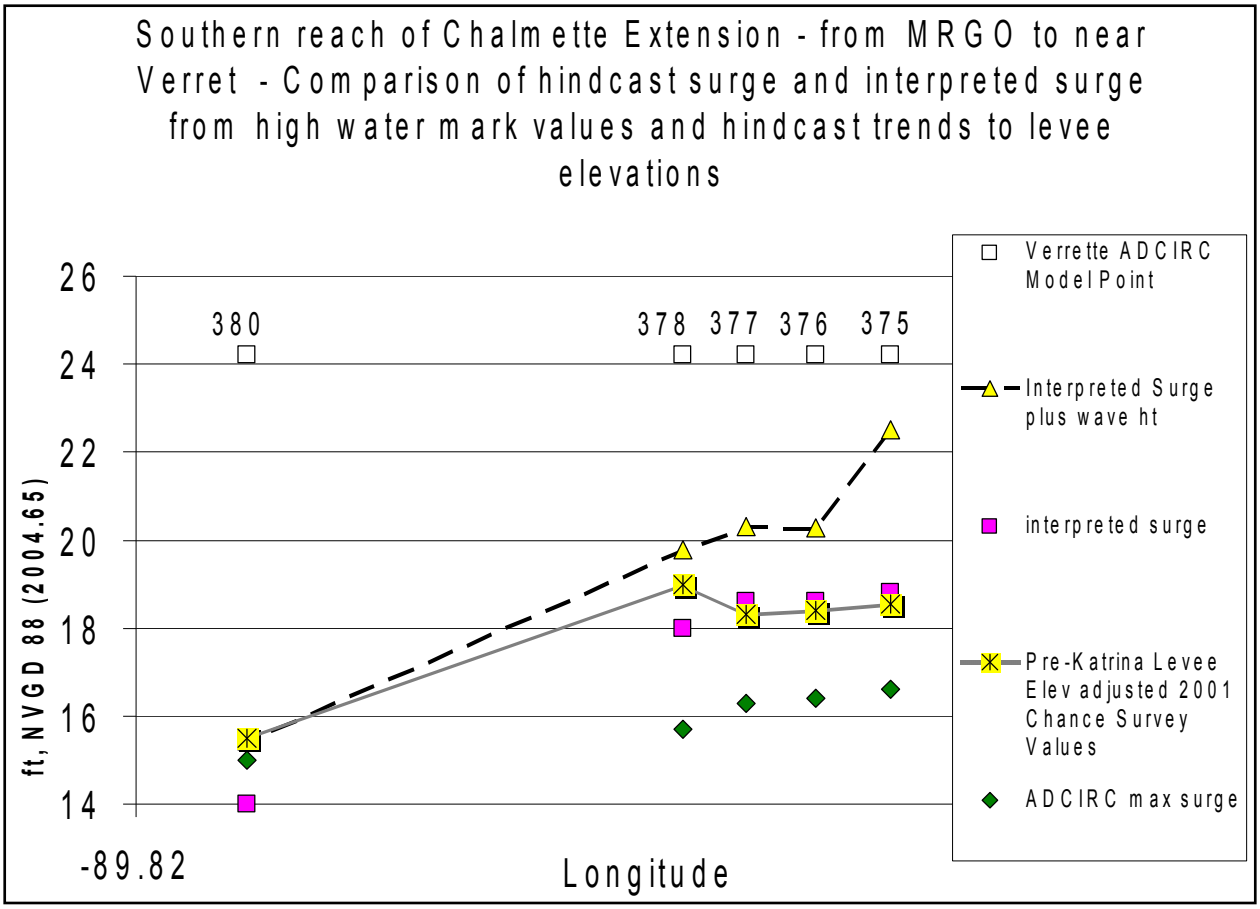

Figure 49. Estimated surges compared to levee elevations from west to east along the Chalmette extension levee at Verret. Data point locations shown in Figure 47. Note that Data point 375 is adjacent to MRGO and is also plotted on Figure 48.

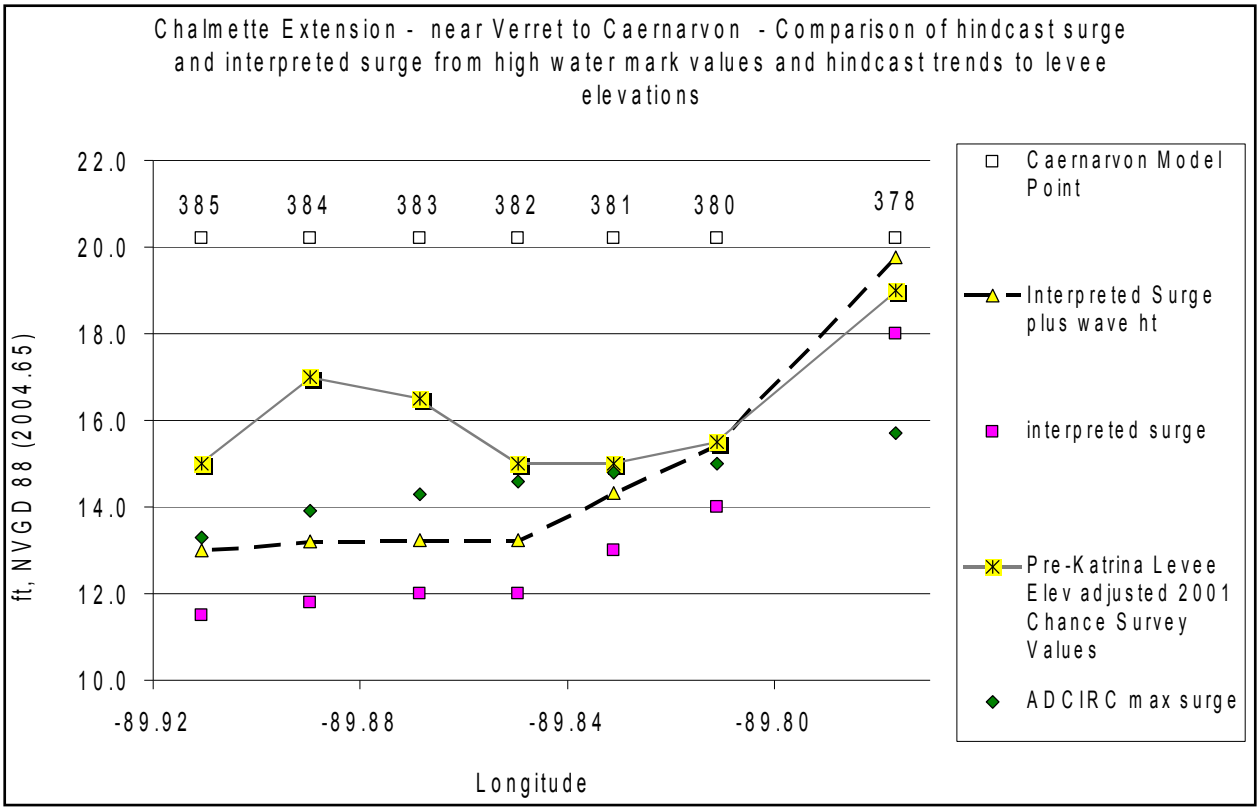

Figure 50. Estimated surges compared to levee heights along the Verret to Caernarvon levee

Figures 49 and 50 illustrate similar comparisons of maximum water level and levee elevation along two reaches of the Chalmette Extension Levee, 1) from MRGO to near the town of Verret and 2) from Verret to Caernarvon. Location of hydraulic data points are shown on Figure 47. Erosion damage was minimal in the first reach primarily because the storm surge was approximately at the levee crown. Erosion damage in the second reach was also minimal and the data shows little to no overtopping. Note the calculated surge is overestimated when the high water mark survey is considered (e.g., interpreted surge is lower than calculated).

Figure 51 shows the approximate location of another set of erosion tests conducted by ERDC/GSL on the relatively undamaged levee near Verret. These tests confirmed the high erodibility resistance of the dark fat clay (CH) soil surface. Figure 52 shows two typical pre-Katrina soil borings along this reach, with an upper clay layer from local borrow covering sandy/silty layers from dredged fill. Figures 53 and 54 show typical minimal erosion damage indicated on LIDAR profiles along this reach. Figure 55 shows the breach at pump station 8, and figure 56 shows the levee crown elevation drop below 15 ft. Note that the modeled hydraulic loading height approximately equaled the levee crown elevation below 15 ft, which explains the observed levee crown integrity and lack of significant erosion along this reach.

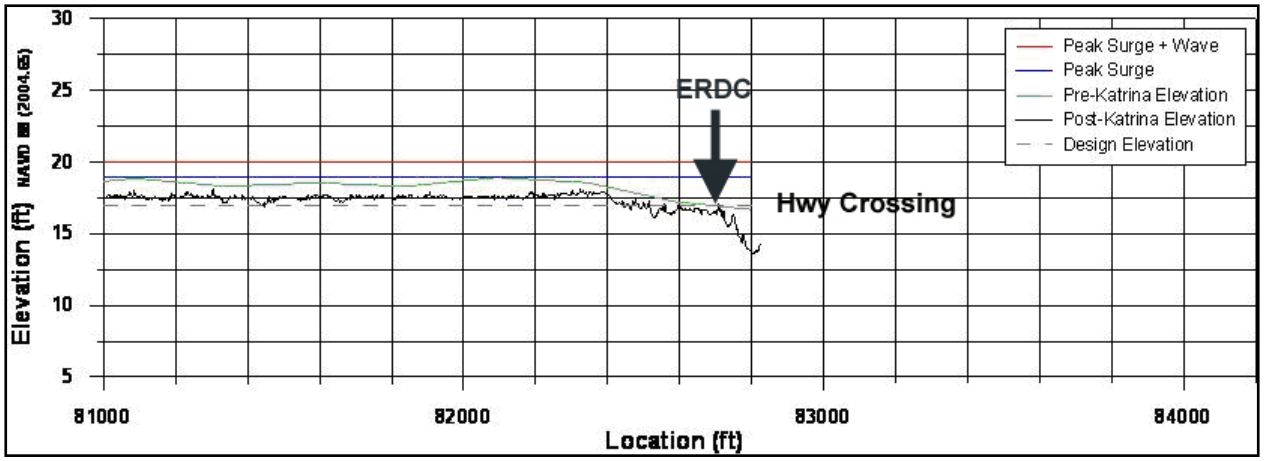

Figure 51. Approximate location of ERDC erosion tests near Verret. Erosion damage was minimal even with the drop in pre-Katrina levee elevation.

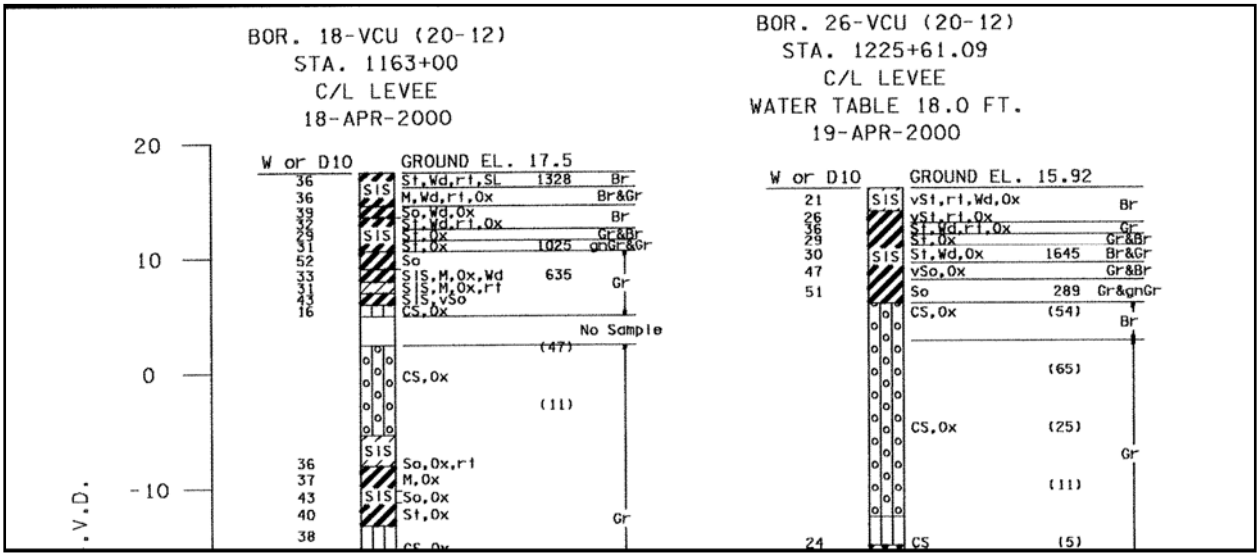

Figure 52. Soil borings in the reach between Verret and Caernarvon, typically consisting of sandy hydraulic fill covered with a clay cap hauled from local borrow area.

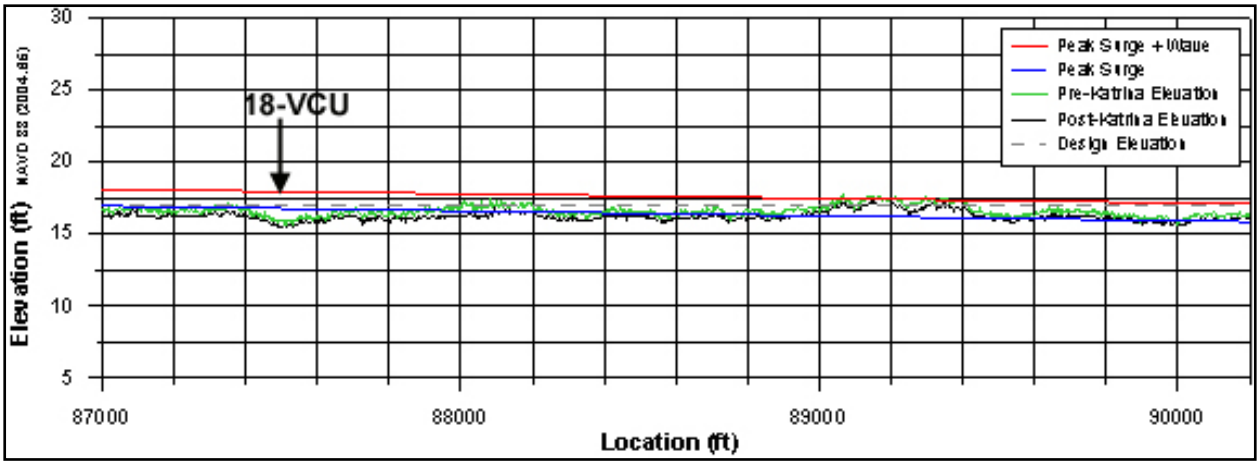

Figure 53. LIDAR plot of levee west of Verret.

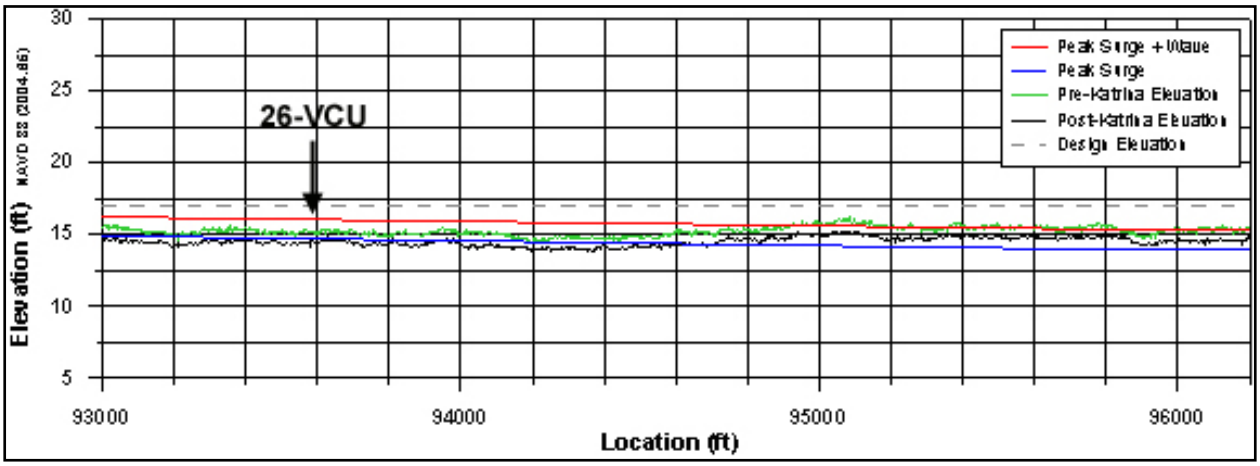

Figure 54. LIDAR plot of levee west of Verret.

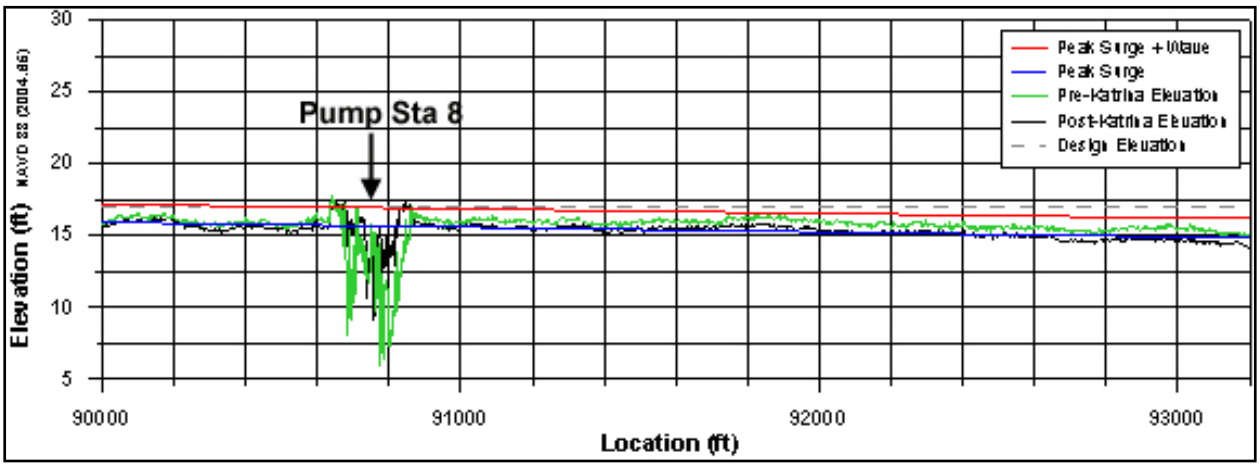

Figure 55. LIDAR plot of levee west of Verret.

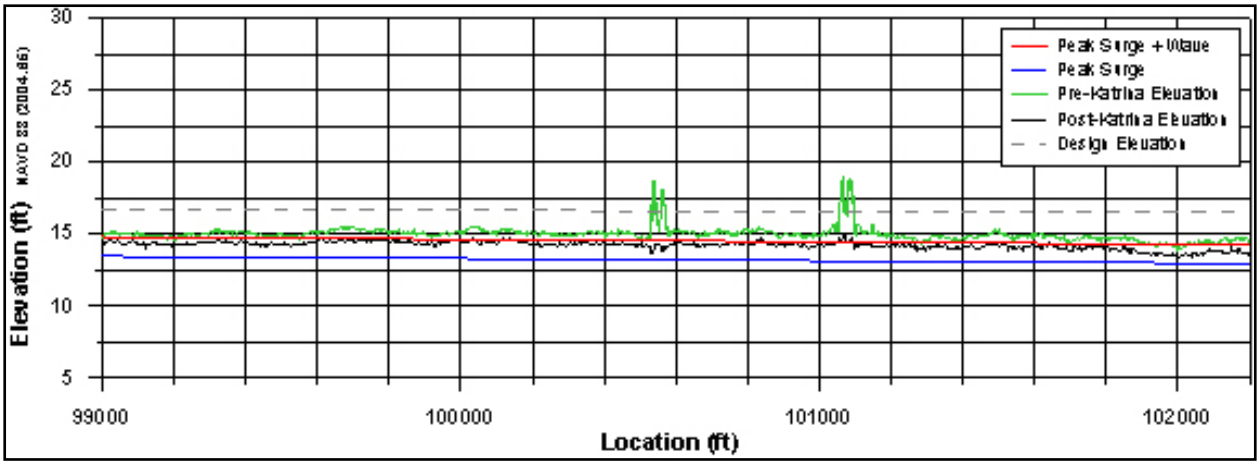

Figure 56. LIDAR plot of levee west of Verret showing drop in levee crown height along the reach near twin pipeline crossing. Note that the modeled hydraulic loading height also drops.

The levee from the MRGO to Caernarvon was typically constructed with a fat clay cap on top of a sandy "core", (see Figure 27) and performed much better than the MRGO levee with fewer breaches and less erosion. The hydraulic loading (storm surge plus wave heights) varied from about 1 ft above the crown in the MRGO vicinity to 3 ft below the crown nearer Caernarvon.

Summary

Two variables played a major role in determining the extent and amount of levee damage. The hydraulic loading (storm surge and wave action) from the hurricane was the driving influence of course, but the levee damage was not a continuous function of overtopping surge and wave heights. The levee response (failure versus functional) was also determined by pre-Katrina geotechnical issues (soil type, soil layering, soil consistency, and levee construction methods).

Combined with visual high-water surveys and numerical computer modeling performed by IPET Storm Team, the storm surge elevations and wave heights during the hurricane were estimated (hindcasted). The wave heights were typically from about 2 ft to 4 ft above the maximum estimated storm surge heights. In general, the extent of damaged (eroded and breached) levees was greater where the overtopping surge and wave heights were greater, as evidenced by miles of missing levee sections along the MRGO that had about 7 ft water overtopping. The most damage-resistant levees (those with smaller amounts of erosion damage) appeared to be those having a fat clay cover with higher stiffness (density). The levee sections having thicker layers of clay (less layering heterogeneity) also appeared to perform better, as did those constructed from hauled borrow soil (versus non-compacted hydraulic fill).

Minimal forensic evidence was available to validate geotechnical correlations to surge elevation since the damaged levee data were taken from historic soil borings at limited locations. Only the most recent (mid 1990s to 2001) soil borings showed the pre-Katrina soil profile since previous borings generally were drilled through levees prior to their final construction lifts. The

near-surface soils that poorly performed were washed away and were unavailable for analysis. Dynamic effects such as erosion progression and dynamic slope stability issues due to cyclic hydraulic loading were also not analyzed due to insufficient hydraulic and geotechnical forensic evidence.

References

U.S. Army Corps of Engineers, New Orleans District. 1971. *Lake Pontchartrain, Louisiana and Vicinity Lake Pontchartrain Barrier Plan Design Memorandum No. 2 – General Supplement No. 4, New Orleans East Back Levee.* New Orleans, LA.

TFG. 2005. St. Bernard Project Information Report.

Wibowo, J., Taylor, P., and Lee, L. 2006. "Soil erosion assessments of New Orleans levees: Post-Katrina visual observations and soil erosion tests," ERDC GSL Technical Report (to be published).

Attachment A
Soil Erosion Assessments of New Orleans Levees: Post-Katrina Visual Observations and Soil Erodibility Tests

by Johannes L. Wibowo, Perry A. Taylor, and Landris T. Lee, Jr., June 2006

Background

This report provides an overview of observed post-Katrina soil erosion on levee structures, primarily in the Orleans and St. Bernard Parishes which took the brunt of overtopping erosion and breaching that caused severe economic impacts. Storm surge water overtopping is a primary functional failure mode for dams, levees, and floodwalls. Overtopping initiates surface erosion on the levee slopes, and progressive erosion leads to breaching which is a structural failure mode. A breached levee / floodwall implies that the structural integrity of the flood-protecting system has failed.

In particular, this report describes preliminary efforts to quantitatively assess the levee soil erodibility using an innovative in-situ erodibility test procedure. Although the majority of earthen levees were reconstructed prior to the subject testing, numerous tests were performed on both the existing and newly reconstructed levee systems in Orleans and St. Bernard Parishes.

Hurricane Katrina Levee Damage

The most prominent failure modes during the Katrina event were overtopping and breaching, based on "proxy" evidence such as eyewitness accounts, high-water marks, and barges resting on top of floodwalls (IPET 2006). Lengthy reaches (miles) of earthen levees and capped levees were overtopped. Some reaches showed signs of initial erosion, others showed signs of progressive erosion, and other reaches contained significant breaching. Similar to levees, lengthy reaches of floodwall were overtopped and were left in various stages of damage ranging from minor scour at the wall base to breaches where complete floodwall sections were flattened. Several stages of erosion and scour patterns were visually observed along numerous levee / floodwall reaches, and almost all patterns appeared to have been initiated on the backside (protected or land side) of the levee / floodwall.

Post-Katrina observations revealed that earthen levee backside erosion was caused by wave and water overtopping before and after the surge height exceeded the levee crest elevation (IPET 2006). If water overtops a levee and washes out (erodes) the backside slope, the lateral stress-resisting ability and the underseepage force-resisting ability will be compromised, depending on the degree of erosion. Progressive erosion of unprotected soil on the backside of levees and floodwalls likely contributed to breaching. Erosion damage at transitions between earthen levees and structures such as flood gates was also observed.

In the New Orleans East, Lakeshore, and St. Bernard Parish basins, approximately 50 miles of earthen levees overtopped but did not breach; approximately 20 miles of earthen levees

overtopped and contained significant breaches; approximately 7 miles of floodwall overtopped but did not breach; and approximately 2 miles of floodwall overtopped and had breaches. The majority of levees and floodwalls failed by overtopping, but did not breach.

In Plaquemines Parish, the Mississippi River mainline levee and the back levee lengths total about 162 miles. There are about 7 miles of floodwall (I-walls and sheetpile). All of the levees in Plaquemines Parish sustained overtopping damage, and there was considerable crown and slope scour along the total length. The mainline levee riverside slope pavement sustained damage from the hundreds of ships and barges that crashed into it. There were also several severe breaches, coinciding with pipeline crossings and with some floodwalls. Five of the 7 miles of floodwall were damaged beyond repair. There were major breaches at sheet pile wing walls at two pump stations in the back levee. A major breach occurred at the Shell pipeline crossing near Nairn, and the West Pointe a la Hache pipeline crossing was severely damaged.

Levee Soil Erodibility

Soil material properties greatly influence surface erodibility and erosion progression rate during overtopping. Cohesive (silt and clay) soils erode due to the formation and migration of a headcut perpendicular to the levee axis (i.e. across the levee section from the backside to the floodside). A headcut is a vertical or near-vertical elevation drop, and migrates upstream due to hydraulic stresses at the overfall, base seepage, weathering, and gravity (Hanson et al 2001). Sandy (non-cohesive) soil erosion involves a sediment transport process as the material is removed in layers. Cohesive soil erosion rates are more strongly influenced by soil material properties such as water content, density, erodibility, shear strength, and compaction effort during construction (Hanson et al 2003). For example, it was found that only a 5-point (5%) decrease in compaction water content caused a 100-fold increase in the breach widening rate for clay soil.

Characterizing soil erodibility is a complicated matter, due to spatial non-homogeneity and variability in soil types, difficulty in selecting accurate engineering properties needed to determine erodibility, and temporal effects during erosion progression such as surface roughness changes which in turn affect the hydraulic stress and turbulence conditions. Soil properties affecting erodability are soil classification (gravel, sand, silt, clay proportions); water content (antecedent moisture); clay mineralology and proportion; soil structure; Atterberg limits; organic content; pore water chemistry (salinity, hardness, quality, pH); in-situ density; erodibility parameters such as the critical shear stress required to initiate soil particle detachment, hydraulic shear stress, and erodibility coefficient; in-situ shear strength, and compaction effort during construction (optimum moisture content and optimum dry density values both specified and as-built).

The rate of erosion is proportional to the applied shear stress in excess of a critical shear stress and is also proportional to an erodibility coefficient (Hanson and Simon 2001). Soils with a lower critical shear stress tend to have a higher erodibility coefficient.

Levee geometry is important when analyzing erosion probability. A 1:3 side slope is steeper than a 1:4 slope, and a stabilizing berm slope acts as an overtopping energy dissipator. Water cascading down a 1:3 slope impacting a 1:20 berm slope would be more likely to initiate erosion than that on a 1:4 slope, and would also depend on slope distance between the crest and the toe, surface roughness, and water depth.

Hydraulic Loading

U.S. Army Corps of Engineers (USACE) guidance is silent on the topic of assessing levee soil erodibility for a levee backside. Guidance is available for designing floodside erosion protection features and hydraulic channel protection. Soil susceptibility to erosion as a function of water velocity is noted for hydraulic design. For example, EM 1110-2-1601 (USACE 1994) for Hydraulic Design lists average allowable water velocities on various channel surface materials (Figure 1).

Channel Material	Mean Channel Velocity, fps
Fine Sand	2.0
Coarse Sand	4.0
Fine Gravel[1]	6.0
Earth	
Sandy Silt	2.0
Silt Clay	3.5
Clay	6.0
Grass-lined Earth (slopes less than 5%)[2]	
Bermuda Grass	
Sandy Silt	6.0
Silt Clay	8.0
Kentucky Blue Grass	
Sandy Silt	5.0
Silt Clay	7.0
Poor Rock (usually sedimentary)	10.0
Soft Sandstone	8.0
Soft Shale	3.5
Good Rock (usually igneous or hard metamorphic)	20.0

Notes:
1. For particles larger than fine gravel (about 20 millimetres (mm) = 3/4 in.), see Plates 29 and 30.
2. Keep velocities less than 5.0 fps unless good cover and proper maintenance can be obtained.

Figure 1. Hydraulic channel velocity for several soil and rock types (USACE 1994)

Figure 2 shows a generalized cross sectional diagram of an overtopped levee (wave dynamics are not illustrated). The water crest height (y) and mean velocity (v) impart a shear stress (τ) on

the backside levee surface having a slope gradient (S). The majority of levees have slope gradients of 1V:3H (S = 0.33) or 1V:4H (S = 0.25).

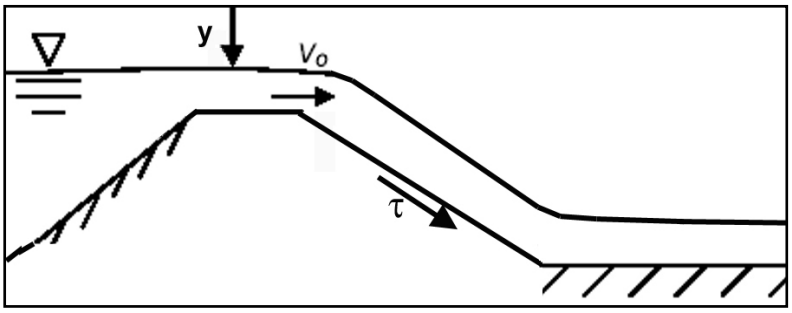

Figure 2. Conceptual diagram of water surge (without waves) overtopping an earthen levee

Overflow velocity and soil shear stress values may be estimated by making simple assumptions regarding the flow regime and using the following equations (Vennard and Street 1975). Assuming the Manning coefficient (n) for grassed levees is approximately 0.03, the friction factor (f) may be estimated as

$f = 258\ (0.03 / 1.49\ y^{0.16})^2$ where y = approximate overtopping crest depth, ft

and

$v = (258 / f)^{1/2}\ (Sy)^{1/2}$, ft/sec

For example, the approximate friction factor and overtopping velocity on a 1V:3H grassed slope with crest height of 1 ft is:

$f = 0.1$

and

$v = 29$ ft/sec

Soil shear stress (τ) is idealized by the equation

$\tau = \gamma y S$, where γ = unit weight of water

For example, the idealized shear stress imposed by a water depth of 1 ft on a 1V:3H slope is:

$\tau = \gamma y S = (63)(1)(0.33) = 21$ psf

These equations are shown only for the purpose of generally estimating the magnitudes of shear stress and overflow velocity for ideal flow. The actual shear stresses and overflow velocities present during the hurricane event were most likely different due to numerous non-ideal variables including turbulence, non-uniform flow fields, and wave dynamics. Figure 3 is a chart for estimating overtopping velocity due to various surge heights (wave effects not included).

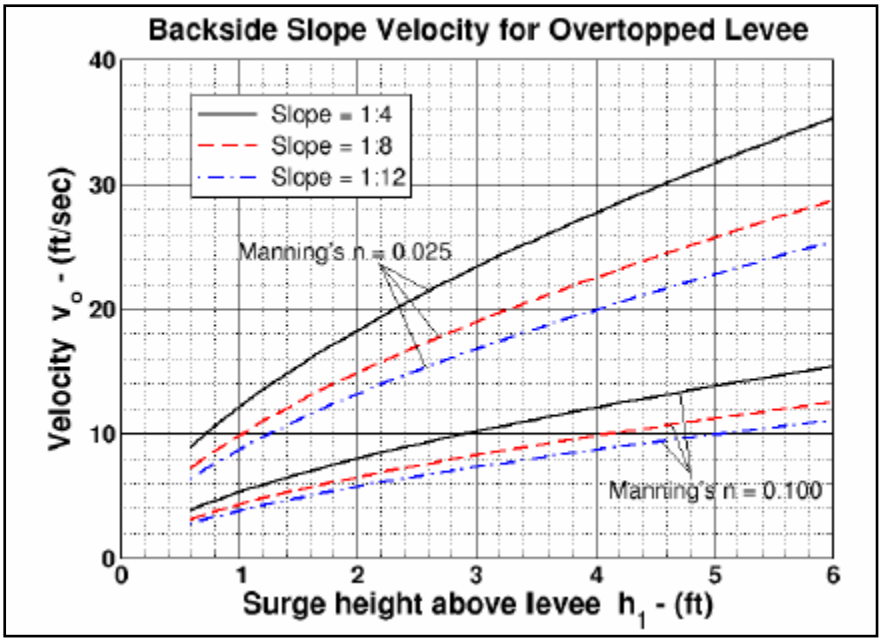

Figure 3. Overtopping velocity as a function of surge height (h_1 = y in above equations) (from Hughes et al 2006)

The New Orleans levee system was surveyed several years prior to and immediately after Katrina using aerial light detection and ranging (LIDAR), and the collected data was immensely useful to the New Orleans District's Task Force Guardian (TFG) who reconstructed the damaged levee system in less than a year after Katrina. Combined with visual high-water surveys and numerical computer modeling performed by ERDC, the storm surge heights and wave heights during the hurricane were estimated. The wave heights typically ranged from 2 ft to 4 ft above the maximum storm surge heights (IPET 2006). Combining the LIDAR elevation data and hydraulic data allowed pre- and post- hurricane comparisons of levee crown heights with erosion depths as well as correlation to hydraulic loading.

Post-Katrina Erosion Observations

An earthen levee that is overtopped will exhibit identifiable stages of backside (landside or protected side) erosion progression (Hunt et al 2005, Fukuoka and Fujita 1988). Figure 4 is an illustration of four erosion progression stages, and the following paragraphs describe erosion progression as a function of time. Photographs taken around the Greater New Orleans area after the storm are included to provide examples of observed erosion stages.

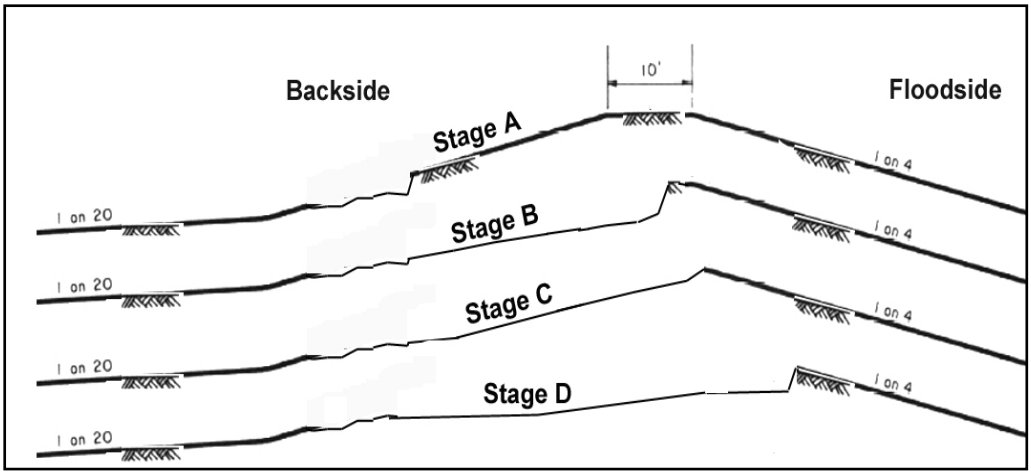

Figure 4. Erosion progression stages

Stage A. Initial overtopping causes surface sheet and rill erosion which develops into a series of cascading overfalls. The highest forces develop from the backside slope down to the backside toe, and the crown is not initially exposed to these large hydraulic forces. The cascading overfalls develop into one large headcut that migrates from the slope to the crest such that the erosion width approximately matches the overtopping width.

Figures 5 and 6 show examples of Stage A initial overtopping erosion on the Citrus Back Levee backside along the north bank of the GIWW in New Orleans East. The levee crown was elevation 14 to 15 ft and storm surge from the GIWW was approximately 15 to 17 ft, so the overtopping crest depth was about 1 to 2 ft, with overtopping velocities approaching 20 fps. Historic soil borings along this reach indicated non-homogeneity in the surficial layers of the levee crest and slopes, and cohesive soils with interbedded layers of silt and/or sand were typical.

Figure 5. Stage A erosion on the Citrus Back Levee

Figure 6. 600’ reach of levee along the north bank of the GIWW (Citrus Back Levee, New Orleans East) between Elaine Pump Station and Paris Road.

Figure 7 shows a closeup of landside slope erosion between the Paris Rd overpass and the Elaine Pump Station on the north bank of the GIWW (Citrus Back Levee, New Orleans East). Erosion damage measured 24’ (length) x 13’ (width) x 8” (depth). Note the headcut that developed up the slope toward the crest.

Figure 7. Another example of Stage A erosion along the Citrus Back Levee

There is a possibility that the erosion shown in Figure 7 was pre-existing, as seen in the pre-Katrina satellite photo below (Fig 8).

Figure 8. Possible pre-existing surface erosion on levee slopes along the north bank of the GIWW (Citrus Back Levee) at N 30deg 0 min 7 sec W 89deg 58min 31 sec. (pre-Katrina image from GoogleEarth website). Possible erosion is evidenced by vegetation distress and bare spots along the levee.

Figure 9 shows backside slope erosion and minor erosion on the stabilizing berm slope along the south bank GIWW levee between Sta. 65+008 and STA. 277+20 in St. Bernard Parish. The General Design section for the south bank GIWW indicated that the levee was built to approximate elevation 14 ft. circa 1970, and an additional lift up to elevation 19 was added circa 1985. Post-Katrina LIDAR along the south bank GIWW showed the uneroded levee crown was up to approximate elevation 16 ft. Storm surge along the GIWW was approximately 15 to 17 ft, causing an estimated overtopping depth of approximately 1 to 2 ft. Drawing 9 of 19, New Orleans District file H-8-45533, shows several layers of stiff lean clay (CL) at centerline top of levee (boring elevation 16.8 ft) from the 5/11/2000 soil boring 5A-CAU, B/L Sta 135+50.

Figure 9. Stage A erosion on south bank GIWW levee, St. Bernard Parish

Figure 10 shows two soil borings in the levee reach east of pump station 15 on the East Back levee (north bank of the GIWW). Borings 42-U and 43-U both had surface soils composed of medium-stiff CL. The location of boring 42-U was approximate Sta 832+00, and boring 43-U was approximately 4000 ft to the east. The modeled storm surge and wave heights at the 42-U location approximately matched the levee crown elevation, but were approximately 0.5ft higher than the crown elevation at the 43-U location. No crown erosion occurred at either location, based on post-Katrina LIDAR surveys, typified in Figure 11 along this reach.

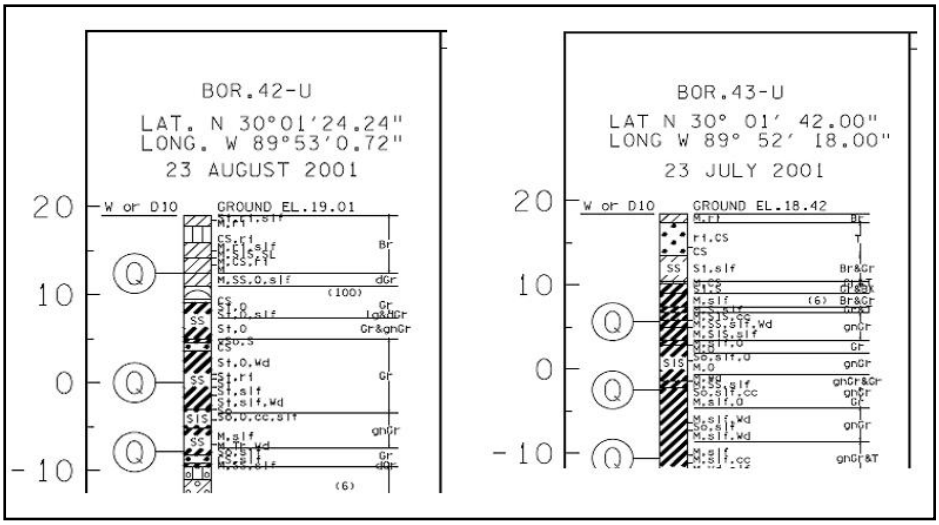

Figure 10. Soil borings 42-U (approximate B/L Sta 832+00) and 43-U (approximate B/L Sta 872+00) west of pump station 15

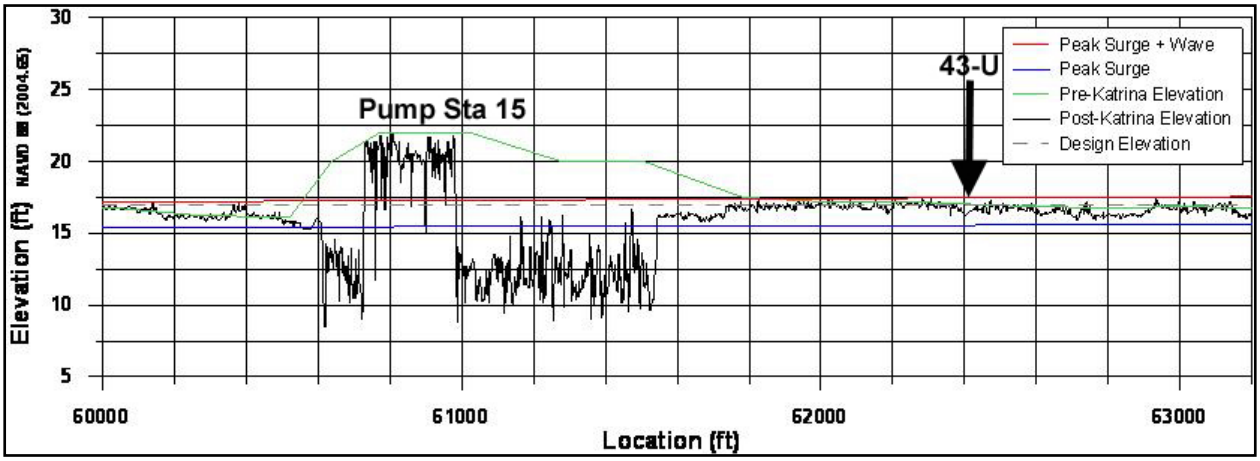

Figure 11. Typical post-Katrina LIDAR profile along the East Back levee west of pump station 15, showing approximate location of soil boring 43-U (from IPET 2006)

Stage B. The headcut continues to migrate from the backside crest (crown) to the floodside crest.

Figure 12 shows soil boring 44-U located at approximate B/L Sta 913+00, east of pump station 15 along the East Back levee (north bank of the GIWW). The surface soil consisted of medium-consistency fat clay (CH). Numerous Stage B incidents occurred along the reach east of pump station 15, with the majority becoming full-blown levee breaches (discussed later). Figure 13 shows the LIDAR profile with surge height approximately at the same elevation as the levee crown and wave height approximately 2 ft higher. Crown scour was approximately 0.5 ft at this location.

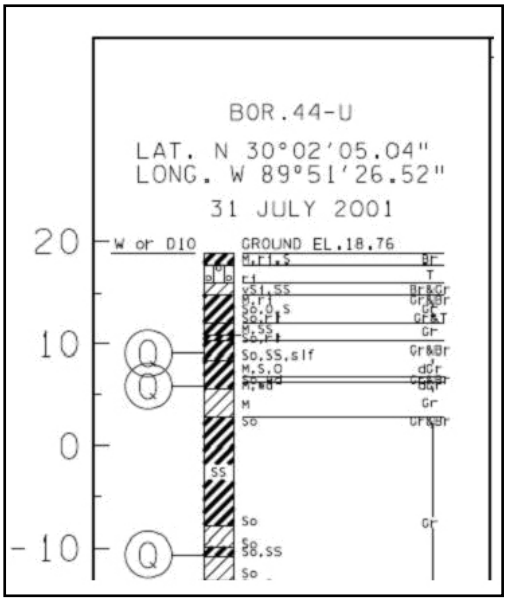

Figure 12. Boring 44-U on north bank of GIWW (East Back levee) east of pump station 15

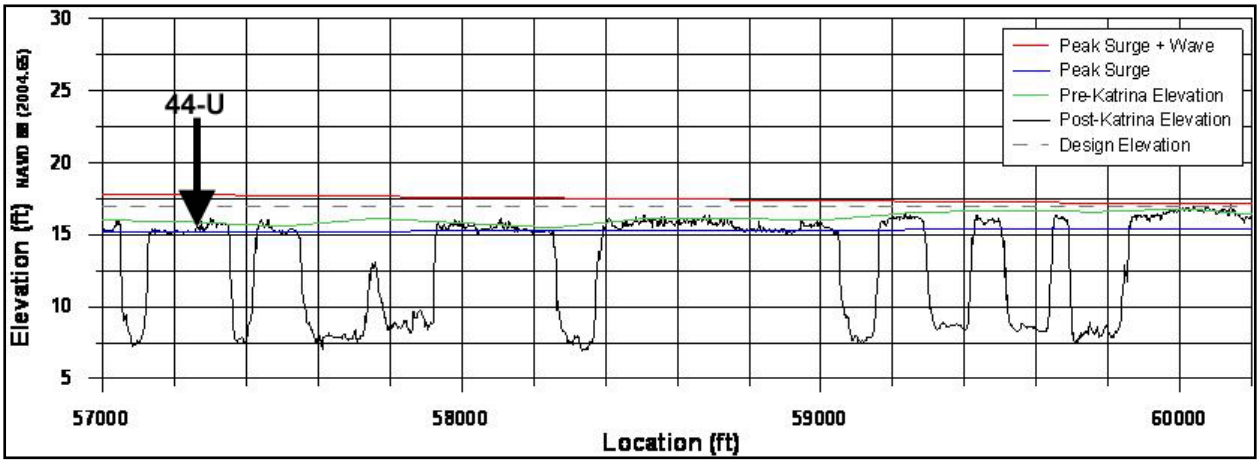

Figure 13. Post-Katrina LIDAR profile east of pump station 15, Orleans East Back levee, north bank of GIWW

Figure 14 shows a short levee section with Stage B erosion on the west side of the IHNC protecting the container terminal between France Rd. and IHNC. The headcut extends to the top crest elevation, and a breach almost developed. The unscoured soil surface is a fat clay and the eroded soil visually appears to be a shell hash mixture of clay and oyster shell fragments.

Figure 14. Crown erosion (stage B) on the remaining west side IHNC levee between IHNC and France Rd. ramp

Figure 15 shows a small section of the levee between Bayous Bienvenue and Dupre, viewed to the south from approximate B/L Sta 570+00. The MRGO is to the left of photo. Approximately 6.2 miles of levee along the MRGO were overtopped and breached at numerous locations. Storm surge along the MRGO was approximately up to 21 ft, so the approximate overtopping depth was about 5 ft along this reach. Soil boring 12BU-CHBD (01-16834) from 2001 at Sta 570+00 (Figure 16) shows the top 1.4 ft of levee (at crown elevation 16) was composed of lean clay (CL), with fat clay (CH) layers underneath. At a depth of 8.5 ft below the crown, a shear Q test indicated cohesion value 270 psf at 51% water content and 68 pcf dry density in a CH layer. At a depth of 16.8 ft, cohesion was slightly higher (396 psf) at 62% water content and 62 pcf dry density, also in a CH layer. This low strength profile indicates that the levee's ability to withstand hydrodynamic pressure loading would be seriously impaired if the levee footprint was reduced. There were numerous locations along this reach where the footprint was significantly reduced due to soil loss on the backside, which most likely accelerated breaching progression.

Figure 15. Stage B crown erosion on remaining levee southeast of Bienvenue Control Structure

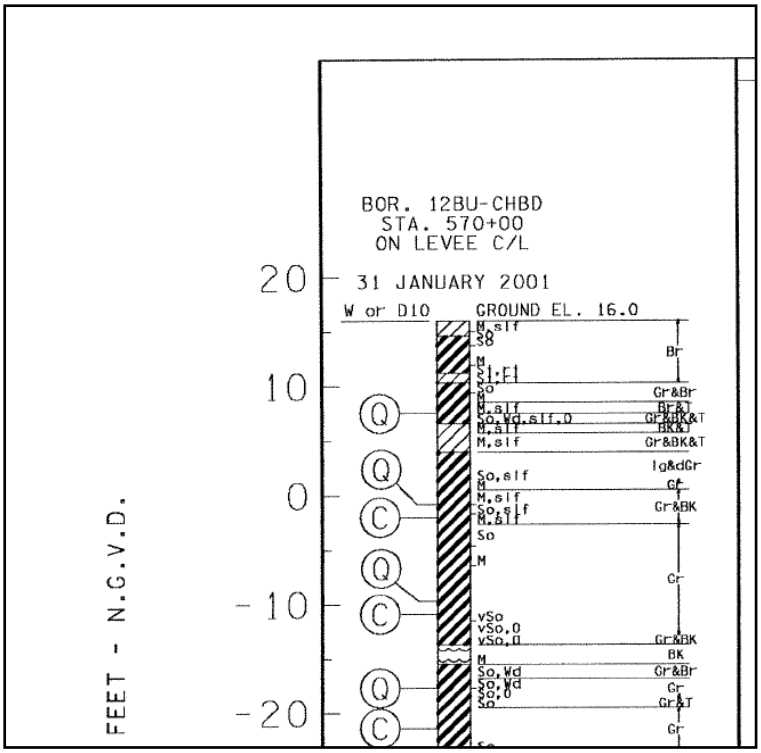

Figure 16. Soil boring 12BU-CHBD approximately located in above Figure 15.

Figure 17 shows the LIDAR profile along the reach where boring 12BU-CHBD was taken. Maximum wave and surge overtopping was approximately 5 ft, with scour depth approximately 6 ft.

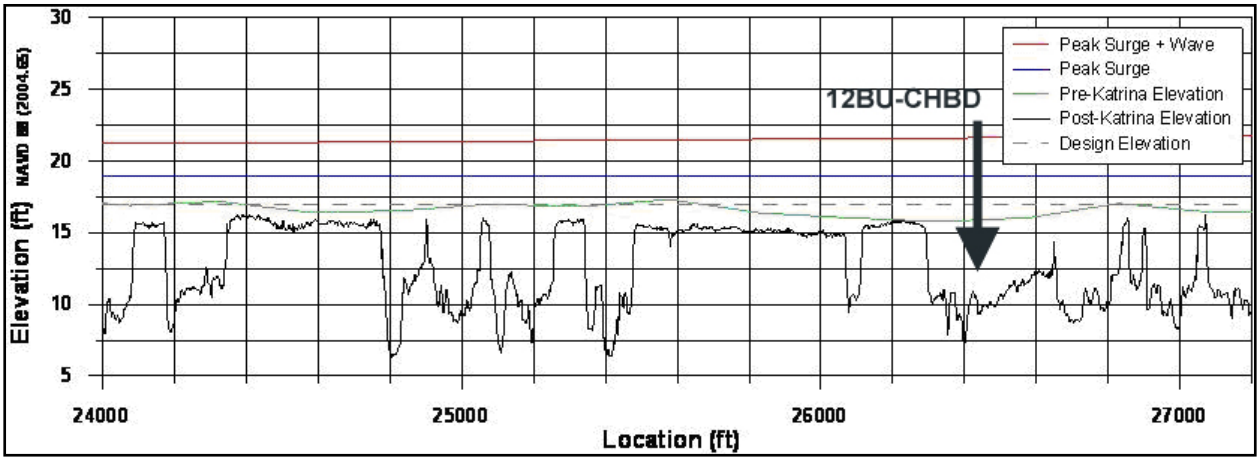

Figure 17. LIDAR plot showing approximate location of soil boring 12BU-CHBD, scour depths, and hydraulic loading (from IPET 2006).

Stage C. The crest drops as a breach begins to develop.

Figure 18 shows Stage C crown scour along approximate B/L Sta 1203+00 to Sta 1230+00 on the St. Bernard levee between the MRGO and the Mississippi River. Crown elevation was

approximately 15 ft, but dropped to about 12 ft for about a mile in this eroded section. Storm surge and wave heights were up to 3 ft higher than the levee along this reach, and this was the only significant breach between Verret and Caervarnon. The levee along this reach was constructed of Mississippi River hydraulic sand fill, capped with local borrow material fat clay intebedded with silt and/or sand lenses, and shaped to grade with Mississippi River batture soil (truck-hauled fill). Similar to other levees' construction materials and history, this section contains heterogeneous soil layering probably compacted to different densities over a half-century or so timeframe. Figure 19 shows a pre-Katrina boring at Sta 1225+61 with a thin surface layer of very stiff lean clay underlain by very stiff fat clay and the hydraulic fill sand.

Figure 18. Stage C breach development on short reach of levee between Verret and Caernarvon

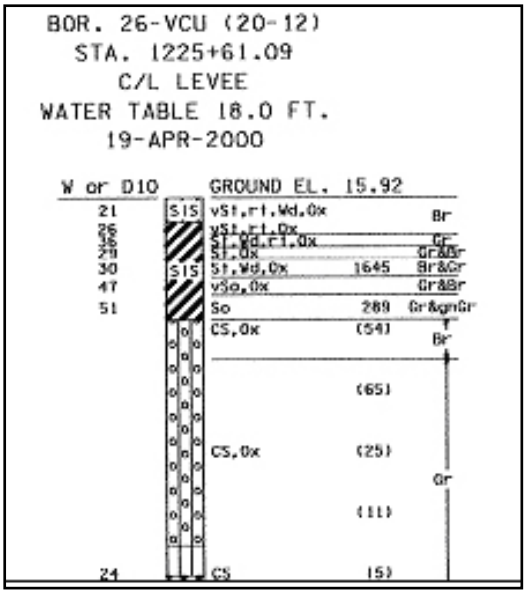

Figure 19. Soil boring taken along the reach between Verret and Caervarnon. Crown height approximately equaled the surge height at this soil boring location.

Figure 20 shows a section of Plaquemines Parish east bank back levee along Reach C (Phoenix to Bohemia, between river miles 59.3 and 44.3). Approximately 3 miles of crown erosion were noted along this 16-mile reach. This levee is approximate elevation 17 ft, and consists of a sand core with hauled-in clay blanket cap. Note the erosion has cut through the clay cap, moving clay blocks as erosion progressed downward to the sand layer.

Figure 20. Stage C breach along Plaquemines Parish levee

Stage D. The breach opening erodes out to the toe and the breach widens.

Figure 21 shows the levee section east of pump station 15 (N.O. East Back Levee) on the north bank of the GIWW. Approximately 12,750 feet of this levee was completely degraded (Station 876+87 B/L to 1101+90 B/L). West of the pump station, 9,800 feet of levee was completely degraded (approx Sta 778+00 to 876+00). The levees in these reaches were constructed from GIWW hydraulic fill in staged lifts over a period of three years. Figures 22 and 23 show soil boring 45U and its LIDAR profile along the reach east of pump station 15. The thin surface layer was composed of medium-consistency lean clay (CL) underlain by stiff CL. Hydraulic loading consisted of an approximate wave height of 2ft and surge height approximately at crown elevation, but the resulting scour depth was approximately 8 ft. Figure 24 shows a localized breach in the levee east of pump station 15 that widened out but stopped before spreading to the adjacent levee, indicating a localized area with higher soil erodibility.

Figure 21. Stage D erosion east of pump station 15, N.O. East Back levee

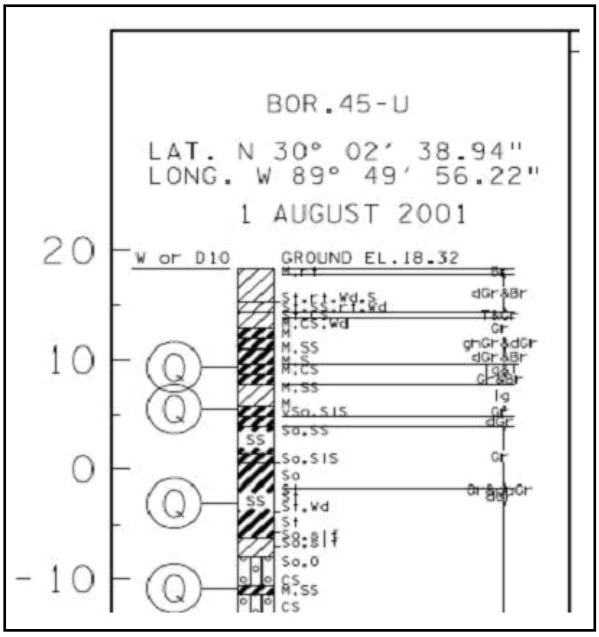

Figure 22. Soil boring 45-U at approximate B/L Sta 1003+00 on the GIWW north bank.east of pump station 15

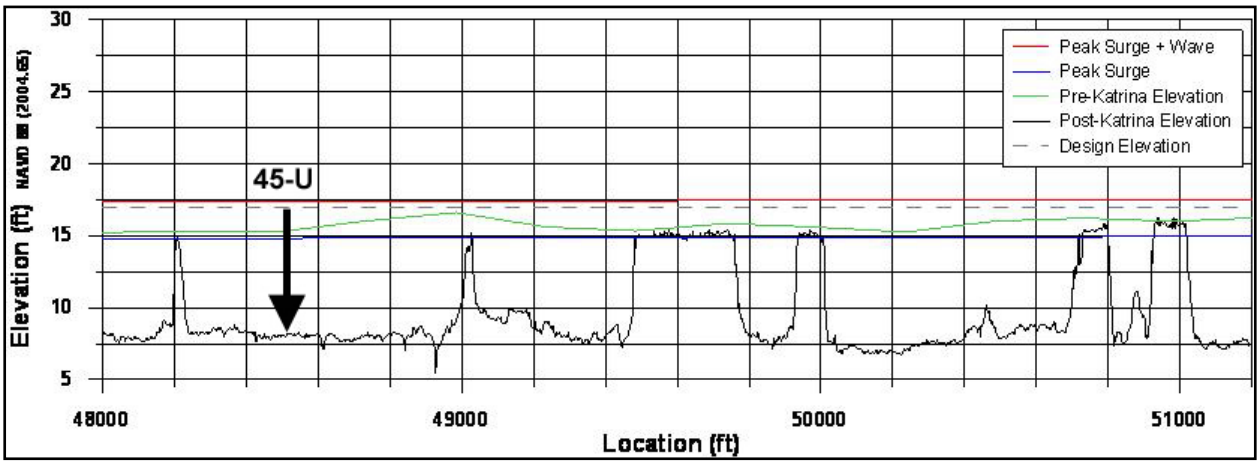

Figure 23. LIDAR profile east of pump station 15 showing approximate location of soil boring 45-U.

Figure 24. Localized Stage D breach east of pump station 15 on the East Back levee

Figures 25 and 26 are photos of a 19,000 ft. levee reach between Bayou Bienvenue (Sta 383+00) and Bayou Dupre (Sta 704+00) that lost approximately 12' of levee height from its original (design) height 17.5 ft, and a 2300 ft levee reach that only lost about 8 ft height. Storm surge and wave overtopping between Bienvenue and Dupre ranged from approximately 3 ft to 7 ft, with the highest overtopping occurring closer to Bayou Dupre (IPET 2006).

Figure 25. Stage D erosion between Bienvenue and Dupre structures, St. Bernard Parish

Figure 26. 2,300 ft. of levee between Bayou Bienvenue (Sta 383+00) and Bayou Dupre (Sta 704+00) that only lost 50% of original height.

Hydraulic fill from the MRGO channel formed the levee between Bienvenue and Dupre. Soil boring 9BU-CHBD (Figure 27) from 2001 at Sta 445+00 shows the top 1.5 ft of the levee (elevation 18.1 ft) was composed of medium stiff lean clay (CL). The underlying layers are mostly fat clay (CH) with interbedded lean clay layers. At a depth of 9.7 ft below the crown, a shear Q test indicated cohesion value 238 psf at 32% water content and 88 pcf dry density in a CH layer. Figure 28 shows the approximate location on the LIDAR plot, indicating approximately 5 ft erosion depth.

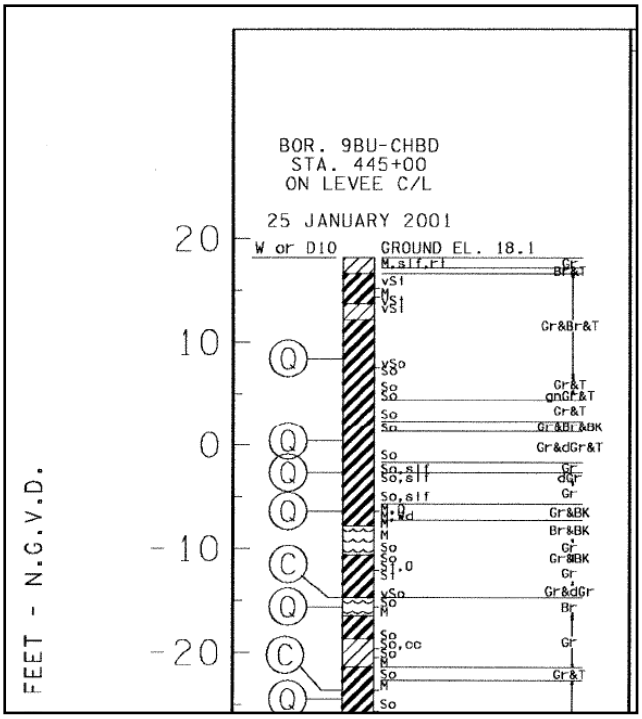

Figure 27. Soil boring 9BU-CHBD at Sta 445+00.

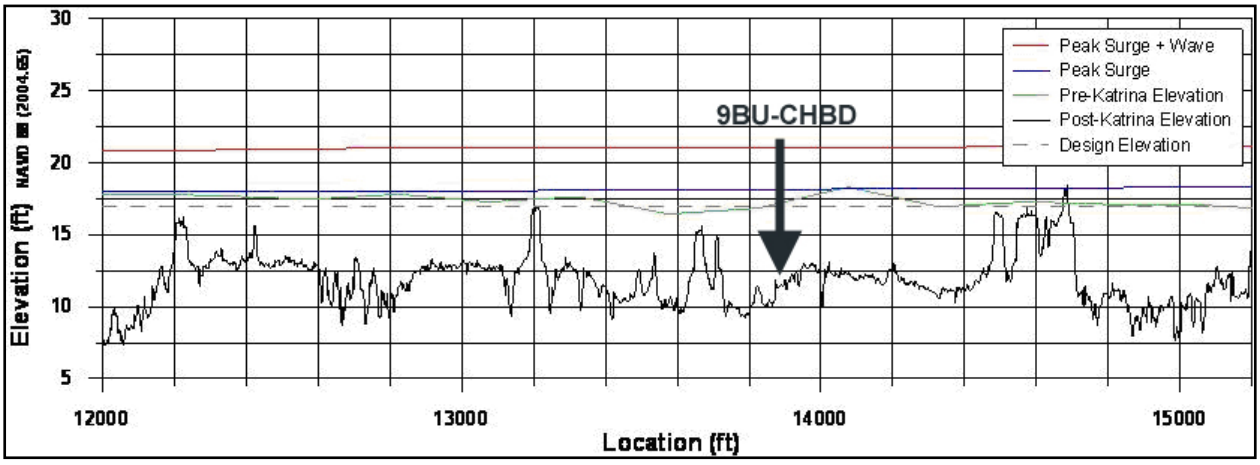

Figure 28. Approximate location of soil boring 9BU-CHBD with scour depth approximately 5 ft from overtopping surge plus wave height 3ft above crown.

Soil boring 11BU-CHBD (Figure 29) from 2001 at Sta 509+00 shows the top 2 ft of levee (elevation 17.4) was composed of soft fat clay (CH), with a 1-ft thick layer of poorly graded sand (SP) underneath. At a depth of 15.4 ft below the crown, a shear Q test indicated cohesion value 238 psf at 56% water content and 64 pcf dry density in a CH layer. Figure 30 shows the approximate location on the LIDAR plot, indicating approximately 10 ft erosion depth. Storm surge plus wave heights were approximately 5ft above the levee crown.

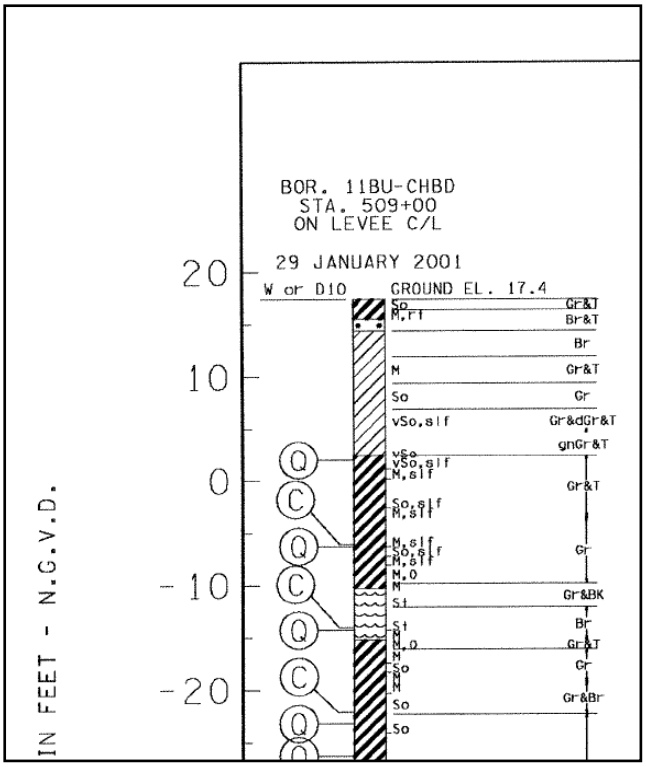

Figure 29. Soil boring 11BU-CHBD at Sta 509+00 with soft clay surface

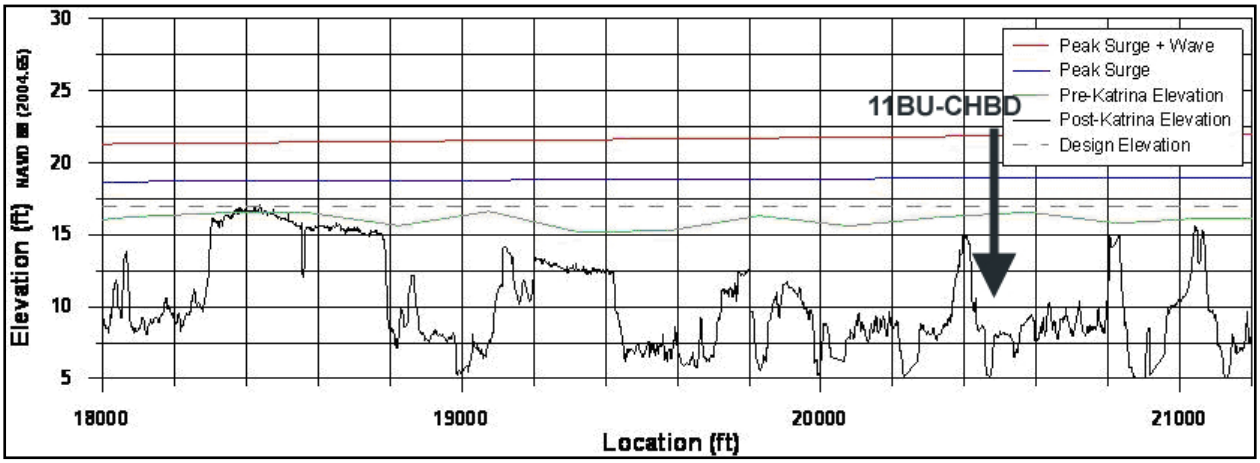

Figure 30. Approximate location and scour near soil boring 11BU-CHBD

Soil boring 18-UBD (Figure 31) at B/L Sta 596+00 shows the top 5.8 ft of levee (elevation 14.4) was composed of sandy silt (SM), with CH layers underneath. At a depth of 12 ft below the crown, a shear Q test indicated cohesion value 396 psf at 27% water content and 95 pcf dry density in a CL layer. Figure 32 shows the LIDAR plot with approximate location and scour depth.

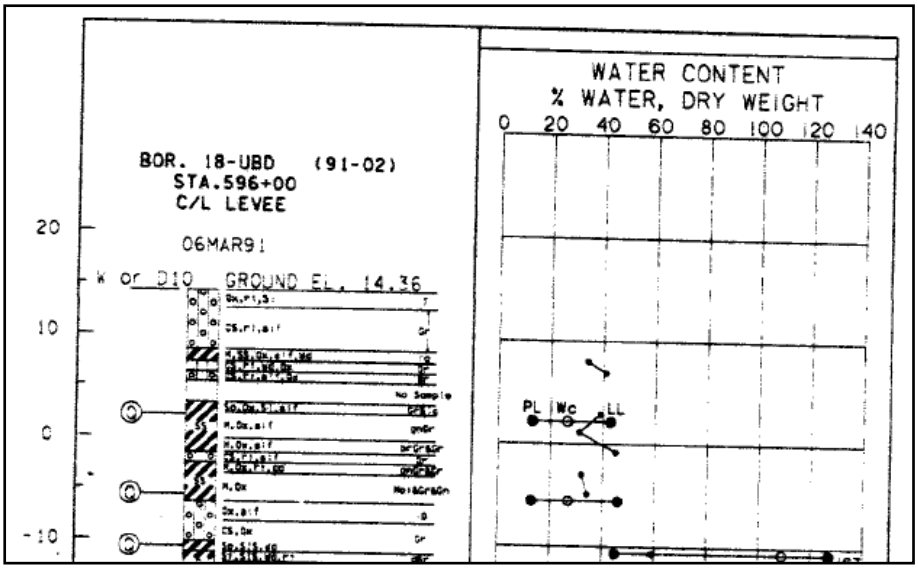

Figure 31. Soil boring 18-UBD.

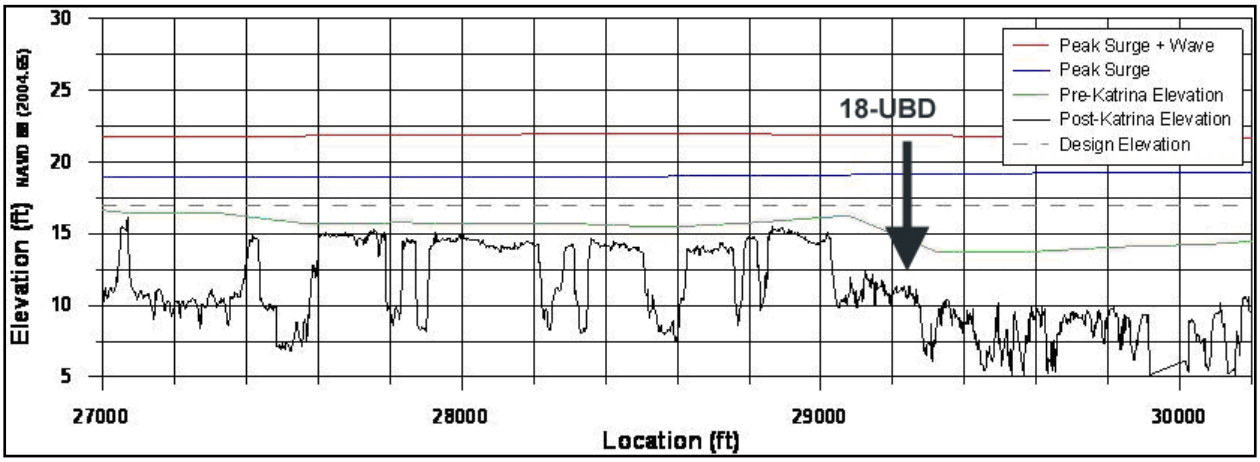

Figure 32. LIDAR plot showing scour depth of approximately 6 ft from 7ft water overtopping (surge plus waves)

Soil boring 13BU-CHBD (Figure 33) at Sta 614+00 shows the top 25 ft of levee (elevation 15.4) was composed of medium fat clay (CH), with organic clays and peats underneath. At a depth of 5 ft below the crown, a shear Q test indicated cohesion value 632 psf at 29% water content and 92 pcf dry density in the CH layer. Figure 34 shows the LIDAR plot with approximate location and scour depth (less than 1ft). Surge plus wave loading was about 7 ft.

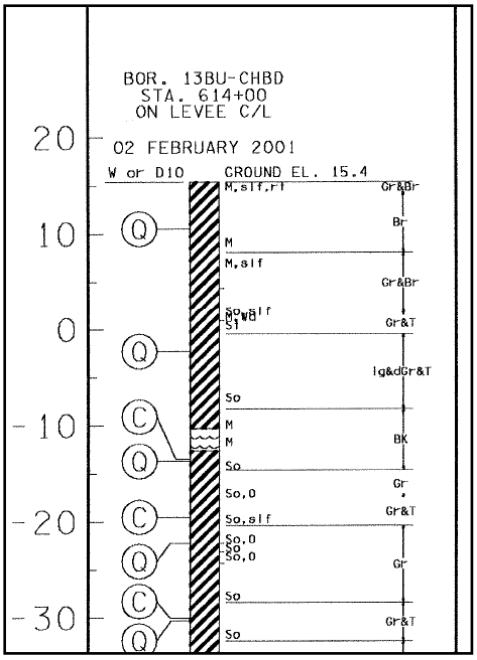

Figure 33. Soil boring 13BU-CHBD at Sta 614+00

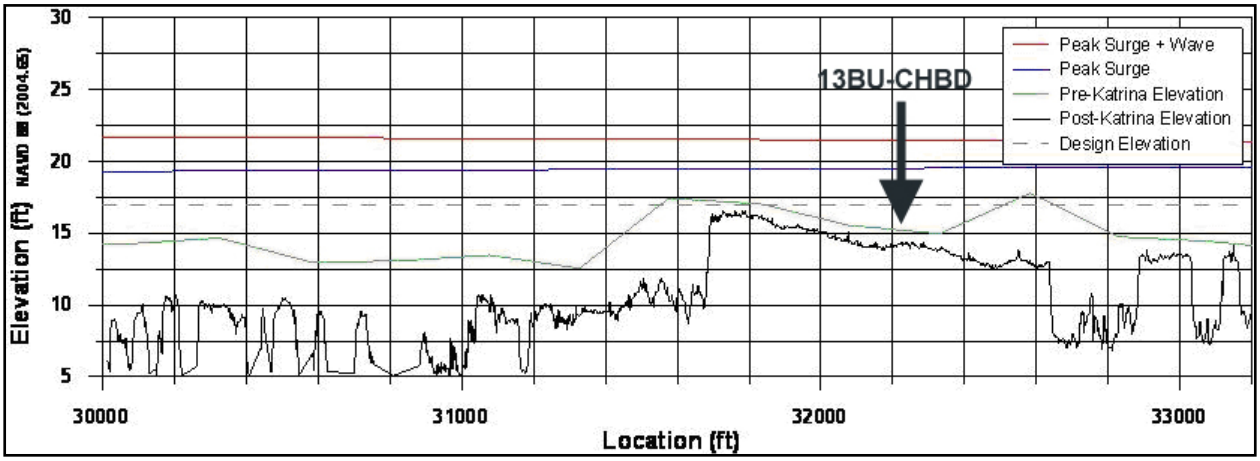

Figure 34. LIDAR plot showing approximate location and scour depth

Figure 35 is a photo of the damage near the Dupre Structure.

Figure 35. Stage D scour at the floodwall / levee at the southeast side of Bayou Dupre control structure

Figure 36 shows a portion of the 8,000 ft. section of the levee immediately southeast of Bayou Dupre (St. Bernard Parish) that was severely damaged and not only lost approximately 12 feet of original levee height but also part of the original levee foundation. The storm surge and waves overtopping this section of levee were approximately 7 ft. above the crown height. Figure 37 shows another portion of the levee southeast of Dupre.

Figure 36. Stage D erosion southeast of Dupre Control Structure

Figure 37. 2,500 ft. of levee from Dupre Control Structure to Sta 1007+91 that lost approximately 8' of elevation.

A soil boring (Figure 38) through the levee crown southeast of Dupre (7600 ft distant) was logged in 1981 and showed the top 3 ft consisted of stiff lean clay (CL), fat clay (CH), silt (ML or MH), and intebedded lenses of silt and/or sand. Any of these layered soil materials may have contributed to erosion initiation and progression. Surge plus wave overtopping was approximately 5 ft along this reach, and the scour depth was approximately 7 ft (Figure 39).

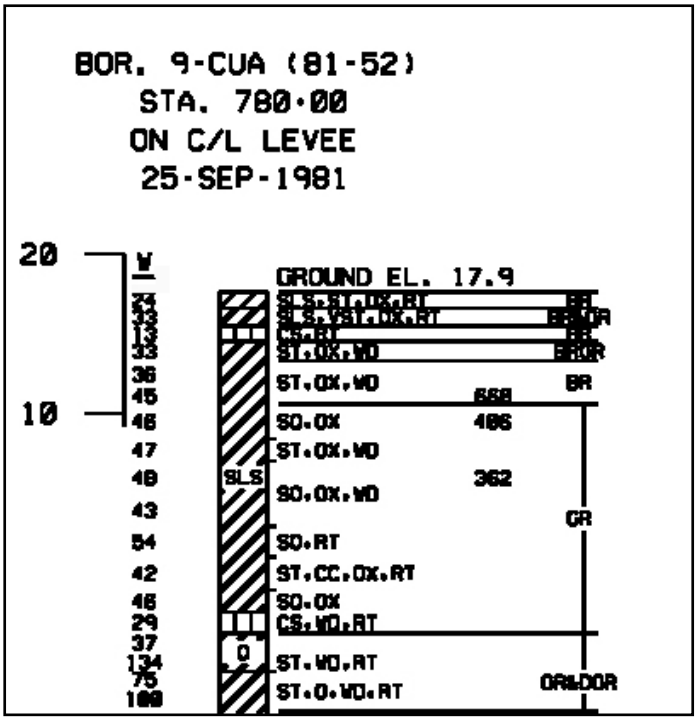

Figure 38. 1981 soil boring at Sta 780+00 near Dupre shows top layer of lean clay (CL) underlain by fat clay (CH), silt (ML or MH), and silt / sand lenses (SLS) in the CH material (from drawing 9 of 10, TFG contract solicitation W912P8-06-R-0002)

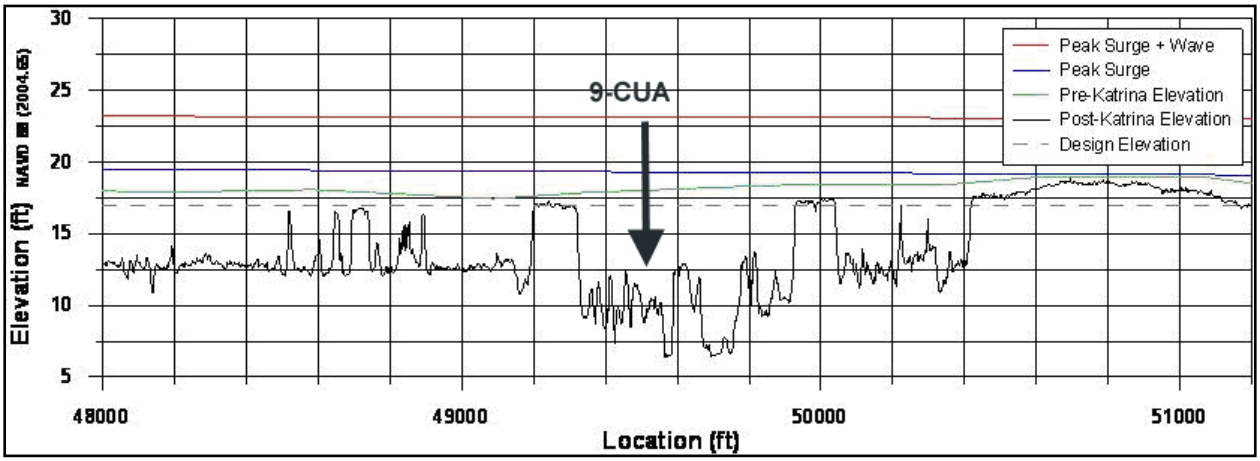

Figure 39. LIDAR plot of approximate location and scour depth.

Figure 40 shows a sheetpile / levee transition along the MRGO southeast of Dupre at B/L Sta 980+58. Note that scour occurred behind the sheetpile wall and minimally beyond the levee transition. Approximate sheetpile elevation was 17 ft and levee crown elevation was 13 ft. Beyond the transition, the levee crown elevation was approximately 17 ft. The approximate surge and wave overtopping drop was 7 ft above the soil at the sheetpile base and 4 ft over the transition levee, thus the overtopping water velocities were different. Nearest soil boring 10-CUHA (Figure 41) from 1991 at Sta 976+00 in the sheetpile reach shows the top 4 ft of levee (elevation 13) was composed of lean silt and clay (ML and CL) with CH layers underneath.

Figure 42 shows the LIDAR plot. An earlier (1985) boring at Sta 989+00 (about 800 ft beyond the sheetpile/levee transition) showed the levee section was composed of fat clay (CH) with interbedded silt lenses (Figure 43). Figure 44 indicates minimal erosion occurred beyond the sheetpile transition.

Figure 40. Sheetpile-to-levee transition showing significant scour behind the sheetpile and minimal erosion on the levee southeast of Dupre.

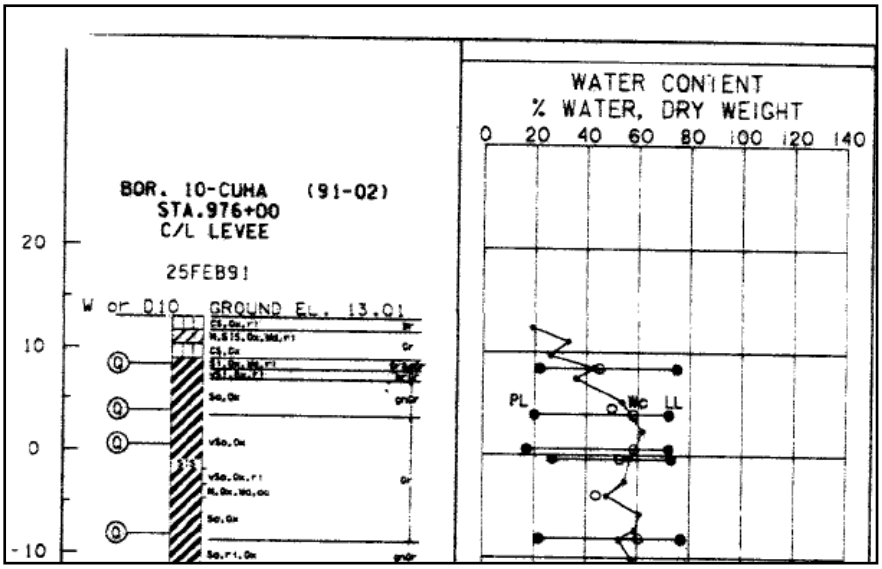

Figure 41. Boring 10-CUHA in the sheetpile reach. Note the soil layering typical of hydraulic fill.

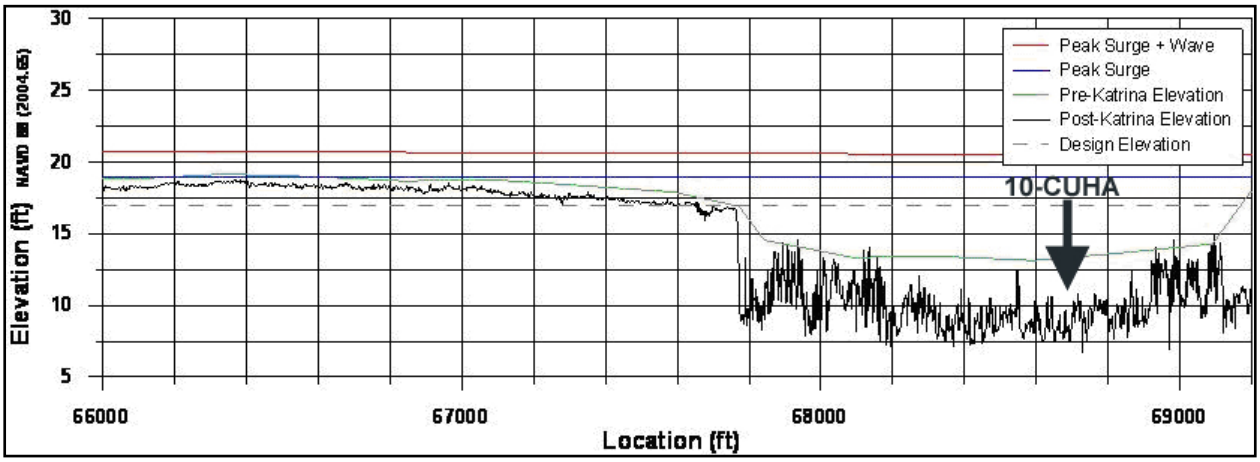

Figure 42. LIDAR plot showing approximate location of soil boring 10-CUHA in the sheetpile reach. Pre-Katrina crown elevation was 13 ft in 1991, and post-Katrina elevation was approximately 6 ft lower, indicating crown subsidence (settlement) in the 14 year period combined with Katrina scour.

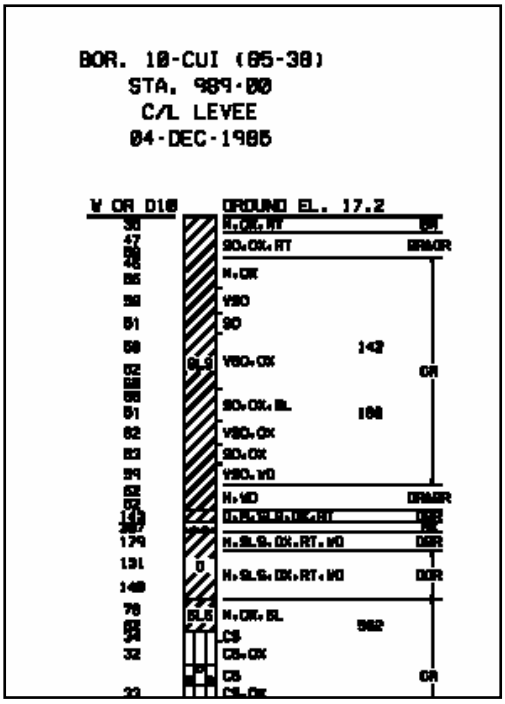

Figure 43. Boring 10-CUI beyond the sheetpile transition to levee. Top layer is fat clay.

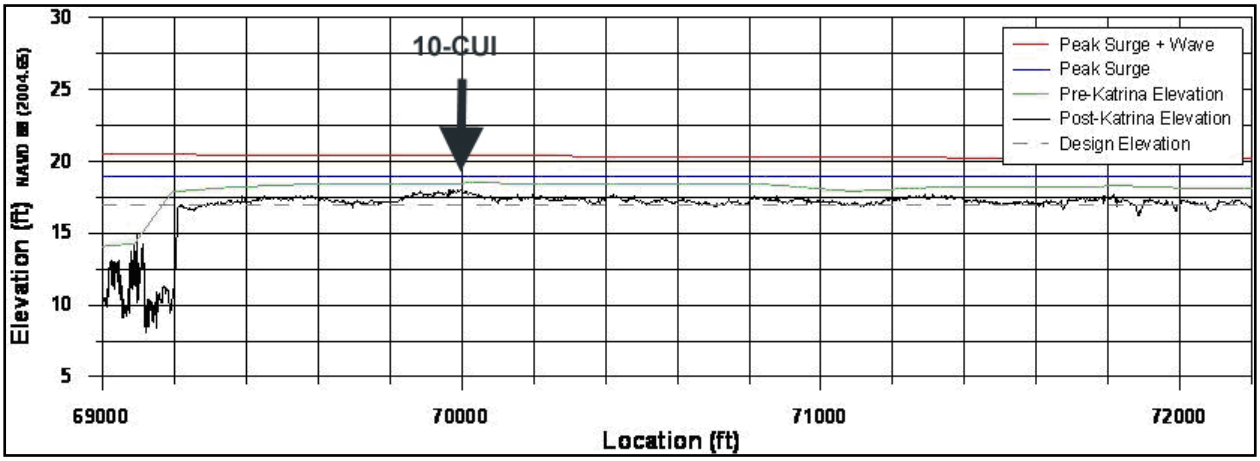

Figure 44. LIDAR plot showing minimal erosion at 10-CUI location.

Figure 45 is a graph of scour depths versus surge/wave loading at selected points along the levee reaches, plotted from the data in Table 1. The soil borings and LIDAR data were compiled by levee crown soil type (SM = silty sand, CL = lean clay, and CH = fat clay); soil consistency (soft, medium, and stiff); erosion depth; and maximum water height (ft) above crown elevation. Figure 45 indicates a lack of correlation between water height and erosion depth, but it does show that fat clays with medium consistency (strength) fared better than soils having lower plasticity and strength.

Table 1
Surface soil and scour versus hydraulic loading. Strengths (consistencies) are soft, medium (med) and stiff. Soils are lean clay (CL), fat clay (CH), and sandy silt (SM)

Boring	Surface soil type	Scour depth, ft	Overtop crest, ft
9BU	med CL	5	2
11BU	soft CH	10	5
12BU	med CL	6	7
18UBD	SM	6.2	7
13BU	med CH	1	7
ERDCM3	med CH	0.7	7
10-CUI	med CH	0.5	6
9-CUA	stiff CL	7	5
44-U	med CH	0.5	1
45-U	med CL	8	2
5A-CAU	stiff CL	0	1

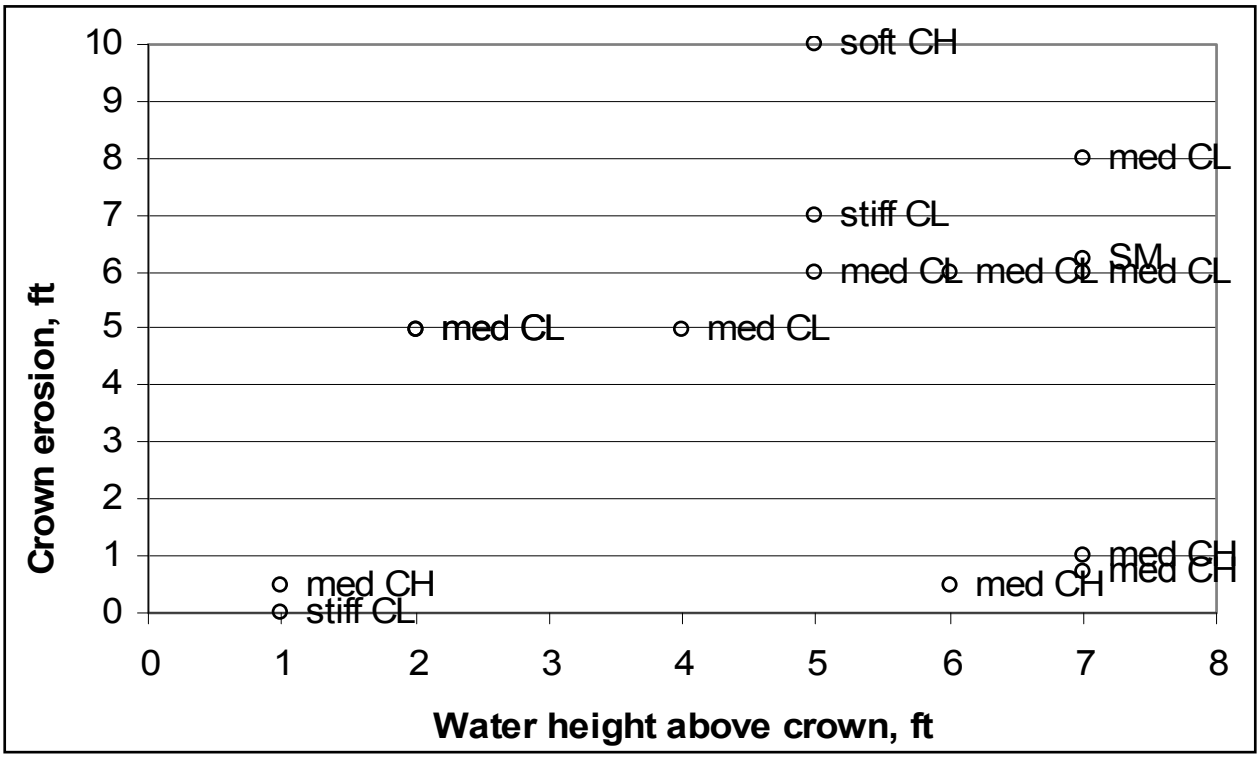

Figure 45. Scour depths versus surge/wave loading from soil borings and LIDAR data plotted from Table 1. Levee surface soil stiffness (strength) and soil type are labeled. Note that medium strength fat clay (med CH) had the least amount of erosion as the hydraulic loading increased.

In-situ Erodibility Assessment

The U.S. Army Corps of Engineers District, New Orleans, tasked ERDC to assess soil erodibility on reconstructed levees in Orleans Parish (East) and St. Bernard Parish. The ERDC team borrowed an innovative device, the Jet Index testing apparatus (owned by the U.S. Department of Agriculture's Research Center at Oxford, MS), rapidly assembled a field-portable support system, and deployed to New Orleans for approximately 3 weeks to conduct over 90 tests on selected existing and reconstructed levees.

Jet Index Test

The Jet Index test consists of placing the testing device on the soil surface and allowing a submerged water jet to impinge on and scour the soil surface. The scoured hole depth is then measured, and analytical procedures determine the soil erodibility parameters. The test method and apparatus were developed by the U.S. Department of Agriculture as a means to predict the erodibility of cohesive bank materials (Hanson et al 2002). Hanson (1991) developed a soil-dependent "jet index" based on the change in maximum scour depth caused by an impinging jet versus time. The test method and apparatus are described in ASTM Standard D5852-00 (ASTM 2000). Figure 46 shows the device.

Figure 46. Jet Index test apparatus. (Detailed description needed?)

The relationship for characterizing cohesive material erodibility is:

$$\varepsilon = k_d (\tau_e - \tau_c)^a$$

where

ε = erosion rate in volume of soil per unit time per unit area

τ_c = critical soil shear stress in Pascals

τ_e = hydraulic stress in Pascals

k_d = erodibility or detachment coefficient

^{a} = exponent assumed to be = 1

When the hydraulic stress becomes greater than the soil's critical shear stress the soil is detached (eroded) at a rate determined by the erodibility coefficient. Soils with a lower critical shear stress tend to have a higher erodibility coefficient.

Levee Erodibility Investigation

Two identical Jet Index test devices were assembled and deployed to New Orleans. Fifteen sites were selected in New Orleans East and St. Bernard, shown in Figure 47. At each site, two concurrent Jet Index tests were conducted on the levee floodside at three separate locations, generally beginning at the levee toe and progressing up the slope. At each of the 15 sites, 6 Jet Index tests were thus conducted, for an overall total of 90 tests. The floodside location was selected due to the water intake requirement for the pump system, and minimized pumping distance, pressure fluctuations, and ongoing construction traffic impacts. It was assumed that the soil materials and construction compaction efforts were the same on both the floodside and the backside, enabling floodside test result conclusions to also be applicable to the levee backside.

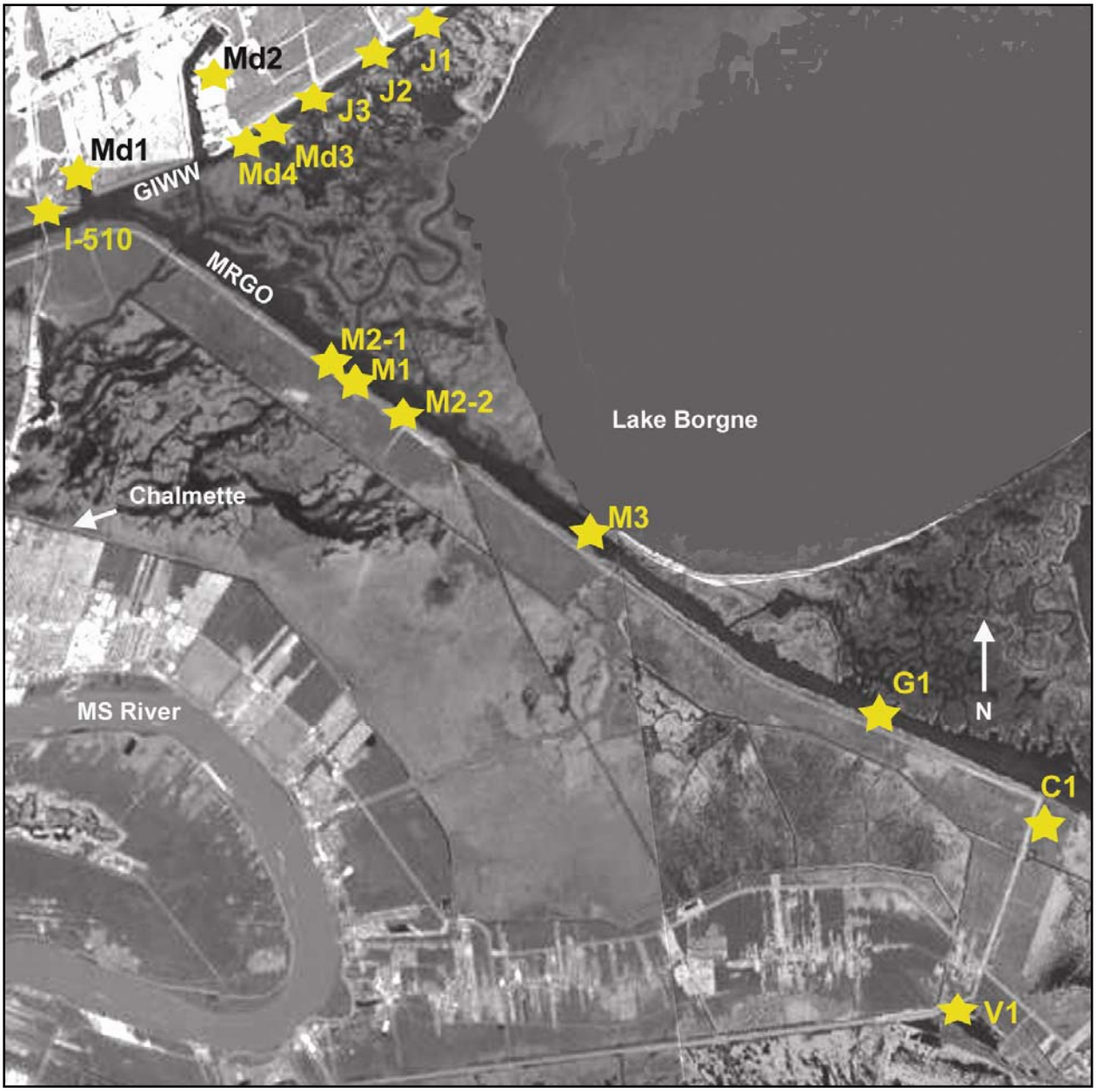

Figure 47. Overview of Jet Index testing sites (15 total) located on New Orleans East and St. Bernard levees.

St. Bernard (MRGO) Levee Tests

The initial Jet Index tests were conducted along the St. Bernard Parish levees (Chalmette Area and Chalmette Extension Hurricane Protection Plan levees). Test locations are shown in Figures 48 and 49, and levee site and soil conditions are summarized in Tables 1 through 9.

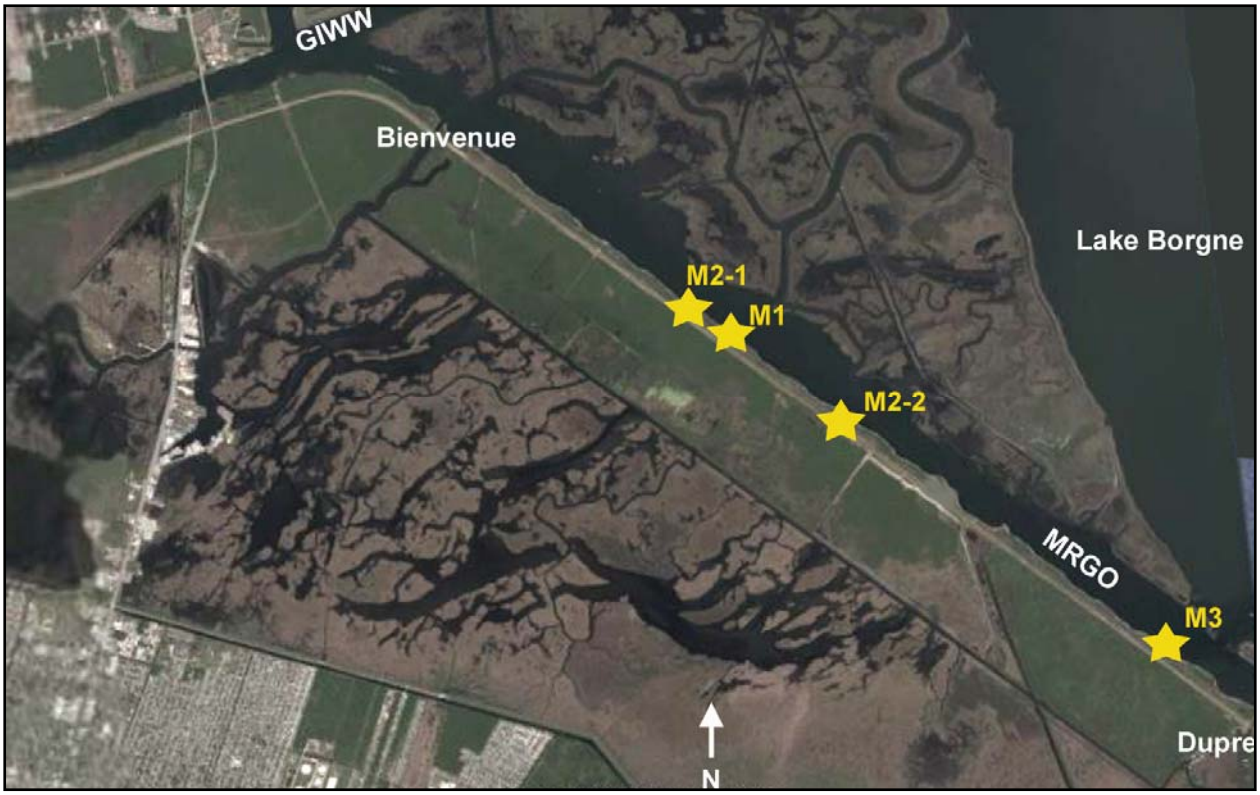

Figure 48. Levee test locations between Bienvenue and Dupre Control Structures

Table 1
Summary of Test Conditions

Site	GPS / Stationing	Visual Soil Class	Compaction Effort	Comments
M1	N29.97691 W89.88841 (Sta 483+00)	Yellow clay	3 dozer passes	MS borrow site
M2-1	Sta 482+00	Dark clay	3 dozer passes	local borrow
M2-2	Sta 520+00	Gray SM/CH	uncompacted	local borrow pit
M3	Sta 674+00	Dark clay w/sand	n/a	Existing levee

These sites (except M3) were located on a levee being reconstructed (backfilled, compacted, graded) by the Corps of Engineers contractor Manson, Inc. Site M3 tests were on overtopped yet uneroded levee material.

The existing conditions were very dry from lack of rainfall and the soils contained surface dessication cracks.

Compaction effort and borrow site information was verbally given by onsite Corps and/or contractor personnel.

Soil tests were conducted on soil immediately adjacent to the Jet Index tests, and are summarized in the following tables. In-situ measurements (water content % and dry unit weight, γ_d) were taken using the Troxler® nuclear density gage, and soil samples were taken to separate

labs for soil classification and Atterberg limit tests (LL= liquid limit, PL= plastic limit, and PI = plasticity index).

Table 2
Adjacent Soil Properties, Site Manson 1 (M1)

Site	Nuclear Density Gage		Lab	
	γ_d pcf	Water %	Soil Class	LL, PL, PI
1A	100	24	CL	41, 13, 28
1B	100	24	“	44, 13, 31
1C	104	21	“	47, 13, 34
1D	104	21	“	45, 13, 32
1E	n/a	n/a	“	45, 13, 32
1F	n/a	n/a	“	41, 14, 27

Table 3
Adjacent Soil Properties, Site Manson 2-1 (M2-1)

Site	Nuclear Density Gage		Lab	
	γ_d pcf	Water %	Soil Class	LL, PL, PI
2-1A	93	19	CH	62, 22, 40
2-1B	77	43	“	86, 26, 60
2-1C	80	33	“	104, 36, 68
2-1D	83	35	“	81, 25, 56
2-1E	81	37	“	71, 20, 51
2-1F	73	45	“	93, 23, 70

Table 4
Adjacent Soil Properties, Site Manson 2-2 (M2-2)

Site	Nuclear Density Gage		Lab	
	γ_d pcf	Water %	Soil Class	LL, PL, PI
2-2A	76	40	CH	112, 38, 74
2-2B	86	33	“	69, 19, 50
2-2C	80	31	“	66, 23, 43
2-2D	81	32	“	58, 20, 38
2-2E	97	24	CL	21, 14, 7
2-2F	100	19	SM	23, 18, 5

Table 5
Adjacent Soil Properties, Site Manson 3 (M3)

Site	Nuclear Density Gage		Lab	
	γ_d pcf	Water %	Soil Class	LL, PL, PI
3A	81	36	CH	86, 25, 61
3B	80	39	"	86, 25, 61
3C	87	38	"	85, 23, 62
3D	80	35	"	89, 24, 65
3E	90	9	SM	19, 13, 6
3F	83	22	CH	89, 24, 65

Figure 49. Levee test locations southeast of Dupre Control Structure

Table 6
Summary of Test Conditions

Site	GPS / Stationing	Visual Soil Class	Compaction Effort	Comments
G1	N29_54_27 W89_47_57	Gray clay	3 dozer passes	local borrow
C1	Sta 1041+00	Yellow clay	3 dozer passes	Slidell borrow
V1	N29_51_14 W89_47_08	Dark gray clay		Existing levee

These sites (except V1) were located on a levee being reconstructed (backfilled, compacted, graded) by the Corps of Engineers contractors Granite, Inc. (site G1) and Clark, Inc. (site C1). The site V1 tests were conducted on overtopped yet uneroded levee material.

The existing conditions were very dry from lack of rainfall and the soil contained surface dessication cracks.

Compaction effort and borrow site information was verbally given by onsite Corps and/or contractor personnel.

Soil tests were conducted on soil immediately adjacent to the Jet Index tests, and are summarized in the following tables.

Table 7
Adjacent Soil Properties, Site Granite 1 (G1)

Site	Nuclear Density Gage		Lab	
	γ_d pcf	Water %	Soil Class	LL, PL, PI
1A	91	30	CH	74, 20, 50
1B	107	18	"	62, 18, 44
1C	114	12	CL	24, 13, 11
1D	108	15	"	22, 12, 10
1E	83	28	CH	59, 16, 43
1F	92	26	"	60, 17, 43

Table 8
Adjacent Soil Properties, Site Clark 1 (C1)

Site	Nuclear Density Gage		Lab	
	γ_d pcf	Water %	Soil Class	LL, PL, PI
1A	100	18	CH	57, 17, 40
1B	92	18	CL	39, 13, 26
1C	84	27	CH	50, 19, 31
1D	85	20	"	66, 17, 49
1E	84	31	"	56, 20, 36
1F	79	28	"	52, 16, 36

Table 9 Adjacent Soil Properties, Site Verret 1 (V1)				
Site	Nuclear Density Gage		Lab	
	γ_d pcf	Water %	Soil Class	LL, PL, PI
1A	100	19	CH	61, 19, 42
1B	98	17	"	63, 17, 46
1C	92	18	"	68, 16, 42
1D	95	18	"	50, 19, 31
1E	92	18	"	59, 21, 38
1F	93	14	"	56, 18, 38

Orleans East Levee Tests

Jet Index tests were conducted along the Orleans East levees (East Back, Michoud, and Citrus Back). Test locations are shown in Figures 50 and 51, and in-situ levee conditions are summarized in the following tables.

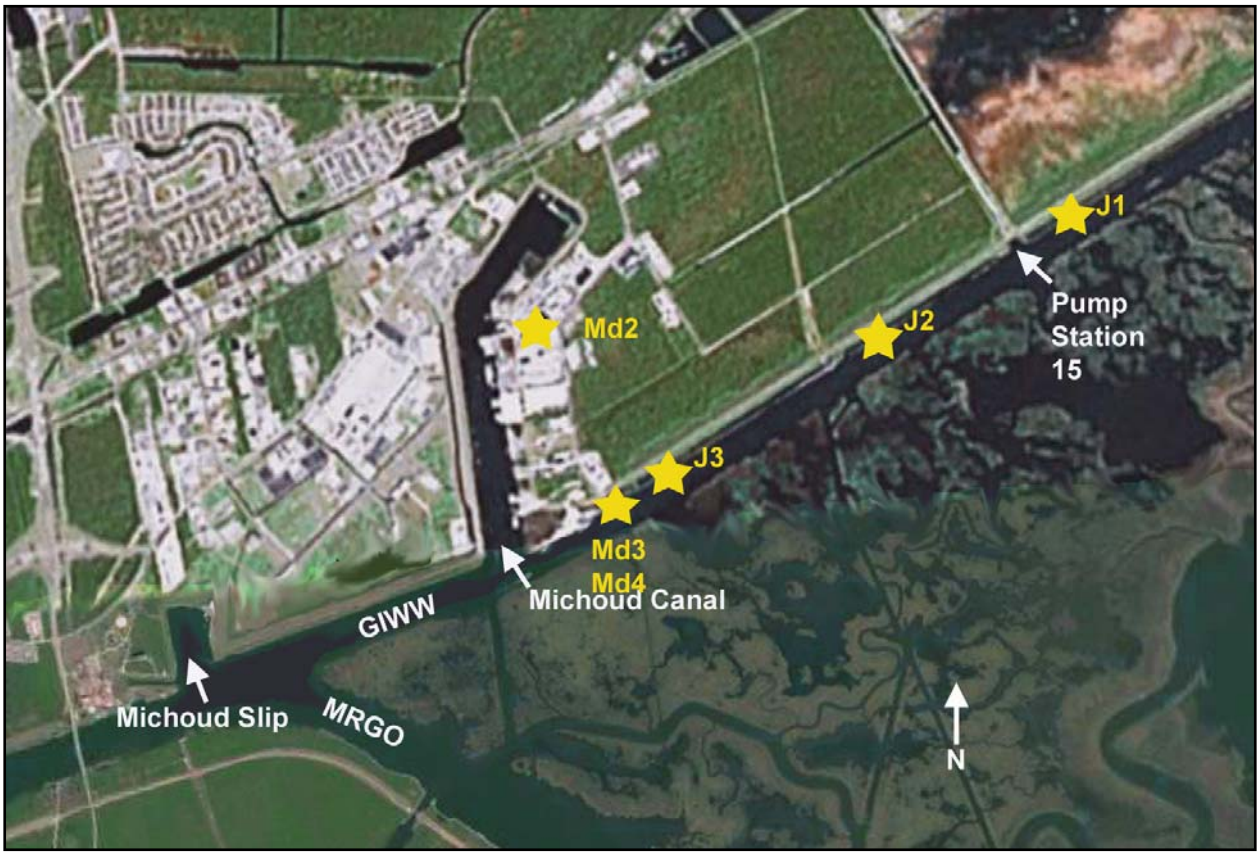

Figure 50. East Back and Michoud Canal levee test locations

Table 10
Summary of Test Conditions

Site	GPS / Stationing	Visual Soil Class	Compaction Effort	Comments
J1	N30_01_57 W89_51_38 (Sta 903+00)	Gray silty clay (CL)	3 dozer passes	Hwy90/MS mix
J2	N30_01_29 W89_52_47 (Sta 836+00)	Tan silty clay (CL)	3 dozer passes	MS borrow
J3	N30_01_09 W89_53_34 (Sta 789+00)	Gray CH/CLHwy90 Yellow CH(Slidell)	uncompacted	Hwy 90 (4 tests) MS (2 tests)
Md2	N30_01_39 W89_54_16 (LoneStar plant)	CH/ML	Roller compacted (90% of optimum)	Hwy 90 borrow
Md3	N30_01_01 W89_53_55 (Air Products site) on lower bench slope	Clay	uncompacted	Bonnet Carre borrow site
Md4	N30_01_01 W89_53_55 (Air Products site) on lower bench slope	Clay	3 dozer passes	Bonnet Carre borrow site

These sites were located on levees being reconstructed (backfilled, compacted, graded) by the Corps of Engineers contractors James, Inc. (sites J1, J2, and J3) and Boh Bros, Inc. (Md sites). Site Md2 was an I-wall levee that had overtopped with minor scour damage.

The existing conditions were very dry from lack of rainfall and the soil contained surface dessication cracks.

Compaction effort and borrow site information was verbally given by onsite Corps and/or contractor personnel.

Soil tests were conducted on soil immediately adjacent to the Jet Index tests, and are summarized in the following tables.

Table 11
Adjacent Soil Properties, Site James 1 (J1)

Site	Nuclear Density Gage		Lab	
	γ_d pcf	Water %	Soil Class	LL, PL, PI
1A	101	14	CL	not available
1B	101	14	"	not available
1C	107	13	"	not available
1D	103	9	"	not available
1E	105	11	"	not available
1F	103	9	"	not available

Table 12
Adjacent Soil Properties, Site James 2 (J2)

Site	Nuclear Density Gage		Lab	
	γ_d pcf	Water %	Soil Class	LL, PL, PI
2A	109	10	CL	not available
2B	110	11	"	not available
2C	108	12	"	not available
2D	112	13	"	not available
2E	114	10	"	not available
2F	113	10	"	not available

Table 13
Adjacent Soil Properties, Site James 3 (J3)

Site	Nuclear Density Gage		Lab	
	γ_d pcf	Water %	Soil Class	LL, PL, PI
3A	104	12	CH	not available
3B	105	10	"	not available
3C	104	11	CL	not available
3D	103	13	"	not available
3E	116	10	"	not available
3F	114	11	"	not available

Table 14
Adjacent Soil Properties, Site Michoud Canal 2 (Md2)

Site	Nuclear Density Gage		Lab	
	γ_d pcf	Water %	Soil Class	LL, PL, PI
2A	95	22	CL	53, 19, 34
2B	101	18	"	45, 18, 27
2C	92	25	CH	58, 20, 38
2D	97	21	"	72, 22, 50
2E	94	20	"	73, 22, 51
2F	92	22	"	57, 19, 30

Table 15
Adjacent Soil Properties, Site Michoud AirProducts 3 (Md3)

Site	Nuclear Density Gage		Lab	
	γ_d pcf	Water %	Soil Class	LL, PL, PI
3A	93	33	CH	89, 26, 63
3B	98	31	“	91, 24, 67
3C	94	31	“	88, 28, 60
3D	88	27	“	91, 26, 65
3E	98	32	“	78, 26, 52
3F	97	30	“	66, 26, 40

Table 16
Adjacent Soil Properties, Site Michoud AirProducts 4 (Md4)

Site	Nuclear Density Gage		Lab	
	γ_d pcf	Water %	Soil Class	LL, PL, PI
4A	88	28	CH	67, 20, 47
4B	-	-	“	66, 21, 45
4C	92	30	“	63, 19, 44
4D	96	29	“	68, 20, 48
4E	96	27	“	79, 23, 56
4F	102	22	“	77, 18, 59

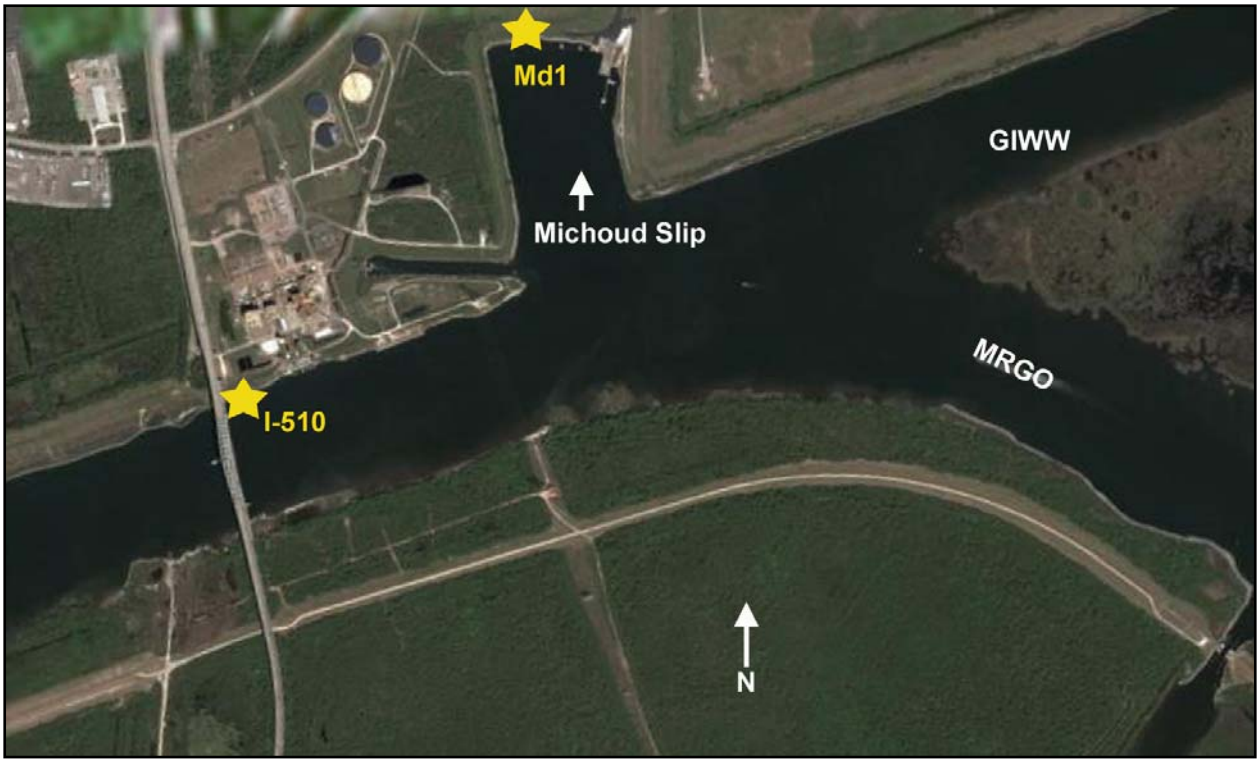

Figure 51. Citrus Back and Michoud levee test locations

Table 17
Summary of Test Conditions

Site	GPS / Stationing	Visual Soil Class	Compaction Effort	Comments
Md1	N30_01_47 W89_55_51 (Sta 46+88)	Gray clay	Sheepsfoot/roller vibratory compacted (90% of optimum)	Hwy 90 borrow
I-510	Below I-510 (Paris Rd) high rise bridge	Brown gray clay		Existing levee

Site Md1 was located on a floodwall levee being reconstructed (backfilled, compacted, graded) by the Corps of Engineers contractor Boh Bros, Inc. Site I-510 was an existing overtopped yet undamaged levee.

The existing conditions were very dry from lack of rainfall and the soil contained surface dessication cracks.

Compaction effort and borrow site information was verbally given by onsite Corps and/or contractor personnel.

Soil tests were conducted on soil immediately adjacent to the Jet Index tests, and are summarized in the following tables.

Table 18
Adjacent Soil Properties, Site Michoud Slip 1 (Md1)

Site	Nuclear Density Gage		Lab	
	γ_d pcf	Water %	Soil Class	LL, PL, PI
1A	89	25	CH	61, 21, 40
1B	96	22	"	59, 21, 38
1C	89	29	"	60, 22, 38
1D	92	27	"	58, 21, 37
1E	81	27	"	62, 21, 41
1F	88	25	"	65, 22, 43

Table 19
Adjacent Soil Properties, Site Paris Rd Bridge I-510 (I-510)

Site	Nuclear Density Gage		Lab	
	γ_d pcf	Water %	Soil Class	LL, PL, PI
1A	85	30	CH	63, 18, 45
1B	88	30	"	64, 18, 46
1C	101	21	CL	48, 14, 34
1D	100	21	"	46, 15, 31
1E	103	16	"	47, 15, 32
1F	101	16	"	48, 15, 33

Jet Index Test Results

Each of the 15 sites (M1 through I-510) typically contained six separate test locations (A through F), and the test results for each location are tabulated below. Two jet index test devices located approximately 6 ft apart horizontally (equal datum elevations) were concurrently collecting data. Viewed from the levee toe looking up the slope toward the crown, the left jet index device tested locations A, C, and E. Concurrently, the right jet index device tested locations B, D, and F. For example, the left jet index device tested location 1A concurrently as the right jet index device tested location 1B.

Table 20
Site M1

Location number	Critical shear stress, τ_c, Pascals	Erodibility coeff, K_d, cm^3/N-sec
1A	31.55	0.05
1B	17.77	0.07
1C	19.14	0.11
1D	6.51	0.10
1E	23.01	0.06
1F	19.96	0.13

Table 21
Site M2_1

Location number	Critical shear stress, τ_c, Pascals	Erodibility coeff, K_d, cm^3/N-sec
2-1-A	0.32	1.58
2-1-B	6.36	0.37
2-1-C	17.25	0.07
2-1-D	11.26	0.16
2-1-E	10.73	0.17
2-1-F	27.69	0.08

Table 22
Site M2_2

Location number	Critical shear stress, τ_c, Pascals	Erodibility coeff, K_d, cm^3/N-sec
2-2-A	21.08	2.00
2-2-B	0.00	42.12
2-2-C	0.02	5.18
2-2-D	9.37	1.59
2-2-E	0.04	293.19
2-2-F	0.02	100.42

Table 23
Site M3

Location number	Critical shear stress, τ_c, Pascals	Erodibility coeff, K_d, cm^3/N-sec
3-A	25.05	0.06
3-B	23.28	0.13
3-C	67.81	0.04
3-D	43.95	0.07
3-E	0.36	68.22
3-F	1.35	85.82

Table 24
Site G1

Location number	Critical shear stress, τ_c, Pascals	Erodibility coeff, K_d, cm^3/N-sec
1A	34.85	0.06
1B	28.58	0.10
1C	5.43	0.66
1D	28.19	0.73
1E	68.90	0.08
1F	9.57	0.00

Table 25
Site C1

Location number	Critical shear stress, τ_c, Pascals	Erodibility coeff, K_d, cm^3/N-sec
1A	38.19	1.46
1B	67.49	0.22
1C	1.99	12.95
1D	10.96	1.67
1E	43.84	0.72
1F	8.87	2.72

Table 26
Site V1

Location number	Critical shear stress, τ_c, Pascals	Erodibility coeff, K_d, cm^3/N-sec
1A	127.77	0.03
1B	80.56	0.06
1C	108.26	0.06
1D	69.01	0.16
1E	39.00	0.29
1F	32.14	0.48

Table 27
Site J1

Location number	Critical shear stress, τ_c, Pascals	Erodibility coeff, K_d, cm^3/N-sec
1A	0.01	10.03
1B	5.50	2.39
1C	15.09	0.83
1D	21.14	0.81
1E	31.64	0.29
1F	0.13	3.41

Table 28
Site J2

Location number	Critical shear stress, τ_c, Pascals	Erodibility coeff, K_d, cm^3/N-sec
2A	66.51	0.07
2B	0.30	2.76
2C	5.97	0.34
2D	15.79	0.82
2E	14.49	0.83
2F	1.05	1.51

Table 29
Site J3

Location number	Critical shear stress, τ_c, Pascals	Erodibility coeff, K_d, cm^3/N-sec
3A	27.42	0.16
3B	25.91	0.34
3C	0.11	2.90
3D	46.47	0.25
3E	5.63	1.24
3F	9.99	0.85

Table 30
Site Md1

Location number	Critical shear stress, τ_c, Pascals	Erodibility coeff, K_d, cm^3/N-sec
1A	22.80	0.23
1B	17.52	2.13
1C	205.11	0.01
1D	121.17	0.03
1E	147.83	0.02
1F	111.98	0.06

Table 31
Site Md2

Location number	Critical shear stress, τ_c, Pascals	Erodibility coeff, K_d, cm^3/N-sec
2A	66.80	0.12
2B	49.20	0.17
2C	67.89	0.08
2D	98.18	0.05
2E	20.41	0.11
2F	20.41	0.11

Table 32
Site Md3

Location number	Critical shear stress, τ_c, Pascals	Erodibility coeff, K_d, cm^3/N-sec
3A	19.52	0.11
3B	22.39	0.15
3C	44.79	0.08
3D	28.83	0.37
3E	20.02	0.40
3F	39.25	0.24

Table 33 Site Md4		
Location number	**Critical shear stress, τ_c, Pascals**	**Erodibility coeff, K_d, cm^3/N-sec**
4A	98.27	0.03
4B	97.05	0.08
4C	93.50	0.04
4D	94.71	0.11
4E	104.60	0.03
4F	33.17	0.09

Table 34 Site I-510		
Location number	**Critical shear stress, τ_c, Pascals**	**Erodibility coeff, K_d, cm^3/N-sec**
1A	4.35	0.30
1B	8.81	0.06
1C	31.64	0.08
1D	137.14	0.06
1E	193.02	0.06
1F	56.89	0.20

All 15 Sites

All data from each of the 15 sites (including all left and right jet index tests) were analyzed to detect the erodibility parameters compared by site. Figures 52 through 55 show the combined plotted data for all sites.

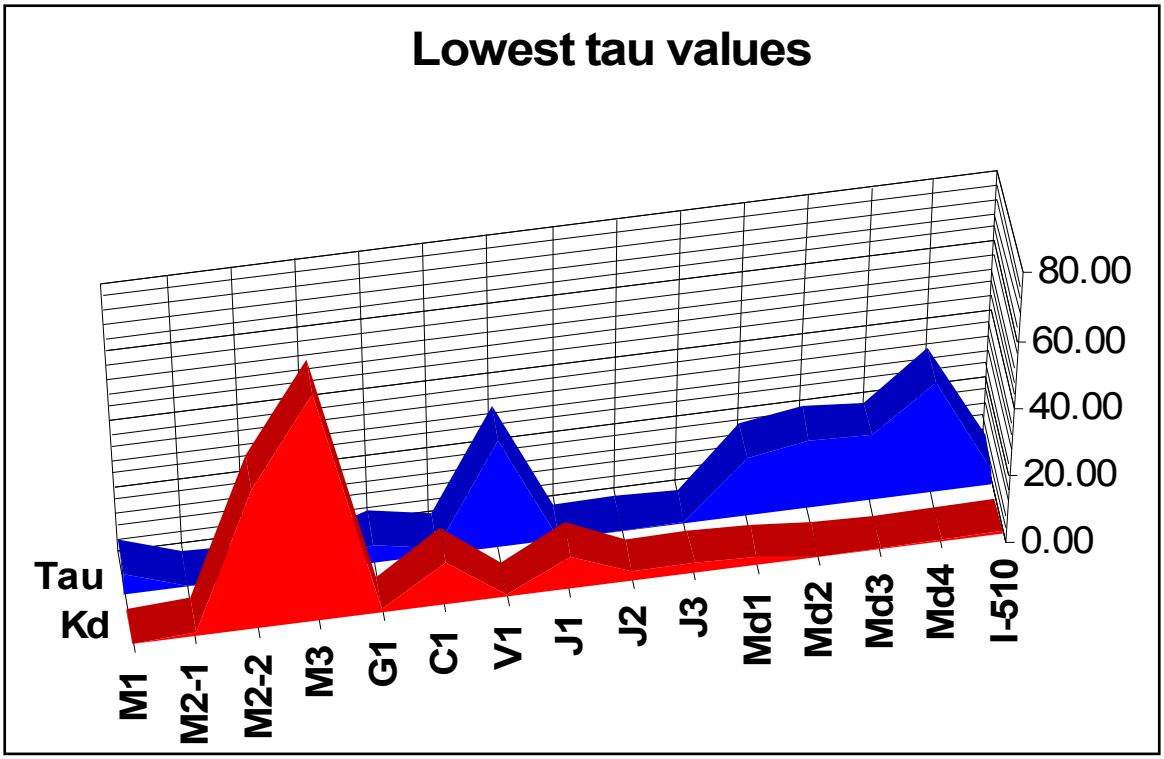

Figure 52. Combined site data plotted by lowest tau (τ_c) values

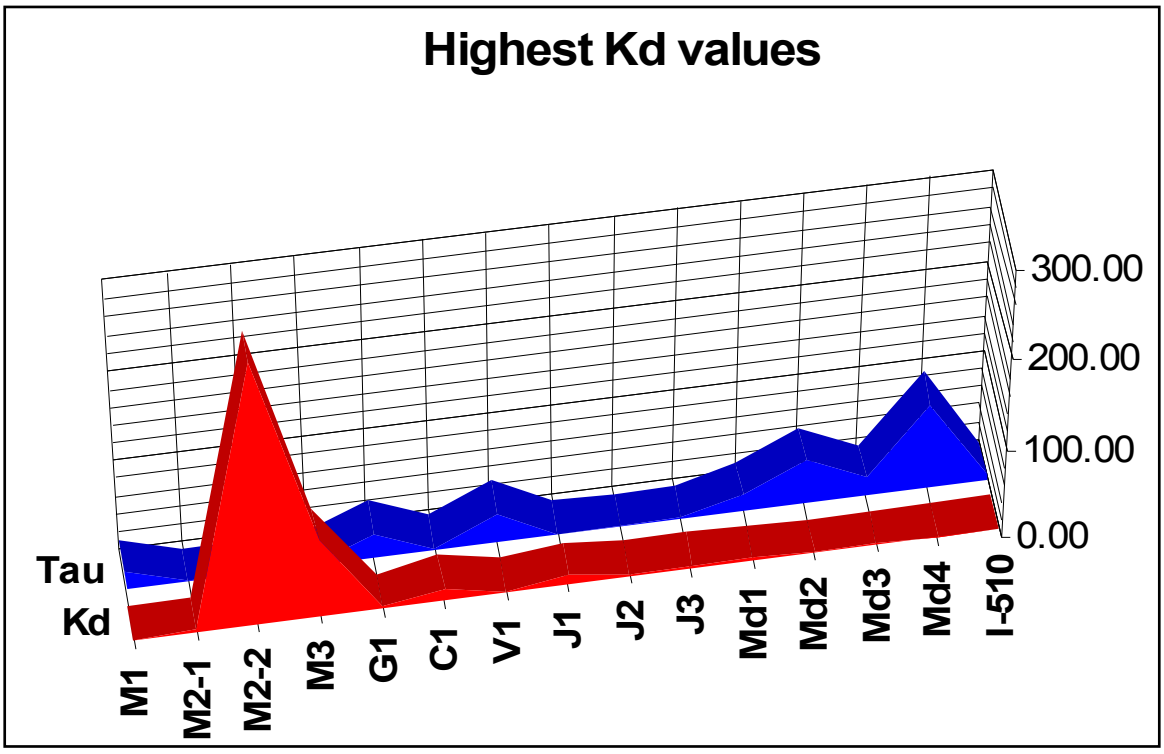

Figure 53. Combined site data plotted by highest Kd values

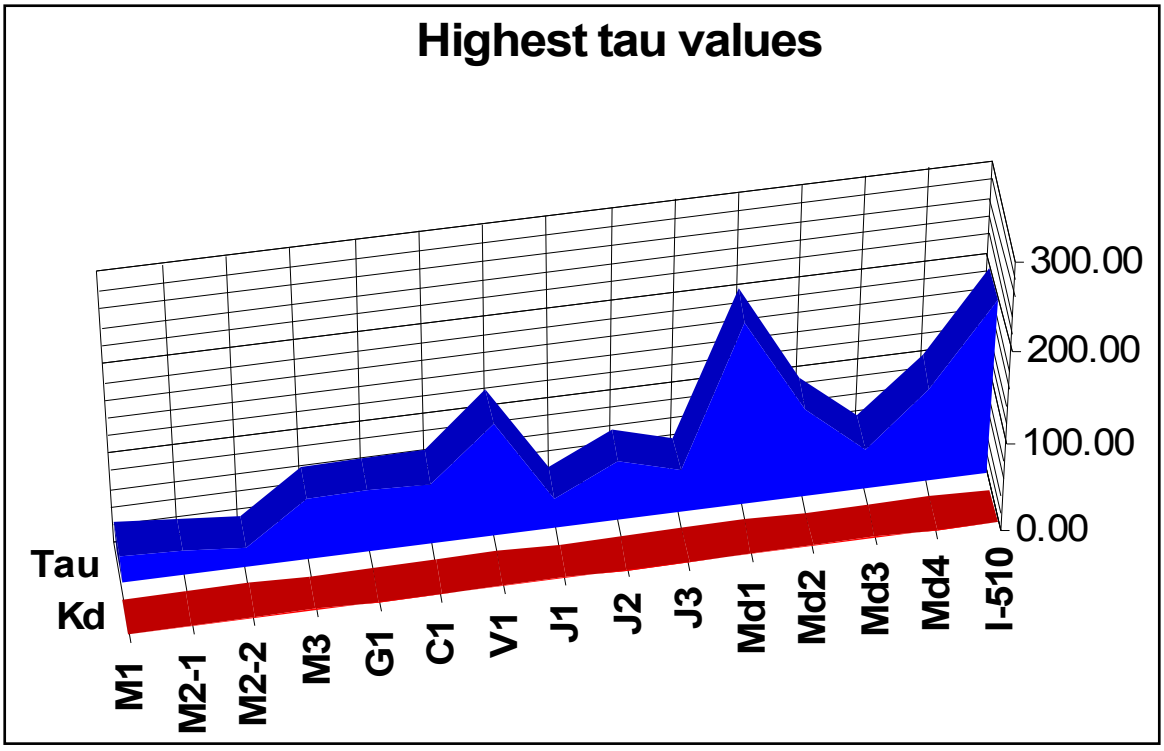

Figure 54. Combined site data plotted by highest tau (τ_c) values

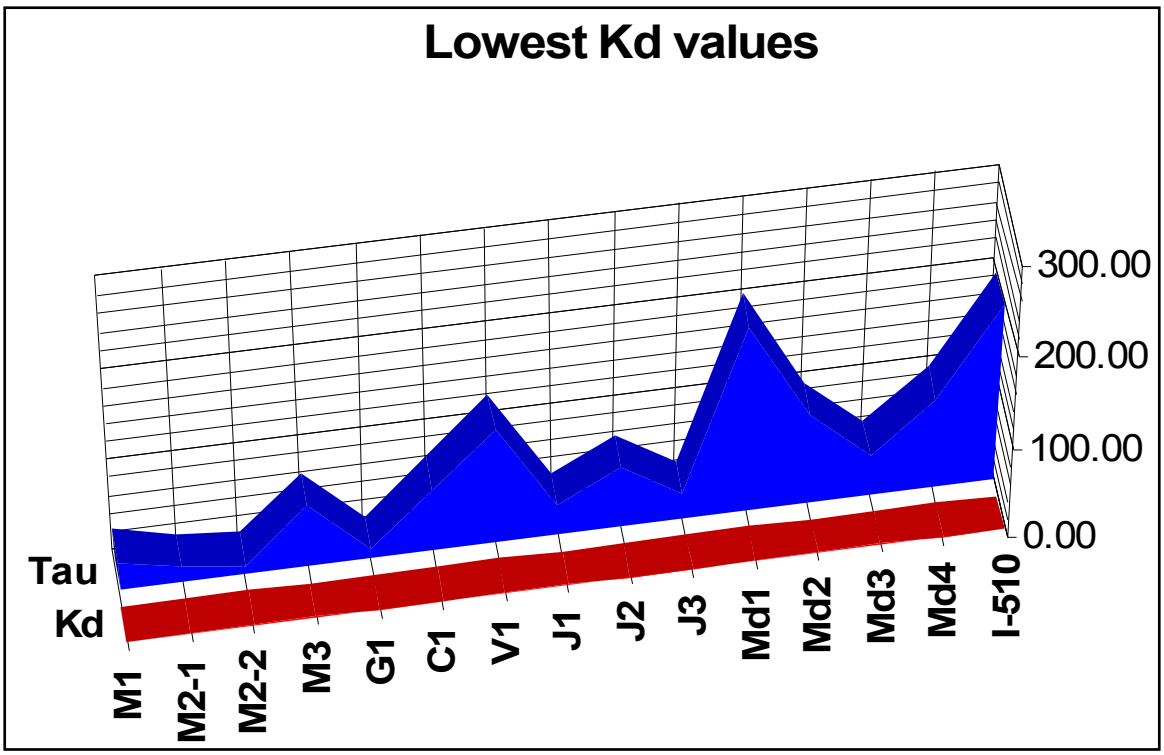

Figure 55. Combined site data plotted by lowest Kd values

Note that the tau (τ_c) and Kd values are generally inversely proportional, i.e. the higher the tau value, the lower the Kd value. A higher τ_c generally indicates lower erodibility (higher erosion resistance).

Erodibility comparisons between sites were obtained by normalizing the tau and Kd values (dividing tau by Kd) and averaging the results (Table 35). Figure 56 illustrates the relative erodibility ranking for each site using the Table 35 data.

Table 35
Relative Erodibility Based on Averaged Data Points From tau / Kd Relationship (the Lower the Number, the Higher the Erodibility)

Site	Averaged tau/Kd values
M1	276
M2-1	125
M2-2	3
M3	478
G1	2051
C1	68
V1	1242
J1	26
J2	177
J3	75
Md1	4960
Md2	737
Md3	192
Md4	1991
I-510	1073

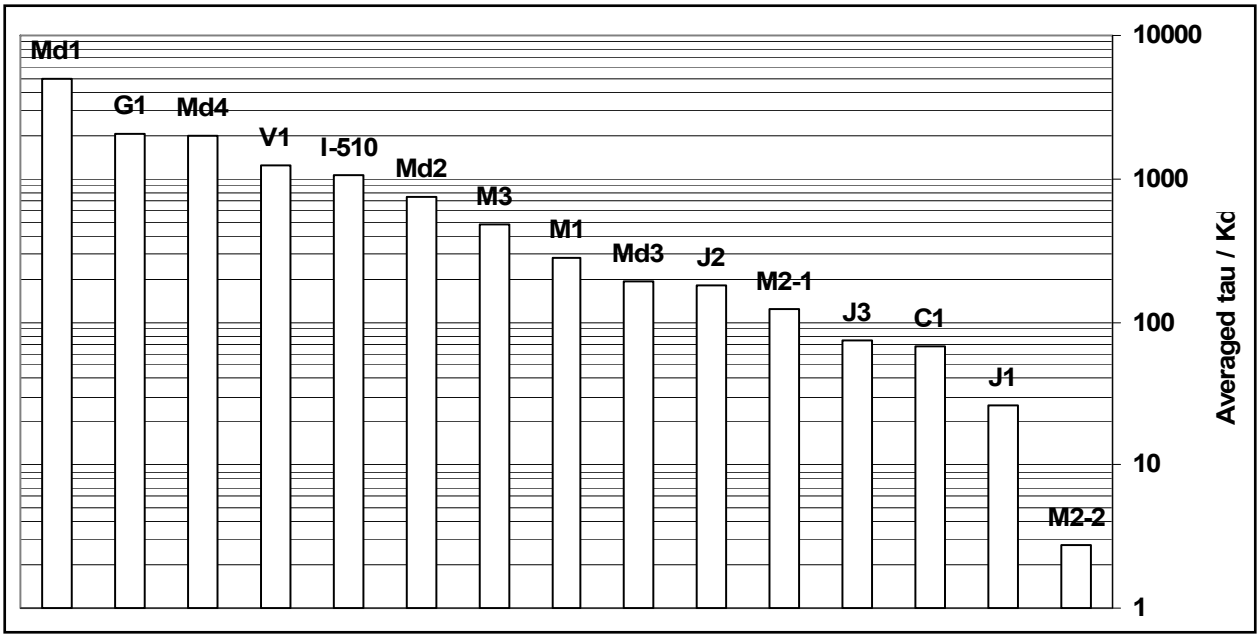

Figure 56. Bar chart showing the relative erodibility ranking for the 15 sites based on averaged results. Note that site Md1 had the highest erosion resistance, and site M2-2 had the lowest erosion resistance.

Comparing each of the 15 sites to one another (Figure 56) shows that the M2-2 site was the most erodible, and the Md1 site was the least erodible. The M2-2 soils were uncompacted, and the Md1 soils were compacted with sheepsfoot and vibratory roller, so it seems reasonable that the soils with higher compaction efforts were less erodible, all other factors being equal. Also note that the top 5 sites having the least erodibility (Md1, G1, Md4, V1, and I-510) included 2 of the surviving levee sites (I-510 and V1). The site M3 erodibility value was in the top half of all sites. Since site M3 was a surviving levee, perhaps its averaged tau/Kd value (500) should be considered as a threshold erodibility value. For example, values greater than 500 indicate erosion resistance, and values less than 500 indicate lower erosion resistance.

Discussion

Hanson and Simon (2001) collected a series of jet index data from various sites around the U.S. (Iowa, Nebraska, and Mississippi) to explore the erodibility of natural streambank materials. Figure _ shows the erodibility index versus critical shear stress for those materials. Erosion resistance was categorized into five levels (very erodible, erodible, moderately resistant, resistant, and very resistant).

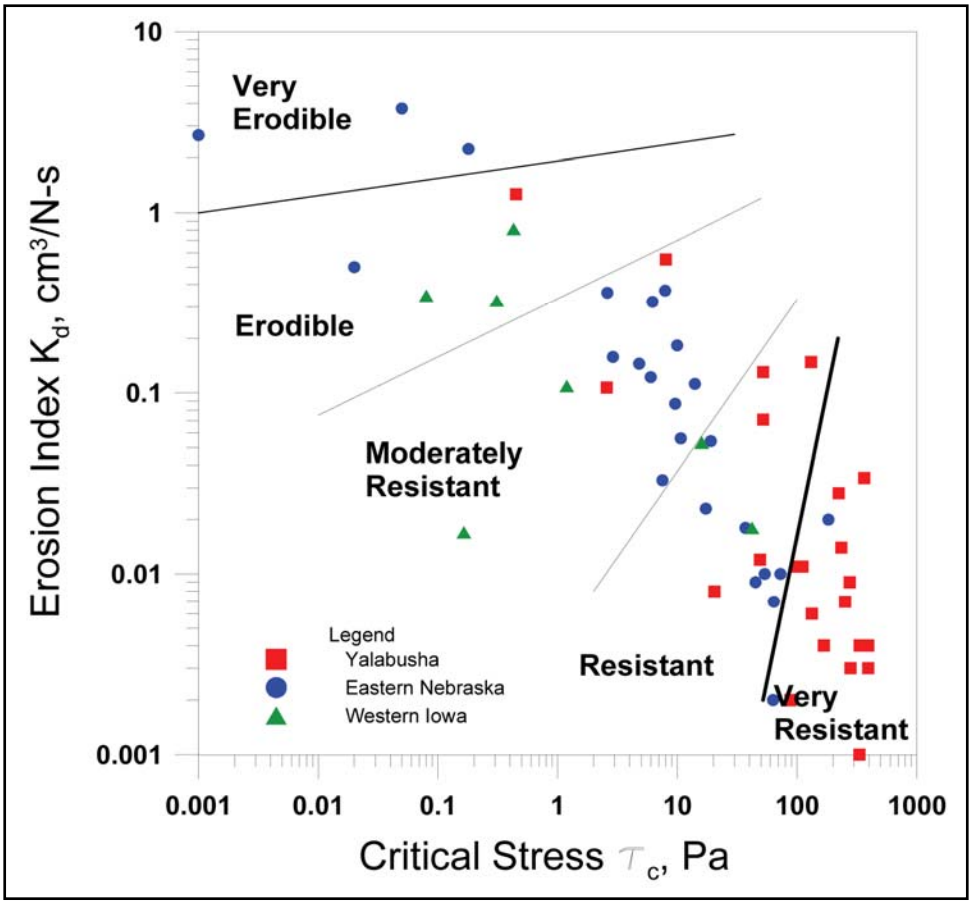

Figure 57. Erosion Index versus critical stress for USDA data (from Hanson and Simon, 2001)

Figure 58 is a summary of the New Orleans data (all 15 sites) displayed in the Hanson and Simon format. The soil erodibility varies widely from highly erodible (site M2-2) to very resistant (site Md1).

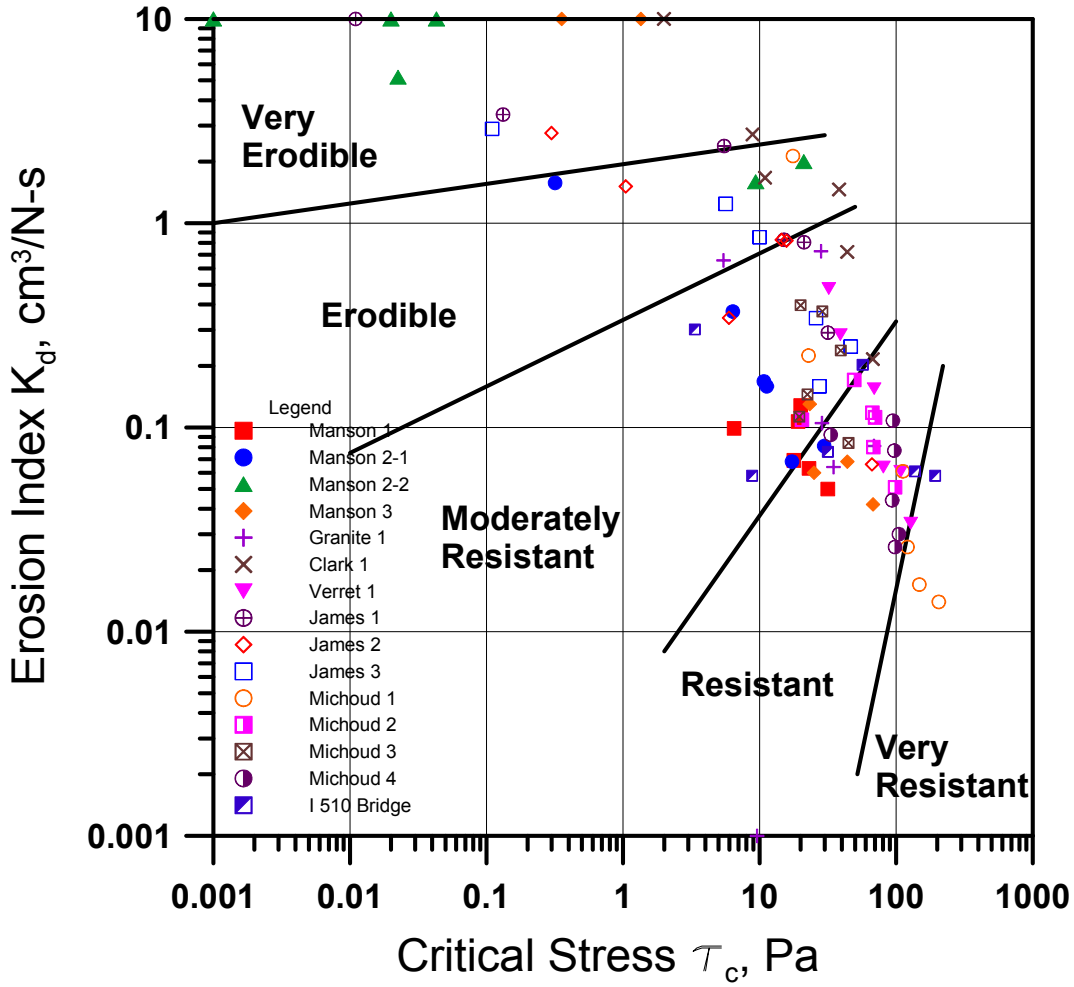

Figure 58.Erosion Index versus critical stress summary for New Orleans data

Figure 59 takes a closer look at the summary data shown above, and includes only the old (existing) levee that was overtopped but was undamaged. Note that most of the data are clustered in the "resistant" category. This figure suggests that erodibility of new levees should at least be within the "resistant" category.

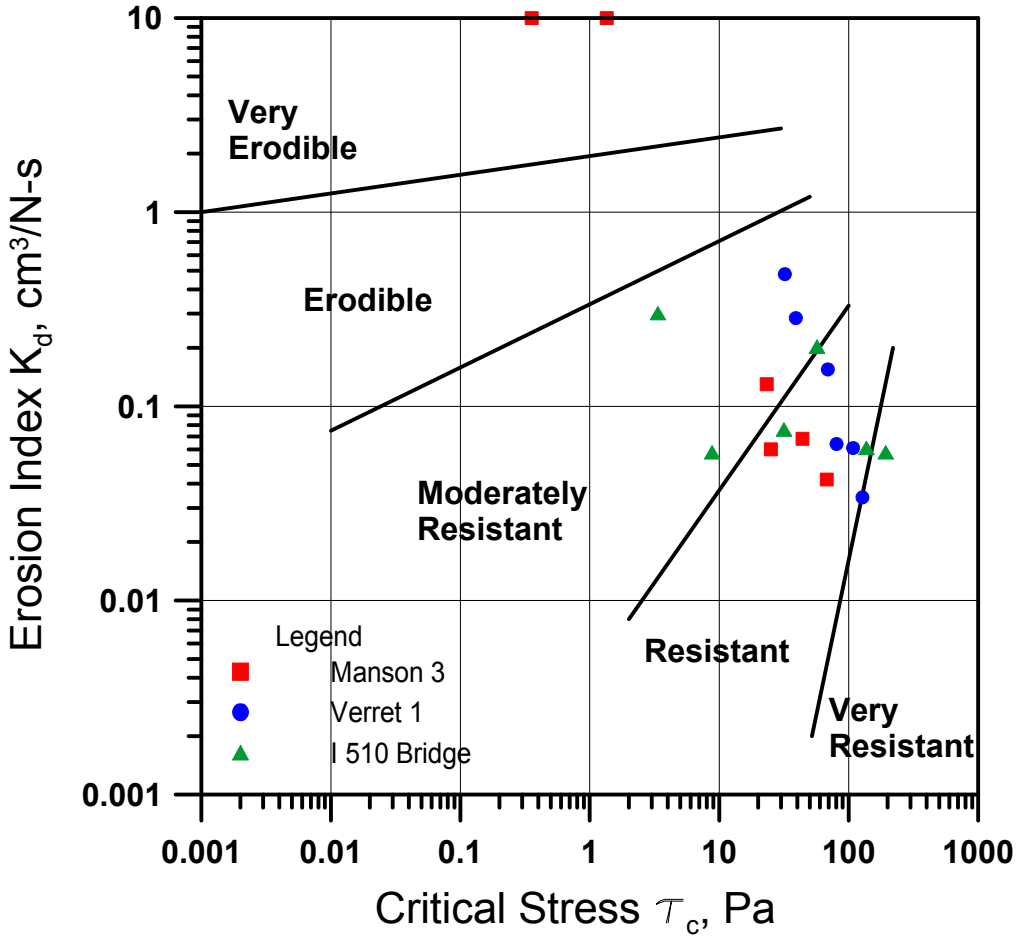

Figure 59. Erosion Index versus critical stress of old (existing) levees in St Bernard Parish and New Orleans East

Figure 60 shows the new (re-constructed) levee materials compacted using the New Orleans District's three-dozer-passes compaction specification. This specification requires a minimum of three dozer passes (6.2 psi minimum track pressure) on materials having water contents ranging from 18% to 28% (CL soils) or 20% to 40% (CH soils). This figure shows that the Michoud 4 (Md4) site has more erosion resistance than the other sites that were compacted with three dozer passes. This was the only compacted material tested that came from the Bonnet Carre borrow site. The Granite 1 (G1) site was also resistant but non-homogeneity (possibly a sand seam or dessication crack) caused the wide scatter. The G1 soil came from a local borrow area.

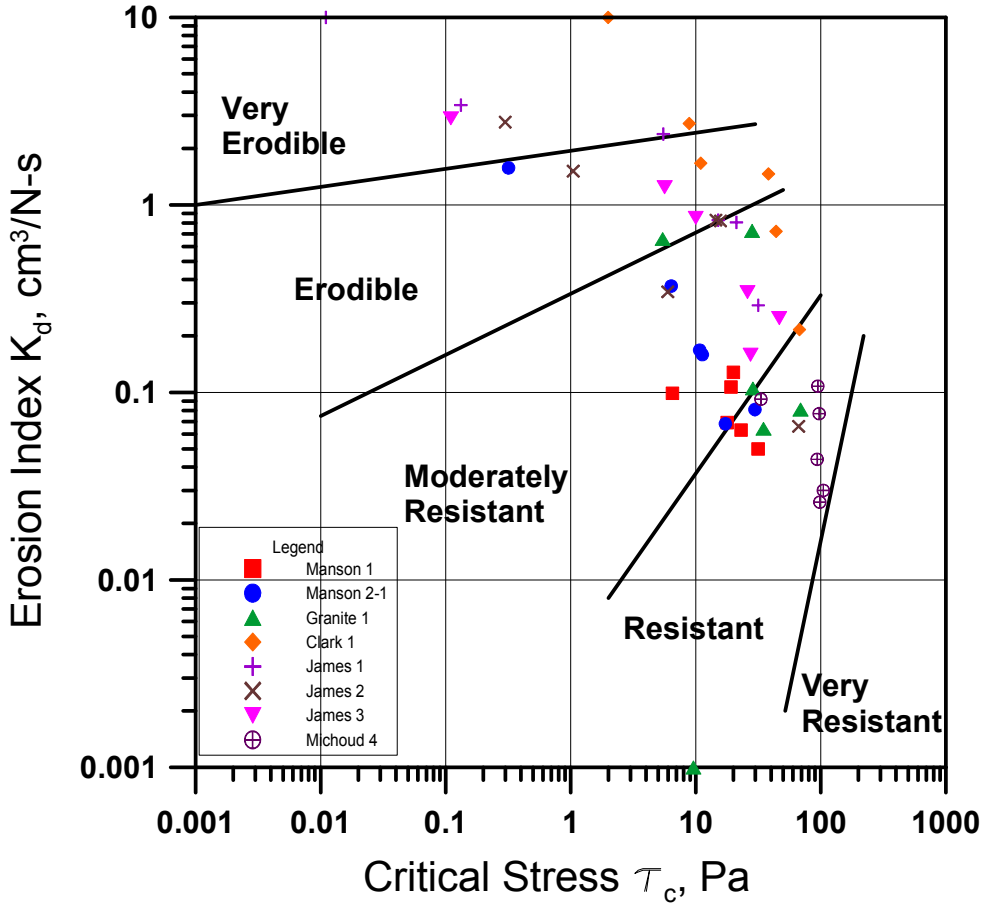

Figure 60. Erosion Index versus critical stress of new levee with three passes compaction

Figure 61 shows the Manson site data. Note that the existing levee site (M3) was the most resistant. The new levee (M1) was the next best.

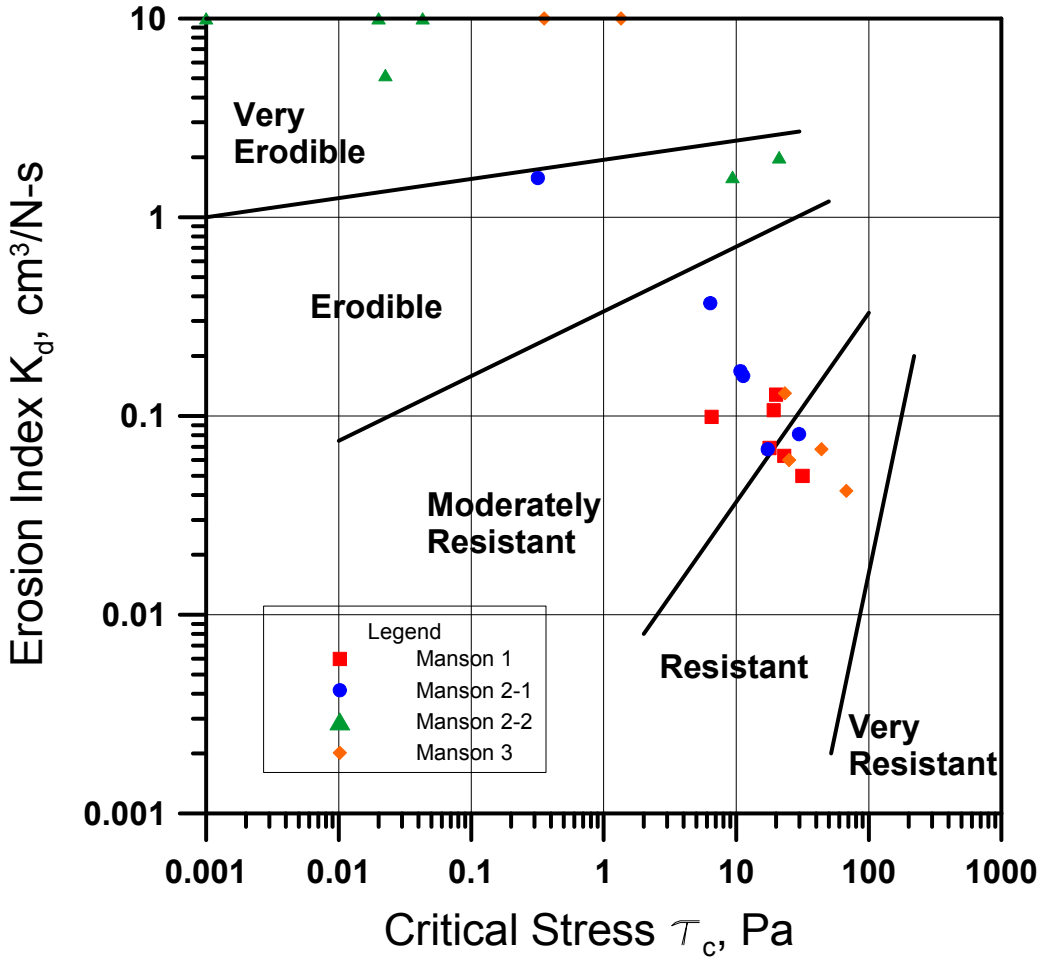

Figure 61. Erosion Index versus critical stress of new and old Manson site levees along the MRGO

Figure 62 shows the old (Verret) and new (Granite and Clark) levees south of Bayou Dupre along the MRGO. The Clark material (C1) was the most erodible of the three materials.

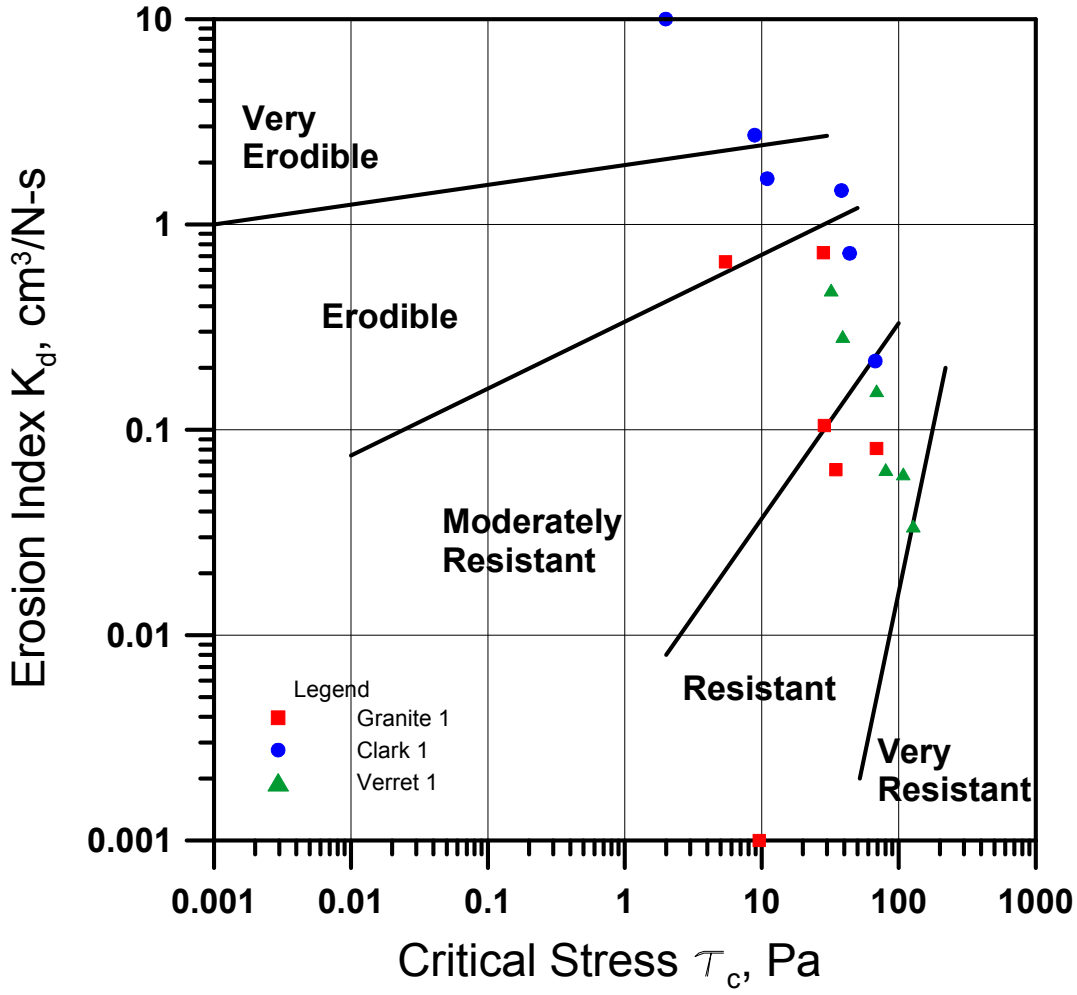

Figure 62. Erosion Index versus critical stress of old (Verret) and new levee south of Bayou Dupre (St. Bernard Parish)

Figure 63 shows the new Levees in New Orleans East (James Sites) and the existing levee (under the I- 510 Bridge). The James 1, 2, and 3 materials were more erodible than the I-510 material.

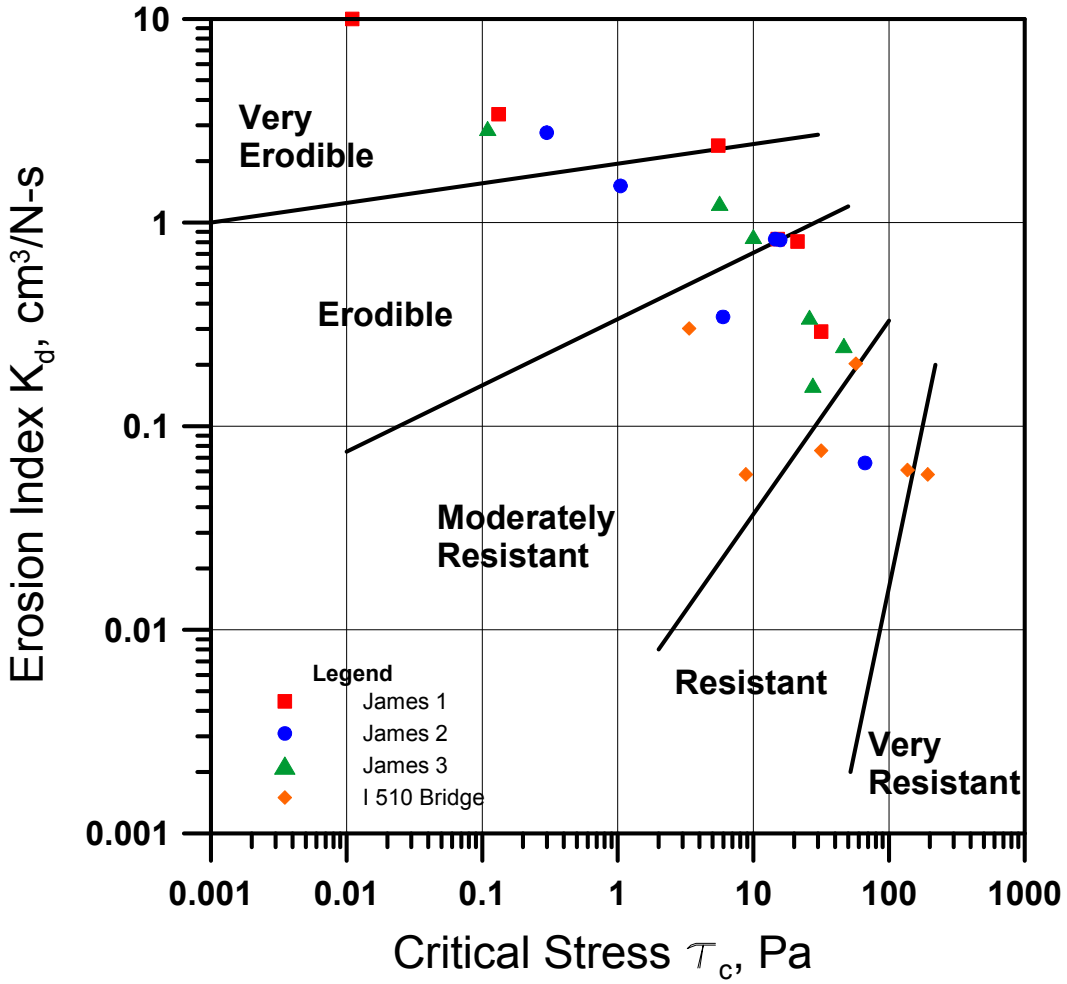

Figure 63. Erosion Index versus critical stress of new levees in New Orleans East (James Sites) and old levee (under I-510 Bridge)

Figure 64 shows the Michoud levee data. The I-wall levees (sites Md1 and Md2) were overtopped but had minor erosion. The sites Md3 and Md4 were on the overtopped and breached Air Products levee / floodwall. The reconstructed soil specifications generally required minimum 90% compaction effort with +5% to -3% water content tolerances for the Boh Bros.Inc constructed Md1 and Md2 sites. Michoud 1 (Md1) material was more resistant than the existing levee sites that were tested, possibly because it was sheepfoot- and vibratory smooth roller-compacted (unlike the other levee sites). The two erodible data points were likely due to localized non-homogeneity. Michoud 2 (Md2) material was the next best possibly due to its compaction method (smooth roller-compacted to minimum 90%). Michoud 3 (Md3) material was from the Bonnet Carre borrow pit but was uncompacted (lower bench slope). The erosion tests show that this levee is categorized as “moderately resistant”. Michoud 4 (Md4) was the Bonnet Carre borrow material compacted with three dozer passes as previously noted. James Construction Inc. built the Md3 and Md4 sites.

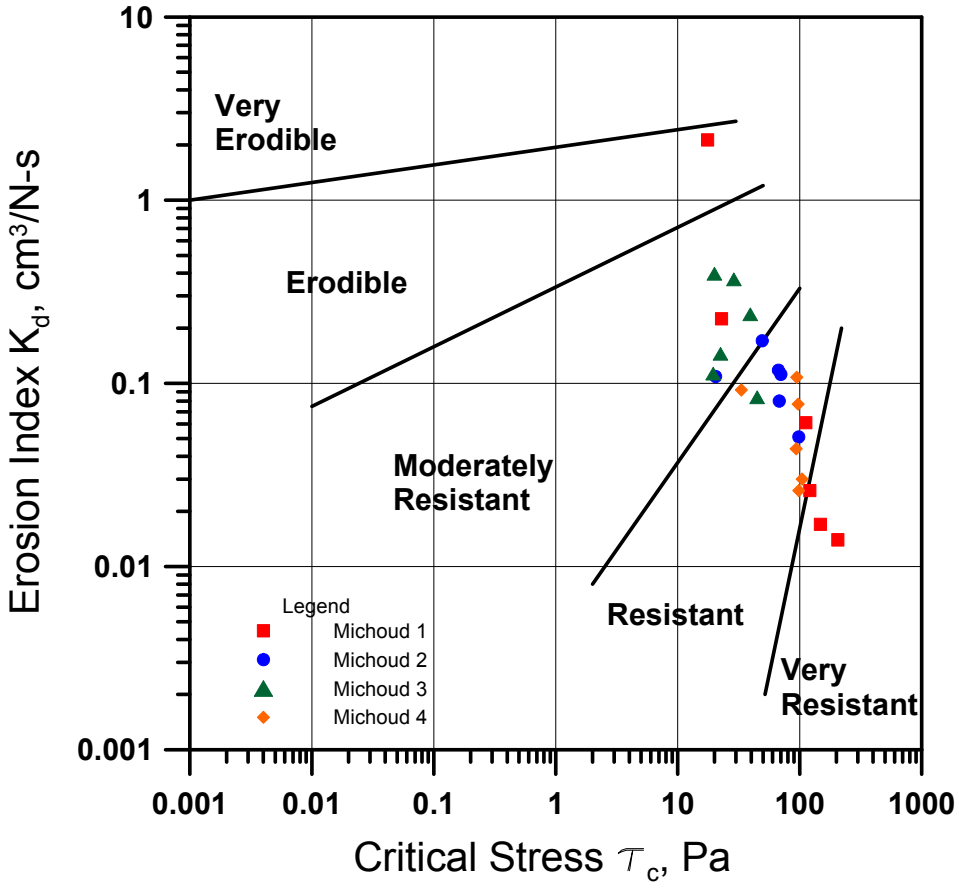

Figure 64. Erosion Index versus critical stress for New Orleans East levee sites (Michoud Canal and Slip sites)

Summary and Conclusions

Two major variables played roles in determining the extent and amount of levee damage caused by Hurricane Katrina. Hydraulic loading (storm surge and wave action) was the driving influence of course, but the levee damage was not a continuous function of overtopping surge and wave heights. Breaches occurred in places where the overtopping was less than 1 ft as well as those with overtopping up to 7 ft. The levee damage was also determined by pre-Katrina geotechnical issues (soil type, soil layering, soil consistency, and levee construction methods).

The lateral extent of damaged (eroded and breached) levees was greater where the overtopping surge and wave heights were greater, as evidenced by miles of missing levee sections along the MRGO that had about 7 ft maximum overtopping. The most damage-resistant levees (those with smaller amounts of erosion damage) appeared to be those having a fat clay cover with higher stiffness (density). The pre-Katrina soil borings showing medium-consistency fat clay (CH) as the crown surface layer withstood the highest overtopping with the least crown erosion. The levee sections having thicker layers of clay (less layering heterogeneity) also appeared to perform better, as did those constructed from hauled borrow soil (versus non-compacted hydraulic fill).

Minimal post-Katrina evidence was available to validate geotechnical correlations to surge height since the damaged levee data were taken from historic soil borings at limited locations. Only the most recent (mid 1990s to 2001) soil borings showed the pre-Katrina soil profile since previous borings generally were drilled through levees prior to their final construction lifts. The near-surface soils that poorly performed were washed away and were unavailable for analysis. Dynamic effects such as erosion progression and dynamic slope stability issues due to cyclic hydraulic loading were also not analyzed due to insufficient hydraulic and geotechnical forensic evidence.

The surface soil materials at fifteen levee sites were tested in-situ with the Jet Index apparatus. The sites were on levees in New Orleans East (Orleans Parish) and St. Bernard Parish, and included three surviving levee sections (overtopped by the storm surge but unbreached). The remaining 12 sites were on levees being reconstructed at the time of the tests.

The test results were plotted to show erosion resistance at each site. A wide range of erodibility was observed on both the existing and new levee materials. The existing (surviving) levee soils were erosion-resistant even with varying surge heights. Since the M3 site had the highest surge and wave loading (up to approximately 7 ft over the levee), and the jet index test results indicated its erosion resistance, it may be considered as a threshold for erodibility. For example, threshold erodibility values taken from the surviving levee sections may be useful for assessing erodibility of reconstructed levees when matched with anticipated hydraulic loading (surge heights).

The compaction effort appeared to influence the erodibility of the materials on the newly-constructed levees. For example, the Md1 levee was reconstructed using the 90% compaction specification and had a much higher jet index value than the G1 levee reconstructed using the 3-dozer-pass specification.

The jet index test method provided in-situ soil erodibility data that varied widely depending on the micro-scale soil conditions under the jet nozzle. The presence of a small root or soil fissure impacted the resultant erodibility coefficient and critical stress values. Performing two concurrent tests located approximately 6 ft apart on the levee surface also yielded varying results depending on micro-scale soil conditions under each nozzle. Extrapolating the data results to quantify an entire levee reach will require more robust spatial coverage (closer spacing and longer extents) as well as micro-scale issues. The jet index test provided a quantitative method to assess erodibility, and further efforts will be required to minimize the impacts of soil non-homogeneity and micro-scale variance for applying broader conclusions.

References

ASTM. 2000. “Standard test method for erodibility determination of soil in the field or in the laboratory by the Jet Index method,” American Society for Testing and Materials Standard Designation D 5852-00, West Conshohocken, PA.

Briaud, J.L., F.C.K. Ting, H.C. Chen, Y. Cao, S.W. Han, and K.W. Kwak. 2001. "Erosion function apparatus for scour rate prediction," *ASCE Journal of Geotechnical and Geoenvironmental Engineering*, Vol 127, No. 2, pp 105 - 113.

Fukuoka, S. and K. Fujita. 1988. "Levee overflow survey and development of the armored levee," *6th Congress, Asian and Pacific Regional Division, Intl Assoc for Hydraulic Research*, Kyoto, Japan, 20-22 July, pp 417 - 424.

Hanson, G.J., K.R. Cook, W. Hahn, and S.L. Britton. 2003. "Evaluating erosion widening and headcut migration rates for embankment overtopping tests," American Society of Agricultural Engineers Paper no. 032067.

Hanson, G.J. and A. Simon. 2002. "Discussion of 'Erosion function apparatus for scour rate predictions'," *ASCE Journal of Geotechnical and Geoenvironmental Engineering*, Vol 128, No. 8, pp 1-2.

Hanson, G.J., A. Simon, and K.R. Cook. 2002. "Non-vertical jet testing of cohesive streambank materials," *American Society of Agricultural Engineers (ASAE) Meeting Paper No. 022119*, St. Joseph, MI.

Hanson, G.J. and A. Simon. 2001. "Erodibility of cohesive streambeds in the loess area of the midwestern USA," *Hydrological Processes*, Vol 15, pp 23 - 38.

Hanson, G.J., K.M. Robinson, and K.R. Cook. 2001. "Prediction of headcut migration using a deterministic approach," *Transactions of the American Society of Agricultural Engineers*, Vol 44(3), pp 525 - 531.

Hanson, G.J. 1991. "Development of a jet index to characterize erosion resistance of soils in earthen spillways," *Transactions of the American Society of Agricultural Engineers*, Vol 36(5), pp 2015 - 2020.

Hunt, S.L., G.J. Hanson, K.R. Cook, and K.C. Kadavy. 2005. "Breach widening observations from earthen embankment tests," *Transactions of the American Society of Agricultural Engineers*, Vol 48(3), pp 1115 - 1120.

Interagency Performance Evaluation Team (IPET). 2006. Interim report I and II, ERDC. website

USACE. 1994. "Design of hydraulic structures," Engineering Manual 1110-2-1601, U.S. Army Corps of Engineers, Washington D.C.

USDA. *Engineering field manual*, U.S. Dept of Agriculture Soil Conservation Service, Washington, D.C.

Appendix 19
FLAC Numerical Analyses of Floodwalls of New Orleans Flood Protection System

SSI Analyses of 17th Street, London North, and London South Breaches

Background

A study was undertaken to analyze the performance of levees and floodwalls used in the New Orleans flood protection system to determine the most likely causes of their damage and failure from Hurricane Katrina. This study was conducted by the Interagency Performance Evaluation Task Force (IPET) and included 2D soil-structure interaction (SSI) numerical modeling. These modeling efforts support an investigation into how individual sections of the floodwall and levee system respond to the computed forces to better understand failure mechanisms and to explain phenomena observed in the field. These SSI analyses were conducted using the PC-based programs, Plaxis (Brinkgreve, 2004) and FLAC (Itasca, 1998). This report presents the results of the FLAC analyses.

Following a sequence of increasingly complex analyses provides a reasonable path when dealing with the challenging task of failure mode analysis. This is especially important since each additional step requires concomitant input data which is usually increasingly difficult to provide. Still the effort involved in SSI analyses offer potential advantages over limit equilibrium (whether or not a simple or more complex material model is used): a) better estimate of failure surface geometry, b) ability to handle strain interaction between stiff and soft materials, particularly if some of the materials may be strain softening, c) ability to obtain a relationship between deformation and safety factor, and d) ability to more easily couple the seepage and stress analyses.

Therefore, concurrent numerical analyses using Plaxis and FLAC were undertaken to provide a more thorough investigation. These coordinated but distinct analyses provided the advantage of comparing results from different numerical analysis software. The expected variations that permitted a measure of the robustness of the estimated results are the use of different model geometries, constitutive models, numerical solution schemes, and the numerical analysts. While the expected differences noted above should provide some variance among the results the

independence of this effort was necessarily constrained. All analyses relied on a common site characterization and material property assessment, system response insight provided by the prior limit equilibrium analyses, and collected field evidence on failure modes and flood water levels (IPET Stability Analyses, 2006). The analyzed sections were closely coordinated and consistent regarding section geometry control points, material properties, boundary conditions and failure mode assumptions.

The FLAC (Fast Lagrangian Analysis of Continua) numerical geotechnical analysis program was selected because it is well recognized, commercially available, and routinely used in geotechnical engineering practice. FLAC is an explicit, finite difference program that uses a Lagrangian formulation for performing large strain analyses. This program is capable of modeling two-dimensional problems in soil-structure interaction with full coupling of the stress-strain and groundwater flow components. Available constitutive models include linear elastic to non-linear plasticity-based models. FLAC also provides the capability of inputting user-defined constitutive models or making minor modifications to built-in models.

One of the distinct and significant differences between the FLAC and Plaxis programs is the method used to solve the equilibrium equations. FLAC uses an explicit solution scheme in which the dynamic equilibrium equations are solved at each of the nodal masses over a series of small timesteps. This dynamic solution process is used for static problems by ensuring enough timesteps are solved to reach equilibrium. Plaxis uses an implicit scheme which involves solution of the entire stiffness matrix of the structure. Although the equations solved in Plaxis are more computationally intensive, a solution may be achieved in significantly fewer steps.

A second key difference between the FLAC and Plaxis analyses is the formulation of the basic soil element. FLAC uses a very simple 4-noded quadrilateral element that is numerically constructed from overlaid pairs of constant strain triangular elements. Although this uncomplicated element allows for extremely fast stress-strain estimates, a relatively fine grid may be required to properly represent the variation of stress and strain within the structure. The finite element used in Plaxis is significantly more complex. In the analyses for the 17th St. Canal, 15-noded elements, each with 12 integration points, were used to model the soil.

Stability analyses were conducted with FLAC to investigate the following failure sections: 17th St. Outfall Canal breach (Station 10+00), and the two breaches on the London Outfall Canal (London North breach near the Robert E. Lee Boulevard bridge Station: 14+00 and London South breach near the Mirabeau St. bridge Station 53+00). The locations of these breached sections are show in Figures 19-1 and 19-2. These figures show two important geologic factors that were significant in the response of these floodwalls. First, the general near-surface geologic setting was mash-swamp deposits providing the possibility of low-strength clay and peat foundation soils. Secondly, a significant sand deposit that trends through the area is very shallow at London's south and north breaches, but found much deeper at 17th St. breach site. The general foundation soils stratigraphy to an approximate depth of 80 ft was idealized and modeled with material zones: levee clay, clay top soil, peat, lacustrine clay, beach sand, bay sound clay, and finally the Pleistocene clays.

A relatively brief description of each analysis is provided since much of the material and geometric description has already been provided in the other IPET reports.

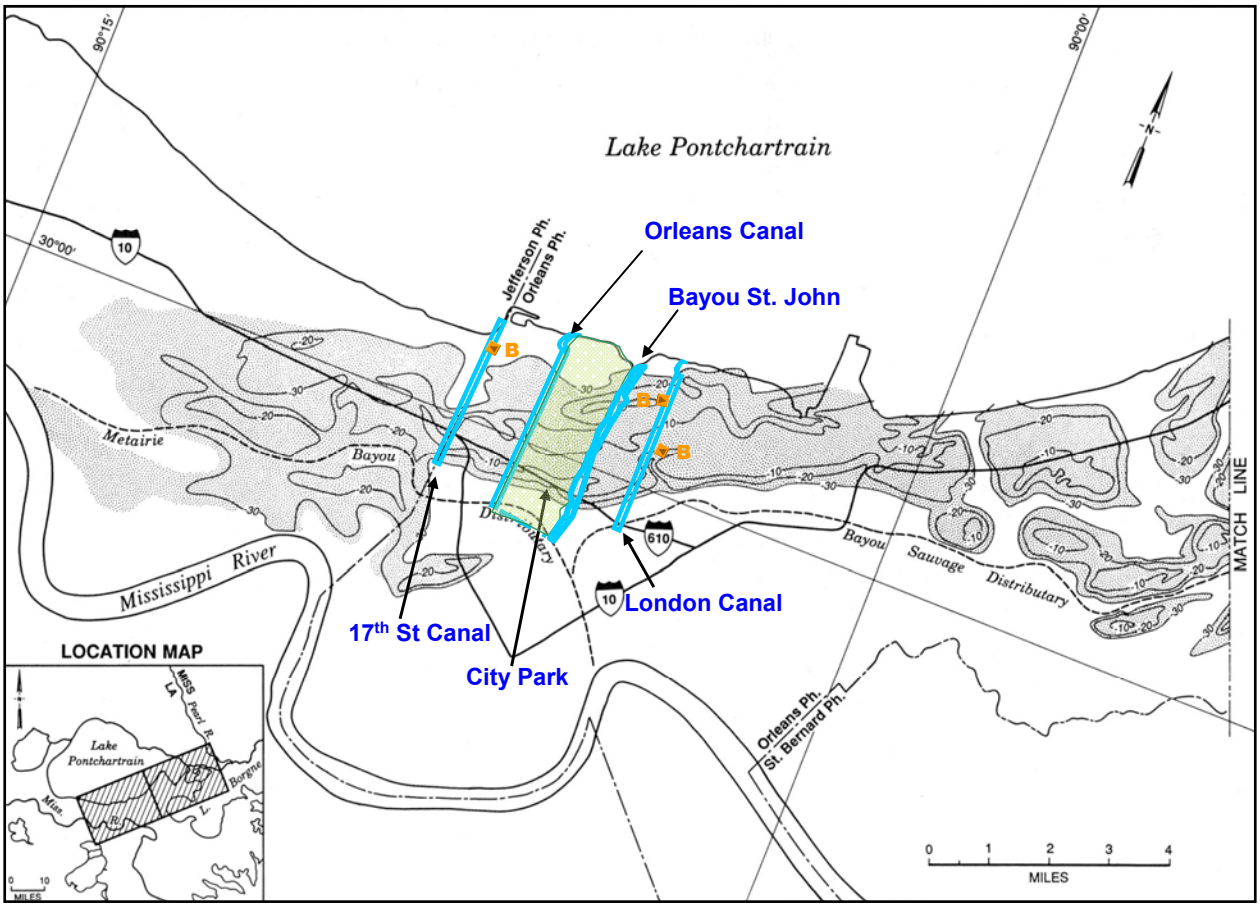

Figure 19-1. Location of breach sections analyzed plotted on a map of depth to beach sand deposit (showing why sands in foundation were important to London Canal breaches and probably not the 17th St. breach)

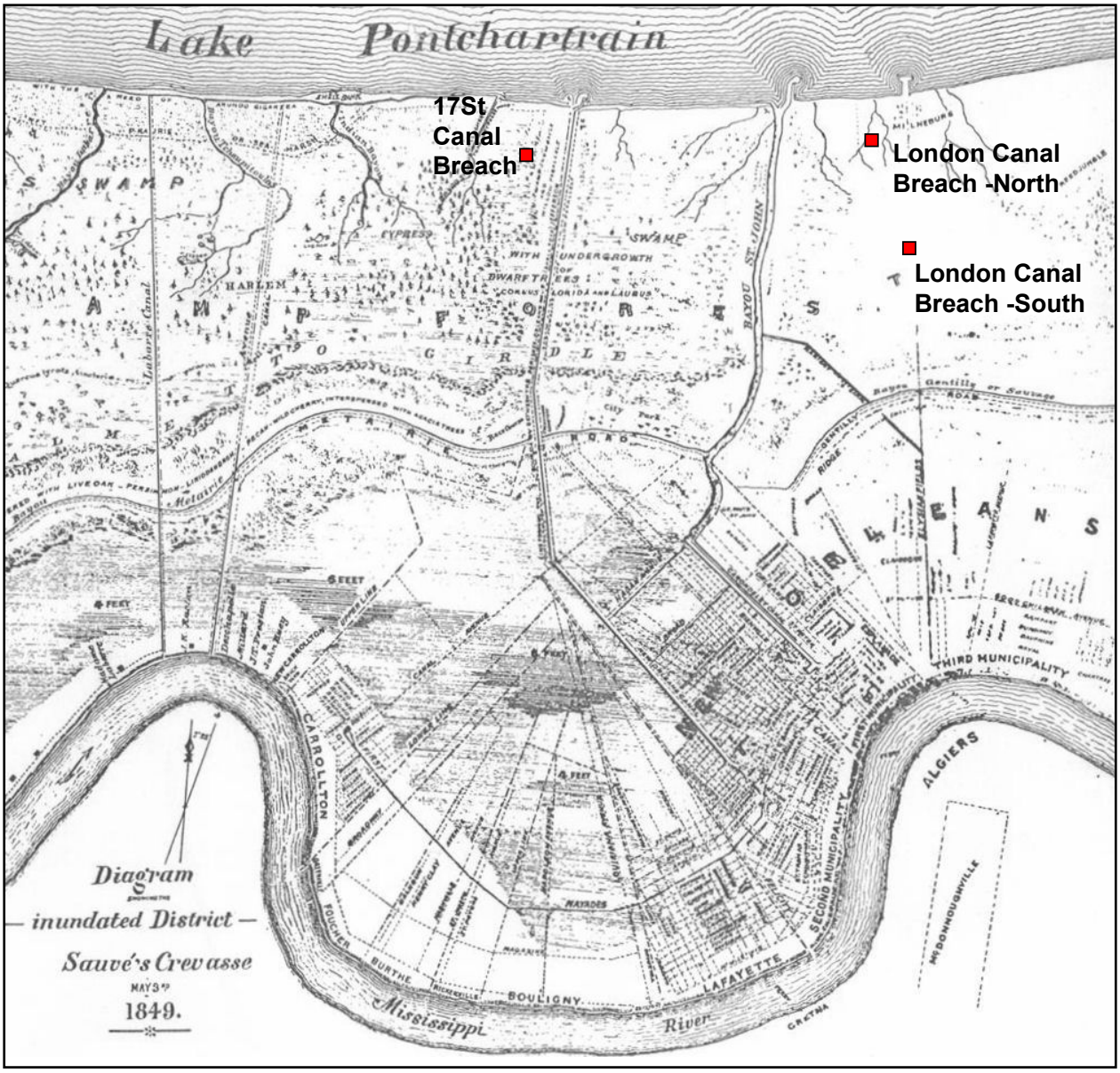

Figure 19-2. Near-surface geologic deposition environment and significant marsh-swamp peat and soft clay conditions

17th St. Outfall Canal Breach Analysis

The 17th St. Outfall Canal breach was analyzed using both a linear-perfectly plastic Mohr-Coulomb model, and a non-linear constitutive model. Both analyses used a total stress approach for representing the undrained behavior of the finer-grained soils. The canal section at Station 10+00 was used in the analysis. This section is composed of concrete and steel sheet-pile I-wall floodwall built into the centerline of the earthen levee. The findings of the limit equilibrium stability analyses showed that given the wall failure at an estimated canal water level of 6.5 ft (all elevations are referenced to NAD88 datum unless noted), introducing a full depth crack from

surface to pile tip resulted in Factor of Safety of 0.88. Without introduction of a crack, the Factor of Safety is 1.62 (IPET, 2006). This assumed crack or gap between the sheet pile wall and canal side embankment is a significant factor in these analyses. The IPET field reconnaissance study documented this condition along intact wall panels adjacent to the London North breach and along the distressed floodwall on the east side across from this breach. This response of the I-walls was also noted in places along the Inner Harbor Navigation Canal. The water level in 17th St. Canal submerged any visual evidence for this breach. The "crack" or gap between the sheet pile wall and soil embankment on the canal side was introduced into the model and its occurrence is supported with simple stress analyses.

Linear-perfectly plastic Mohr-Coulomb Analysis

This FLAC analysis uses a simple plasticity based model where the failure envelope follows the Mohr-Coulomb criterion and all stress increments below the failure envelope are considered linear elastic. The use of such a simple model can be acceptable when the strength of the material governs the behavior and other effects such as stiffness or potential strain softening are secondary. The Mohr-Coulomb model appeared suitable for this evaluation given the characterization provided for the various soil units: linearly-varying undrained strengths and average secant stiffness (E_{50}) as a simple multiple of undrained strength.

The two primary objectives of this analysis were 1) to determine if a failure consistent with the observed behavior would be predicted by FLAC using the provided site characterization, and 2) to provide a basis of comparison to other analyses performed on the same section. A thorough evaluation of the response, including sensitivity or parametric studies, was not performed.

Approach

The general development of the FLAC model was kept consistent with the Plaxis and limit equilibrium analyses by strictly adhering to the provided site interpretation. Key parameters provided for the FLAC analysis included the stratigraphic and geometric description, unit weights, undrained strength for fine grained soils, drained strength for the Beach Sand layer, and average secant elastic modulus (E_{50}) for the fine grained soils. A tensile strength was also assumed for the fine grained soils to permit the prediction of a gap adjacent to the sheet pile wall. Soil properties were assigned element by element to provide for smoothly changing properties consistent with the specified variations.

The floodwall was represented with the structural beam elements included in the FLAC program. Structural properties for the wall were input as provided. The beam element interacted with the soil grid through interface elements on each side of the structure. These interface elements were assigned zero tensile strength and assumed to have a relatively low shear strength equal to 2/3 of the adjacent soil strength.

A total stress formulation based on the undrained strengths and stiffnesses was used to evaluate the response to the flood loading.

The analysis was performed in small strain mode to eliminate the potential grid distortion caused when predicted element strains become very large. Large strain analyses can be useful when the predicted deformations have a significant influence on the stability of the section. Such changes in stability are often the result of a decrease in driving force or an increase in the resisting or buttressing force. However, the initial deformations predicted for the levee were dominated by lateral sliding with relatively little change expected in the stability. The small strain formulation is considered adequate for predicting the modest displacements related to impending failure. However, the magnitude and pattern of the very large displacements associated with failure may be influenced by this simplification.

The FLAC grid is shown in Figure 19-3. As can be seen, the model space is well sampled and uniform allowing the simple quadrilateral zone elements to accurately capture the model response.

Solution procedure

The steady state pore pressure distribution resulting from a canal water surface elevation of 1 ft was estimated using a seepage analysis. The boundary conditions were consistent with the Plaxis analysis and relative values of hydraulic conductivity were assumed. The seepage analysis produced a reasonable distribution of pore pressures across the grid as shown in Figure 19-4. The effect of the sheet pile wall on the pore pressures and flow vectors is clearly seen.

The initial state of effective stress in the model was estimated using a sequence of elastic and plastic analyses. The objective of these analyses was to establish an initial state of stress that was in equilibrium and that had values of horizontal effective stresses that reflected the geometry and strength of the material. Drained strengths were assumed during the plastic analyses to help achieve this goal. Although a more refined estimate of the initial stress state could be made using a non-linear constitutive model and imposing the loading or construction history, initial stress states are difficult to accurately estimate given the many unknowns and the stress redistribution that may occur with time. The initial stress state is shown in Figure 19-5, and contours of the fraction of mobilized shear strength are shown in Figure 19-6.

The flood analysis was performed incrementally to reduce the dynamic response related to the loading of each flood increment. Water levels were increased in the canal a maximum of 0.5 to 1.0 feet per increment. Equilibrium conditions were achieved at each increment before increasing the water surface elevation (WSE).

The development of a gap between the sheet pile wall and soil on the canal side of the levee had been identified as potentially critical prior to performing the FLAC analysis. A subroutine was added that automatically determined if a crack could occur based on the prediction of horizontal effective stress between the wall and soil. The subroutine was executed at the end of the calculations for each flood stage. This routine checked the stresses in the uppermost element against the wall. If the horizontal effective stresses were found to be compressive, then the routine assumed a crack would not propagate and the solution for the next flood increment would begin. However, if the effective stresses in the element were tensile, then the crack was assumed to propagate across that element: the interface would be removed and the full hydrostatic force

and pore pressure was applied to the edge of the soil element as well as the wall. The analysis was then stepped to equilibrium and crack propagation was evaluated across the next lower element. Pressures within the crack were updated at every flood increment.

Although the crack subroutine appeared to produce a final gap consistent with expectations, there are a couple of uncertainties with this approach. First, crack propagation depends upon accurate prediction of horizontal effective stresses. As this is not an easy task to accurately achieve, it would be reasonable to include a safety factor in the crack propagation routine. In addition, the Mohr-Coulomb model may not give the best prediction of horizontal stresses at states below failure. And second, the above routine used the effective stress in the soil element to estimate tensile conditions. This effective stress was based on the pore pressure predicted in the soil, which was typically less than the hydrostatic pressure based on the current flood stage. Because the crack propagates along the predefined interface between the wall and soil, and the opening of the crack could expose the crack tip to the full hydrostatic pressure, it seems reasonable to revise the routine so that the effective stress is based on the hydrostatic pressure rather than the predicted pore pressure.

Analysis Results and Discussion

Using the assumptions for crack formation described above, the crack was estimated to initiate during the first flood increment which had a WSE of 2.0 feet. The initial crack or gap was 5 ft deep, which gradually increased to the full 16 foot depth when the WSE reached 9.5 ft. The initiation and growth of a crack is shown to greatly increase the displacements and leads to a response indicative of impending failure. Figure 19-7 shows the predicted maximum displacements of the wall and soil as well as crack depth versus WSE. In comparison, the Plaxis analysis used a different crack initiation criteria based on hydrostatic pressure exceeding total horizontal stress. This approach has the crack initiate at WSE of 6.5 ft and extend to the marsh-lacustrine clay interface which is 2 ft above the sheet pile tip. In this analysis, the crack started at a lower flood stage but developed slower, not reaching this depth until a WSE of 8.5 ft.

The predicted response following formation of a full depth crack to the tip of the sheet pile shows a failure surface beginning at base of sheet pile and extending horizontally near the top of the Lacustrine Clay layer until turning upward and exiting the surface roughly 60 ft from wall on protected side. This is illustrated in Figures 19-8 and 19-9 which show deformed shapes and contours of maximum shear strain. The model also predicts that at a WSE of 10 ft there is sufficient wall movement, approximately 7 ft, to assume the wall section is breached. Also, although the model was in equilibrium but certainly breached for 10 ft WSE, an additional 0.5 ft rise in the water level produced additional deformations, and the modeled section could not reach equilibrium. Furthermore, the predicted wall displacements at lower flood levels such as 8.5 ft are still considerable, greater that 2 ft, Figure 19-11, which may be sufficient to separate individual wall panels and initiate a breach before the unstable condition posed by the 10.5 WSE. Accommodating over 2 feet of displacement would require a broad smooth intact deformation of a section of wall panels. The field reconnaissance documented severe distress to the wall section directly across from the London north breach that was near failure and had a gap

of approximately 2 ft at the top of soil embankment. The predicted failure surface is clearly displayed in Figure 19-9 in contour plots of maximum shear strain.

The development of the failure mode is further clarified in Figure 19-10, which shows estimated contours for the fraction of mobilized shear strength at three water levels: WSE = 4, 7, and 10.5 feet. Significant zones of the Lacustrine Clay are predicted to be highly stressed from the start of flood loading. Full instability of the section occurs as the marsh/peat and topsoil zones become highly stressed.

The representation of material properties for the soil was relatively simple. This was particularly true with respect to the assumption of linear stiffness and the relatively uniform undrained strengths. Also the numerical simplifications made in the analyses are factors which probably contributed to estimating smaller deformation than the other analyses and a higher WSE for section instability. Nevertheless, even hampered with these conservative and simplifying assumptions and approaches significant deformation is predicted for this section providing insight into the probable failure mechanism. Although a more refined modeling of soil properties and sensitivity evaluation could permit a better assessment of actual or potential response, the modeling and analysis described above appears to have been adequate to identify a critical response mode of the structure.

Conclusions

This analysis supports the field observations, aspects of the limit equilibrium analyses, and the Plaxis SSI analyses that a predominately translational instability breached this section at WSE less than 10.5 ft. The current model properties produce a failure surface initiating close to pile tip elevation near the top of the lacustrine clay layer. In comparison, another study being conducted by the National Science Foundation (Seed et al, 2006) report a similar failure mode, but at a higher elevation within the Marsh layer. The FLAC model also shows a kinematic response that approximately matches the field observed intact block displacement of protected side of levee embankment and heaving and over-thrusting of foundation soil layers beyond the levee toe.

The introduction of "crack" or gap between the canal side sheet pile wall and levee soil embankment was a dominant factor in inducing this failure mode. Continuing analyses involving alternative crack formation criteria support a gap formation evolution that results in failure at a WSE elevation closer to the field reported 8.5 ft. This shows the importance in this phenomenon in controlling failure behavior and should be further studied.

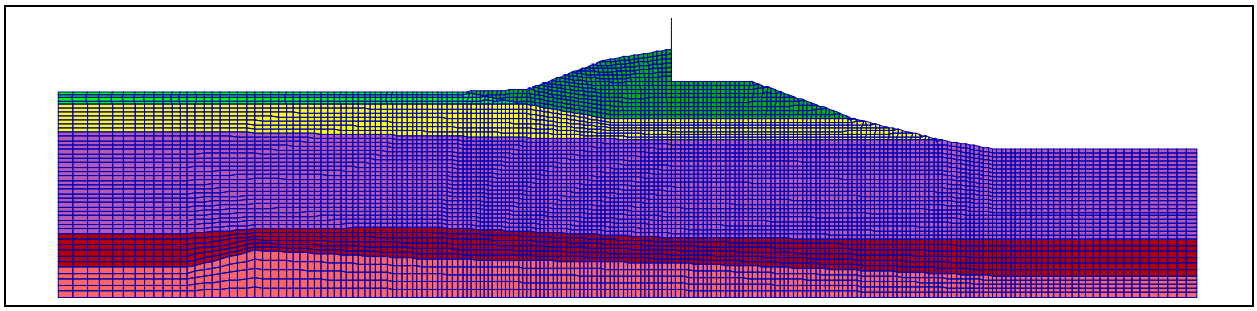

a. FLAC grid

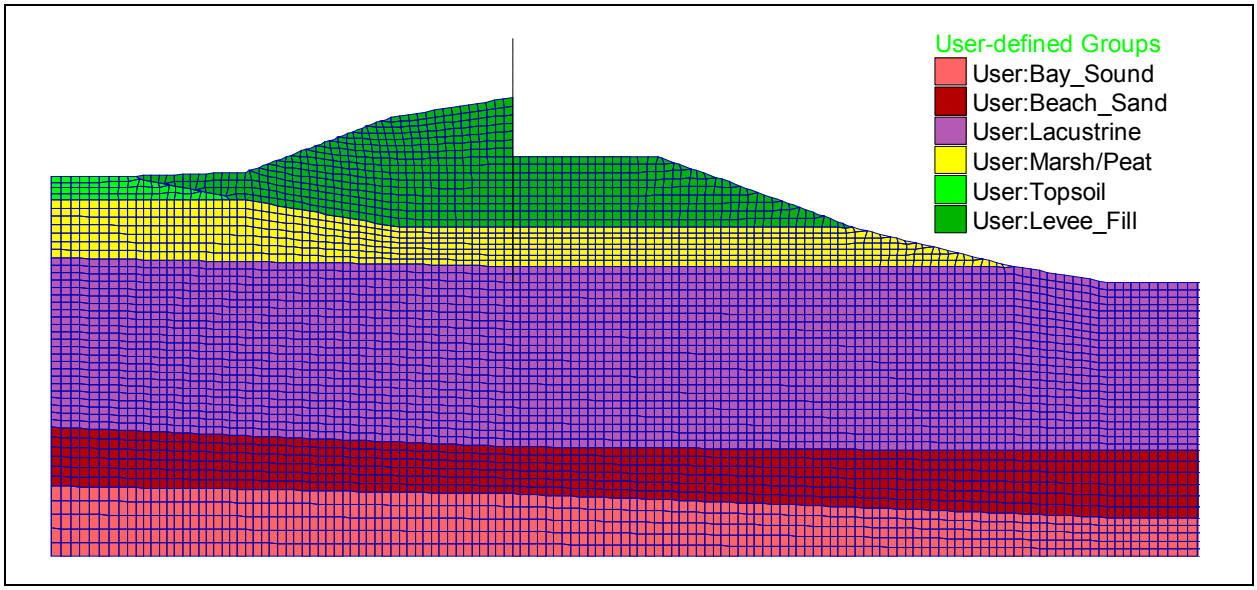

b. FLAC grid at levee

Figure 19-3. FLAC model geometry for 17th St. breach

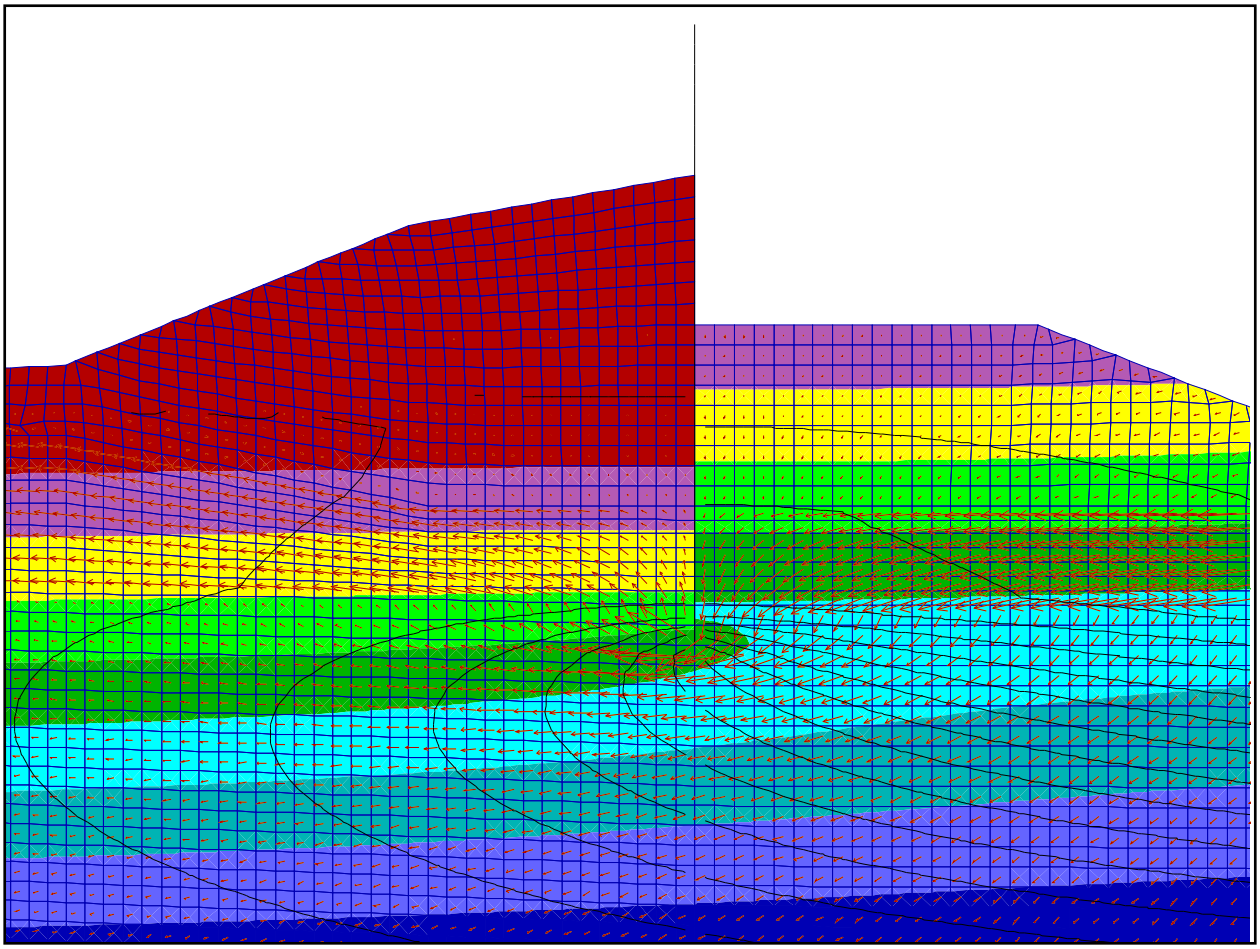

Figure 19-4. Estimated pore pressures, flow vectors, and contours of head at levee for 17th St. breach sta. 10+00

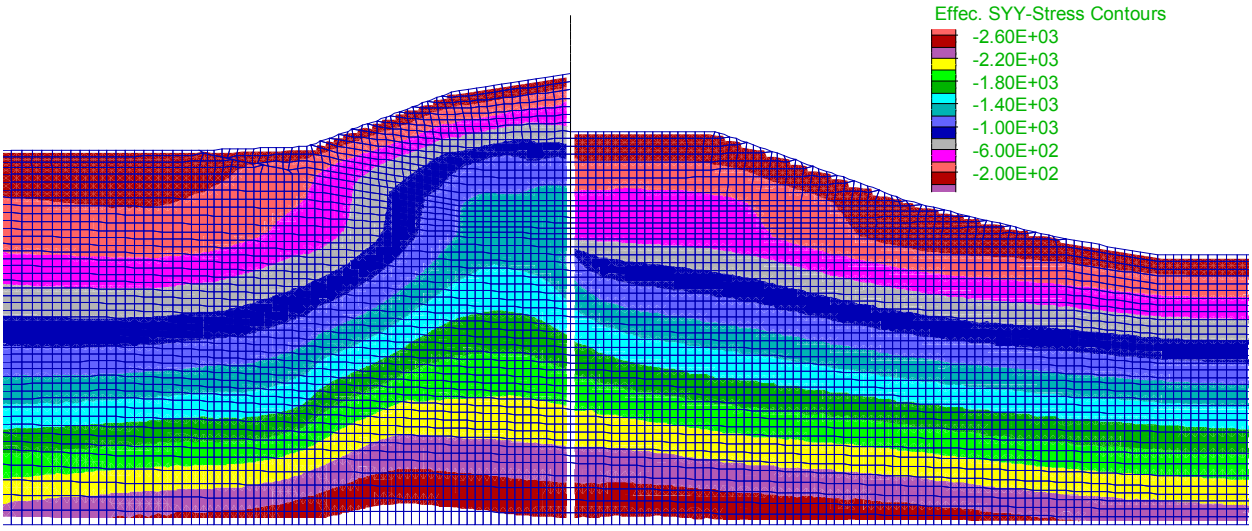

a. Vertical effective stress

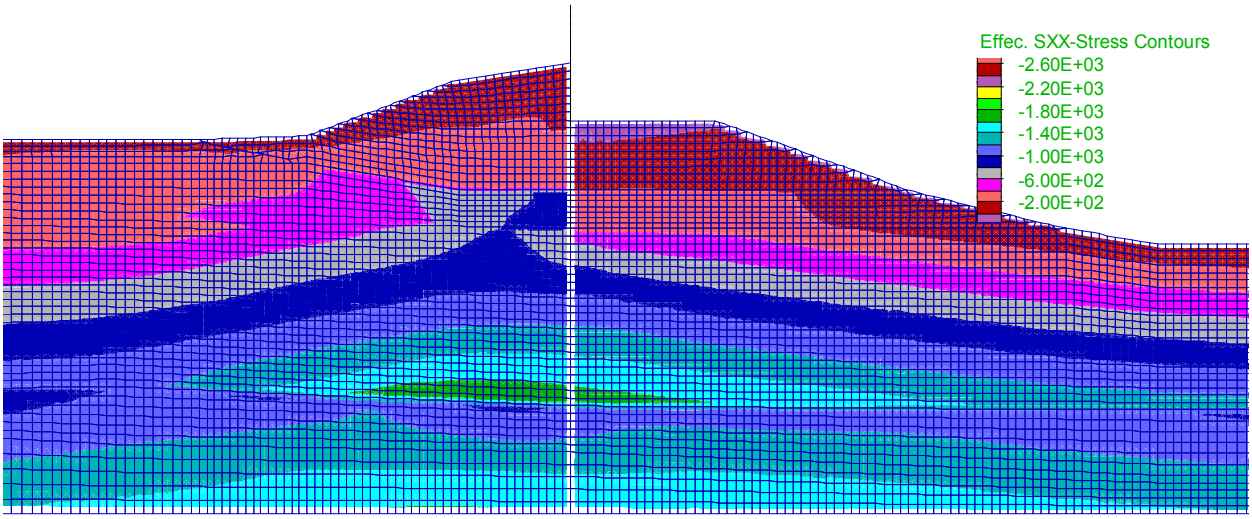

b. Horizontal effective stress

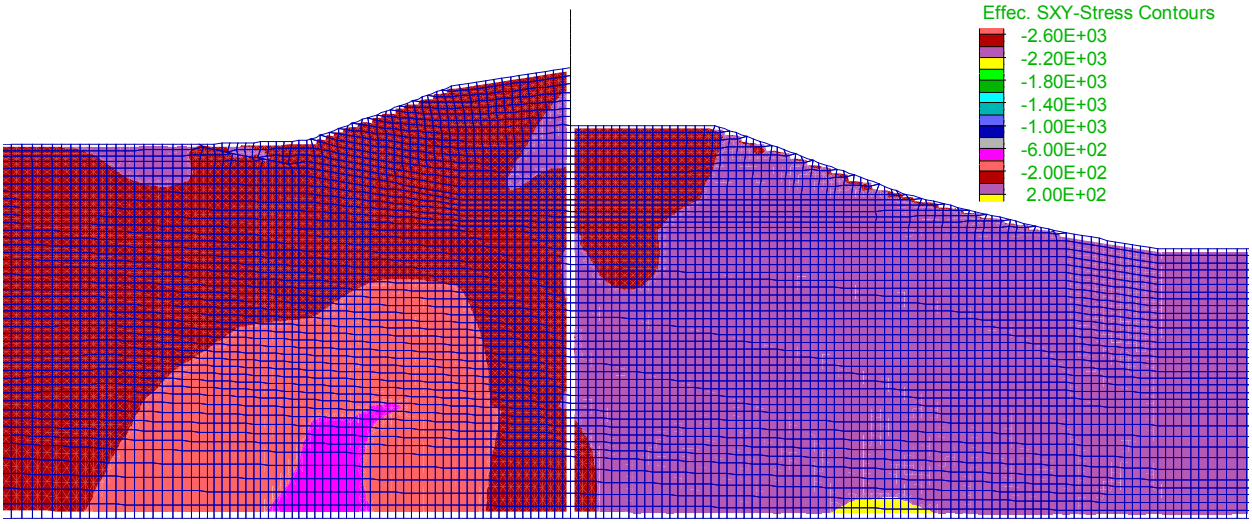

c. Horizontal Shear Stress

Figure 19-5. Estimated stresses for initial conditions for 17th St breach sta. 10+00

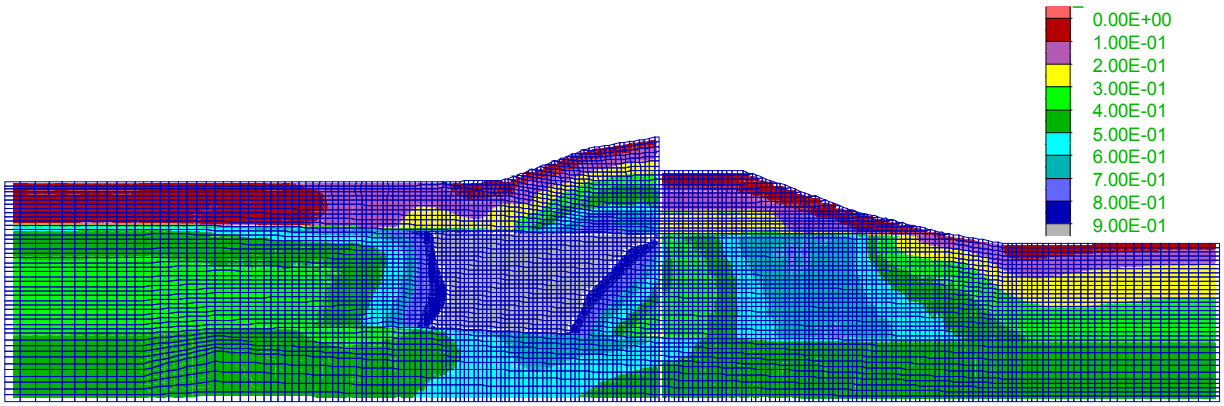

Figure 19-6. Fraction of mobilized shear strength for initial conditions and undrained strengths for 17th St. breach sta. 10+00

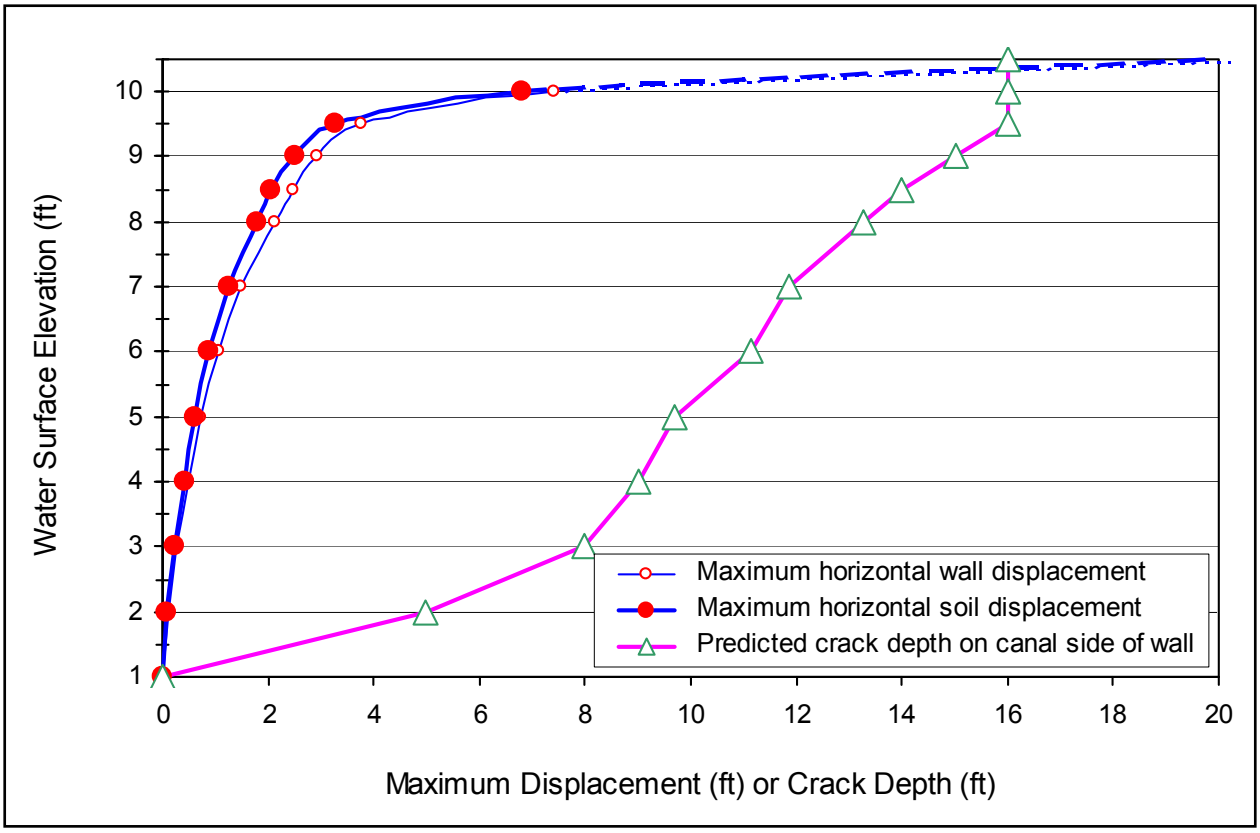

Figure 19-7. Predicted maximum horizontal displacement and crack depth versus WSE for 17th St. breach sta. 10+00

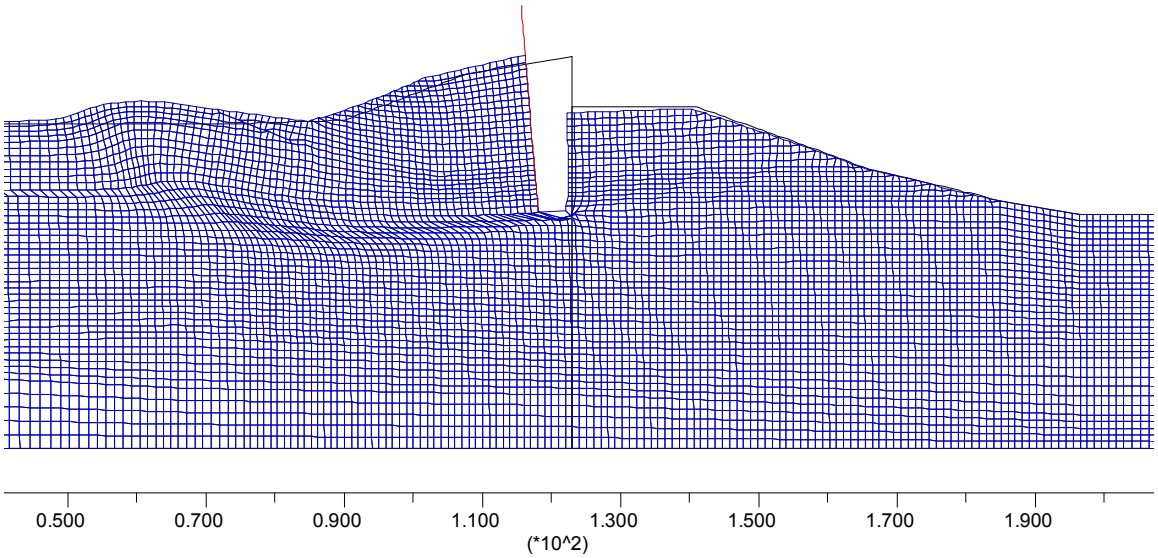

a. WSE = 10.0 feet (displacement shown at true scale, model at equilibrium)

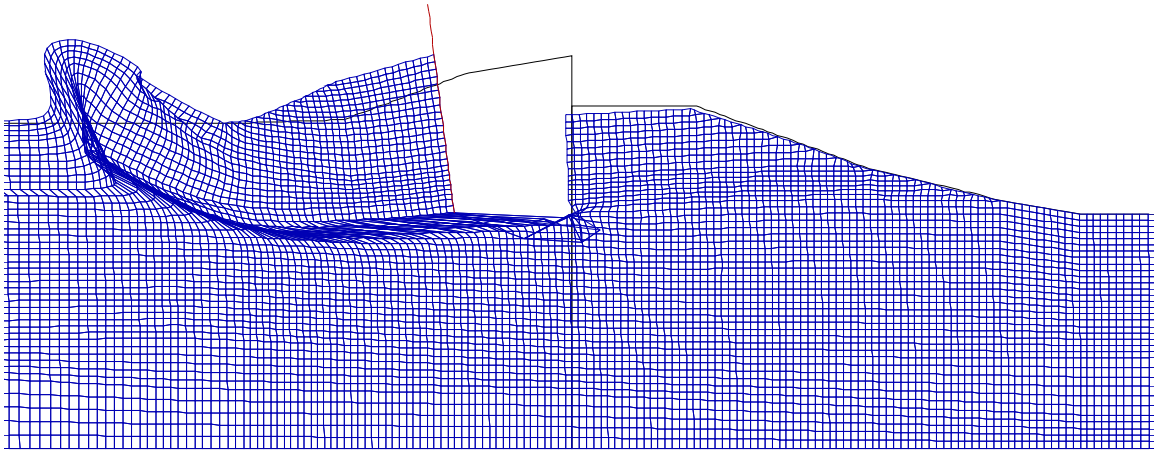

b. WES =10.5 feet (displacement shown at true scale, model NOT at equilibrium

Figure 19-8. Estimated deformed shape for 17th St. breach Sta. 10+00

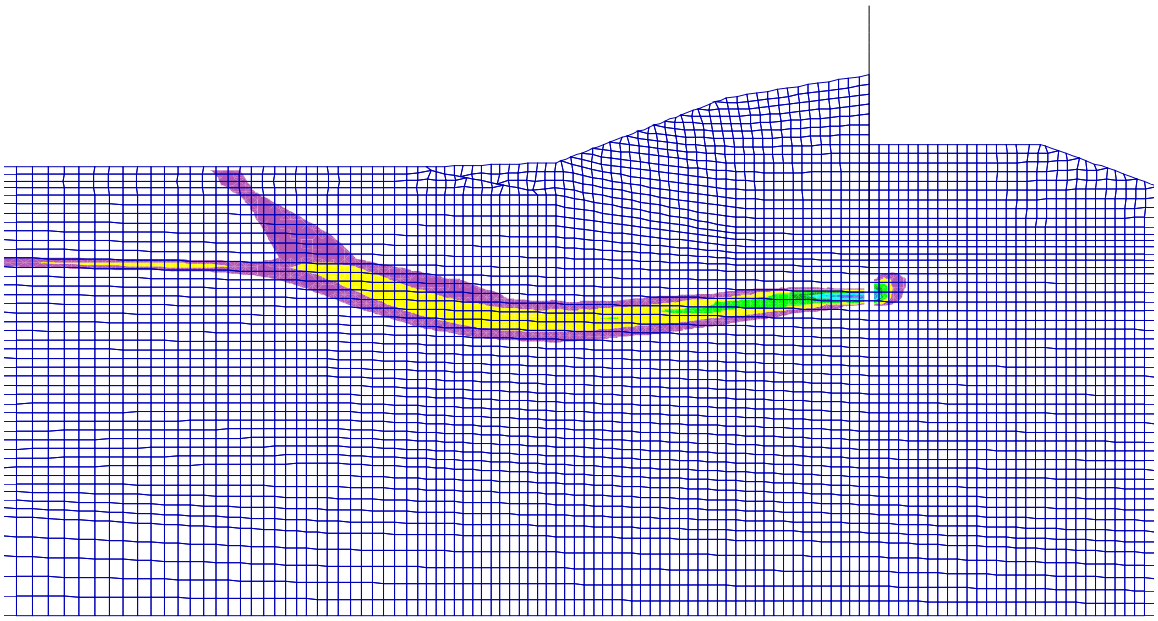

a) WSE =10.0 feet (contour increment = 50% shear strain)

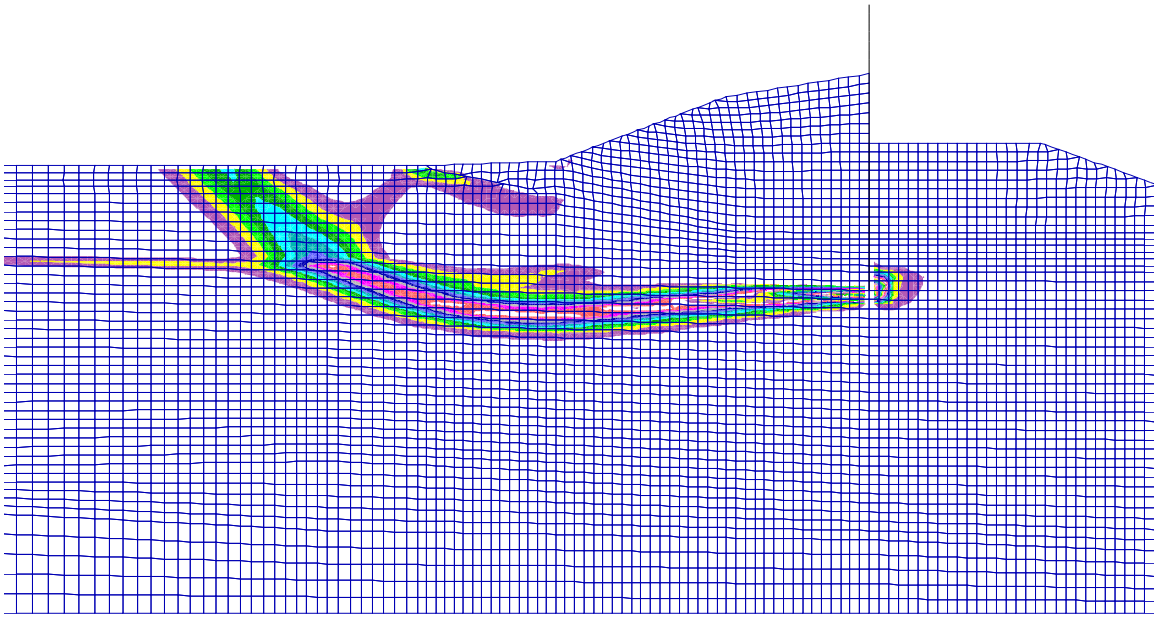

b) WSE = 10.5 feet (contour increment= 50% shear strain)

Figure 19-9. Estimated contours of maximum shear strain Mohr-Coulomb model for 17th St. breach sta. 10+00

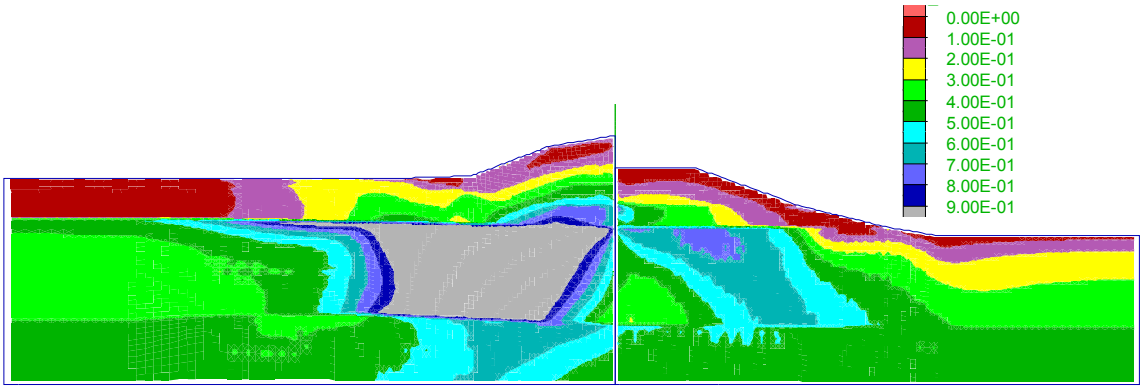

a. WSE = 4 feet

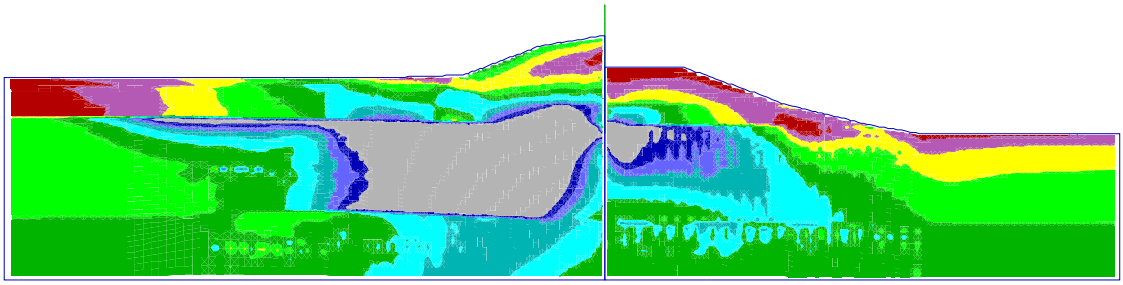

b. WES = 7 feet

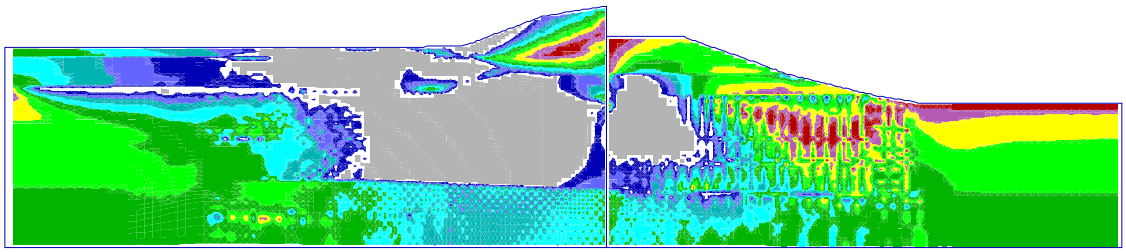

c. WSE = 10.5 feet

Figure 19-10. Estimated fraction of mobilized shear strength for 17th St breach sta. 10+00

Figure 19-11. Estimated deformed shape for WSE=8.5 for entire model (a) and near levee crest with 5x exaggeration (b) for 17th St. breach sta. 10+00

Nonlinear Constitutive Model Analysis

Approach. The levee section at Station 10+00 of the 17th St. Canal in New Orleans was also analyzed using FLAC with a user-defined nonlinear soil model for the Katrina high water elevation of 8.5 ft. The geometry and undrained strengths are consistent with the Plaxis analyses. For the current analysis, a simple case was run with Young's modulus (Eu_50) of E50=92·Su for all clays (value assigned for lacustrine clay). This model is being run next for the case consistent with the Plaxis analysis which used assigned softer properties of E50=48·Su for the levee and peat clays. The nonlinear model used was developed by Wang et al, Geomatrix Consultants, Inc. (Wang 1990) and requires additional model parameters (G_{max} and h_r) for total stress analysis.

The analysis presented here used a simple relation to define these two parameters. For G_{max}, $2 \cdot G_{50} = E_{u\_50}/(2/(1+\nu))$ was used. Another parameter $h_r = 0.77$ was chosen to give a secant modulus $G = 0.5G_{max}$ at a strain level $\varepsilon = S_u/G_{max}$. The unit weight, undrained soil strength, and model parameters are presented in Table 19-1. The undrained strength of the clay for each zone was specified consistent with values used in the slope stability analyses. These strengths vary horizontally and increase with depth at the rate of 11psf/foot to account for the appropriate confining stresses.

The model profile showing the finite difference grid and the soil layers is presented in Figures 19-12 and 19-13.

Table 19-1. Soil Properties and Model Parameters for Levee Section at 17th Street Canal, Station 10+00

Description	Soil Type	gt, pcf	gt/g	Su, psf	f, deg	E50=92*su	n, Poisson	G, psf	K,psf	Gmax	hr
Fill/Top soil	1	109	3.39	900	0	82800	0.47	28163	690000	56327	0.77
Marsh (Canal side)	2	80	2.48	350	0	32200	0.47	10952	268333	21905	0.77
Marsh (Protected side)	4	80	2.48	150	0	13800	0.47	4694	115000	9388	0.77
	4	80	2.48	250	0	23000	0.47	7823	191667	15646	0.77
	4	80	2.48	300	0	27600	0.47	9388	230000	18776	0.77
	4	80	2.48	350	0	32200	0.47	10952	268333	21905	0.77
	4	80	2.48	400	0	36800	0.47	12517	306667	25034	0.77
	4	80	2.48	450	0	41400	0.47	14082	345000	28163	0.77
Lacustrine	5	109	3.39	Table	0	Table	0.47	Table	Table	Table	0.77
Beach Sand	6	120	3.73	1500		138000	0.47	46939	1150000	93878	0.77
Bay Sound	7	125	3.88	5000		460000	0.47	156463	3833333	312925	0.77

The analysis was performed in the following steps: build model and apply initial water level, estimate initial stress conditions, apply flood load, introduce crack between floodwall and soil levee, and finally introduce an interface along failure surface defined by non-interface model.

In building the model, a simple contrived construction history was implemented based on current geometry. The construction steps were first to bring soil foundation and levee embankment to canal side bench level (elevation -2.5 feet), insert sheet pile and floodwall (floodwall top elevation of 12.5 ft and sheet pile tip at elevation -18.5 ft), continue building levee embankment to final crest elevation of 5 ft on protected side. In building the numerical model the grid space was first generated and the soil was constructed layer by layer by turning on gravity for each layer. The newly added layer was a load increment for the previously constructed layers, so that the non-linear soil model can be properly invoked by simulating natural deposition and construction events to better compute the resultant static stresses within the levee embankment and foundation. The concrete I-wall and sheet piles were simulated by linear elastic beam elements using the properties assigned by the Plaxis team.

Next, the water pressures for pre-Katrina water levels were applied; a normal canal water elevation of 0.5 was used. The normal water pressures were developed based on water level of elevation -0.5 ft on the canal side levee with a tail-water level elevation -5 on the protected side.

The phreatic surface was generated using FLAC's 'Water Table' option which assigns pore pressures based on this static head in-lieu of ground water flow generated phreatic surface.

This model was then solved to equilibrium and all computed grid node displacements reset to zero. These analysis steps resulted in an estimate of pre-Katrina static effective stresses for before applying the Katrina flood loading.

The Katrina flood water level was applied in one step using FLAC's 'Water Table' option and applied water pressure to levee on the canal side to compute the displacements. The solution was obtained using FLAC's 'dynamic on' option, because the 9 feet high Katrina water (from elevation -0.5' to elevation 8.5') was simulated as an 'impact' loading while in reality such water might be raised in a few hours. The computed displacements oscillated until they reached steady values. Only the stabilized displacements were used. This loading produced a displacement of the floodwall of approximately 1 foot, but resulted in a stable section that did not predict failure. This simplified loading procedure (i.e. apply Katrina water in one step) may overly predict the levee's deformation compared with raising the water foot by foot and computing the stabilized displacement for each water increment. This conclusion for non-failure is based on the modeled single wall panel section and assumes that the wall panels can accommodate this amount of differential displacement which is beyond the scope of the current 2-D model.

Based on the results of the slope stability analyses, and the hydraulic fracturing criteria used in the Plaxis analyses, it was assumed that a crack or gap will develop next to the concrete wall and sheet pile (on the canal side), down to the elevation of the tip of the pile. The development of such a crack was verified by comparing the pore water pressure with total horizontal stress in the soil layers (as shown in Figure 19-18). For the water level at the Katrina high flood level (elevation 8.5 feet), the pore pressures in the soil profile were generally greater than the total horizontal normal stress (computed at normal pool water level at elevation -0.5 ft) down to about elevation -19 feet.

Accordingly, the soil column adjacent to the wall above the pile tip (elevation -18.5 feet) was removed (nulled). The removal of the soil (i.e., an excavation process) allows the canal water to fill the void, and boundary water pressures were then applied normal to the sheet-pile wall and the opposite side soil face as well as the base of the excavated column.

The water level is raised to the specified flood level, and the calculation is continued to compute the total wall movement as a result of the formation of the crack and the rise in the water level. Again, the crack was assumed to form in one step down to the pile tip, and the displacement induced due to the application of the water pressure in the crack was computed in the FLAC's 'dynamic on' mode. The computed displacements oscillated until they reached steady values and only the stabilized displacements were used.

In addition to the simulation of the crack formation, and before raising the water level to the specified flood level, a horizontal interface layer was included at the pile tip level (El. -18.5 feet) on the protected side, with a specified undrained shear strength equal to the strength calculated for the Lacustrine clay layer at the same elevation. This interface feature allows FLAC to

compute larger displacement along the upper portion of the weak clay layer when the water level is raised to the Katrina flood level at elevation 8.5 ft (or 10.5 ft).

Analysis Results and Discussion. The material zones, beam elements simulating the floodwall and sheet piles and the normal pool water are shown in Figure 19-12. The finite difference grid used for the FLAC analysis is shown in Figure 19-13. The computed total vertical stress and pore water pressure at normal pool water level are presented in Figure 19-14 and 19-15, respectively. The pore water pressure contours using Katrina water at elevation 8.5 ft are presented in Figure 19-16.

Computed displacements of the floodwall due to water levels associated with the high Katrina flood levels, but ignoring the effects of crack or gap formation between the floodwall and the levee berm (at the canal side) were less than 1 foot, but the levee slopes were stable with no indication of impending failure (Figure 19-17).

Pore water pressures associated with Katrina high flood water level exceeded the total horizontal normal stresses computed from normal pool water level in the clay layers down to about elevation 19 feet, indicating the potential for crack formation between the levee soil and the sheet pile wall (Figure 19-18).

The possible crack formation was simulated in the analyses. The computed deformations of the pile wall and the levee slopes when simulating the effect of cracking resulted in horizontal deformation of about 1.2 ft (Figure 19-19).

When incorporating a horizontal interface at the top of the soft lacustrine clay layer (at the elevation of pile tip), the computed deformation for the Katrina flood water level at El. 8.5 ft was about 5 to 6 ft, indicating the potential for failure (Figure 19-20).

Conclusion. The representation of material properties using a nonlinear constitutive model for the soil was more sophisticated but also more dependent on an estimate of initial stresses. The modeling and analysis described above appears to also have identified a critical failure mode for this structure.

This analysis also supports the field observations, aspects of the limit equilibrium analyses, and the Plaxis SSI analyses that a predominately translation instability breached this section at a canal water flood level at elevation 8.5 ft. The current model properties produce a failure surface initiating close to pile tip elevation near the top of the lacustrine clay layer. The FLAC model also shows a kinematic response that approximately matches the field observed intact block displacement of the protected side of levee embankment and heaving and over-thrusting of foundation soil layers beyond the levee toe.

However, the introduction of “crack” or gap between the canal side sheet pile wall and levee soil embankment and use of an interface along the failure surface were needed to induce significant displacements (5 to 6 ft) and probable failure. Continuing analyses with lower stiffnesses for the levee and marsh deposits may alter these results. Use of this non-linear soil model may be important in obtaining a better estimate of initial stresses effecting the formation of the crack or gap needed to trigger this failure mode.

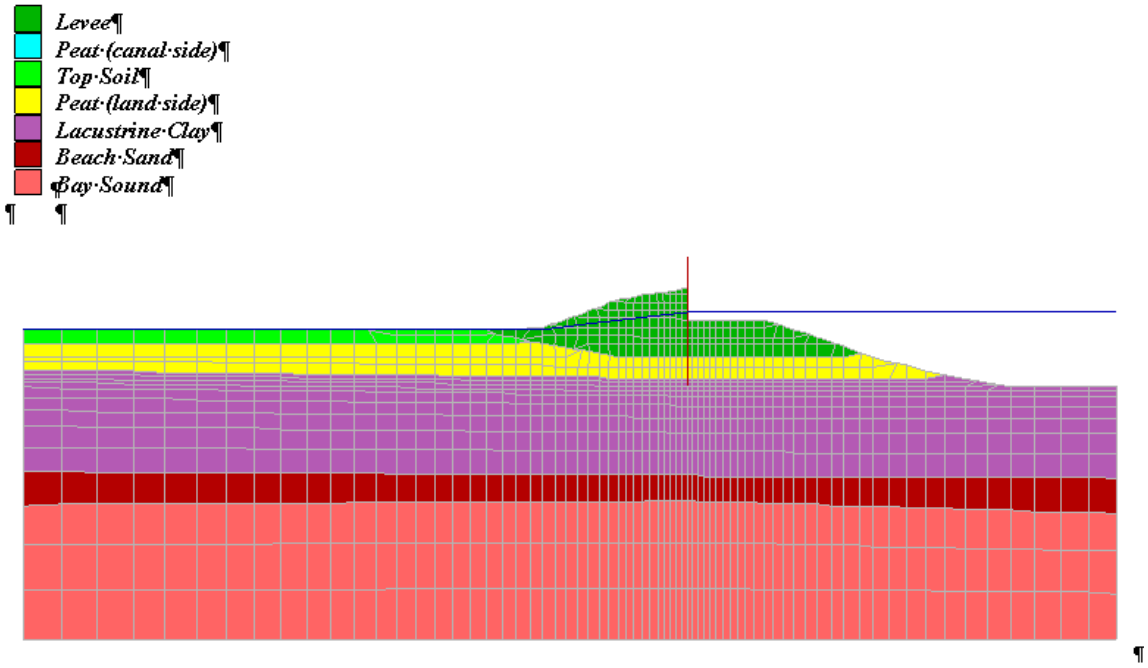

Figure 19-12. Soil zones, levee wall and sheet piles and normal Pool for 17th St. breach sta. 10+00

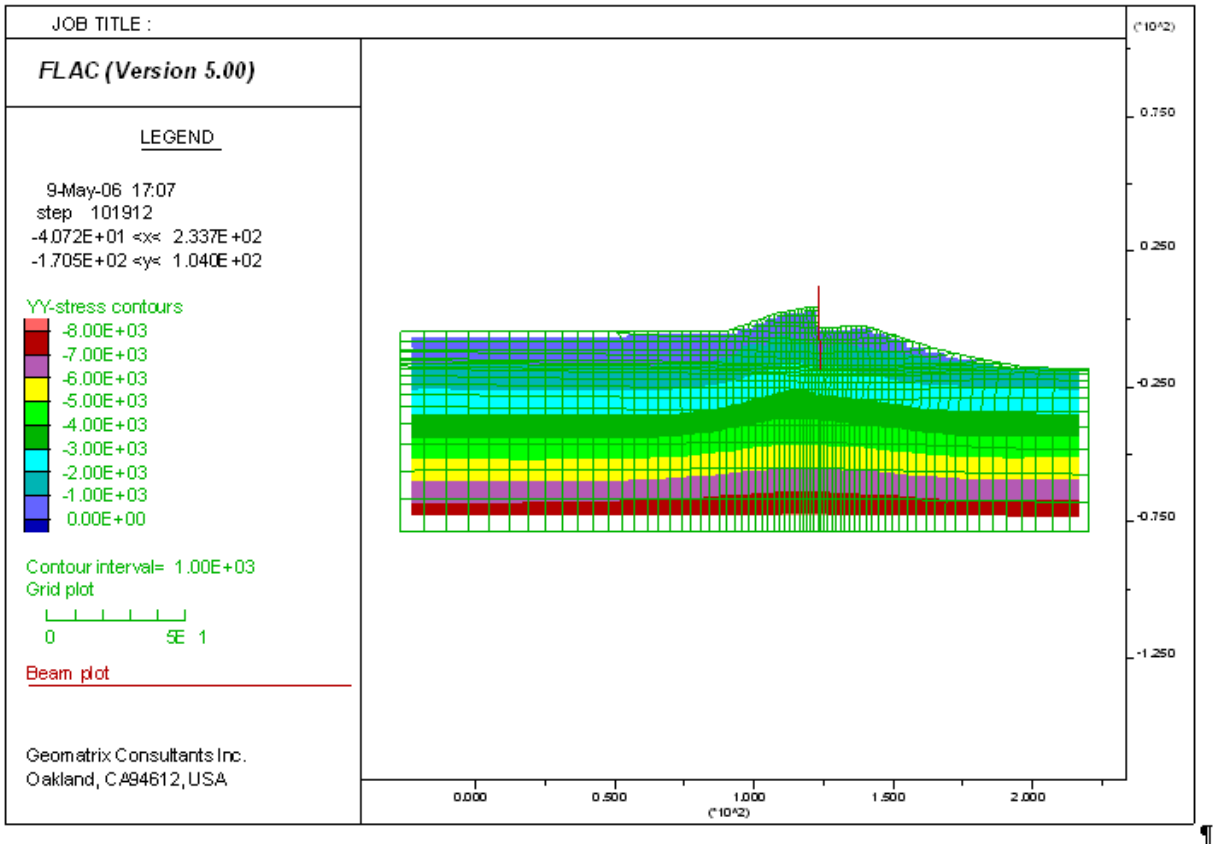

Figure 19-13. FLAC model (grid) used for the analysis of 17th St. breach sta. 10+00

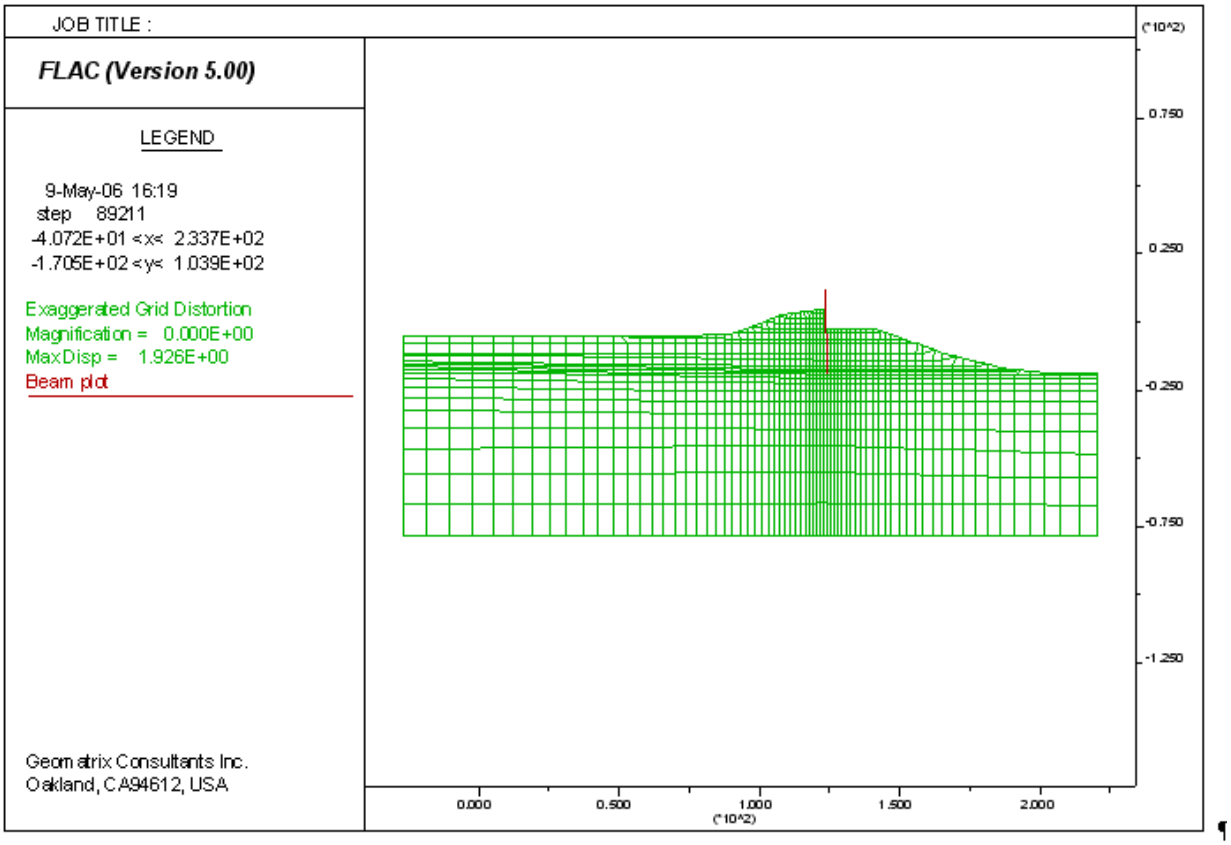

Figure 19-14. Contours of vertical total stress at normal pool water level, elevation -0.5 feet 17th St. breach sta. 10+00

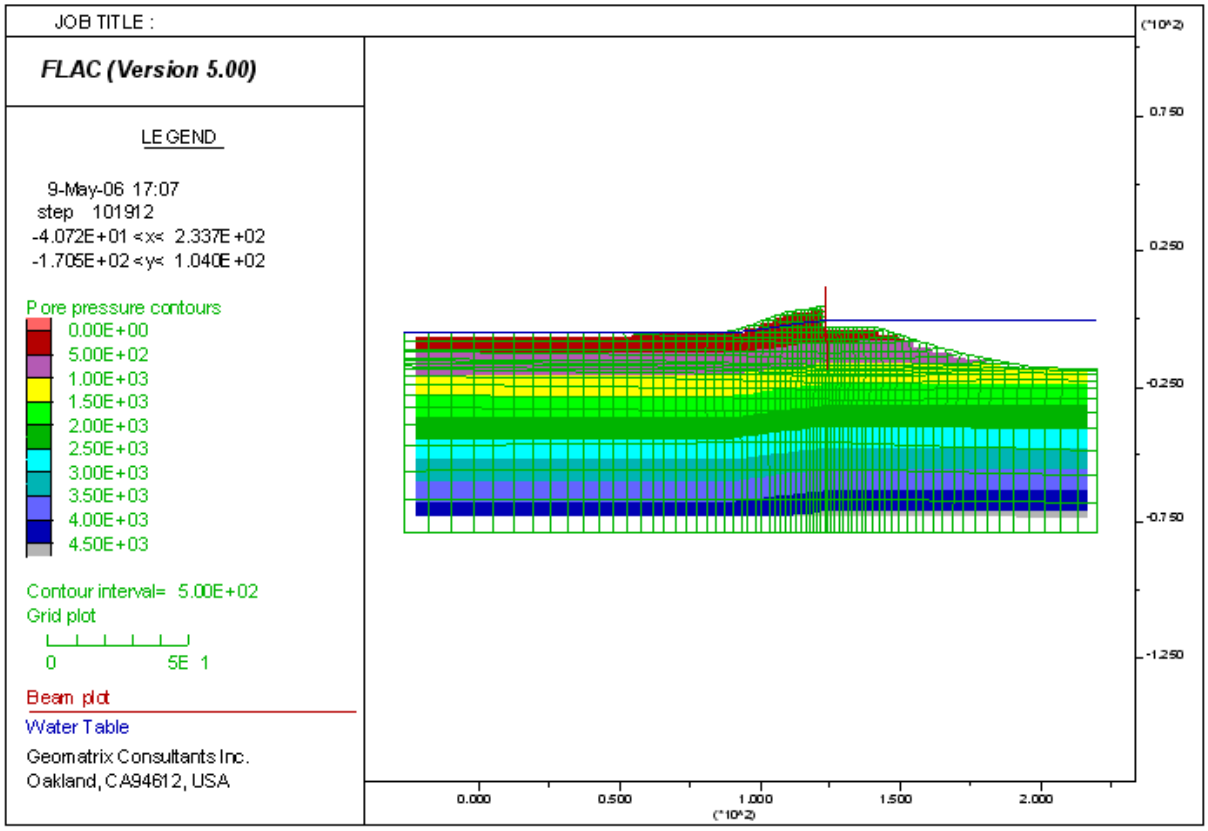

Figure 19-15. Contours of pore pressure at normal pool water at El. +0.5 feet, nonlinear model 17th St. breach sta. 10+00

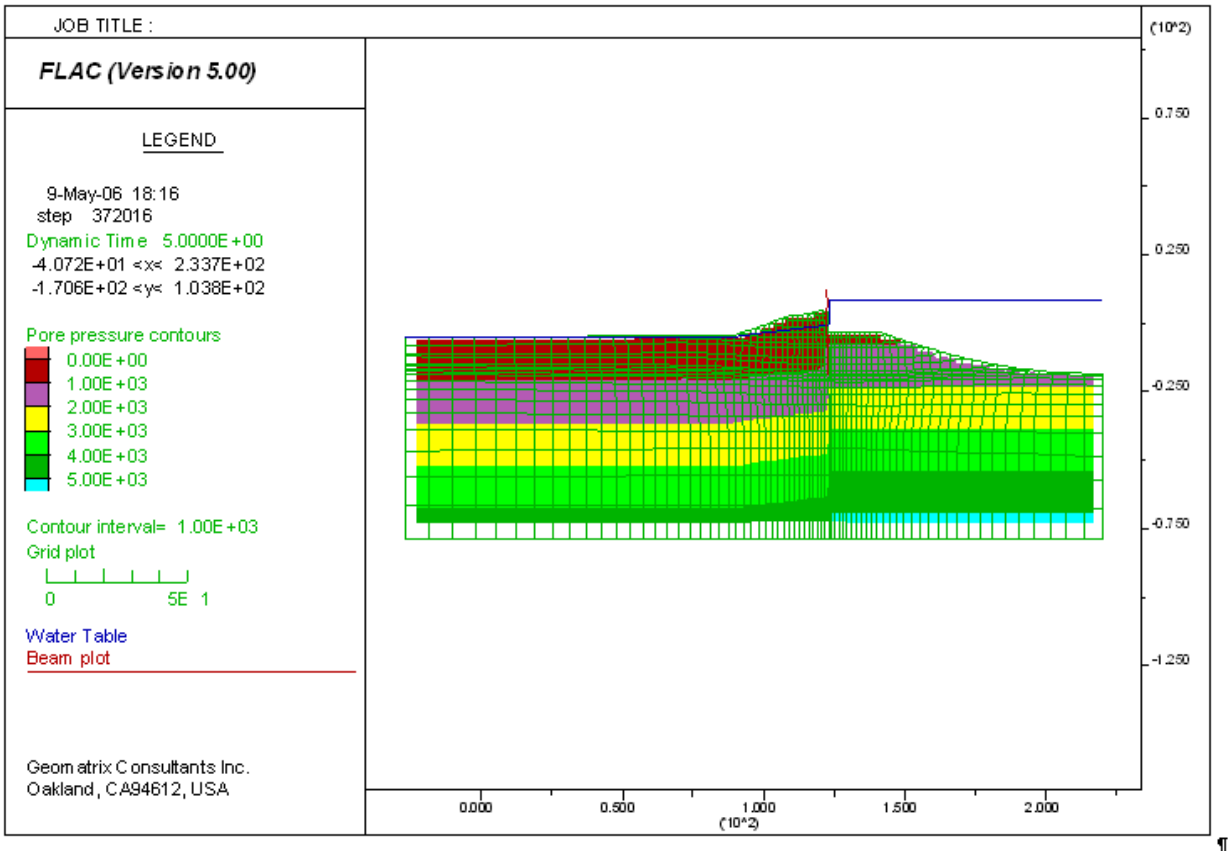

Figure 19-16. Contours of pore pressure, Katrina flood water level at El. +8.5 feet, nonlinear model 17th St. breach sta. 10+00

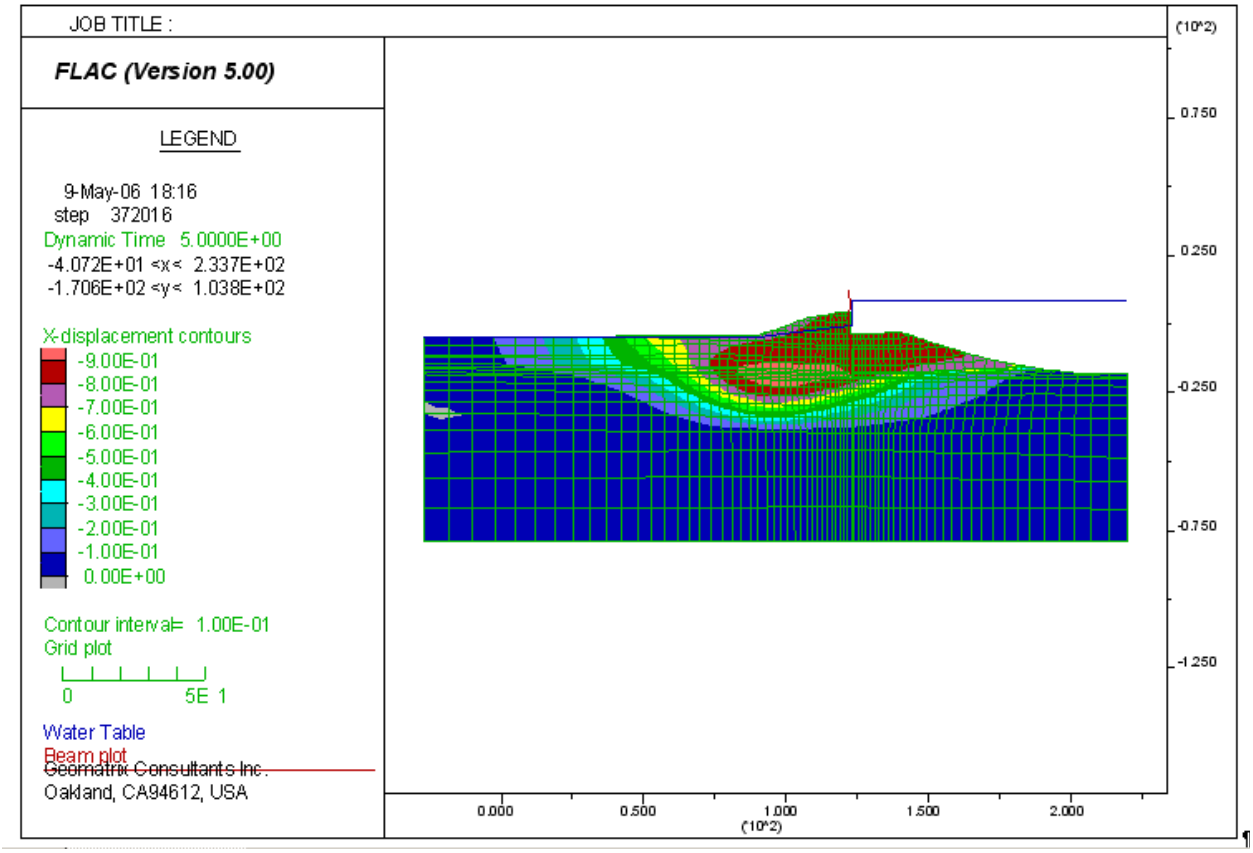

Figure 19-17. Contours of horizontal displacement, Katrina flood water level at El. +8.5 feet, non-linear model 17th St. breach sta. 10+00

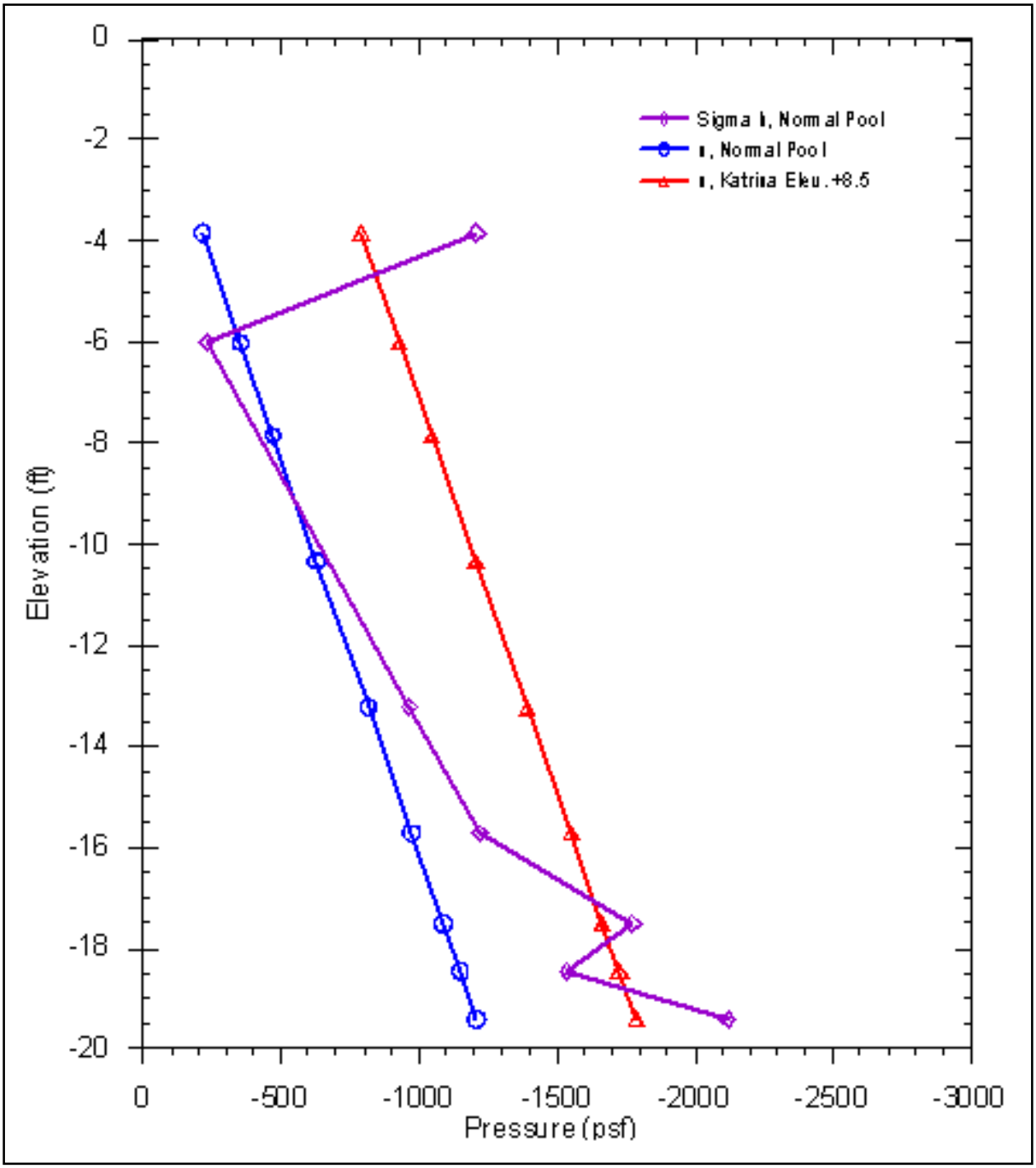

Figure 19-18. Comparison of water pressure and horizontal total stress 17th St. breach sta. 10+00

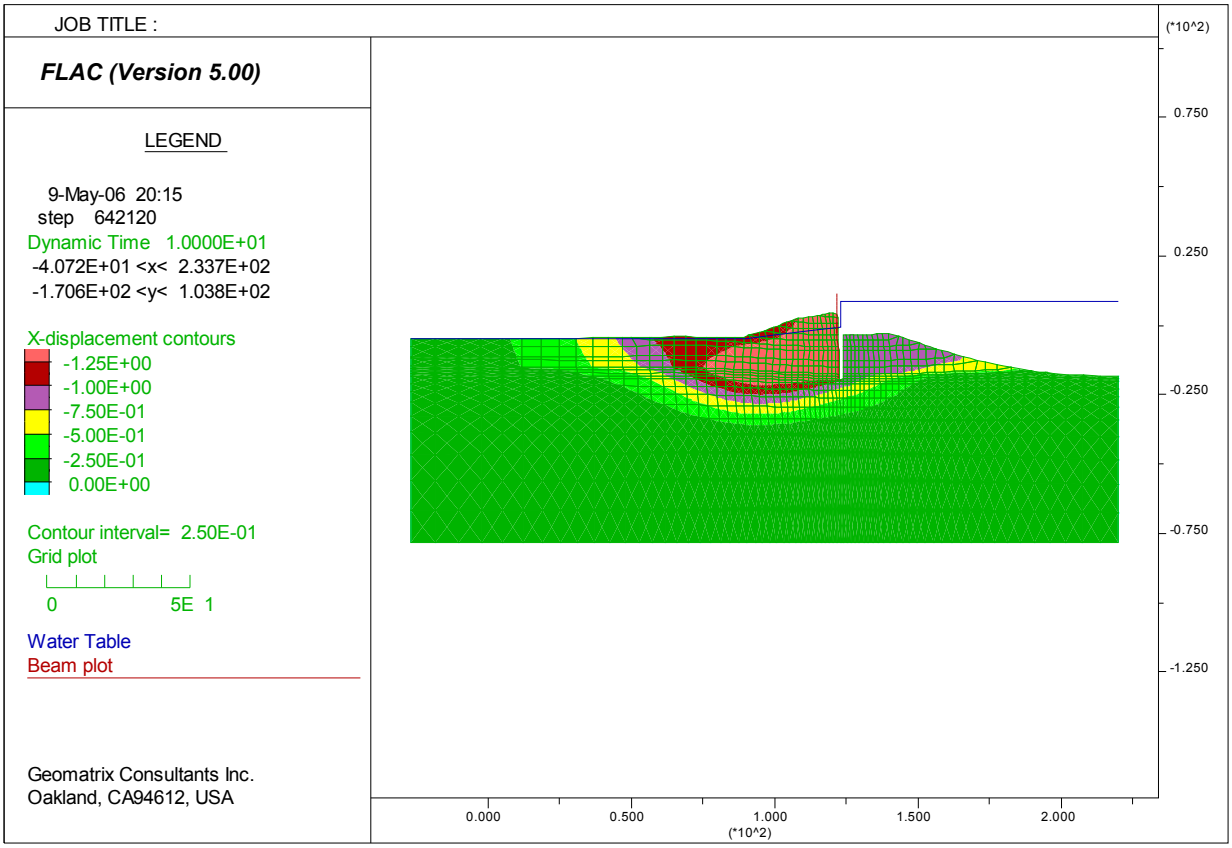

Figure 19-19. Contours of horizontal displacement with crack simulation, Katrina flood water level at El. +8.5 feet, non-linear model 17th St. breach sta. 10+00

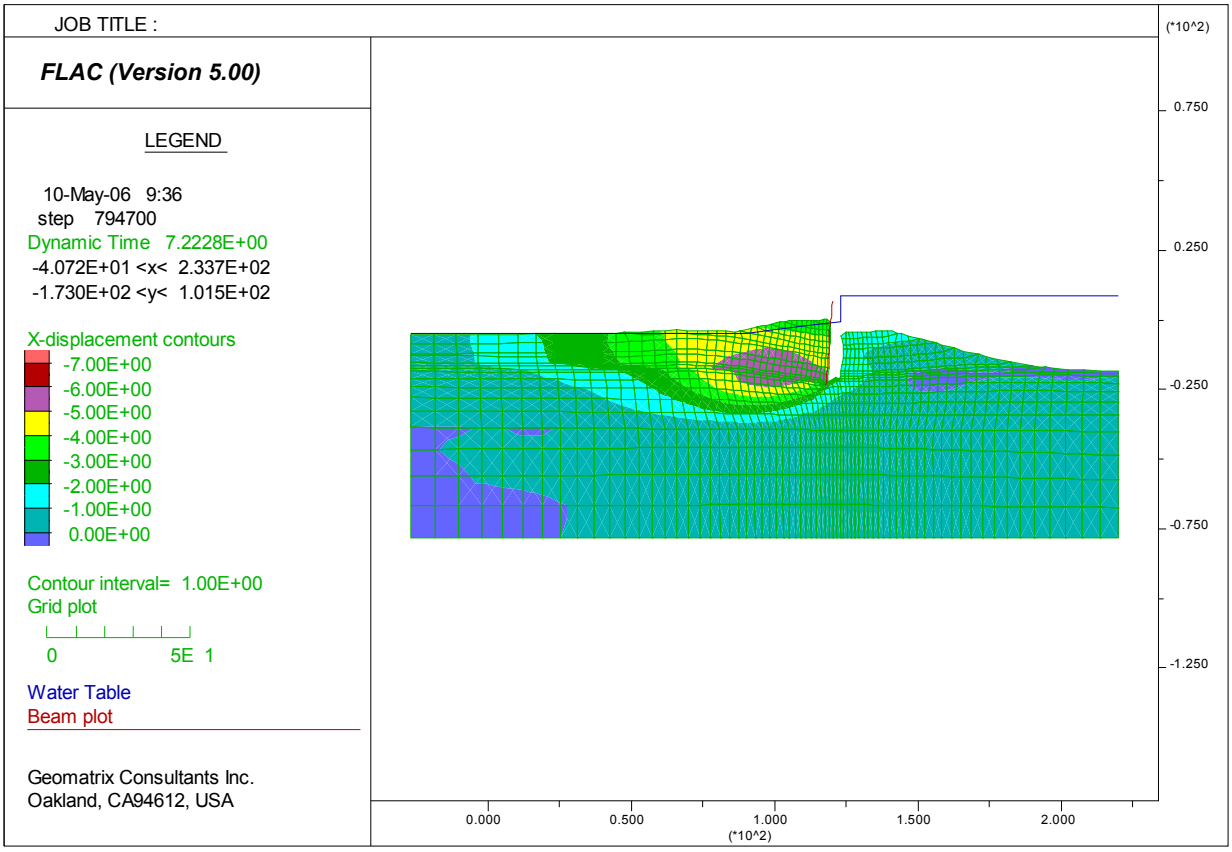

Figure 19-20. Deformed grid (with crack simulation and interface) Katrina flood water level at El. +8.5 feet, non-linear model for 17th St. breach sta. 10+00

London Canal North Levee Breach Analysis

The London Avenue Outfall Canal – North (near Robert E. Lee Bridge) was estimated to have breached around 7:00 AM to 8:00 AM, an hour later then the London South breach. This section is composed of concrete and steel sheet-pile I-wall floodwall built into the centerline of the earthen levee. The findings of the limit equilibrium stability analyses showed that the wall begun failure at canal water level between 8.2 and 9.5 ft (NAD88). One case analyzed for a water level just before the estimated breach resulted in a slope stability Factor of Safety of 1.00 for a canal water level of 8.1 ft (IPET, 2006). This report further concludes that field evidence and slope instability analyses show that the most likely mode of failure is sliding instability. Seepage studies also show that erosion and piping was another possible mode of failure. The high water pressures in the sands and the movement of the wall toward the protected side, forming a gap or crack on the canal side between the wall and earth embankment, were allowed to act directly on wall and high uplift pressures on marsh and clay deposits overlying the sands. Field evidence showed intact crest sliding and heaving at the toe.

The levee section at Station 14+00 of the London Avenue Canal (North Breach) in New Orleans was analyzed using a finite difference program, FLAC, with the Mohr –Coulomb model

and a user-defined nonlinear soil model for the Katrina high water at Elevation 9 feet. The soil profile shows that there are sand layers below the Marsh-clay layers, and the pile tip just penetrates the top sand layer. The effective stress and strength in the sand layer may be reduced due to water flow resulting from the Katrina high water load. In order to model these variations, a user-defined effective stress model (Wang, 1990) was used for the Beach Sand layer 1 (shown in yellow on the attached Figure 19-21). For other materials, the Mohr-Coulomb model was used for faster solution speed. The geometry, undrained strength and Young's modulus (Eu_50) values for the Mohr-Coulomb model are consistent with those used in the other analyses (Plaxis and limit equilibrium stability analyses). The unit weight, undrained soil strength, and model parameters are presented in Table 19-2.The nonlinear model used in this analysis requires additional model parameters (G_o , h_r, k_r, and d) for effective stress analysis. A $K_{2max} = 40$ for sandy material was estimated for $D_r = 40\%$ of Beach Sand layer 1. This $K_{2max} = 40$ was correlated with model parameter G_o. Parameter $h_r = 0.77$ was used to give a secant modulus $G = 0.5G_{max}$ at a reference strain level $\gamma = \tau_f/G_{max}$ in which τ_f is the soil strength. Two more parameters (k_r and d) are needed if excess pore water pressure generation is allowed. These parameter values were estimated for Beach Sand 1 with SPT of about 10. The unit weight and model parameters for the Beach Sand 1 layer are presented in Table 19-3 that uses the nonlinear effective stress model.

Approach

The analysis was performed using the mechanical and ground water flow modes of the FLAC program. To expedite the computational process, in the present analysis, the Mohr-Coulomb model was used in all the soil layers in the profile except for Sand Layer 1 as described above. For this layer, the non linear effective stress model was used in the analysis.

The following steps were used in the analysis:

1. Build numerical model. The grid was generated first. The soil profile was constructed layer by layer by turning on gravity for each layer. For the London Canal (North) section, 'construction' was simulated from the bottom of the profile to the crest of the levee. The newly added layer was a load increment for the previously constructed layers, so that the non-linear soil model can properly be used to compute the static stresses within the levee embankment.

2. Construct the two floodwalls (sheet pile and concrete wall), both are simulated by beam elements.

3. Apply normal pool water pressure (at El -0.5 feet) on the levee at the canal side, and develop the phreatic surface (from El. -0.5 feet on the canal side, to El. -4.4 feet on the protected side), and compute the wall deformation at the normal pool level.

4. Let FLAC balance the effective stresses as prior Katrina's static stresses and reset all computed displacement to zero (before raising the water level to specified Katrina levels).

5. Raise the water level to the assumed Katrina high water level at Elevation 9 feet, and apply water pressure to the levee on the canal side in one step. The new phreatic surface corresponding to the assumed Katrina water level was developed using FLAC's 'water flow on' option and assumed water level at ground surface level at the protected side. The displacement due to the Katrina high water level was computed using FLAC's 'dynamic on' option. Because the high Katrina flood water (at elevation 9') was simulated as an 'impact' loading while in reality such water might raised in a few hours, this simplified loading procedure (i.e. apply Katrina water in one step) may overly predict the levee's deformation compared with raising the water foot by foot and computing the stabilized displacement for each water increment. In the dynamic mode, the computed displacements were oscillated to reach steady values and only the stabilized displacements were used. This simplified procedure resulted in a displacement of the floodwall of approximately 3 inches, which did not cause failure.

6. Based on the results of the slope stability and seepage analyses, and the hydraulic fracturing criteria used by the Plaxis team, it was assumed that a crack will develop next to the concrete wall and sheet pile (on the canal side), and would extend down to the elevation of the top of the sand layer. The development of such a crack was verified by comparing the pore water pressure from Katrina water level at elevation 9' with the total horizontal stress computed from normal water level in the soil layers (as shown in figure below). For the water level at the Katrina High flood level (at Elevation 9 feet), the pore pressures in the clay layers were generally greater than the total horizontal normal stress down to about Elevation -13 feet.

7. Accordingly the soil column adjacent to the wall above the El. -12.9 feet was removed (nulled) to simulate the crack development. The removal of the soil (i.e., the excavation process) allows the canal water to fill the void between the levee berm and the floodwall. Thus the water pressure was then applied normal to the sheet-pile wall and to the opposite soil face, as well as at the base of the excavated soil column.

8. The water is allowed to flow through the crack into the sand layer below. The flow computation is then performed and the water flow vectors are computed and are shown on Figures 3-7 and 3-8. The increase in pore water pressure in the sand layer results in a reduction in the effective stress, and a corresponding decrease in the shear strength of this layer.

9. The flow calculation is terminated, and the mechanical calculation is continued to compute the total wall movement as a result of the formation of the crack, the rise in the water level, and the increased pore pressures in the sand layer below the tip of the sheet pile. This results in computed large movement of the wall towards the protected side. Again, the crack was assumed to form in one step down to the top of the beach sand 1, and the displacement induced due to the application of the water pressure in the crack was computed in the FLAC's 'dynamic on' mode.

Analysis Results and Discussion

The material zones, beam elements simulating the floodwall and sheet piles, and the normal pool water are shown in Figure 19-21. The finite difference grid used for the FLAC analysis is shown in Figure 19-22. The computed total vertical stress and pore water pressure at normal pool water level are presented in Figures 19-23 and 19-24, respectively. The pore water pressure contours using Katrina canal water level at elevation 9 ft are presented in Figure 19-25.

Computed displacements of the floodwall due to water levels associated with the high Katrina flood levels but ignoring the effects of crack formation between the floodwall and the levee berm (at the canal side) were of the order of 3 inches. The levee slopes were stable, with no indication of impending failure.

Pore water pressures associated with Katrina high flood water level exceeded the total horizontal normal stresses computed from normal pool water level in the clay layers down to about elevation 13 feet as shown in Figure 19-26, indicating the potential for crack formation between the levee soil and the sheet pile wall.

The possible crack formation was simulated in the analysis, and water flow into the underlying sand layer indicated significant increases in the pore pressures, and a corresponding reduction in effective stresses and shear strength. The water flow vector in the sand layers is presented in Figure 19-27. The detailed flow vectors and the simulated crack are presented in Figure 19-28.

The computed deformations of the pile wall and the levee slopes when simulating the effects of cracking and seepage flow into the underlying sand layer resulted in horizontal deformations exceeding 4 feet as shown in Figures 19-29 and 19-30. The computations were terminated at about 4 feet due to numerical problems with distorted elements, prior to reaching a stable configuration, indicating the potential for continued large movements.

The deformed shape of levee profile indicates that there was about 4 feet of upwards movement (bulging) in the top soil at the protected site, beyond the toe of the levee as shown in Figure 19-31. This is believed to be induced by the pore water pressure due to water flow into the top sand layer through the crack behind the wall. This bulging could indicate rupture of the overlying clay layer that would result in piping and possible failure.

Table 19-2
Soil Property and Mohr –Coulomb Model Parameters

Mohr Coulomb Model	Soil Type	γt pcf	Su, psf	ϕ, deg	E50=92*su	ν, Poisson	G psf	K psf	Vs, fps
Levee Fill	1	109	900	0	82800	0.47	28163	6.90E+05	assumed
Sheet Pile	2	125							
Silt on Bottom of Canal	3	100	100	0	9200	0.47	3129	7.67E+04	
	4	80	300	0	27600	0.47	9388	2.30E+05	
Marsh (Canal Side)	4	80	400	0	36800	0.47	12517	3.07E+05	
Clay	5	109	350	0	32200	0.47	10952	2.68E+05	
Beach Sand 2	7	122		36	0	0.47	5455901	8.91E+07	1200
Beach Sand 3	8	118		32	0	0.47	7182609	1.17E+08	1400
Bay Sound	9	125	5000	0	460000	0.47	156463	3.83E+06	

Table 19-3
Soil Property and Effective Stress Model Parameters for Beach Sand 1

Effective Stress Model	Soil Type	ϕ	G_o	h_r	k_r	d	F_p	ν, Poisson	b	γ_t, pcf
Beach Sand 1	6	31	418	1	1	2	1	0	2	118

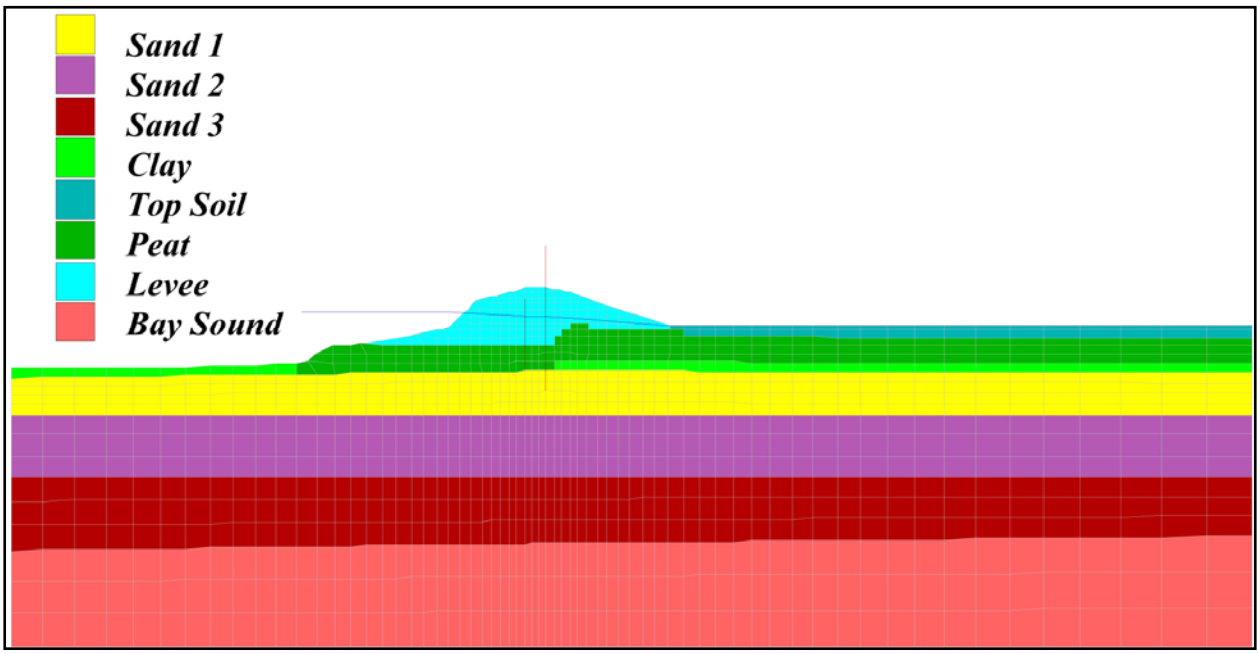

Figure 19-21. Soil zones, levee wall and sheet piles at normal pool for London north breach sta. 14+00

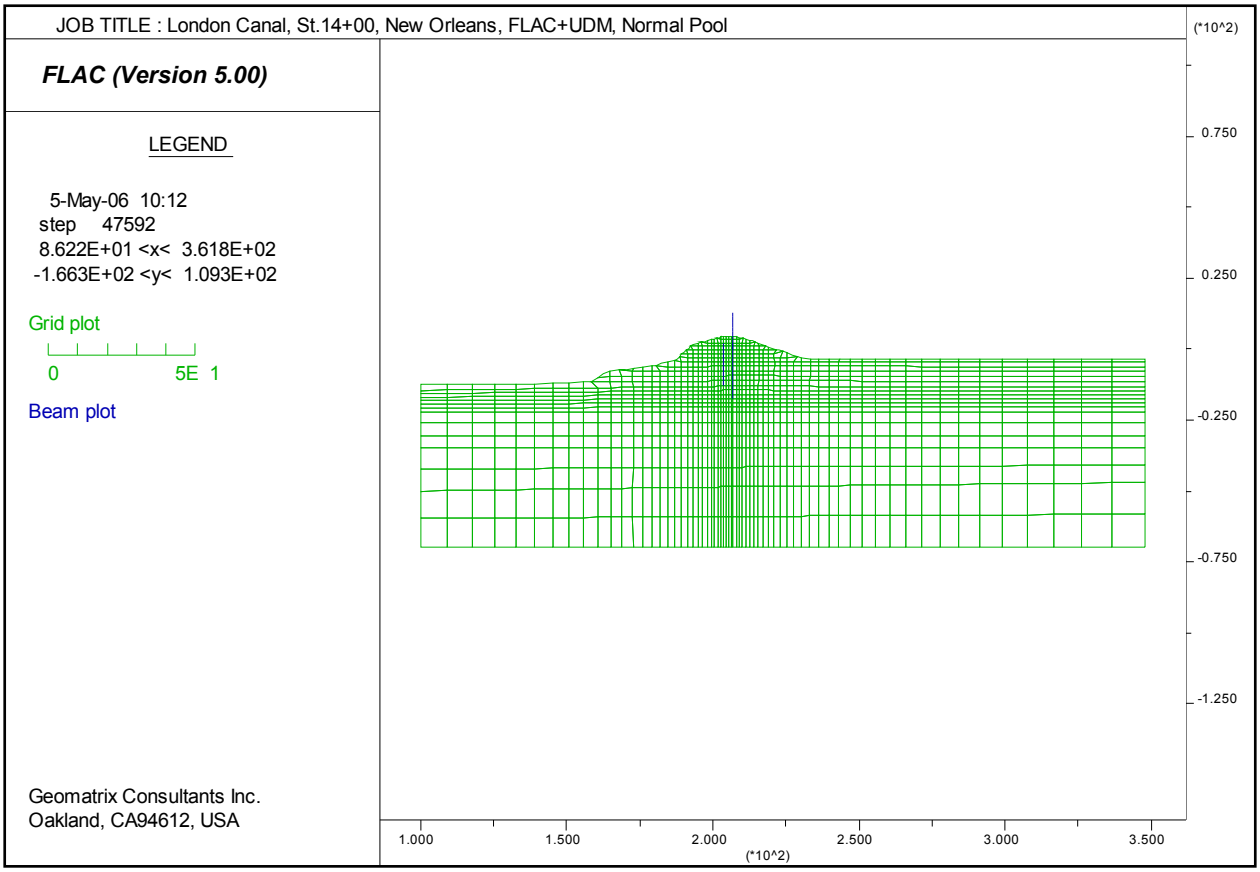

Figure 19-22. FLAC model (grid) used for analysis of London north breach sta. 14+00

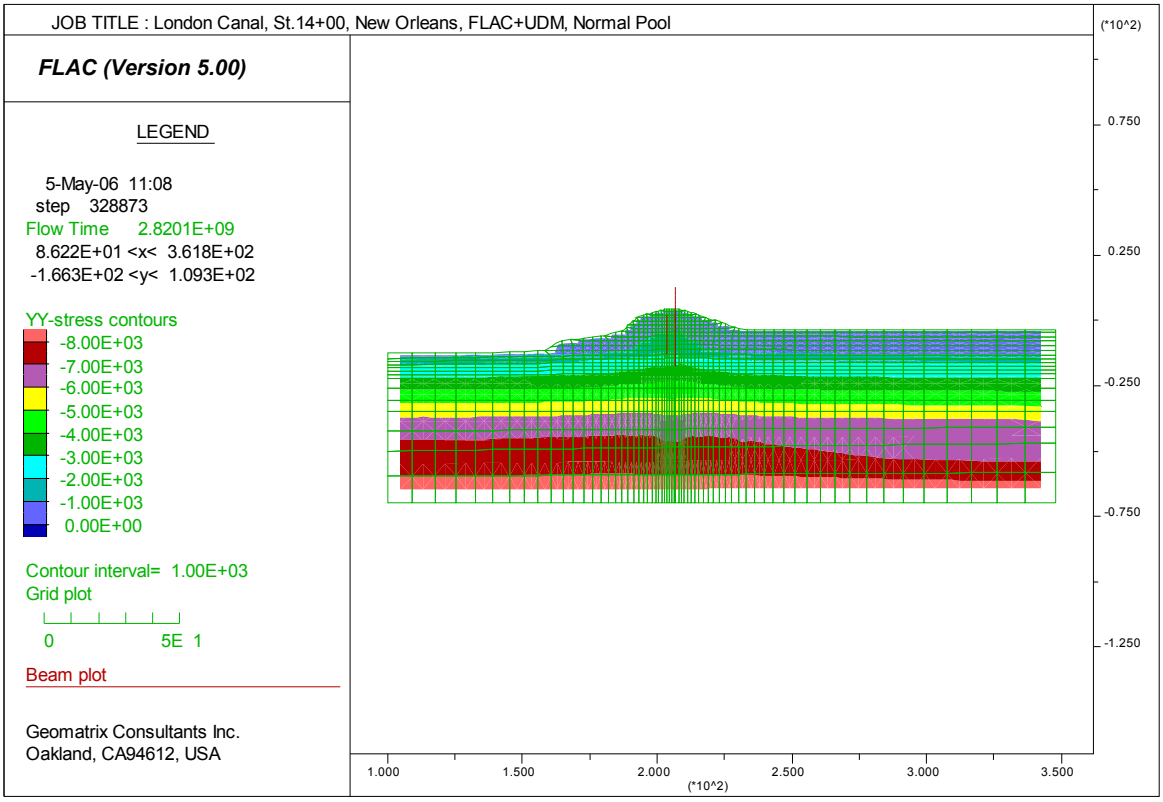

Figure 19-23. Contours of vertical total stress at normal pool water level, Elevation -0.5 feet for London north breach sta. 14+00

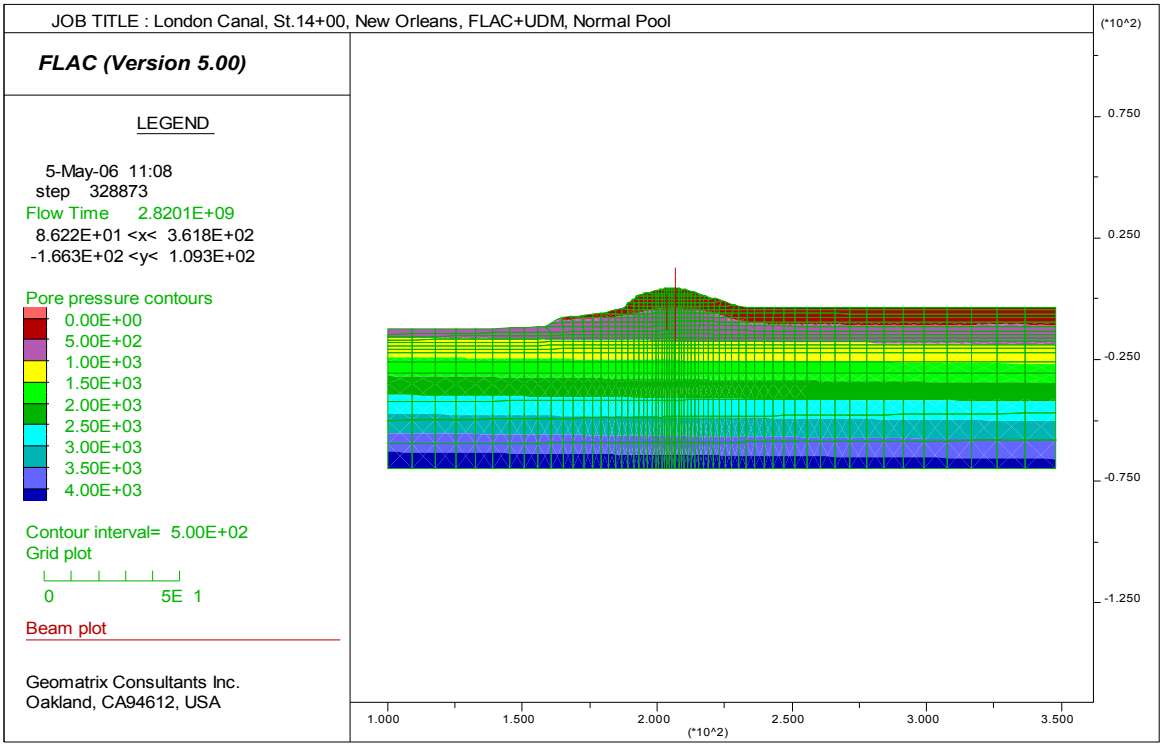

Figure 19-24. Contours of pore water pressure at normal pool water level, Elevation -0.5 feet for London north breach sta. 14+00

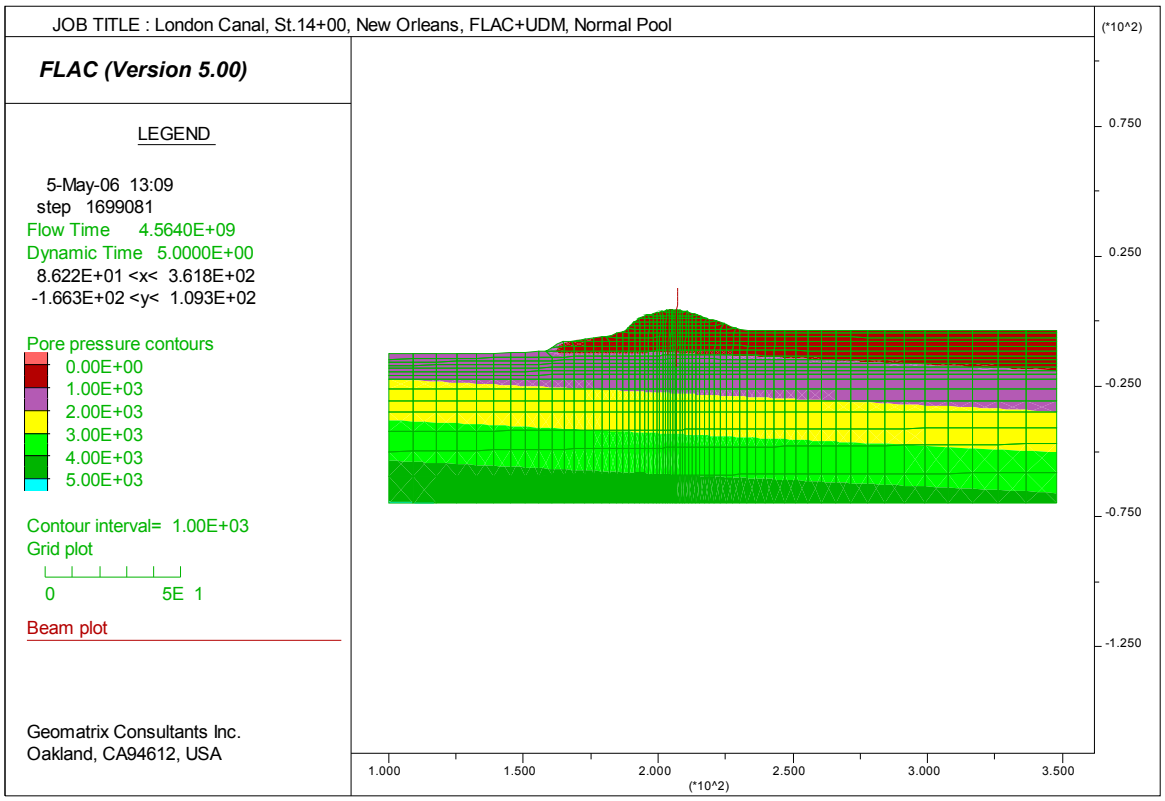

Figure 19-25. Contours of pore water pressure at Katrina Flood Water Level at Elevation 9 feet for London north breach sta. 14+00

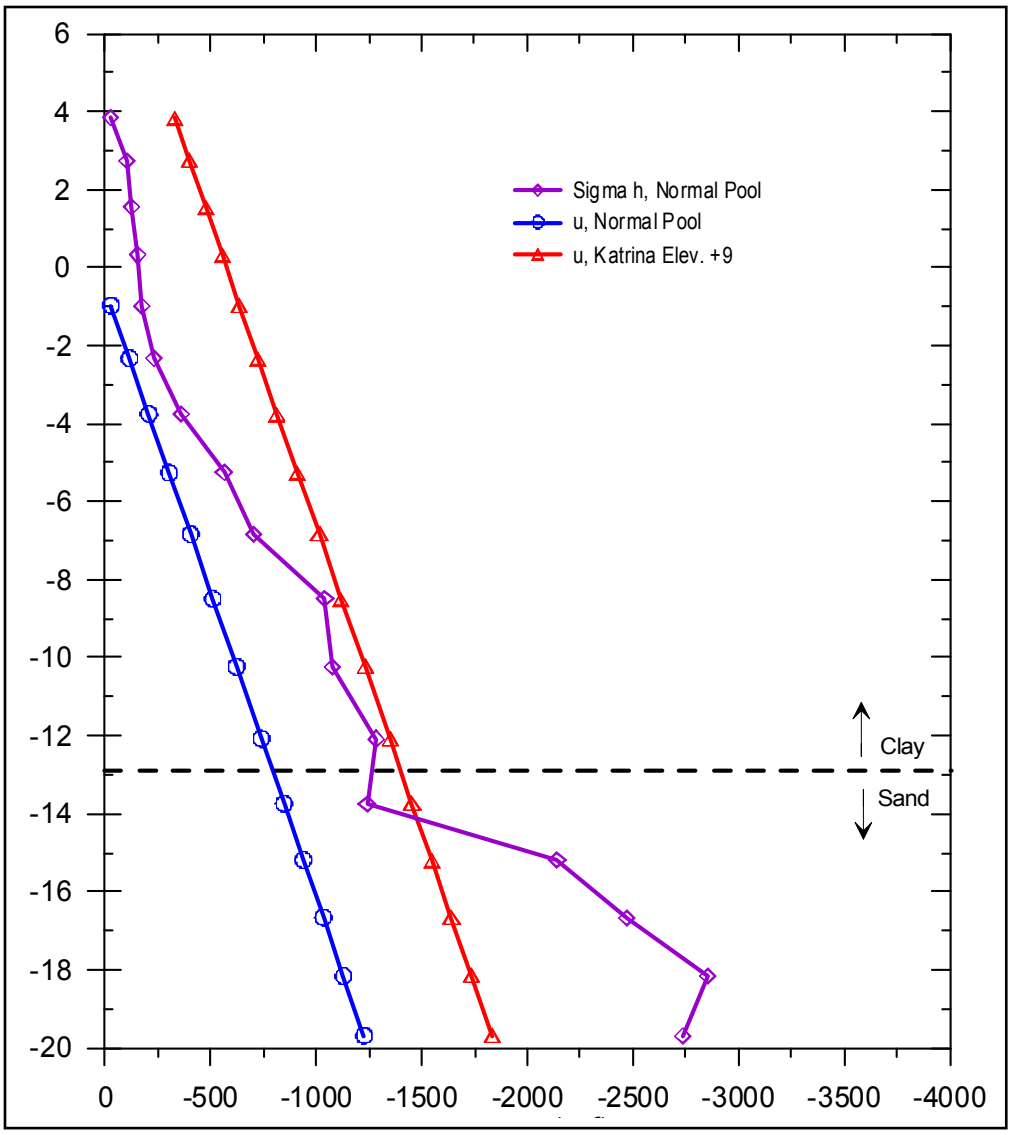

Figure 19-26. Comparison between water pressure and horizontal total stress for London north breach sta. 14+00

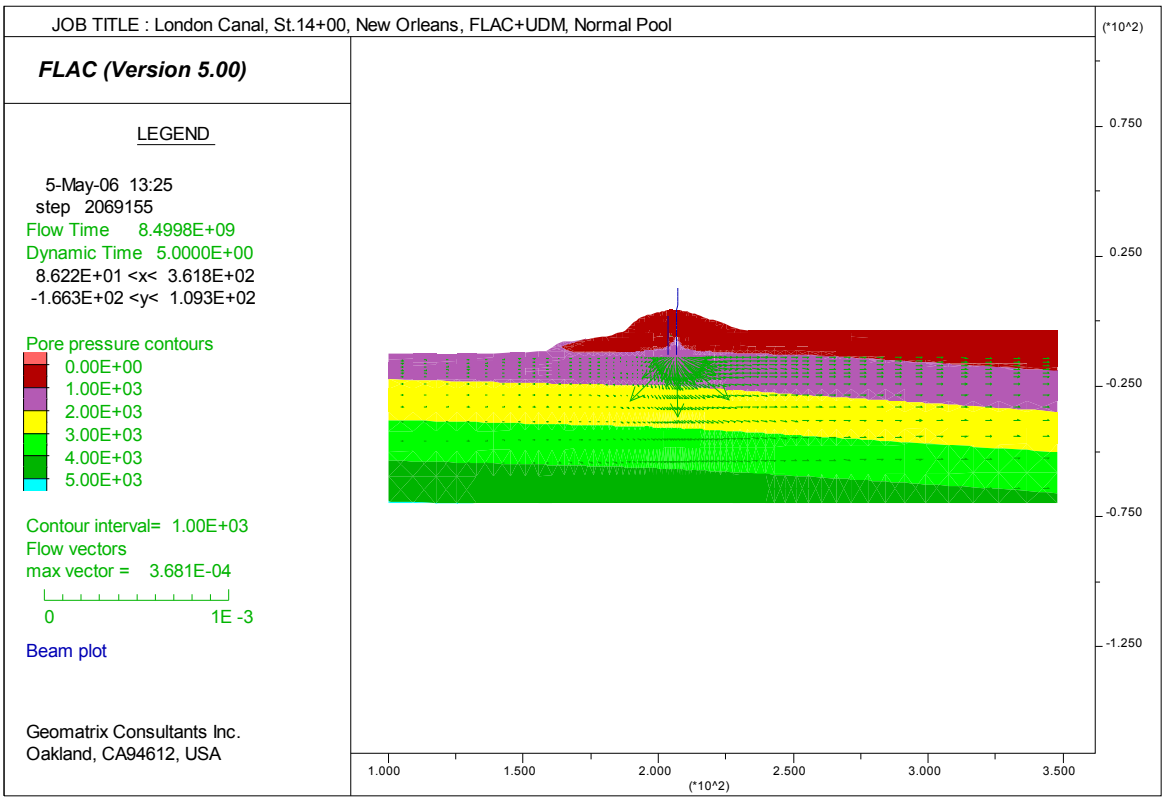

Figure 19-27. Water flow vectors through the crack (behind the wall) into sand layer for London north breach sta. 14+00

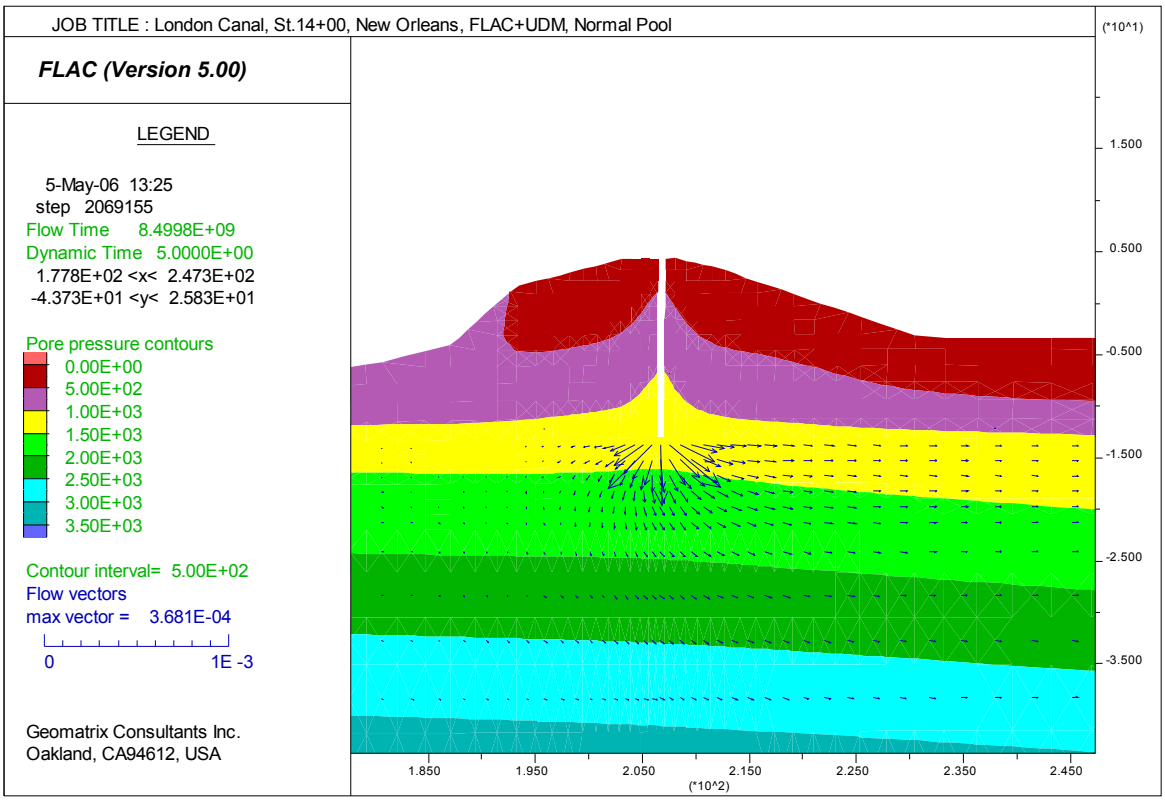

Figure 19-28. Detailed flow vectors from near tip of pile and into top sand layer for London north breach sta. 14+00

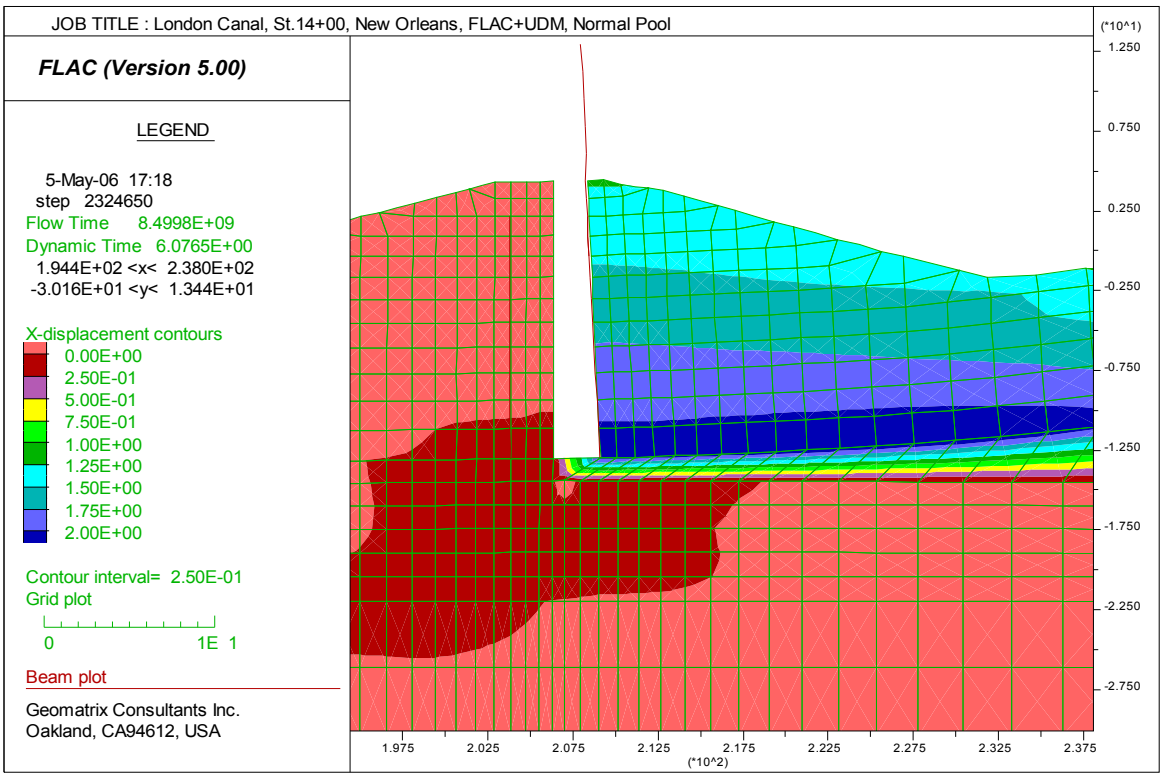

Figure 19-29. Wall moved two feet (computation terminated due to bad geometry at bottom of crack) for London north breach sta. 14+00

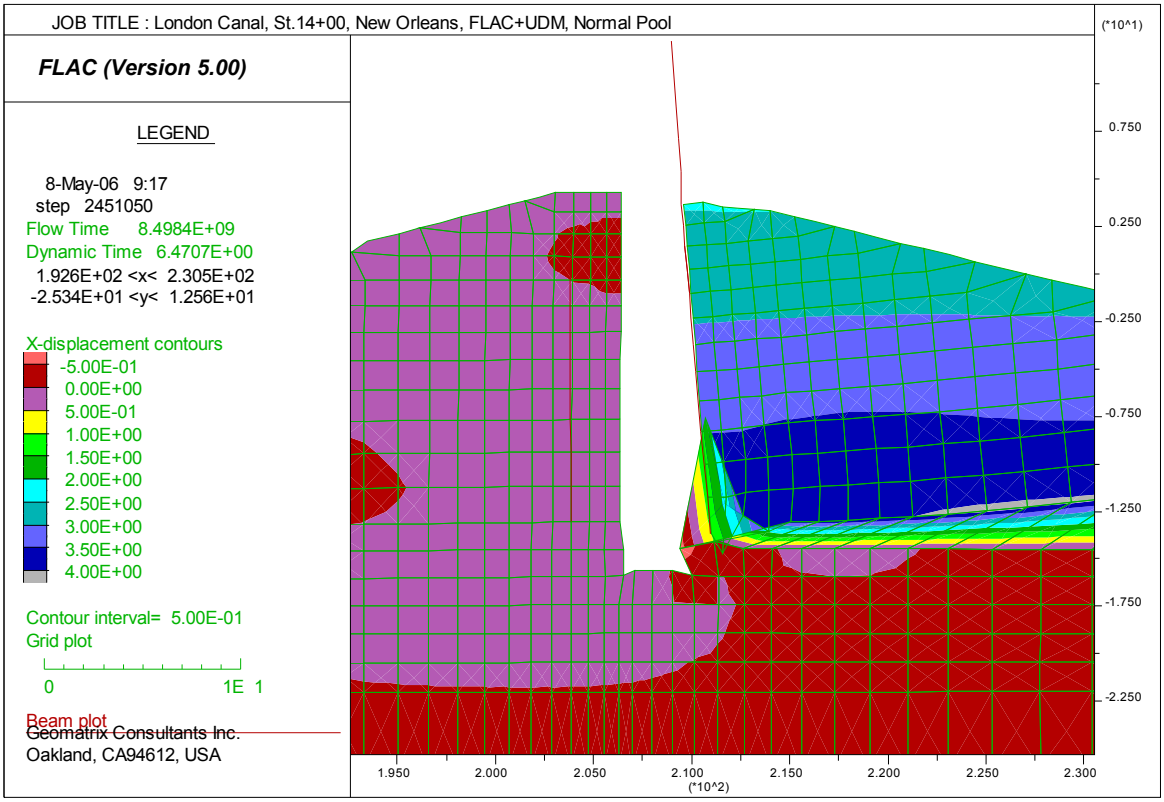

Figure 19-30. Wall moved four feet, unstable due to bad geometry at bottom of crack, (bad zones were removed to allow computation to continue) for London north breach sta. 14+00

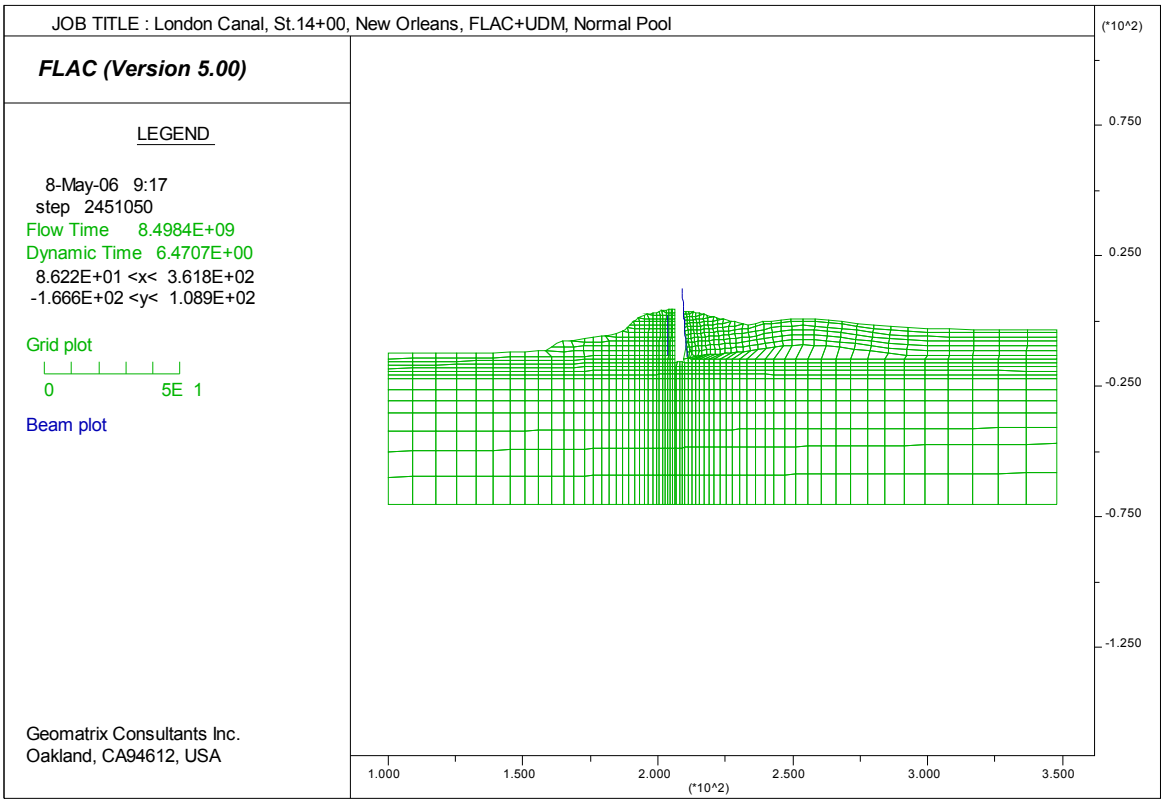

Figure 19-31. Deformed shape at wall movement of four feet showing bulging beyond the toe (computation terminated due bad geometry) for London north breach sta. 14+00.

London South – Mirabeau Breach Analysis

Analysis Approach

An analysis of the Mirabeau breach on the London South Canal using FLAC was performed, although the analysis had not reached a conclusion by the time of this report. The general methodology follows that described for the Mohr-Coulomb analysis performed for the 17th St. Canal breach. Geometry and material properties were provided for the analysis in an effort to maintain consistency with the Plaxis evaluation. In addition to the range of parameters supplied for the 17th St. analysis, values of hydraulic conductivity were also provided for the Mirabeau Breach section.

The simple Mohr-Coulomb model was selected because the initial analyses showed that seepage predictions and the resulting loss of effective stress in the sand were likely to be critical mechanisms. As with the 17th St. analysis, the FLAC model can be easily modified to use a nonlinear effective stress model if needed.

The FLAC model developed to analyze the Mirabeau breach is shown in Figures 19-32 and 19-33. This model includes a special wedge of material just downstream of the toe. This zone is identical to the remaining marsh-topsoil material. However, it has been isolated and connected to the remaining soil grid using interface elements. The presence of this wedge provides some additional flexibility in evaluating the effect of high pore pressures beneath the marsh deposits.

Analysis Results and Discussion

A seepage analysis using the groundwater flow capability of FLAC was performed to estimate the initial steady-state pore pressures. This analysis of steady state conditions highlighted the importance of seepage to the stability of this section of levee. The cross section provided for analysis has Beach Sand extending continuously beneath the levee section and forming the bottom of the canal. Since this layer is assigned a permeability value of $1.5x10^{-2}$ cm/sec, the direct connection to canal water allows for high pore pressures to be quickly transmitted beneath the levee section. The effect of this is exacerbated by the low unit weight of only 80 pcf assigned to the topsoil and marsh layer. The buoyant weight of this material is so low that it provides little effective restraining force due to dead weight on the underlying sand. Given these input parameters, the predicted pore pressures for steady state in the sand below the toe of the levee are sufficient to exceed the total overburden weight of the overlying marsh deposit.

It is likely that the steady state pore pressures were not this high in the absence of serious stability issues with this section. Assigning a vertical permeability of 10X the horizontal permeability to the sand layer was sufficient to modestly but significantly reduce the pore pressures at the toe. It may be possible that the surface of the sand exposed in the canal had become silted so that a thin layer of reduced permeability material was essentially lining the canal. A 2-ft-thick layer of material at the bottom of the canal with a permeability of $1.5x10^{-4}$ cm/sec was found to significantly reduce the initial pore pressures at the toe. The

presence of a silted layer would also reduce the pore pressure response during the flood loading. Unfortunately, the presence or description of this potential silted layer is not known. Although the development of such a layer appears reasonable, it may also be periodically removed by dredging. Initial pore pressures estimated using the above assumptions are shown in Figures 19-34 to 19-36.

In the analyses completed to date, instability of the section appears to begin as the pore pressures along the top of the sand exceed the buoyant weight of the overlying material. This occurrence tends to begin somewhat below the toe of the levee. Unless the seepage is restricted by a silted layer in the canal, these high pressures occur at very low flood stages. An initial deformation response due to high pore pressures is shown in Figure 19-37.

Based on the available information, the FLAC analyses clearly show that seepage is a critical issue in the behavior of this levee. These analyses have not yet identified a likely failure mechanism due to uncertainties in the actual permeability's and resulting pore pressures. A more thorough study might include an organized set of parametric studies to evaluate ranges in permeability assumptions and distributions. The likelihood of a crack between the sheet pile wall and levee fill contributing to the failure might also be evaluated as part of this study. Investigating the effect of material loss at the toe might be evaluated by systematic mining of the toe and foundation to define conditions associated with failure. The relative narrowness of the breach also suggests a potential 3D influence in the failure.

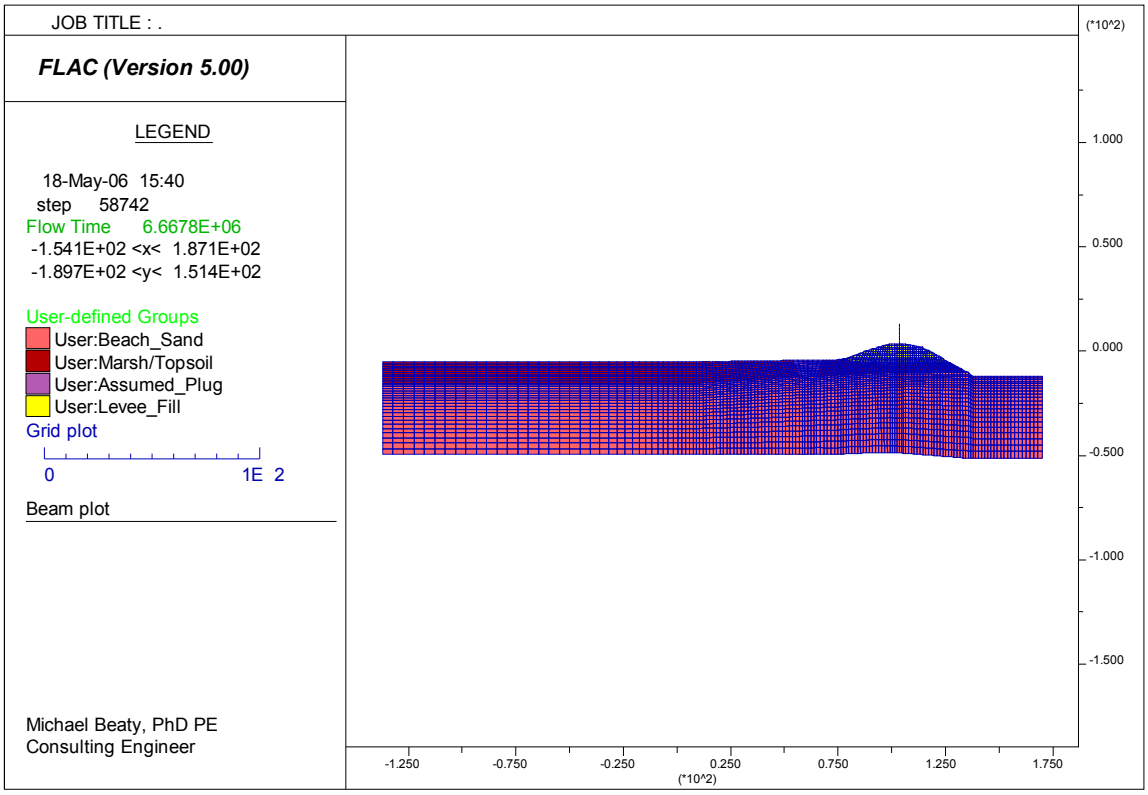

Figure 19-32. FLAC grid for London South breach sta. 53+00. (Mirabeau breach)

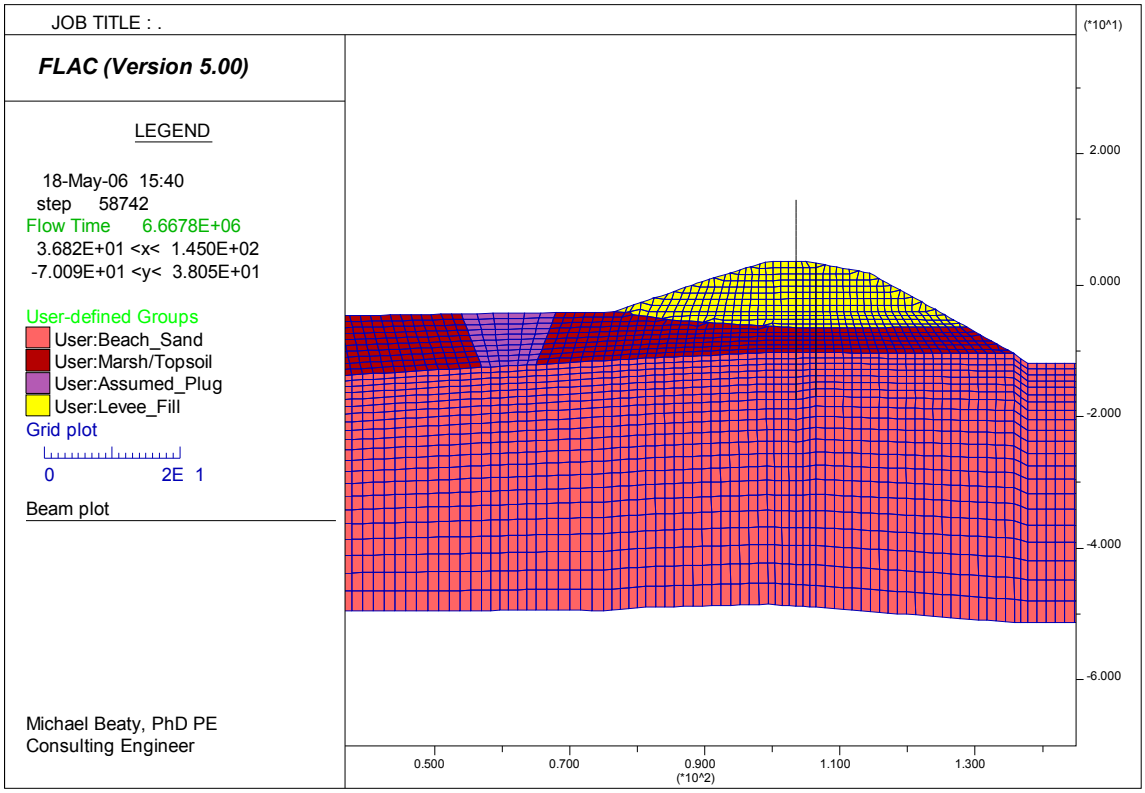

Figure 19-33. FLAC grid near levee for London South breach sta. 53+00

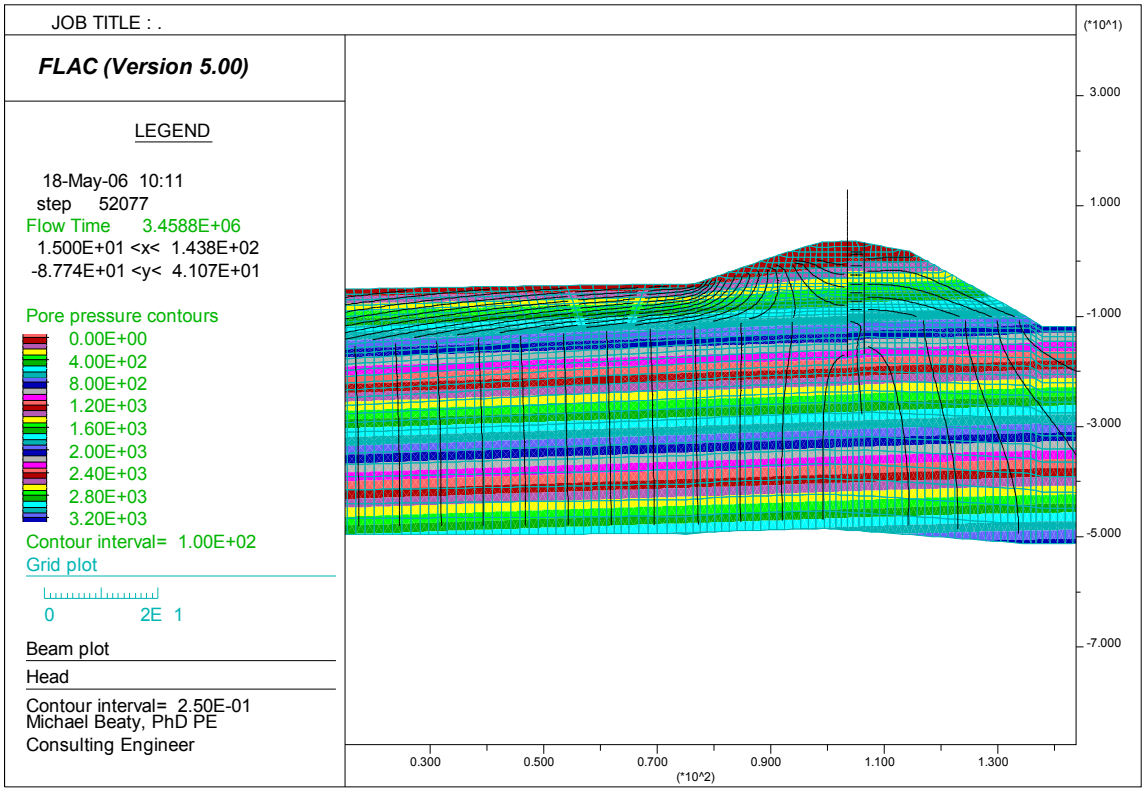

Figure 19-34. Predicted initial pore pressures for basic FLAC model for London South breach sta. 53+00

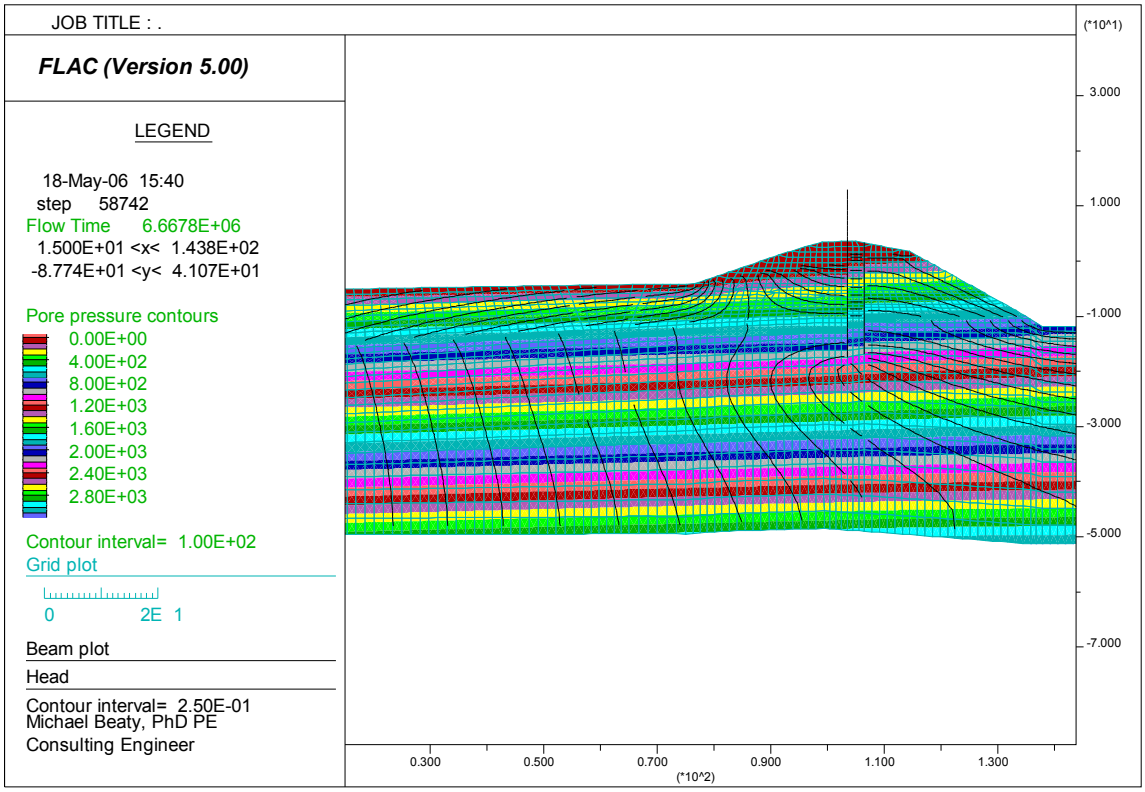

Figure 19-35. Predicted initial pore pressures for Kv = 10x Kh. for London South breach sta. 53+00

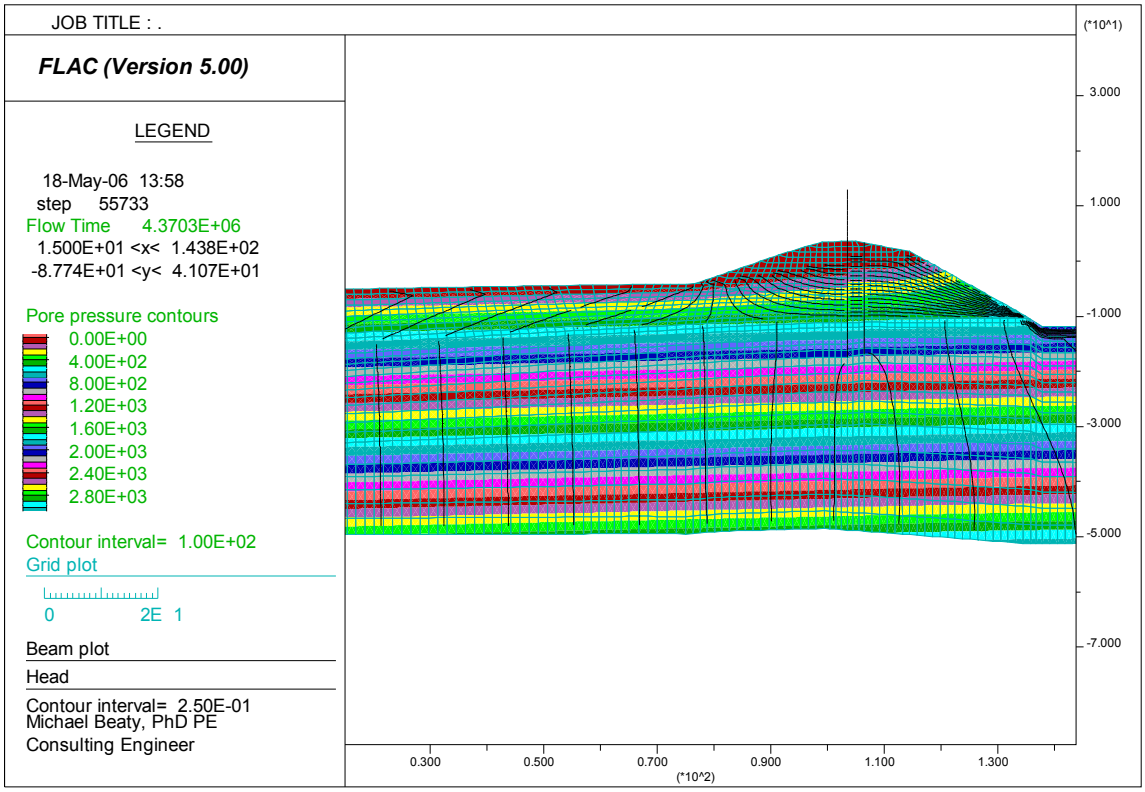

Figure 19-36. Predicted initial pore pressures for 2-foot-thick silted layer for London South breach sta. 53+00

.

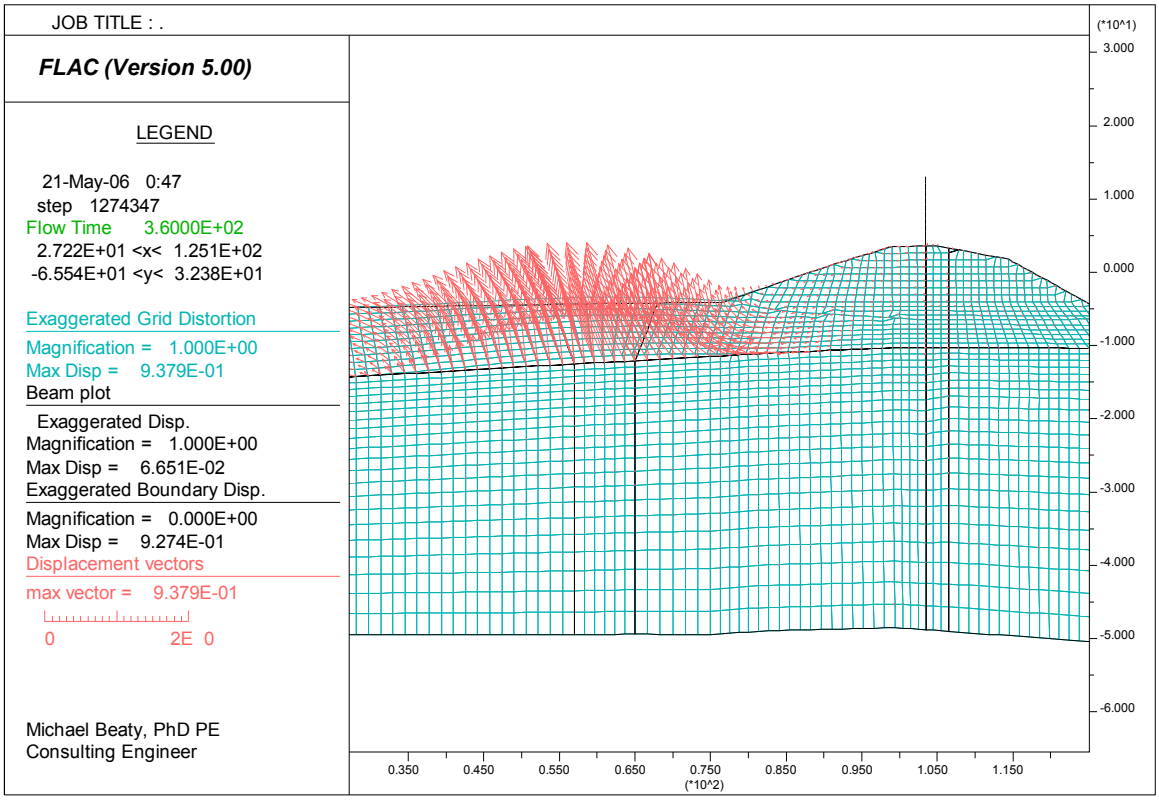

Figure 19-37. Estimated of initial bulge in marsh-topsoil layer due to high pore pressures in underlying sand (assumes Kv = 10x Kh in sand and WSE = 4.5 feet in canal) for London South breach sta. 53+00

.

Conclusion

Two-dimensional SSI numerical modeling analyses were conducted by IPET as part of a study undertaken to analyze the performance of levees and floodwalls used in the New Orleans flood protection system. The overall objective was to determine the most likely causes of their damage and failure from Hurricane Katrina. This report documents the findings from the analyses using the FLAC numerical geotechnical analysis program. FLAC is an explicit, finite difference program that uses a Lagrangian formulation for performing large strain analyses. This program is capable of modeling two-dimensional problems in soil-structure interaction with full coupling of the stress-strain and groundwater flow components. Available constitutive models include linear elastic to non-linear plasticity-based models. FLAC also provides the capability of inputting user-defined constitutive models or making minor modifications to built-in models.

The analysis approach considered and adopted where appropriate findings based on the field investigation and limit-equilibrium stability and seepage analyses conducted prior to these analyses. This enabled a consistent, thorough study based on site-specific field data and a progression of increasingly complex analyses, appropriately constrained by their respective assumptions and findings.

Stability analyses were conducted to investigate the following failure sections: east side 17th St. Outfall Canal breach sta. 10+00, and the two breaches on the London Outfall Canal (London North breach west side - near the Robert E. Lee Bridge Sta. 14+00 and London South breach east side - near the Mirabeau St. Bridge Sta. 53+00). Two important geologic factors that significantly contributed to the response of these floodwalls were the general near-surface geologic setting being (1) marsh-swamp deposits providing the possibility of low strength clay and peat foundation soils and the (2) shallowest sand deposit that trends through the area is very shallow at London's south and north breaches but found relatively deeper at 17th St. breach. The general foundation soils stratigraphy to an approximate depth of 80 ft was idealized and modeled by material zones: levee clay, clay top soil, peat, lacustrine clay, beach sand, bay sound clay, and finally the Pleistocene clays. The failure modes identified in these analyses involved the marsh and lacustrine clays for the 17th St. breach. For both breaches on the London canal, the shallower beach sands also played a dominant part with the overlying clays in the resulting failures.

The FLAC analyses of the 17th St. breach employing both simple to complex soil models resulted in the same general failure surface and strong dependence on formation of a gap (crack) between the floodwall sheet pile and canal side embankment to effect large wall movements and resulting failure. This gap is a triggering mechanism when coupled with the current soil model and estimated flood water level (elevation 8.5) to produce a failure that begins near the sheet pile tip near the top of the lacustrine clay layer. This analysis support the field observations, aspects of the limit equilibrium analyses, and the Plaxis SSI analyses that a predominately translation instability breached this section. The FLAC model also shows a kinematic response that approximately matches the field observed intact block displacement of protected side of levee embankment and heaving and over-thrusting of foundation soil layers beyond the levee toe. The range of computed wall deformation for the Katrina Flood water level at El. 8.5 ft was 5 to 6 feet indicating the potential for failure for the non-linear soil model and just over 2 ft for the Mohr-Coulomb model.

The FLAC analyses for the London south breach sta. 53+00 clearly show that seepage is a critical issue in the behavior of this levee. These analyses have not yet identified a likely failure mechanism due to uncertainties in the actual permeability's and resulting pore pressures. A more thorough study might include an organized set of parametric studies to evaluate ranges in permeability assumptions and distributions. In support of the Plaxis analyses the likelihood of a crack between the sheet pile wall and levee fill contributing to the failure should also be evaluated as part of further studies. Investigating the effect of material loss at the toe might be evaluated by systematic mining of the toe and foundation to define conditions associated with failure. The relative narrowness of the breach also suggests a potential 3D influence in the failure.

The FLAC analysis of the London north breach sta. 14+00 supports field evidence and slope stability analyses that concluded the most likely mode of failure is sliding instability. However, seepage studies also show that erosion and piping was another possible mode of failure or strongly coupling factor. It is interesting that this breach displays a combination of failure modes from both 17th St. and London South. The high water pressures in the sands and the movement of the wall toward the protected side forming a gap or crack on canal side between the wall and earth embankment allowed high water pressures to act directly on wall and high uplift pressures on marsh and clay deposits overlying the sands. Field evidence showed intact crest sliding and heaving at the toe which is also supported by the model response. The possible crack formation was simulated in the analysis, and water flow into the underlying sand layer indicated significant increases in the pore pressures, and a corresponding reduction in effective stresses and shear strength. The computed deformations of the pile wall and the levee slopes resulted in horizontal deformations exceeding four feet. The deformed shape of levee profile indicates that there was about 4 feet of up-wards movement (bulging) in the top soil at the protected site, beyond the toe of the levee. This is may have been induced by the pore water pressure due to water flow into the top sand layer through the gap behind the wall. This bulging could indicate rupture of the overlying clay layer that would result in piping and possible failure.

The introduction of a "crack" or gap between the canal side sheet pile wall and levee soil embankment was a dominant factor in inducing failure modes at 17th St and London North. Continuing analyses involving alternative criteria to support gap initiation and evolution that results in failure should be undertaken. Use of non-linear soil models may be important in obtaining a better estimate of initial stresses effecting the formation of the crack or gap needed to trigger this failure mode.

In summary, the FLAC analyses results were generally consistent with Plaxis results showing the same dominant failure modes for the same approximate canal water levels. This is also in agreement with the limit equilibrium stability analyses. However, these SSI analyses did not consider 3-D effects and given the relatively narrow breach zones it is possible these 2-D idealizations could over-predict the effect of lower water levels in triggering failure of the floodwall sections. Therefore the findings of these analyses may be conservative in this sense but provide important insight into the performance of the analyzed I-wall floodwalls which will be useful for improving future designs and assessments.

References

Beaty, M. H., and Byrne, P. M. (2001). "Observations on the San Fernando dams." Proc., *4th Int. Conf. on Recent Adv. in Geot. Earthquake Engrg. and Soil Dyn (CD-Rom).*, Univ. of Missouri-Rolla.

Beaty, M., and Byrne, P.M. (1998). "An Effective Stress Model for Predicting Liquefaction Behavior of Sand. In P. Dakoulas, M.Yegian, and R.D. Holts (Eds.), Geotechnical Earthquake Engineering and Soil Dynamics III, ASCE Geotechnical Special Publication No. 75 Vol.1, Proceedings of a Specialty Conference (pp 766-777). Seattle; ASCE.

Brinkgreve, R. B. J., Broere, W., and Waterman, D., ed. (2004). *Plaxis 2D – Version 8.* Plaxis B.V. The Netherlands: Delft University of Technology.

Byrne, P. M., Park, S. S., Beaty, M., Sharp, M., Gonzalez, L., and Abdoun, T. (2004). "Numerical Modeling of Liquefaction and Comparison with Centrifuge Tests," *Canadian Geotechnical Journal*, 41, 193-211.

Interagency Performance Evaluation Task Force (IPET), 2006. Interim Report on Performance of 17th St. Outfall Canal, New Orleans."

Interagency Performance Evaluation Task Force (IPET), 2006. Interim Report on Performance of London Outfall Canal, New Orleans."

Itasca Consulting Group, Inc., 2005. "FLAC – Fast Lagrangian Analysis of Continua, Version 5.0 User's Manual," Minneapolis, Minnesota: Itasca.

Seed, R. B., Abdelmalak, R. I., Athanasopoulos, A. G., Bea, R. G., Boutwell, G. P., Bray, J. D., Briaud, J.-L., Cheung, C., Collins, B. D., Cobos-Roa, D., Cohen-Waeber, J., Ehrensing, L., Farber, D., Hanenmann, M., Harder, L.F., Inamine, M. S., Inkabi, K. S., Kammerer, A. M., Karadeniz, D., Kayen, R.E.**,** Moss, R. E. S., Nicks, J., Nimala, S., Pestana, J. M., Porter, J., Rhee, K., Riemer, M. F., Roberts, K., Rogers, J. D., Storesund, R., Thompson, A., Govindasamy, A. V., Vera-Grunauer, X., Wartman, J., Watkins, C. M., Wenk, E., and Yim, S. (2006). "Investigation of the Performance of the New Orleans Flood Protection Systems in Hurricane Katrina on August 29, 2005.*"* Report No. UCB/CCRM – 06/01, Draft Final Report, May 22, 2006.

Wang, Z.L., 1990, "Bounding Surface Hypoplasticity Model for Granular Soils and its Applications," Ph.D. Dissertation, University of California Davis, U.M.I., Dissertation Information Service, Order No. 9110679, Ann Arbor, MI 48106.

Wang, Z.L., and Makdisi, F.I. 1999. "Implementing a Bounding Surface Hypoplasticity Model for Sand into FLAC Program," Proceedings of the FLAC Symposium on Numerical Modeling in Geomechanics, Minneapolis, Minnesota, September 1-3.

Appendix 20
Glossary for Performance of Levees and Floodwalls

Breach – The loss of the crest of a levee and/or the loss of a floodwall leading to an opening or a rupture that allows water to flow into a protected area.

Centrifuge model tests – Scale model tests conducted using a centrifuge to apply acceleration larger than the acceleration of gravity so that the stresses within the model are the same as the stresses in the full-scale prototype, resulting in behavior that closely simulates full-scale field behavior.

Clay – An aggregate of microscopic and submicroscopic particles derived from the chemical decomposition of rock constituents. Clay is cohesive and sticky over a wide range of water contents. For classification purposes, soil particles smaller than 0.002 mm.

Coefficient of variation – A measure of the dispersion of a probability distribution. It is calculated by dividing the standard deviation of a distribution by its mean value.

Cohesion – Attraction between very fine soil particles caused by intermolecular forces. Also, shear strength of soil at zero normal stress.

Cohesionless – Describes a soil with no cohesion, and no tendency for particles to stick together.

Cone Penetration Test (CPT) – An in-situ test in which an instrumented cone-tipped rod is pushed into the ground at a constant rate, while measuring tip resistance, side friction, and in some cases pore pressure.

COV – Coefficient Of Variation.

CPT – Cone Penetration Test.

CPTU – A cone penetration test in which pore pressures are measured during penetration.

Crest – The top of the levee.

Critical slip surface – The potential slip surface with the lowest factor of safety.

Cross-section – A view as seen in a plane cutting through a structure. The levee cross sections used in the analyses described here are vertical, at right angles to the levee axes.

Crown – The top of a levee.

Elevation – The height of a point above a known reference level or datum.

Erosion – Dislodgement and transportation of soil by flowing water.

Factor of safety – A measure of the stability of a slope – the shear strength of the soil divided by the shear stress required for equilibrium.

Finite element analysis – A method for numerical analysis of stresses and deformations.

Friction angle (ϕ) – A parameter used to characterize the shear strengths of soils.

Harr's Method – A method for analyzing groundwater flow.

Head – See hydraulic head.

Hydraulic gradient – Change in hydraulic head divided by the distance over which the change occurs.

Hydraulic head – A measure of the amount of energy in groundwater, often expressed in ft = ft-lb/lb.

Hydrostatic water pressure – The pressure exerted by water that is not moving.

IPET – Interagency Performance Evaluation Task Force.

I-wall – A type of flood wall consisting of sheetpiles embedded within a levee, and projecting above the levee crest. In cross section view, the wall is "I" shaped.

Lacustrine clay – Clay formed by deposition of soil particles in a lake.

Lane's Weighted Creep Ratio – The ratio of the length of flow, measured along the base of a hydraulic structure, divided by the net hydraulic head across the structure. The length of flow is weighted by dividing horizontal flow distances by 3.0.

Lognormal distribution – In probability and statistics, the probability distribution of a random variable whose logarithm is normally distributed.

Marsh – An organic soil formed in marshy areas – contains mineral as well as organic matter.

Method of Planes – A method of slope stability analysis used by the New Orleans District of the Corps of Engineers. It involves calculation of factors of safety based on a wedge mechanism consisting of three planes.

Overburden pressure – The vertical stress on the ground resulting from the weight of overlying soil.

Passive resistance – Resistance of the ground to horizontal or sub-horizontal forces.

Peat – A fibrous or amorphous aggregate of macroscopic and microscopic fragments of partially decayed vegetable matter.

Permeability – A measure of the ease with which water flows through soil.

Piezometer – An instrument for measuring hydraulic head and water pressure.

Piping – A phenomenon involving erosion due to groundwater flow, resulting in formation of an eroded pipe-like feature in the ground.

Pore pressure – The pressure in water in the voids of a soil.

Pressure – Force divided by the area over which it acts.

Probability of failure – A number that indicates the likelihood of failure.

Progressive failure – A type of failure involving a sequence of events; a progressively worsening condition leading eventually to failure.

Sand – A cohesionless soil, consisting predominantly of soil particles ranging in size from 0.074 mm to 4.76 mm.

Sand boil – A feature resulting from upward flow of groundwater, transporting sand to the ground surface.

Scour – Erosion of soil particles by flowing water.

Seepage – Flow of water through the ground.

Shear strength – The maximum shear stress that a soil can sustain.

Sheetpile – One of a series of interlocking thin steel members – sheetpiles are driven into the ground to form a wall for retaining soil or for reducing the flow of water through the ground.

Silt – A fine-grained soil consisting predominantly of particles ranging in diameter from 0.002 mm to 0.074 mm.

Sinkhole - A depression in the ground surface caused by collapse of the roof of an underground hole, often associated with underground erosion and piping.

Slope stability analysis – An analysis performed to determine the degree of stability of a slope.

Spencer's Method – An accurate numerical method of slope stability analysis.

SPT – Standard Penetration Test.

Standard deviation – A measure of statistical dispersion of values of a variable.

Standard Penetration Test (SPT) – An in-situ dynamic penetration test designed to provide information on the geotechnical properties of soils. In this test, a thick-walled soil sampler is driven 18 inches into the ground by consecutive blows from a 140 lb. hammer dropped from a height of 30 inches. The number of blows required to advance the sampler 12 inches (after it has already been advanced 6 inches) is the blow count N. The value of N provides information about the density and strength of the soil, and is used in many empirical geotechnical engineering correlations.

Station – A location along a line, frequently expressed in terms of hundreds of feet plus feet. For example, Station 8+30 indicates a point 830 ft from the reference point.

Taylor Series – A mathematical relationship that can be used to represent a wide range of mathematical functions by a power series.

Toe – The lowest part of an embankment, levee, or dam, where the slope merges with the adjacent ground surface.

T-wall – A type of flood wall that looks like an inverted "T" in cross section, usually supported on deeply penetrated bearing piles, and usually with a sheet pile wall beneath it to cut off seepage.

Underseepage – Flow of water beneath a structure, through the ground.

Undrained conditions – The condition under which there is no flow of water into or out of a mass of soil in the length of time that the soil is subjected to a change in load.

Unit weight – The weight of soil per unit volume, often expressed in pounds per cubic foot.

Uplift pressure – Upward water pressure exerted on a structure or lower permeability soil layer by water pressure in the ground beneath.

Vane shear test – An in-situ shear test involving rotation around a vertical axis of an x-shaped device to measure the shear strength of soil.

Wave effect – An increase in pressure, above hydrostatic pressure, caused by waves.

Appendix 21
Regional Geology and History

Summary Abstract

The geologic history of the New Orleans area significantly influences the engineering properties of the foundation soils beneath the levees. Geologic and engineering data gathered from the different levee failures identifies a spatially complex geomorphic landscape, caused by Holocene sea level rise, development of different Mississippi River delta lobes, and the distributary channels associated with delta development. Overlying the Pleistocene surface beneath the New Orleans area are predominantly fine-grained, shallow water depositional environments and related sediments associated with bay sound (or estuarine), nearshore-gulf, sandy beach, lacustrine, interdistributary, and paludal (marsh and swamp) environments. These environments define the New Orleans area history during the Holocene, and comprise the levee foundation for the different failure areas. A relict barrier beach ridge is present in the subsurface along the southern shore of Lake Pontchartrain. This relict beach blocked the filling of the lake with fluvial-deltaic sediments, impacted the supply and texture of sediment being deposited by advancing distributary channels, and influenced the engineering properties of these soils. Marsh and swamp soils beneath the failure area at the 17th Street Canal are much thicker in comparison to those beneath the London Avenue Canal because of the influence of the beach complex, and are thickest in the Industrial Canal area. Additionally, man's activities in New Orleans during historic time contributed to the spatial complexity of this area and affected the engineering properties of the foundation soils. Man's activities included construction of drainage and navigation canals, pumping ground water drainage, hydraulic filling of the Lake Ponchartrain lake front, and construction of levees to prevent the river from flooding low lying areas. Man's activities, combined with the geologic setting and subsidence in this region are responsible for the unique landscape that created the New Orleans area. Historic settlement and subsidence in the New Orleans area has been most severe on the back barrier side of the Pine Island Beach. Subsidence didn't contribute to the poor performance of the levee failures. However, subsidence has impacted the datum of many of the benchmarks in the city upon which engineering decisions and design were based and affected levee height and the level of flood protection.

Introduction

A review of the geology and geologic history of coastal Louisiana is presented to establish the general framework for the soils and stratigraphy beneath the New Orleans levee failures. Geologic processes active during the past 5,000 years directly relate to the development of the land mass upon which the New Orleans area is situated, and the resulting stratigraphy beneath the levee failures at the 17th Street, London Avenue, and Inner Harbor Navigation Canals (IHNC). Failures of six I-wall reaches and one earthen levee occurred at these three canals. These canals were responsible for the extensive flooding in the New Orleans metropolitan area following Hurricane Katrina. Levees in the IHNC area were mainly overtopped by storm surge during Hurricane Katrina, while levees at the 17th Street and London Avenue Canals were not overtopped, but failed at water levels below their design height. Geologists working in support of USACE flood control projects in the Lower Mississippi Valley (LMV) have typically classified the geology beneath structures and levees according to specific depositional environments. These lithostratigraphic units are associated with diagnostic fluvial and deltaic processes, and are classified according to soil texture, sedimentary structures, organic content, fossils, and associated engineering properties. USACE geologists has been involved with studies of the New Orleans area geology since the 1940s and have applied an engineering geology classification to the underlying stratigraphy (Fisk, 1944; Schultz and Kolb, 1954; Kolb and Van Lopik, 1958 and 1965; Kolb, 1962; Montgomery, 1974; Kolb, Smith, and Silva; 1975; Britsch and Dunbar,1990; Saucier, 1994; Dunbar et al. 1994 and 1995; Dunbar, Torrey, and Wakeley, 1999).

Physiography and Setting

The city of New Orleans is situated in Jefferson and Orleans Parishes along the eastern edge of the Mississippi River's deltaic plain. Broad natural levees associated with the Mississippi River, Bayou des Familles, and Bayou Metairie are the most prominent physiographic features in the area (Figure 1). Surface elevations are generally near sea level and range from approximately 15 ft above sea level along the crests of the Mississippi River levees to below sea level over much of the area north of the river. Increased urban reclamation of low lying areas occurred after World War II by draining the cypress swamps that were present north of the city to meet the demands for expansion and population growth. A map of the greater New Orleans area from 1849 is presented in Figure 2, showing the extensive swamps and major physiographic features north of the river, before the advent of 20th Century urbanization. Continuous pumping of surface and ground water drainage to support residential development has contributed to the desiccation of these swamp and marsh soils, and has lowered the ground surface to below sea level for a significant portion of the city. Levees that encircle the city and continuous pumping of surface water are required to keep the sea from reclaiming the "Crescent City." Sea level rise of approximately of 1 to 3 ft during the next century due to global warming will provide even greater challenges to local, state and Federal officials and engineers tasked with protecting this historic American city, and other cities along our nation's coasts.

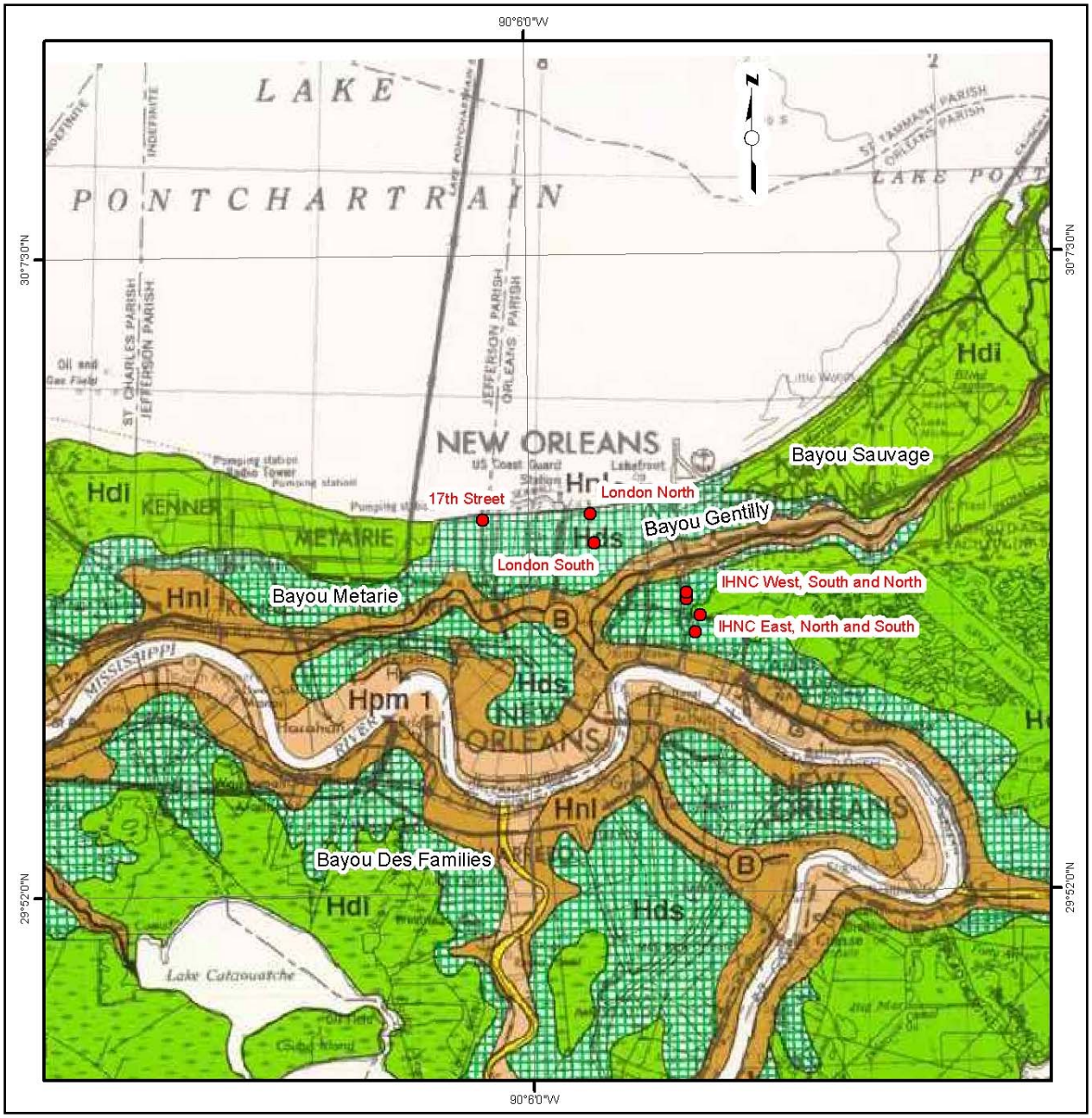

Figure 1. General map of the New Orleans area geology showing the limits of the different surface depositional environments (Saucier 1994). Map symbols are as follows: H = Holocene, d = deltaic, i = interdistributary, s = inland swamp, nl = natural levee, pm1 = point bar (most recent meander belt), B=St. Bernard distributary channel. Bayous Metarie/Gentilly and Des Families are abandoned St. Bernard

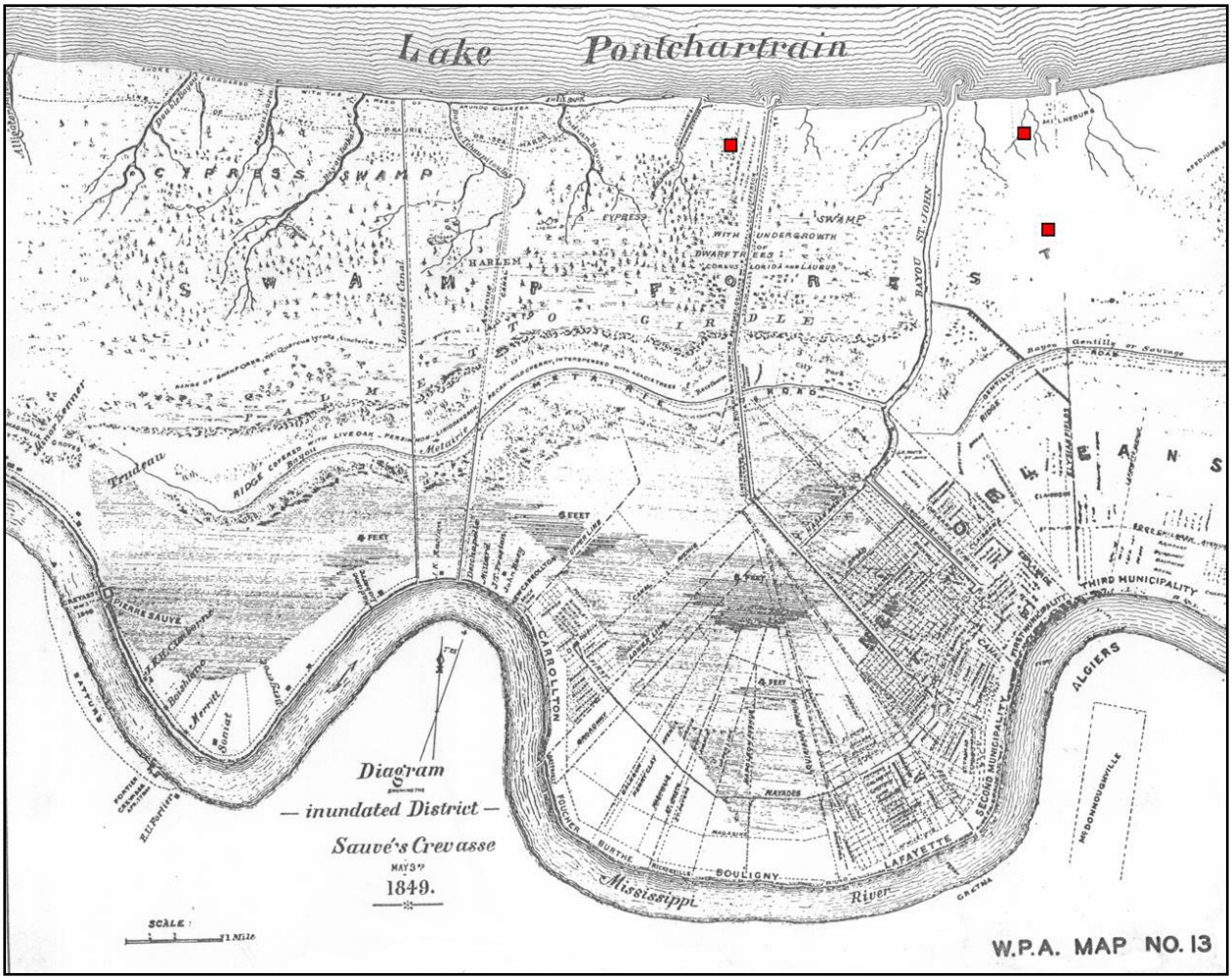

Figure 2. New Orleans area map from 1849 showing the locations of the Bayous Metairie and Gentilly distributary channel, the cypress swamps north of the city, and locations of 17th Street, London North, and South Canal breaches (marked by red squares, beginning from left to right and going clockwise). Bayous Metairie and Gentilly merge into the Bayou Sauvage distributary channel east of the New Orleans area. From Work Projects Administration (1937)

Geologic History

A geologic history has been developed for the Mississippi River's deltaic plain based upon thousands of engineering borings drilled during the past 50 years, thousands of radiocarbon age dates from organic deltaic sediments, and numerous geologic studies conducted in this region (Kolb and Van Lopik 1958a, 1958b, and 1965; Kolb 1962; Kolb, Smith, and Silva 1975; Kolb and Saucier 1982; Frazier 1967; Saucier 1963 and1994; May et al.1984; Britsch and Dunbar 1990; Dunbar et al. 1994, 1995). More than 10,000 borings have been drilled in the greater New Orleans area during the past 50 years in support of foundations for the many engineered structures. Boring data identifies a complex geology that is related to the different course shifts by the Mississippi River and formation of its deltas during Holocene time (Figure 3). Continental glaciers covered much of North America 15,000 years before the present, with sea level

approximately 350 ft below the present level and the Gulf shoreline significantly farther seaward than its present location (Kolb, Smith, and Silva 1975). The ancestral Mississippi River and its tributaries were entrenched into the underlying Pleistocene surface below Baton Rouge, and had developed a broad drainage basin, approximately 25 miles wide, with the axis of this entrenchment in the vicinity of Houma, approximately 45 miles southwest of New Orleans. Global warming and glacial melting caused eustatic sea-level rise, which stabilized between 4,000 to 6,000 years ago, and was 10 to 15 ft lower than the present level (Figure 4).

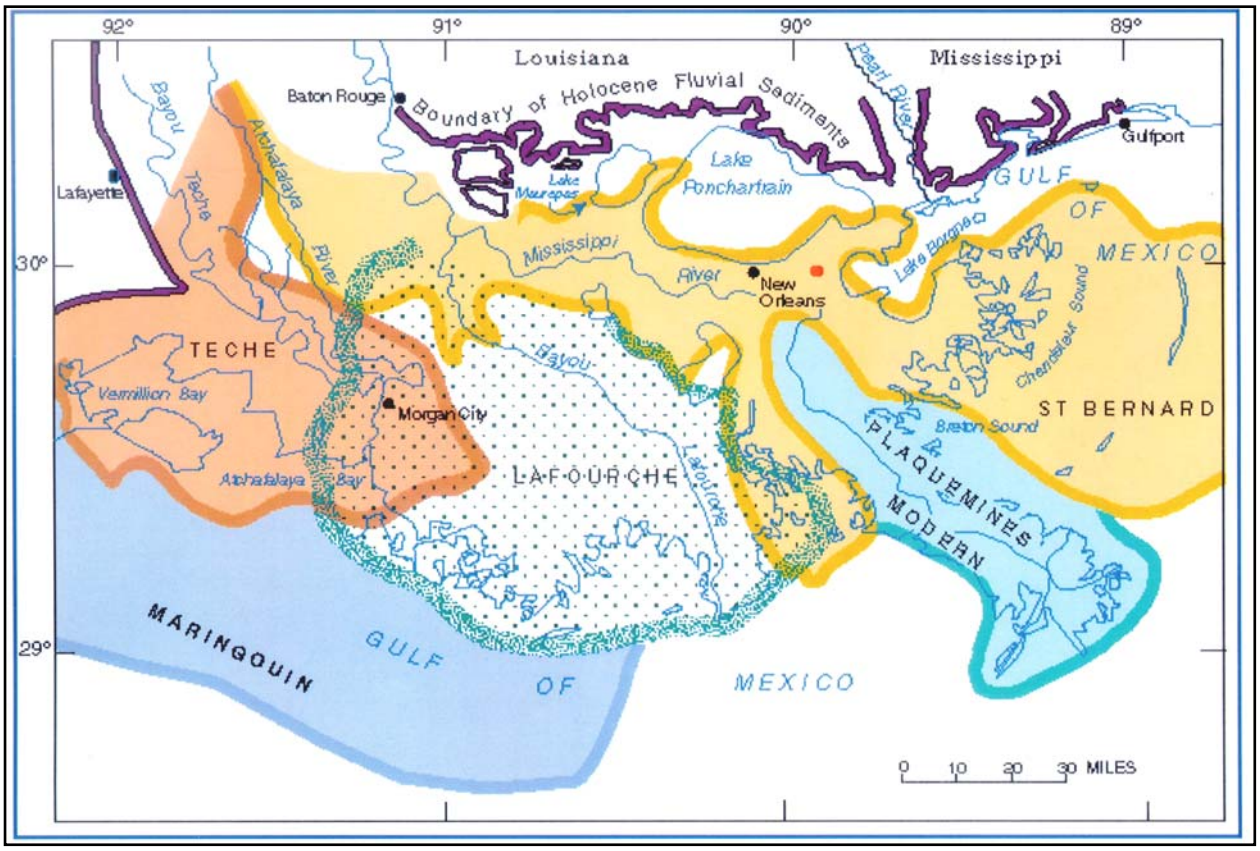

Figure 3a. Holocene deltas of the Mississippi River (after Fraizer, 1967)

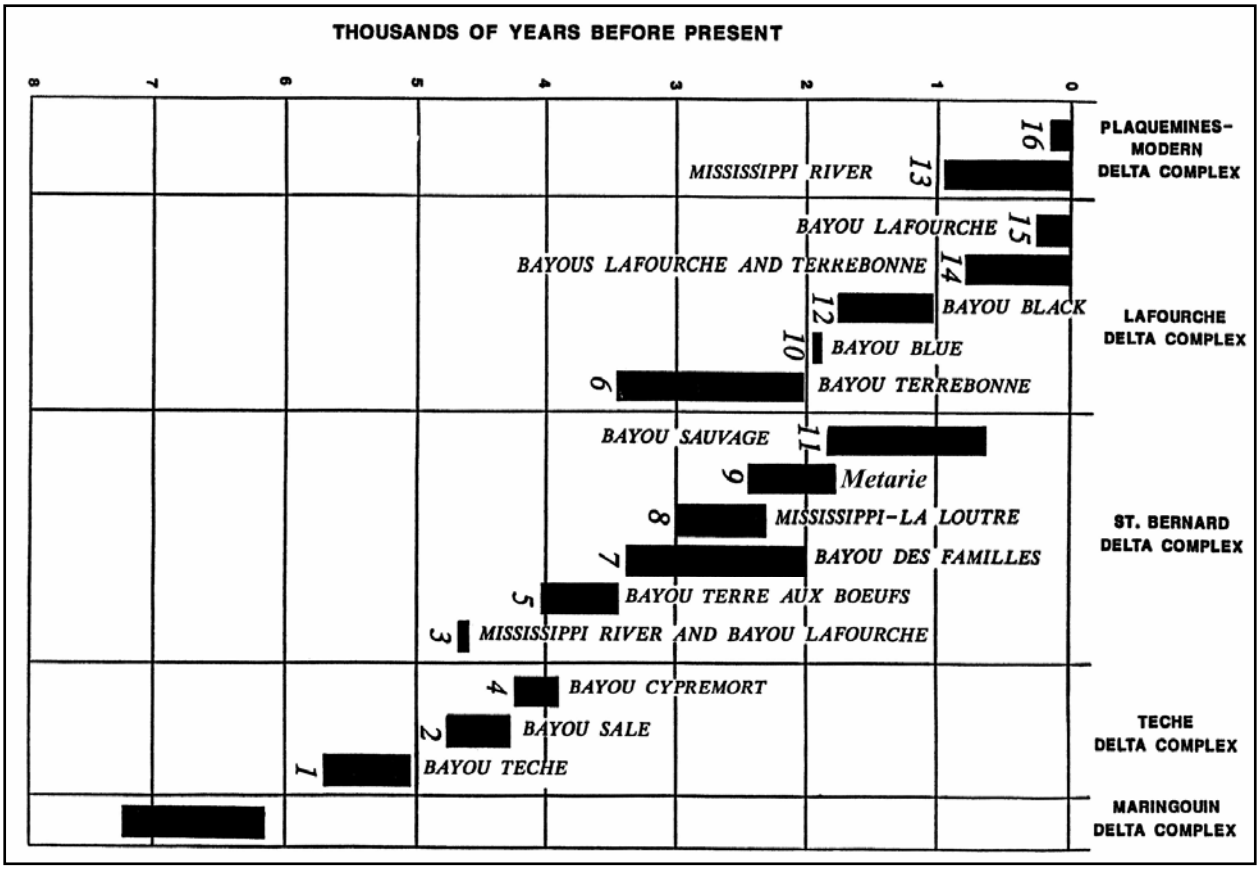

Figure 3b. Chronology of major Holocene distributary channels (after Fraizer, 1967)

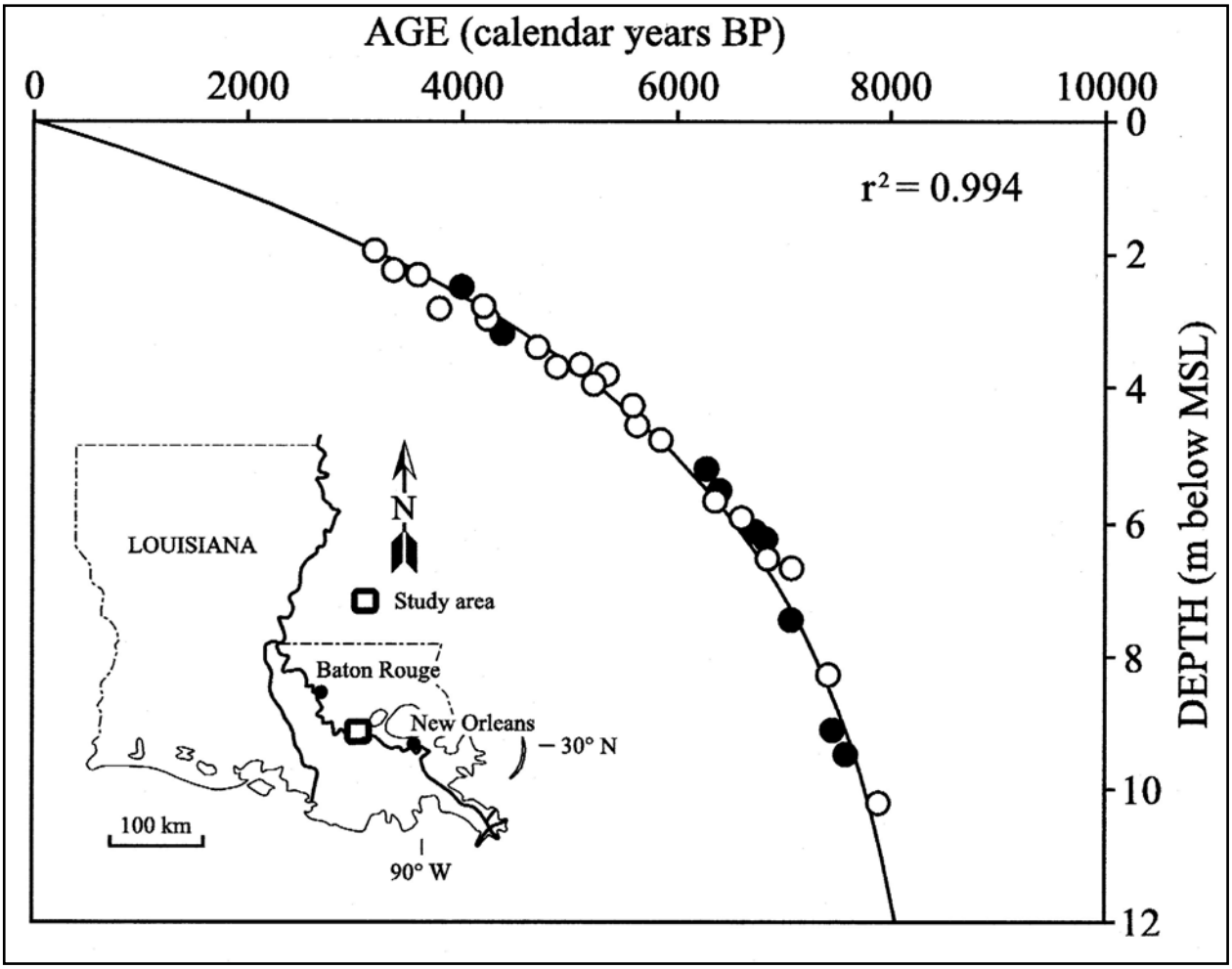

Figure 4. Holocene sea level curve for the Eastern Mississippi River deltaic plain based on carbon-14 dating of basal peats from the transgressive contact at the Holocene and Pleistocene contact (Tornqvist et al. 2004).

Holocene sea level rise drowned the drainage valley and tributary network of the ancestral Mississippi River and caused massive deposition of fluvial sediment within this broad alluvial valley. Creation of the present-day deltaic plain began with the sea level near its present stand. Coastal Louisiana is the product of numerous, but generally short-lived delta systems that have built seaward by deposition of fluvial transported sediment. These deltas have been subsequently reworked and modified by coastal transgressive processes. Five major deltaic systems have built seaward during the past 7,000 years as shown in Figure 3 (after Frazier, 1967).

Each delta system contains a network of several major distributary channels and numerous smaller channels that terminate at the sea's edge where they discharge transported sediment to the sea. Collectively, this network of seaward prograding and bifurcating distirbutary channels forms a short-lived delta lobe complex. Relative ages of these deltas and the major distributrary channels (Figure 3b) are well established by radiocarbon dating of the sediments in these systems (Kolb and Van Lopik 1958a; Fisk, 1960; McFarlan, 1961; Frazier 1967; Smith, Dunbar, and Britsch, 1984). The first major advance of a delta into the New Orleans area occurred by the

St. Bernard system approximately 3,500 to 4,000 years ago via several major distributary channels (see Figures 1 and 3b). The land in the New Orleans area was established by this delta system. Partial Mississippi River flow continued to pass through the New Orleans reach following abandonment of this delta for the Lafourche delta complex south of Donaldsonville. After abandonment of the Lafourche system, approximately 500 years before present, Mississippi River flow returned to the present course. Historic construction of levees has prevented the river from seeking a different and shorter route to the Gulf. Active deltaic growth is occurring at the mouth of the Mississippi River and at the mouth of the Atchafalaya River.

Geologic Structure and Faulting

Holocene sediments underlying New Orleans are part of the seaward thickening wedge of Quaternary sediments that dip gently to the south and fill the Gulf of Mexico basin. Geologic structures within this sedimentary prism are piercement salt domes and growth faults. No salt domes are present beneath the greater New Orleans area. Faulting has been identified in the subsurface throughout the deltaic plain and in the Pleistocene deposits exposed at the surface north of Lake Pontchartrain (Wallace 1966, Snead and McCulloh 1984; Gagliano, 2005; Dokka, 2006). These faults are generally not considered tectonically active (i.e., U.S. Army Corps of Engineers (USACE) usage that implies Holocene movement and capable of producing large magnitude earthquakes that affect engineered structures). Instead, they are related to sedimentary loading, compaction, and consolidation of sediments in the Gulf of Mexico basin. Detailed study of the Pleistocene deposits by Kolb, Smith, and Silva (1975) did not identify faulting in the New Orleans area. Their study identified only one nearby fault in Lake Pontchartrain. Recognition of this fault was based on closely spaced borings and geophysical data. Subsequent geologic mapping of the eastern deltaic plain by Dunbar et al. (1994, 1995) did not identify any Holocene faults based solely on boring and engineering data. Surface faults occurring in Holocene sediments by movement in the underlying Pleistocene deposits are difficult to detect because unconsolidated sediments tend to warp rather than shear. Better resolution of Holocene and Pleistocene stratigraphy using seismic data, combined with closely space borings, and a dense network of elevation benchmarks are needed to determine whether Holocene movement in deltaic sediments are associated with the underlying Pleistocene fault structure.

Geologists in the New Orleans District generally evaluate the presence of faulting in studies of the subsurface stratigraphy during boring programs to determine the geotechnical properties of the foundation for the proposed structures. Additionally, radiometric dating of organic sediments is routinely conducted as part of the site investigations to determine geologic based subsidence histories for the area under study. Fault movements are generally factored into the subsidence history for the structure. Evidence of faulting would be reflected by subsidence, especially if the rates are abnormally high. Furthermore, land loss and engineering geology mapping studies by the New Orleans District have been evaluated for the presence of faults, as linear trends in land loss may define their presence (Dunbar, Britsch, and Kemp, 1992; Britsch and Dunbar, 1993 and 2005). In the New Orleans area, no evidence of faulting was identified at the canal levee failures from the boring and stratigraphic evidence gathered and evaluated by the IPET team during focused studies at these areas. Stratigraphic evidence obtained and evaluated from these sites indicates other mechanisms are responsible for the different canal failures.

Holocene Environments of Deposition

The geology in the Lower Mississippi Valley and the New Orleans has traditionally been defined by USACE geologists according to depositional environments. Surface environments include natural levee, point bar, inland swamp, fresh marsh, and abandoned distributary channels (see Figure 1). Distributary channels are associated with two major St. Bernard distributary systems, the Bayou des Familles-Barataria and the Bayou Metairie-Sauvage system (Figure 3b). The Bayou Des Familles-Barataria extends due south from the Mississippi River and was active approximately 2,000 to 3,400 years before present (Figure 1), while the Bayou Metairie-Sauvage-Gentilly course is located north of the Mississippi River and was active about 2,500 to 700 years before the present (Frazier 1967, Saucier 1963). These distributary systems filled the shallow water in the New Orleans area with fluvial-deltaic sediments. Overbank deposition from these active distributary channels has formed well developed natural levees that transition to inland swamps and low-lying marsh environments. Sediments within these different environments generally become finer-grained with increasing distance from the distributary channels, and have a corresponding increase in organic content.

USACE foundation and regional geologic studies show the Holocene fill ranges from 70 to 80 ft thick across much of the New Orleans area, and is composed of stacked depositional environments, related to shifting delta systems and their seaward advancement and growth. Where the Mississippi River has scoured in the bends of the river, the Holocene fill exceeds depths greater than 150 ft thick (Dunbar, Torrey, and Wakeley, 1999; Saucier, 1994). Major deltaic environments overlying the Pleistocene surface in the vicinity of the canal failures include nearshore gulf, bay sound-estuarine, intradelta, relict beach, lacustrine, and interdistributary environments (Dunbar et al. 1994, 1995). Regional geologic maps and cross sections from the Louisiana Coastal Plain and the greater New Orleans area are presented on a USACE geology website of the Lower Mississippi Valley (LMV) and show the vertical and horizontal limits of these different environments of deposition in the subsurface (see Corps geology website for the LMV to obtain maps and cross-sections at *lmvmapping.erdc.usace.army.mil*). Similarly, cross-sections were developed from the boring information at the different failure sites where they define the vertical and horizontal limits of these environments in the subsurface, presented in discussions about each breach site in Volume 5 of the IPET report.

Correlations between depositional environments and the engineering properties of the soils that form these lithostratigraphic units are summarized in Table 1 (Kolb and Van Lopik, 1965). A detailed discussion and presentation of the physical and engineering properties characteristic of these different depositional environments is beyond the scope of this study. A comprehensive description of these environments is provided in several USACE studies (Kolb and Van Lopik 1958a, 1959b, and 1965; Kolb 1962; Montgomery 1974; Kolb, Smith, and Silva 1975; Saucier 1994), which are presented at the above LMV geology website.

Table 1a. Selected engineering properties of deltaic depositional environments, soil texture, water content, and unit weight (Kolb, 1962; Kolb and Van Lopik,1965)

DEPOSITIONAL TYPES	LITHOLOGY PERCENT 0 25 50 75 100	REMARKS
NATURAL LEVEES		Disposed in narrow bands flanking the Mississippi River and its abandoned courses and distributaries. Elevation varies from 25 feet near Baton Rouge to sea level.
POINT BAR		Usually found flanking the more prominent bends of present and abandoned courses. Thickness in excess of 100 feet.
PRODELTA CLAYS		Fat clay in offshore areas and at depth beneath deltaic plain. Thickness ranges between 50 and 400 feet.
INTRA DELTA		Coarse portion of subaqueous delta. Intricately interfingered deposits. Disposed in broad wedges about abandoned courses and major distributaries.
INTERDISTRIBUTARY		Forms clay wedges between major distributaries. Minor amounts of silts and fine sands typically occur in very thin but distinct layers between clay strata.
ABANDONED DISTRIBUTARY		Form belts of clayey sediments from a few feet to more than 1000 feet in width and from less than 10 to more than 50 feet in depth.
ABANDONED COURSE		Form belts of fairly coarse sediment in abandoned Mississippi River courses. Lower portion filled with sands, upper portion with silts and clays. Coarsest fill near point of diversion.
SWAMP		Tree-covered organic deposits flanking the inner borders of the marsh and subject to fresh-water inundation. Deposits 3 to 10 feet thick.
MARSH		Forms 90 percent of land surface in the deltaic plain. Ranges from watery organic oozes to fairly firm organic silts and clays. Average thickness 15 feet.
ABANDONED TIDAL CHANNELS		Found principally in peripheral marsh areas. Average depths on the order of 25 feet. Widths average 200 feet. Filling varies from peat to organic clay.
SAND BEACH		Border the open gulf except in areas of active deltaic advance. May be a mile or more wide and more than 10 miles long. Sand may pile as high as 30 feet and subside to depths 30 feet below gulf level.
SHELL BEACH		Border landward shores of protected bays and sounds and marshland lakes. Vary from 25 to 200 feet in width and from 2 to 6 feet in height. Lengths usually less than a mile.
LACUSTRINE		Deposits vary in thickness from 2 to 25 feet. Stratification in clayey lacustrine deposits is poorly developed or lacking.
REEF		Active reefs found principally in bay-sound areas. Buried reefs 5 to 10 feet thick a common occurrence within deltaic plain. Reach dimensions of 1/2-mile wide and 10-miles long.
BAY-SOUND		Relatively coarse sediments on bottoms of bays and sounds. Thickness between 3 and 20 feet.
NEARSHORE GULF		Found at the borders of the open ocean seaward of the barrier beaches. Thickness normally increases with distance from shore.
SUB-STRATUM		Massive sand and gravel deposits filling entrenched valley and grading laterally into nearshore gulf deposits. Material becomes coarser with depth.
PLEISTOCENE		Ancient former deltaic plain of Mississippi River. Consists of environments of deposition and associated lithology similar to those found in Recent deltaic plain. Depth of this ancient, eroded surface increases in a southerly and westerly direction in southeastern Louisiana.

LEGEND

GRAVEL (>2.0 MM) SAND (2.0–0.05 MM) SILT (0.05–0.005 MM)

CLAY (<0.005 MM) ORGANIC MATERIAL SHELL

Table 1b. Selected engineering properties of deltaic depositional environments (Kolb 1962 and Kolb and Van Lopik1965)

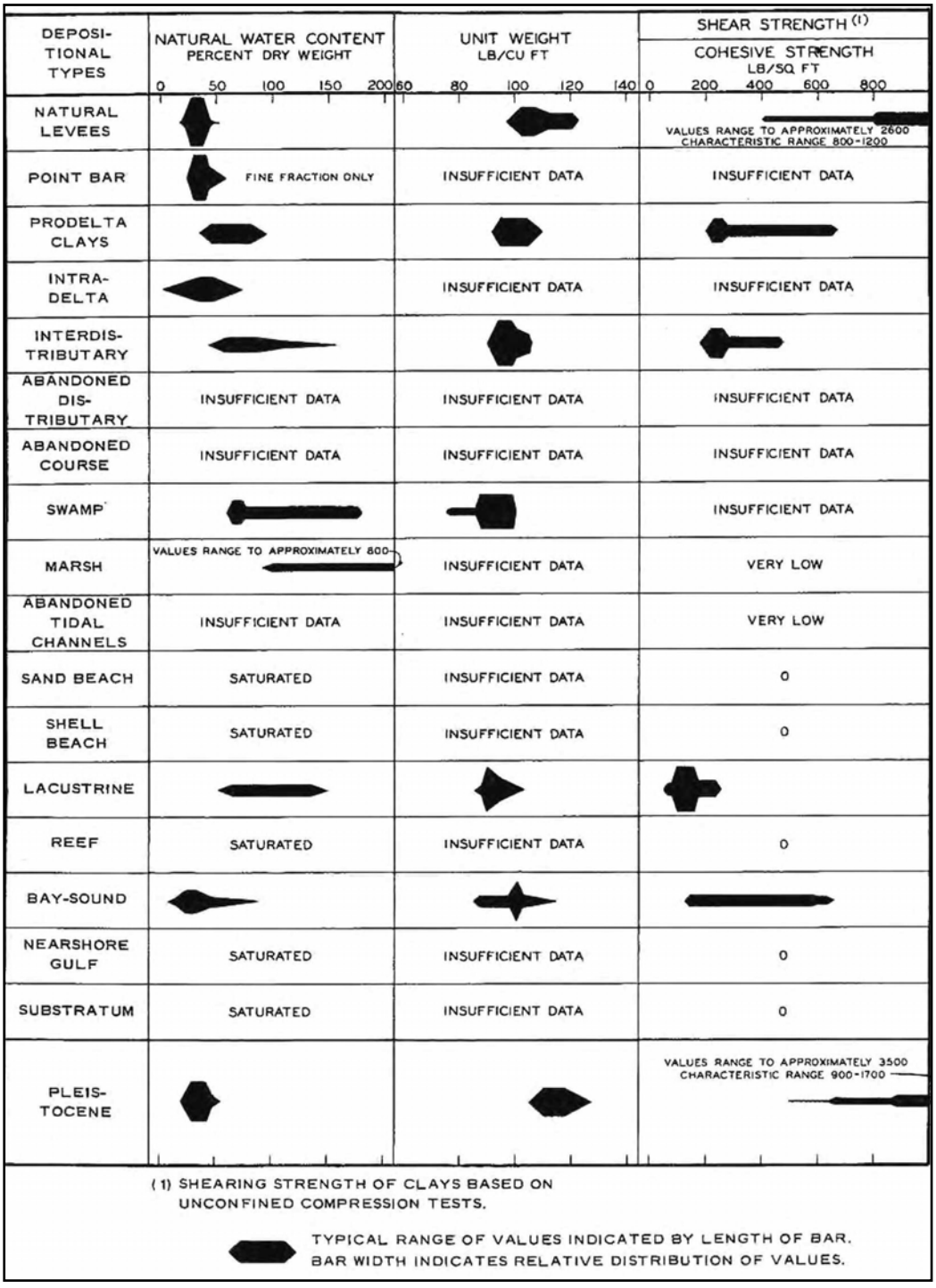

Classification of the subsurface stratigraphy beneath the failure sites by the IPET investigation team was made according to depositional environments from the available boring data. Geologic cross sections at each failure area were prepared from the available boring data to

support the engineering analyses of the failure mechanisms. Interpretation of the underlying stratigraphy is based on the Corps classification of depositional environments gained from more than 50 years of corporate experience in geologic mapping and evaluation of fluvial deltaic deposits in the costal plain in support of foundation studies for various flood control projects (Fisk 1944; Schultz and Kolb, 1954; Kolb and Van Lopik 1958a, 1958b, and 1965; Kolb, Smith and Silva, 1975; Saucier and Kolb, 1982, Saucier 1994). Engineering properties of fluvial-deltaic soils are uniquely related to their origin, their age, local current and wave conditions, sedimentary structures, and the subsequent geomorphic processes and man-made changes that have occurred after their deposition. The greatest contrast in engineering properties occurs between the high and low energy depositional environments and sediment age, namely whether the sediments are Holocene or Pleistocene.

A prominent buried beach ridge lies between Lake Ponchartrain and the Mississippi River that has directly influenced levee foundation properties and contributed to the subsequent failures at the 17th Street and London Canals (Figure 5). A relatively stable, but lower (10 to 15 ft lower than present) sea level 4,000 to 5,000 years ago, permitted sediments from the Pearl River east of New Orleans area to be concentrated by longshore drift, forming a prominent sandy spit or barrier beach complex known as the Pine Island Beach (Saucier 1963 and 1994). The levee breach at the 17th Street Canal was located on the protected or back barrier side of this beach system, while both of the London Avenue Canal levee breaches were located on the main axis, where the maximum sand thickness occurs. Consequently, soft soils at the 17th Street break are much thicker and finer-grained than those beneath the London Canal. Foundation soils at the 17th Street Canal levee are dominated by clay while those at the London Canal are composed mainly of sand. Levee failures in the Inner Harbor Navigation Canal (IHNC) area are located on the seaward side of the beach complex and south of the Bayou Metairie-Sauvage distributary system. The Pine Island Beach trend prevented this distributary system from completely filling Lake Ponchartrain with sediment. Because of the high sediment rates and close proximity to the Bayou Metairie-Sauvage distributary and the present course of Mississippi River, the IHNC area has thick deposits of fine-grained soils consisting of natural levee and inland swamp.

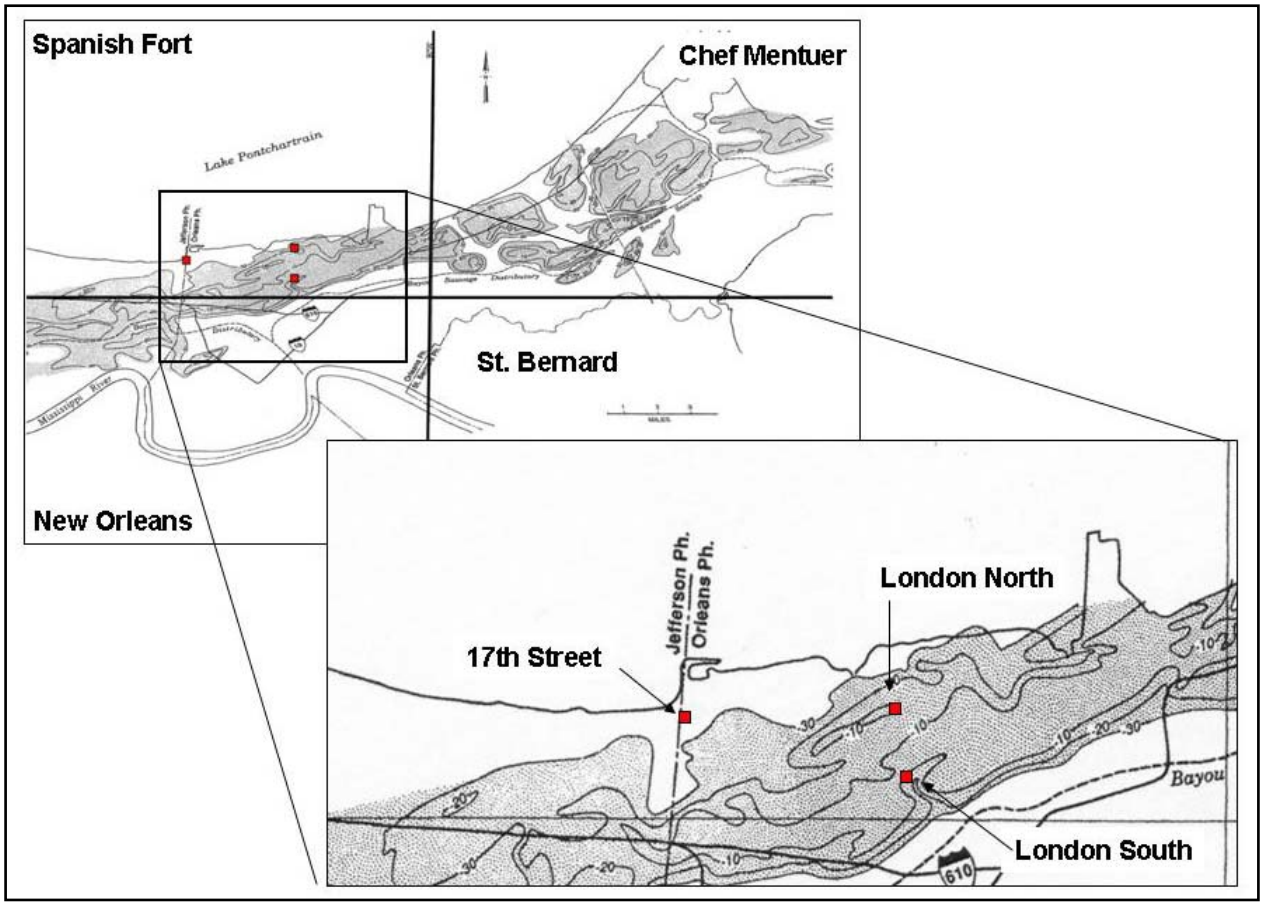

Figure 5. Contour map of the buried Pine Island Beach with elevations in ft MSL (Saucier, 1994) London Canal levee failures are located along the main axis of the buried beach. The 17th Street Canal levee break is located on the protected or back barrier side of the beach ridge. Back barrier side was dominated by fine-grained deposition from advancing St. Bernard distributary channels into low-energy lacustrine environment. The Bayou Metarie - Gentilly distributary channel is located on the seaward side of the barrier beach.

Subsidence and settlement

Loss of wetlands in Coastal Louisiana are among the most severe in the United States. Historic rates have been as high as 42 square miles per year during the mid 1960s. During the period between 1983 and 1990, loss rates were at about 25 square miles per year (Britsch and Dunbar, 1993 and 2005). Because of Hurricanes Katrina and Rita, rates are in excess of 200 sq miles/year (Times-Picayune, 11 October 2006). Loss wetlands in the Mississippi River deltaic plain are related to a combination of factors, including erosion by wave and storm surges, global sea level rise, regional subsidence from sedimentary loading of the Gulf of Mexico Basin, local subsidence due to compaction and consolidation of the Holocene deltaic sediments, oil and ground water extraction, movement along Quaternary faults, movement of the underlying Jurassic salt layer, movement of salt domes, and impacts caused by man's activities.

Man's activities have included construction of levees, the building of flood control and diversion structures, dredging of navigation and petroleum canals, and the dewatering and pumping of low lying coastal plain areas to support agricultural and urban development. Subsidence in the Louisiana coastal zone and the New Orleans area involves both sea level rise and the general lowering of the land surface because of the different natural and man-made mechanisms listed above. Further contributing to the wetland loss has been the confinement of the Mississippi River to a fixed course by levee construction and bank stabilization, which has prevented fluvial transported sediments from reaching the distal parts of its former floodplain during the annual flooding, and the creation of new land areas by crevassing, channel avulsion, and formation of new deltas. In the New Orleans area, subsidence has been severe, due in large part to historic dewatering of swamp and marsh soils, and because of the lack of new sediment from reaching low lying areas on the floodplain from levee confinement. Active land building by fluvial-deltaic processes in coastal Louisiana has been restricted to the Mississisippi and Atchafalaya River deltas.

Subsidence rates in the in the Louisiana Coastal Plain and the New Orleans area have been the focus of several recent studies (Dixon et. al, 2006; Meckel, ten Brink, and Williams, 2006; Miller and Douglas, 2004; Shinkle and Dokka, 2004; Burkett, Zilkoski, and Hart, 2003; Penland et al. 1989). Subsidence rates reported for the New Orleans area are variable (Figure 6). Subsidence rates are generally higher in the low lying areas near the lake front as compared to the natural levees flanking the active channel and its distributaries. Generally, the low lying swamp areas (Figure 2) are more compressible due to their fine-grained texture and higher water contents, as compared to the natural levees soils with lower water contents and coarser-grained textures. Current, short-term estimates of subsidence in the New Orleans area average about 5 mm/year (Dixon et al., 2006; Burkett, Zilkowki, and Hart, 2003). Geological estimates of long-term subsidence in the New Orleans area based on carbon-14 dating of buried peats and organic sediments, and they indicate the general background rate is about 0.5 to 1 ft per century, or about 1.5 to 3 mm/year (from unpublished USACE C-14 data and Kolb and Van Lopik, 1958, respectively). Short-term subsidence rates in the New Orleans area are nearly 3 to 4 times higher than the background rate determined from geologic time scales spanning several thousand years. The geologic background rate also incorporates sea level rise as a component, since peats are assumed to form at the land-water interface within coastal marsh settings, and thicken in response to deltaic sedimentation and continued marsh growth under a rising sea level.

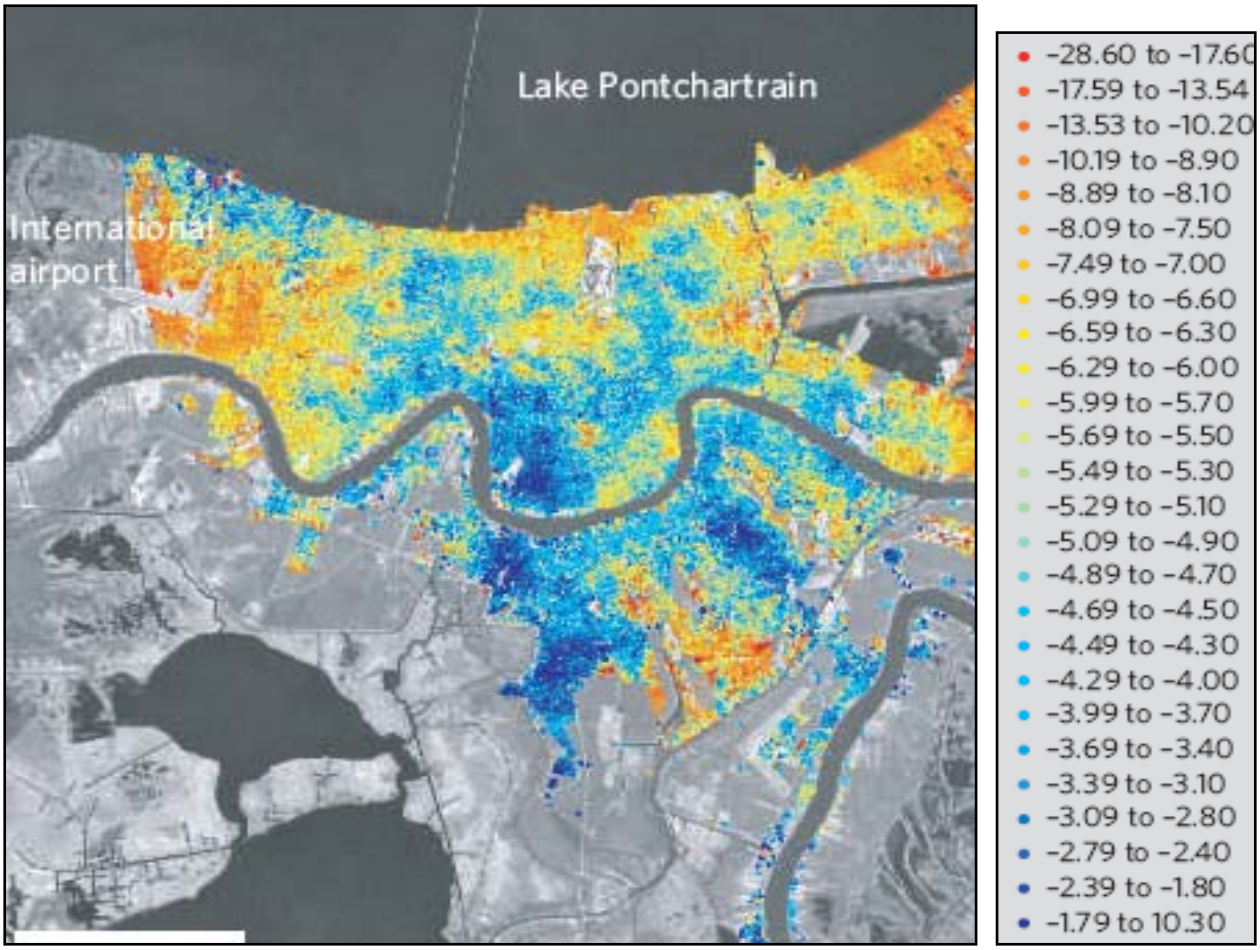

Figure 6. New Orleans area subsidence rates in mm/yr, based on 33 Radarsat satellite scenes from 2002 and 2005 (Dixon et al., 2006). Rates are generally highest near the Lake Ponchartrain shoreline. Lake front area contains dredge fill from early 1900s. This area also corresponds to the protected or back barrier side of the buried Pine Island beach complex (Figure 5).

An underlying cause for the higher historic subsidence rates in the New Orleans area has been the construction of drainage canals during the 20th Century, and dewatering of the organic (swamp and marsh) soils shown in Figure 2 to accommodate the increased demands for land development and population growth. Lowering of ground water levels by construction of drainage canals and pumping of surface drainage has caused a corresponding net reduction in soil volume, oxidation of the dewatered organic sediments, and an overall decline in surface elevation throughout the city. Data presented by Saucier and Kolb (1982) estimates total subsidence in the Kenner area of Eastern Jefferson Parish may be as much as 70-in. since dewatering began (Figure 7). Saucier and Kolb referred to this human induced subsidence as "settlements," because of its underlying engineering origin. Added to the settlements from dewatering are the secondary affects of residential construction and loading of the ground surface by building foundations (Eustis Engineering Company, 1984).

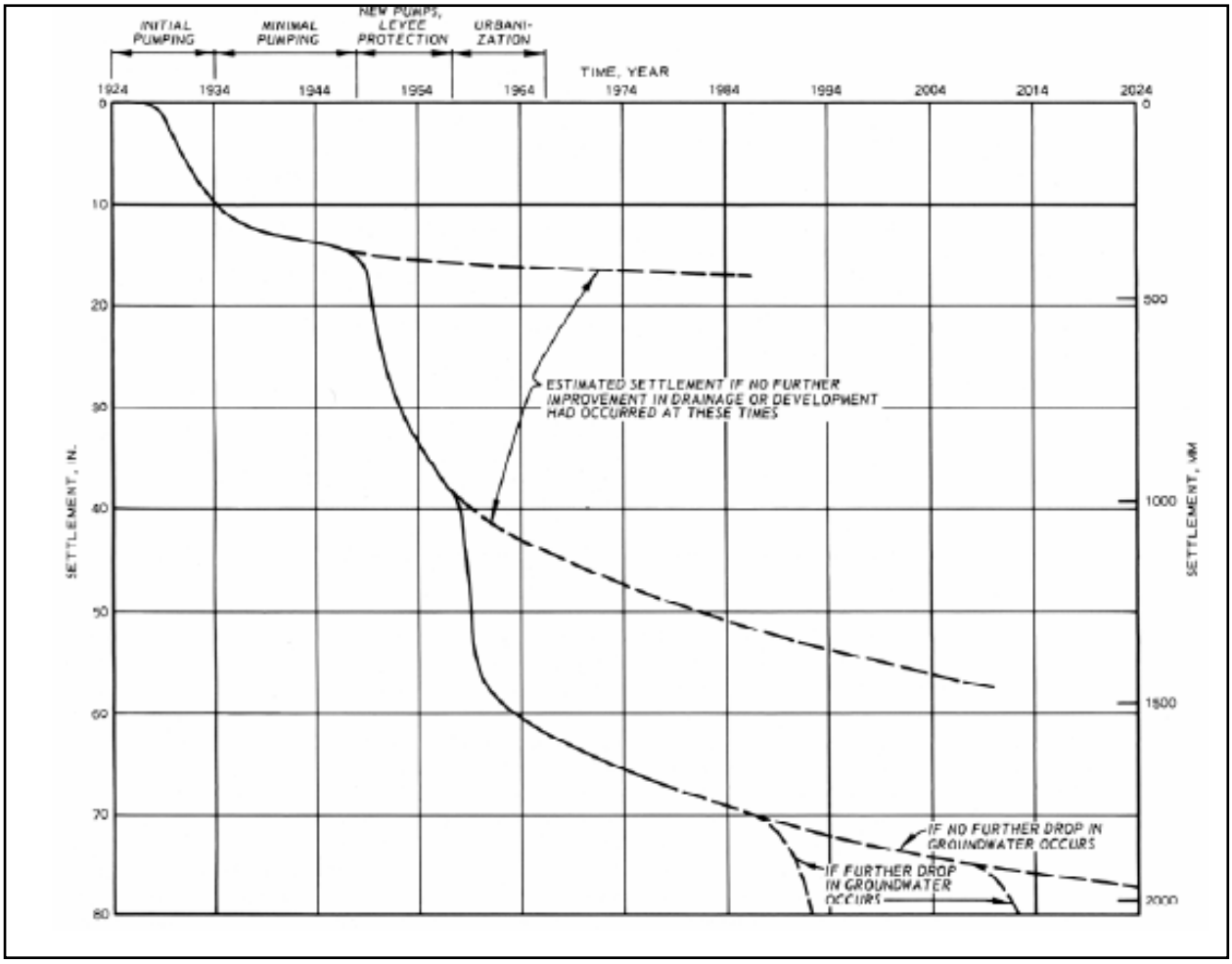

Figure 7. Estimated settlement history in the Kenner area due to dewatering of near surface organic sediments by drainage canals and pumping (from Kolb and Saucier (1982) using unpublished data by Traughber and Gore). Dewatering of organic sediments causes volume reduction in these sediments and results in oxidation, which lowers the ground surface.

Site specific, cumulative changes in surface elevation in Orleans Parish have been identified in a study by URS (2006). Comparison of historic 5 meter elevation data, relative to a constant datum between 1895 and 2002, indicates total subsidence and/or "settlement" in some parts of the city ranges from 8 to 10 ft (Figure 8). Positive land gain in Figure 8 corresponds to early 1900s dredge filling to create the New Orleans lake front. Highest values of elevation decline during the past 100 years are in areas underlain by thick marsh and swamp deposits. Furthermore, these areas are located on the back barrier side of the buried Pine Island beach, consisting of 70 to 80 ft thick, unconsolidated Holocene deltaic sediments. Boring data and cross sections developed from this area identifies the underlying geology as consisting in descending order and increasing age as 8 to 12 ft thick sequence of 3,000 year or less paludal (marsh and swamp) deposits, 20 to 25 ft thick lacustrine sediments, 10 to 20 ft thick sand that is part of the Pine Island Beach complex, and 30 to 40 ft thick fine-grained, bay sound deposits that overlie the stable Pleistocene surface (Schultz and Kolb, 1954; Kolb and Van Lopik, 1958a; Fisk, 1960; Kolb, Smith, and Silva, 1975; Dunbar et al., 1994 and 1995; USACE, 1988, 1989, and 1990).

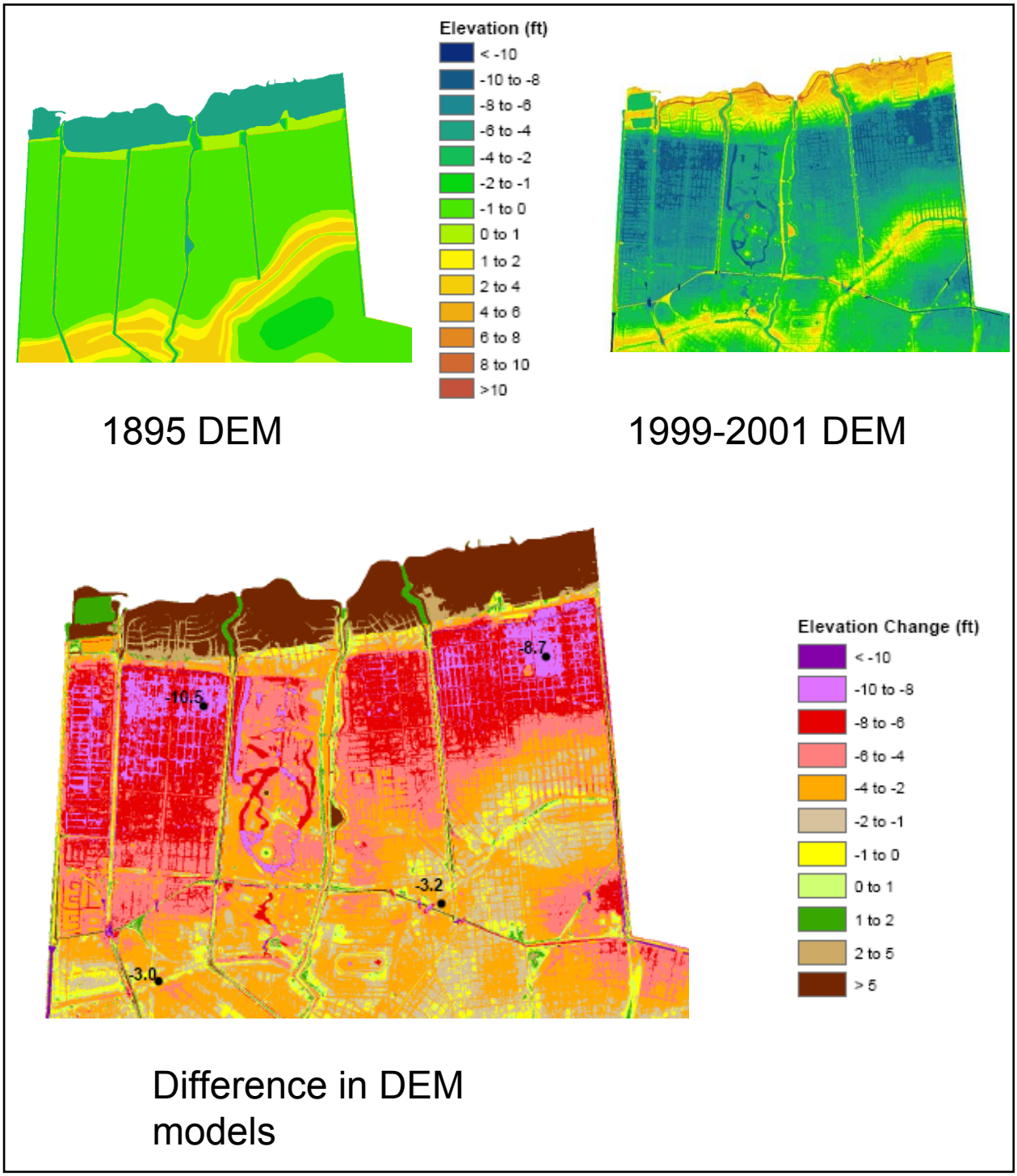

Figure 8. Changes in ground surface elevation between 1895 and 2001 (URS, 2006). Comparison is based on 1895 historic topographic map and 1999-2001 digital elevation models (DEMs). Locations of failures are identified by open circles, from left to right are 17th Street Canal, London Canal North breach (top), and London

Settlements beneath the drainage canals are considerably less than the adjoining residential areas in Figure 8. Historic settlements are probably less severe because of construction related

compaction of the foundation by the added weight of the levee during its initial dredging during the late 1800s and early 1900s and continued maintenance of levee height since this time. Figure 7 suggests that settlements are most severe after the initial dewatering process occurs, and then stabilizes at a constant background rate. Present day surface elevations near the landside toe of the levee breaches are generally between -5 and -6 ft NAVD88. Considering that the original swamp surface was probably 1 to 2 ft above sea level before urbanization began (Figure 2), large settlements of more than 70 in. are the norm, rather then the exception during historic time in the New Orleans area. Both short-term (man-made) and long-term (geologic) mechanisms are involved in the subsidence problem beneath the city.

Another historic perspective of New Orleans subsidence rates is provided by elevation measurements from the ALCO1931 benchmark during a 53 year record of measurements (Figure 9). This benchmark is located on the west side of the Hammond Highway Bridge, near the Coast Guard Station, and near where the 17th Street Canal breach occurred. An elevation difference of -2.095 ft relative to NAVD88(2004.65) or -2.345 ft relative to MSL in 2005 was reported for this benchmark for the 53 year period of record. The net difference in elevation includes changes in the survey datum (or spheroid model of the earth used) and a component of subsidence. By subtracting the difference in survey datum from the overall value, the resultant value corresponds to historic subsidence changes at this location during the period of record, and generally 40 to 50 years after canal construction and dewatering have occurred. At the ALCO1931 location, it has been estimated that the datum changes account for about 0.19 ft or 2.28-in.of the total measured difference (Garster, personal communication). Subtracting the datum component from the total difference, yields a subsidence component of -1. 905 ft (580.6 mm) relative to NAVD88(2004.65) and -2.155 ft (656.8 mm) relative to the Mean Sea Level (MSL) datum. This net difference corresponds to an annual subsidence rate of 0.43-in./yr (10.95 mm/year) relative to NAVD88(2004.65), or 0.49-in./year (12.4 mm/year) relative to MSL (which incorporates sea level rise) for the 53 year period of record. These rates correspond to cumulative subsidence rates of between 3.59 to 4.07 ft (1.095 to 1.24 m) per century, and probably accurately reflect the latter stages of the subsidence curve in Figure 7 in areas that have undergone dewatering.

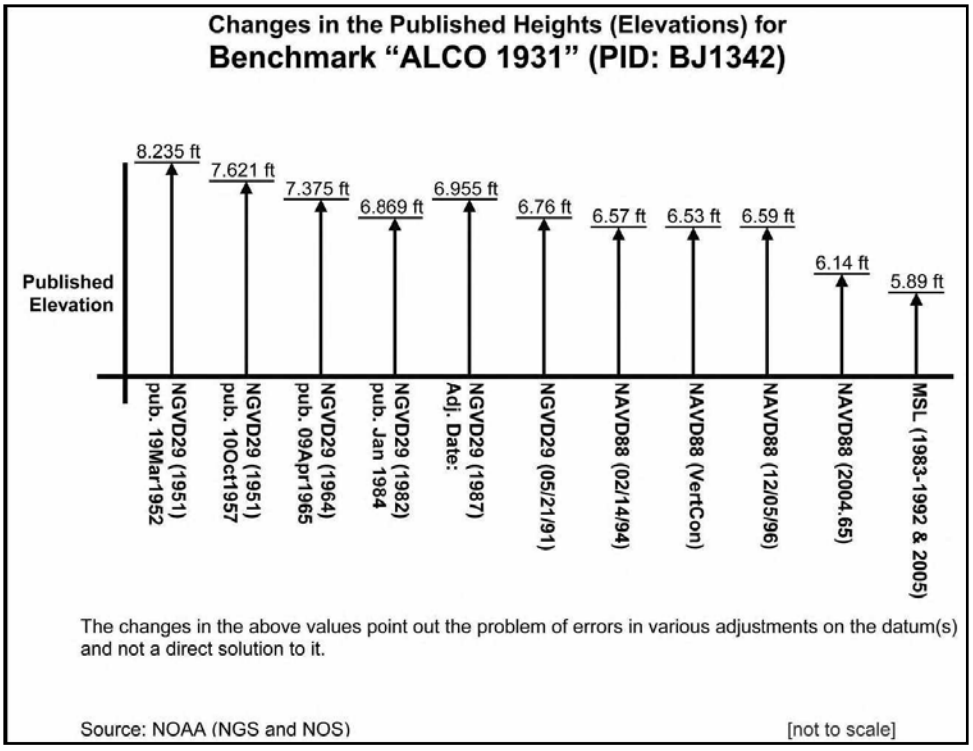

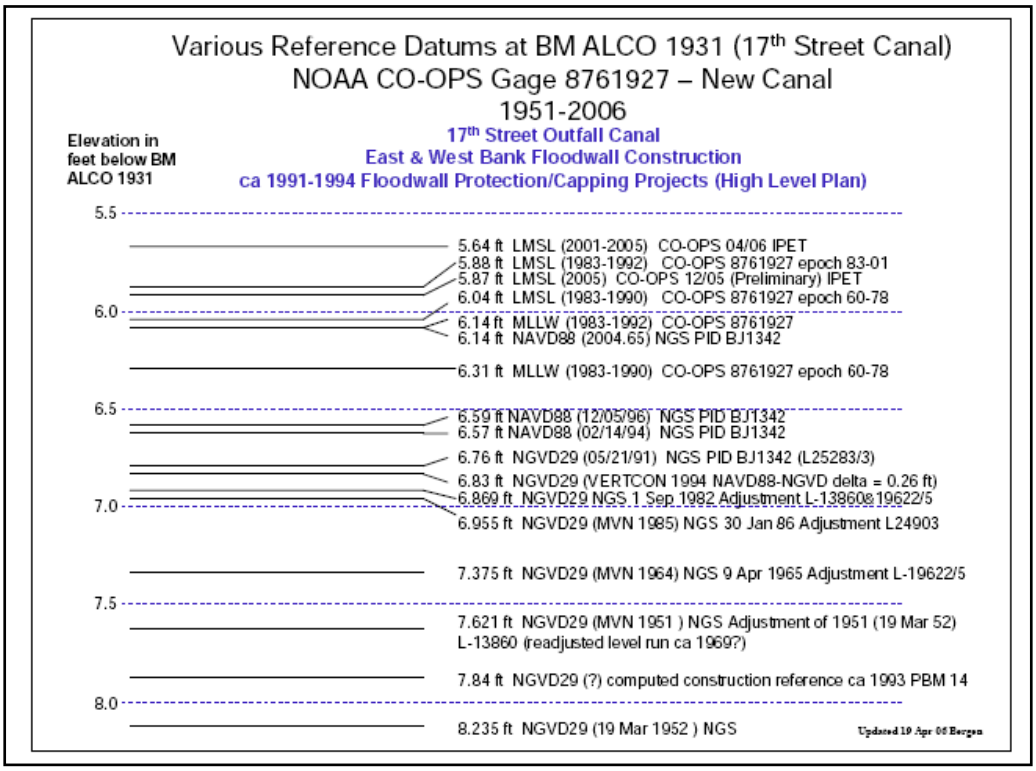

Figure 9. Changes in elevation reported for the ALCO benchmark, near the Hammond Highway Bridge at 17th Street Canal (from IPET, Chpt 2, Figures 69 and 33, respectively). Reported elevations reflect changes in the datum (spheroid model used), man-made settlement, and local subsidence since 1952. A net difference of 2.345 ft is identified for the benchmark over the nearly 50 year record of measurements.

Subsidence rates identified by the various methods described above in Figures 6 though 9 are important for understanding the short and long term impacts to engineered structures, and designing effective solutions for flood protection in New Orleans. Hurricane protection of the drainage canal levees consisted of I-wall and T-wall construction during the early 1990s. Changes in elevation due to subsidence was generally not incorporated into the design of I walls and T-walls for hurricane protection. Impacts to levee stability and subsequent levee performance from changes in elevation due to subsidence were nonexistent or negligible. In terms of levee performance, no reports of differential settlements have been reported during the annual levee inspections, nor were they documented by the current IPET investigation. If significant subsidence had occurred, it may have caused deformation between I-wall panels, which may have compromised the integrity of the hurricane protection system, and resulted in poor performance. Short term subsidence was not an issue factoring into the poor performance of the I-walls at the canal levee failures.

No structural impacts to levee performance are attributed to subsidence during Hurricane Katrina, except in terms of the level of protection afforded from the design flood height. Height of the flood protection wasn't at levels authorized by Congress because of poor understanding and effective resolution of the different benchmark datum's that were incorporated into the engineering of the flood protection system. Congress authorized a level of protection that was not achieved because of faulty resolution of the datum and historic changes from subsidence.

With a forward look to the future for Coastal Louisiana, the New Orleans District currently has no funding for a systematic, district wide program for monitoring subsidence within man-made and natural settings. All of the subsidence rate calculations are long-term estimates, or short term estimates from a few site specific benchmarks. In order to effectively address subsidence and its implications for flood protection, a district wide program for monitoring subsidence using the latest technology must be implemented. Important to this program will be a dense network of benchmarks upon the levees and its structural components, as opposed to only highway benchmarks, that accurately measure the subsidence rates across the Louisiana Coastal Plain for effective solutions that mitigate subsidence, land loss, and flood protection.

Summary

Inland swamp and marsh soils form the foundations for the levees and these soils require special attention for effective engineering of structures. Urban reclamation of low-lying areas has impacted the surface topography during historic time and has involved draining the cypress swamps that were present north of the city to meet the demands for city expansion and population growth. Continuous pumping of surface and ground water drainage are necessary to keep ground water levels below residential development. This process has directly contributed to the desiccation of the underlying swamp and marsh soils, and lowered much of the ground surface below sea level over a significant portion of the city. Levees that encircle the city and continuous pumping into the drainage canals are now required to prevent flooding. A buried beach ridge is located between the south shore of Lake Ponchartrain and the Mississippi River, and has directly affected levee foundation and engineering properties at the 17th Street and London Avenue Canals. The thickness of inland swamp and marsh deposits at the canals are

controlled by the presence of the buried relict beach and their proximity to prehistoric distributary channels, which created the land area beneath New Orleans. Swamp and marsh soils are thickest behind the beach ridge and the IHNC area, and are the thinnest over the axis of the beach ridge. Focused geologic studies of the levee breaches indicate weak lacustrine soils were responsible for the levee failure at the 17th Street Canal. High storm surges in the canals appear to have elevated pore pressures in the pervious beach sands that ultimately contributed to the levee failures at the London Avenue Canal. Further east in the IHNC area, the hurricane generated storm surge overtopped and scoured the soil foundations behind the vast majority of I-walls that failed. Ultimately, the lessons that emerge from Hurricane Katrina are that the geology and associated hazards imposed by weak and pervious foundation soils must be clearly defined and better understood. Subsidence was not a factor in the poor performance of the failed levee sections. A dense network of benchmarks is needed on Corps levees and structures to effectively characterize long-term subsidence trends.

References

Britsch, L. D. and Dunbar, J. B. (1990). "Geomorphic investigation of Davis Pond, Louisiana." Technical Report GL-90-12, U.S. Army Engineer Waterways Experiment Station, Vicksburg, MS.

Britsch, L. D. and Dunbar, J. B. (1993), "Land Loss Rates: Louisiana Coastal Plain," Journal of Coastal Research, Vol. 9, No. 2, p. 324-328.

Britsch, L. D. and Dunbar, J. B. (2005), "Land Loss Maps of the Louisiana Coastal Plain, Plates 1 through 7" Technical Report ERDC/GSL-TR-05-13, Engineer Research and Development Center, Vicksburg, MS, (available at lmvmapping.erdc.usace.army.mil).

Burkett, V. R., Zilkoski, and Hart, D. A. (2003), "Sea level rise and subsidence: Implications for flooding in New Orleans, Louisiana," U.S. Geological Survey Subsidence Interest Group Conference, Open File Report 03-308, Galveston, TX.

Dixon, T. H., Amelung, F., Ferretti, A., Novali, F., Rocca, F., Dokka, Sella, G., Kim, S., Wdowinski, S., Whittman, D., "Subsidence and flooding in New Orleans," Nature, Vol. 441, p. 587-588.

Dunbar, J. D., Torrey, V. H., and Wakeley, L. D. (1999), "A case history of embankment failure: geological and geotechnical aspects of the Celotex levee failure, New Orleans, Louisiana," Technical Report GL-99-11, USAE Waterways Experiment Station, Vicksburg, MS.

Dunbar, J. D., Britsch, L. D., and Kemp E. B., (1992), "Land Loss Rates Rates, Report 3, Louisiana Coastal Plain," Technical Report GL-90-2, USAE Waterways Experiment Station, Vicksburg, MS.

Dunbar, J. B., Blaes, M. Dueitt, S., and Stroud, K. (1994). "Geological investigation of the Mississippi River deltaic plain, Report 2 of a Series." Technical Report GL-84-15, U.S. Army Engineer Waterways Experiment Station, Vicksburg, MS.

Dunbar, J. B., Blaes, M., Dneitt, S., and May, J. (1995). "Geological investigation of the Mississippi River deltaic plain, Report 3 of a Series." Technical Report GL-84-15, U.S. Army Engineer Waterways Experiment Station, Vicksburg, MS.

Eustis Engineering Company (1984), "Geotechnical Investigation, Soil Stratification and Foundation Conditions for Residential Development, New Orleans, Louisiana," For City of New Orleans and Sewerage and Water Board of New Orleans, Eustis Engineering Company, Metairie, LA.

Fisk, H. N. (1960), "Recent Mississippi River sedimentation and peat accumulation,"4th International Congress, Carboniferous stratigraphy and geology, Heerlen, Holland, 1958, Compte Rendu, p. 187-199

Frazier, D. E. (1967). "Recent deltaic deposits of the Mississippi River: Their development and chronology." Transactions 17th annual meeting, Gulf Coast Association of Geological Societies.. San Antonio, TX.

Gagliano, S. M. (2005), "Effects of Earthquakes, Fault Movements, and Subsidence on the South Louisiana Landscape," Louisiana Civil Engineer, Journal of the Louisiana Section of the American Society of Civil Engineers, Vol. 13, No. 2, p. 5-7 and 19-22.

Kolb, C. R. (1962). "Distribution of soils bordering the Mississippi River from Donaldsonville to Head of Passes." Technical Report No. 3-601, U.S. Army Engineer Waterways Experiment Station, Vicksburg, MS.

Kolb, C. R., and Saucier, R. T. (1982). "Engineering geology of New Orleans." Reviews in Engineering Geology, Geological Society of America, 5, 75-93.

Kolb, C. R., Smith, F. L., and Silva, R. C. (1975), "Pleistocene sediments of the New Orleans-Lake Pontchartrain area." Technical Report S-75-6, U.S. Army Engineer Waterways Experiment Station, Vicksburg, MS.

Kolb, C. R., and VanLopik, J. R. (1958a). "Geology of the Mississippi River deltaic plain." Technical Report No. 3-483, Vol 1 and 2, U.S. Army Engineer Waterways Experiment Station, Vicksburg, MS.

Kolb, C. R., and VanLopik, J. R. (1958b). "Geological investigation of the Mississippi River-Gulf Outlet Channel." Miscellaneous Paper No. 3-259, U.S. Army Engineer Waterways Experiment Station, Vicksburg, MS.

Kolb, C. R., and VanLopik, J. R. (1965). "Depositional environments of the Mississippi River Deltaic Plain." In Deltas in their geologic framework, editor Martha Lou Shirely and James A Ragsdale, Houston Geological Society, Houston, TX.

May, J. R., Britsch, L. D., Dunbar, J. B., Rodriguez, J. P., and Wlonsinski, L. B. (1984). "Geological investigation of the Mississippi River Deltaic Plain." Technical Report GL-84-15, U.S. Army Engineer Waterways Experiment Station, Vicksburg, MS.

McFarlan, E. (1961), "Radiocarbon dating of Late Quaternary deposits, South Louisiana," Geological Society of America Bulletin, Vol. 72, p. 129-162.

Meckel, T. A., ten Brink, U. S., and Williams, S. J. (2006), "Current subsidence rates due to compaction of Holocene sediments in southern Louisiana," Geophysical Research Letters, Vol. 33, L11403, p. 1-5.

Miller, L. and Douglas, B. C. (2004), "Mass and volume contributions to twentieth-century global sea level rise," Nature, Vol. 428, p. 406-409.

Montgomery, R. L. (1974). "Correlation of engineering properties of cohesive soils bordering the Mississippi River from Donaldsonville to Head of Passes, LA." Miscellaneous Paper S-74-20, U.S. Army Engineer Waterways Experiment Station, Vicksburg, MS.

Penland, S., Ramsey, K. E., McBride, R. A., Moslow, T. F., and Westphal, K. A. (1989), "Relative sea level rise and subsidence in Louisiana and the Gulf of Mexico," Coastal Geology Technical Report No. 3, Louisiana Geological Survey, Baton Rouge, LA.

Saucier, R. T. (1963). "Recent geomorphic history of the Pontchartrain Basin, Louisiana." Technical Report 16, Part A, United States Gulf Coastal Studies, Coastal Studies Institute, Contribution No. 63-2, Louisiana State University, Baton Rouge, LA.

Saucier, R. T. (1994), "Geomorphology and Quaternary Geologic History of the Lower Mississippi Valley." Volumes I and II, U.S. Army Engineer Waterways Experiment Station, Vicksburg, MS.

Saucier, R. T. and Kolb, C. R. (1982), "Engineering geology of New Orleans," Geological Society of America, Reviews in Engineering Geology, Vol 5, p. 75-91

Schultz, J. R. and Kolb, C. R. (1954), "Geological Investigation of the New Orleans Harbor Area," Technical Memorandum 3-391, USAE Waterways Experiment Station, Vicksburg, MS.

Shinkle, K. D. and Dokka, R. K. (2004), "Rates of vertical displacement at benchmarks in the Lower Mississippi Valley and Northern Gulf coast," NOAA Technical Report NOS/NGS 50, US Department of Commerce, Washington, DC.

Smith, L. M., Dunbar, J. B., and Britsch, L. D. (1986), "Geomorphological investigation of the Atchafalaya Basin, Area West, Atchafalaya Delta, and Terrebonne Marsh," Technical Report GL-86-3, USAE Waterways Experiment Station, Vicksburg, MS.

Snead, J. I., and McCulloh, R. P. (1984). "Geologic map of Louisiana, scale 1:500,000, Baton Rouge, LA."

Tormqvist, T. E., Gonzalez, J. L., Newsom, L. A., van der Borg, K., de Jong, A. F., Van, R. J., (2002), "Reconstructing Background Rates of sea-level rise as a tool for forecasting coastal wetland loss, Mississippi Delta," Eos, Transactions, American Geophysical Union, Vol. 83, No. 46, p. 525-531.

URS (2006), "A century of subsidence: change in New Orleans DEMs relative to MGL 1895 to 1999/2002," Poster prepared for Federal Emergency Management Agency, URS Inc, Baton Rogue, LA.

US Army Corps of Engineers (1988), "Design Memorandum No. 19, General Design, Orleans Avenue Outfall Canal," US Army Corps of Engineers, New Orleans District, New Orleans, LA.

US Army Corps of Engineers (1989), "Design Memorandum No. 19A, General Design, London Avenue Outfall Canal," US Army Corps of Engineers, New Orleans District, New Orleans, LA.

US Army Corps of Engineers (1990), "Design Memorandum No. 20, General Design, 17th.St. Outfall Canal," US Army Corps of Engineers, New Orleans District, New Orleans, LA.

Wallace, W. E. (1966). "Fault and salt map of South Louisiana." Gulf Coast Association of Geological Societies, 16.

Works Progress Administration of Louisiana (1937), Some data in regard to foundations in New Orleans and vicinity, New Orleans, LA, p. 243.

Appendix 22
General Comments About the IPET Geology in Response to the Third Report of the NAE/NAE/NRC Committee on New Orleans Regional Hurricane Protection Projects, Dated Wednesday, 25 October 2006

Comments by NAE/NRC, Regional Geology (p.6)

Volume V of the June 1, 2006 Final Draft is entitled "The Performance—Levees and Floodwalls." Within Volume V, there are references to system wide data; data in the appendices (p. V-12-10), though useful, are limited. *The main text fails to provide the type of an overview of regional geology and synthesis of geologic processes that are required to establish a context for evaluating the hurricane protection system.* Attention was drawn to this deficiency in this committee's first report (NAE/NRC, 2006a), and a summary of the regional geology was included in subsequent IPET reports. Although reference to regional geology is made in Appendix II, Volume V, the level of discussion is somewhat limited: regional geology is described in a single paragraph in Volume V in the June 1, 2006 report, and is absent from the Executive Summary. *The IPET report (in Volume V) should include a summary of regional geology to explain respective elevation differences across the New Orleans area, identify localized problems with soft clay deposits and underseepage conditions, and offer reasons for present and future subsidence and settlement issues.* A comprehensive assessment of the geology and its engineering implications establishes governing principles that affect performance of various hurricane protection structures across the region.

Response by Joe Dunbar

I agree more should have been said about the geology. A more detailed overview of the geology and stratigraphy was not included because of scheduling. Numerous activities in support

of the IPET project prevented developing the detailed description that was needed. A paper by J. B. Dunbar and L. D. Britsch for the upcoming GeoDenver conference in February 2007 will serve as additional background information for the geology. This paper has been modified to include a discussion of historic subsidence rates in the New Orleans area.

In regards to subsidence, the Corps generally did not factor subsidence into the overall design of the hurricane protection system for the canal levees. In fact, top of levee elevations were below levels authorized by Congress because of subsidence in benchmarks that were used to establish the design elevations. Many of these benchmarks were found to have large vertical changes in elevation, and were not updated to correct for the effects of historic subsidence. As identified by Chapter 2 of the IPET report, the benchmarks used for design purposes were at much higher levels than elevations measured in 2005 after Hurricane Katrina.

The Corps has not developed a program to monitor subsidence over the long term, especially along its flood control levees. The Geology Section at the District has advocated a program to study the subsidence problem for the past 10 to 15 years by installing a network of benchmarks on their engineered structures and levees to study general trends as a function of the underlying geology and historic activities by man. To date, no significant funding has been authorized to study this complex issue in a meaningful program. Currently, the New Orleans District has a long term database of subsidence rates based on radiocarbon dating of peat sediments from recent borings, but historic rates during the life history of the structure are tied to a only a few benchmarks. Preliminary studies have been conducted by the Corps and ERDC in land loss mapping and geology mapping of the coastal plain to support a study of subsidence.

One of the reasons for the lack of general type studies such as subsidence by the New Orleans District is due in part to the change in the Corps funding policy during the early 1990's, which require general studies to be tied directly to ongoing projects as part of the total project management concept. This change eliminated many of the background studies that were previously possible, and were routinely conducted by the District. Also, contributing to the lack of general background studies has been the interagency coordination among the local, State, and Federal agencies, where decisions are often times made by committee and/or group thinking. A by-product of this process is that local agencies will perform parts of studies as their contribution to the cost-share to the project. This process has fragmented or eliminated the research previously performed by the District and/or failed to provide the information needed by the District to support the big picture during life cycle evaluations.

Comments by NAE/NRC, Site Characterization (p. 9)

The quality of the site characterization studies is key determinant for successful diagnosis of geotechnical failures. In previous reports, this committee has expressed reservations about site investigation methods and interpretation presented in the IPET reports. The site investigations carried out by IPET are not consistent with current geotechnical engineering practice. This section summarizes these primary limitations. Site stratigraphy should integrate observations from borehole logs, field probing tests (notably piezocone penetration records), and local geological knowledge. It is unclear how this process has been carried out to re-construct cross-

sections of the state of the levees prior to Hurricane Katrina. The reports lack detailed plans showing how site investigations relate to surveyed features of the breaches, and the cross-sections are generally hand-drawn. The soils data, which are provided through the public website, are not well organized. A parallel study by Seed et al. (2006) shows a more detailed interpretation of the stratigraphy at the 17th Street Canal breach site.

Comments by Joe Dunbar

Introduction

The NAE/NRC has assumed that the NSF (2006) report (i.e., Seed et al., 2006) was the gold standard by which the IPET geology data should be judged. Apparently the NAE/NRC authors were favorably impressed with the NSF report. They draw attention to the detailed interpretations about the geology, and negatively describe the hand drawn cross sections that were initially presented in the earlier version of the IPET report. The overall tone of the above comments, combined with unfavorable comments published in the NSF report, and the news press by the NSF about the geology, call into question the credibility of the Corps interpretation of the geology, particularly at the 17th Canal breach. The NAE/NRC has questioned the quality of the site characterization studies that were performed by IPET, and indirectly they disparage the qualifications and/or abilities of the IPET and District geologists involved with the design studies or the post-failure investigations into the causes for the different levee failures. I want to state at the onset of this response that the geology at the 17th Street Canal (USACE, 1990) was correctly defined based on standards that were defined and used by USACE in the classification of the New Orleans area stratigraphy. In the sections that follow, I will provide answers to many of the questions that have been raised by the different review groups and an explanation of the IPET interpretation for the stratigraphy. Appendix A of this paper includes various Figures from the NSF (2006) report that are cited in this paper and show the stratigraphy at the 17th Street Canal site. NSF (2006) figures in Appendix A are included for discussion and comparison purposes.

IPET, ASCE, and NSF Field Studies

Before we address the 17th Street Canal failure geology, it is necessary to provide some general background information about the IPET/ASCE/NSF field studies. It should be noted that one of the first tasks assigned to me as a member of the newly formed IPET study team was to serve as a Katrina levee failure tour guide for the combined ASCE and NSF study teams in late September and early October 2005. In this capacity, one of my primary duties was to describe the geology at each site to the ASCE and NSF teams using the cross-sections from the original General Design Memorandum (GDM) for each canal furnished by the Mississippi Valley Division (MVD) geotechnical staff. This information was also furnished in notebooks to members of the ASCE and NSF teams. My long history in mapping the geology of the Louisiana Coastal Plain (LCP) for the New Orleans District made me an immediate subject matter expert for this job. I had the opportunity to observe each site numerous times, photograph my

observations, and gather data during the many visits to these different areas during a nearly 3 month period spent in the New Orleans area.

IPET Support to NSF Geology Team

The NSF team sent a geologist to investigate the New Orleans area in February 2006 to characterize the geology of the levee failures. The NSF geologist was not part of the original ASCE/NSF/IPET review team at each site in September and October 2005 when much of the failure evidence was still visible at the various failure sites. Following a newspaper article in February 2006 by the Times-Picayune about the poor job the Corps had done in defining the geology for the design of 17th Street Canal (see Appendix B), I was asked to participate in a teleconference at ERDC with senior members of the IPET investigative team and the NSF geologist. Based on this conversation, I concluded that the NSF geologist had very little experience in the Mississippi River deltaic plain and was unfamiliar with many of the previous USACE regional studies that had been performed and methods the USACE had developed to classify deltaic plain soils. I furnished the NSF geologist with the LMV Geology Website (Dunbar, Myers, and Jackson, 2005) to download the basic geology references and published studies to better assist his efforts. The IPET team also coordinated a meeting with Mr. E. Burton Kemp, retired Chief, Geology Section, New Orleans District, to provide the NSF geologist with background information to support his investigation at the various levee breaks.

General Background

A few comments about my background and experience in the Louisiana Coastal Plain require mention as many of the NAE/NRC review team members were probably unaware of the qualifications of many of the individual IPET team members. I am a senior research geologist with the Engineer Research and Development Center (ERDC), formerly Waterways Experiment Station (WES), Engineering Geology and Geophysics Branch (EGGB), with nearly 28 years of experience in the coastal plain of Louisiana. I was directly involved with site characterization studies of the canal levee failures for the IPET team, and had numerous opportunities to witness the field evidence before it was destroyed by the repair and clean-up process.

Geologic interpretations about the site stratigraphy are based in large part on the understanding of Mississippi River coastal plain processes, and the unique work experiences of the geologist in conducting site investigations in the coastal plain. Understanding the site stratigraphy beneath the different levee failures, correctly interpreting this stratigraphy, and correlating this information to the general framework that has been developed for the Mississippi River's deltaic plain are critically important for the correct resolution of the levee failure mechanisms. Important to this process, is an understanding of deltaic processes, knowledge of delta chronology, recognition of deltaic depositional environments in soil cores, their sedimentological characteristics, and the engineering properties of these environments. Knowledge about and experience with coastal plain processes and interpretation of its stratigraphy are the basis for understanding, properly investigating the various canal levee failures, and accurately determining the failure mechanisms.

My work experience at ERDC-WES includes a long history with the New Orleans District in support of engineering geology, cultural resource, and wetland loss projects. This work experience includes geomorphic mapping of the surface and subsurface geology for nearly half of the quadrangles that comprise the Mississippi River's deltaic plain (May et al., 1984; Dunbar et al. 1994 and 1995). This mapping was conducted as part of the Corps of Engineers, Lower Mississippi Valley (LMV) Engineering Geology Mapping Program (Dunbar, Myers, and Jackson, 2005). In support of cultural resource investigations in the coastal plain, I have co-authored two studies which involved geomorphic mapping, interpretation of site stratigraphy from numerous shallow and deep soil cores, including radiography of these cores, and radiometric dating of organic sediments from these cores to evaluate the distribution and the context of archaeological sites as a function of Holocene delta lobe chronology (Smith, Dunbar, and Britsch, 1988; Britsch and Dunbar, 1990). In addition, I was involved with several studies of Mississippi River flow slide failures below Baton Rogue, Louisiana, including a site investigation of a levee failure in the New Orleans area (Torrey, Dunbar, and Peterson, 1988; Dunbar and Torrey, 1991; Dunbar, Torrey, and Wakeley, 1999). Finally, my work experience in the coastal plain has included land loss studies of the Mississippi River deltaic and chenier plains, which are the underlying basis for many of the wetland restoration efforts by the New Orleans District in coastal Louisiana (Dunbar, Britsch, and Kemp, 1992; Britsch and Dunbar, 1993 and 2005).

The New Orleans area geology has largely been defined by the branch that I am member, and a brief history here is appropriate to gain a sense of historical perspective and past involvement in this area. This branch was originally established at WES by the Mississippi River Commission (MRC) in 1948, after H. N. Fisk, a professor at Louisiana State University (LSU) and a geologic consultant to the MRC, took a full-time position with Humble Oil Company in Houston, Texas. The primary mission for the Geology Branch as it was known in 1948 was to conduct studies of the geology in the LMV (including the LCP) to support flood control engineering by the MRC. Past members of this branch involved with the geology mapping program in the LMV have included (in alphabetical order): Messrs. Louis D. Britsch, Charles R. Kolb, Arthur R. Fleetwood, Ellis L. Krinitzsky, Rufus J. LeBlanc, John R. May, P. R. Mabrey, Roger T. Saucier, John R. Schultz, R. C. Silva, Fred L. Smith (later became Chief of Geology Section, New Orleans District), Lawson M. Smith, William B. Steinriede, and Jack R. Van Lopik. The alluvial mapping program lasted for approximately 50 years, and supported ongoing flood control projects by the Corps, and would later serve as the basis for many environmental and cultural resource studies.

The Mississippi River deltaic plain mapping program was eventually completed with publication of three mapping folios by May et. al (1984; note the authors for this folio are J. R. May, L. D. Britsch, J. B. Dunbar, J. P. Rodriguez, and L. B. Wlosinski;) and Dunbar et al. (1994 and 1995). I believe it is appropriate to say that I am one of two remaining members of this long serving alluvial mapping team at WES, and the other member is Mr. Louis D. Britsch, who is currently the senior geologist in the New Orleans District. Because of my many years of experience and history in the alluvial valley, I was asked to serve on the peer review group for the comprehensive update of the "Geology of the Alluvial Valley and its Chronology" by Dr. Roger T. Saucier (1994). The Engineering Geology Branch later merged with the Geophysics

Branch during the mid-1990s and later WES would merge with the other Corps Labs in the nation to form ERDC.

In summary, a significant amount of geologic data and studies have been published by the USACE and ERDC-WES in particular on the geology of the LMV. Most of these studies are available at a public website (lmvmapping.erdc.usace.army.mil) that presents the Geology of the Lower Mississippi Valley. I am largely responsible for scanning these maps and development of this website along with my associates Mr. William M. Myers, and Ms. Sarah Jackson. Many of the pioneering geology studies in the LMV sponsored by the MRC and Corps Districts during the past 50 years are the basis upon which the levee failure stratigraphy has been characterized by the Districts and both the IPET and NSF study teams. One has only to review the many geology references in Chapter 3 of the NSF report to see the impact that WES (ERDC) had on defining the geology of this region.

With respect to background and knowledge of the New Orleans area geology, I had the opportunity to map the surface and subsurface geology for the Chef Menteur, New Orleans, Spanish Fort, and St. Bernard, Quadrangles as part of the USACE geology mapping program (Dunbar et. al, 1994 and 1995 available at website: lmvmapping.erdc.usace.army.mil). For those unfamiliar with these quadrangles, they represent the Greater New Orleans area. As part of the mapping process, I literally examined thousands of borings from the New Orleans area and developed numerous cross sections of the stratigraphy from these borings. This process involved the analyses of a large boring data set and classification of this boring information into depositional environments using soil texture, color, consistency, sedimentological properties, fossils, engineering properties, and other information contained on the boring logs. Additionally, the LMV boring database at WES contained the borings from the earlier mapping efforts (see Schultz and Kolb, 1954; Kolb and Van Lopik, 1958a and 1959b; Kolb, Smith, and Silva, 1975). Also, part of the mapping process involved visiting various private engineering companies in New Orleans and Baton Rouge to obtain boring data to define the subsurface stratigraphy for the quadrangles being mapped. I provide this information to shed light on the magnitude of the LMV mapping program, and to highlight my more than casual knowledge of the geology and stratigraphy of the New Orleans area.

During the mapping of the New Orleans area, I was very privileged to have input from Dr. Roger T. Saucier, as well as lengthy discussions with him about the depositional environments and the Holocene setting for this area. For those unfamiliar with Dr. Saucier's background, he was raised in New Orleans, obtained a PhD from LSU on the Geomorphology of the Ponchartrain Basin (Saucier, 1963), had a long career at WES in both the Geotechnical and Environmental Labs (in Geotechnical Lab much of which was spent mapping the geology in the LMV), and worked part-time as a consultant in the New Orleans area. Dr. Saucier's work as a consultant in New Orleans bears mention here, as he furnished me a copy of an engineering geology report and set of detailed plates that he helped prepare as part of a report for Eustis Engineering Company (1984), titled "Soil Stratification and Foundation Conditions for Residential Development," for the City of New Orleans and the Sewerage and Water Board. Illustrations presented in Dr. Saucier's (1994) report on the top of Pleistocene surface and Pine Island Beach in the New Orleans area based in part on his work as a consultant for Eustis

Engineering, which involved a review of literally thousands of borings (Saucier, personal communication).

The point that I want to make in presenting my background and that of the organization that I work for is summarized by the following NAE/NRC statement "*Site stratigraphy should integrate observations from borehole logs, field probing tests (notably piezocone penetration records, and local geological knowledge "*(NAE/NRC, p. 9)," I believe it is a true statement that as the IPET geologist, I have more than just a "local knowledge" about the geology of the New Orleans area. Furthermore, I believe it is also a true statement that without the added benefit of having examined the numerous borings and CPTs that were drilled as part of the IPET investigations at each failure area, I have "integrated observations of the stratigraphy" from the many years spent, and the thousands of boring logs that I have reviewed, and hundreds of soil cores carefully examined and logged as part of the geologic mapping program for the New Orleans area and the deltaic plain region as a whole. This local knowledge serves as the basis for the IPET investigations of the levee failures. The "*integrated observations of the stratigraphy*" was apparently useful to the NSF team as they presented a cross section which I developed during the early 1990s for the Spanish Fort Quadrangle (see NSF report, Chapter 3, Figure 3-14, p. 3-36). This section passes almost directly through the different canal levee failures. Furthermore, the geology defined by this section is relatively accurate in light of the recent data collection efforts.

Unified Soils Classification System (USCS)

A modification to the Unified Soils Classification System (USCS) by the New Orleans District in May 1949 (Kolb and Van Lopik, 1958a, p. 27) has a direct bearing on the interpretation of New Orleans area stratigraphy and its engineering properties. The modified USCS is presented as Figure 1 and has been exclusively used by the New Orleans District and Eustis Engineering Company to describe and characterize the soils from local borings. I draw attention to this modified USCS version because of its importance as a tool to classify soft deltaic soils, and its specificity in differentiating and classifying these soils according to their Plastic and Liquid Limits and organic content. A generally unknown fact is that modification of the USCS is possible, providing it maintains the basic soil groups (USCS, 1963, p. 27). The modified classification has been used exclusively to characterize soils in the levee foundations and in the post failure borings by Eustis Engineering Company.

For those unfamiliar with Eustis Engineering, this geotechnical firm is located in New Orleans and has conducted a significant amount of the drilling, soil sampling, and lab analyses for the original foundation borings for the hurricane design improvements, and the foundation borings for the post-Katrina repairs of the levees. Eustis Engineering Company was founded in 1946 by Joseph B. Eustis in Vicksburg, MS. Mr. Eustis was a former WES employee, actively involved with the study of underseepage of levees in the LMV (USACE, 1941), before opening his own firm and moving to New Orleans in 1948. During his career at WES, Mr. Eustis would work for and later study under Dr. Cassagrande from Harvard University, who was a consultant to the MRC for under seepage research in the LMV.

17th Street Canal Failure

Introduction. A primary disagreement exists between the IPET and the NSF studies concerning the stratigraphy beneath the 17th Street Canal failure, and the horizon where the failure originated. A fundamental question emerges as to which interpretation of the geology and stratigraphy best describes the field evidence. Questions have been raised as to how the IPET team conducted the site investigations at the breach sites. Critical to this process was the collection of all the available information, repeated site visits, and observations by the IPET team, collection of field evidence, carefully describing and documenting this evidence, determining the site conditions prior to the failure, and evaluating these data to determine the underlying causes for the poor performance and subsequent levee failure.

Activities conducted as part of the geology study included a review of USACE foundation studies (primarily existing levee borings and associated laboratory soil test data), historic photographs and imagery for each breach area, historic maps, post-Katrina hydrographic surveys from the canals, new geotechnical borings that were drilled to characterize the stratigraphy and obtain associated laboratory soils test data, and frequent visits and observations at each site. Stratigraphic and geotechnical data were obtained by borings, backhoe trenches, soil profiles, and careful study of the debris trail at the breaks and in the nearby neighborhoods.

Field Methods. The17th Street failure was about 400-ft-wide, and occurred at the east (Orleans Parish) side of the 17th Street Canal near the Hammond Highway Bridge (Figure 2). A nearly intact section of the levee, measuring approximately 100 × 200 ft, was displaced about 50 ft east of its original location during the failure (see Figure 2). Soil profiles were mapped along the exposed face of the displaced block during the IPET data collection effort. Geotechnical and CPT borings were drilled in the failure zone. Drilling wasn't possible at some locations within the breach zone because of the rock fill or the debris in the breach. Borings were drilled into and adjacent to the displaced levee soil mass. Backhoe trenches were also dug along the southern edge of the transposed levee section on two separate occasions, the first time was to expose the stratigraphy of the displaced block, and the second time to obtain representative samples for centrifuge testing. Backhoe trenches were used to help determine the failure mechanism from study of the soils and stratigraphy. Additionally, a study of the debris trail in the neighborhood was conducted to provide visual clues about the swamp/marsh stratigraphy, determine its geographic extent, and see whether there was stratigraphic and sedimentological evidence in the debris trail to support where the failure horizon was located.

17th Street Stratigraphy and Environments of Deposition. Soils data from borings were grouped into distinct depositional environments, based on sedimentological, stratigraphic, and engineering characteristics of soils that have been correlated for each environment (see Table 1). This classification process is based on several previous studies of Mississippi River deltaic plain stratigraphy and its sediments by the USACE (Schultz and Kolb, 1954; Kolb and Van Lopik, 1958a, 1958b, and 1965; Kolb, 1963; Kolb, Smith, and Silva, 1975; Montgomery, 1974; Saucier, 1994; and Dunbar et al., 1994, 1995, 1999). Soil type, bedding, fossils, and organics contained within these lithostratigraphic units have been correlated with general engineering properties in Table 1, and are an important clue as to the depositional environment. Water content and soil consistency are especially important engineering properties. These studies along with a

comprehensive study by Eustis Engineering Company (1984) and Frazier (1967) represent the best chronostratigraphic and engineering geology data that have been developed for this area. These studies represent the basic foundation upon which much of the canal stratigraphy has been defined.

Numerous geologic cross-sections were prepared from the available boring data to classify the stratigraphy according to unique depositional facies and environments. Post-failure cross-sections were produced using exiting borings and new borings drilled specifically for this purpose. These sections incorporated accurate hydrographic and ground survey data, and included the identification of both man-made and natural features that were observed in the breach zone. In addition to the post-failure cross sections, pre-failure sections were developed at these same locations from the boring information, and these sections incorporated historic photography, imagery, and digital elevation data prior to the failure. These data were spatially rectified to a common datum and integrated into ESRI's ArcView Geographic Information Systems (GIS) software to manipulate these different data sets to produce accurate cross-sections of the embankment geometry and the underlying stratigraphy. Pre-failure cross-sections were then used for the engineering and slope stability analyses using a variety of software packages.

The basic stratigraphy at the 17th Street failure consists of man-made fill (levee and/or foundation fill), an organic horizon (swamp/marsh), lacustrine (lake), relict beach (Pine Island beach sand), bay sound-estuarine, and Pleistocene deposits. A representative east to west cross-section with a view looking to the south is presented in Figure 3. This section identifies the fundamental features at the 17th Street failure site: the translated levee block, the underlying stratigraphy according to environments of deposition, the post failure surface topography that was determined from hydrographic and ground surveys, pre and post failure engineering borings from which the section was constructed, and identification of the slip surface beneath the displaced levee section in borings and backhoe trenches. Equally important for understanding the complex stratigraphy of this area is an understanding of the Holocene chronology of sedimentation. A critically important chronostratigraphic event in soil cores from this site was the switch from a shallow water or lake setting, to a terrestrial setting represented by marsh and then followed by swamp vegetation. This stratigraphy is a function of sea level rise, delta lobe development, and the formation and abandonment of distributary channels within this area.

Various components of the cross-section in Figure 3 are individually described in the following sections. Locations of referenced borings from the representative cross-section at 17th Street are shown in Figure 2. Only selected borings are presented in Figure 2 from the many that were drilled at this site to avoid crowding in the illustration due to overlapping boring labels. The intent of the discussion about the17th Street stratigraphy is to keep the presentation of information as simple as possible and to the point to address questions that have been raised about the IPET study methods. Only a few of the depositional environments identified in Table 1 are present and relevant to the breach stratigraphy. A detailed presentation of these depositional environments follows, and incorporates the recent boring data in the discussion about the site stratigraphy.

Backhoe Trench at the Displaced Levee Section. A backhoe trench was dug along the southern edge of the displaced levee section to obtain stratigraphic and chronological

information. The backhoe trench exposed a continuous, soft, grey, highly plastic, "wet" clay layer approximately 1 ft thick, at a 20- to 30-degree angle near the base of the displaced soil block (see Figure 4). This grey clay layer has been interpreted to represent the slide surface, and closely matches the lacustrine horizon beneath the marsh horizon as determined from the boring data. The clay layer had a consistency of soft peanut butter, and upon close inspection showed signs of basal drag as the clay layer overrode the underlying marsh surface, and produced the saw-tooth pattern visible in Figure 4 at the bottom of the clay layer. Additionally, radiocarbon age dating of peat sediments above and below the shear surface identifies an identical age for the upper and lower peat samples, corresponding to an age of 2,990 (+/- 60 and 70 years, respectively) before the present at the base of the peat (marsh) horizon (Appendix C). Locations of the C-14 samples and respective dates are shown in Figure 3, and were located between borings B-14 and B-15.

Studies of Peat and Marsh Thickness

The radiocarbon age dates obtained from the translated soil block are noteworthy, since they are exactly consistent with the chronology of Mississippi River sedimentation that was developed much earlier by Fisk (1960) in a study of peat accumulation in the New Orleans area, and summarized by Kolb, Smith, and Silva (1975) to characterize the development of this area. Fisk's (1960) study indicates peat thickness in the New Orleans area is generally between 8 to 16 ft thick across much of the Northern New Orleans area as shown by Figure 5, and that peat formation generally began about 3,000 years ago, based on radiocarbon age dates taken from the base of the organic stratigraphic sequence (see Figure 6, age dates are shown in the organic section at various depths). A comprehensive study much later by Eustis Engineering Company (1984) for the City of New Orleans and the Sewer and Water Board confirms the organic thickness is less than 20 ft across Orleans Parish based on a review of several thousand borings.

Carbon-14 age dates of 2,900 years before the present from the organic horizon immediately above and below the shear surface are critically important dates. These dates almost precisely match those obtained by Fisk (1960) for the base of the organic section in the New Orleans area. Peat sediments above the shear zone are from the base of the organic fill according to age and stratigraphic position, since the grey shear zone clay is from the lacustrine (lake) horizon. Furthermore, borings B-14 and B-15 corroborates this fact by the measured depth of the peat/lacustrine contact in these borings. These borings are examined in greater detail in the next section.

The IPET age dates from the base of the 17th Street peat (marsh environment) are consistent with the chronology and filling history previously identified by Fisk (1960), Saucier (1963; p.72, p.74, and p. 104), and Kolb, Smith, and Silva (1975, p. 4) for the New Orleans area. Interdistributary deposits on the south side of the Pine Island Beach ridge, and lacustrine deposits on the north side of the beach ridge generally transition from a shallow water to a terrestrial or marsh setting beginning about 3,000 years ago. The marsh environment later transitions to a swamp type setting, which was representative of the conditions that were observed by the first European settlers to this region. The transition to wood dominated

vegetation was dependent on sediment supply and the subsequent development of the various distributary networks by the St. Bernard and Modern Delta Complexes in this area.

Seventeen Street Boring Data, Engineering Properties, and their Relationship to Depositional Environments. Boring logs used to construct the cross section in Figure 3 are examined in greater detail in this section to provide a better understanding of the classification process that was used to separate the soils and underlying stratigraphy into distinct depositional environments. Soil texture, color, consistency, water content, organic content, and other relevant textural and stratigraphic properties were used to separate soils types defined by borings into distinct depositional environments. Most of the borings shown in Figure 3 were drilled by Eustis Engineering Company along with the subsequent laboratory analyses and testing of the soil samples from these borings. Additionally, USACE drilling crews from the Vicksburg District drilled several geotechnical borings (see Figure 2) and all the CPT borings (not shown) at the 17th Street canal to support the IPET geotechnical study. Borings B-1 through B-13 were drilled by Eustis Engineering Company in support of the levee repairs for the 17th Street canal. Borings B-14 and B-15 were drilled ontop of the displaced levee section to support the IPET studies at the 17th Street failure.

Borings B-14 and 15 were drilled to help characterize the stratigraphy of the displaced levee section, and to provide a reference to compare against other post-Katrina borings that were drilled by Eustis Engineering Company at this site. Eustis Engineering Company was contracted by the New Orleans District to drill borings for the engineering analyses for the subsequent repairs and to support the IPET studies of the displaced levee section. Boring logs and lab test data are based on the modified USCS in Figure 1 to characterize the stratigraphy. All phases of drilling, soil sampling, and laboratory classification of samples from borings B-14 and B-15 were observed by the author along with New Orleans District personnel to gain a better perspective and understanding of the laboratory classification procedures that were used by Eustis laboratory personnel to describe the soil samples and derive laboratory test data. The vast majority of borings that were drilled during the past 25 years at the 17th Street and London canal sites was performed by Eustis Engineering Company for the USACE, New Orleans District, or architectal and engineering (A&E) contractors involved with design of the hurricane protection of the levees.

Boring data from B-14 is presented in Figures 7a through 7f, and includes a graphical log of soil texture (Figure 7a), laboratory summary data sheet (Figure 7b), and photographs of the extruded soil samples from this boring (Figures 7c through 7f). Similarly, boring B-15 is presented in Figures 8a through 8f. Only soil samples from borings B-14 and B-15 were photographed to provide a visual record of these cores. Boring logs for B-6 and B-3 are presented as Figures 9 and 10, while design borings 61 through 64 are presented as Figures 11 through 14 respectively. Original design borings are evaluated to compare with the new borings. Much of the controversy of the 17th Street Canal stratigraphy stems from the interpretation of the original design borings by the NSF, particularly boring 64.

A review and discussion of each boring follows, and it is again stressed that soil texture, color, consistency, water content, organic content, and other relevant textural and stratigraphic properties were used to separate the soils beneath the levees into distinct depositional

environments as shown in Figure 3. Stratigraphic and sedimentological symbols identified on the different graphical logs and lab summary data sheets are defined at the bottom of Figure 7a.

Boring B-14. Boring B-14 was drilled on top of the eastern edge of the displaced levee section, and to the right (east) of the soft grey clay horizon in Figure 4. The boring was positioned to avoid the shear zone shown in Figure 4 in the subsurface. The surface elevation for boring B-14 was at 0 ft NGVD. Prior to Hurricane Katrina, the surface elevation at this location was about -6 ft NAVD 88 based on the five-meter digital elevation model (DEM) for New Orleans in 2001. It is estimated that eastward horizontal translation of the soil mass, combined with overtopping of the levee toe by the horizontally displaced levee mass, has thickened (and compressed) the swamp/marsh horizon, adding approximately 4 to 5 ft of organic sediments at this location, after correcting for the datum differences (NAVD vs. NGVD). This concept is indicated by Figure 3. Furthermore, because of the horizontal movement, this section should contain a much thicker organic horizon as compared to areas nearby, where there was no addition of soil mass during the failure.

Boring B-14 clearly identifies distinct differences in physical properties between the swamp/marsh, the underlying lacustrine environment, and the former beach environment (Pine Island Beach) that is below the lacustrine stratigraphic horizon. The swamp/marsh unit is characterized by soft, very wet, dark grey to black organic clays that range from CHOA to CHOC (see Figure7b) to peats. Water contents are generally above 100 percent and range above 200 percent for peat as shown by Figures 7a and 7b. Wood fragments and roots are common throughout the swamp/marsh sequence. It is unclear from the organic stratigraphy where the maximum disturbance and deformation occurred, and whether it affected the entire organic column, or only portions of the organic zone. Soil texture and water contents are relatively uniform, except for sample 5b where the water content dropped to 45 percent. Just above this sample, there is an inclined clay seam in sample 5a (see Figures 7b and 7d). Generally, bioturbation (i.e., mixing and churning of the soil column) by organisms and roots will destroy layering, unless there are high sedimentation rates. As shown by the cross section in Figure 3, it was judged that there was overall disturbance throughout the organic horizon. The thickness of the organic horizon is about 10.7 ft based on the boring data in B-14.

A sharp contact occurs at 12 ft in B-14 (see Figure 7d). There is a noticeable change in soil color from dark grey and black to grey, a significant reduction in the water content to below 100 percent (ranges from 30 to 96 percent), a large reduction in organic content to minor or trace amounts, and perhaps the most diagnostic characteristic, the presence of shells and/or shell fragments. Distinct changes in both the physical and engineering properties occur below 12 ft depth, and correspond to a rapid transition to lacustrine type sediments. These sediments are characterized by thin beds and lamina of silt and/or fine sand. The layering is very pronounced at the midpoint of the lacustrine sequence, and possibly corresponds to deeper water (see Figures 7d and 7e). Near the contact with upper marsh/swamp unit and at the lower beach sand, shells and shell fragments are more abundant, and bedding features are reduced, possibly due to bioturbation (sediment mixing) by shallow water organisms which tends to destroy the original bedding features. Shells are generally more pronounced near the base and near the top of the lacustrine unit, suggesting that a combination of shallow water and/or abundant sediment/nutrient supply were more favorable to bottom dwelling organisms, and reflect their

marked abundance in the stratigraphic record near the transitions between depositional environments. The lacustrine environment is underlain by the relict beach sand (Pine Island Beach, see Saucier 1963 and 1964) at 36 ft depth. The beach sand is underlain by bay sound deposits at 43.5 ft and the Pleistocene surface at around 80 ft (Figure 3).

Boring B-15. Boring B-15 was drilled on top of the western half of the displaced levee section (Figure 2), and to the left (west) of the soft grey clay horizon in Figure 4. The boring was positioned to intersect the shear zone in the subsurface. The surface elevation for boring B-15 was also at 0 ft NGVD. Prior to Hurricane Katrina, the surface elevation at this location was about -6 ft NAVD 88 based on the five-meter digital elevation model (DEM) for New Orleans in 2001. Horizontal displacement of the soil mass along the shear zone has added approximately 4 to 5 ft of organic sediments at this location. This concept is indicated by Figure 3. The thickness of the organic horizon is about 6.9 ft, based on stratigraphic data from B-15 (see Figures 8b, 8c, and 8d, samples 3, 4, and 5). Included within this 6.9 ft organic zone was a 1.2 ft thick gray clay layer, which corresponds to the shear zone shown in Figure 4. This soft grey clay closely matches the lacustrine clay layer below the organic horizon. Organic sediments were classified as peat and CHOA to CHOC clays. Water contents were above 200 percent in the organic horizon.

The beginning of the lacustrine (lake) horizon in B-15 is at 9.7 ft (sample 5, Figure 8d), and is manifested by a soft grey clay. Lake clays have a significant reduction in water content as compared to the overlying organic rich (swamp/marsh) horizon. Water contents drop below 100 percent in the lacustrine layer (see Figure 8b). Organic matter is present in trace amounts, and the presence of shells or fragments is a diagnostic clue to the lake origin for these sediments. Light colored lamina, lenses, and thin beds of silt are another common characteristic of sediments belonging to the lake environment (see Figures 8c to 8e).

Boring B-6. The next boring in our review of the stratigraphy in Figure 3 is boring B-6, drilled as part of the post-failure repairs by Eustis Engineering Company. This boring has been projected into the section as shown by its location in Figure 3. The boring was located at the toe of the failed levee section. The levee section was pushed horizontally across this area, and consequently, the upper stratigraphy is expected to be disturbed. The boring was drilled in October 2005 after the rock fill was placed in the breach zone. Data from the 2001 DEM identifies a ground elevation prior to the failure somewhere between -4 and -5 ft NAVD88 (-2.5 to -3.5 NGVD). Top of ground elevation is near 0 ft NGVD for boring B-6. Boring and laboratory logs are presented as Figures 9a and 9b, respectively.

This boring was drilled to 77 ft depth, or about 5 ft into the oxidized Pleistocene surface. The boring log identifies the presence of gravel at approximately a depth of 6 ft in Figures 9a and 9b, indicating at least 6 ft of disturbance in the upper part of the boring. The swamp/marsh zone ends at the bottom of the organic clay layer (CHOC) in samples 5B2 and 5C (see Figure 9b). The lacustrine contact is marked by a sharp reduction in water content at about 13 ft depth, where it is below 100 percent in sample 5D. No organic designation (i.e., CHOA - CHOC) occurs below this depth, and the log identifies the presence of mostly soft, inorganic clays (CH4), silt lenses, organics (only as a modifier), lower plastic clays (CH3, CL6) and shell fragments at 14.7 ft. These characteristics are diagnostic for the lacustrine stratigraphic unit. Lake sediments end at

the top of the sand layer, which corresponds to the back barrier side of the Pine Island Beach. This 8 ft thick sandy layer is underlain by laminated and thinly bedded, medium to stiff clays (CH4, CH3, CL6) bay sound-estuarine deposits, which overlie the Pleistocene surface at around 72 ft. The Pleistocene surface was exposed to oxidation and weathering before the advent of sea level rise 10,000 years ago, giving it the stiff to very stiff consistency and diagnostic tan, light brown, and/or olive grey color. The Pleistocene surface was probably a tree covered upland forest when glacial maximum and sea level minimum occurred prior to 10,000 years ago.

The presence of a CH4 layer above the organic horizon and below the gravel in samples 5A and 5B1(Figure 9b), and water contents between 55 and 70 percent, suggest that the grey clay shear zone layer maybe present in this boring as well. Compare the characteristics of B-6, samples 5A and 5B1, to those in boring B-14 (i.e., samples 5A and 5B1, observed in Figure 8d), where the shear zone is know to exist. The physical and engineering properties for these samples are nearly identical. As this is a projected boring into Figure 3, the contact between the organic zone and the lacustrine layer was incorporated into this section. The elevation profile of the section was derived from the 31 August 2005 survey data, before the breach was filled during the emergency repairs. The general stratigraphy in relationship to the elevation profile was judged to be more important, than shallow features from nearby borings that were projected into the section. The surface of this profile will be discussed following the presentation and discussion of all the boring data.

Boring B-3. Boring B-3 was drilled for the repair and is located in the canal as shown by Figure 2. The canal was dredged into the lacustrine unit at this location as indicated by boring data in Figure 10 and by hydrographic multibeam data from the 26 September 2005 survey in Figure 11. Stratigraphic data from this boring does not identify the swamp/marsh horizon that is present in nearby borings (Figure 3). Multibeam data indicates the canal was dredged to about 20 ft deep in front of the failure reach sometime prior to Hurricane Katrina. Boring data identifies the presence of organic material at the base of the canal instead of sediments characteristic of the swamp/marsh horizon. Lacustrine clay properties are similar to those previously identified and the stratigraphy is consistent with other borings that have been examined above.

Original Design Borings 61 to 64. These borings were drilled in 1981 for the levee design for the hurricane protection by an A&E firm, Modjeski and Masters, Inc., Consulting Engineers, New Orleans, LA. The borings were sampled mainly by a 3-in. Shelby tube. There is no record in the general design memorandum in Volume I whether the sampling was continuous or at a fixed 5 ft interval, nor is this information presented on the boring logs in Volume II (USACE 1990). Because the borings were drilled by an A&E firm, the modified USCS used by the New Orleans District in Figure 1 was not applied to these borings during the laboratory classification and testing (Mr. Lloyd Held, Retired President, Eustis Engineering Company, personal communication).

Much of the confusion surrounding the stratigraphy at the 17th Street Canal site by the NSF team is derived from the interpretation of the design borings in the vicinity of the breach, especially boring 64 (Times-Picayune, 3 February 2006 (Appendix B), NSF, 2006; Chpt. 8, Figure 8.33, p. 8-67; Figure 8.69, p. 8-99). As the cross section in Figure 3 incorporates soils

data from borings 62 through 64, the individual logs from these borings are presented (see Figures 12 through 16) and described. Boundaries have been drawn on each log to separate the lithology in each boring into associated depositional environments. Included at the bottom of each log are the laboratory soil test results. Engineering data are presented at the bottom of each log and consist of water content (%), dry and wet density (lbs/cubic ft), and unconfined compressive strength (lbs/square foot). Elevations of the boring logs are referenced to the Cario Datum, which corresponds to 20.434 ft Mean Gulf Level (WPA, 1937, p. 4). To derive the corresponding value for MGL, subtract 20.434 for the reported Cario elevation in the boring log.

Identified on borings 61 through 64 are the boundaries for the depositional environments. Boundaries separate the soils into levee fill, swamp-marsh, lacustrine, relict beach, and/or bay sound-estaurine deposits. Borings 61 through 64 are generally consistent with the physical soil properties previously observed and described for borings B-14, B-15, B-6, and B3. However, the upper part of the lacustrine interval shown in boring 64 has been erroneously interpreted by the NSF to represent a thick marsh horizon, based on the description of organics and wood layers for this interval. The presence of shell in this interval was ignored and is considered diagnostic of the lacustrine environment, combined with the lower water content, as shown by the laboratory soil test data (compare samples 6 and 7 test results). Boring 63 is located on the west bank of the canal, opposite of boring 64, also identifies shell fragments and a trace of organic matter in this interval, which is consistent with a lacustrine origin describe above and shown by the photographs of the lacustrine soil from B-14 and 15.

The incorrect interpretation of boring 64 by the NSF is primarily due to the poor description of the soil stratigraphy in boring 64. Because of local cost share requirements for Federal Water Projects, borings were contracted by the Sewer and Water Board to an A&E firm to meet their part of the cost share obligation. However, these borings were not classified in accordance with the modified USCS in Figure 1 for the New Orleans District (Mr. Lloyd Held, Eustis Engineering Company, personal communication). Recall that the modified USCS in Figure 1was adapted by the New Orleans District in May 1949 to better characterize highly organic and high water content deltaic soils. No requirements were specified for the modified USCS by the Sewer and Water Board or Modjeski and Masters.

Other Stratigraphic and Chronological Data. Stratigraphic and chronologic data are available to verify the lacustrine origin in boring 64, instead of the swamp/marsh origin interpreted by the NSF for the disputed interval between 20 and 30 ft depth. Data supporting a lacustrine origin includes the soil stratigraphy from two nearby borings (i.e., borings B-4 and 7, see Figure 2). Boring B-4 is presented in Figure 16 (soil profile in Figure 16a and lab summary data sheet in 16b) and was drilled in the canal; while boring B-7 is presented in Figure 17 (soil profile in Figure 17a and lab summary in Figure 17b) and was drilled at the landside toe of the old levee. If the marsh horizon extends to a depth of 30 ft as indicated by the NSF study, then these two borings should contain deep organic soils. Examination of the profile and lab logs for B-4 identifies marsh type conditions to a depth of only 20 ft. Below this depth, no organics are observed in B-4. Soils types below 20 ft are primarily highly plastic, inorganic clays (CH3 and CH4). If marsh were present to a depth of 30 ft, then the log should show the presence of CHOA, CHOB, or CHOC soil types, the water contents should be above 100 percent at a minimum, and

sediment color should reflect the higher organic content by their dark grey color. None of these conditions exist in B-4.

Examination of boring B-7in Figure 17 identifies a similar trend. Soils data from this boring identifies organics to a maximum depth of only about 8 ft. Below this depth, the presence of shell fragments, water contents below 100 percent, grey soil color, and inorganic soil texture (CH3, CH4, and CL6) all define a lacustrine origin for the underlying stratigraphy.

Lake Ponchartrain Borings. A lacustrine interpretation of the stratigraphy in boring 64 for the 20 to 30 ft depth interval is supported by examination of soil logs and engineering laboratory data from Lake Ponchartrain borings in Figures 18 through 20 (Eustis Engineering Company, 1966). The purpose for presenting logs of lake cores is to compare the lake stratigraphy to boring data from the 17th Street Canal area. Lake borings were drilled in support of the Jefferson Parish Lakefront Development. Borings B-1 and B-2 were drilled in the lake and these borings sampled the bottom sediments from Lake Ponchartrain (see Figures 18 through 20). Descriptions of the lake sediments and associated engineering properties are generally identical to those identified in borings beneath the swap/marsh horizon. One has only to review these boring and lab logs from the Lake Ponchartrain borings to observe these similarities. In boring B-1, the bottom of the lake in February1966 was in 12 ft deep water, located about 500 ft from the current shoreline, and contained very soft grey clay with organic matter and humus layers (compare to Figure 15, boring 64, and note the similarities).

Chronological Data. A deep marsh horizon identified for boring 64 by the NSF must agree with the regional chronology developed for this area, which is based on the published radiometric age dates of organic sediments presented in Kolb and Van Lopik (1958a); Fisk (1960), McFarlan, (1961), Saucier (1963), and Frazier (1967). The chronology that has been developed for this area generally does not support a 30 ft deep marsh horizon as reported by the NSF (Times-Picayune, 3 February 2006 (Appendix B); NSF, 2006; Chpt. 8, Figure 8.33, p. 8-67; Figure 8.69, p. 8-99). The chronology that has been established for this region indicates shallow water or lake conditions at a depth of 30 ft and not marsh.

Abandoned Slough or Drainage Channel. The NSF reports in Chapter 3 the possible existence of a slough, tidal, or drainage channel at the 17th Street Canal breach (p. 3-11, Figure 3-16, p. 3-37). This slough or channel was shown on the 1936 WPA Map 1 (WPA, 1937), and was a compilation of earlier historic maps of this region, including the 1872 map by Valery Sulakowski. The channel is shown in Figure 3.16 (Appendix A) as intersecting the 17th Street Canal approximately midway between Stafford and Spencer Avenues. If we assume for purposes of this discussion that the position of the abandoned drainage channel or slough was correct, and boring 64 was positioned in the exact center of this now abandoned channel, then the underlying stratigraphy may represent a slough, abandoned tidal channel or localized drainage channel, but not a 30 ft deep marsh. Furthermore, it is very unlikely that this relatively short channel would be 30 ft deep, since the channel length is relatively short, the drainage area is inconsequential, and volume of water that is potentially discharged would be minimal. It is estimated the channel width would be on the order of 50 to 100 ft maximum based on its short size in Figure 3.16. If the channel were subjected to filling from sedimentation, then a marsh horizon would be

established only during the latter stages of filling. It is difficult to envision a thick marsh setting that corresponds to an active drainage channel.

This channel was so insignificant or ephemeral that it doesn't even register on the 1849 WPA (1937, Plate 13, see Figure 21a) map, the 1895 MRC map of the New Orleans area (see Figure 21b), or the 1895 Sewer and Water Board map (URS, 2006). The NSF identifies a 30 ft deep marsh section at boring 64 (i.e., Figures 8-33 and 8-69) and this position is believed to be erroneous for a variety of reasons, including sedimentological characteristics of the boring data, engineering properties, and local chronologic data. Furthermore, this position doesn't support evidence from nearby borings, hydrographic survey data, or the stratigraphic information obtained from the debris field in the immediate vicinity of the breach.

Hydrographic Survey Data. Conclusive evidence for a lacustrine origin for the interval between 20 to 30 ft depth is obtained from two sources. The first is the hydrographic survey data from the breach zone, made immediately after the failure. The second is stratigraphic information identified from the debris field surrounding the breach, particularly in the immediate vicinity of boring 64. Debris field data are described in the next section. High water bathymetric surveys were made two days after the failure on 31 August 2005 (see Figure 22). These surveys show the ground surface elevation from within the failure zone at -18 ft NGVD, before rock filling was initiated to dewater the city. Elevation data from these surveys are incorporated into the cross section in Figure 3, and are supplemented by land surveys that were performed after dewatering. Survey data from the 17th Street breach site in Figure 3 and Figure 22a clearly shows that material was removed from mainly landside of the I-wall. Foundation soils were removed from the lacustrine horizon during the failure, especially within the immediate vicinity of boring 64 (see Figure 22b, stations 8+00 and 8+50). Furthermore, the tip of the sheet pile was driven to the top of the lacustrine layer as shown by the cross section in Figure 3. An important point to take away from the post-failure hydrographic survey data in Figure 22b is the ground surface elevation behind the missing I-wall panels after the failure, especially near boring 64. Nowhere does the surface elevation behind boring 64 extend to more than -18 ft NGVD. Additionally, the failure was confined only to the landside of the levee as shown by Figures 3, 11, and 22b.

Debris Evidence. Critical evidence was obtained from the debris field to support the lacustrine interpretation for the disputed horizon in boring 64. The debris field identifies the lacustrine layer as the horizon where the levee failure occurred. A careful study of the debris field was made during the IPET study. Large intact masses or blocks of foundation soils from beneath the levee were displaced and transported into the neighborhood by the surge of water from the failure. These large soil blocks were deposited in the streets, front lawns, and between houses. The larger soil blocks were located and studied during the IPET investigation to provide additional information about the stratigraphy and origin of the failure horizon. At several locations, the lower lacustrine grey clay horizon was still firmly attached to the overlying marsh strata (locations shown in Figures 22a and 23a). An unbroken contact between the lower lacustrine horizon and the overlying marsh horizon is an important discovery and unequivocally identifies the lacustrine horizon as being the weak soil horizon for the foundation failure of the levee.

One of the most significant occurrences was located near boring 64 at 6942 Bellairie Drive (see Figure 22a and 23a, western location). This 6 ft block of soil was transported only a short distance from the breach. The soil block was located approximately 150 ft north and east of its original position, and was only a short distance from boring 64 (Figure 23b). The soil block was orientated in a semi-horizontal position in the probable direction of current flow, and was behind the remains of a garage that was transported due east of its original location. The stratigraphy of this soil block consisted of approximately 3 ft of marsh and 3 ft section of lacustrine soils. Clearly visible in the photographs in Figures 23b and 23c are whole shells that are embedded in the lower lacustrine grey clay matrix. Dark grey to black organic marsh soils are directly above the lake clays. The contact between these two different depositional settings was firmly attached to each other, was very distinct, and was relatively sharp, as opposed to being a gradual transition. Also present nearby were logs that were 2 to 3 ft in diameter and were embedded in the upper swamp section of the organic sequence.

Many of the organic soil blocks in the neighborhood showed the transition from marsh at the base to swamp at the top. The swamp sequence contains the wood, roots, logs, and stumps. One of the main reasons for many large soil blocks being transported over relatively large distances from the breach was the buoyancy offered by the organic soils and their high wood content at the top of the stratigraphic sequence. This buoyancy permitted many of these soil blocks to rest upright in their original stratigraphic position. Furthermore, the tensile strength due to the interlocking organic mass allowed many of these soil blocks to be transported relatively intact over large distances. An example of this phenomenon is shown in Figure 23d, and corresponds to the center location highlighted in Figure 23a. This soil block was located on the front lawn of a home at 335 Spencer Avenue, approximately midway between the 17th Street Canal and the four lane highway known as Fluer de Lis. This soil block was prevented from moving further eastward on Spencer Avenue by a tree in the front yard of this home. At the base of this relatively intact organic mass was a soft grey lacustrine clay, which either corresponds to the grey lacustrine shear zone or represents the lacustrine contact with the overlying swamp/marsh horizon. It is more likely that the grey clay corresponds to the shear zone as the consistency was very soft and contained trace amounts of embedded organics. The important point about this soil block is the mass of the block, its spatial location from the breach opening, and the presence of the underlying lacustrine clay.

The third soil block that is noteworthy was located at 6901 Fluer de Lis. This block of soil was at the intersection of Spencer Avenue and the north lane of Fluer de Lis (eastern location in Figure 23a). This soil block was located about 1,180 ft east of the failed levee. The organic soil block at this location was less than 5 ft long, and contained the underlying lake clay, which was firmly attached to the base of the organic sequence (Figures 23e and 23f). The characteristics of the lake clay at the base of this soil block indicate it is from the lacustrine horizon, instead of being part of the shear zone

Lacustrine and Marsh Transition. The generally sharp contact between the lake clay and overlying marsh horizon was observed in numerous borings and in a few of the soil blocks from the 17th Street area. This well defined contact indicates the transition from open water or lake conditions to a marsh type setting was relatively rapid. The IPET interpretation of the 17th Street stratigraphy generally indicates a single well defined swamp/marsh depositional unit, grading

upward from a marsh to a swamp setting. The presence of wood, logs, and stumps are interpreted to occur in the middle to upper part of the organic sequence (Figure 24). The IPET position differs sharply from the NSF position, which indicates stumps occur near the base of the organic sequence and also at the top of the sequence (NSF, 2006, Chapter 3, Figures 3-18 and 3-19, p. 3-39 and 3-40).

The NSF (2006) report cites a historical reference for stumps in two swamp horizons (WPA, 1937, Chapter 1). This reference is from a historical account of several hundred foundation borings from buildings in the downtown area of New Orleans, and historic maps and photographs. The original purpose for publishing the 1937 WPA study was to document the foundation conditions in the New Orleans area, and attempt to describe the geologic conditions as they were understood at that time. The vast majority of cases identified in the 1937 publication were from the downtown area, where most of the active construction was occurring prior to this time period, as opposed to the Lake Ponchartrain shoreline area, which was generally sparsely inhabited.

Schultz and Kolb (1954, p. 19) also reported on the presence of two distinct swamp horizons in their study of the New Orleans Harbor area. However, their description appears to be a general reference to the earlier WPA (1937) document, instead of first hand observations associated with results of their study of the New Orleans area. From current knowledge of the New Orleans area geology, it is known that conditions are generally different on either side of the Bayou Metarie ridge, a natural topographic feature located north of the downtown area. This ridge is a former St. Bernard Distributary Channel and is shown on historic maps in Figures 21a and 21b. To illustrate the differences north and south of the Metairie Ridge, a cross section from the earlier Schultz and Kolb (1954) study is presented as Figure 25. This section shows the geology along the length of the New Basin Canal from levee borings along either side of the canal. This canal was located approximately 2,200 ft east of the 17th Street Canal, and was later filled during the 1960s. This filled canal corresponds to the park land between the Ponchartrain and West End Boulevards, which was used by FEMA following Hurricane Katrina to separate the flood debris for disposal. The canal is historically old. It is identified on New Orleans maps from the 1849 and 1895 time periods (see Figure 22a and 22b). This canal extended into the downtown New Orleans area as shown by these historic maps. The purpose for presenting this cross section is to illustrate the differences in the subsurface geology north and south of the Metairie Ridge.

North of the Metairie Ridge are buried beach sands, brackish and fresh water lake deposits, and an upper organic layer. South of the Metairie ridge are brackish and fresh water lake deposits, and an upper organic layer, which merges with Mississippi River natural levee deposits. The cross section by Schultz and Kolb in Figure 25 shows the presence of two organic horizons south of Bayou Metairie. Interestingly, Schultz and Kolb didn't mention these borings in this section displaying the dual organic horizon and supporting the 1937 account of there being two swamp horizons. Conditions north of the Metairie Ridge in the 17th Street Canal area are significantly different from those observed in the downtown area by the WPA (1937). Boring data and field evidence from the 17th Street Canal area indicates only a single well defined swamp/marsh horizon, instead of two horizons, and the organic horizon grading upward from a marsh to a swamp type setting. The cross section in Figure 25 identifies only a single organic horizon north of the Metairie Ridge as being about 10 ft thick, and accurately reflecting

conditions that were observed in the 17th Street Canal area. Considering how this area was filled and the general chronology that has been developed, the transition from a marsh setting to a swamp type setting is logical and consistent with the observed data. Again, this section is nearby (i.e., 2,200 ft east) and closely parallels the 17th Street Canal north of Veterans Avenue.

Subsurface conditions north and south of the Metairie Ridge are different. A dual swamp horizon possibly occurs south of the ridge because of the geographical extent and the different chronological ages of the various nearby distributary systems (i.e., Bayou Metairie, Bayou Sauvage, Bayou des Families, Bayou La Loutre, Unnamed Bayou, and the Modern Mississippi River Course – see Saucier, 1963; Fraizer, 1967; and Kolb, Smith, and Silva, 1975), and their association with the different Holocene delta lobes (i.e., primarily the St. Bernard versus the Modern Mississippi River delta lobes). Fraizer (1967) shows many of these distributary systems were not completely abandoned, but continued to receive partial flow following delta switching. The concept of a single master Mississippi River channel similar to today's single channel system is a recent event and doesn't represent prehistoric conditions (Frazier, 1967). Local subsidence and the different ages of these delta systems and their affiliated distributary systems are responsible for creating this dual swamp horizon south of the Metairie Ridge as originally reported in the downtown area by the WPA (1937). The presence of the Pine Island Beach trend and Bayou Metairie-Sauvage against the southern edge of the beach complex prevented a massive influx of sediment into the area north of the Metairie Ridge and prevented Lake Ponchartrain from being filled by these different delta lobes and their associated distributaries. If a dual swamp horizon exists north of the ridge, logically it would occur along the immediate margins of the buried beach ridge, especially on the south side, and not along the extreme back barrier side of the ridge in the vicinity of the 17th Street Canal area.

IPET Summary of 17th Street Canal Data. Geologic information from borings, the debris field, and chronostratigraphic data evaluated during the IPET study indicates the upper lacustrine unit as the weak soil, and the horizon where the levee failure initiated. This finding is further supported by the hydrographic survey data taken during the high water after the failure. The survey data identifies material being removed from the lacustrine horizon, which is entirely consistent with evidence from the debris field, backhoe trenches, and the boring data. These findings are integrated with local knowledge of the New Orleans area geology and its chronology, which has largely been defined by various comprehensive studies by the USACE. Furthermore, the geology as originally defined by the earlier foundation studies was correct, based on the results of the focused IPET investigation.

NSF Geology Interpretation. The NAE/NRC comments cited at the beginning of this response indicate the NSF (2006) report was more detailed and apparently the standard by which the IPET geology data were judged. The pointed reference by the NAE/NRC to the NSF report suggests the IPET geology and stratigraphy at the 17th Street Canal site were lacking in detail or were in error. Alternatively, the IPET position indicates parts of the NSF site geology for the 17th Street Canal site are simply incorrect. The NSF position fails to reconcile the IPET field evidence, especially stratigraphic data observed in the debris field, and information from hydrographic surveys from the breach. Additionally, their interpretation doesn't fit the established chronology and stratigraphy that has been developed for this region. The NSF report presents descriptions and illustrations about the geology in Chapters 3 and 8. Major differences

exist between the IPET and NSF positions, some of which have been discussed above. Also, many of the illustrations presented in the NSF report are contradictory to each other as we will examine in greater detail in the following sections.

Geologic interpretations by the NSF at odds with IPET position involve cross-sections in Chapter 3, Figures 3.18 (p 3-39) and 3.19 (p 3-40). These illustrations show the shear zone occurs in the middle part of the organic horizon. This position directly opposes the various types of evidence gathered by the IPET study, which has the shear zone in the lacustrine horizon as described above. Furthermore, the NSF position is at odds with illustrations in Chapter 8, in Figures 8.26 (p. 8-62), 8.27 (p. 8-63), and 8.67 (p. 8-97). Illustrations in Chapter 8 identify the failure zone occurring at the base of the marsh horizon, and above a new deltaic environment labeled "*Intermixing Zone*." However, in Chapter 3, in Figures 3.18 and 3.19 of the NSF report, they indicate the failure is within the swamp deposits with no intermixing zone shown. Clearly, the various chapters in the NSF report are in complete disagreement with each other regarding the general stratigraphy. And, this is the "gold standard" by which the NAE/NRC reviewers judged the IPET geology and stratigraphy!

Intermixing Zone Versus Lacustrine. A description of the Intermixing Zone environment and the underlying lacustrine environment are described by the NSF (2006, p. 3-14) in the classification of the CPT data as follows:

- **Intermixing Zone:** This zone consists of mixture of *soft clays, silt lenses with little or no organic material*. The thickness of intermixing zone ranges from 3 ft to 8.5 ft on the east bank of the canal. No intermixing zone is interpreted on the west bank of the canal. However the contact between marsh and intermixing zone is highly irregular and should be correlated with borehole data.

- **Lacustrine Deposits:** Lacustrine deposits consist of *clays to organic clays with thin silt and fine sand lenses*. *No organic matter* is found in these deposits. The thickness of lacustrine deposits is around 17-19 ft on the west bank of the canal and 15-22 ft on the east bank of the canal. The depth at which lacustrine deposits encountered ranges from -17 (on the west side) to 14-23 (on the east side).

The underlying origin for the intermixing zone environment in the NSF report is undocumented. From the name given to this environment and the brief description provided above, it can only be concluded that lacustrine conditions favorable to formation of soft clay, silt lenses, and little organic material are indicative of this environment. In fact, a review of these two descriptions identifies no discernable differences between them. Intermixing zone appears to form in an open water or a lake setting. There are no significant organics in either of these two environments; otherwise intermixing zone would represent a marsh. The descriptions of these two environments are nearly identical, with soft clays, low organic content, and silt and/or fine sand lenses. These descriptions are consistent with the boring data observed from Lake Ponchartrain borings, which are representative of lacustrine conditions (see Figures 19 and 20). Furthermore, the presence of shells is ignored, and these were observed in most of the borings that the NSF describes as being part of the intermixing zone. Both lacustrine and intermixing clays are grey in color from descriptions in the text (p.3-12) and Figure 8.33 (p. 8-67).

A fundamental question emerges as to why it was necessary to create a whole new depositional environment when the basic properties are identical. These properties include soil texture, stratigraphic characteristics, and engineering properties (note the lab logs from borings presented earlier). It's quite ironic that the IPET stratigraphy was criticized by the NAE/NRC reviewers for not integrating with the local geology, when the NSF saw the need to establish a brand new environment instead of working within the established deltaic plain framework.

If intermixing zone represents a slough, as intimated in the NSF report by Figure 3.16 (p.3-41), then the limits of this prehistoric slough should have been defined and stratigraphic differences documented for this site. The problem with this viewpoint is the historic maps and the boring data do not readily support this position. Also, a slough should have a limited geographic extent, perhaps 50 to 100 ft maximum channel width. The slough shouldn't range 500 ft wide as shown by Figure 8.33 of the NSF report. It is doubtful whether the slough would extend horizontally any appreciable extent. The southern limits of the breach are where the failure likely initiated, based on the orientation of the displaced levee section and the debris field observed along Bellaire and Spencer Avenues. This area is outside of the slough according to Figure 3.16 in the NSF report, where the slough intersects midway between Spencer and Stafford Avenues and shouldn't extend much beyond 25 to 50 ft either side of the location shown. Also, the intermixing zone doesn't extend to the west side of the canal, which further indicates a limited horizontal extent (see description above). Little or no organic material is present in the intermixing zone sediments according to the NSF description of this environment presented above. Yet boring 64 represents a deep marsh section according to the NSF position in Figures 8.33 and 8.69, but an intermixing zone interpretation in Figures 8.26 and 8.27. These interpretations are completely at odds with each other. Further adding to this confusion is the description in the legend in Figures 8.26 and 8.27 for intermixing zone, which identifies a mix of gray clays and marsh materials. These different descriptions and cross-sections all contradict one another.

The intermixing zone environment described above isn't consistent with the lithostratigraphic units that have been established for the deltaic plain (see Table 1 for list of primary environments). This environment exactly matches and corresponds with the lacustrine or lake environment that has been recognized by previous workers in the Mississippi River deltaic plain. Furthermore, engineering properties of soils from the lacustrine environment are fairly consistent as evidenced by the laboratory test results from the many borings that have been presented in this paper which the NSF would attribute to the "intermixing zone environment." The lacustrine grey clay observed in the soil block near boring 64 would represent "intermixing zone" sediments according to the new NSF definition for this horizon. Consequently, the displaced soil block near boring 64 identifies the failure zone as occurring within the NSF intermixing zone based on the intact contact between the grey "intermixing" clay (IPET lacustrine clay) and the overlying marsh horizon, instead of the swamp horizon shown by the NSF illustrations in Figures 3.18, 3.19, 8.26, and 8.27. The IPET interpretation of the 17th Street Canal stratigraphy rejects the "Intermixing Zone" classification.

Missing Hydrographic Survey Data. The NSF interpretation of the stratigraphy and failure mechanisms generally ignores the hydrographic surveys from the 17th Street Canal that were run shortly after the failure (Figure 22). These surveys show foundation soils being removed to about

the -18 ft NGVD elevation, which is completely ignored by the NSF cross-section in Figures 8.26, 8.27, and 8.67. Their interpretation in these illustrations doesn't fit the known survey data from this breach.

Incorrect Wall Geometry. The NSF cross-section in Figures 8.26, 8.27, and 8.67 show the pre-failure canal side embankment being above the water level in the canal. This position is incorrect (see Figure 26). The canal side embankment was lowered to approximately -1 ft elevation, below the level of the canal, many years earlier because of slope stability concerns with the canal side embankment.

Boring Data Errors. Other errors are present in the NSF cross sections in Figures 8.26 and 8.27. Stratigraphic contacts in Figures 8.26 and 8.27 between the lacustrine grey clay, the underlying beach sands, and bay sound deposits are incorrect. The NSF section shows the beach sand as occurring from about -34 to -48 ft elevation, or to the bottom of the cross-sections. However, in boring B-6, the sand elevation occurs between -35 and -42 ft (see Figure 9); boring B-3, the sand elevation occurs between -39 and -47 ft (see Figure 10), and boring 64 (Figure 15) shows 1.5 ft of bay sound clay at the end of the boring. The boring stratigraphy and contacts are ignored in the NSF sections.

Additionally, the cross-section shows the sand contact rising to around -26 ft east of the canal in the vicinity of Bellaire Street. The sand at this elevation is incorrect based on boring data presented in Figure 25 from the New Basin Canal and Figure 27. Borings 391 and 394 in Figure 25 are located in the centerline of the canal, 2,200 ft due east of the 17th Street Canal breach, and at the same approximate latitude as the breach. These borings identify the contact with the beach sand at about -34 ft MGL. This value is consistent with published contour maps from the beach sand by Saucier (1994) in Figure 27.

IPET and NSF Stratigraphy Summary. In the preceding sections we have examined both the IPET and NSF positions regarding the stratigraphy at the 17th Street Canal failure. Interpretation of the site stratigraphy by the IPET is based on the boring data, physical properties of the soils, laboratory soil test data, engineering soil properties, previous studies, established chronology and framework, historic maps of this area, and the available field evidence. Field evidence includes backhoe trenches, hydrographic survey data, and the stratigraphy from the debris field. The IPET study indicates the failure was in the underlying lacustrine horizon. The "Intermixing Zone" is not recognized as being a unique deltaic depositional environment, but is considered part of the lacustrine environment. Examination of boring data and laboratory test data from the 17th Street Canal site supports a lake (lacustrine) environment beneath the marsh horizon, entirely consistent with published studies of this region.

Various chapters in the NSF report are in complete disagreement with each other regarding the general stratigraphy for this site. The NSF position identifies the swamp/marsh horizon as being the horizon where the failure occurred. Interpretations about the site stratigraphy are generally not supported by previously published studies, historic map data, existing survey data, and the field evidence. The NSF cross-sections contain errors of omission and misinterpretation about stratigraphy in the existing boring data.

A famous fourteen century English logician and Francisan friar, William of Ockham, is credited with Occam's razor, which states: "…the explanation of any phenomenon should make as few assumptions as possible, eliminating, or "shaving off," those that make no difference in the observable predictions of the explanatory hypothesis or theory. In short, when given two equally valid explanations for a phenomenon, one should embrace the less complicated formulation" (Wikipedia).

References

Britsch, L. D. and Dunbar, J. B. (1990). "Geomorphic investigation of Davis Pond, Louisiana." Technical Report GL-90-12, U.S. Army Engineer Waterways Experiment Station, Vicksburg, MS.

Britsch, L. D. and Dunbar, J. B. (1993), "Land Loss Rates: Louisiana Coastal Plain," Journal of Coastal Research, Vol. 9, No. 2, p. 324-328.

Britsch, L. D. and Dunbar, J. B. (2005), "Land Loss Maps of the Louisiana Coastal Plain, Plates 1 through 7" Technical Report ERDC/GSL-TR-05-13, Engineer Research and Development Center, Vicksburg, MS, (available at lmvmapping.erdc.usace.army.mil).

Dunbar, J. D., Torrey, V. H., and Wakeley, L. D. (1999), "A case history of embankment failure: geological and geotechnical aspects of the Celotex levee failure, New Orleans, Louisiana," Technical Report GL-99-11, USAE Waterways Experiment Station, Vicksburg, MS.

Dunbar, J. D., Britsch, L. D., and Kemp E. B., (1992), "Land Loss Rates Rates, Report 3, Louisiana Coastal Plain," Technical Report GL-90-2, USAE Waterways Experiment Station, Vicksburg, MS.

Dunbar, J. B., Blaes, M. Dueitt, S., and Stroud, K. (1994). "Geological investigation of the Mississippi River deltaic plain, Report 2 of a Series." Technical Report GL-84-15, U.S. Army Engineer Waterways Experiment Station, Vicksburg, MS.

Dunbar, J. B., Blaes, M., Dneitt, S., and May, J. (1995). "Geological investigation of the Mississippi River deltaic plain, Report 3 of a Series." Technical Report GL-84-15, U.S. Army Engineer Waterways Experiment Station, Vicksburg, MS.

Dunbar, J. B., Myers, W. M., Jackson, S., 2006. "Lower and Middle Mississippi Valley Engineering Geology Mapping Program Website," lmvmapping.erdc.usace.army.mil, Engineer Research and Development Center, Geotechnical and Structures Laboratory, Vicksburg, MS

Eustis Engineering Company (1966), "Metairie Shore, Jefferson Parish Lakefront Development," Supplemental Report, Volume IV, Soils and Foundation Study, New Orleans, LA.

Eustis Engineering Company (1984), "Geotechnical Investigation, Soil Stratification and Foundation Conditions for Residential Development, New Orleans, Louisiana," For City of New Orleans and Sewerage and Water Board of New Orleans, Eustis Engineering Company, Metairie, LA.

Fisk, H. N. (1960), "Recent Mississippi River sedimentation and peat accumulation,"4th International Congress, Carboniferous stratigraphy and geology, Heerlen, Holland, 1958, Compte Rendu, p. 187-199

Frazier, D. E. (1967). “Recent deltaic deposits of the Mississippi River: Their development and chronology.” Transactions 17th annual meeting,Gulf Coast Association of Geological Societies.. San Antonio, TX.

Kolb, C. R. (1962). “Distribution of soils bordering the Mississippi River from Donaldsonville to Head of Passes.” Technical Report No. 3-601, U.S. Army Engineer Waterways Experiment Station, Vicksburg, MS.

Kolb, C. R., and Saucier, R. T. (1982). “Engineering geology of New Orleans.” Reviews in Engineering Geology, Geological Society of America, 5, 75-93.

Kolb, C. R., Smith, F. L., and Silva, R. C. (1975), “Pleistocene sediments of the New Orleans-Lake Pontchartrain area.” Technical Report S-75-6, U.S. Army Engineer Waterways Experiment Station, Vicksburg, MS.

Kolb, C. R., and VanLopik, J. R. (1958a). “Geology of the Mississippi River deltaic plain.” Technical Report No. 3-483, Vol 1 and 2, U.S. Army Engineer Waterways Experiment Station, Vicksburg, MS.

Kolb, C. R., and VanLopik, J. R. (1958b). “Geological investigation of the Mississippi River-Gulf Outlet Channel.” Miscellaneous Paper No. 3-259, U.S. Army Engineer Waterways Experiment Station, Vicksburg, MS.

Kolb, C. R., and VanLopik, J. R. (1965). “Depositional environments of the Mississippi River Deltaic Plain.” In Deltas in their geologic framework, editor Martha Lou Shirely and James A Ragsdale, Houston Geological Society, Houston, TX.

May, J. R., Britsch, L. D., Dunbar, J. B., Rodriguez, J. P., and Wlonsinski, L. B. (1984). “Geological investigation of the Mississippi River Deltaic Plain.” Technical Report GL-84-15, U.S. Army Engineer Waterways Experiment Station, Vicksburg, MS.

McFarlan, E. (1961), “Radiocarbon dating of Late Quaternary deposits, South Louisiana,” Geological Society of America Bulletin, Vol. 72, p. 129-162.

Mississippi River Commission, (1975), “Master Index, Upper and Lower Mississippi River Surveys for Period 1879-80 to 1928 and Some Historic Maps Prior to this Period,” US Army Corps, Mississippi River Commission, Vicksburg, MS.

Montgomery, R. L. (1974). “Correlation of engineering properties of cohesive soils bordering the Mississippi River from Donaldsonville to Head of Passes, LA.” Miscellaneous Paper S-74-20, U.S. Army Engineer Waterways Experiment Station, Vicksburg, MS.

National Science Foundation (2006). “Investigation of the Performance of the New Orleans Flood Protection Systems in Hurricane Katrina on August 29,2005,” Volumes I and II, National Science Foundation and the University of California, Berkeley, CA, http://www.ce.berkeley.edu/~new_orleans/

Saucier, R. T. (1963). “Recent geomorphic history of the Pontchartrain Basin, Louisiana.” Technical Report 16, Part A, United States Gulf Coastal Studies, Coastal Studies Institute, Contribution No. 63-2, Louisiana State University, Baton Rouge, LA.

Saucier, R. T. (1994), "Geomorphology and Quaternary Geologic History of the Lower Mississippi Valley." Volumes I and II, U.S. Army Engineer Waterways Experiment Station, Vicksburg, MS.

Saucier, R. T. and Kolb, C. R. (1982), "Engineering geology of New Orleans," Geological Society of America, Reviews in Engineering Geology, Vol 5, p. 75-91

Schultz, J. R. and Kolb, C. R. (1954), "Geological Investigation of the New Orleans Harbor Area," Technical Memorandum 3-391, USAE Waterways Experiment Station, Vicksburg, MS.

Smith, L. M., Dunbar, J. B., and Britsch, L. D. (1986), "Geomorphological investigation of the Atchafalaya Basin, Area West, Atchafalaya Delta, and Terrebonne Marsh," Technical Report GL-86-3, USAE Waterways Experiment Station, Vicksburg, MS.

URS (2006), "A century of subsidence: change in New Orleans DEMs relative to MGL 1895 to 1999/2002," Poster prepared for Federal Emergency Management Agency, URS Inc, Baton Rogue, LA.

U S Army Corps of Engineers (1941), "Investigation of Underseepage Lower Mississippi River Levees," Technical Memorandum No.184-1, U.S. Army Engineer, Waterways Experiment Station, Vicksburg, MS.

US Army Corps of Engineers (1963), "The Unified Soils Classification System," Technical Memorandum No. 3-357, U.S. Army Engineer, Waterways Experiment Station, Vicksburg, MS.

US Army Corps of Engineers (1988), "Design Memorandum No. 19, General Design, Orleans Avenue Outfall Canal," US Army Corps of Engineers, New Orleans District, New Orleans, LA.

US Army Corps of Engineers (1989), "Design Memorandum No. 19A, General Design, London Avenue Outfall Canal," US Army Corps of Engineers, New Orleans District, New Orleans, LA.

US Army Corps of Engineers (1990), "Design Memorandum No. 20, General Design, 17th.St. Outfall Canal," US Army Corps of Engineers, New Orleans District, New Orleans, LA.

Works Progress Administration of Louisiana (1937), Some data in regard to foundations in New Orleans and vicinity, New Orleans, LA, p. 243.

DEGREE OF PLASTICITY		SOIL CLASSIFICATION	LETTER AND CORRELATION SUBSCRIPT	GRAIN-SIZE PERCENTAGES		APPARENT PLASTICITY RANGE		
				SAND	CLAY	LIQUID LIMIT	PLASTICITY INDEX	
FINE – GRAINED SOILS	HIGH	FAT CLAY	CH_4 CH_3 CH_2	0-20 0-20 0-20	70-100 50-70 40-50	70-110 55-80 50-60	45-75 30-55 25-40	
		FAT CLAY (SANDY)	CH_{3-S} CH_{2-S} CH_1	20-50 20-30 30-60	50-70 40-50 40-50	50-70 50-60 50	25-50 25-40 30	
		FAT ORGANIC CLAY	ABOVE "A" LINE CH_{OA} CH_{OB} CH_{OC}	BELOW "A" LINE OH_A OH_B OH_C	40-80	ABOVE "A" LINE 50+ 75+ 100+	 22+ 40+ 60+	
	LOW	LEAN CLAY	CL_6 CL_4	0-20 0-20	30-40 20-30	40-50 28-43	20-35 10-25	
		SANDY CLAY	CL_{6-S} CL_5 CL_{4-S} CL_3	20-30 30-60 20-38 38-60	30-40 30-40 20-30 20-30	40-50 30-45 25-40 20-35	20-35 15-30 8-20 3-15	
		LEAN ORGANIC CLAY	CL_{OA} CL_{OB} CL_{OC}		10-40	30+ 50+ 70+	10+ 25+ 40+	
	SLIGHT	SILT	ML_3 ML_2	0-20 0-20	5-15 5-20	25-28 22-28	2-6 0-6	
		SANDY SILT	ML_{2-S} ML_1	20-45 45-60	5-20 0-15	17-28 15-20	0-6 0-6	
		ORGANIC SILT	OL_4 OL_2	0-20 0-20	20-30 5-20	30-40 28-40	6-15 2-10	
		ORGANIC SANDY SILT	OL_{2-S} OL_1	20-45 45-60	5-20 0-15	28-35 30	0-6 0-5	
SAND & SANDY SOILS – NONE TO SLIGHT PLASTICITY		CLAYEY SAND	SC_{5-S} SC_{3-S} SC_1	60-70 60-80 60-90	30-40 20-30 10-20	>28	>6	MINUS 35 MESH
		SILTY SAND	SM_1	60-80	0-15	<28	<6	
		SAND	SM_{1-S} SP	80-90 90-100	0-20 0-10	NONPLASTIC		
FIBROUS ORGANIC SOILS		PEAT	PT			200+		

Figure 1. Unified soil classification system (USCS) adapted to New Orleans District soils in May 1949 (from Kolb and Van Lopik, 1958a). Soils logged for original hurricane design borings and post Katrina borings by US Army Corps and Eustis Engineering Company were classified by the modified USCS.

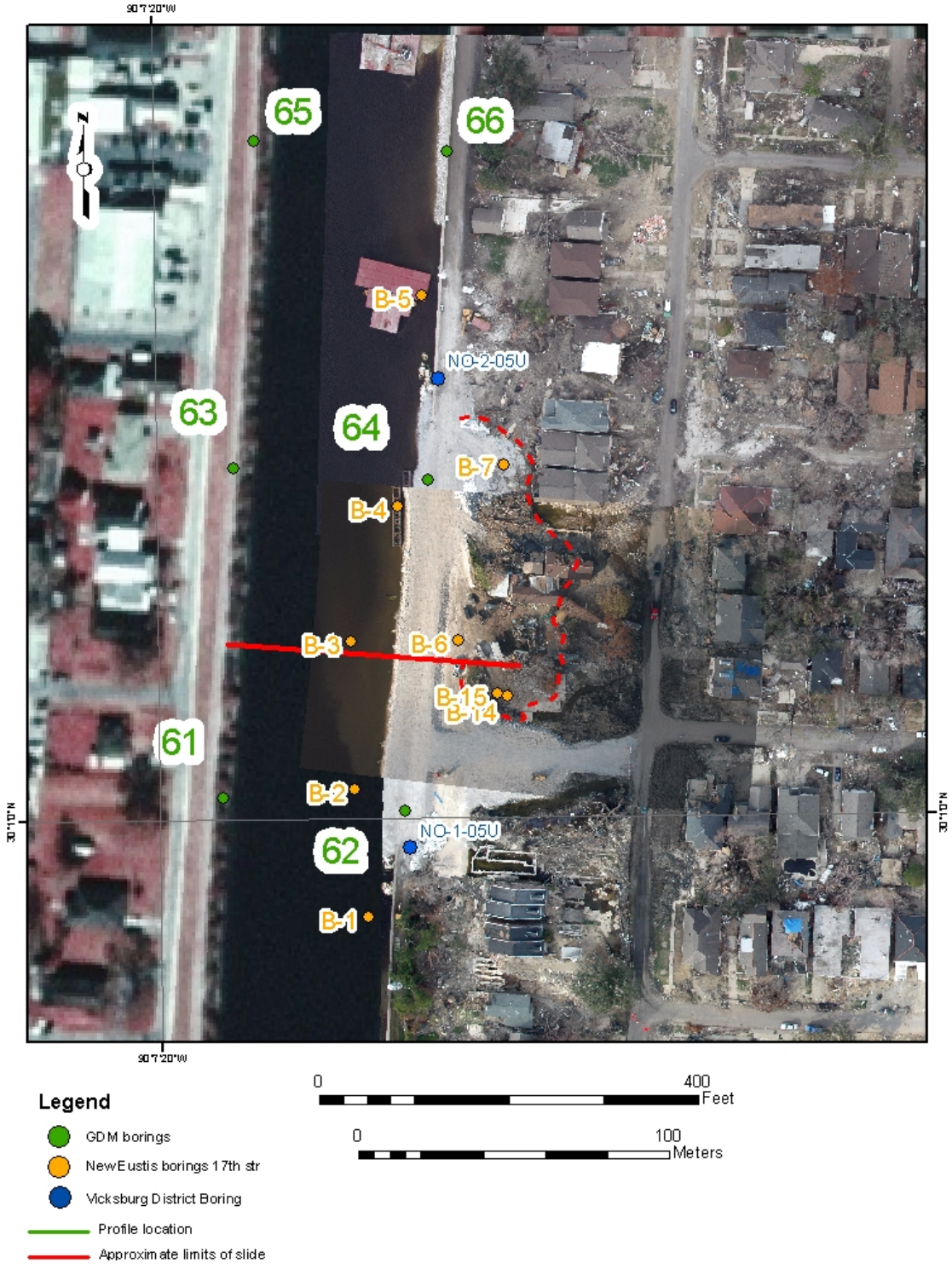

Figure 2. Aerial photographs from November 2005 of the 17th Street failure showing locations of selected pre and post failure borings, representative geological cross-section, and general limits of the displaced levee block (dashed red line). Borings 14 and 15 are on top of the translated levee block, on either side of slip surface that was uncovered by backhoe trench that was excavated at southern edge of the displaced levee section.

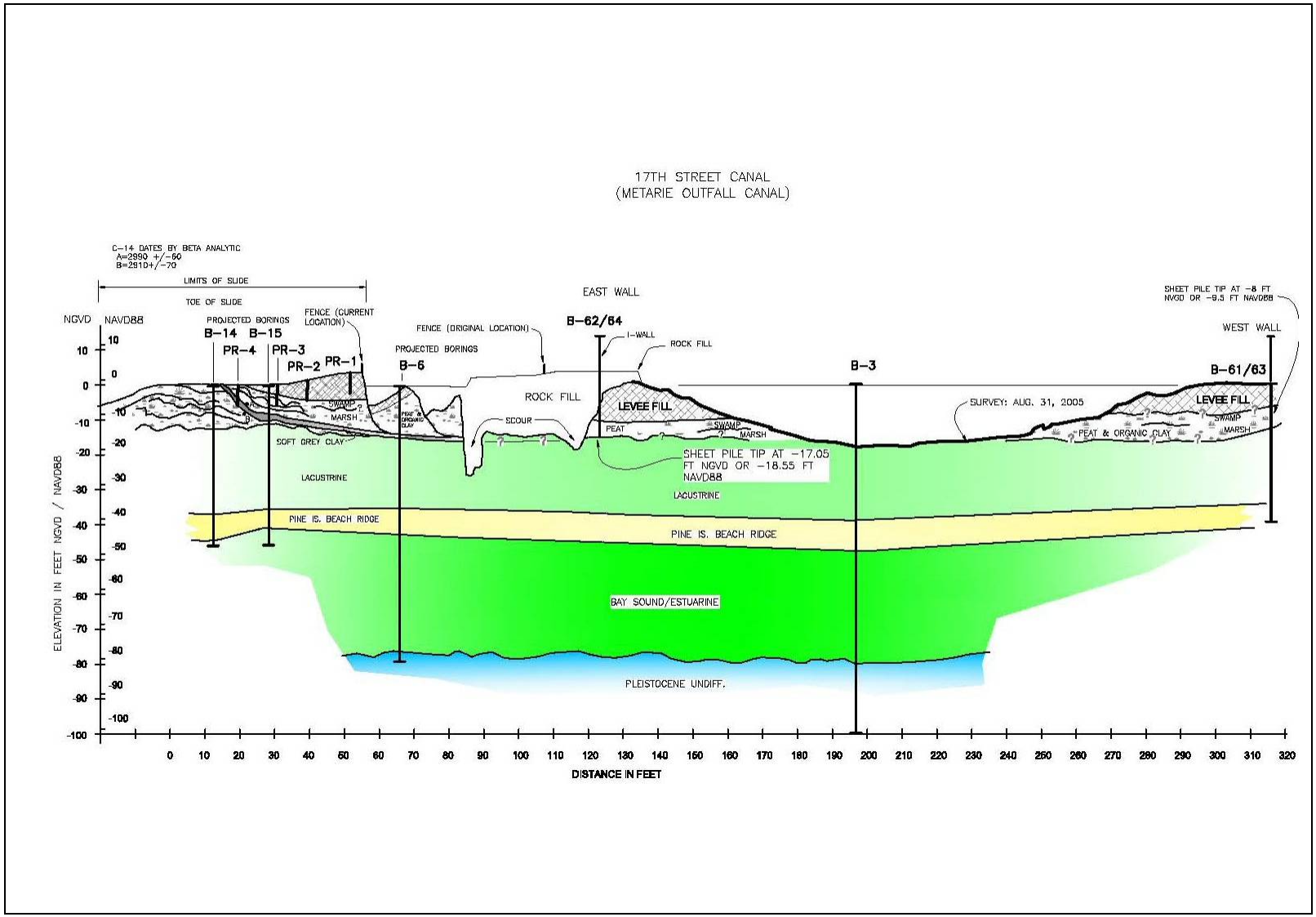

Figure 3. Representative cross section from 17th Street Canal levee failure. Cross-section is view looking south and shows the underlying stratigraphy, pre and post-failure engineering borings, surface topography from hydrographic and ground surveys.

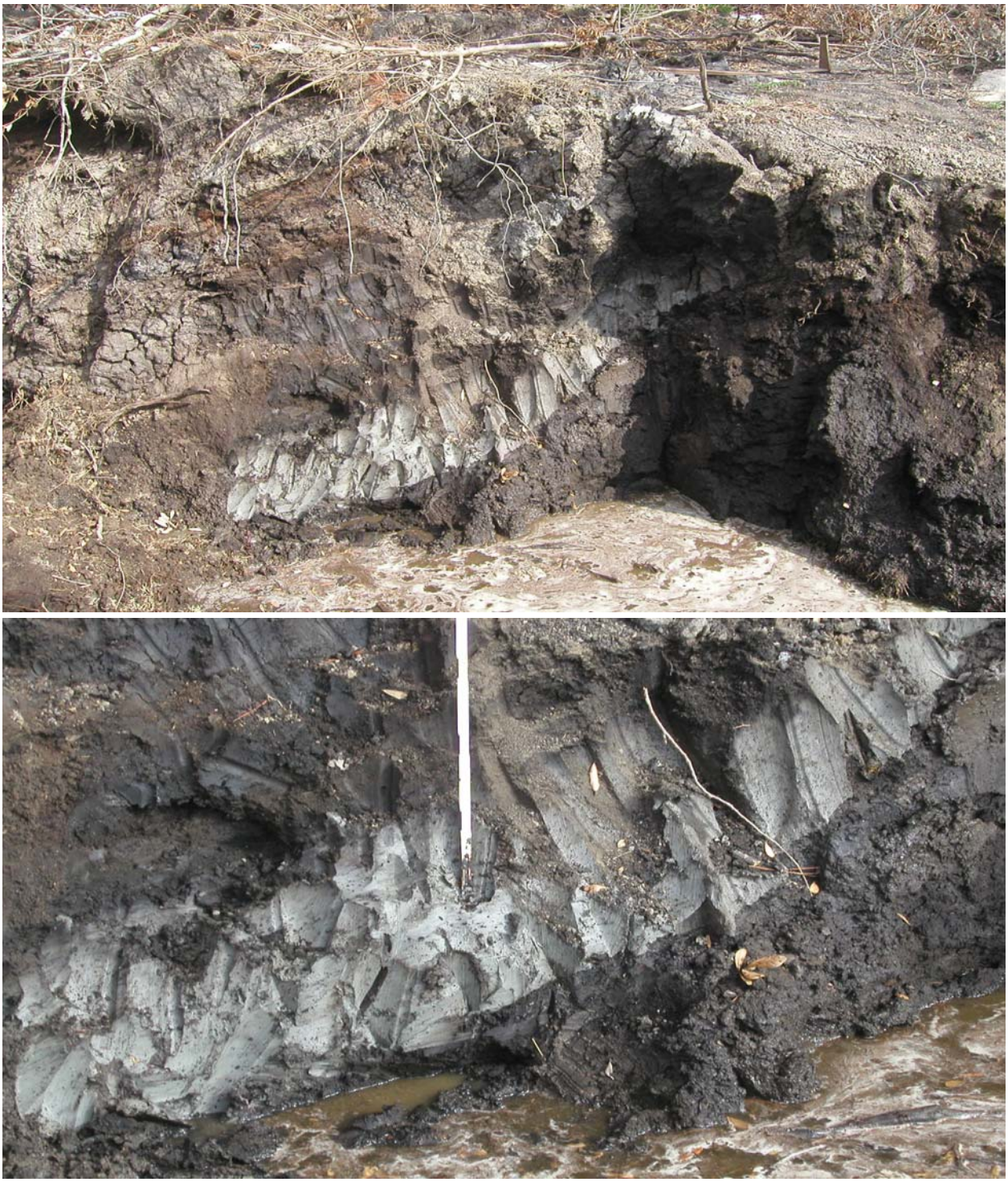

Figure 4. Failure plane at the 17th Street Canal breach showing soft lacustrine clay that was displaced overtop the marsh at the levee toe. The marsh above and below the clay is the same layer as confirmed by carbon-14 age dating.

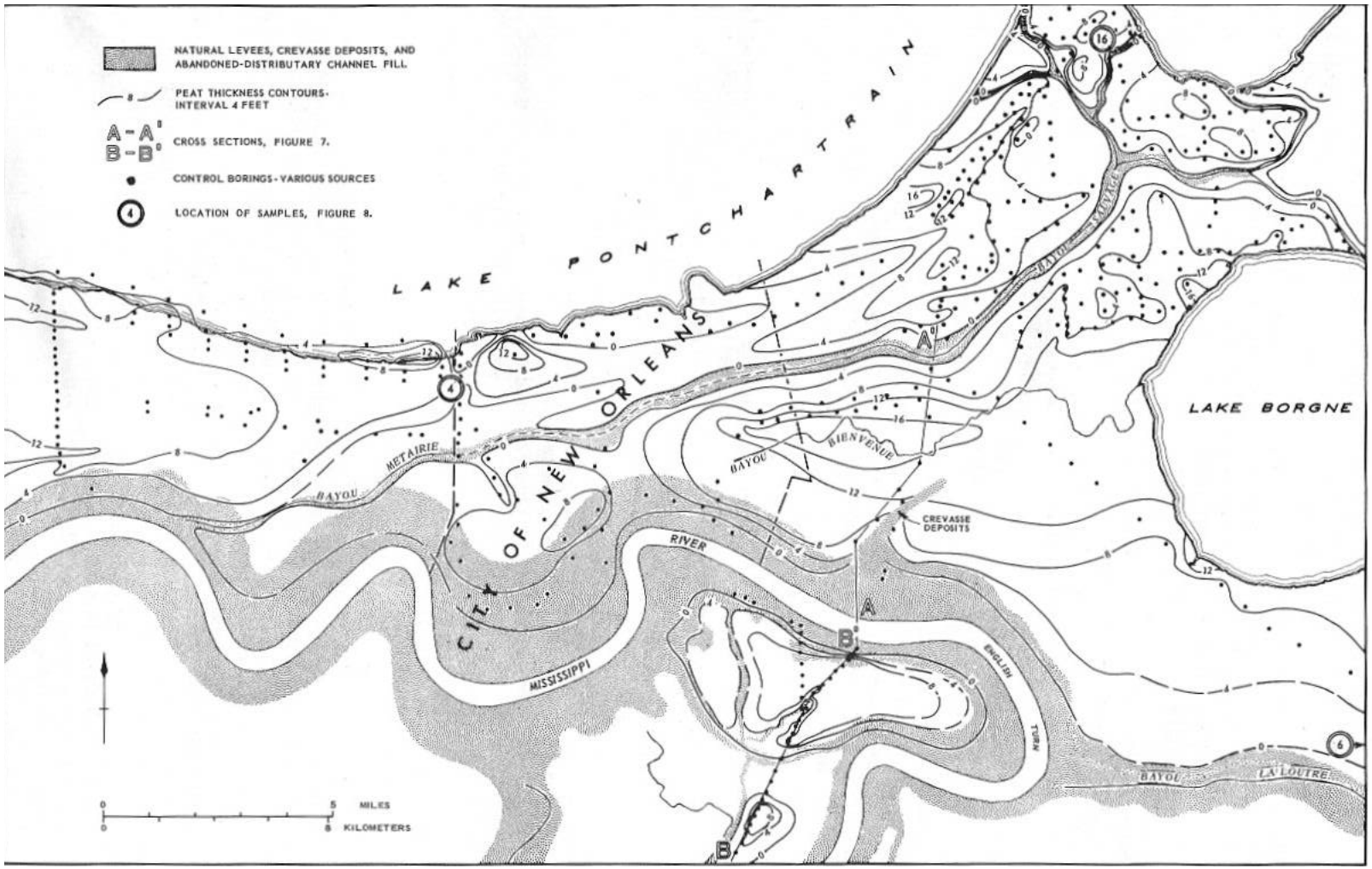

Figure 5. Map of peat thickness in the New Orleans area which is generally between 8 to 16 ft thick (from Fisk, 1960).Cross-section A-A' and B-B' referenced above are presented in Figure 6. The 17th Street canal break is located north of sample location 4 in map.

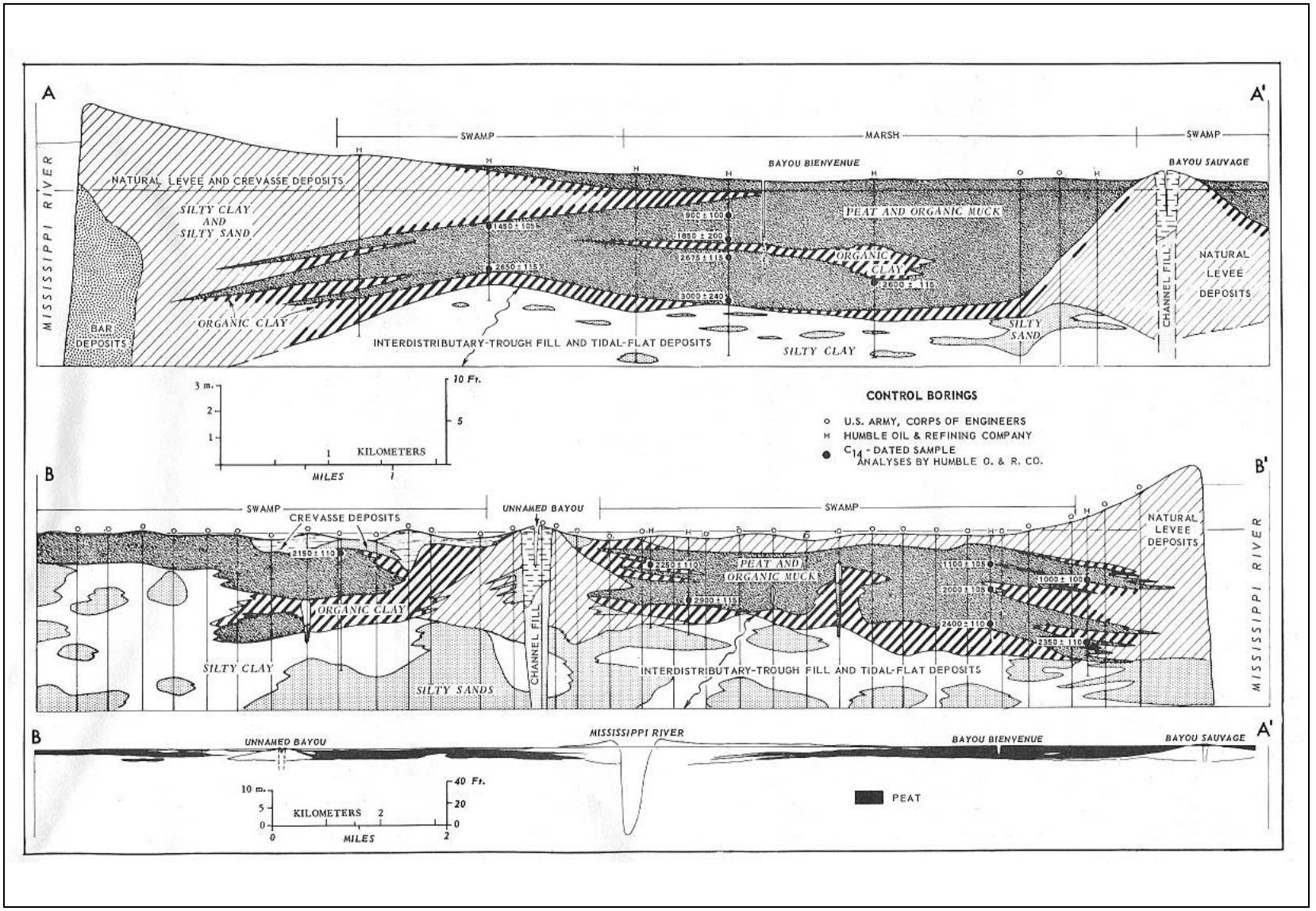

Figure 6. Section A-A' and B-B' from Figure 5 (Fisk, 1960); note the radiocarbon age dates shown at the base of the organic fill are consistent with dates obtained from base of organic fill at the 17th Street levee break in the displaced levee block.

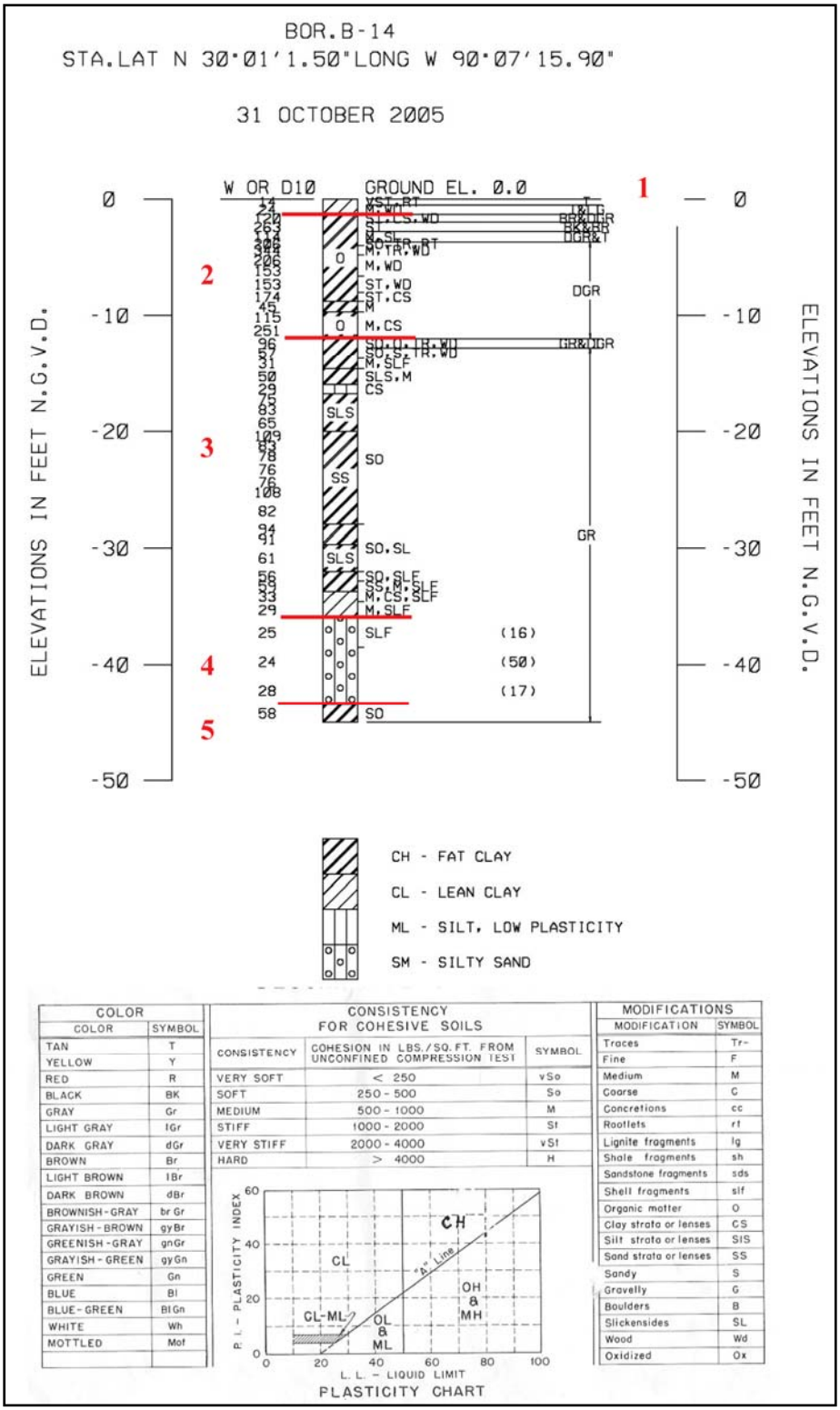

Figure 7a. Boring log for B-14 (see Figure 2 for location), see Figure 8b for lab summary and Figures 8c through 8f for photographs of soil samples. Boundaries between depositional environments are identified in red: 1) levee fill, 2) swamp/marsh, 3)lacustrine, 4) relict beach, and 5)bay sound.

SUMMARY OF LABORATORY TEST RESULTS

Project: U.S.A.C.E. - 17TH STREET CANAL AND IN SITU TESTING AT LONDON AVE

Project Number: 19115
Boring: B-14

Current Date: 11/3/2005

Sample Number	Depth in Feet	Visual Classification		USCS	W%	SPT	Sample Notes
1	0.0-0.5	VST T CL6 W/ RT	1	CL6	14		
2A	0.5-1.33	M T & LGR CL6 W/ WD		CL6	24		
2B	1.3-1.97	ST BR & DGR CHOB W/ WD, LYS CH		CHOB	120		0.6-0.7 LYS CH
3A1	2.0-2.5	ST BK & BR CHOC		CHOC	263		VERY BRITTLE
3A2	2.5-2.83	M DGR & T CHOA W/ SL		CHOA	114		0.1-0.3 LYS CH
3B	2.8-3.72	M DGR & BK CHOB W/ LYS CH		CHOB	166		0.4-0.5 LYS CH
3C	3.7-4.03	SO DGR CHOC W/ TR-RT		CHOC	206		
4A	4.0-4.83	M DGR CHOC W/ TR-WD		CHOC	313		
4B	4.8-5.72	M DGR CHOC W/ WD	2	CHOC	206		
4C	5.7-6.62	M DGR CHOB W/ WD		CHOB	153		
4D	6.6-6.93	ST DGR CHOB W/ WD		CHOB	153		
5A	8.0-8.83	ST DGR CHOB W/ LYS CH		CHOB	174		0.5-0.7 LYS CH ON 30 DEG ANGLE
5B	8.8-9.72	M DGR CH4		CH4	45		
5C	9.7-10.62	M DGR CHOA W/ LNS CH		CHOA	115		
5D	10.6-11.52	M DGR CHOC W/ LNS CH		CHOC	251		
6A	12.0-12.83	SO GR & DGR CH4 W/ O, TR-WD		CH4	96		
6B	12.8-13.72	SO GR CH4 W/ ARS SM, TR-WD		CH4	57		
6C	13.7-14.62	M GR CH2 W/ SIF		CH2	37		
6D	15.5-16.42	M GR CH2 W/ LYS ML	3	CH2	50		0.6-0.9 LYS ML
7A	16.0-16.83	GR ML2 W/ LYS CH		ML2	29		0.7-0.8 LYS CH
7B	16.8-17.72	SO GR CH4 W/ ARS & LNS ML		CH4	75		
7C	17.7-18.62	SO GR CH4 W/ ARS & LNS ML		CH4	83		
7D	18.6-19.52	SO GR CH3 W/ LNS & LYS ML		CH3	65		0.3-0.5 LYS ML
8A	20.0-20.83	SO GR CH4 W/ LNS SM		CH4	109		
8B	20.8-21.72	SO GR CH4 W/ LNS SM		CH4	83		
8C	21.7-22.62	SO GR CH4 W/ LNS SM		CH4	78		
8D	22.6-23.02	SO GR CH4 W/ LNS SM		CH4	76		
9A	24.0-24.83	SO GR CH4 W/ LNS SM		CH4	76		
9B	24.8-25.72	SO GR CH4 W/ LNS SM		CH4	108		
9C	25.7-26.62	SO GR CH4 W/ LNS SM		CH4	83		
10A	28.0-28.83	SO GR CH4 W/ SL		CH4	94		
10B	28.8-29.72	SO GR CH4 W/ SL		CH4	91		
10C	29.7-30.2	SO GR CH4 W/ SL, LNS ML		CH4	61		
11A	32.0-32.83	SO GR CH3 W/ ARS & LNS SM, SIF		CH3	56		
11B	32.8-33.72	M GR CH3 W/ LNS & LYS SP, SIF		CH3	59		0.1-0.3 LYS SP
11C	33.7-34.62	M GR CL5 W/ LYS CH, SIF		CL5	33		0.0-0.2 LYS CH
11D	34.6-35.27	M GR CL3 W/ SIF		CL3	29		
12	36.0-38.5	GR SM1 W/ SIF		SM1	25	16	
13	38.5-41	GR SM1	4	SM1	24	50	
14	41.0-43.5	GR SM1		SM1	28	17	
15	43.5-46	SO GR CH2	5	CH2	58	WOH	WOH = WEIGHT OF HAMMER

Figure 7b. Lab test results for B-14 (see modified USCS in Figure 1 for soil texture classification). Properties most often used to classify deltaic soils into depositional environments are texture, water content, organic content, and presence of shells (sif). Note photographs of soil samples are presented in Figures 7c through 7f. Boundaries between depositional environments marked by red lines,1 = fill, 2 = swamp/marsh, 3 = lacustrine; 4= relict beach, 5 =bay sound-estaurine. Based on soil texture, color, water content, consistency, absence or presence of shells, laminations, and/or other soils structure properties.

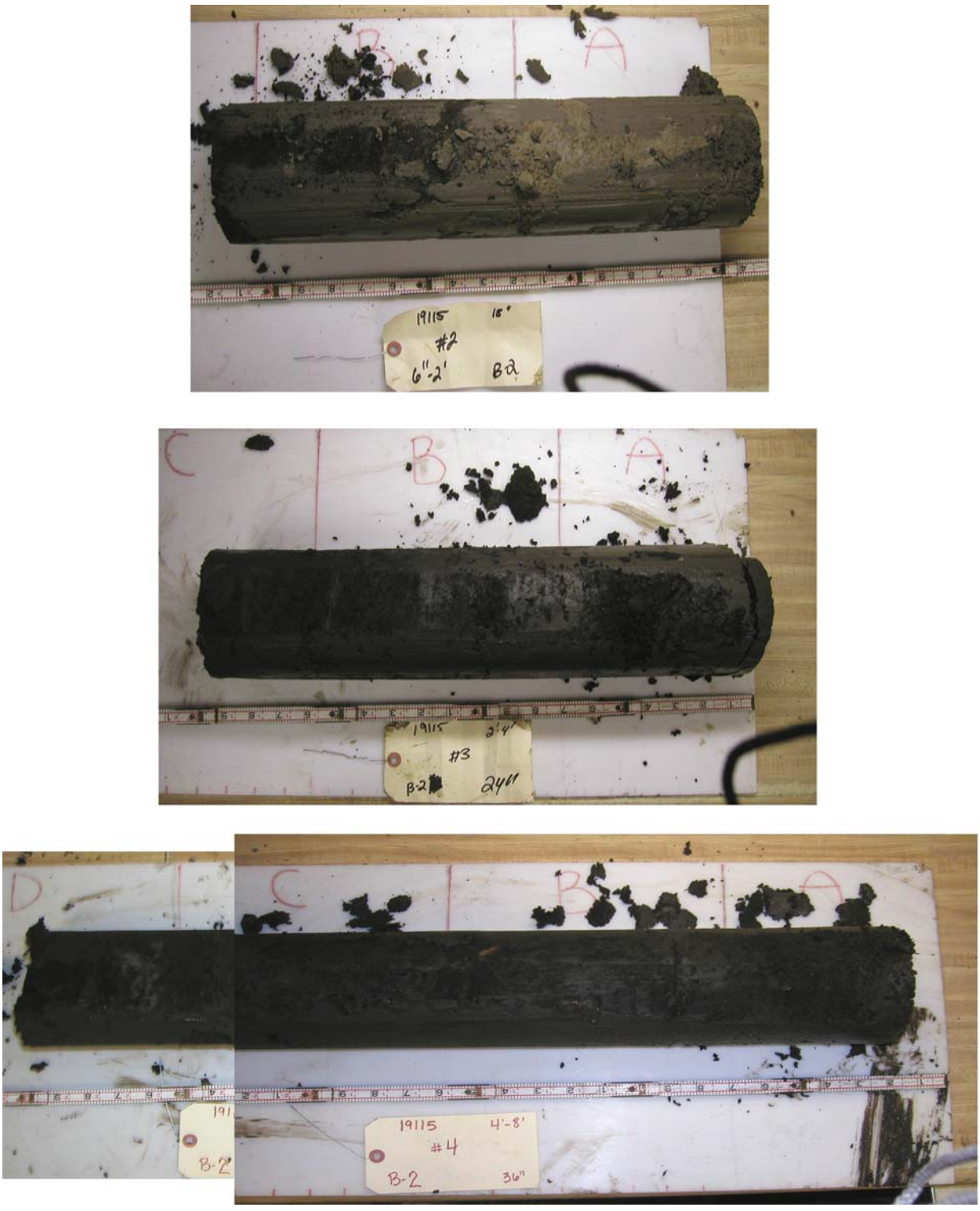

Figure 7c. Boring B-14, samples 2 (top), 3 (center), and 4 (bottom), 0.5 to 2 ft, 2 to 4 ft, and 4 to 8 ft, respectively. Top of samples are at right and bottom at left. Sample 2 from levee fill, and samples 3 and 4 are in the swamp/marsh environment--note the high water and the high organic content as indicated by the CHOA to CHOC designation (see Figures 1 and 7b). Presence of wood pieces and roots are common in samples. Samples from west edge of displaced levee section and are disturbed.

Figure 7d. Boring B-14, samples 5 (top), 6 (center), and 7 (bottom), 8-12 ft, 12-16 ft, and 16-20 ft; respectively; sample 5 is from swamp/marsh environment, and samples 6 and 7 are from the lacustrine environment. Note the darker color, higher water and organic contents for sample 5 (Figure 7b, CHOA to CHOC). Lighter grey color, lower water and organic contents, shell fragments (white specs), and laminations and lenses of silt and/or fine sand are diagnostic of lacustrine (lake) sediments

Figure 7e. Boring B-14, samples 8 (top), 9 (center), and 10 (lower); depths from 20 to 24 ft, 24 to 28 ft, 28 to 32 ft, respectively. See boring and lab logs in Figures 7a and 7b for descriptions. All three samples are from the lacustrine stratigraphic unit. This unit characterized by soft to medium grey clay, note the presence of light colored silt and/or fine sand lenses, laminations, and thin beds. Water content ranges between 29 and 109 percent. Samples were merged in photographs above by bedding features between adjacent photos, and may not align with the sample board in background between photos. Samples 12, 13, 14, and 15 are split spoon samples and not photographed.

Figure 7f. Boring B-14, sample 11; depth from 32 to 36 ft, view of lacustrine grey clay, note the shell fragments near base of sample (left side), overlying and merging with the relic beach sand at 35 to 40 ft (Figure 3). See Figure 7b for lab summary descriptions.

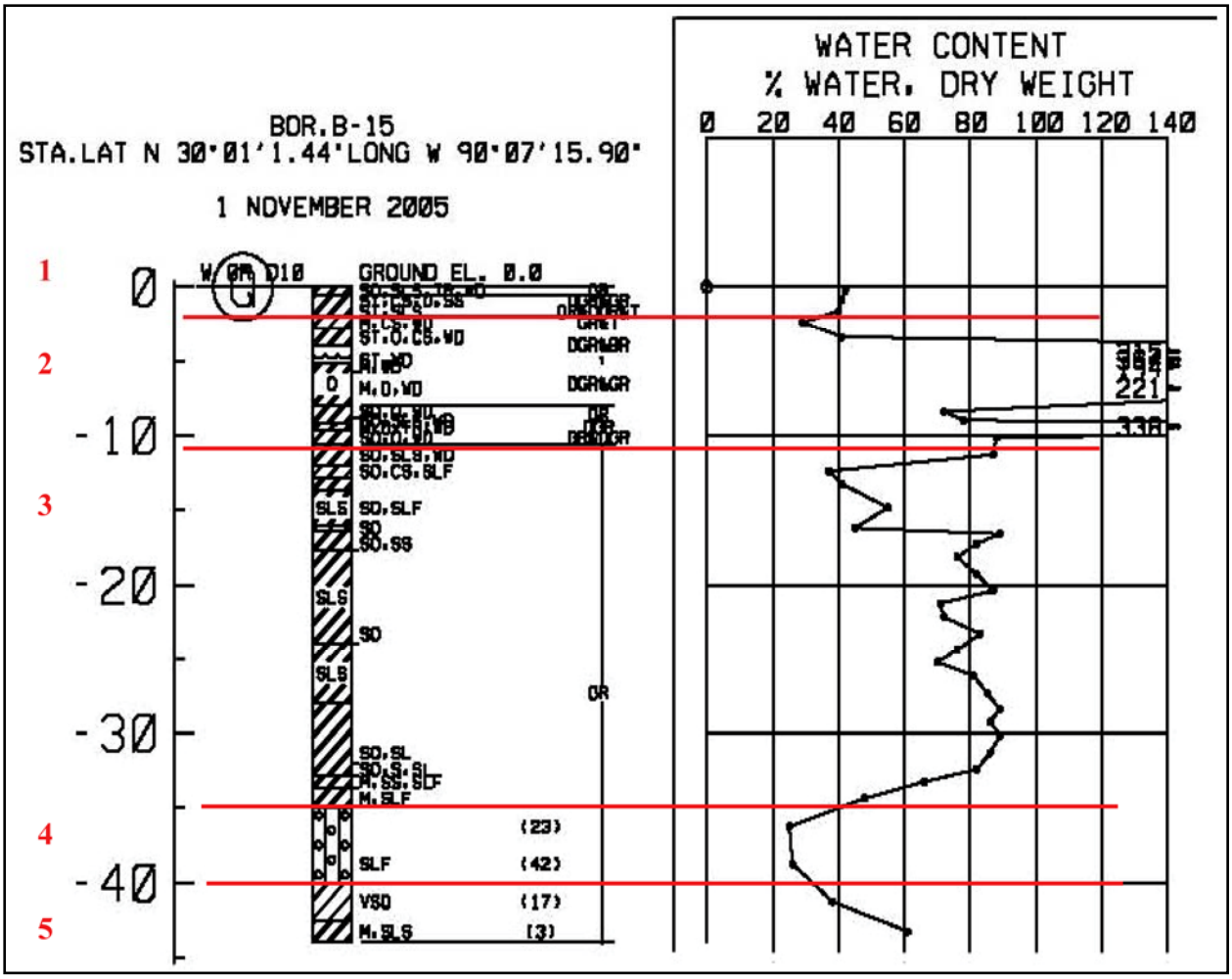

Figure 8a. Boring log for B-15 (see Figure 2 for location), see Figure 8b for lab summary and Figures 8c through 8f for photographs of soil samples. Boundaries between depositional environments are identified in red: 1) levee fill, 2) swamp/marsh, 3) lacustrine, 4) relict beach, and 5) bay sound.

SUMMARY OF LABORATORY TEST RESULTS

Project: U.S.A.C.E. - 17TH STREET CANAL AND IN SITU TESTING AT LONDON

Project Number: 19115
Boring: B-15

Current Date: 11/3/2005

Sample Number	Depth in Feet	Visual Classification		USCS	W%	SPT	Sample Notes
1	0.0-0.5	SO GR CH3 W/ ARS ML, TR-WD		CH3	42		
2A	0.5-1.33	ST DGR & GR CH4 W/ LYS CH & PT, ARS SM		CH4	41		0.5 - 0.6 LYS CH, 0.6 - 0.8 LYS PT
2B	1.3-1.97	ST GR, DGR & T CH4 W/ LNS ML & PT	1	CH4	40		0.4 - 0.5 LYS ML, 0.5 - 0.7 LYS PT
3A	2.0-2.83	M GR & T CL6 W/ WD, LYS CH		CL6	29		0.0 - 0.3 DISTURBED CH
3B	2.8-3.3	ST DGR & BR CHOA W/ LYS CH & CL, WD		CHOA	71		0.0 - 0.1 LYS CL, 0.1 - 0.2 LYS CH
4A	4.0-4.83	ST DGR & BR PT W/ WD	2	PT	315		VERY BRITTLE
4B1	4.8-5.13	ST DGR & BR PT W/ WD		PT	364		
4B2	5.1-5.68	M DGR & GR CHOA W/ WD		CHOA	194		TEST SAMPLE
4C	5.7-6.62	M DGR & GR CHOB W/ WD, LYS PT		CHOB	221		0.6 - 0.9 LYS PT
5A	8.0-8.83	SO GR CH4 W/ ARS ML, O, WD		CH4	72		
5B1	8.8-9.22	SO GR CH4 W/ ARS ML, O, WD		CH4	78		
5B2	9.2-9.7	M DGR CHOC W/ TR-WD		CHOC	338		
5C	9.7-10.62	SO GR & DGR CH4 W/ O, WD, LYS CHOC		CH4	88		0.0-0.1 0.2- 0.3 LYS CH
5D	10.6-11.02	SO GR CH4 W/ LNS ML, WD		CH4	87		
6A	12.0-12.83	SO GR CL6 W/ ARS CH, SIF		CL6	37		
6B	12.8-13.72	SO GR CH2 W/ SIF	3	CH2	41		
6C	13.7-14.2	SO GR CH3 W/ LNS & LYS ML, SIF		CH3	55		0.0-0.2 LYS ML
7A1	16.0-16.42	SO GR CL6		CL6	45		
7A2	16.4-16.82	SO GR CH4 W/ LNS SM		CH4	89		
7B	16.8-17.72	SO GR CH4 W/ LNS SM		CH4	82		
7C	17.7-18.62	SO GR CH3 W/ LNS LYS ML		CH3	76		
7D	18.6-19.52	SO GR CH3 W/ LNS & LYS ML		CH3	82		
8A	20.0-20.83	SO GR CH4 W/ LNS ML		CH4	87		
8B	20.8-21.72	SO GR CH4 W/ LNS ML		CH4	71		
8C	21.7-22.62	SO GR CH4 W/ LNS ML		CH4	72		
8D	22.6-23.18	SO GR CH4 W/ LNS ML		CH4	83		
9A	24.0-24.83	SO GR CH4 W/ LNS ML, SL		CH4	76		
9B	24.8-25.72	SO GR CH4 W/ LNS ML, SL		CH4	70		
9C	25.7-26.62	SO GR CH4 W/ LNS ML, SL		CH4	81		
9D	26.6-27.02	SO GR CH4 W/ LNS ML, SL		CH4	85		
10A	28.0-28.83	SO GR CH4 W/ SL		CH4	89		
10B	28.8-29.72	SO GR CH4 W/ SL		CH4	86		
10C	29.7-30.62	SO GR CH4 W/ SL		CH4	89		
10D	30.6-31.52	SO GR CH4 W/ SL		CH4	86		
11A	32.0-32.83	SO GR CH4 W/ ARS SM, SL		CH4	82		
11B	32.8-33.72	SO GR CH3 W/ ARS & LNS SM, SIF		CH3	66		
11C	33.7-34.62	M GR CH2 W/ SIF		CH2	48		
12	35.0-37.5	GR SM1 W/ SIF	4	SM1	25	23	
13	37.5-40	GR SM1 W/ SIF		SM1	26	42	
14	40.0-42.5	VSO GR CL3		CL3	38	17	
15	42.5-44	M GR CH3 W/ ARS ML	5	CH3	61	3	

Figure 8b. Lab test results for B-15 (see modified USCS in Figure 1 for soil texture classification). Photographs of soil samples described above are presented in Figures 8c through 8f. Boundaries between environments are identified in red; 1 = fill, 2 = swamp/marsh, 3 = lacustrine; 4= relict beach, 5 =bay sound-estaurine. Based on soil texture, color, water content, consistency, absence or presence of shells, laminations, or other soils structure.

Figure 8c. Photographs of soil samples from B-15, samples 2 through 4, 0.5 to 8 ft depth; samples 2 and 3 from the levee fill, sample 4 from the swamp/marsh environment--note the high water content identified in Figures 8a and 8b, and the high organic content as indicated by the CHOA to CHOC designation for sample 3 (see Figure 1). Presence of wood pieces and roots are common in samples.

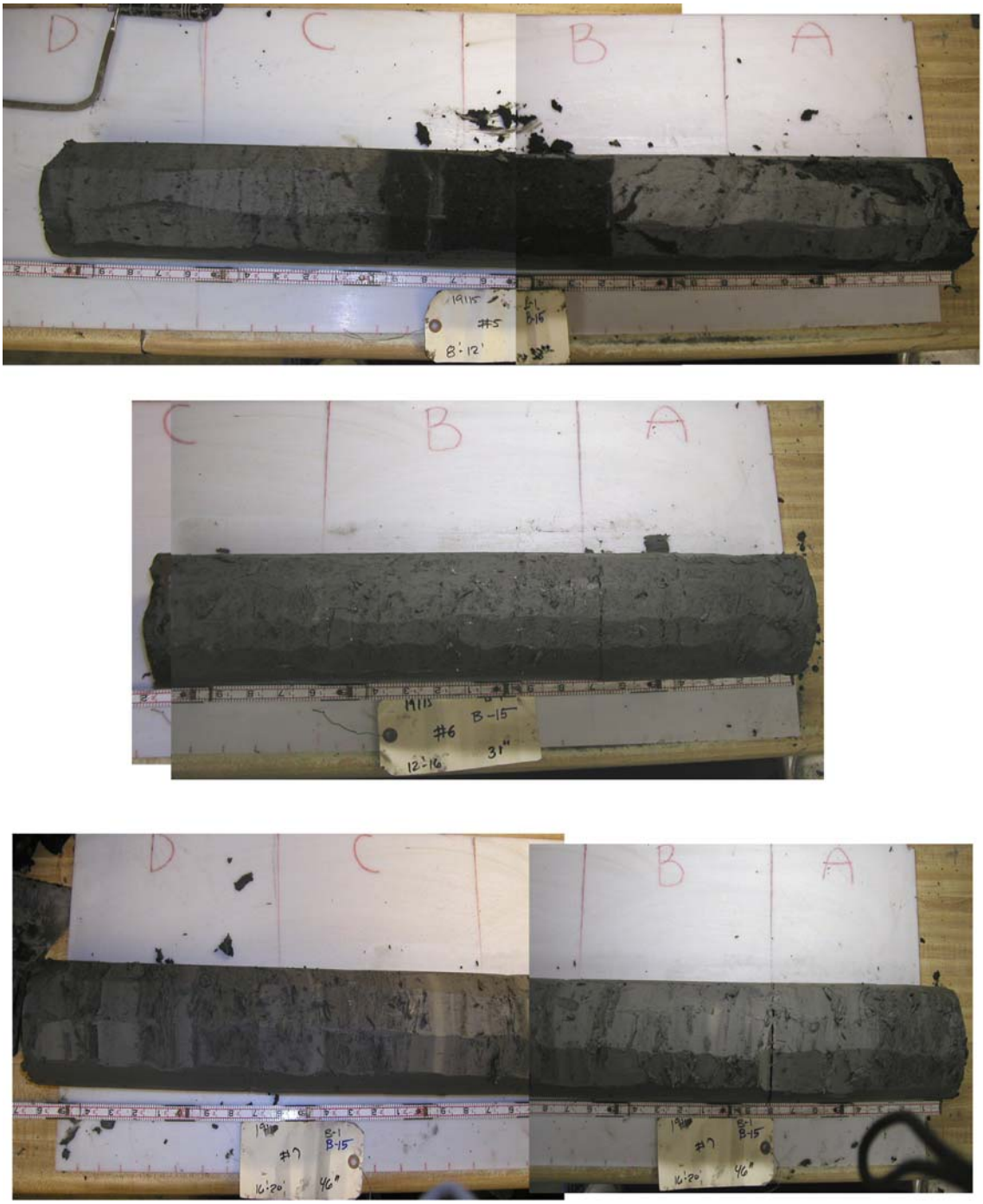

Figure 8d. Boring B-15, samples 5 (top), 6 (center), and 7 (lower); depths from 8 to 12 ft, 12 to 16 ft, 16 to 20 ft, respectively. See boring and lab logs in Figures 8a and 8b for descriptions. Sample 5 at top (right) contains the slip surface which is grey clay with distorted inclusions of peat in parts A and upper half of B. Shear zone is underlain by nearly 1 ft of peat (marsh deposits). Marsh deposits above and below grey clay layer have age date of 2,900 years. Lacustrine deposits begin in 5C at 10.6 ft. Note the sharp contact with the lacustrine deposits, and the distinct change to soft grey clay with trace organics and most importantly shell fragments (white specs) and silt and fine sand laminations. Note the change in water content between marsh and lacustrine in boring and lab logs. Bioturbation occurs in upper part of the lacustrine stratigraphic unit.

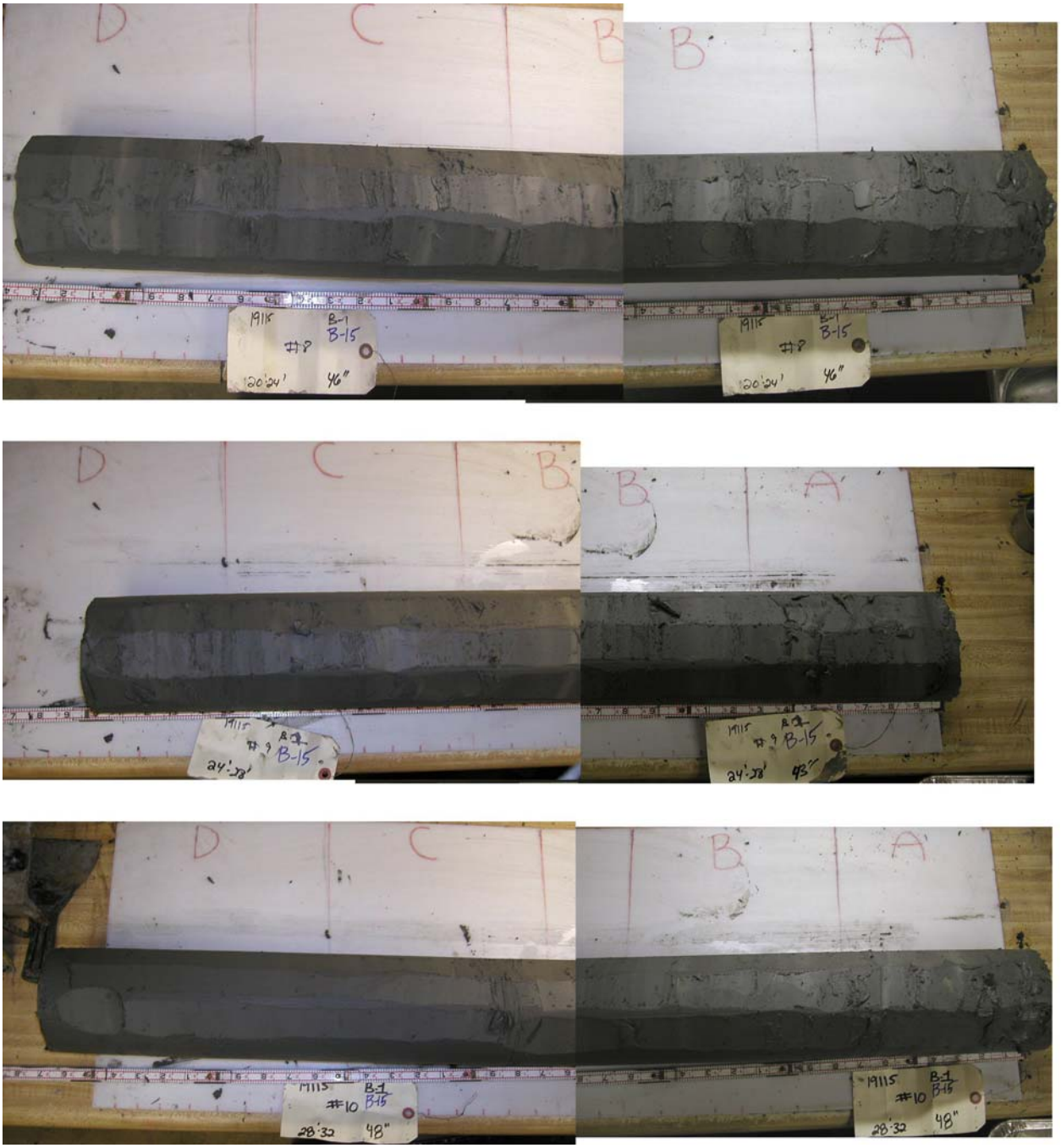

Figure 8e. Boring B-15, samples 8 (top), 9 (center), and 10 (lower); depths from 20 to 24 ft, 24 to 28 ft, 28 to 32 ft, respectively. See boring and lab logs in Figures 8a and 8b for descriptions. All three samples are from the lacustrine stratigraphic unit. This unit characterized by grey clay, note the presence of light colored silt and fine sand lenses, laminations, and thin beds. Also, note the water content in boring and lab logs ranges between 37 and 89 percent. Samples are merged in photographs above by bedding features between adjacent photos, and may not align with the sample board in background.

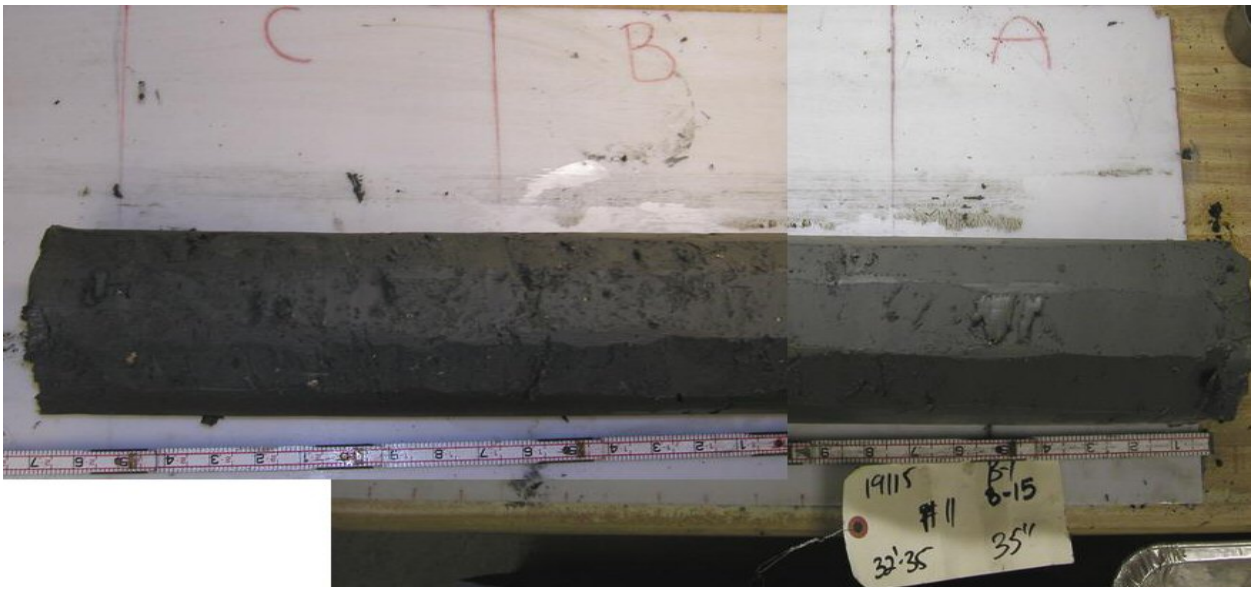

Figure 8f. Boring B-15, sample 11; depth from 32 to 35 ft, view of lacustrine grey clay, note shell fragments near base (left side) above the relic beach sand at 35 to 40 ft (see Figure 3). Samples 12, 13, 14, and 15 are split spoon samples from the relict beach and are not shown.

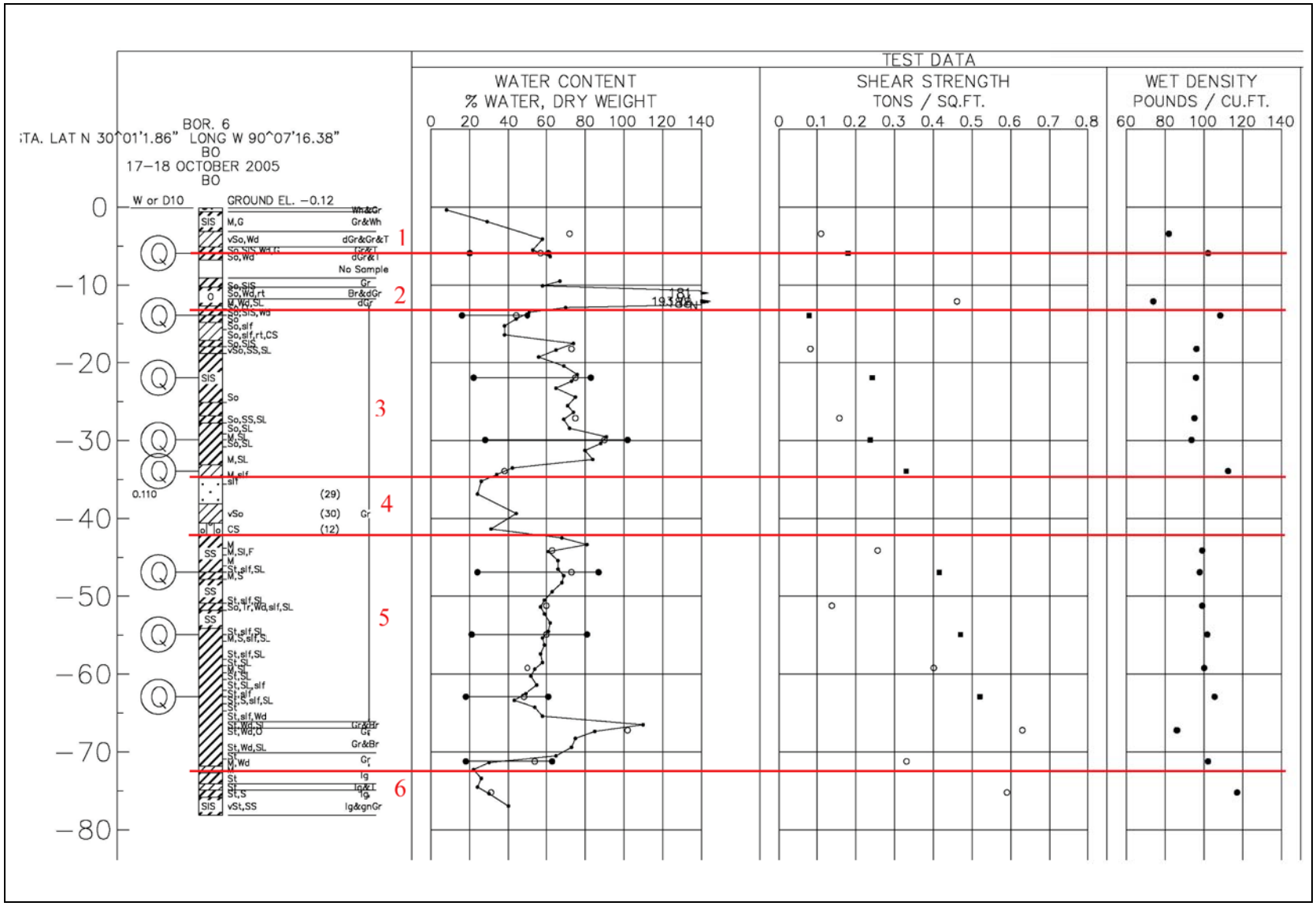

Figure 9a. Soil profile for Boring B-6; 1 = rock fill and levee fill, 2 = swamp/marsh, 3 = lacustrine, 4 = relict beach sand, 5 = bay sound/estuarine, 6 = Plesistocene.

SUMMARY OF LABOR. ORY TEST RESULTS

Project: USACE - 17TH STREET CANAL Assigned By: _____

Project Number: 19080 Current Date: 11/4/2005
Boring: B-6

Sample Number	Depth in Feet	Visual Classification	USCS	E(f)	W%	Dry Dens (pcf)	Wet Dens (pcf)	Sat %	Shear Test Type	Angle	Cohesion (psf)	Unconf. Comp. Str.	LL	PL	PI	TORVANE (tsf)	Other Tests
1	0.0	WH & GR GP	GP		8												
2	0.5	M GR & WH CH3 W/ ARS ML, G	CH3		29												
3A	3.0	VSO DGR, GR & T CL6 W/ WD	CL6	6	72	48	82	77	UC	--	221	443				0.230	
4A	6.0	SO GR & T CH3 W/ ARS ML, WD, G	CH3		53												
4B	6.8	SO GR & T CH3 W/ ARS ML, WD	CH3		62												
5A	9.0	SO GR CH4 W/ LNS & ARS ML	CH4		67												
5B1	9.8	SO GR CH4 W/ LNS & ARS ML	CH4		58												
5B2	10.2	SO BR & DGR CHOC W/ WD, RT	CHOC		181												
5C	11.7	M DGR CHOC W/ WD, SL	CHOC	10	193	25	74	92	UC	--	921	1841				0.350	
5D	12.6	SO GR CH4 W/ LNS ML, O	CH4		70												
6A	13.0	SO GR CH3 W/ LNS & ARS ML, WD	CH3		51												
6B	13.8	SO GR CH3 W/ LYS & ARS CL	CH3		44												
6C	14.7	SO GR CL6 W/ SIF	CL6		38												
6D	15.6	SO GR CL6 W/ SIF, RT, LYS CH	CL6		38												
7A	17.0	SO GR CH4 W/ LNS & ARS ML	CH4		74												
7B	17.8	VSO GR CH4 W/ LNS SM, SL	CH4	6	73	56	96	96	UC	--	166	333				0.130	
7C	18.7	SO GR CH3 W/ LNS & LYS ML	CH3		56												
7D	19.6	SO GR CH3 W/ LNS & LYS ML	CH3		69												
8A	21.0	SO GR CH4 W/ LNS ML	CH4		76												
8B	21.8	SO GR CH4 W/ LNS ML	CH4		73												
8C	22.7	SO GR CH4 W/ LNS ML	CH4		65												
8D	23.6	SO GR CH4 W/ LNS ML	CH4		75												
9A	25.0	SO GR CH4 W/ SL	CH4		71												
9B	25.8	SO GR CH4 W/ SL	CH4		74												
9C	26.7	SO GR CH4 W/ SL, LNS SM	CH4	5	75	54	95	95	UC	--	316	632				0.200	
9D	27.6	SO GR CH4 W/ SL	CH4		72												
10A	29.0	M GR CH4 W/ SL	CH4		91												
10B	29.8	M GR CH4 W/ SL	CH4		88												
10C	30.7	M GR CH4 W/ SL	CH4		80												
10D	31.6	M GR CH4 W/ SL	CH4		84												
11A	33.0	M GR CL5 W/ SIF	CL5		42												
11B	33.8	M GR CL5 W/ SIF	CL5		34												
11C	34.7	GR SP W/ SIF	SP		26												
12	35.5	GR SM1	SM1		24												
13	38.0	VSO GR CL3	CL3		44												
14	40.5	GR SM1 W/ ARS CH	SM1		31												
15A	42.0	M GR CH3 W/ LYS & LNS SP	CH3		68												

1
2
3
4

Shear Zone ?

Figure 9b. Lab summary data sheet for Boring B-6; 1=rock fill and levee fill, 2 = swamp/marsh, 3=lacustrine, 4=relict beach sand, dashed line above organic (CHOC) may correspond to gray clay shear zone shown in Figure 4 (continued).

SUMMARY OF LABOR..ORY TEST RESULTS

Project: USACE - 17TH STREET CANAL Assigned By: _____

Project Number: 19080
Boring: B-6

Current Date: 11/4/2005

Sample Number	Depth in Feet	Visual Classification	USCS	E(f)	W%	Dry Dens (pcf)	Wet Dens (pcf)	Sat %	Shear Test Type	Angle	Cohesion (psf)	Unconf. Comp. Str.	LL	PL	PI	TORVANE (tsf)	Other Tests
15B	42.8	M GR CH3 W/ LYS & LNS SP	CH3		81												
15C	43.7	M GR CH3 W/ ARS & LNS SM, SIF	CH3	6	63	61	99	95	UC	--	514	1029				0.300	
15D	44.6	M GR CH3 W/ LYS & LNS SP	CH3		66												
16A	46.0	ST GR CH4 W/ LNS & ARS SM, SIF, SL	CH4		66												
16B	46.8	ST GR CH4 W/ LNS & ARS SM, SIF, SL	CH4		69												
16C	47.7	ST GR CH4 W/ LNS & ARS SM, SIF, SL	CH4		68												
16D	48.6	ST GR CH4 W/ LNS & ARS SM, SIF, SL	CH4		63												
17A	50.0	ST GR CH4 W/ LNS SM, SIF, SL	CH4		59												
17B	50.8	ST GR CH4 W/ LNS SM, SIF, SL	CH4		57												
17C	51.7	ST GR CH4 W/ LNS SM, SIF, SL	CH4		59												
17D	52.6	ST GR CH4 W/ LNS SM, SIF, SL	CH4		62												
18A	54.0	ST GR CH4 W/ SIF, SL	CH4		61												
18B	54.8	ST GR CH4 W/ SIF, SL	CH4		58												
18C	55.7	ST GR CH4 W/ SIF, SL	CH4		59												
18D	56.6	ST GR CH4 W/ SIF, SL	CH4		57												
19A	58.0	ST GR CH4 W/ SL	CH4		58												
19B	58.8	ST GR CH4 W/ SL	CH4		54												
19C	59.7	ST GR CH4 W/ SL	CH4		52												
19D	60.6	ST GR CH4 W/ SL, SIF	CH4		55												
20A	62.0	ST GR CH4 W/ SIF	CH4		49												
20B	62.8	ST GR CH4	CH4		43												
20C	63.7	ST GR CH4	CH4		54												
20D	64.6	ST GR CH4 W/ SIF, WD	CH4		58												
21A	66.0	ST GR & BR CH4 W/ WD, SL	CH4		110												
21B	66.8	ST GR & BR CH4 W/ WD, SL	CH4		85												
21C	67.7	ST GR & BR CH4 W/ WD, SL	CH4		75												
21D	68.6	ST GR & BR CH4 W/ WD, SL	CH4		73												
22A	70.0	ST GR CH4	CH4		65												
22B	70.8	ST LGR & BR CL6 W/ WD	CL6		30												
22C	71.7	M LGR CL6	CL6		22												
22D	72.6	ST LGR CH2	CH2		26												
23A	74.0	ST LGR & T CL6	CL6		24												
23B	74.8	VST LGR & GNGR CH4 W/ LNS & ARS ML & SM	CH4		30												
23C	75.7	VST LGR & GNGR CH4 W/ LNS & ARS ML & SM	CH4		40												

5

6 = Pleistocene

Figure 9c. Lab summary data sheet for Boring B-6; 5=bay sound-estuarine over Pleistocene.

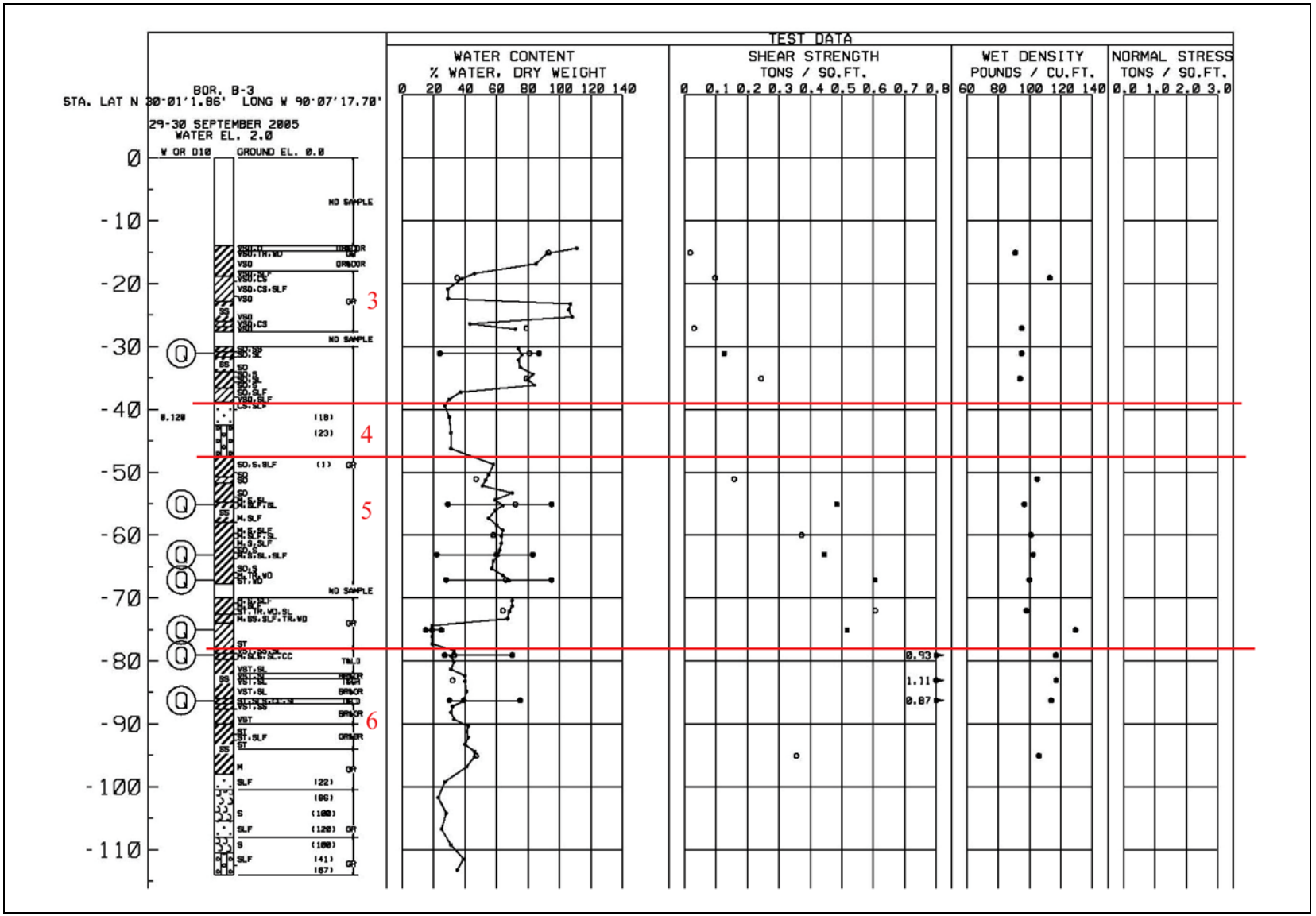

Figure 10a. Soil profile for Boring B-3; 3 = lacustrine, 4= relict beach, 5 = bay sound-estaurine, 6 = Pleistocene.

SUMMARY OF LABOR. ORY TEST RESULTS

Project: USACE - 17TH STREET CANAL Assigned By: _____

Project Number: 19080 Current Date: 11/4/2005
Boring: B-3

Sample Number	Depth in Feet	Visual Classification	USCS	E(f)	W%	Dry Dens (pcf)	Wet Dens (pcf)	Sat %	Shear Test Type	Angle	Cohesion (psf)	Unconf. Comp. Str.	LL	PL	PI	TORVANE (tsf)	Other Tests
NS	0.0	WATER	NS														
1A	14.0	VSO GR & DGR CH4 W/ O	CH4		111												
1B	14.8	VSO GR CH4 W/ TR-WD	CH4	3	93	47	91	97	UC	--	37	74				0.070	
1C	15.7	VSO GR & DGR CH4	CH4		85												
2A	18.0	VSO GR CH2 W/ SIF	CH2		46												
2B	18.8	VSO GR CL4 W/ ARS CH	CL4	20	35	84	113	94	UC	--	196	391				0.110	
2C	19.7	VSO GR CL4 W/ LYS CH, SIF	CL4		29												
3A	22.0	VSO GR CL4	CL4		29												
3B	22.8	VSO GR CH3 W/ LNS & LYS SM	CH3		107												
3C	23.7	VSO GR CH3 W/ LNS & LYS SM	CH3		106												
3D	24.6	VSO GR CH3 W/ LNS & LYS SM	CH3		108												
4A	26.0	VSO GR CL4 W/ LYS CH	CL4		43												
4B	26.8	VSO GR CH4	CH4	4	79	53	95	98	UC	--	61	122				0.110	
NS	27.7	NO SAMPLE	NS														
5A	30.0	SO GR CH4 W/ LNS SM	CH4		74												
5B	30.8	SO GR CH4 W/ SL	CH4		76				UU	0			87	24	63	0.200	
5C	31.7	SO GR CH4 W/ LNS SM	CH4		74												
5D	32.6	SO GR CH4 W/ LNS SM	CH4		75												
6A	34.0	SO GR CH4 W/ ARS SM	CH4		83												
6B	34.8	SO GR CH4 W/ SL	CH4	4	79	53	94	96	UC	--	488	976				0.230	
6C	35.7	SO GR CH4 W/ ARS SM	CH4		84												
6D	36.6	SO GR CL5 W/ SIF	CL5		37												
7A	38.0	VSO GR CL3 W/ SIF	CL3		30												
7B	38.8	GR SP W/ ARS CH, SIF	SP		27												
8	40.0	GR SP	SP		30												PD
9	42.5	GR SM1	SM1		31												
10	45.0	GR SM1	SM1		31												
11	47.5	SO GR CH3 W/ ARS SM, SIF	CH3		58												
12A	50.0	SO GR CH2	CH2		55												
12B	50.8	SO GR CL5	CL5	8	47	72	105	93	UC	--	316	632				0.280	
12C	51.7	SO GR CH2	CH2		51												
12D	52.6	SO GR CH2	CH2		70												
13A	54.0	M GR CH4 W/ ARS SM, SL	CH4		59												
13B	54.8	M GR CH4 W/ LNS SM, SIF, SL	CH4		72	55	95	95	UU	0	970		95	29	66	0.300	
13C	55.7	M GR CH3 W/ ARS & LNS SM, SIF	CH3		59												
13D	56.6	M GR CH3 W/ ARS & LNS SM, SIF	CH3		55												
14A	58.0	M GR CH3 W/ ARS SM, SIF	CH3		60												

3
4
5

Figure 10b. Lab summary data sheet for Boring B-3; 3 = lacustrine, 4= relict beach, 5 = bay sound-estaurine

SUMMARY OF LABOR...ORY TEST RESULTS

Project: USACE - 17TH STREET CANAL Assigned By: _____

Project Number: 19080
Boring: B-3

Current Date: 11/4/2005

Sample Number	Depth in Feet	Visual Classification	USCS	E(f)	W%	Dry Dens (pcf)	Wet Dens (pcf)	Sat %	Shear Test Type	Angle	Cohesion (psf)	Unconf. Comp. Str.	LL	PL	PI	TORVANE (tsf)	Other Tests
14B	58.8	M GR CH3 W/ ARS SM, SIF	CH3		64												
14C	59.7	M GR CH4 W/ SIF	CH4	3	58	64	101	95	UC	--	745	1490				0.350	
14D	60.6	M GR CH3 W/ ARS SM, SIF	CH3		63												
15A	62.0	SO GR CH4 W/ ARS SM	CH4		62												
15B	62.8	M GR CH4 W/ ARS SM, SL, SIF	CH4		60	63	100	96	UU	0	890		83	22	61	0.370	
15C	63.7	SO GR CH4 W/ ARS SM	CH4		58												
15D	64.6	SO GR CH4 W/ ARS SM	CH4		57												
16A	66.0	M GR CH4 W/ TR-WD 5	CH4		64												
16B	66.8	ST GR CH4 W/ WD	CH4		66	59	98	95	UU	0	1210		95	28	67	0.400	
NS	67.7	NO SAMPLE	NS														
17A	70.0	M GR CH4 W/ ARS SM, SIF	CH4		70												
17B	70.8	M GR CH4 W/ SIF	CH4		70												
17C	71.7	ST GR CH4 W/ TR-WD, SL	CH4	3	64	60	98	95	UC	--	1213	2425				0.400	
17D	72.6	M GR CH4 W/ SIF, TR-WD, LYS SM	CH4		67												
18A	74.0	ST GR CL3	CL3		19												
18B	74.8	ST GR CL3 6	CL3		19	105	124	82	UU	0	1033		25	15	10	0.650	
18C	75.7	ST GR CL3	CL3		19												
18D	76.6	ST GR CL3	CL3		19												
19A	78.0	VST T & LGR CH3 W/ LNS SM, SL	CH3		33												
19B	78.8	M T & LGR CH3 W/ LNS & LYS ML, SL, CC	CH3		33	86	115	92	UU	0	933		70	27	43	0.625	
19C	79.7	VST T & LGR CH3 W/ LNS SM, SL	CH3		33												
19D	80.6	VST T & LGR CH3 W/ LNS SM, SL	CH3		31												
20A	82.0	VST BR & GR CH4 W/ LNS SM, SL	CH4		40												
20B	82.8	VST T & GR CH4 W/ LNS SM, SL	CH4	3	32	88	117	94	UC	--	2212	4424				0.875	
20C	83.7	VST BR & GR CH4 W/ LNS SM, SL	CH4		41												
21A	86.0	ST T & LGR CH4 W/ LNS ML, CC, SL	CH4		39	81	113	96	UU	0	1746		75	30	45	0.800	
21B	86.8	VST BR & GR CH3 W/ LNS SM	CH3		32												
21C	87.7	VST BR & GR CH2	CH2		31												
21D	88.6	VST BR & GR CH2	CH2		33												
22A	90.0	ST GR & BR CH3 W/ ARS & LNS SM	CH3		42												
22B	90.8	ST GR & BR CH3 W/ ARS & LNS SM	CH3		41												
22C	91.7	ST GR & BR CH3 W/ ARS & LNS SM, SIF	CH3		42												
22D	92.6	ST GR & BR CH4 W/ ARS & LNS SM	CH4		40												
23A	94.0	M GR CH4 W/ LNS SM	CH4		46												
23B	94.8	M GR CH4 W/ LNS SP	CH4	9	47	72	106	93	UC	--	712	1424				0.380	
23C	95.7	M GR CH3 W/ LNS SM	CH3		41												
24	98.0	GR SP W/ SIF	SP		27												

Figure 10c. Lab summary data sheet boring B-3, 5 = bay sound-estaurine, 6 = Pleistocene

SUMMARY OF LABOR. ORY TEST RESULTS

Project: USACE - 17TH STREET CANAL Assigned By: _____

Project Number: 19080
Boring: B-3

Current Date: 11/4/2005

Sample Number	Depth in Feet	Visual Classification	USCS	E(f)	W%	Dry Dens (pcf)	Wet Dens (pcf)	Sat %	Shear Test Type	Angle	Cohesion (psf)	Unconf. Comp. Str.	LL	PL	PI	TORVANE (tsf)	Other Tests
25	100.5	SI W/ SP	SI		23												
26	103.0	SI W/ SP	SI		28												
27	105.5	GR SP W/ SIF	SP		25												
28	108.0	SI W/ SP	SI		31												
29	110.5	GR SM1	SM1		39												
30	112.5	GR SM1	SM1		35												

Figure 10d. Lab summary data sheet boring B-3

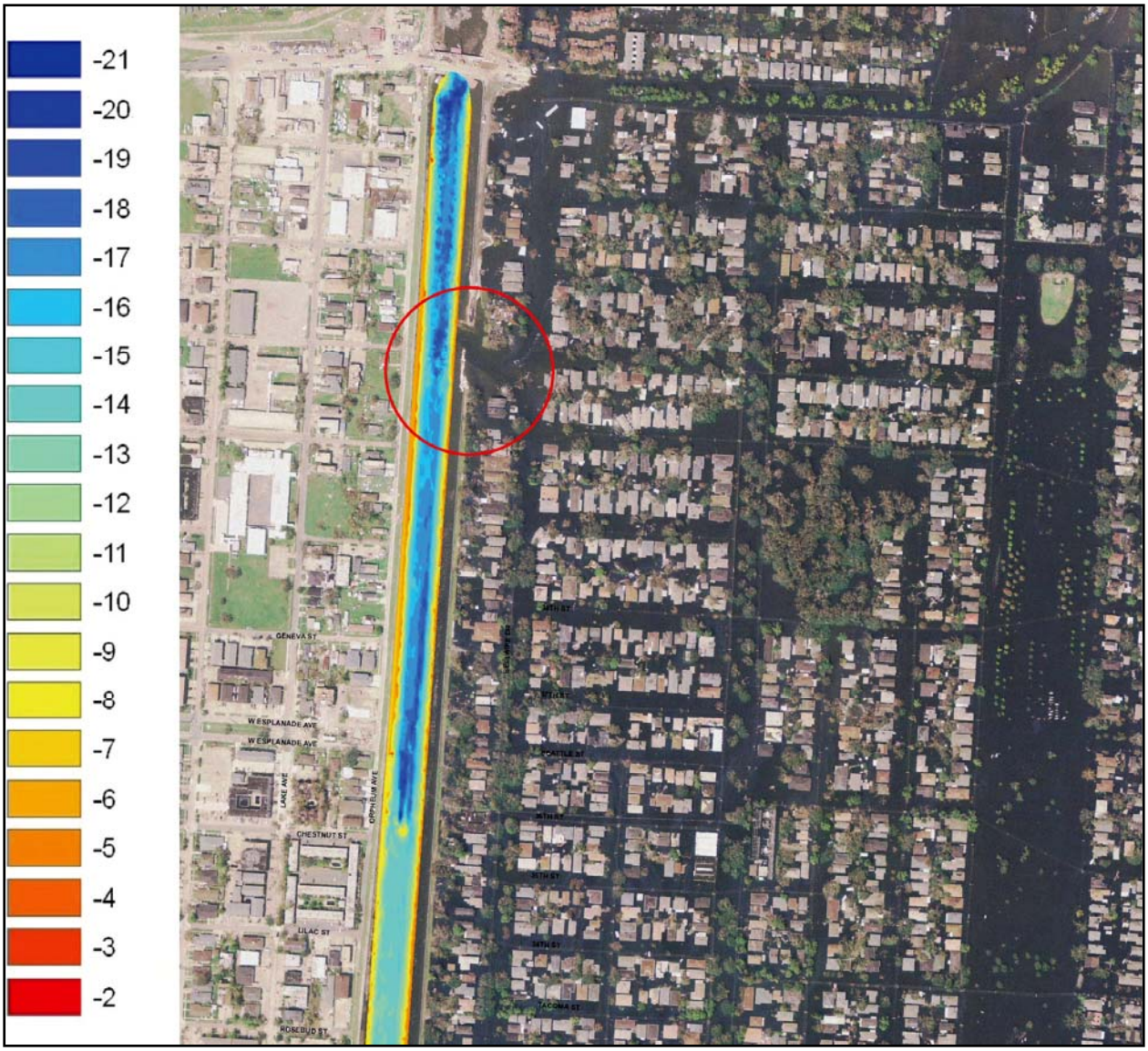

Figure 11. Multibeam elevation data from 17th Street canal from 26 September2006, values in ft NAVD88, note the elevation (or depth) of the canal adjacent to levee failure (area in red), also note the dredge cut mark near the lower (southern end) of the photo.

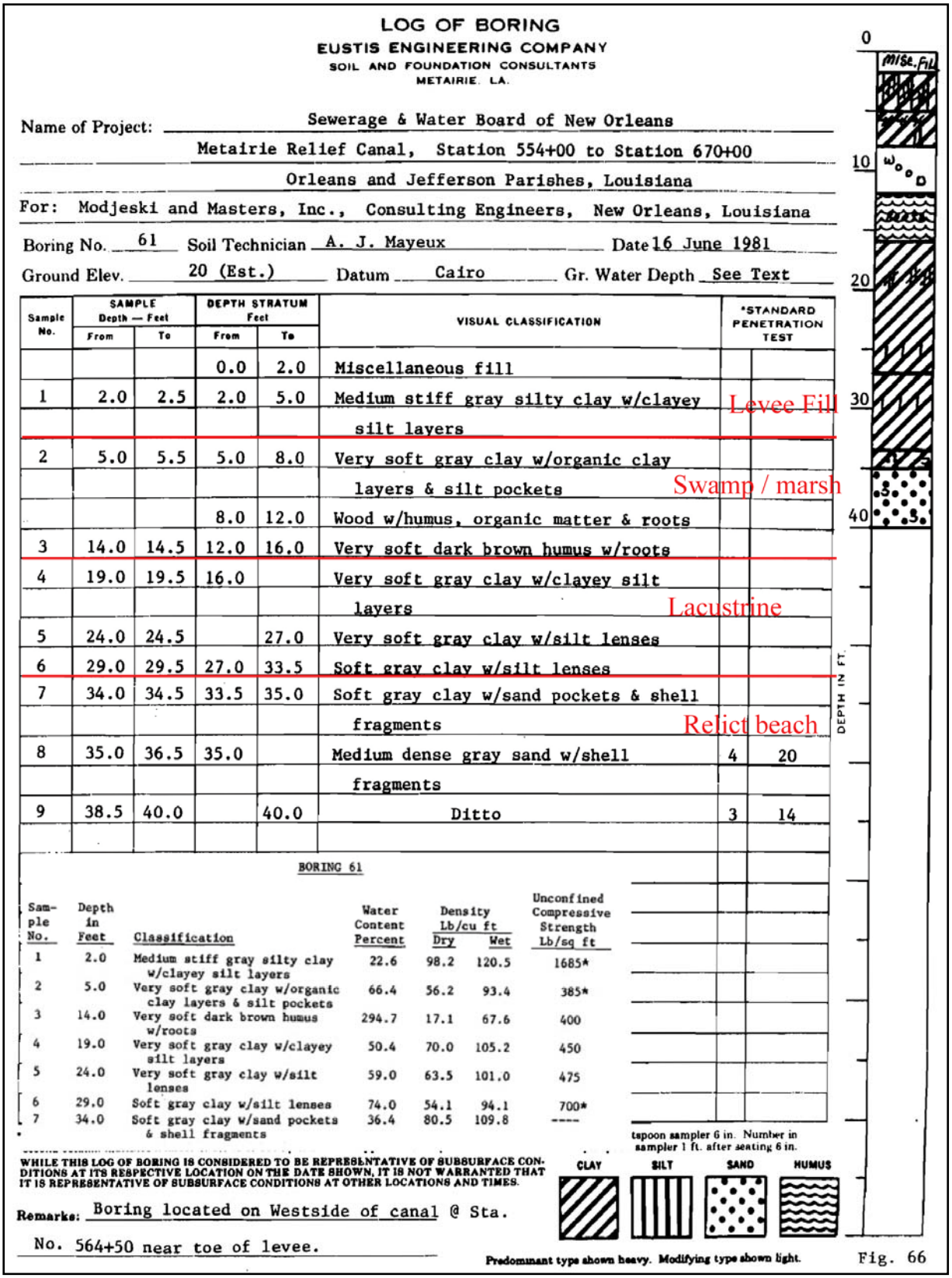

LOG OF BORING

EUSTIS ENGINEERING COMPANY

SOIL AND FOUNDATION CONSULTANTS

METAIRIE, LA.

Name of Project: Sewerage & Water Board of New Orleans

Metairie Relief Canal, Station 554+00 to Station 670+00

Orleans and Jefferson Parishes, Louisiana

For: Modjeski and Masters, Inc., Consulting Engineers, New Orleans, Louisiana

Boring No. 61 Soil Technician A. J. Mayeux Date 16 June 1981

Ground Elev. 20 (Est.) Datum Cairo Gr. Water Depth See Text

Sample No.	SAMPLE Depth — Feet From	To	DEPTH STRATUM Feet From	To	VISUAL CLASSIFICATION	*STANDARD PENETRATION TEST	
			0.0	2.0	Miscellaneous fill		
1	2.0	2.5	2.0	5.0	Medium stiff gray silty clay w/clayey silt layers		
2	5.0	5.5	5.0	8.0	Very soft gray clay w/organic clay layers & silt pockets		
			8.0	12.0	Wood w/humus, organic matter & roots		
3	14.0	14.5	12.0	16.0	Very soft dark brown humus w/roots		
4	19.0	19.5	16.0		Very soft gray clay w/clayey silt layers		
5	24.0	24.5		27.0	Very soft gray clay w/silt lenses		
6	29.0	29.5	27.0	33.5	Soft gray clay w/silt lenses		
7	34.0	34.5	33.5	35.0	Soft gray clay w/sand pockets & shell fragments		
8	35.0	36.5	35.0		Medium dense gray sand w/shell fragments	4	20
9	38.5	40.0		40.0	Ditto	3	14

BORING 61

Sample No.	Depth in Feet	Classification	Water Content Percent	Density Lb/cu ft Dry	Density Lb/cu ft Wet	Unconfined Compressive Strength Lb/sq ft
1	2.0	Medium stiff gray silty clay w/clayey silt layers	22.6	98.2	120.5	1685*
2	5.0	Very soft gray clay w/organic clay layers & silt pockets	66.4	56.2	93.4	385*
3	14.0	Very soft dark brown humus w/roots	294.7	17.1	67.6	400
4	19.0	Very soft gray clay w/clayey silt layers	50.4	70.0	105.2	450
5	24.0	Very soft gray clay w/silt lenses	59.0	63.5	101.0	475
6	29.0	Soft gray clay w/silt lenses	74.0	54.1	94.1	700*
7	34.0	Soft gray clay w/sand pockets & shell fragments	36.4	80.5	109.8	----

tspoon sampler 6 in. Number in sampler 1 ft. after seating 6 in.

WHILE THIS LOG OF BORING IS CONSIDERED TO BE REPRESENTATIVE OF SUBSURFACE CONDITIONS AT ITS RESPECTIVE LOCATION ON THE DATE SHOWN, IT IS NOT WARRANTED THAT IT IS REPRESENTATIVE OF SUBSURFACE CONDITIONS AT OTHER LOCATIONS AND TIMES.

Remarks: Boring located on Westside of canal @ Sta. No. 564+50 near toe of levee.

CLAY SILT SAND HUMUS

Predominant type shown heavy. Modifying type shown light.

Fig. 66

Figure 12. Design boring 61 and lab data (USACE, 1990)

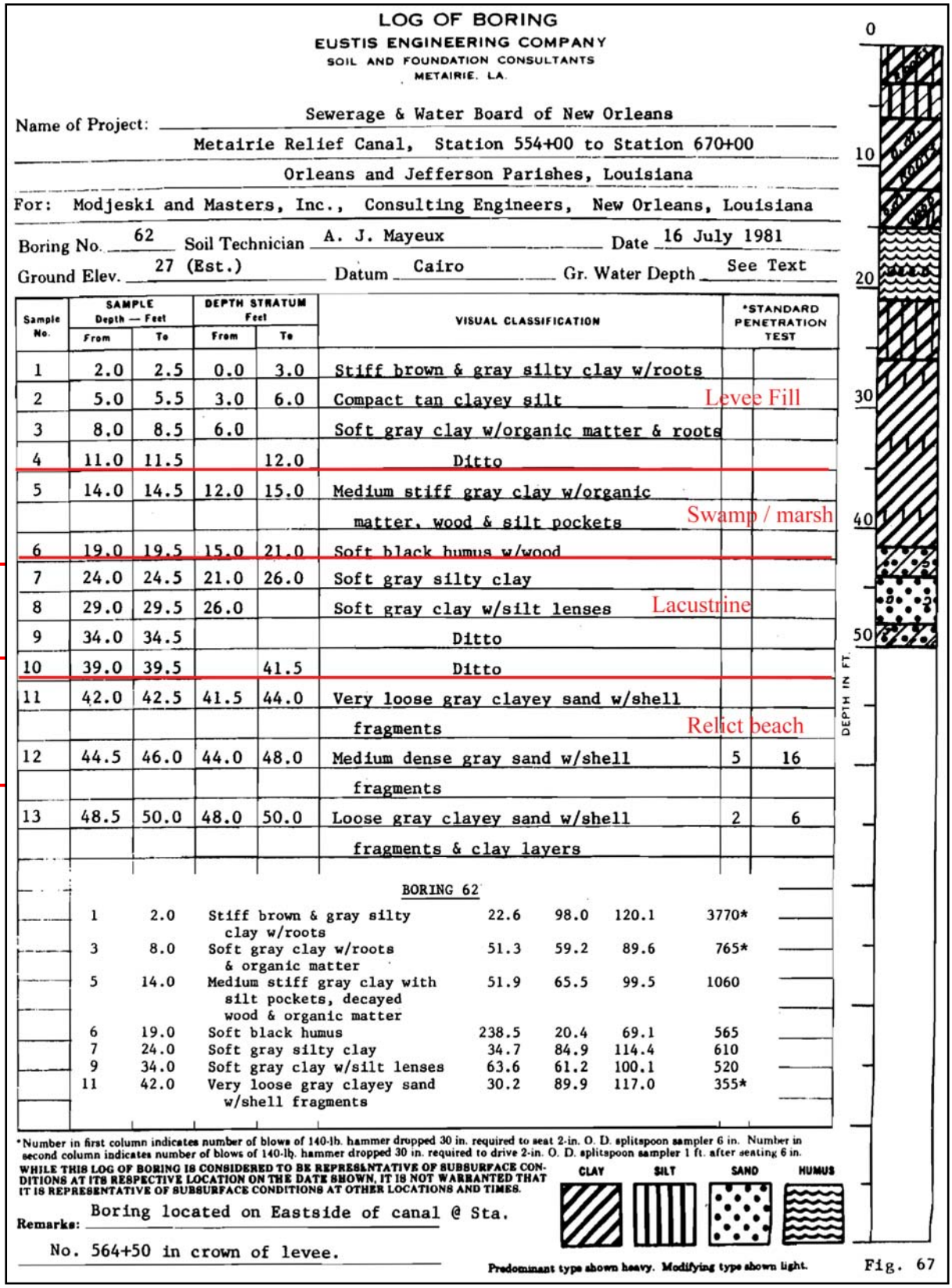

LOG OF BORING

EUSTIS ENGINEERING COMPANY

SOIL AND FOUNDATION CONSULTANTS

METAIRIE, LA.

Name of Project: Sewerage & Water Board of New Orleans

Metairie Relief Canal, Station 554+00 to Station 670+00

Orleans and Jefferson Parishes, Louisiana

For: Modjeski and Masters, Inc., Consulting Engineers, New Orleans, Louisiana

Boring No. 62 Soil Technician A. J. Mayeux Date 16 July 1981

Ground Elev. 27 (Est.) Datum Cairo Gr. Water Depth See Text

Sample No.	SAMPLE Depth — Feet From	To	DEPTH STRATUM Feet From	To	VISUAL CLASSIFICATION	*STANDARD PENETRATION TEST	
1	2.0	2.5	0.0	3.0	Stiff brown & gray silty clay w/roots		
2	5.0	5.5	3.0	6.0	Compact tan clayey silt		
3	8.0	8.5	6.0		Soft gray clay w/organic matter & roots		
4	11.0	11.5		12.0	Ditto		
5	14.0	14.5	12.0	15.0	Medium stiff gray clay w/organic matter, wood & silt pockets		
6	19.0	19.5	15.0	21.0	Soft black humus w/wood		
7	24.0	24.5	21.0	26.0	Soft gray silty clay		
8	29.0	29.5	26.0		Soft gray clay w/silt lenses		
9	34.0	34.5			Ditto		
10	39.0	39.5		41.5	Ditto		
11	42.0	42.5	41.5	44.0	Very loose gray clayey sand w/shell fragments		
12	44.5	46.0	44.0	48.0	Medium dense gray sand w/shell fragments	5	16
13	48.5	50.0	48.0	50.0	Loose gray clayey sand w/shell fragments & clay layers	2	6

Levee Fill

Swamp / marsh

Lacustrine

Relict beach

BORING 62

1	2.0	Stiff brown & gray silty clay w/roots	22.6	98.0	120.1	3770*
3	8.0	Soft gray clay w/roots & organic matter	51.3	59.2	89.6	765*
5	14.0	Medium stiff gray clay with silt pockets, decayed wood & organic matter	51.9	65.5	99.5	1060
6	19.0	Soft black humus	238.5	20.4	69.1	565
7	24.0	Soft gray silty clay	34.7	84.9	114.4	610
9	34.0	Soft gray clay w/silt lenses	63.6	61.2	100.1	520
11	42.0	Very loose gray clayey sand w/shell fragments	30.2	89.9	117.0	355*

*Number in first column indicates number of blows of 140-lb. hammer dropped 30 in. required to seat 2-in. O. D. splitspoon sampler 6 in. Number in second column indicates number of blows of 140-lb. hammer dropped 30 in. required to drive 2-in. O. D. splitspoon sampler 1 ft. after seating 6 in.

WHILE THIS LOG OF BORING IS CONSIDERED TO BE REPRESENTATIVE OF SUBSURFACE CONDITIONS AT ITS RESPECTIVE LOCATION ON THE DATE SHOWN, IT IS NOT WARRANTED THAT IT IS REPRESENTATIVE OF SUBSURFACE CONDITIONS AT OTHER LOCATIONS AND TIMES.

Remarks: Boring located on Eastside of canal @ Sta. No. 564+50 in crown of levee.

CLAY SILT SAND HUMUS

Predominant type shown heavy. Modifying type shown light.

DEPTH IN FT. 0 10 20 30 40 50

Fig. 67

Figure 13. Design boring 62 and lab data (USACE, 1990)

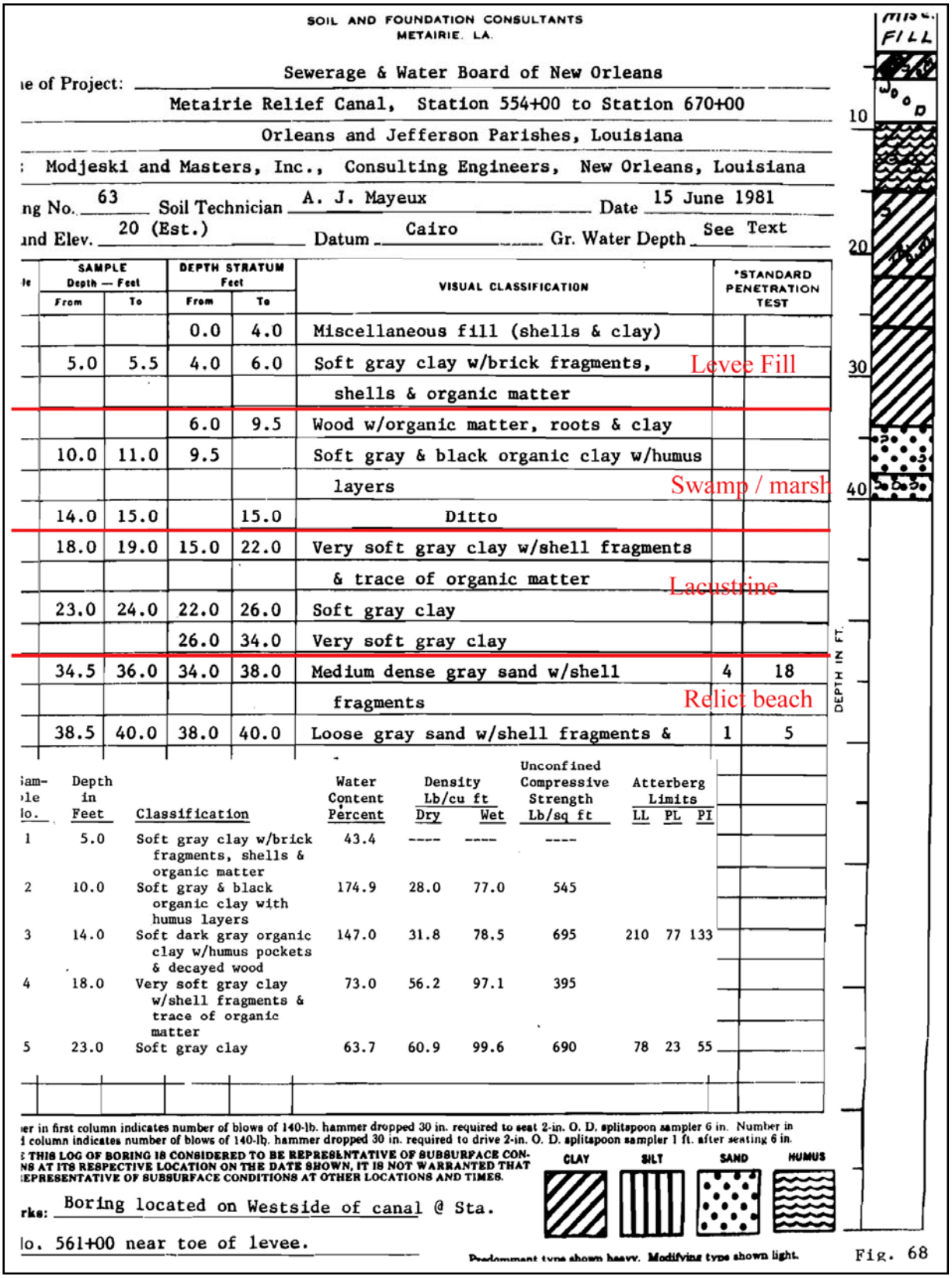

SOIL AND FOUNDATION CONSULTANTS
METAIRIE, LA.

ıe of Project: Sewerage & Water Board of New Orleans
Metairie Relief Canal, Station 554+00 to Station 670+00
Orleans and Jefferson Parishes, Louisiana
: Modjeski and Masters, Inc., Consulting Engineers, New Orleans, Louisiana
ng No. 63 Soil Technician A. J. Mayeux Date 15 June 1981
ınd Elev. 20 (Est.) Datum Cairo Gr. Water Depth See Text

le	SAMPLE Depth — Feet From	To	DEPTH STRATUM Feet From	To	VISUAL CLASSIFICATION	*STANDARD PENETRATION TEST	
			0.0	4.0	Miscellaneous fill (shells & clay)		
	5.0	5.5	4.0	6.0	Soft gray clay w/brick fragments, shells & organic matter		
			6.0	9.5	Wood w/organic matter, roots & clay		
	10.0	11.0	9.5		Soft gray & black organic clay w/humus layers		
	14.0	15.0		15.0	Ditto		
	18.0	19.0	15.0	22.0	Very soft gray clay w/shell fragments & trace of organic matter		
	23.0	24.0	22.0	26.0	Soft gray clay		
			26.0	34.0	Very soft gray clay		
	34.5	36.0	34.0	38.0	Medium dense gray sand w/shell fragments	4	18
	38.5	40.0	38.0	40.0	Loose gray sand w/shell fragments &	1	5

ıam-ple lo.	Depth in Feet	Classification	Water Content Percent	Density Lb/cu ft Dry	Density Lb/cu ft Wet	Unconfined Compressive Strength Lb/sq ft	Atterberg Limits LL	PL	PI
1	5.0	Soft gray clay w/brick fragments, shells & organic matter	43.4	----	----	----			
2	10.0	Soft gray & black organic clay with humus layers	174.9	28.0	77.0	545			
3	14.0	Soft dark gray organic clay w/humus pockets & decayed wood	147.0	31.8	78.5	695	210	77	133
4	18.0	Very soft gray clay w/shell fragments & trace of organic matter	73.0	56.2	97.1	395			
5	23.0	Soft gray clay	63.7	60.9	99.6	690	78	23	55

ıer in first column indicates number of blows of 140-lb. hammer dropped 30 in. required to seat 2-in. O. D. splitspoon sampler 6 in. Number in d column indicates number of blows of 140-lb. hammer dropped 30 in. required to drive 2-in. O. D. splitspoon sampler 1 ft. after seating 6 in.

: THIS LOG OF BORING IS CONSIDERED TO BE REPRESENTATIVE OF SUBSURFACE CONDITIONS AT ITS RESPECTIVE LOCATION ON THE DATE SHOWN, IT IS NOT WARRANTED THAT IEPRESENTATIVE OF SUBSURFACE CONDITIONS AT OTHER LOCATIONS AND TIMES.

rks: Boring located on Westside of canal @ Sta. lo. 561+00 near toe of levee.

CLAY SILT SAND HUMUS

Predominant type shown heavy. Modifying type shown light.

Fig. 68

Figure 14. Design boring 63 and lab data (USACE, 1990)

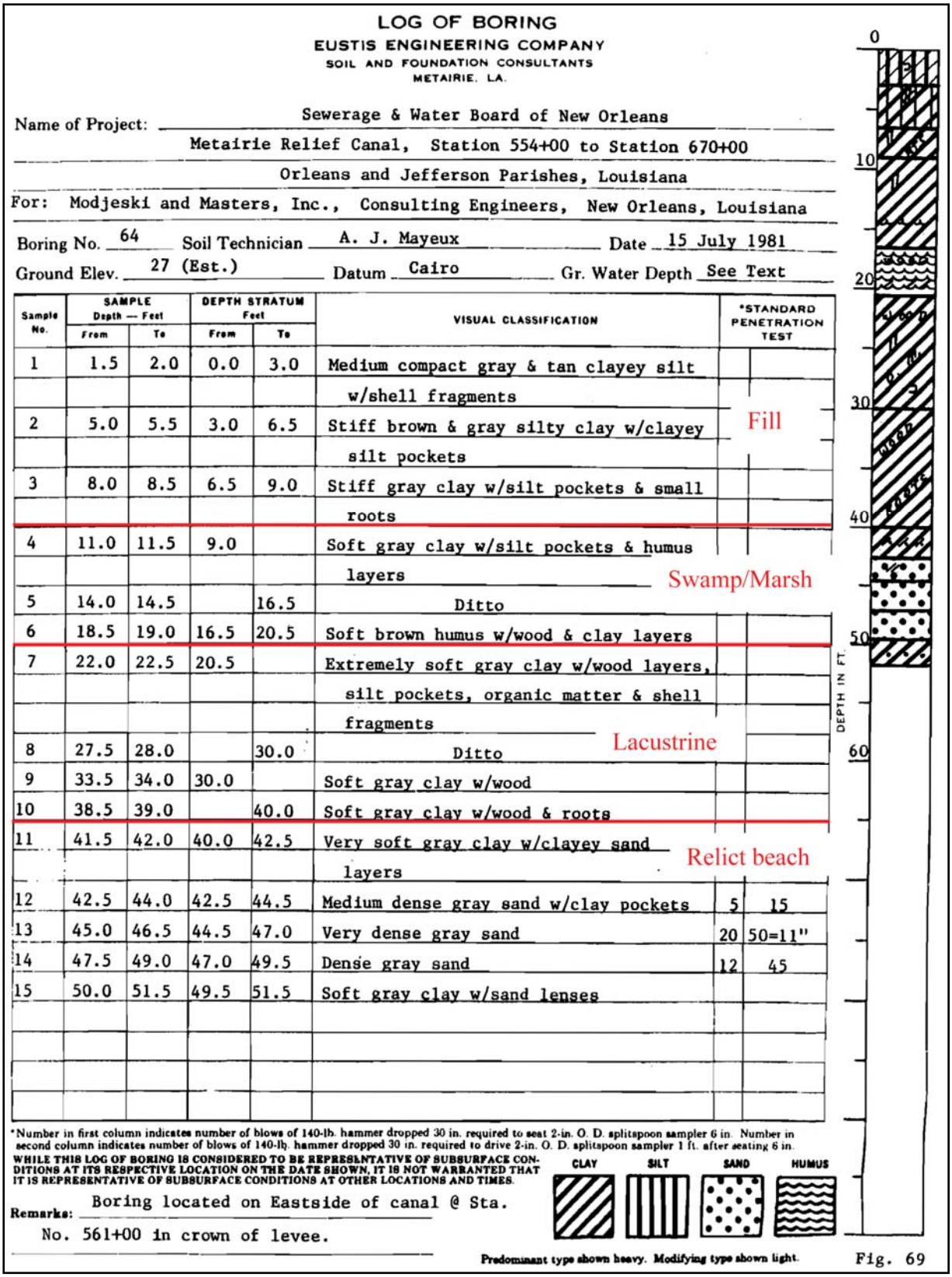

LOG OF BORING

EUSTIS ENGINEERING COMPANY

SOIL AND FOUNDATION CONSULTANTS

METAIRIE, LA.

Name of Project: Sewerage & Water Board of New Orleans

Metairie Relief Canal, Station 554+00 to Station 670+00

Orleans and Jefferson Parishes, Louisiana

For: Modjeski and Masters, Inc., Consulting Engineers, New Orleans, Louisiana

Boring No. 64 Soil Technician A. J. Mayeux Date 15 July 1981

Ground Elev. 27 (Est.) Datum Cairo Gr. Water Depth See Text

Sample No.	SAMPLE Depth — Feet From	To	DEPTH STRATUM Feet From	To	VISUAL CLASSIFICATION	*STANDARD PENETRATION TEST	
1	1.5	2.0	0.0	3.0	Medium compact gray & tan clayey silt w/shell fragments		
2	5.0	5.5	3.0	6.5	Stiff brown & gray silty clay w/clayey silt pockets		
3	8.0	8.5	6.5	9.0	Stiff gray clay w/silt pockets & small roots		
4	11.0	11.5	9.0		Soft gray clay w/silt pockets & humus layers		
5	14.0	14.5		16.5	Ditto		
6	18.5	19.0	16.5	20.5	Soft brown humus w/wood & clay layers		
7	22.0	22.5	20.5		Extremely soft gray clay w/wood layers, silt pockets, organic matter & shell fragments		
8	27.5	28.0		30.0	Ditto		
9	33.5	34.0	30.0		Soft gray clay w/wood		
10	38.5	39.0		40.0	Soft gray clay w/wood & roots		
11	41.5	42.0	40.0	42.5	Very soft gray clay w/clayey sand layers		
12	42.5	44.0	42.5	44.5	Medium dense gray sand w/clay pockets	5	15
13	45.0	46.5	44.5	47.0	Very dense gray sand	20	50=11"
14	47.5	49.0	47.0	49.5	Dense gray sand	12	45
15	50.0	51.5	49.5	51.5	Soft gray clay w/sand lenses		

Fill

Swamp/Marsh

Lacustrine

Relict beach

DEPTH IN FT. 0 10 20 30 40 50 60

*Number in first column indicates number of blows of 140-lb. hammer dropped 30 in. required to seat 2-in. O. D. splitspoon sampler 6 in. Number in second column indicates number of blows of 140-lb. hammer dropped 30 in. required to drive 2-in. O. D. splitspoon sampler 1 ft. after seating 6 in.

WHILE THIS LOG OF BORING IS CONSIDERED TO BE REPRESENTATIVE OF SUBSURFACE CONDITIONS AT ITS RESPECTIVE LOCATION ON THE DATE SHOWN, IT IS NOT WARRANTED THAT IT IS REPRESENTATIVE OF SUBSURFACE CONDITIONS AT OTHER LOCATIONS AND TIMES.

Remarks: Boring located on Eastside of canal @ Sta. No. 561+00 in crown of levee.

CLAY SILT SAND HUMUS

Predominant type shown heavy. Modifying type shown light.

Fig. 69

Figure 15a. Design boring 64 (USACE, 1990)

BORING 64

2	5.0	Stiff brown & gray silty clay w/clayey silt pockets	19.6	99.2	118.6	2950*
4	11.0	Soft gray clay w/silt pockets	40.4	78.3	110.0	705
6	18.5	Soft brown humus w/clay layers & wood	246.6	----	----	----
7	22.0	Extremely soft gray clay w/silt pockets, organic matter & shell fragments	61.2	63.1	101.7	205
9	33.5	Soft gray clay	65.9	62.1	103.0	765
11	41.5	Very soft gray clay	71.4	57.2	98.1	335

Figure 15b. Lab data for design boring 64 (USACE, 1990)

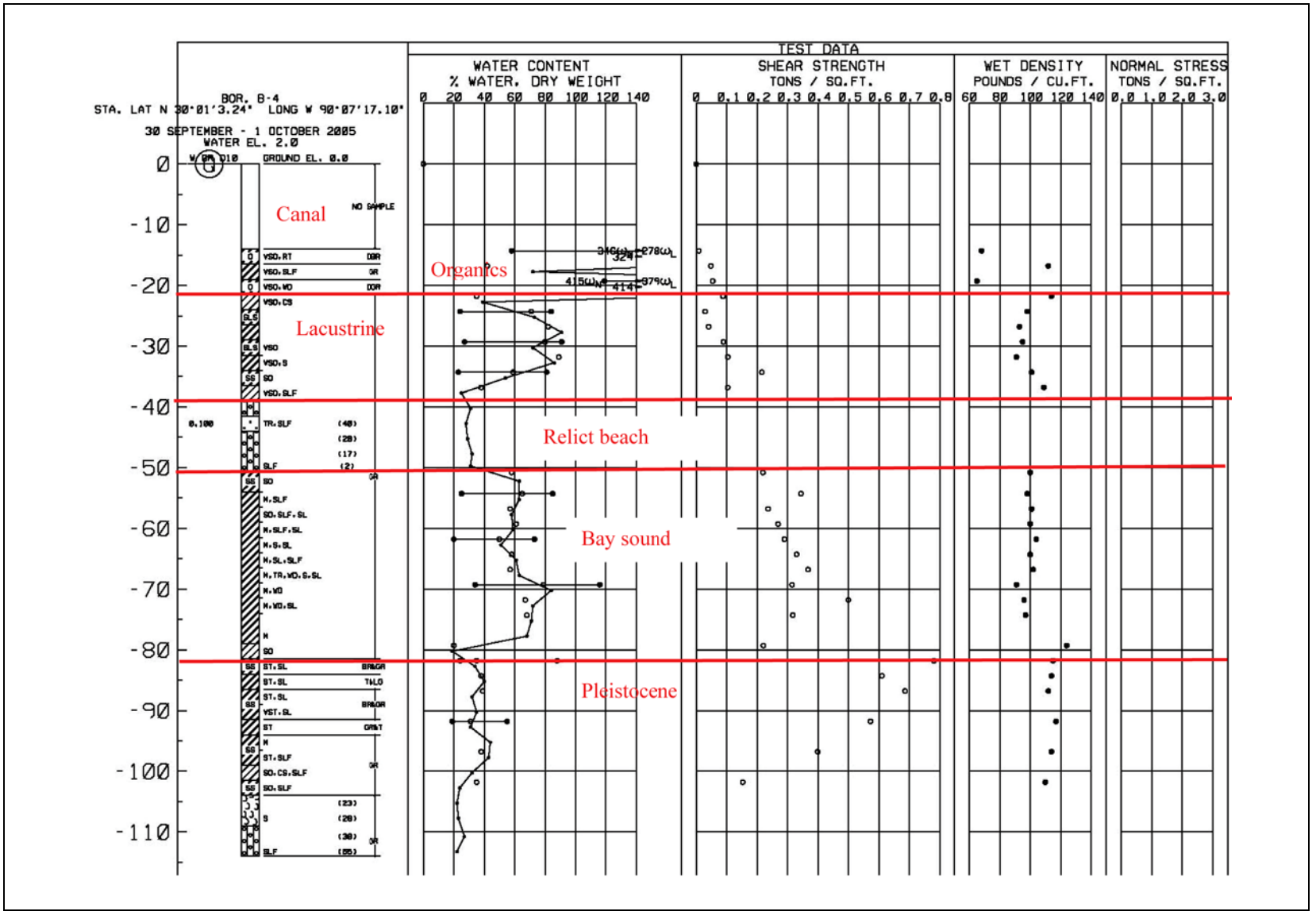

Figure 16a. Boring log for B-4

SUMMARY OF LABOR. ORY TEST RESULTS

Project: USACE - 17TH STREET CANAL Assigned By: _____

Project Number: 19080
Boring: B-4

Current Date: 11/4/2005

Sample Number	Depth in Feet	Visual Classification	USCS	E(f)	W%	Dry Dens (pcf)	Wet Dens (pcf)	Sat %	Shear Test Type	Angle	Cohesion (psf)	Unconf. Comp. Str.	LL	PL	PI	TORVANE (tsf)	Other Tests
NS	0.0	WATER	NS														
1	14.0	VSO DBR CHOC W/ RT	CHOC	10	346	15	68	94	UC	--	17	33	276	58	218		
2	16.5	VSO GR CH2 W/ SIF	CH2	14	42	79	112	99	UC	--	96	192				0.130	
3	19.0	VSO DGR CHOC W/ WD	CHOC	2	415	13	65	91	OB	--	112	223	379	119	260	0.100	
4	21.5	VSO GR CL4 W/ LYS CH	CL4	12	35	85	114	95	UC	--	175	349				0.070	
5	24.0	VSO GR CH3 W/ LNS ML	CH3	1	71	58	98	98	OB	--	59	117	84	24	60	0.070	
6	26.5	VSO GR CH4	CH4	4	82	51	93	96	UC	--	82	163				0.070	
7	29.0	VSO GR CH4 W/ LNS ML	CH4	2	80	53	95	98	OB	--	178	355	91	27	64	0.150	
8	31.5	VSO GR CH4 W/ ARS SM	CH4	5	89	48	91	95	UC	--	207	413				0.150	
9	34.0	SO GR CH3 W/ ARS & LNS SM	CH3	5	59	63	101	95	OB	--	432	863	81	23	58	0.200	
10	36.5	VSO GR CL5 W/ SIF	CL5	7	38	79	109	90	UC	--	206	412				0.150	
11	39.0	GR SM1	SM1		31												
12	41.5	GR SM1	SM1		28												
13	44.0	GR SM1	SM1		29												
14	46.5	GR SM1	SM1		32												
15	49.0	GR SM1 W/ SIF	SM1		31												
16	50.5	SO GR CH3 W/ LNS SM	CH3	4	58	63	100	94	UC	--	438	875				0.330	
17	54.0	M GR CH4 W/ SIF	CH4	5	65	59	98	94	OB	--	688	1376	85	25	60	0.400	
18	56.5	SO GR CH4 W/ SIF, SL	CH4	5	57	64	101	94	UC	--	473	945				0.370	
19	59.0	M GR CH4 W/ SIF, SL	CH4	7	61	62	100	95	UC	--	537	1073				0.350	
20	61.5	M GR CH4 W/ ARS SM, SL	CH4	5	50	69	104	94	OB	--	580	1159	73	20	53	0.370	
21	64.0	M GR CH4 W/ SL, SIF	CH4	11	58	63	100	93	UC	--	659	1318				0.400	
22	66.5	M GR CH4 W/ TR-WD, ARS SM, SL	CH4	6	57	65	102	95	UC	--	735	1470				0.390	
23	69.0	M GR CH4 W/ WD	CH4	3	79	51	91	91	OB	--	630	1259	116	34	82	0.400	
24	71.5	M GR CH4 W/ WD SI	CH4	8	67	58	96	93	UC	--	1000	2000				0.450	
25	74.0	M GR CH4	CH4	5	68	58	97	94	UC	--	634	1267				0.370	
26	76.5	M GR CH4	CH4		68												
27	79.0	SO GR CL3	CL3	7	20	103	124	86	UC	--	442	883				0.230	
28	81.5	ST BR & GR CH4 W/ LNS SM, SL	CH4	2	35	85	115	95	UC	--	1562	3124	88	24	64	1.250	
29	84.0	ST T & LGR CH4 W/ SL	CH4	4	38	82	114	97	OB	--	1220	2440				1.250	
30	86.5	ST BR & GR CH4 W/ LNS SM, SL	CH4	7	39	81	112	95	UC	--	1372	2744				1.000	
31	89.0	VST BR & GR CH4 W/ LNS SM, SL	CH4		35												
32	91.5	ST GR & T CH2	CH2	5	31	90	117	93	UC	--	1145	2289	55	19	36	0.625	
33	94.0	M GR CH3 W/ ARS & LNS SM	CH3		44												
34	96.5	ST GR CH4 W/ LNS SM, SIF	CH4	11	38	83	114	96	UC	--	798	1596				0.500	
35	99.0	SO GR CL3 W/ LYS CH, SIF	CL3		32												
36	101.5	SO GR CH3 W/ LNS & LYS SP, SIF	CH3	4	35	81	110	87	OB	--	305	610				0.300	

Organics

Lacustrine

Relict beach

Bay sound

Pleistocene

Remarks: _____
EUSTIS ENGINEERING COMPANY, INC.

Checked by: _____
File Name: 19080

Figure 16b. Lab summary data sheet for boring B-4 (continued)

SUMMARY OF LABOR ORY TEST RESULTS

Project: USACE - 17TH STREET CANAL Assigned By: _____

Project Number: 19080
Boring: B-4

Current Date: 11/4/2005

Sample Number	Depth in Feet	Visual Classification	USCS	E(f)	W%	Dry Dens (pcf)	Wet Dens (pcf)	Sat %	Shear Test Type	Angle	Cohesion (psf)	Unconf. Comp. Str.	LL	PL	PI	TORVANE (tsf)	Other Tests
37	104.0	SI W/ ARS SM	SI		22												
38	106.5	SI W/ ARS SM	SI		23												
39	109.0	GR SM1 W/ SIF	SM1		27												
40	112.5	GR SM1 W/ SIF	SM1		22												

Figure 16c. Lab summary data sheet for boring B-4.

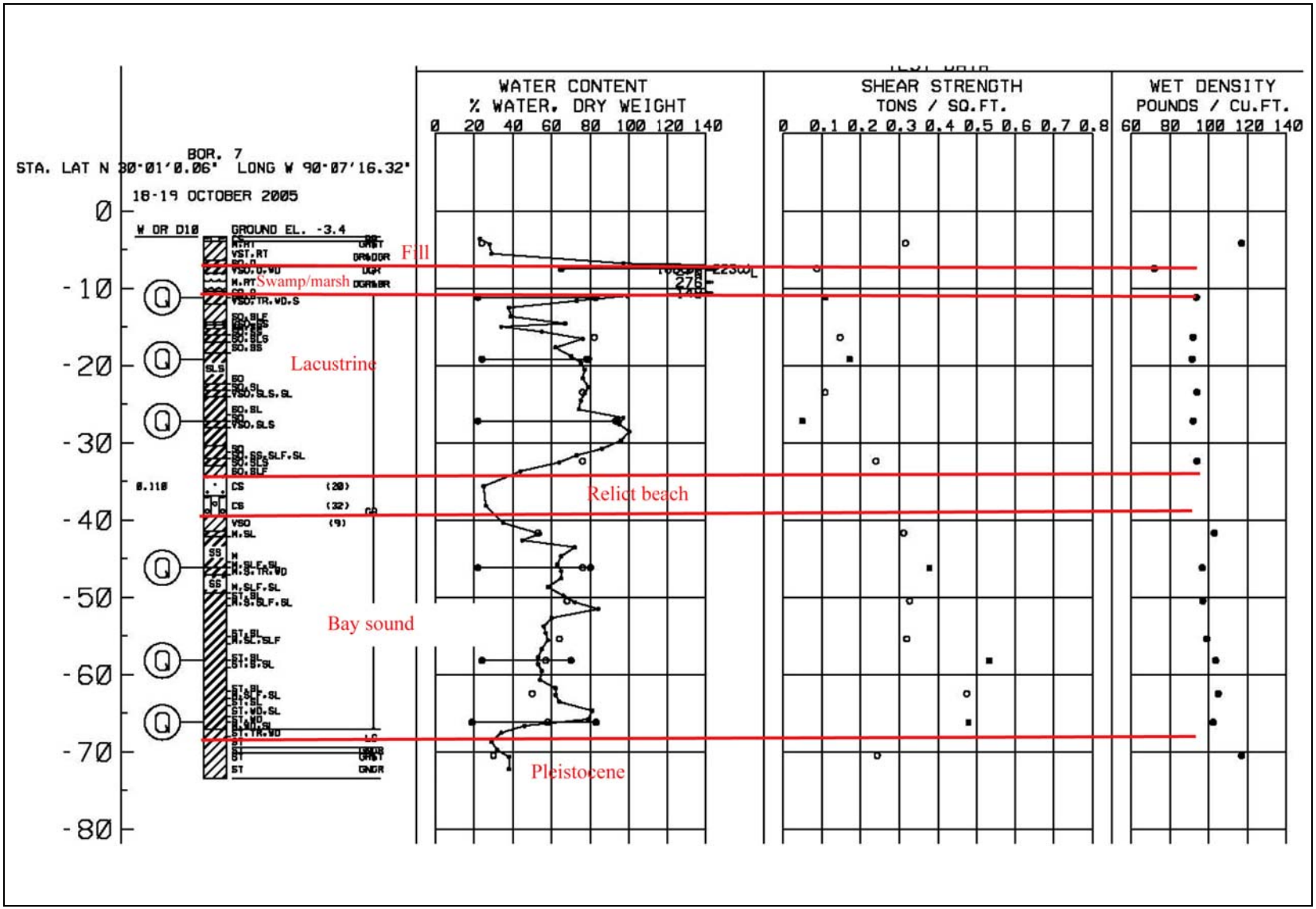

Figure 17a. Boring log for B-4

SUMMARY OF LABORATORY TEST RESULTS

Project: USACE - 17TH STREET CANAL Assigned By: _____

Project Number: 19080
Boring: B-7

Current Date: 11/4/2005

Sample Number	Depth in Feet	Visual Classification	USCS	E(f)	W%	Dry Dens (pcf)	Wet Dens (pcf)	Sat %	Shear Test Type	Angle	Cohesion (psf)	Unconf. Comp. Str.	LL	PL	PI	TORVANE (tsf)	Other Tests
1	0.0	BR SM1 W/ ARS CH	SM1		23												
2A	0.5	M GR & T CL6 W/ RT	CL6	9	24	94	117	83	UC	--	632	1265				0.875	
2B	1.3	VST GR & DGR CL5 W/ RT	CL5		29												
3A	3.0	SO GR & DGR CH4 W/ O	CH4		97												
3B	3.8	VSO DGR CHOB W/ WD	CHOB	7	186	25	72	89	UC	--	174	349				0.270	
3C	4.7	M DGR & BR PT W/ RT	PT		276												
4A1	7.0	SO DGR & BR CHOB	CHOB		148												
4A2	7.4	SO GR CH4 W/ O	CH4		99												
4B	7.8	SO GR CH4 W/ WD	CH4		73												
4C	8.7	SO GR CL6 W/ SIF	CL6		38												
4D	9.6	SO GR CL6 W/ SIF	CL6		39												
5A1	11.0	VSO GR CH4 W/ LNS SM	CH4		67												
5A2	11.4	SO GR CL4 W/ LNS SM	CL4		34												
5B	11.8	SO GR CH3 W/ LNS & LYS SM	CH3		55												
5C	12.7	SO GR CH3 W/ LNS & LYS SM	CH3		76												
5D	13.6	SO GR CH3 W/ LNS & LYS SM	CH3		62												
6A	15.0	SO GR CH4 W/ LNS & LYS ML	CH4		70												
6B	15.8	SO GR CH4 W/ LNS ML	CH4		75												
6C	16.7	SO GR CH4 W/ LNS ML	CH4		77												
6D	17.6	SO GR CH4 W/ LNS ML	CH4		76												
7A	19.0	SO GR CH4 W/ SL	CH4		79												
7B	19.8	VSO GR CH4 W/ LNS SM, SL	CH4	4	76	53	94	95	UC	--	217	435				0.100	
7C	20.7	SO GR CH4 W/ SL	CH4		75												
7D	21.6	SO GR CH4 W/ SL	CH4		74												
8A	23.0	SO GR CH4	CH4		97												
8B	23.8	SO GR CH4	CH4		95												
8C	24.7	SO GR CH4	CH4		100												
8D	25.6	SO GR CH4	CH4		96												
9A	27.0	SO GR CH4 W/ LNS SM	CH4		86												
9B	27.8	SO GR CH4 W/ LNS SM, SIF, SL	CH4		73												
9C	28.7	SO GR CH3 W/ LNS SM, SIF, SL	CH3		64												
9D	29.6	SO GR CL5 W/ SIF	CL5		44												
10	31.0	GR SM1 W/ ARS CH	SM1		25												
11	33.5	GR SM1 W/ ARS CH	SM1		26												
12	36.0	VSO GR CL3	CL3		35												
13A	38.0	M GR CH2 W/ SL	CH2	2	53	68	103	95	UC	--	622	1244				0.270	
13B	38.8	M GR CH3 W/ ARS & LNS SM	CH3		45												

Fill

Swamp/Marsh

Lacustrine

Relict beach

Bay sound

Remarks: _____ Checked by:

Figure 17b. Lab summary data sheet for boring B-7 (continued)

SUMMARY OF LABORATORY TEST RESULTS

Project: USACE - 17TH STREET CANAL Assigned By: _____

Project Number: 19080
Boring: B-7

Current Date: 11/4/2005

Sample Number	Depth in Feet	Visual Classification	USCS	E(f)	W%	Dry Dens (pcf)	Wet Dens (pcf)	Sat %	Shear Test Type	Angle	Cohesion (psf)	Unconf. Comp. Str.	LL	PL	PI	TORVANE (tsf)	Other Tests
13C	39.7	M GR CH3 W/ ARS & LNS SM	CH3		72												
13D	40.6	M GR CH3 W/ ARS & LNS SM	CH3		65												
14A	42.0	M GR CH3 W/ LNS SM, SIF, SL	CH3		63												
14B	42.8	M GR CH3 W/ LNS SM, SIF, SL	CH3		65												
14C	43.7	M GR CH3 W/ LNS SM, SIF, SL	CH3		65												
14D	44.6	M GR CH3 W/ LNS SM, SIF, SL	CH3		58												
15A	46.0	ST GR CH4 W/ SL	CH4		66												
15B	46.8	ST GR CH4 W/ SL	CH4		72												
15C	47.7	ST GR CH4 W/ SL Bay sound	CH4		84												
15D	48.6	ST GR CH4 W/ SL	CH4		60												
16A	50.0	ST GR CH4 W/ SL	CH4		56												
16B	50.8	ST GR CH4 W/ SL	CH4		57												
16C	51.7	M GR CH4 W/ SL, SIF	CH4	2	64	60	99	96	UC	--	639	1277				0.350	
16D	52.6	ST GR CH4 W/ SL	CH4		55												
17A	54.0	ST GR CH4 W/ SL	CH4		53												
17B	54.8	ST GR CH4 W/ SL	CH4		53												
17C	55.7	ST GR CH4 W/ SL	CH4		55												
17D	56.6	ST GR CH4 W/ SL	CH4		54												
18A	58.0	ST GR CH4 W/ SL	CH4		62												
18B	58.8	ST GR CH4 W/ SL	CH4		62												
18C	59.7	ST GR CH4 W/ SL	CH4		64												
18D	60.6	ST GR CH4 W/ WD, SL	CH4		81												
19A	62.0	ST GR CH4 W/ WD	CH4		79												
19B	62.8	ST GR CH4 W/ WD	CH4		46												
19C	63.7	ST LGR CL6 W/ TR-WD	CL6		34												
19D	64.6	ST LGR CL6	CL6		29												
20A	66.0	ST GNGR CL6	CL6		32												
20B	66.8	ST GNGR CL6 Pleistocene	CL6		38												
20C	67.7	ST GNGR CL6	CL6		38												

Remarks: _____
EUSTIS ENGINEERING COMPANY, INC.

Checked by: _____
File Name: 19080

Figure 17c. Lab summary data sheet for boring B-7

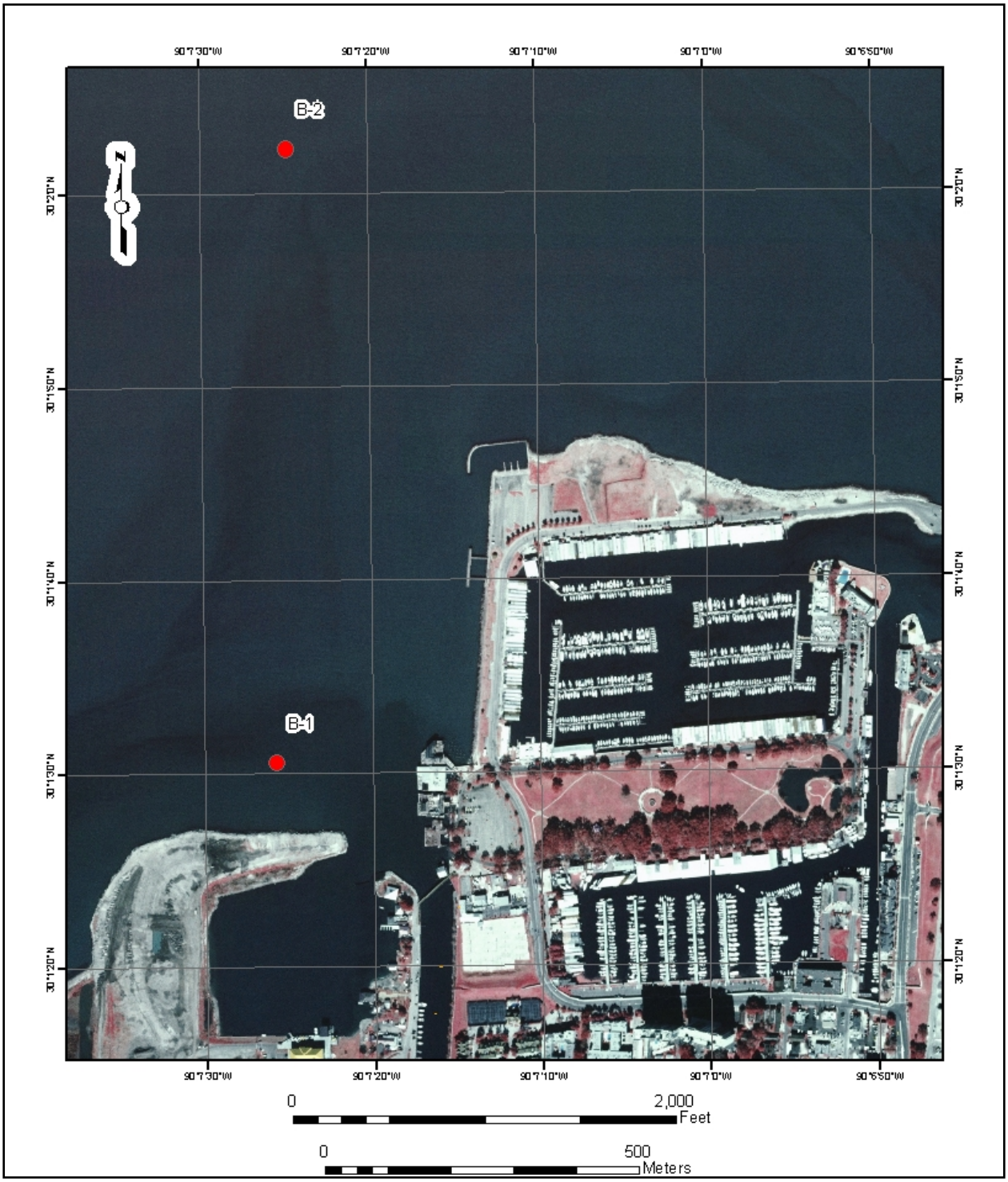

Figure 18. Lacustrine borings at the mouth of the 17th Street Canal to identify the general physical and engineering properties of lake sediments. Boring and laboratory soil test logs for B-1 and B2 are presented in Figures 19 and 20, respectively.

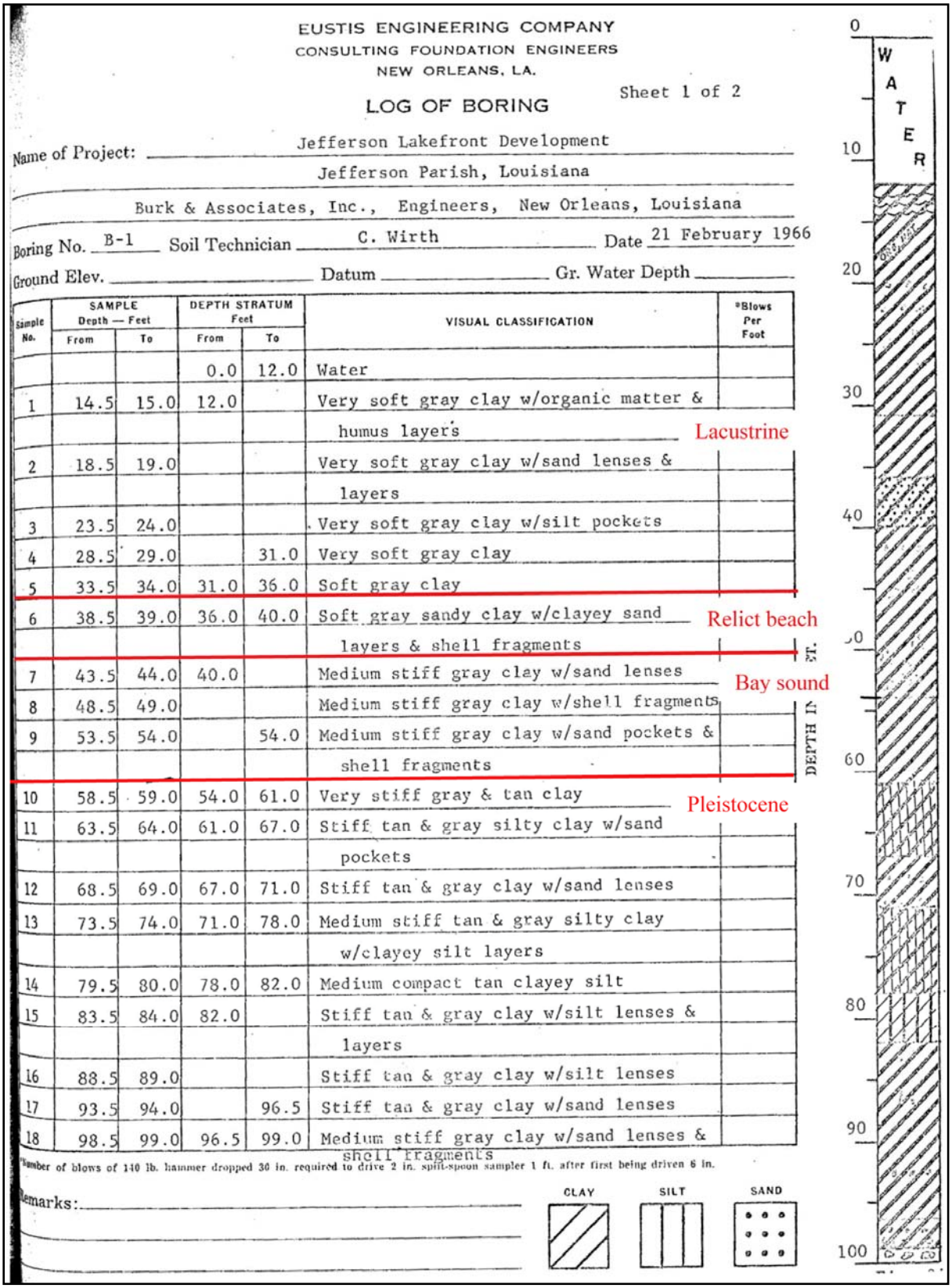

EUSTIS ENGINEERING COMPANY
CONSULTING FOUNDATION ENGINEERS
NEW ORLEANS, LA.

LOG OF BORING

Sheet 1 of 2

Name of Project: Jefferson Lakefront Development
Jefferson Parish, Louisiana

Burk & Associates, Inc., Engineers, New Orleans, Louisiana

Boring No. B-1 Soil Technician C. Wirth Date 21 February 1966

Ground Elev. _____ Datum _____ Gr. Water Depth _____

Sample No.	SAMPLE Depth — Feet From	To	DEPTH STRATUM Feet From	To	VISUAL CLASSIFICATION	*Blows Per Foot
			0.0	12.0	Water	
1	14.5	15.0	12.0		Very soft gray clay w/organic matter & humus layers	
2	18.5	19.0			Very soft gray clay w/sand lenses & layers	
3	23.5	24.0			Very soft gray clay w/silt pockets	
4	28.5	29.0		31.0	Very soft gray clay	
5	33.5	34.0	31.0	36.0	Soft gray clay	
6	38.5	39.0	36.0	40.0	Soft gray sandy clay w/clayey sand layers & shell fragments	
7	43.5	44.0	40.0		Medium stiff gray clay w/sand lenses	
8	48.5	49.0			Medium stiff gray clay w/shell fragments	
9	53.5	54.0		54.0	Medium stiff gray clay w/sand pockets & shell fragments	
10	58.5	59.0	54.0	61.0	Very stiff gray & tan clay	
11	63.5	64.0	61.0	67.0	Stiff tan & gray silty clay w/sand pockets	
12	68.5	69.0	67.0	71.0	Stiff tan & gray clay w/sand lenses	
13	73.5	74.0	71.0	78.0	Medium stiff tan & gray silty clay w/clayey silt layers	
14	79.5	80.0	78.0	82.0	Medium compact tan clayey silt	
15	83.5	84.0	82.0		Stiff tan & gray clay w/silt lenses & layers	
16	88.5	89.0			Stiff tan & gray clay w/silt lenses	
17	93.5	94.0		96.5	Stiff tan & gray clay w/sand lenses	
18	98.5	99.0	96.5	99.0	Medium stiff gray clay w/sand lenses & shell fragments	

*Number of blows of 140 lb. hammer dropped 30 in. required to drive 2 in. split-spoon sampler 1 ft. after first being driven 6 in.

Remarks: _____

CLAY SILT SAND

0 WATER 10 20 30 40 50 60 70 80 90 100 DEPTH IN FT.

Lacustrine
Relict beach
Bay sound
Pleistocene

Figure 19a. Boring B-1 drilled in Lake Pontchartrain (Eustis Engineering Company, 1966). Values shown are in feet. Boring location shown in Figure 18.

Subsoil Investigation
Jefferson Lakefront Development
Jefferson Parish, Louisiana

Burk & Associates, Inc., Engineers, New Orleans, Louisiana

SUMMARY OF LABORATORY TEST RESULTS

BORING 1

Sample No.	Depth Below Water Surface in Feet	Classification	Water Content Percent	Density Lbs./Cu.Ft. Dry	Density Lbs./Cu.Ft. Wet	Unconfined Compressive Strength Lbs./Sq.Ft.	Atterberg Liquid Limits
1	14.5	Very soft gray clay w/trace of organic matter	77.2	55.1	97.6	290	94
2	18.5	Very soft gray clay w/sand layers	63.1	62.7	102.3	335	70
3	23.5	Very soft gray clay w/silt lenses	70.3	58.5	99.6	430	80
4	28.5	Very soft gray clay	83.1	52.5	96.1	430	
5	33.5	Soft gray clay	85.7	50.9	94.5	565	161
6	38.5	Soft gray sandy clay w/sand pockets & shells	37.6	----	-----	----	
7	43.5	Medium stiff gray clay w/sand lenses	70.3	57.7	98.3	1190	71
10	58.5	Very stiff tan & gray clay	27.5	98.1	125.1	4345	67
11	63.5	Stiff tan & gray silty clay w/sand pockets	27.3	97.2	123.7	2135	45
12	68.5	Stiff tan & gray clay w/sand lenses	36.4	85.8	117.0	2015	
13	73.5	Medium stiff gray silty clay w/clayey silt layers	30.1	91.9	119.6	1320	
14	79.5	Medium compact tan clayey silt	30.5	91.3	119.1	$\phi=4^{\circ}$ c=400*	
15	83.5	Stiff tan & gray clay w/silt lenses	34.1	88.1	118.1	2165	
16	88.5	Ditto	47.2	75.2	110.7	2810	72
17	93.5	Ditto	41.4	81.1	114.7	2730	
18	98.5	Medium stiff gray clay w/sand lenses & shell fragments	33.3	90.2	120.2	2200	

*Quick Triaxial Shear Test.

ϕ = Angle of internal friction;
c = Cohesion in pounds per sq. ft.

Fig.78

EUSTIS ENGINEERING COMPANY
CONSULTING FOUNDATION ENGINEERS

Figure 19b. Lab log for boring B-1, drilled in Lake Ponchartrain (Eustis Engineering Company, 1966). See Figure 19a for sample intervals and stratum intervals.

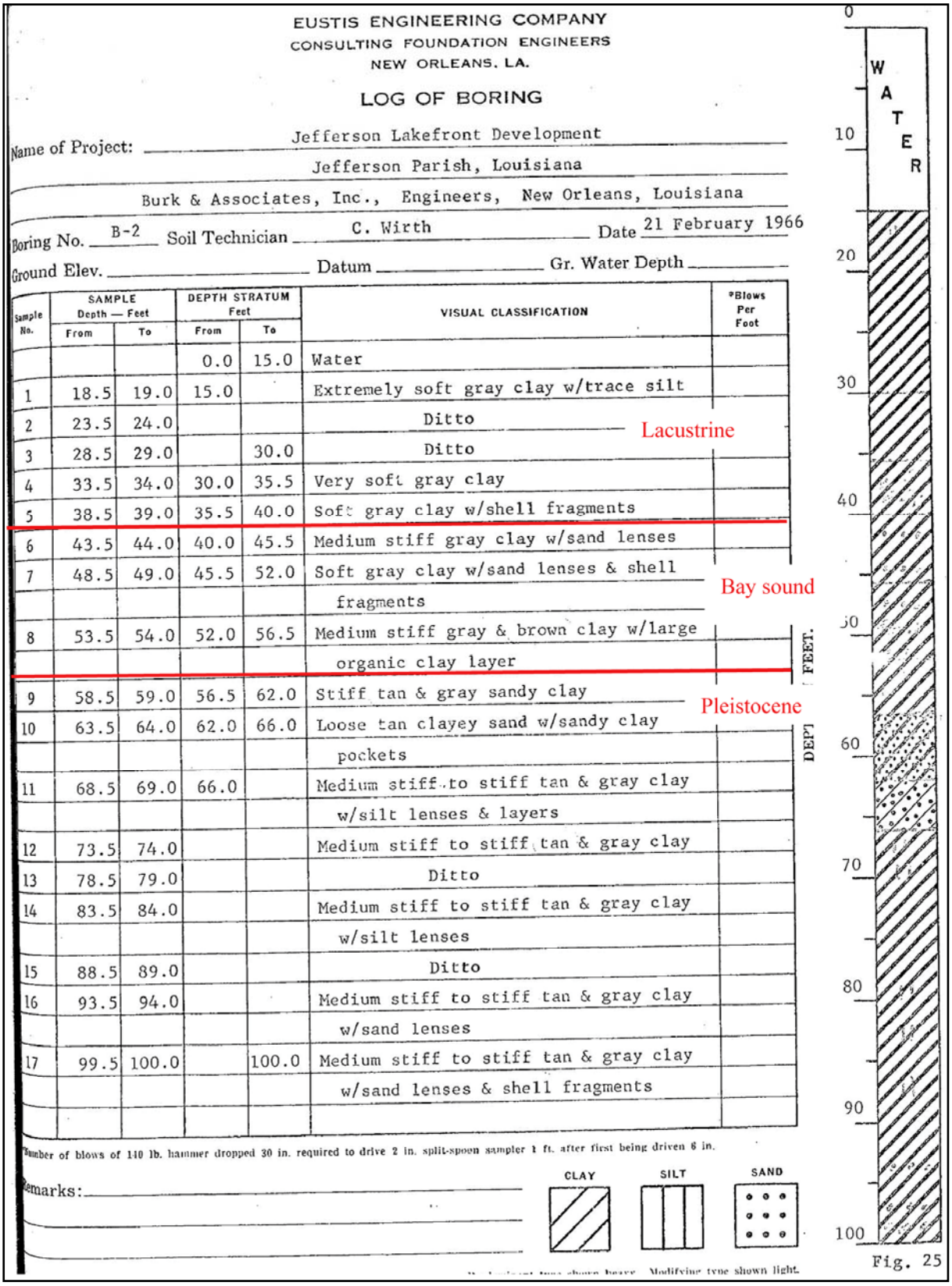

EUSTIS ENGINEERING COMPANY
CONSULTING FOUNDATION ENGINEERS
NEW ORLEANS, LA.

LOG OF BORING

Name of Project: Jefferson Lakefront Development
Jefferson Parish, Louisiana
Burk & Associates, Inc., Engineers, New Orleans, Louisiana

Boring No. B-2 Soil Technician C. Wirth Date 21 February 1966
Ground Elev. _____ Datum _____ Gr. Water Depth _____

Sample No.	SAMPLE Depth — Feet From	To	DEPTH STRATUM Feet From	To	VISUAL CLASSIFICATION	*Blows Per Foot
			0.0	15.0	Water	
1	18.5	19.0	15.0		Extremely soft gray clay w/trace silt	
2	23.5	24.0			Ditto	
3	28.5	29.0		30.0	Ditto	
4	33.5	34.0	30.0	35.5	Very soft gray clay	
5	38.5	39.0	35.5	40.0	Soft gray clay w/shell fragments	
6	43.5	44.0	40.0	45.5	Medium stiff gray clay w/sand lenses	
7	48.5	49.0	45.5	52.0	Soft gray clay w/sand lenses & shell fragments	
8	53.5	54.0	52.0	56.5	Medium stiff gray & brown clay w/large organic clay layer	
9	58.5	59.0	56.5	62.0	Stiff tan & gray sandy clay	
10	63.5	64.0	62.0	66.0	Loose tan clayey sand w/sandy clay pockets	
11	68.5	69.0	66.0		Medium stiff to stiff tan & gray clay w/silt lenses & layers	
12	73.5	74.0			Medium stiff to stiff tan & gray clay	
13	78.5	79.0			Ditto	
14	83.5	84.0			Medium stiff to stiff tan & gray clay w/silt lenses	
15	88.5	89.0			Ditto	
16	93.5	94.0			Medium stiff to stiff tan & gray clay w/sand lenses	
17	99.5	100.0		100.0	Medium stiff to stiff tan & gray clay w/sand lenses & shell fragments	

Lacustrine
Bay sound
Pleistocene

*Number of blows of 140 lb. hammer dropped 30 in. required to drive 2 in. split-spoon sampler 1 ft. after first being driven 6 in.

Remarks:

CLAY SILT SAND

Modifying type shown light.

0 WATER 10 20 30 40 50 60 70 80 90 100 DEPTH IN FEET.

Fig. 25

Figure 20a. Boring B-2 drilled in Lake Pontchartrain (Eustis Engineering Company, 1966). Values shown are in feet. Boring location shown in Figure 18.

Subsoil Investigation
Jefferson Lakefront Development
Jefferson Parish, Louisiana

Burk & Associates, Inc., Engineers, New Orleans, Louisiana

SUMMARY OF LABORATORY TEST RESULTS

BORING 2

Sample No.	Depth Below Water Surface in Feet	Classification	Water Content Percent	Density Lbs./Cu.Ft. Dry	Density Lbs./Cu.Ft. Wet	Unconfined Compressive Strength Lbs./Sq.Ft.	Atterberg Liquid Limits
1	18.5	Extremely soft gray clay	82.4	52.9	96.5	155	
2	23.5	Extremely soft gray clay w/silt lenses	81.0	53.3	96.5	175	77
3	28.5	Ditto	93.4	48.7	94.2	230	
4	33.5	Very soft gray clay	92.9	47.9	92.4	375	109
5	38.5	Soft gray clay w/sand pockets & shell fragments	74.2	55.6	96.9	505	
6	43.5	Medium stiff gray clay w/sand lenses	93.1	47.9	92.5	1090	102
7	48.5	Soft gray clay w/sand lenses & shell fragments	55.0	66.7	103.4	440	
8	53.5	Medium stiff gray & brown clay w/organic clay layers	103.0	43.7	88.7	1275	149
9	58.5	Stiff tan & gray sandy clay	25.8	100.6	126.6	2810	51
10	63.5	Loose tan clayey sand w/sandy clay pockets	24.4	100.7	125.3	$\phi=0^{o}$ c=420*	23
11	68.5	Medium stiff tan & gray clay w/silt layers	30.6	93.6	122.2	1845	
12	73.5	Ditto	31.1	92.2	120.9	2100	43
13	78.5	Stiff tan & gray clay w/silt lenses	34.4	88.3	118.7	2890	
14	83.5	Ditto	34.0	88.2	118.1	2915	
15	88.5	Ditto	43.8	78.5	112.9	3675	
16	93.5	Ditto	42.0	80.6	114.5	2295	60
17	99.5	Ditto	36.0	86.6	117.8	1380	

*Quick Triaxial Shear Test.

ϕ = Angle of internal friction;
c = Cohesion in pounds per sq. ft.

Fig. 79

EUSTIS ENGINEERING COMPANY
CONSULTING FOUNDATION ENGINEERS

Figure 20b. Lab log for boring B-2, drilled in Lake Pontchartrain (Eustis Engineering Company, 1966). See Figure 20a for sample intervals and stratum intervals.

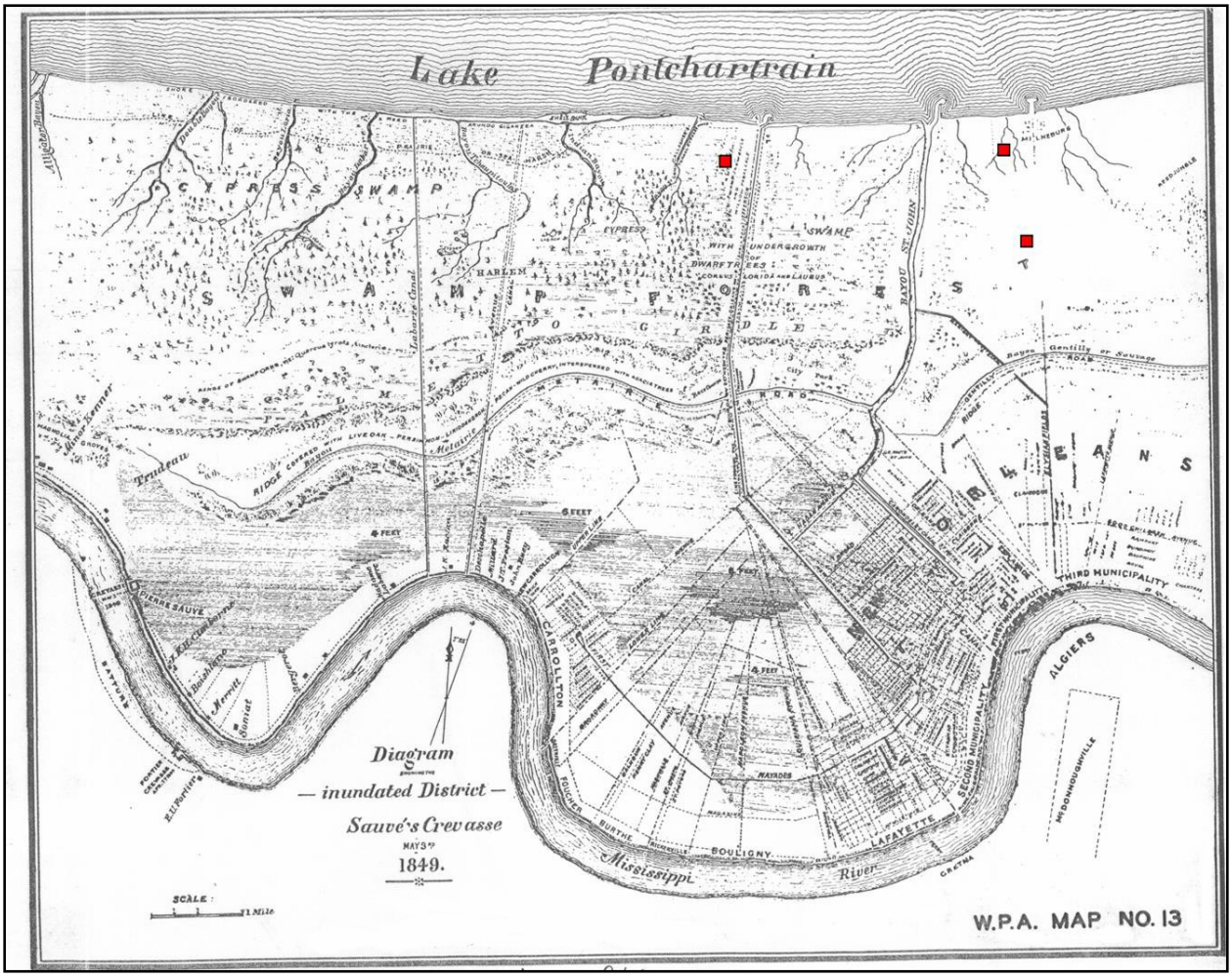

Figure 21a. General map of the New Orleans area from 1849 showing major drainage and topographic features (WPA, 1937, Plate 13). The 17th Street and London Canals breaks are shown on the map with the 17th Street canal break as the western most location. No significant drainage is present at the 17th Street canal area.

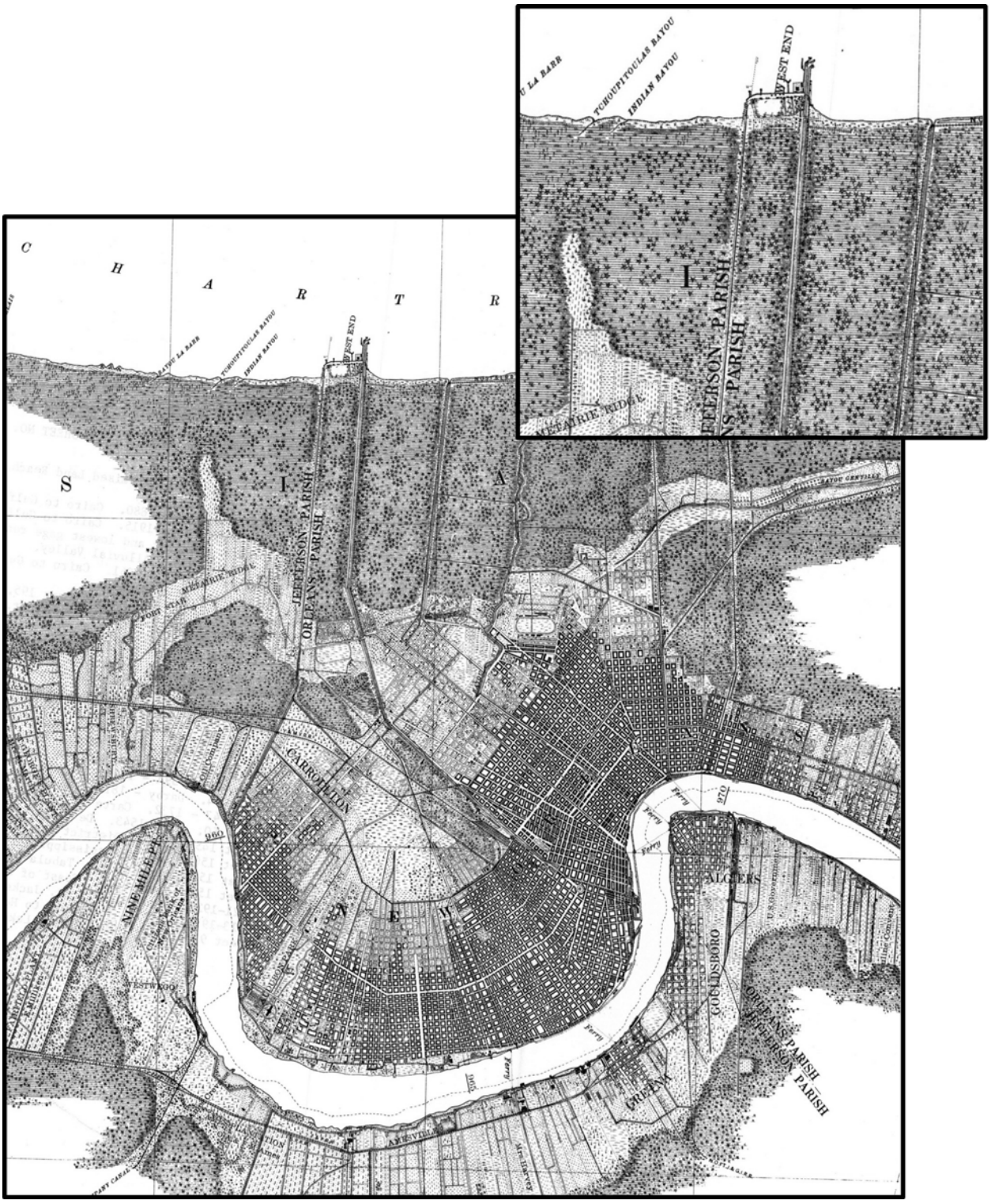

Figure 21b. General map of the New Orleans area from 1895 showing major drainage and topographic features (MRC, 1975). Enlarged map view shows there were no significant drainage features identified in the 17th Street Canal area.

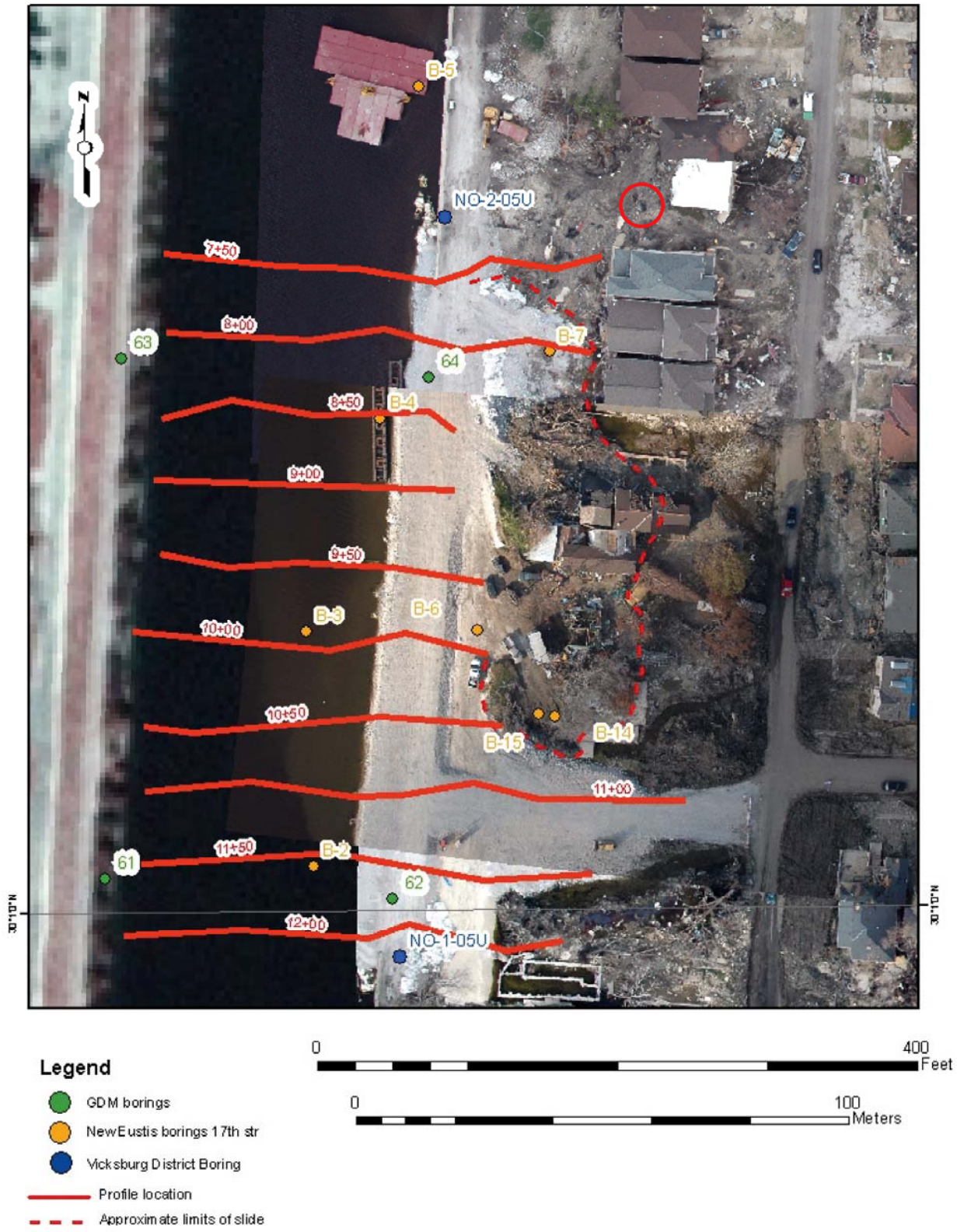

Figure 22a. Hydrographic survey profiles from the 17th Street canal from 31 August 2005. See Figure 22b for survey profiles. The area circled in red in upper part of the photo represents a large soil mass from the foundation which shows the intact lacustrine and marsh contact (see Figure 23).

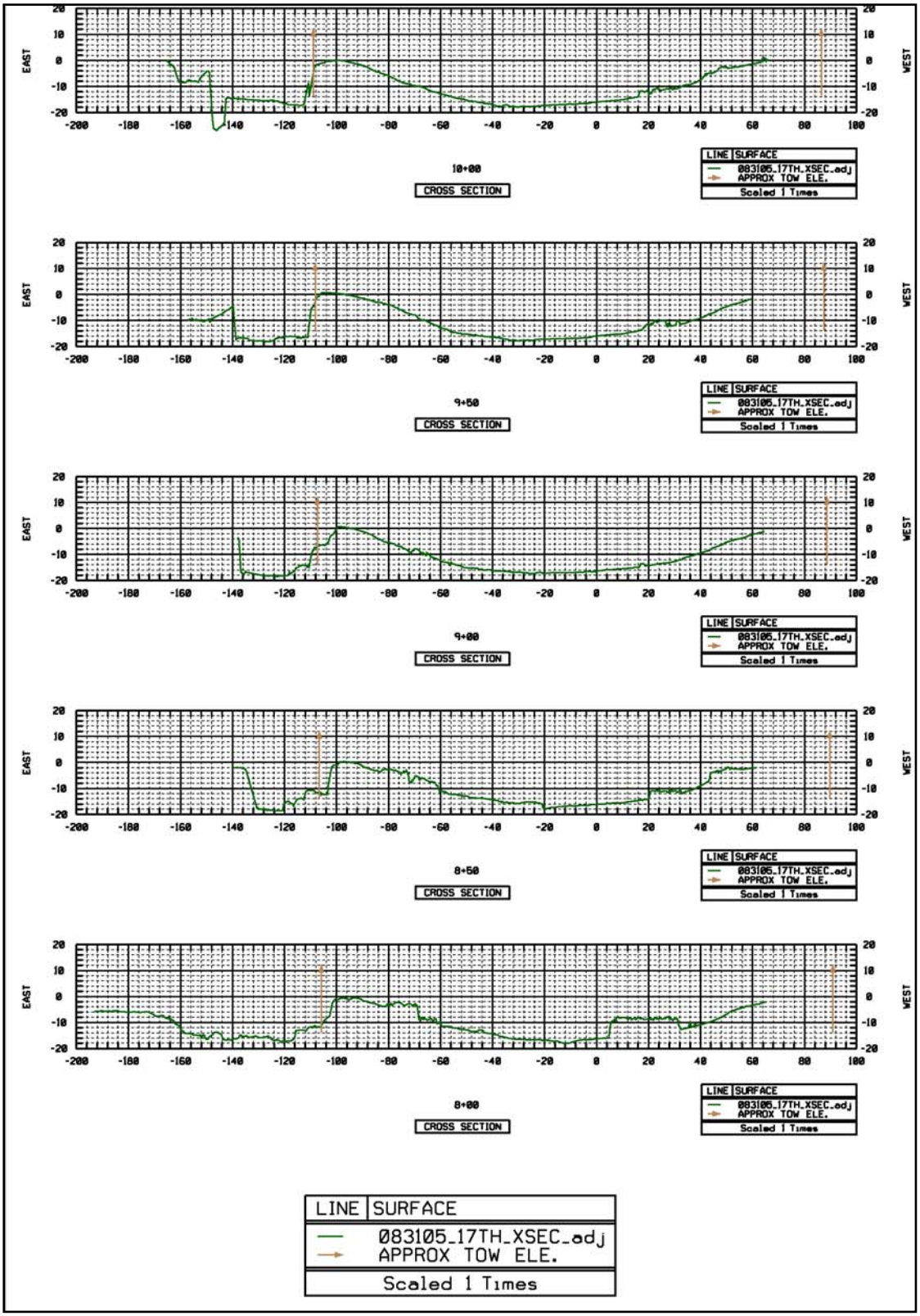

Figure 22b. Hydrographic survey profiles from the 17th Street canal area (see Figure 21a for survey locations). Boring 64 is at located midway between stations 8+00 and 8+50. Brown vertical line represents the estimated position of the I-wall.

Figure 23a. November 2005 photograph showing locations where the grey lake clay and overlying marsh contact was observed. The accompanying photographs show close-up views of the swamp/marsh/lacustrine stratigraphy. The presentation of sites in the accompanying photographs is in a west to east direction in the above photograph. Sites are designated as west (Figures 23b and 23c), center (Figure 23d), and east (Figures 23e and 23f).

Figure 23b. Block of soil from levee foundation near boring 64, showing the intact marsh and lacustrine contact. A six foot folding rule is stretched across the soil mass. Upper photo shows the general setting (see Figures 22 and 23a for location). Lower photo shows block with about 3 ft of marsh and 3 ft of grey lacustrine clay. Whole shells are embedded within the grey lacustrine soils near the base of the soil block, where the shovel tip is located. Close-up view is shown in Figure 23c.

Figure 23c. Close-up view of the grey lacustrine clay that formed the levee foundation in the vicinity of boring 64. The soil block shows whole shell and fragments embedded throughout the grey clay. Note the shell below the shovel with clay embedded into the interior of the shell. This grey lacustrine clay was firmly attached to the overlying marsh soils as shown by Figure 23b.

Figure 23d. Grey lacustrine clay at base of organic soil block (bottom photo). Swamp soils at top of soil mass where the wood and roots are present. Generally, most of the soil blocks were orientated with wood part upward and/or laying in direction of water current.

Figure 23e. Grey lacustrine clay at base of organic soil block (bottom photo). Close-up view of the lake clay in Figure 23f. Location is identified in Figure 23a and corresponds to the eastern site.

Figure 23f. Close-up view of the grey lake clay from the soil block at the intersection of Spencer Avenue and north bound lane of Fluer de Lis.

Figure 24. View of Bellaire Drive on 3 October 2005 looking northeast from near intersection of Bellairie Drive and Spencer Avenue. Soil blocks were transported by force of moving water into the neighborhood, especially along Spencer Avenue, Stafford Avenue and 40th Street. A general observation from the survey of soil blocks in the neighborhood was the stratigraphic position of the swamp, which was observed to be at the top of the organic horizon.

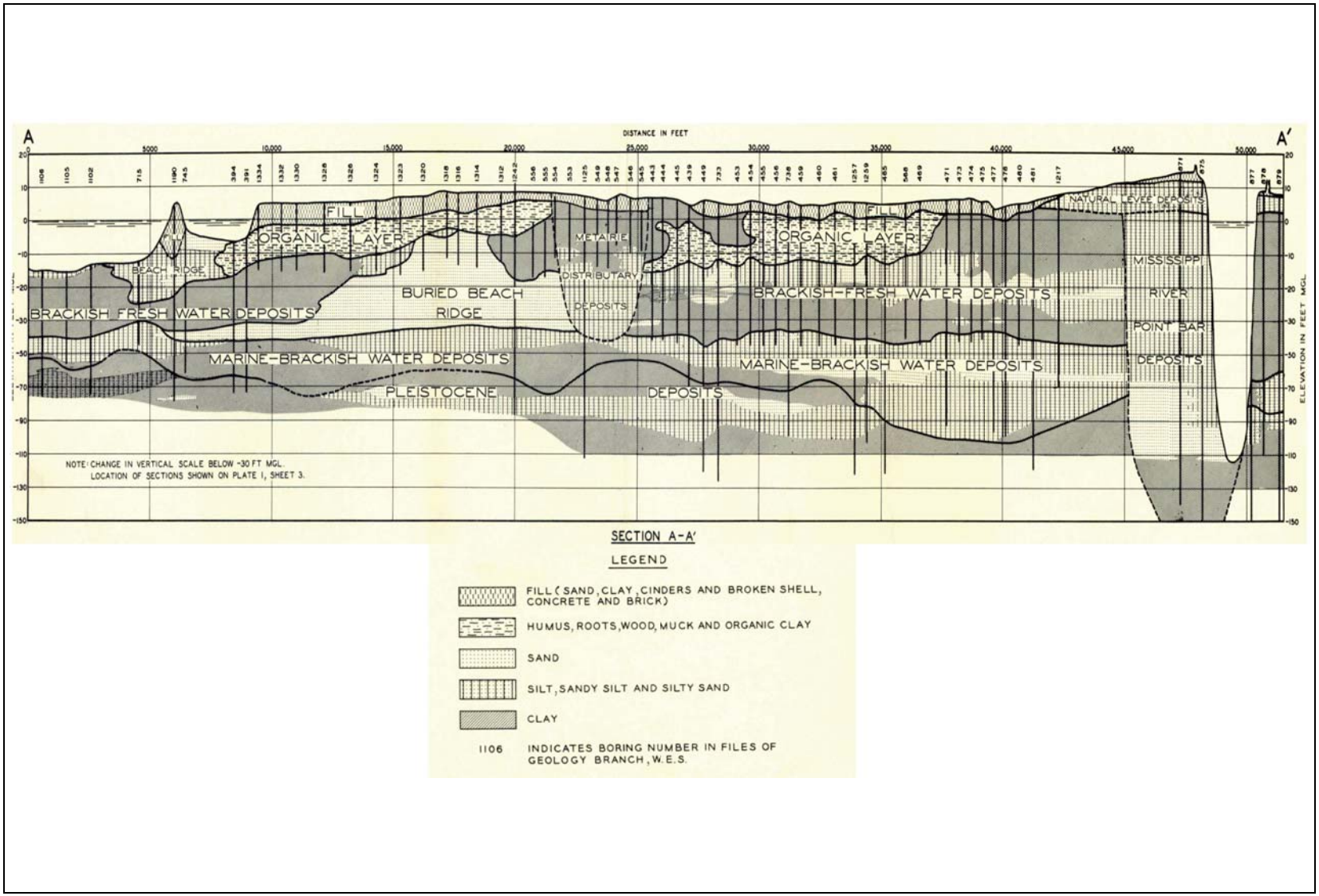

Figure 25. Cross-section from Schultz and Kolb (1954) showing the stratigraphy along the New Basin Canal, approximately 2,200 ft east of 17th Street Canal.

Figure 26. View of the 17th Street Canal looking south toward Veterans Avenue. Note the Orleans Parish side (left) of the canal has no embankment section above the water level, while the Jefferson Parish side (right) has an exposed embankment section. Approximately 20 measurements were made from top of wall in a southerly direction from the breach on the Orleans Parish side with a weighted tape measure to determine the water depth to the top of the embankment. These measurements indicate the water level was approximately 1 ft deep on the canal side adjacent to the I-wall.

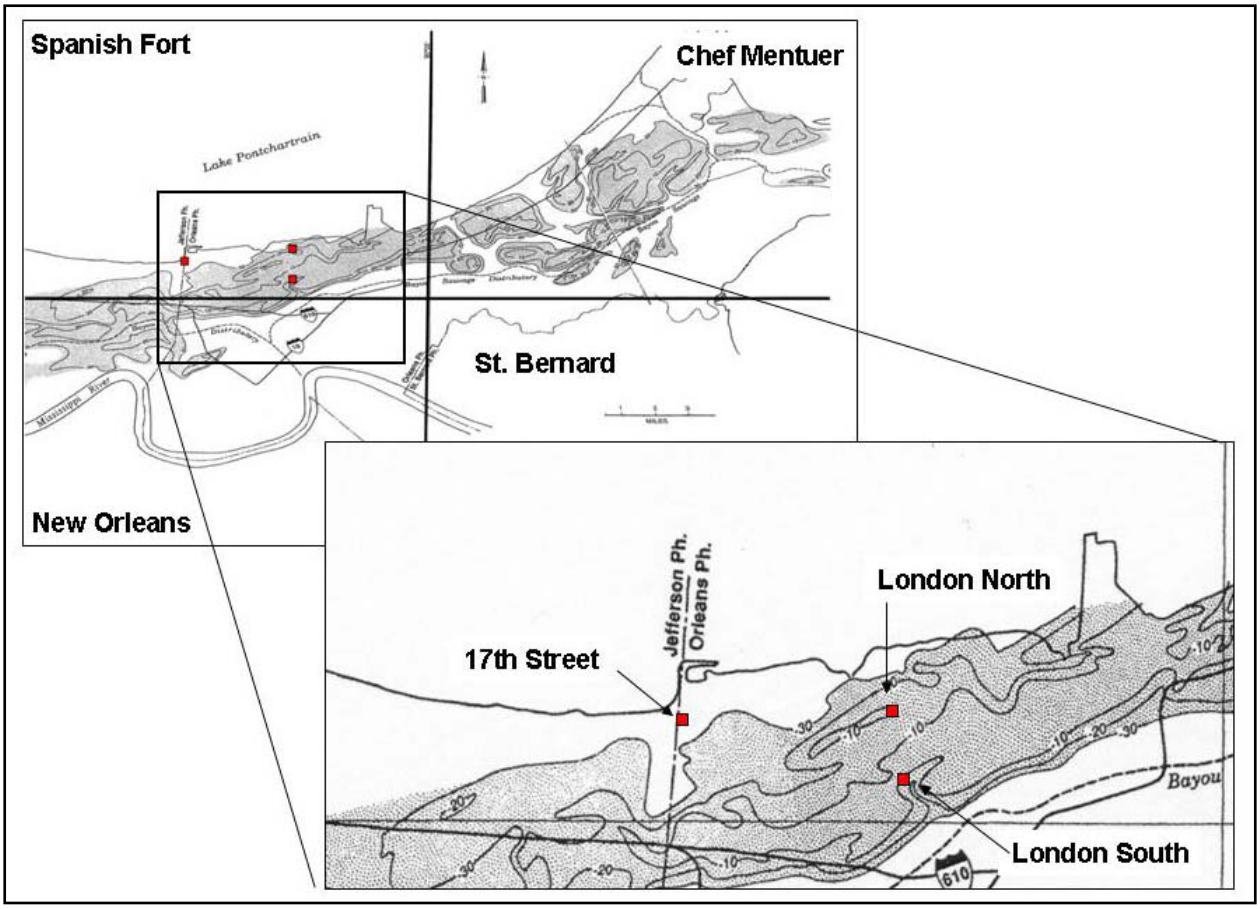

Figure 27. Contour map of the Pine Island Beach showing the elevation to the beach sand as being in excess of -30 ft NGVD at the 17th Street Canal levee breach (Saucier, 1994).

Appendix 23
Analysis of the Stability of Michoud Canal

Introduction

No levee or I-wall failures occurred in the Michoud Canal area during Hurricane Katrina. The Michoud Canal area is protected by a series of I-walls constructed on top of a levee section. Figure 1 is an aerial photograph showing the plan view of the Michoud Canal. Along a portion of the west I-wall is a series of sand drains that were installed to relieve the high pore pressures during high water events. Sections of the I-wall were overtopped by wave action, but this did not lead to breaching of the protection. Post-Katrina damage reports identify a section of I-wall along the west bank, approximately 200 ft south of the pump station, as leaning a few inches toward the canal side[1]. It is uncertain whether this displacement occurred before or during Hurricane Katrina. A photograph showing this section of the I-wall is shown in Figure 2a. Figure 2b shows erosion that occurred on the protected side due to overtopping of the I-wall.

Construction of the Michoud Canal and the Gulf Intercoastal Waterway (GIWW) occurred in 1942. I-wall construction and capping occurred in the 1970s in response to Hurricane Betsy in 1965. Reference documents relating to the design and stability analyses of the Michoud Canal area are presented in U.S. Army Corps of Engineers (USACE) Design Memoranda[2,3]. The GDM shows that the design water level was 3 ft below the top of the floodwall. The elevations of the top of the floodwall vary along the canal and are about 2 ft higher on the west side than on the east.

Possible Modes of Failure Investigated

The purpose for this study of the Michoud Canal area is to compare the I-wall and embankment characteristics in this area, which did not fail, to other areas that experienced failure

[1] Bob Grubb, MVN, personal communication., May 18, 2005
[2] Mississippi River – Gulf Outlet, Design Memorandum No. 1, General Design Michoud Canal, Department of the Army, New Orleans District, Corps of Engineers, July 1973.
[3] Lake Pontchartrain, LA and vicinity, Lake Pontchartrain Barrier Plan, Design Memorandum No. 2, General Design, Citrus Back Levee, Department of the Army, New Orleans District, Corps of Engineers, August 1967.

in order to better evaluate the Katrina-related failure mechanisms and analysis procedures. The post-Katrina reconnaissance revealed that overtopping by waves had eroded some soil adjacent to the wall on the protected side along some sections of the I-wall. Figure 2b shows some minor scour damage on the protected side of the levee on the west bank near the pump house area. It appeared that waves breaking over the top of the floodwall scoured and eroded the levee on the protected side of the I-wall, exposing the supporting sheet piles. This erosion was not severe enough to cause the sheet piles to lose their foundation support.

Other possible modes of failure considered were sliding instability and piping and erosion from underseepage. Piping and erosion from underseepage were unlikely problems because the I-walls were founded in a clay levee fill, a marsh layer made up of organics, clay, and silt, overlying a clay layer. Because of the thicknesses, the sufficiently low permeabilities of these materials, and the relatively short duration of the storm, the factors of safety for this failure mode were considered to be higher than for other conditions and were, therefore, not calculated. Global stability, determined by limit equilibrium analyses, was the primary focus of the study presented in this report.

Stratigraphy

The stratigraphy at the Michoud Canal area was developed from available boring data and published geologic cross sections[2,3,4]. The locations of existing borings and the six new investigation locations are shown in Figure 1. At each new location, rotary borings, cone penetration tests (CPT), and vane shear tests (VST) were conducted. The cross section developed for analysis, located on the west side of the Michoud Canal at Station 4+00, is shown in Figure 3. This cross section is approximately 100 ft north of the pump house, at the south end of the west wall. This section was selected for analysis because of the close proximity to existing exploratory borings. No sand drains were located at this section; therefore this section has the potential to be more unstable than I-wall sections to the north containing sand drains. The sand drains are located along the protected side of the levee near a drainage ditch to relieve pressures in the underlying foundation sands beginning at Station 11+00 and ending at Station 52+50.

The general stratigraphy at the site consists of six depositional units, listed in descending order as (a) levee fill, (b) marsh and swamp (termed marsh 1 and marsh 2), (c) interdistributary clay, (d) intradelta or relic beach sand, (e) nearshore gulf deposits, and (f) Pleistocene deposits. Specific engineering properties of these different depositional units are described in greater detail below.

[4]Dunbar, J. B., Blaes, M. Dueitt, S., and Stroud, K. (1994). "Geological investigation of the Mississippi River deltaic plain, Report 2 of a Series," Technical Report GL-84-15, U.S. Army Engineer Waterways Experiment Station, Vicksburg, MS.

Sources of information on shear strengths

The sources of shear strength data include tests reported in the General Design Memoranda and tests conducted on specimens taken as part of the post-Katrina IPET investigation. Unconfined compression tests (UC), Q triaxial tests (UU), cone penetration tests, and vane shear tests were available to assess the shear strength of the site materials. The CPT data at the Michoud site were inconsistent, and were used mainly to define the contact between the interdistributary clay and the silty sand. The data were used to a lesser extent in the determination of the undrained shear strength of the cohesive soil layers.

Very little data on the levee fill material is available from the GDM borings in the area of interest. The undrained shear strength used for the original design, s_u =500 psf, was also used for the levee fill strength in this analysis. The moist density of the embankment was assumed to be 110 pcf. The levee fill material is not involved in calculated mechanisms of instability for the case of a gap between the sheet pile wall and the adjacent soil, so the value of shear strength used has little influence on the results of the analysis.

Underlying the levee fill is a marsh/swamp unit approximately 15 ft thick. This layer is composed of soft organic material (in the form of roots, wood, and disseminated organics), silt, and clay. Samples taken from the marsh/swamp layer showed a difference in the total unit weight between the upper portion and lower portion; therefore it was divided into two layers, termed marsh 1 and marsh 2, for the analysis. The marsh 1 layer was about 4 ft thick under the crest of the levee, and about 10 ft thick beneath the toe of the levee. The marsh 2 layer was about 3 ft thick under the crest of the levee and about 4 ft thick under the toe of the levee.

The strengths of the foundation soils were interpreted based on the data presented on Figures 4 and 5. These figures show the strength results obtained in the proximity of Station 4+00 from explorations conducted at the centerline and toe, respectively. These figures show the data obtained from cone penetration tests, UC tests, Q tests, and vane shear tests. The vane shear test results were adjusted using Bjerrum's[5] correction for strain rate effects based on plasticity index. These figures also compare the strength interpretations used in this analysis (IPET strengths) with the strengths used in the original design (GDM strength).

The data show that the marsh layers are stronger beneath the levee crest where they have been compressed under the weight of the levee, and weaker at the toe of the levee and beyond, where they have been subjected to a smaller consolidation stress. The marsh 1 layer was assigned a value of undrained shear strength equal to 700 psf beneath the levee crest and 400 psf beneath the levee toe. These shear strength values compare well to the numeric averages of 697 psf and 405 psf for the Q and UC tests conducted in this layer for undisturbed specimens taken beneath the crest and toe, respectively. The shear strength values adopted for the marsh 2 layer were 500 psf beneath the levee crest and 400 psf beneath the levee toe, which are close to the numeric averages of 483 psf and 387 psf measured from Q and UC tests. The total unit

[5] Bjerrum, L., "Embankments on Soft Ground." *Proceedings*, *Conference on Performance of Earth and Earth-Supported Structures*, ASCE, Vol. II, 1972, pp. 1-54.

weight values of the marsh 1 and marsh 2 soils were determined to be 105 and 80 pcf, respectively.

Beneath the marsh layers is a layer of interdistributary clay. The clay appears to be normally consolidated throughout its depth. Based on the shear strength results, the undrained shear strength increased at a rate of approximately 12 psf/ft, resulting in a value of undrained strength ratio, s_u/p', of 0.26. The average saturated unit weight of the clay is about 109 pcf. It should be noted that in Figures 4 and 5, the undrained shear strength in the interdistributary clay is calculated based on the effective stress and undrained strength ratio, and is not based solely on the measured strength data.

Underlying the clay is a silty sand layer. This layer was assumed to have a drained friction angle of 35 degrees and a saturated unit weight of 120 pcf. The friction angle is justified on the basis of CPT soundings MC-1.06, MC-1T and MC-1TA where correlations of the CPT data with Standard Penetration Blowcounts (N_{60}) show that the blowcounts ranged between 30 and 50 blows and averaged about 40 blows. The silty sand layer was assumed to be drained in the stability analyses.

Stability Analysis for Michoud Canal at Station 4+00

Slope stability analyses were performed for the Station 4+00 cross section. The elevation of the top of the floodwall for this section was 19.7 ft NAVD88. The sheet pile beneath penetrated to elevation -10 ft NAVD88, which was within the marsh 2 layer. A drainage ditch is located 100 ft toward the protected side of the levee floodwall.

Slope stability analyses were performed using UTEXAS4[6] and SLIDE[7]. All analyses were performed using Spencer's Method[8]. Circular failure surfaces were analyzed using both UTEXAS4 and SLIDE, and UTEXAS4 was also used to analyze non-circular slip surfaces. Four main cases were evaluated. Cases 1 and 2 considered canal water levels of 15.5 ft NAVD88. Cases 3 and 4 considered canal water levels of 19.7 ft NAVD88. The first canal water level represents the peak hydrograph level measured by staff gages recorded during the storm. The second water level represents the elevation of the top of the wall. For both of these water levels, analyses were performed with and without a water-filled gap behind the wall.

As stated previously, undrained strengths were used to characterize the levee fill, marsh 1, marsh 2, and interdistributary clay layers. However, the silty sand layer was treated as a drained material, and pore pressures in this layer were calculated using the finite element seepage engine built into SLIDE. For these analyses, the protected side hydraulic boundary, located approximately 220 ft from the flood wall, was assumed to be a constant head boundary, with a head elevation of -3 ft NAVD88. The drainage ditch was also considered to be a constant head boundary at the same head elevation. The finite element seepage analyses were conducted in the

[6] Available from Shinoak Software, 3406 Shinoak Drive, Austin, TX 78731.
[7] Available from Rocscience Inc., 31 Balsam Avenue, Toronto, Ontario, Canada M4E 3B5.
[8] Spencer, E. (1967) "A Method of Analysis of the Stability of Embankments Assuming Parallel Inter-Slice Forces," *Geotechnique*, Institution of Civil Engineers, Great Britain, Vol. 17, No. 1, March, pp. 11-26.

same manner, with the same hydraulic material properties, as reported for the Orleans Canal, and details can be found in Appendix 10. None of the critical failure surfaces extended into the silty sand layer; therefore the undrained strengths of the cohesive soil layers above the silty sand layer controlled the stability of the section analyzed. The results of these analyses are presented in Table 1.

Table 1
Results of Slope Stability Analysis for Michoud Canal Station 4+00.

Case	Water Elevation (ft) NAVD88	Strength Model	Crack	Factor of Safety UTEXAS4 non-circular	Factor of Safety UTEXAS4 circular	Factor of Safety SLIDE circular
1	15.5	IPET	No	1.243	1.357	1.368
2	15.5	IPET	Yes	1.023	1.100	1.099
3	19.7	IPET	No	1.098	1.179	1.182
4	19.7	IPET	Yes	0.835	0.919	0.924

Cases 1 and 2 were computed using the peak water level of the hydrograph (elev. 15.5 ft NAVD88). Case 1 represents the results for the *no gap* situation where the factor of safety was computed by UTEXAS4 to be 1.351. Case 2 was computed for the case where a gap is present, and the value of factor of safety was determined by UTEXAS4 to be 1.091. The values of factor of safety determined with UTEXAS4 and SLIDE were very close, with UTEXAS4 normally providing a very slightly lower factor of safety. This can be attributed to the different critical surface search procedures used between the two programs. The critical slip surfaces for Cases 1 and 2 determined from the SLIDE analyses are shown in Figures 6 and 7.

Cases 3 and 4 were computed for a canal water level located at the top of the I-wall (19.7 ft NAVD88). The factor of safety for Case 3, the *no gap* condition, was computed by UTEXAS4 to be 1.172. The factor of safety for Case 4, the *gap* condition, was computed by UTEXAS4 to be 0.921. The critical slip surfaces determined using SLIDE for Cases 3 and 4 are presented in Figures 8 and 9.

Figures 6 through 9 show that for all cases, the critical slip surface extended to the bottom of the interdistributary clay, but did not extend into the intradelta beach sand layer. Also, for all cases, the critical circle exited at the toe of the drainage ditch. These results show that the stability of this cross section is influenced by the close proximity of the ditch to the levee and floodwall.

Because no gap was observed at Michoud, Case 1 (Figure 6) is the best representation of actual conditions, with a calculated factor of safety in excess of 1.3. Case 2 shows that if a gap had developed, it would have reduced the factor of safety significantly, but the wall would have remained stable. Cases 3 and 4, for water levels higher than observed, show that higher water levels would have reduced the factor of safety considerably, and indicate that if a gap had developed with the water level at the top of the wall, failure would have occurred.

Probabilities of Failure

A probability of failure analysis was performed for Cases 1 and 2. Probabilities of failure have been estimated using an approximate technique based on the Taylor Series method. The coefficient of variation of the average clay strength (interdistributary deposit) and the average marsh layer strength (for marsh 1 and marsh 2) were estimated to be 25%. The friction angle in the beach sand was assumed to vary from 30 to 40 degrees.

The Taylor Series numerical method[9] was used to estimate the standard deviation (σ_F) and the coefficient of variation of the factor of safety (COV_F). Values of F_{MLV} and $F_{Su\pm1\sigma}$ for each material were calculated for Station 4+00 of the Michoud Canal and are presented in Table 2. As shown in Table 3, the probability of failure for Cases 1 and 2 are 2% and 40%, respectively. The fact that a gap did not form behind the wall has a very significant effect on the calculated probability of failure.

Table 2
Slope Stability Analysis for Michoud Canal Station 4+00 for Probabilistic Analysis

Case	Water Elevation (ft) NAVD88	Strength Model	Gap	Factor of Safety UTEXAS4	Factor of Safety SLIDE
Case 1					
Case 1a	15.5	IPET Strength	No	1.357	1.368
Case 1b	15.5	Fill -25%	No	1.305	1.317
Case 1c	15.5	Fill +25%	No	1.409	1.419
Case 1d	15.5	Marsh 1 -25%	No	1.309	1.318
Case 1e	15.5	Marsh 1 +25%	No	1.377	1.411
Case 1f	15.5	Marsh 2 –25%	No	1.308	1.315
Case 1g	15.5	Marsh 2 +25%	No	1.384	1.420
Case 1h	15.5	Interdistributary –25%	No	1.167	1.170
Case 1i	15.5	Interdistributary +25%	No	1.542	1.552
Case 1j	15.5	Beach Sand ϕ = 30	No	1.336	1.368
Case 1k	15.5	Beach Sand ϕ = 40	No	1.357	1.368
Case 2					
Case 2a	15.5	IPET Strength		1.100	1.099
Case 2b	15.5	Fill -25%		1.100	1.099
Case 2c	15.5	Fill +25	Yes	1.100	1.099
Case 2d	15.5	Marsh 1 -25%	Yes	1.099	1.099
Case 2e	15.5	Marsh 1 +25%	Yes	1.101	1.099
Case 2f	15.5	Marsh 2 –25%	Yes	1.059	1.040
Case 2g	15.5	Marsh 2 +25%	Yes	1.134	1.146
Case 2h	15.5	Interdistributary –25%	Yes	0867	0.873
Case 2i	15.5	Interdistributary +25%	Yes	1.333	1.311
Case 1j	15.5	Beach Sand ϕ = 30	Yes	1.095	1.099
Case 2k	15.5	Beach Sand ϕ = 40	Yes	1.100	1.099

[9]Wolff, T. F. (1994). "Evaluating the reliability of existing levees." Report, Research Project: Reliability of Existing Levees, prepared for the U.S. Army Engineer Waterways Experiment Station, Geotechnical Laboratory, Vicksburg, MS.

Table 3
Calculated Probabilities of Failure for Michoud Canal, Sta 4+00

Case	Water level (ft) NAVD88	F_{MLV}	COV_F	Probability of failure
Case 1 (no gap)	15.5	1.357	15%	2%
Case 2 (gap)	15.5	1.091	25%	40%

F_{MLV} = most likely value of factor of safety
COV_F = coefficient of variation of factor of safety

Summary

The results of the analyses described in the preceding sections are consistent with the performance of the I-wall along the canal, indicating that the IPET strength model and method of stability analysis provide a suitable basis for evaluating the performance of the Michoud Canal I-wall during Hurricane Katrina. The Michoud Canal stability analysis followed the same general procedures used in the analyses of the 17th St. Canal, the London Avenue Canal, the Orleans Avenue Canal, and the IHNC flood control structures reported in other appendices of the IPET report.

The calculated factors of safety for Station 4+00 were about 20% lower for the gap condition compared to the no gap condition. The undrained strength of the interdistributary clay is important in the stability analyses since the majority of the failure plane is located in this layer. The beach sand layer, modeled as a drained material, did not influence the analysis because failure surfaces did not extend down to this layer.

At Station 4+00, the top of the earthen levee was approximately 14.0 ft (NAVD 88). With the canal water level at the peak of the hydrograph (15.5 ft, NAVD 88), only 1.5 ft of water was acted on the cantilever I-wall. Since the factor of safety is greater than unity for the gap condition, it seems likely that the I-wall would have remained stable even if a gap had formed behind the wall. For the *no gap* case, the probability of failure was only 2%. For the case with a gap, the calculated probability of failure was much higher (40%).

If the static water level had reached the top of a wall, and a gap did not form, the calculated factor of safety is still greater than unity, indicating that the wall would remain stable. However, had a gap formed under this high water level, the calculations indicate that the wall would have failed.

The true hydraulic loading of the I-wall at Station 4+00 may have been somewhere between Cases 2 and 4 (15.5 ft and 19.7 ft NAVD88). Evidence of scour on the protected side of the I-wall indicates that some overtopping due to wave action had occurred, but this loading by waves was apparently of too short duration to be equivalent to the static water loading represented by Case 4 (19.7 ft NAVD88).

Similar to other cases analyzed as part of the IPET study, the use of non-circular failure surfaces resulted in factors of safety that were about 5% less than the values calculated using circular failure surfaces.

Post-Katrina Improvements in the Pumphouse Area of Michoud Canal

A significant effort was made to improve the stability of the pumphouse area of Michoud canal after Katrina. The work was performed during the year 2006. These improvements include:

1. Installation of 19 relief wells between Station 0+00 and 13+30 to relieve pore pressures in the sand layer.

2. An 80-foot long sheet pile was installed from Station 0+05 to Station 13+00 to provide a deeper seepage barrier through the full thickness of the sand layer this area.

3. The stickup height of the I-wall was reduced by rasing the top of the levee, and the levee slopes were flattened to improve stability. In addition, wave berms and riprap were added to improve erosion resistance.

4. The entire crest of the levee was paved to provide a greater level of protection against overtopping.

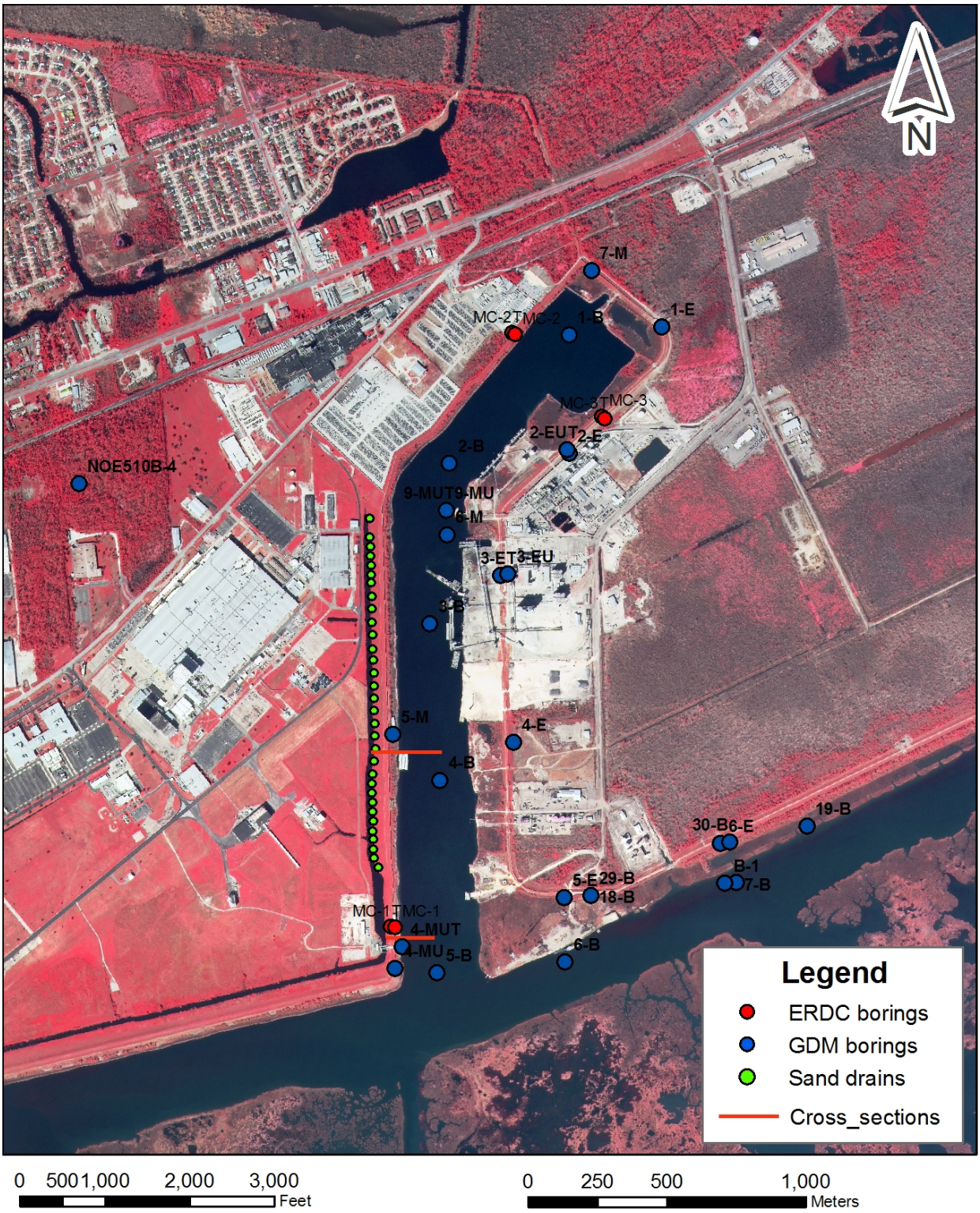

Figure 1. Aerial Photograph of Michoud Canal

Figure 2a. Post-Katrina photographs of Michoud Canal I-Wall at pump station.

Figure 2b. Post-Katrina Photographs of Michoud Canal I-Wall showing erosion from overtopping waves.

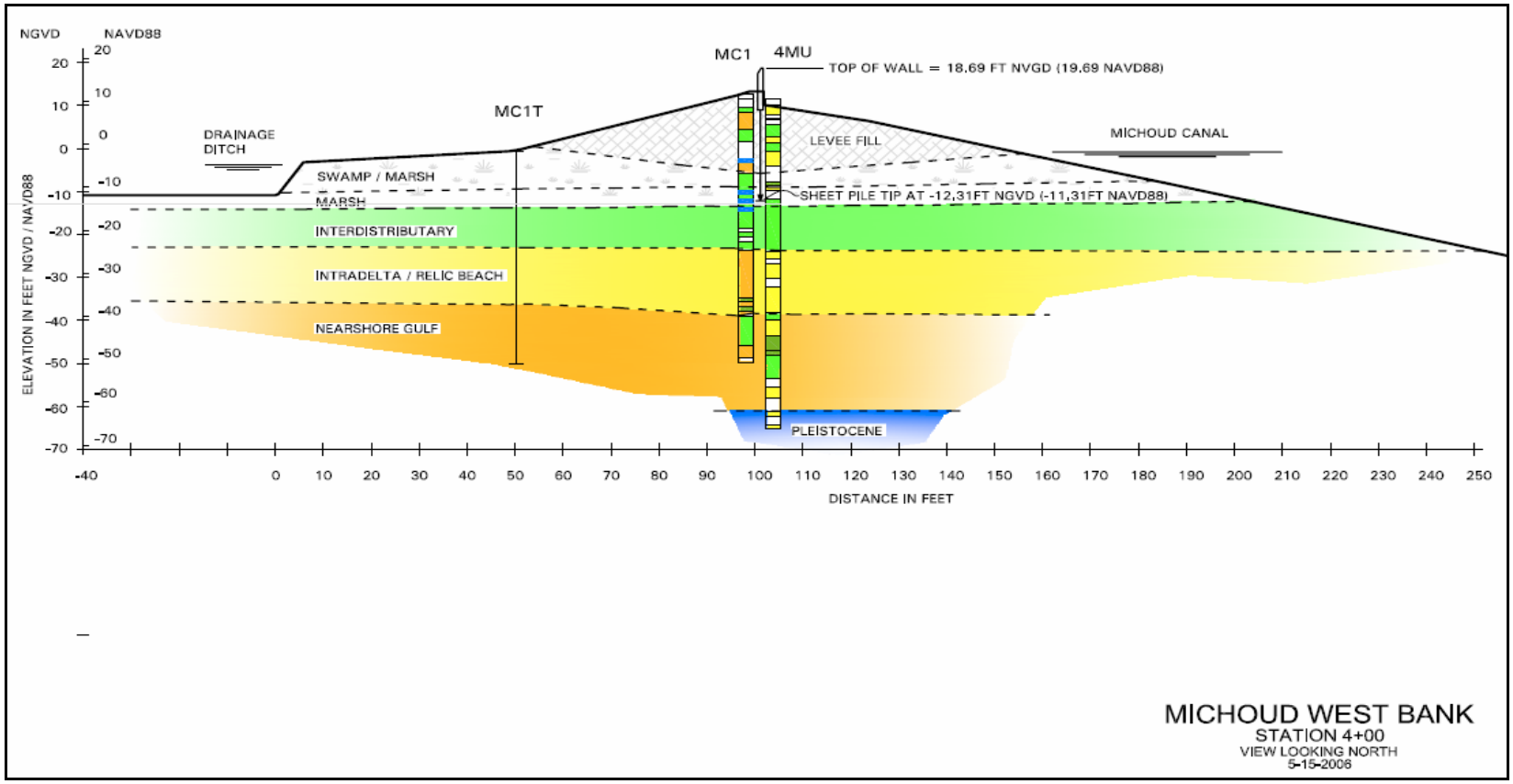

Figure 3. Geologic Cross Section of Sta. 4+00

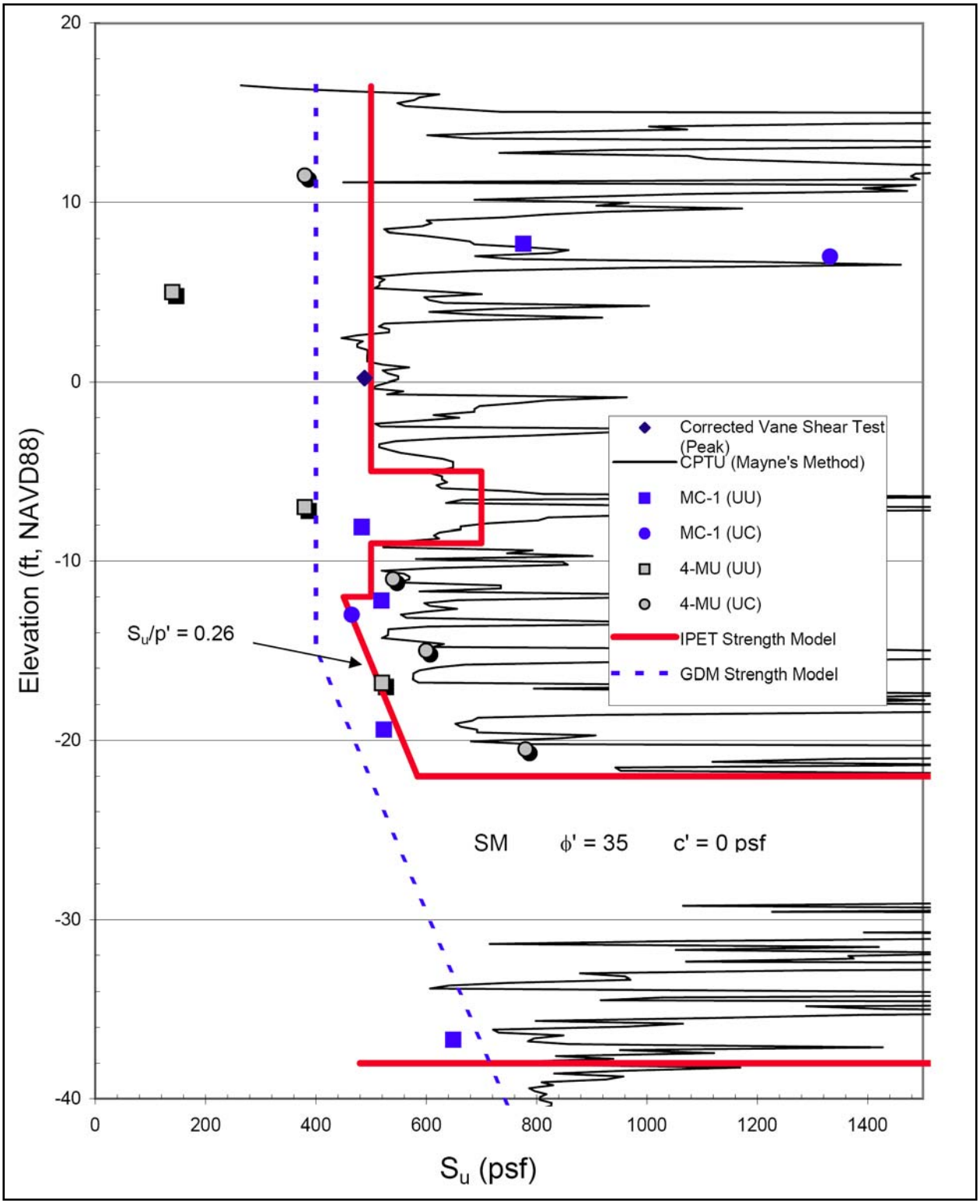

Figure 4. Michoud Canal, Sta. 4+00, Centerline Shear Strength

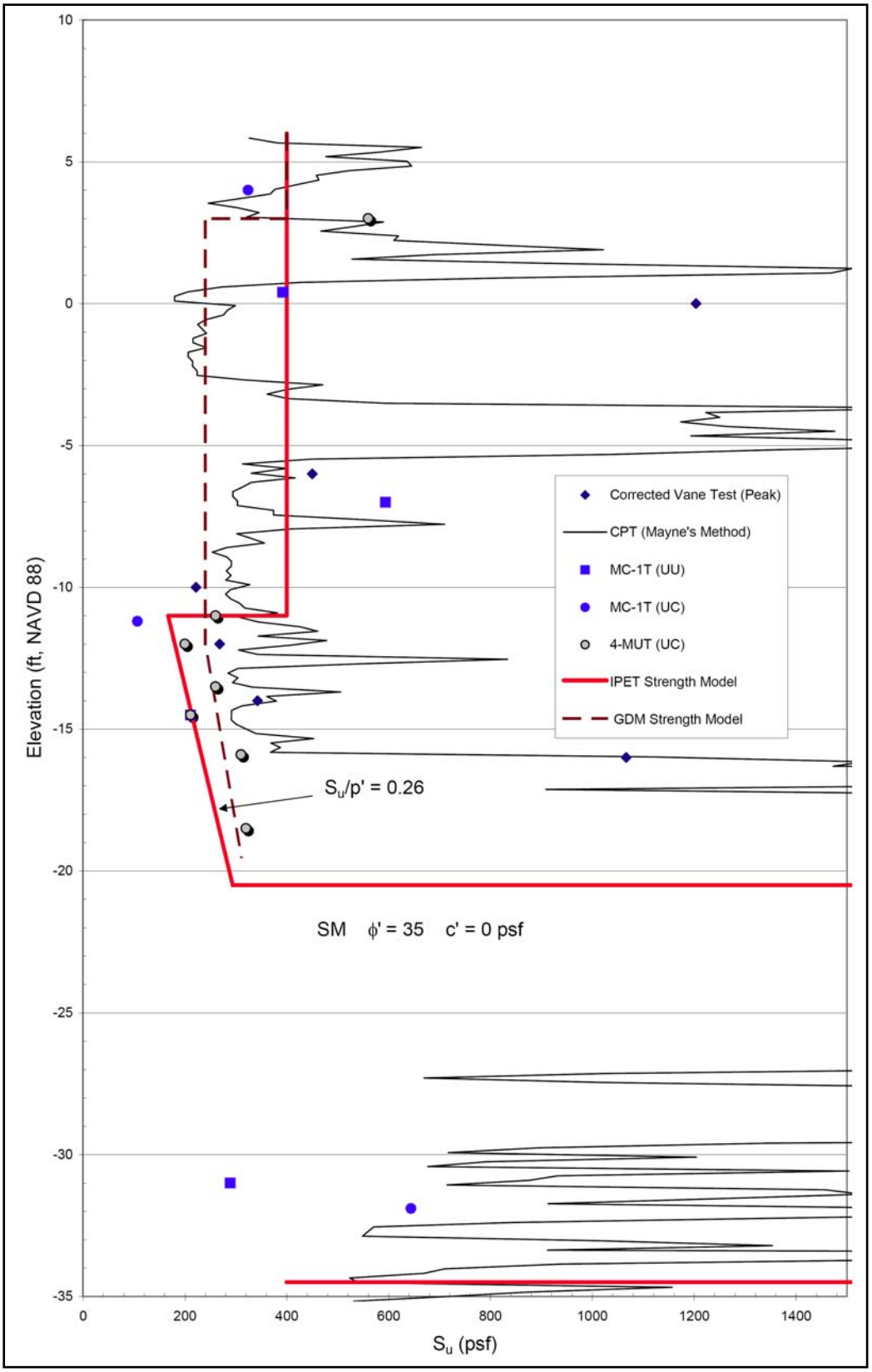

Figure 5. Michoud Canal, Sta. 4+00, Toe Shear Strengths.

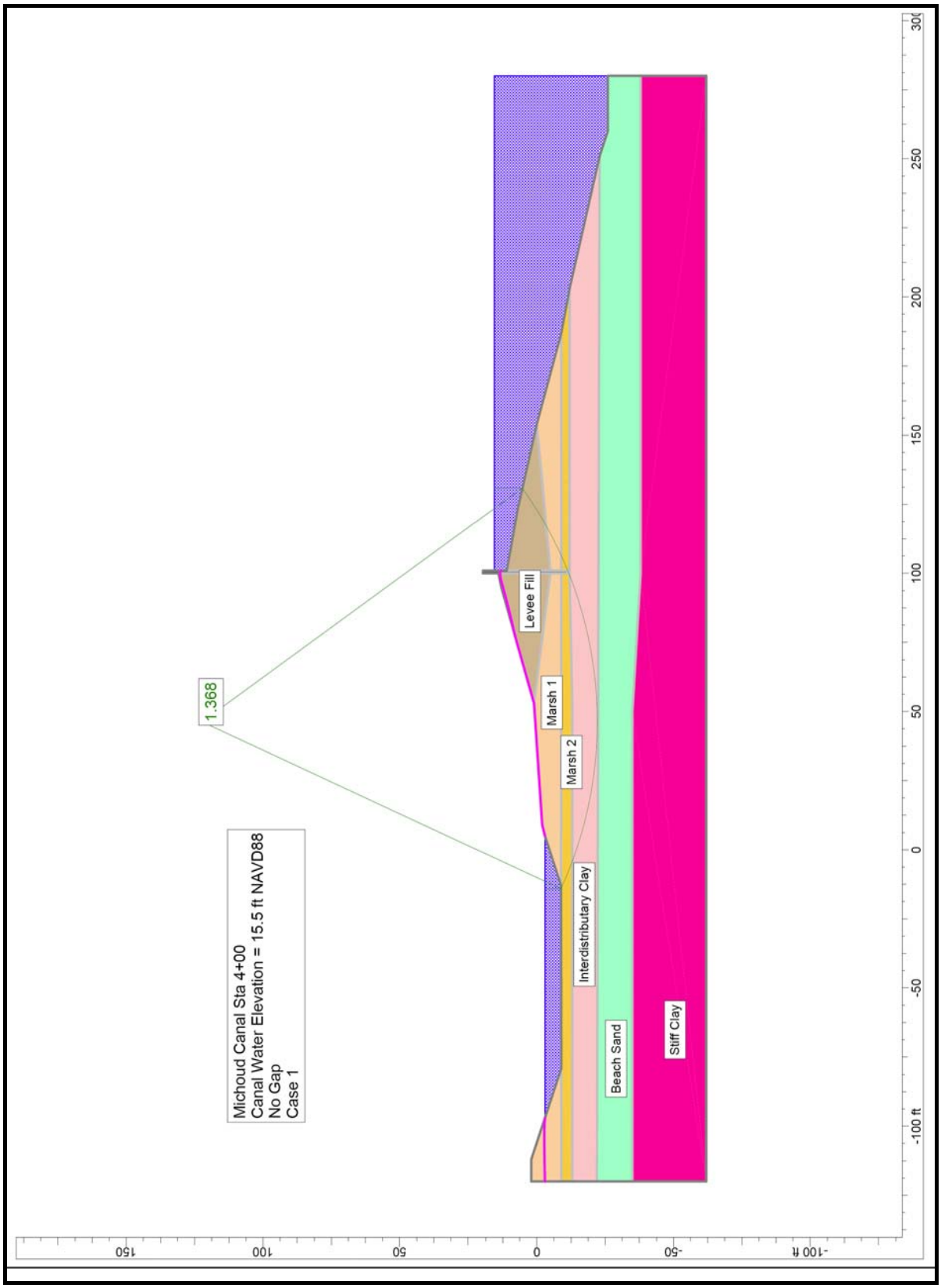

Figure 6. Michoud Canal, Sta. 4+00 – Case 1, Hydrograph Canal Water Level (15.5 ft, NAVD 88), no gap.

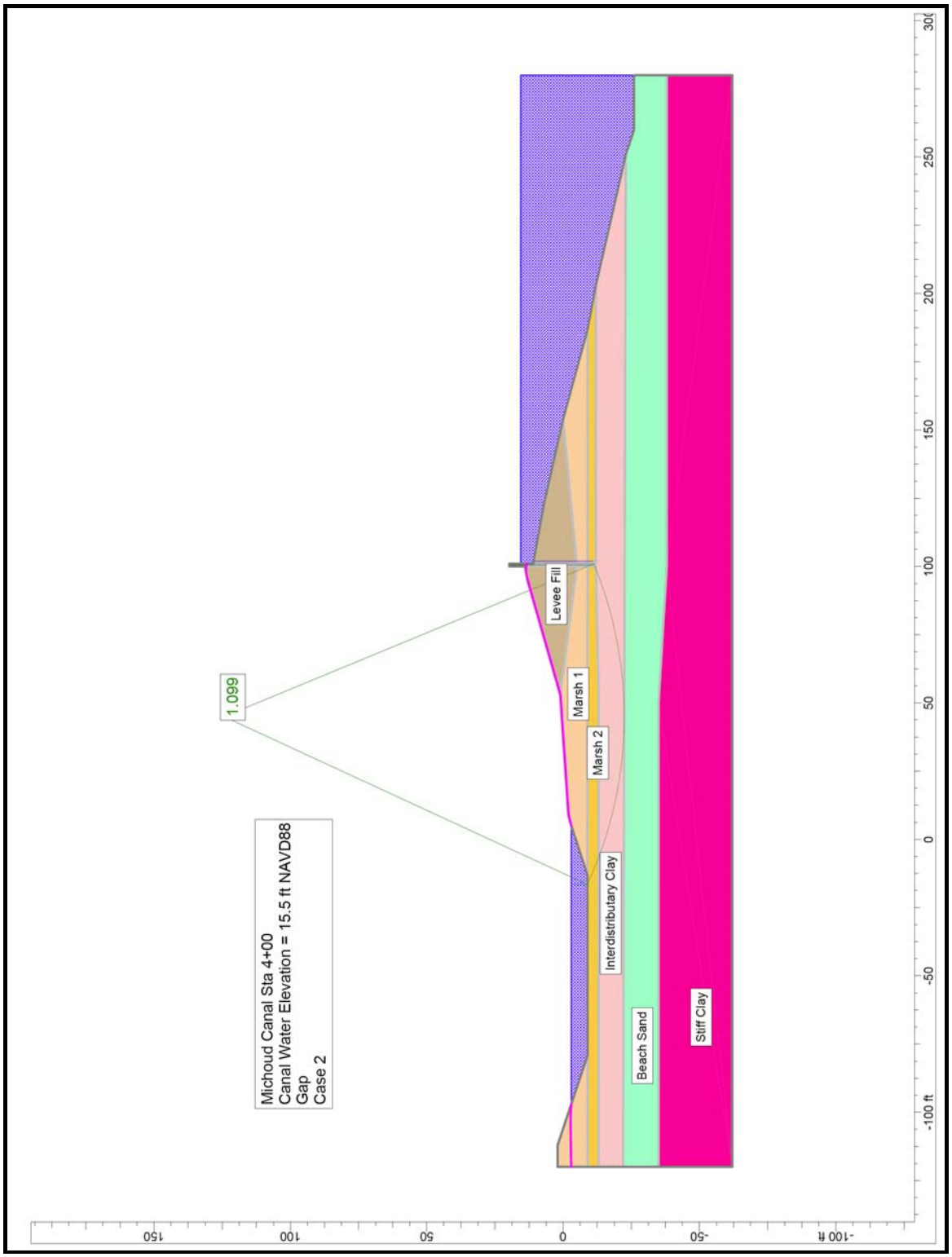

Figure 7. Michoud Canal, Sta. 4+00 – Case 2, Hydrograph Canal Water Level (15.5 ft, NAVD 88), with gap.

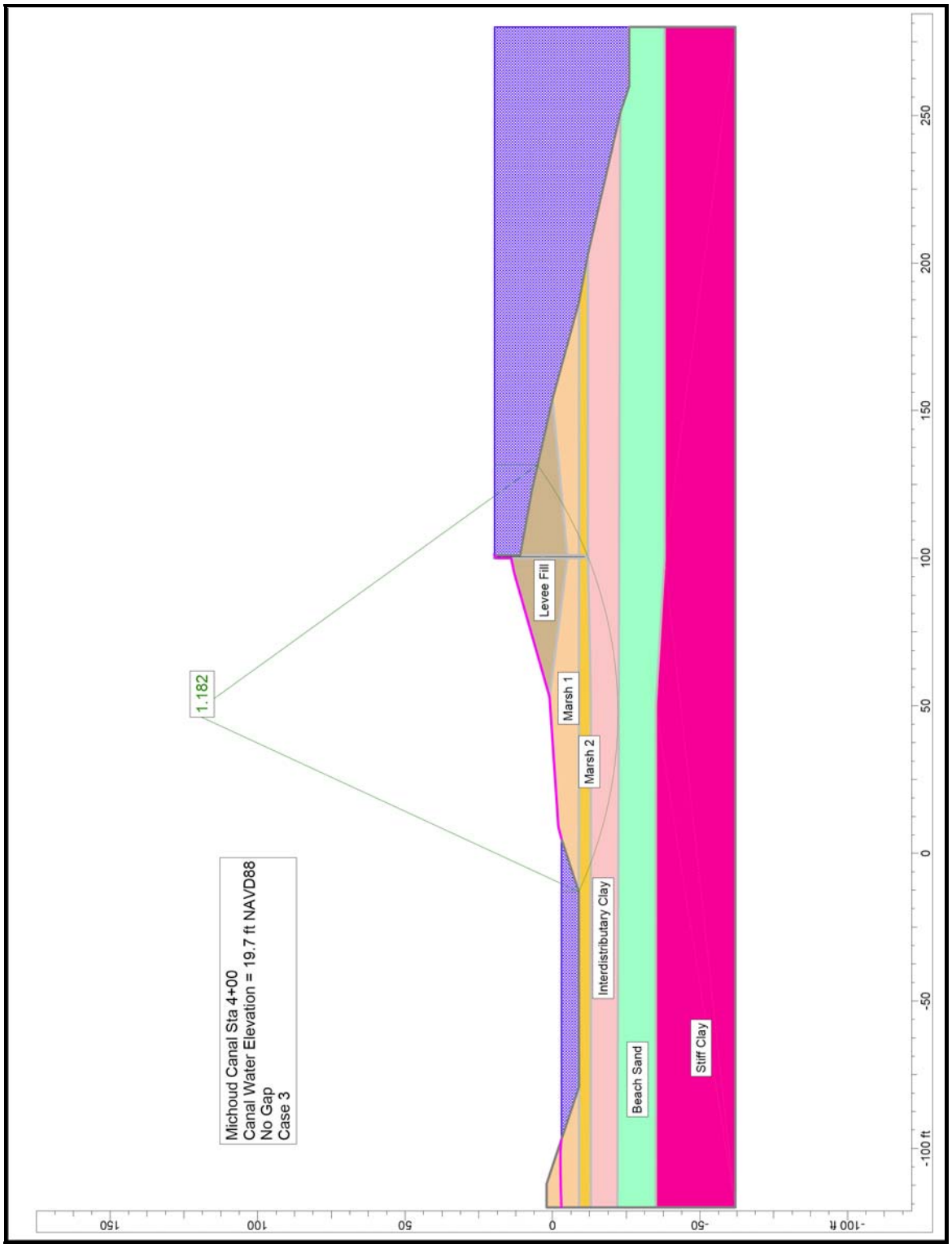

Figure 8. Michoud Canal, Sta. 4+00 – Case 3, Top of Wall - Canal Water Level (19.7 ft, NAVD88), no gap.

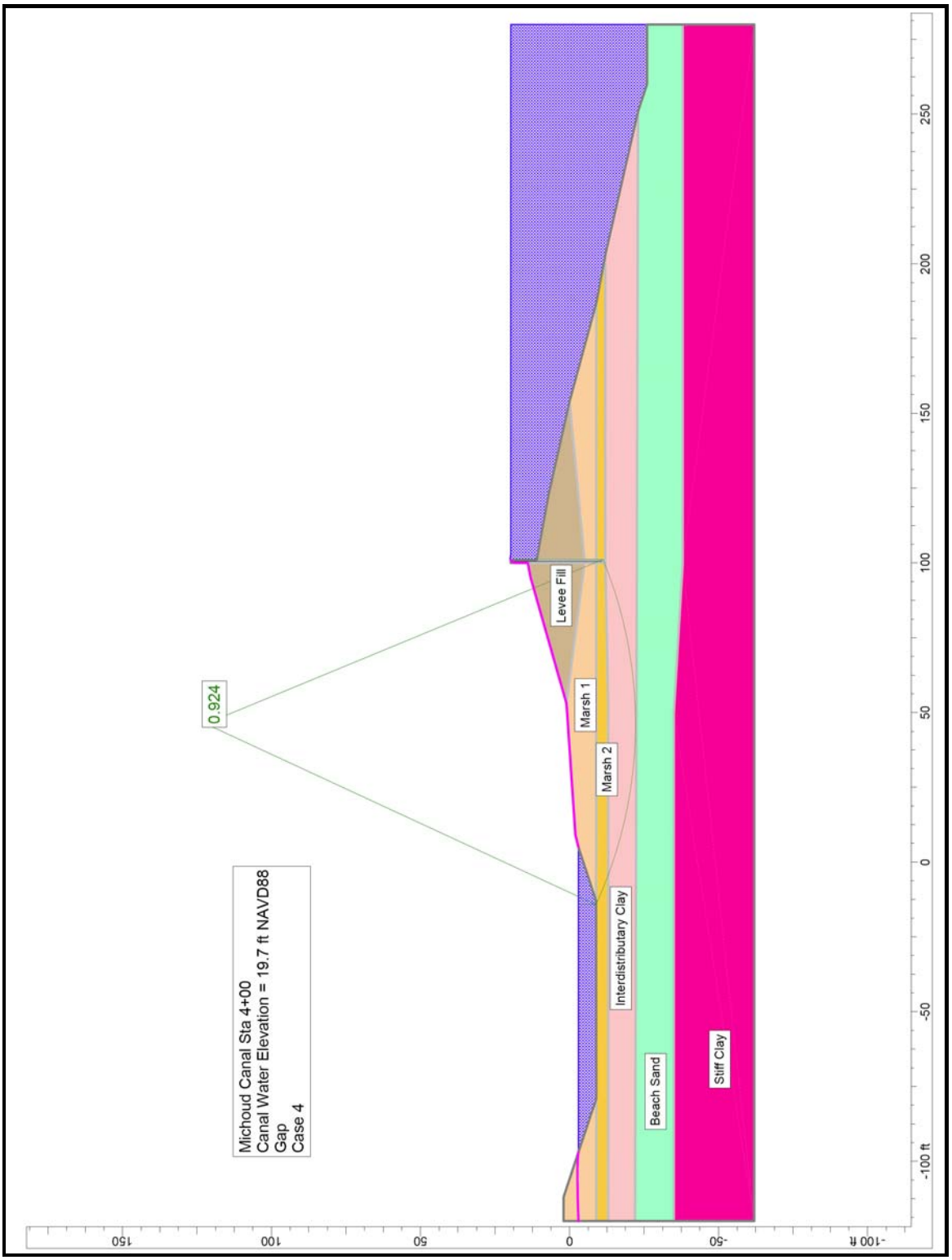

Figure 9. Michoud Canal, Sta. 4+00 – Case 4, Top of Wall - Canal Water Level (19.69 ft, NAVD88), with gap.